



ISSN 1454-8518

**ANNALS
OF THE UNIVERSITY OF
PETROȘANI**

ELECTRICAL ENGINEERING

VOL. 9 (XXXVI)

**UNIVERSITAS PUBLISHING HOUSE
PETROȘANI - ROMANIA 2007**

EDITOR OF PUBLICATION

Prof.dr.eng. Ioan-Lucian BOLUNDUȚ: Email: ibol@upet.ro

ADVISORY BOARD

Prof. Dr. Eng. Pop Emil - University of Petroșani, *Romania*; **Acad. Prof. Dr. Pivnyak Ghenadi** – National Mining University of Ukraine; **Prof. Dr. Eng. Munteanu Radu** - Tehnical University of Cluj-Napoca, *Romania*; **Acad. Prof. Dr. Eng. Dašić Predrag** - High Technological Technical School, Krusevac, *Serbia and Montenegro*, **Prof. Dr. Eng. Cierpisz Stanislaw** – Silesian University of Technology, Poland; **Prof. Dr. Eng. Bitoleanu Alexandru** - University of Craiova, *Romania*; **Prof. Dr. Eng. Păsculescu Mihai** - University of Petroșani, *Romania*; **Acad. Prof. Dr. Eng. Coloși Tiberiu** - Tehnical University of Cluj-Napoca, *Romania*; **Prof. Dr.Eng. Szabo Willibald** – “Transilvania” University of Brașov, *Romania*; **Prof. Dr. Eng. Poantă Aron** - University of Petroșani, *Romania*; **Prof. Dr. Eng. Manolea Gheorghe** - University of Craiova, *Romania*; **Prof. Dr. Eng. Vasilevici Alexandru** - Politechnical University of Timișoara, *Romania*; **Assoc. Prof. Dr. Dubois Daniel** - University of Liège, *Belgium*; **Assoc. Prof. Dr.Eng. Kovács Ernő** - University of Moskolc, *Hungary*; **Prof. Dr. Eng. Klepikov Vladimir Borisovich** – National Technical University of Kharkov, Ukraine; **Prof. Dr. Eng. Trușcă Vasile** - University “Politehnica” of Bucharest, *Romania*; **Prof. Dr. Eng. Fotău Ion** - University of Petroșani, *Romania*

EDITORIAL BOARD

Editor-in-chief:

Prof. Dr. Eng. Fotău Ion	University of Petroșani
Assoc.Prof. Dr.Eng Marcu Marius	University of Petroșani

Associate Editors:

Prof. Dr. Eng. Poantă Aron	University of Petroșani
Assoc.Prof. Dr.Eng Uțu Ilie	University of Petroșani
Assoc.Prof. Dr.Eng. Pătrășcoiu Nicolae	University of Petroșani

Editor Secretary:

Assistant Eng. PhD Student Dobra Remus	University of Petroșani
--	-------------------------

Editorial office address:

University of Petroșani, 20 University Street, 332006 Petroșani, Romania,
Phone: (40) 254/54.29.94; 54.25.80; 54.25.81; 54.33.82;
Fax: (40) 254/54.34.91; 54.62.38, Telex: 72524 univp, E-mail: marcu@upet.ro

This publication is with international distribution. It is sending in 28th countries.

CONTENTS

Dašić Predrag, Nedeff Valentin, Curčić Srećko, Analysis and evaluation of software tools for life cycle assessment	6
Dumitru Cazacu., Constantin Stanescu, Aspects concerning the computation of microstrip lines parameters	16
Gabriel Nicolae Popa, Iosif Popa, Sorin Deaconu, Classical power supply solutions for low pressure mercury lamps	22
Susana Arad, Victor Arad, Bogdan Bobora, Mihaela Bobora, Coal/petcoke conversion like auxiliary fuel at S.C. carpatcement holding S.A Deva branch	28
Liviu Blanaru, Sorin Cureleanu, Anghel Stoichitoiu, Coal-main basic resource in the energy production	34
Sorin Burian, Ionescu Jeana, Daire Marius, Moldovan Lucian, Comparative study on the types of protection for the electric apparatus intended for use in explosive atmospheres	37
Tiberiu Csaszar, Sorin Burian, Marius Darie, Conditions for interconnecting intrinsic safety circuits supplied by linear and non-linear sources intended for use in potentially explosive atmospheres	43
Miltiade Cărlan, Horia Goia, Simona Dzițac, Consideration viewing the optimal dimensioning of the maintenance team from thermo-electric power plants	49
Ioan Felea, Horia Goia, Simona Dzițac, Contributions to implement the reliability centered maintenance at the thermo-electric plants	55
Teodor Tabacaru-Barbu Diagnostic testing for asynchronous motors	61
Dragoș Pasculescu, Constantin Brindusa, Electric frames with linear induction motor propulsion systems electric traction scheme	67
Andrei Ceclan, Dan Doru Micu, Dan Micu, Emil Simion, Electromagnetic device design synthesis	72
Iosif Popa, Gabriel Nicolae Popa, Sorin Deaconu, Electronic time relays with different functions with T.T.L. integrated circuits	77
Corina Cuñan, Ioan Baci, Establishing of the effects produced by the passive filters of rc type on the sinusoidal voltage source	83
Leonard Lupu, Nicula Vatavu, Florin Paun, Improvement methods and technical tests for technical equipment intended for use in area with combustible dusts	87
Doru Visan, Daniela Mardare, Adriana Busoniu, Ileana Marcu Increase of energetic efficiency at S.E.Paroseni plant concerning of environmental European rules	91
Dan Stoia, Mihai Cernat, Integrated starter-generator machines for hybrid automotive vehicles	97
Sorin Deaconu, Gabriel Nicolae Popa, Iosif Popa, Ioan Rodean, Modern system for monitoring and diagnosis of the mechanical and electrical defects for high capacity induction motors	107
Mircea Risteiu, Adrian Tulbure, Moise Achim, Cosmin Covaciu, New approach in measurement-based power network modeling by using smart sensors	111
Sorin Burian, Jana Ionescu, Marius Darie, Possibilities to protect against explosion the low current circuits made of micro-drivings	120
Piotr Gawor, Sergiusz Boron, Power supply and design problems of longwall installations of rated voltage above 1 kV in underground coal mines	126
Maria Orban, Cristinel Popescu, Sorin Cureleanu, Liviu Blanaru, Problem viewing the drive of large power machines from coal extraction industry	133
Victor Vaida, Reflections on the qualification of the generation units for providing the service consisting in reactive power within the voltage secondary control range	138

Niculina Vătavu, Adrian Jurca, Florina Muntean Berzan, Researches on the risk factors when using electro-insulating materials in construction of technical equipment intended for use in areas with explosion hazards.....	147
Marius Marcu, Ilie Utu, Florin Popescu, Leon Pană, Simulation software for static switch controllers.....	153
Nicolae Dan, Visalon Dan, Some results in solving field engineering problems using finite element method.....	160
Florin Adrian Păun, Leonard Lupu, Florina Muntean Berzan, Standardization test methods used at assessment of product conformity with the requirements of preventing the explosive atmosphere ignition by electrostatic discharges.....	164
Leon Pană, Ion Fotău, Horia Șerban Stochastic models for reliability analysis of protection systems.....	168
Jenica Ileana Corcău, Study dynamic of a synchronous generator with electronic load.....	174
Constantin Brîndușa, Mihai Păsculescu, Dragoș Păsculescu Tensions invertors with commutation on three levels. Mathematical modeling; structural diagram.....	183
Constantin Brîndușa, Mihai Păsculescu, Dragoș Păsculescu Tensions invertors with commutation on two levels. Mathematical modeling; structural diagram.....	188
Ioan Baci, Corina Cunțan, The analysis of the lc-type passive filters' influence upon the power supply network of a resistive consumer using the LabView program.....	192
Sorin Cureleanu, Liviu Blanaru, Anchel Stoichitoiu The lignite role as the primary source in the electrical energy supply in Romania.....	196
Adrian Marius Jurca, Mihaela Părăian, Emilian Ghicioi, Nicula Vătavu The new European concept of explosion protection for the non-electrical equipment intended for use in explosive atmospheres.....	199
Ioan Vasii, The optimal operating ranges of the steam generators with natural circulation working on powdered coal in the romanian power plants.....	205
Visalon Dan, Nicolae Dan Theoretical aspects in solving field engineering problems using finite element method.....	211
Andreea Brîndușa, Iosif Kovacs, Adriana Bociat Thermoenergetic block on coal pollution vector water hydroconveyer for ashes.....	215
Andreea Brîndușa, Iosif Kovacs Thermoenergetic block on coal pollution vector: burning gas.....	218
Constantin Brîndușa, Mihai Păsculescu, Marius Popescu, Urban frame with static converter and asynchronous motors. Direct field orientation.....	222
Visalon Dan, Carol Zoller, Using graphical programming vee pro 6 software for function simulation of the grinding aggregates to maintain optimum specific energy consumption.....	226
Jenica Ileana Corcău, Voltage electronic regulator for aircraft.....	232
Dragoș Pasculescu, Constantin Brindusa Wear valuation of braking activ material at urban electric frames brake regime.....	237
Remus Dobra PC to CY8C29466 microcontroller serial communication method.....	242
Corneliu Mândrescu, Olimpiu Stoicuța, Analysis of the luemberger extended estimator used within a vectorial type electrical driving system with an induction motor.....	246
Monica Leba, Emil Pop, Petre Vamvu, Approach on distributions for control systems with relay type nonlinearities.....	254
Gabriela Bucur, Liviu Bucur, Automatic wig welding control using feedforward neural network.....	260

Roxana-Adina Irimia, Alina-Nicoleta Vlăsceanu , Electronic government–reflections over the design of a regional development strategy.....	266
Adrian Tulbure, Mircea Rîsteiu , <i>Embedded-system zur steuerung leistungselektronischer module</i>	272
Aron Poanta, Dan Dojcsar, Bogdan Sochirca , Equipment used in priming of the blasting cartridge with cypress microcontroller.....	278
Luminița Popescu, Florin Grofu, Marian Popescu , <i>Experimental model for predictive control of the pumping aggregates used for water drain in roșia mining pit</i>	286
Luminița Popescu, Olaru Onisifor Florin Grofu , <i>Experimental model for monitoring a pumping aggregate used for water drain in roșia mining pit</i>	292
Cristina Popa, Cristian Patrascioiu , <i>FCC Model predictive control</i>	298
Nicolae Pătrășcoiu, Adrian Marius Tomuș , <i>Gas monitoring system based on Modbus protocol and virtual instrumentation</i>	309
Popescu Marius-Constantin , <i>Hybrid neural network for prediction of process parameters in injection moulding</i>	312
Otilia Cangea , Informatic viruses detection using heuristic algorithms.....	320
Egri Angela, Sirb Vali Chivuța , <i>Modeling for industrial and manufacturing systems</i>	326
Cristina Popescu , <i>Neural network techniques for mobile robot navigation</i>	332
Valentin Casavela , <i>Program conceived in the visual studio.net mediu, for a capital devaluation calculation and displaying</i>	338
Emil Pop, Ioana Camelia Tabacaru Barbu, Maria Pop , Renewable energy resources possibilities use in jiu valley.....	343
Nicolae Pătrășcoiu, Adrian Marius Tomuș , Resistive bridge controled by virtual instrumentation.....	351
Laurențiu Alboteanu, Gheorghe Manolea, Florin Ravigan, Adrian Nour <i>Strategies of control for solar panels positioning systems</i>	357
Corneliu Mândrescu, Olimpiu Stoicuța , <i>Synthesis of the luemberger extended estimator used within a vectorial-type electrical driving system with an induction motor</i>	365
Mircea Rîsteiu, Adrian Tulbure , Zigbee development setup for measurement-based web modeling and simulation.....	373
Andreea Brîndușa, Iosif Kovacs , <i>Thermoenergetic block on coal. Pollution vector: Evacuated water</i>	381
Dašić Predrag,, Ječmenica Ratomir, Šerifi Veis <i>One classification example of decision support systems</i>	385
Liviu Dumitrașcu, Gabriel Marcu, Dorel Dusmanescu <i>Implementing within an object-oriented language (java) the UML modelling concepts</i>	392

ANALYSIS AND EVALUATION OF SOFTWARE TOOLS FOR LIFE CYCLE ASSESSMENT

PREDRAG DAŠIĆ*, VALENTIN NEDEFF**, SREĆKO ĆURČIĆ***

Abstract: Life-cycle assessment (LCA) is a methodology for analyzing and systematic evaluation of environmental aspects of a product or service system through all stages of its life cycle. LCA was chosen to be worldwide used tool in the 1990s for environmental management in the form of ISO 14040 series. There is a large number of developed software tools for LCA nowadays in the world. This paper analyzes and evaluates software tool: GaBi, KCL-ECO, LCAiT, PEMS, SimaPro and TEAM for product and process LCAs.

Keywords: LCA (*Life-Cycle Assessment*), LCE (*Life-Cycle Engineering*), LCI (*Life-Cycle Inventory*), LCIA (*Life-Cycle Impact Assessment*), software tools

1. INTRODUCTION

Life cycle is consecutive and interlinked stages of a product system, from raw material acquisition or generation of natural resources to the final disposal.

Product and process life cycle topics are [7, 12-13]:

- LCA (*Life-Cycle Analysis*),
- LCA (*Life-Cycle Assessment*),
- LCC (*Life-Cycle Cost*),
- LCD (*Life-Cycle Design*),
- LCI (*Life-Cycle Inventory*),
- LCIA (*Life-Cycle Impact Assessment*),
- LCM (*Life-Cycle Management*),
- LCS (*Life-Cycle Strategy*),
- SCM (*Supply Chain Management*) etc.

* *High Technological Technical School, Kosanciceva 36, 37000 Krusevac, Serbia and Montenegro*

** *University of Bacău*

*** *Technical Faculty Cacak, Svetog Save 65, 32000 Cacak, Serbia and Montenegro*

All listed topics for life-cycle incorporate all scientific areas called LCE (*Life-Cycle Engineering*).

Methodology for the life-cycle and sustainability analysis of manufacturing processes is given in paper [6].

LCA (*Life Cycle Assessment*) is a methodology used to evaluate the potential environmental impact of a product, process or activity throughout its entire life cycle by quantifying the use of resources ("inputs" such as energy, raw materials, water) and environmental emissions ("outputs" to air, water and soil) associated with the system that is being evaluated.

The most important applications are:

- Analysis of the contribution of the life cycle stages to the overall environmental load, usually with the aim to prioritise improvements on products or processes and
- Comparison between products for internal or external communications.

The first predecessor of LCA was the REPA (*Resource and Environmental Profile Analysis*) in the 1960s and 1970s. First studies that were performed by REPA were for Coca Cola Company and Mobil Corporation. Interest studies continued through the 1980s as more sophisticated analysis [2].

Modern LCA methodology is root in the development of standards through the 1990s. The SECAT (*Society for Environmental Toxicology and Chemistry*, available on Web site: <http://www.setac.org/>) in 1991 published "A Technical Framework for Life Cycle Assessments" [3] as a first international LCA standard. Detailed LCA methodologies were specified in 1995 by Nordic Council of Ministers.

ISO (*International Organization for Standardization or International Standards Organization*, available on Web site: <http://www.iso.org/> or <http://www.iso.ch/>) released for the first time a general introductory framework on LCA (ISO 14040 standard) in 1997, and the ISO 14040 to 14043 standard series in late 1990s and early 2000s.

A partnership was launched in 2002 between UNEP (*United Nations Environment Programme*, available on Web site: <http://www.unep.org/>) and SETAC in order to form the UNEP/SETAC Life-Cycle Initiative to evaluate products using practical tools and services to achieve sustainable development (available on Web site: <http://www.unep.org/pc/sustain/lcinitiative/home.htm>) and other initiatives [8].

In June 1992 a society for LCA called SPOLD (*Society for Promotion of LCA Development*) was established, which is available on Web site: <http://www.spold.org/> or <http://lca-net.com/spold/>.

Application of LCA is given in paper [1], LCA in industry and business in paper [10], evaluation of environmental impacts in LCA [9] and integrating LCA analysis and LCA in paper [25].

Structure of the life cycle assessment (LCA) is show in figure 1 [5, 6].

2. STANDARDIZATION OF LCA

According to ICS (*International Classification for Standards*), LCA is categorized in the 13th field for "Environment, health protection and safety" and 020th

group (ICS=13.020) for "Environmental protection" and 60th subgroup (ICS=13.020.60) for "Product life-cycles".

The international ISO standards in frame subgroup "Product life-cycles" (ICS=13.020.60) specifically designed for LCA applications are [14-20, 24]: [ISO 14040:1997](#), [ISO 14041:1998](#), [ISO 14042:2000](#), [ISO 14043:2000](#), [ISO/TR 14047:2003](#), [ISO/TS 14048:2002](#) and [ISO/TR 14049:2000](#).



Fig.1 Structure of the Life Cycle Assessment (LCA)

The ISO 14040 to 14043 standards describes the method presenting the different options for the release of LCA. The ISO 14040 standards are a general standard for the LCA area and were issued in 1997 from ISO subcommittee ISO TC 207/SC 5 (available on Web site: <http://www.tc207.org/>). Based on a goal and scope definition, the environmental impacts of the important elements are scrutinized in a so-called inventory analysis [14]. After that, the impacts are assessed and interpreted in order to improve the sustainability and the environmental friendliness of the analyzed product. According to ISO 14040, the general framework of LCA is illustrated in figure 2 [14, 24].

The ISO 14040:1997 standard outlines the principles and the conduct of LCA studies and how to reduce the overall environmental impact of products and services [14].

The ISO 14041:1998 standard in conjunction with ISO 14040 specifies requirements and procedures to define the goal and scope for life cycle assessment, performing, interpreting and reporting a LCI (*Life-Cycle Inventory*) analysis [15]. The ISO 14042:2000 standard provides guidance on a general framework for the LCIA (*Life-Cycle Impact Assessment*) phase of LCA, and the key features and inherent limitations of LCIA [4, 16].

The ISO 14043:2000 standard summarizes the final phase of the LCA procedure, including the LCI (*Life-Cycle Inventory*) analysis and LCIA (*Life-Cycle Impact Assessment*) [17].

The ISO 14047:2003 standard provides examples of application of ISO 14042 [18] and ISO 14049:2000 standard provides examples of application of ISO 14041 [20].

The ISO 14048:2002 standard provides the requirements and a structure for a data documentation format, to be used for transparent and unambiguous documentation and exchange of LCA (*Life-Cycle Assessment*) and LCI (*Life-Cycle Inventory*) data [19].

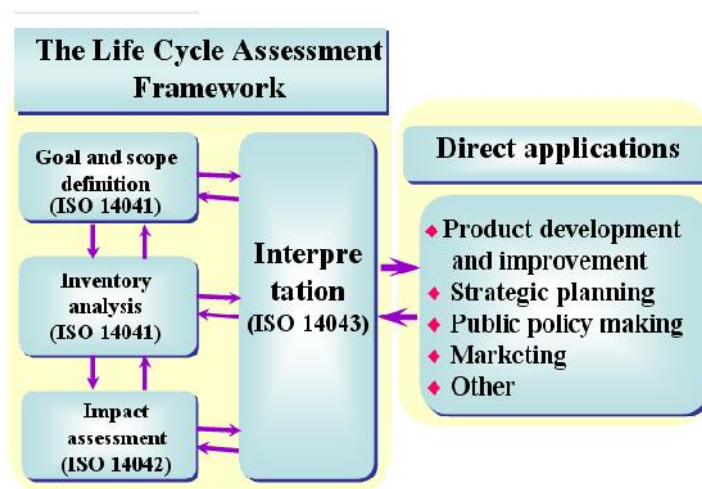


Fig.2 The framework of LCA with four interrelated phases, according to the ISO 14040 standard [13]

3. SOFTWARE TOOLS FOR LCA

Today there is a large number of developed software tools for LCA, whose review is given in book [3] and paper [4]. The list of the most important software tools for product and process LCAs given in alphabetical order is as follows [5, 7-8, 21-22, 26-30, 32-34]:

- ACE (*Active Community / Stakeholder Engagement Software*), available on Web site: <http://www.activ.com/>,
- AME (*A Modeling Environment*), available on Web site: <http://helios.bto.ed.ac.uk/ierm/ame/>,
- ATHENA, available on Web site: http://www.athenasmi.ca/ath_model/model_main.htm,
- Boustead Model, available on Web site: <http://www.boustead-consulting.co.uk/>,
- BeCost, available on Web site: <http://pim.vtt.fi/becost/html/index.htm>,
- CLEAN (*Comprehensive Least Emissions Analysis*),

- CMLCA (*Chain Management by LCA*), available on Web site: <http://www.leidenuniv.nl/interfac/cml/ssp/software/cmlca/index.html>,
- CMSS (*Compliance Management Software Solutions*), available on Web site: <http://www.amadeussolutions.com/>,
- CUMPAN (*Computerunterstützte umweltorientierte Produktbilanzierung*), available on Web site: <http://www.debis.de/debis/systemhaus/>,
- DEEDS (*Design for Environment Decision Support*), available on Web site: <http://sun1.mpce.stu.mmu.ac.uk/pages/projects/dfc/deeds/deeds.html>,
- ECO-it (*Ecological - Indicator Tool*), available on Web site: <http://www.pre.nl/eco-it.html>,
- EcoLab (*Ecological - Lab*), available on Web site: <http://www.port.se/ecolab/default.htm>,
- EcoMan (*Ecological - Manager*), available on Web site: <http://www.fal.com/software/ecoman.html>,
- EcoPack (*Ecological - Package*),
- EcoPro, available on Web site: http://www.sinum.com/htdocs/e_software_ecopro.shtml,
- Eco-Quantum (*Ecological Quantum*), available on Web site: <http://www.ecoquantum.nl/>,
- EcoScan (*Ecological - Scan*), available on Web site: ; <http://www.ind.tno.nl/en/product/ecoscan/> or <http://www.luna.nl/turtlebay/>,
- EcoSoft (*Ecological - Software*), available on Web site: <http://www.ibo.at/ecosoft.htm>,
- EcoSys (*Ecological - Systems*),
- EDIP (*Environmental Design of Industrial Products*), available on Web site: <http://www.mst.dk/activi/08030000.htm>,
- EMS (*Environmental Management Software*), available on Web site: <http://www.esp-net.com/>,
- ENVEST II, available on Web site: <http://www.bre.co.uk/envest/> or <http://invest2.bre.co.uk/account.jsp>,
- EPS 2000 (*Environmental Priority Strategies 2000*), available on Web site: <http://www.assess.se/software.htm>,
- EUKLID, available on Web site: http://www.ivv.fhg.de/sysana_soft.html,
- GaBi (*Ganzheitliche Bilanzierung*), available on Web site: <http://www.gabi-software.de/software.html> or http://www.pe-consulting-group.com/software_gabi.html or http://www.ikpgabi.uni-stuttgart.de/deutsch/gabi_soft.html,
- GBA (*Green Building Advisor*), available on Web site: <http://www.greenbuildingadvisor.com/>,
- GDM (*Green Design and Manufacturing*), available on Web site: <http://greenmfg.me.berkeley.edu/green/Home/Index.html>,
- IDEA (*International DataBase for Eco-profile Analysis*), available on Web site: <http://www.iiasa.ac.at/>,
- IdeMat (*Identification Materials*), available on Web site: <http://www.io.tudelft.nl/research/dfs/ideimat/index.htm>,

-
- IRIS (*Integrated Risk Information System*), available on Web site: <http://www.epa.gov/iris/intro.htm>,
 - JEM-LCA (*Japan Environment Management - LCA*),
 - KCL-ECO (*Keskuslaboratorio – Centrallaboratorium Ab - Ecology*), available on Web site: <http://www.kcl.fi/eco/softw.html>,
 - LCAdvantage (*LC Advantage*), available on Web site: <http://www.battelle.com/>,
 - LCAiT (*LCA Inventory Tool*), available on Web site: <http://www.lcait.com/01.html>,
 - LCAPIX, available on Web site: <http://www.kmlmtd.com/pas/index.html>,
 - LCASys (*LCA Systems*),
 - LCE (*Life Cycle Explorer*), available on Web site: <http://www.sylvatica.com/>,
 - LEGEP, available on Web site: <http://www.legep.de/>,
 - LIMS (*Life Cycle Interactive Modeling System*),
 - LISA (*LCA in Sustainable Architecture*), available on Web site: <http://www.lisa.au.com/>,
 - MIET (*Missing Inventory Estimation Tool*), available on Web site: <http://www.leidenuniv.nl/cml/ssp/software/miet/index.html>,
 - OGIP (*Optimisation of Global Demands in Terms of Costs, Energy and Environment within an Integrated Planning Process*), available on Web site: <http://www.the-software.de/BauenUmwelt.html>,
 - PEMS (*Pira Environmental Management System*), available on Web site: <http://www.pira.co.uk/pack/environmental.htm>,
 - PHASETS (*Phases in the Design of a Model of a Technical System*),
 - PIA (*Product Improvement Analysis*), available on Web site: <http://www.pira.co.uk/>,
 - POEMS (*Product Oriented Environmental Management Systems*), available on Web site: http://www.ecobalance.com/uk_m_poems.php,
 - RAVEL (*Rail Vehicle Eco-efficient Design*),
 - REGIS, available on Web site: http://www.sinum.com/htdocs/e_software_regis.shtml,
 - REPAQ (*Resource and Environmental Profile Analysis Query*), available on Web site: <http://www.fal.com/software/REPAQ.html>,
 - SEEA (*System of Integrated Environmental and Economic Accounting*), available on Web site: <http://unstats.un.org/unsd/environment/software.htm>,
 - SimaPro (*System for Integrated Environmental Assessment of Products*), available on Web site: <http://www.pre.nl/simapro/>,
 - SimaTool (*System for Integrated Environmental Assessment of Tool*),
 - SoFi (*Software for Sustainability Reporting of Financial Service Providers*), available on Web site: <http://www.sofi-software.com/> or http://www.pe-consulting-group.com/software_sofi.html,
 - SWAMI (*Strategic Waste Minimization Initiative*), available on Web site: <http://www.er.doe.gov/epic/html/SWAMI.stm>,
 - TCace (*Total Cost Assessment*), available on Web site: <http://www.tcace.com/> and <http://www.sylvatica.com/tcace.htm>,

- TEAM (*Tool for Environmental Analysis and Management*), available on Web site: http://www.ecobalance.com/uk_team.php,
- TEMIS (*Total Emission Model for Integrated Systems*),
- TIET (*Teleworking Impact Estimation Tool*), available on Web site: <http://greenmfg.me.berkeley.edu/green/SoftwareTools/Telework/>,
- Umberto, available on Web site: <http://www.umberto.de/en/home/>,
- WISARD (*Waste - Integrated Systems Assessment for Recovery and Disposal*), available on Web site: http://www.ecobalance.com/uk_wisard.php,
- WPC (*Web-Based Paper Calculator*), available on Web site: <http://www.ofee.gov/recycled/cal-index.htm> and etc.

4. EVALUATION OF SOFTWARE TOOLS FOR LCA

Out of a large number of software tools for LCA listed in chapter 3 an analysis was performed of ten chosen software tools: GaBi, KCL-ECO, LCAiT, PEMS, SimaPro and TEAM (table 1) [11, 26]. The following criteria were taken into consideration: Functionality, Flexibility, Database, User – friendliness, Software properties, Service and Cost. The evaluation ranges from 1 (very negative) to 5 (very positive). As this is a very subjective evaluation method we decided to disclose the results and publish a non-aggregated rating for each tool and criterium. Even these ratings are based on subjective impressions, therefore other individuals may come to different findings.

According to evaluation in paper [11, 26] the new releases of software tools: GaBi, KCL-ECO, LCAiT, PEMS, SimaPro and TEAM for LCA are the most interesting software tools on the market.

In table 2 is presented a condensed and comparative evaluation of these unique software tools (GaBi, KCL-ECO, LCAiT, PEMS, SimaPro and TEAM) features for product and process LCAs [23].

5. CONCLUSION

All listed topics for life-cycle (LCA, LCC, LCD, LCI, LCIA, LCM, LCS etc.) incorporate all scientific areas called LCE (*Life-Cycle Engineering*).

The general standard for the LCA area is ISO 14040 standards and was issued in 1997 by ISO subcommittee ISO TC 207/SC 5.

There is a large list of software tools for LCA, for example: BEES, CMLCA, CUMPAN, ECO-it, EcoMan, EcoPro, EDIP, GaBi, KCL-ECO, LCAiT, PEMS, REGIS, REPAQ, SDES, SimaPro, TEAM, TRACI, Umberto etc.

New releases of software tools: GaBi, KCL-ECO, LCAiT, PEMS, SimaPro and TEAM for LCA are the most interesting software tools on the market.

Table 1. Evaluation of the software tools for product and process LCAs

Characteristics	GaBi	KCL-ECO	LCAiT	PEMS	SimaPro	TEA M
Functionality	5	4	4	3	2	4
Flexibility	3	3	3	3	3	4
Database	4	2	4	3	4	5
User – friendliness	5	4	3	2	2	3
Software properties	3	4	3	3	3	2
Service	5	3	4	3	3	5
Cost	4	2	3	3	5	2

Table 2. A condensed and comparative evaluation of these unique software tools for LCA features

Characteristics	GaBi	KCL-ECO	LCAiT	PEMS	SimaPro	TEA M
Graphical Interface	✓	✓	✓	✓		✓
Data Protection	✓		✓	✓	✓	✓
Unit Flexibility	✓	✓	✓		✓	✓
Use of Formulas	✓	✓				✓
Uncertainty Analysis	✓	✓		✓		✓
Impact Assessment	✓	✓	✓	✓	✓	✓
Comparison of Results	✓			✓	✓	✓
Graphical Display of Results	✓	✓	✓	✓	✓	✓

REFERENCES

- [1] **Allen, D. T.:** *Applications of life-cycle assessment. In: Environmental Life-Cycle Assessment.* Edited by M. A. Curran. New York (USA): McGraw-Hill, 1996, pp. 5.1-5.17. ISBN 0-07-015063-X.
- [2] **Assies, J. A.:** *Life cycle assessment in a historical perspective. In: Environmental Assessment of Products: A Course on Life Cycle Assessment.* Edited by B. Pedersen. Helsinki (Finland): UETP – Environmental Engineering Education (EEE), 1993. ISBN 951-9110-83-6.
- [3] *A technical framework for life cycle assessments.* Pensacola (FL - USA): Society for Environmental Toxicology and Chemistry (SETAC), 1991. – 134 pp.
- [4] **Bare, C. J.; Pennington, W. D. and Udo de Haes, A. H.:** *Life cycle impact assessment sophistication – international workshop. International Journal of Life Cycle Assessment*, Vol. 4 (1999), No. 5, pp. 299 – 306. ISSN 0948-3349.
- [5] **Bruno, P. and Katrien, P.:** *PRESCO Work Package 2: Inter-comparison and benchmarking of LCA-based environmental assessment and design tool. Final report, Lozenberg (Belgium): Practical Recommendations for Sustainable Construction (PRESCO), 2005. – 74 pp. Available on Web site: http://www.etn-presco.net/generalinfo/PRESCO_WP2_Report.pdf.*
- [6] **Culaba, A. B. and Purvis, M. R. I.:** *A Methodology for the life-cycle and sustainability analysis of manufacturing processes. Journal of Cleaner Production*, Vol. 7 (1999), pp. 435 – 445. ISSN 0959-6526.

- [7] **Dašić, P.:** *Encyclopedia of the Technical and ICT Abbreviations* (in preparation in Serbian language). Electronic Edition. Trstenik: High Technical Mechanical School. ISBN 86-83803-12-0.
- [8] **Dašić, P.;** Nedeff, V.; Petropoulos G.: Internet resources and software tools for life cycle assessment. Plenary and Invitation paper. In: *Proceedings on CD-ROM of 6th International Conference "Research and Development in Mechanical Industry - RaDMI 2006"*, Budva, Montenegro, 13-17. September 2006. Edited by Predrag Dašić. Kraljevo: Faculty of Mechanical Engineering and Trstenik: High Technical Mechanical School, 2006, pp. 68-87. ISBN 86-83803-21-X.
- [9] *Evaluation of environmental impacts in life cycle assessment*. Meeting report, Brussels, Belgia, 29-30. November 1998 and Brighton, 25-26. May 2000. Paris: United Nations Environment Programme (UNEP), 2003. – 97 pp. ISBN 92-807-2144-5. Available on Web site: http://www.unep.org/pc/sustain/reports/lcini/UNE.%20P_US%20EPA%20LCIA%20mtg%20report.pdf.
- [10] **Frankl, P. and Rubik, F.:** *Life cycle assessment in industry and business*. Heidelberg (Germany): Springer, 2000. – 279 pp. ISBN 3-540-66469-6.
- [11] **Frühbrodt, E.:** LCA software review – An up-to-date overview of the European market. *Workshop on life cycle data for assessment of environmental performance of EEE and EU funded RTD activities on EEE ecodesign*. Brussels, 9 October 2002. Available on Web site: http://europe.eu.int/comm/enterprise/electr_equipment/eee/workshop9-10-02/present/lcasoftware.pdf.
- [12] **Hauschild, M.; Alting, L. and Poll, C.:** Life cycle engineering – from methodology to enterprise culture. Keynote paper. In: *Proceedings of 11th International CIRP Life Cycle Engineering Seminar: Product Life Cycle – Quality Management Issues*, Belgrade, Serbia and Montenegro, 20 - 22. June 2004. Edited by Leo Alting and Vidosav Majstorović. Belgrade: Faculty of Mechanical Engineering and Association Serbia and Montenegro for Quality and Standardization (JUSK), 2004, pp. 7-15. ISBN 86-903197-3-5.
- [13] **Herrmann, C.; Mateika, M.:** Quality aspects of life cycle strategies. In: *Proceedings of 11th International CIRP Life Cycle Engineering Seminar: Product Life Cycle – Quality Management Issues*, Belgrade, Serbia and Montenegro, 20 - 22. June 2004. Edited by Leo Alting and Vidosav Majstorović. Belgrade: Faculty of Mechanical Engineering and Association Serbia and Montenegro for Quality and Standardization (JUSK), 2004, pp. 57-61. ISBN 86-903197-3-5.
- [14] ISO 14040:1997 Environmental management -- Life cycle assessment -- Principles and framework. Geneve: International Organization for Standardizations (ISO).
- [15] ISO 14041:1998 Environmental management -- Life cycle assessment -- Goal and scope definition and inventory analysis. Geneve: International Organization for Standardizations (ISO).
- [16] ISO 14042:2000 Environmental management -- Life cycle assessment -- Life cycle impact assessment. Geneve: International Organization for Standardizations (ISO).
- [17] ISO 14043:2000 Environmental management -- Life cycle assessment -- Life cycle interpretation. Geneve: International Organization for Standardizations (ISO).
- [18] ISO/TR 14047:2003 Environmental management -- Life cycle impact assessment -- Examples of application of ISO 14042. Geneve: International Organization for Standardizations (ISO).
- [19] ISO/TS 14048:2002 Environmental management -- Life cycle assessment -- Data documentation format. Geneve: International Organization for Standardizations (ISO).
- [20] ISO/TR 14049:2000 Environmental management -- Life cycle assessment -- Examples of application of ISO 14041 to goal and scope definition and inventory analysis. Geneve: International Organization for Standardizations (ISO).

[21] *Life cycle assessment (LCA) – A guide to approaches, experiences and information sources*. Environmental Issues Series No. 6, Copenhagen: European Environment Agency (EEA), 1998. – 119 pp. Available on Web site: <http://reports.eea.eu.int/GH-07-97-595-EN-C/en/Issue%20report%20No%206.pdf>.

[22] *Life cycle assessment tools to measure environmental impacts: Assessing their applicability to the home building industry*. Final report, Washington (DC – USA): U.S. Department of Housing and Urban Development (HUD) User, 2001. – 49 pp. Available on Web site: <http://www.huduser.org/Publications/PDF/lifecycle.pdf>.

[23] **Menke, M. D.; Davis, A. G. and Vigon, W. B.:** *Evaluation of life cycle assessment tools*. Canada: Hazardous Waste Branch, 1996. – 59 pp. Available on Web site: <http://eerc.ra.utk.edu/ccpct/pdfs/LCAToolsEval.pdf>.

[24] **Nedeff, V.; Dašić, P.; Petropoulos, G.:** Standardization of life cycle assessment. *U zborniku radova XXXIII Simpozijuma o operacionim istraživanjima - SYM-OP-IS 2006*, Banja Koviljača, 03 - 06. oktobra 2006. Editor: Dragan Radojević. Beograd: Institut Mihajlo Pupin, 2006, s. 73-76. ISBN 86-82183-07-2.

[25] **Norris G. A.:** Integrating life cycle cost analysis and LCA, *International Journal of Life Cycle Assessment*, Vol. 6 (2001), No. 2, pp. 118-121. ISSN 0948-3349.

[26] **Rice, G.; Clift, R. and Burns, R.:** LCA software review: comparison of currently available European LCA software. *International Journal of Life Cycle Assessment*, Vol. 2 (1997), No. 1, pp. 53 – 59. ISSN 0948-3349.

[27] **Rizzoli, A. E. and Young, W. J.:** Delivering environmental decision support systems: software tools and technique. *Environmental Modeling & Software*, Vol. 12 (1997), No. 2-3, pp. 237-249. ISSN 1364-8152.

[28] *SimaPro 6 – Introduction to LCA with SimaPro*. Amersfoort (Netherlands): Pré Consultants BV, 2004. – 71 pp. Available on Web site: <http://www.pre.nl/download/manuals/UserManual.pdf>.

[29] *SimaPro 6 Tutorial*. Amersfoort (Netherlands): Pré Consultants BV, 2004. – 59 pp. Available on Web site: <http://www.pre.nl/download/manuals/TutorialWood.pdf>.

[30] **Spatari, S.:** Using **Gabi 3** to perform life cycle assessment and life cycle engineering. *International Journal of Life Cycle Assessment*, Vol. 6 (2001), No. 2, pp. 81 – 84. ISSN 0948-3349.

[31] **Tan, R. R. and Culaba, A. B.:** Sensitivity analysis of the life-cycle inventories of electricity and hydrogen as energy vectors for the Philippine automotive transport sector. *Asean Journal of Chemical Engineering*, Vol. 2 (2002), No. 1, pp. 21-29. ISSN 1655-4418.

[32] **Unger, N.; Beigl, P. and Wassermann, G.:** General requirements for LCA software tools. In: *Proceedings of Complexity and Integrated Resources Management - Transactions of the 2nd Biennial Meeting of the International Environmental Modelling and Software Society (iEMSs 2004)*, Vol. 3. Osnabrück, Germany, 14 - 17. June 2004. Edited by Claudia Pahl-Wostl, Sonja Schmidt, Andrea E. Rizzoli and Anthony J. Jakeman. Manno (Switzerland): International Environmental Modelling and Software Society (iEMSs) and Osnabrück (Germany): University of Osnabrück, Institute of Environmental Systems Research Resource Flow Management, 2004. pp. 468-473. ISBN 88-900787-1-5. Available on Web site: <http://www.iemss.org/iemss2004/pdf/infotech/ungegene.pdf>.

[33] **Weidema, B. P. and Mortensen, B.:** *Results of a test of LCA-software with statistical functionality*. Note for the Danish Environmental Protection Agency (EPA), Lyngby: Institute for Product Development, 1997.

[34] **Wenzel, H.; Hauschild, Z. M. and Alting, L.:** *Environmental assessment of products. Vol. 1: Methodology, tools, techniques and case studies in product development*. London (UK): Chapman & Hall, 1997. – 576 pp. ISBN 0-412-80800-5.

ASPECTS CONCERNING THE COMPUTATION OF MICROSTRIP LINES PARAMETERS

DUMITRU CAZACU*, CONSTANTIN STANESCU**

Abstract: This paper deals with the computation of the lineal capacity and characteristic impedance for a microstrip line configuration using Green functions. Also the influence of the artificial boundaries of the computational domain on the surface electric charge distribution using finite element method was performed. Parametric analysis was performed in order to evaluate the influence. The results are compared with those from literature and a good agreement is observed.

Keywords: microstrip, green functions, finite element parametric analysis.

1. INTRODUCTION

Accurately computation of propagation characteristics of the signals is crucial for designing the integrated circuits and reducing the errors before the manufacturing stage. Determining the propagation parameters is also useful to the design of the multilayer passive electronics devices used in electronics and telecommunications. The importance of the multilayer microstrip lines have increased constantly in the field of the high speed integrated circuits for microwaves and millimeters waves. The static capacitance of a system is an important parameter in the design of the system. In new digital electronic system, the trend is toward higher clocking frequencies. The integral equation method implemented numerically by the method of moments [1], the finite difference method [2], the finite element method [3], the spectral domain Green's function approach [4]. One of the factors that influence the computational resources when a finite element analysis is performed is the distance where the artificial field domain boundary should be placed, in order to minimize the resources and yet not affect the parameters of the device. This paper deals with the influence of this factor on the surface charge microstrip line distribution.

* *Ph.D. at the University of Pitesti , cazacu_dumitru@yahoo.com*

** *Ph.D. at the University of Pitesti stancosty@gmailcom*

1 PROBLEM FORMULATION

It was shown in a rigorous way that in the low frequency limit the microstrip line can be analyzed as a static field problem and that the propagation constant and characteristic impedance are determined by the low frequency distributed capacitance and inductance.

There are a variety of methods for solving the 2D electrostatic laplacian fields.

Considering a Fourier series development of the charge density ρ_s of the form

$$\rho_s(x) = \sum_{n=1,3,\dots}^{\infty} \cos \frac{n\pi x}{2a} \quad (1)$$

and performing some processing's the following expression for the potential V is obtained:

$$V(x, y) = \sum_{n=1,3,\dots} \int_{-w/2}^{w/2} \frac{\cos(w_n x) \cos(w_n x')}{\varepsilon_0 w_n a (\sin(w_n h) + \varepsilon_g \cosh(w_n h))} \left\{ \frac{\sinh(w_n y)}{\sinh(w_n y) e^{-w_n (y-h)}} \right\} \rho_s(x') dx' \quad (2)$$

where $\omega_n^2 = \left(\frac{n\pi}{2a}\right)^2$, with $x = \pm a$ is the distances where the electric walls where placed.

Where the upper term is for $y \leq h$ and the lower is for $y \geq h$. The factor multiplying the charge density represents the Green's function for this problem, $G(x, y, x', y')$.

Expressing the integral equation (2) in a form that can be interpreted as representing the capacitance C between a conducting strip in air above a ground plane with spacings $h_e, 2h_e, 3h_e$, etc. and using the conformal mapping technique, the expression for the capacitance results [5] :

$$C = \frac{[(1 + \varepsilon)/4\varepsilon_g]Ca(h)}{1 + Ca(h) \sum_{m=1}^M \eta^m \frac{1}{Ca[(m+1)h]}} \quad (3)$$

The effective dielectric constant for a microstrip line is given by

$$\varepsilon_{ff} = \frac{C}{Ca} \quad (4)$$

where C_a is the capacity of the air filled line.

Computing the ε_{eff} using the Schneider-Hammerstaad formula [6] the characteristic impedance, for a lossless line, can be computed using the following expression:

$$Z_c = \sqrt{\varepsilon_{eff} \varepsilon_0 \mu_0} \frac{1}{C} \quad (5)$$

2 PROBLEM SOLUTION

2.1 Characteristic impedance computation

The characteristic impedance was determined implementing the equations (3), (4), (5). In Table.1 and Table 2 obtained values for different relative permittivities ε_r . are compared with the results from the literature. The number in brackets represents the terms number necessary to obtain a numerical convergence of 10^{-3} . It can be seen that the results are in good agreement with [7], [8].

Table 1

w/h	$\varepsilon_r = 6.0$		
	Z, Ω	$Z_{[9]}$, Ω	$Z_{[10]}$, Ω
0,1	134,790 ⁽¹⁴⁾	134,7143	134,72
0,2	112,3435 ⁽¹⁵⁾	112,4978	112,50
0,4	90,1907 ⁽¹⁵⁾	90,3807	90,385
0,7	72,6731 ⁽¹⁷⁾	72,7845	72,789
1	61,8295 ⁽¹⁷⁾	61,8807	61,885
2	42,3945 ⁽¹⁷⁾	42,2886	42,293
4	26,5168 ⁽²⁰⁾	26,4489	36,454
10	12,7164 ⁽²⁴⁾	12,7179	12,726

Table 2

w/h	$\varepsilon_r = 9.6$		
	Z, Ω	$Z_{[9]}$, Ω	$Z_{[10]}$, Ω
0,1	108,8966 ⁽²⁵⁾	109,0053	109,01
0,2	90,6873 ⁽²⁵⁾	90,948	90,952
0,4	72,6937 ⁽²⁵⁾	72,9718	72,975
0,7	58,4817 ⁽²⁷⁾	58,6731	58,676
1	49,6899 ⁽²⁷⁾	49,8175	49,821
2	33,9644 ⁽²⁹⁾	33,9308	33,934
4	21,1733 ⁽³²⁾	21,1389	21,143
10	10,1130 ⁽⁴⁰⁾	10,1186	10,125

2.2 Evaluation of boundary influence of the surface charge density computation

In order to study the influence of the positioning on the surface charge density of a microstrip line (Fig.1) the dimensions and H were parameterized using the parameter p a parametric analysis was performed then with varying from 0.1 to 1 with a constant step of 0.1.

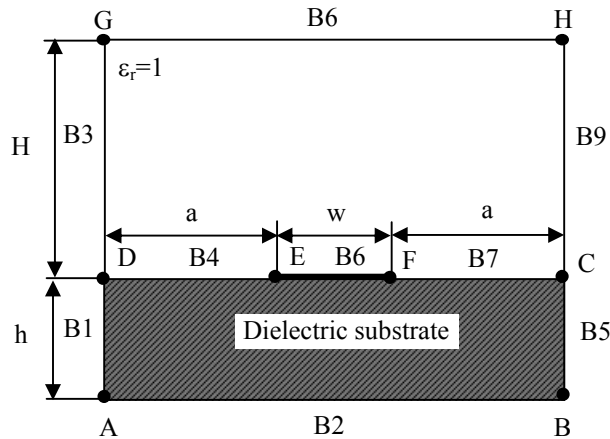


Fig.1 The positioning on the surface charge density of a microstrip line

The geometry used is presented in Fig.1, where geometric initial dimensions are: the strip width $w = 0.2$, the substrate thickness $h = 0.1$, $a = 0.1$, the outer boundary height $H = 0.1$.

The surface charge distribution was determined performing an parametric electrostatic analysis with p as a parameter.

2.2.1 Finite element electrostatic analysis

The equation to be solved is:

$$\Delta V = 0 \quad (6)$$

where V is the electrostatic potential.

First the strip was set up to a 1 V potential and the boundary to 0 V (ground). Because the dielectric is not homogenous at the boundaries between the two media a continuity boundary condition were set, that specifies that the normal component of the electric displacement is continuous across the interior boundary:

$$\vec{n} \cdot (\vec{D}_1 - \vec{D}_2) = 0 \quad (7)$$

For the initial geometry a 962 second order Lagrange elements mesh was produced. Then a electrostatic analysis using a stationary direct solver (UMFPACK) [8] was performed. A number of 1987 DOFs were computed 1.312 s, on a 512M RAM 1.1GHz machine and the electrostatic potential distribution has resulted.

2.2.2 Parametric analysis

The implementation of the parametric analysis was in Comsol Multiphysics (Comsol Multiphysics ver.3.2, Copyright(c) 1994-2005 by Comsol AB, www.comsol.com)

A multiphysics coupling between the Parameterized geometry application mode and electrostatics was applied [9]. This application mode is used to study how the physics changes when the geometry changes, as a function of time or of a parameter. The set unknowns are the electrical potential and the dx and dy displacements. On some boundaries and points some constraints were applied. The boundaries adjacent to the points with parameterized constraints using a p parameter: B1, B8, B3, B9 and B5 were scaled using similarity transformations.

This option is used when the displacement on the boundaries and points were prescribed. The software translates, rotates and scales the boundary so that the constraints at the end points are satisfied.

Also on other boundaries some linear displacement on ox and oy were applied. The point settings for the moving points were parameterized with p.

Then the current solution was used as an initial solution for a parametric analysis that computed also the dx and dy displacement.

2.2.3 Results

A number of 5961 DOF were solved in 27.33 s on the same machine. The number of DOFs indicates the efficiency of the deformed mesh application mode.

Representing the surface charge distribution for each p value the following curves were obtained (Fig.2).

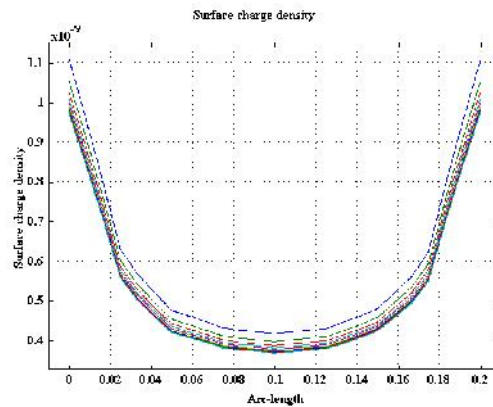


Fig.2 Representing the surface charge distribution

The charge distribution is wider when p increases. It can be noted that the character of the curves meet the analytical character that results from conformal mapping technique. It is known that an isolated infinitely long conducting strip of width w and with total charge Q per meter the charge distribution is given by [5] :

$$\rho_s(x) = \frac{2Q}{\pi w \sqrt{1 - x^2 / (w/2)^2}} \quad (8)$$

3 CONCLUSIONS

The characteristics impedance of some microstrip line configurations were computed and the results met those from the literature. Also the influence of the computation domain on the surface charge distribution was performed and the results are in good agreement with the analytical results. It seems that for this kind of geometrical variation, by expanding the microstrip geometry uniformly after ox and oy the surface charge distribution follows the analytical one. Other types of variations will be considered as well as multilayered structures.

REFERENCES

- [1] **Wei, C., Harrington, R.F.**, *Multiconductor Transmission lines in Multilayered Dielectric Media*, *IEEE Trans. Microwave Theory Techn.*, MTT-32 (1984), pp.439-449.
- [2] **Elsherbeni A.Z.** et.al., *Minimization of the coupling between a two conductor microstrip transmission line using finite difference method*, *Progress in Electromagnetics Research*, *PIER 12*, 1-35, 1996.
- [3] **J.K.Lee, D.Sun, Z.Cendes**, *Full wave analysis of dielectric wave guides using vector finite elements*, *IEEE Trans.Magn.*, vol.39, Nr.8, pp.1262-1271, August 1991.
- [4] **K.S.Oh , D.Kusnetov**, *Capacitance computation in a multilayered dielectric medium using closed form spatial Green's functions*, *IEEE Trans.MTT.*, vol42, pp.1443-1453, 1994.
- [5] **Collin R.**, *Foundations for microwave engineering*, McGraw-Hill, 1992.
- [6] **E.O.Hammerstaad**, *Accurate models for microstrip computer-aided design*, *IEEE MTT-S Int.Microwave Symp.Dig.*, pp. 407-409, 1980.
- [7] **V.Urbanavicius, R.Martavicius**, *Model of the microstrip line with a non-uniform dielectric*, *Electronics and electrical engineering*, ISSN 1392-1215 2006, Nr.3 (67).
- [8] **Cheng K.K.K., Everard K.A.** *Accurate formulas for efficient calculation on the characteristic impedance of microstrip lines*, *IEEE Trans.on Microwave Theory and Techniques*, 1991, vol.MTT-39, No.9, pp.1658-1661.
- [9] **COMSOL** *Electromagnetics User's Guide* ver.3.2. www.comsol.com

CLASSICAL POWER SUPPLY SOLUTIONS FOR LOW PRESSURE MERCURY LAMPS

GABRIEL NICOLAE POPA *, IOSIF POPA **, SORIN DEACONU**

Abstract. The world trend in lighting installations is to change the old incandescent lamps with fluorescent lamps. The paper presents the low-pressure mercury lamps study, when supply through magnetic ballast are and glow starter for different line voltage and improving power factor for these lamps.

Keywords: lamps, fluorescent, low-pressure mercury, supply.

1. INTRODUCTION

Each lighting installation is designed to produce a level of illumination adequate for those working area. Adequate illumination should be maintained to reduce eyestrain, improve moral, increase safety and increase production.

Today, there are neraly 6000 different lamps being manufacturing in six categories: incandescent, fluorescent, mercury vapor, metal halide, high pressure sodium and low pressure sodium. The last five categories can be termed as gas discharge lamps. Fluorescent and low pressure sodium lamps operate on low pressure gaseous discharge and the mercury vapor, metal halide and high pressure sodium lamps operate on high-pressure gaseous discharge.

Luminous efficacy [lm/W] measure of the lamp's ability to convert input electric power [W] into output luminous flux [lm].

Electric gas discharge lamps convert electrical energy into light by the kinetic energy of moving electrons, which becomes radiation as a result of collision process. The process is collision excitation of atoms in a gas, the electrons take the lowest

* Ph.D. Lecturer eng., Electrotechnical Department, Faculty of Engineering Hunedoara, "POLITEHNICA" University of Timișoara, Romania

** Ph.D. Associate professor eng., Electrotechnical Department, Faculty of Engineering Hunedoara, "POLITEHNICA" University of Timișoara, Romania

energy atomic levels and appear the emission of electromagnetic radiation. This radiation is not continuous, it consists in a number of separate spectral lines. Through different gas, the luminous efficacy can be varied.

Compared with incandescent lamps, gas discharge lamps have the following advantages: transforming 20-30% of the electric input into light energy output; the rated life is up to 20000 h and the lamp characteristics are maintained up to end of life. Fluorescent lamps are more efficient than incandescent lamps of an equivalent brightness because more of the energy input is converted into light and less into heat.

Sixty percent of all fluorescent lamps contained 10 mg Hg or less and for the rest of lamps contained between 10-100 mg Hg [2].

2. FLUORESCENT LAMPS CHARACTERISTICS

In fig.1 is presented the structure of low-pressure mercury lamp.

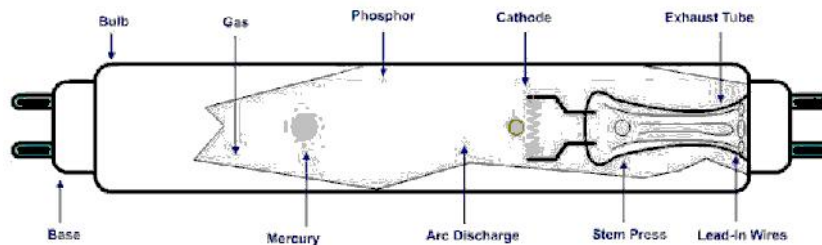


Fig.1. Low-pressure mercury lamp

It is supposed that the lamp is supplied at d.c. voltage.

In fig.2.a is u-i characteristics when a lamp is alone operated from a d.c. voltage source. The slope of the curve has the impedance:

$$Z = \frac{du}{di} \quad (1)$$

Z is negative that causes a problem for operating lamps. The starting voltage U_s is higher than the steady-state operation voltage is needed to establish ionization in the gas. After the discharge begins, the operating point of the discharge lies to the right of the curve and the electron density n_e increases continuously in time. The discharge current increases without any regulation and the lamp is destroyed.

From these reasons the gas discharge lamp cannot be directly connected to a voltage source and an impedance must be placed between the lamp and the voltage source to limit the current [1,3].

In fig.2.b is presented the effect of series resistance in stabilizing the current lamp.

$$U_{AB} = U_R + U_{La} \quad (2)$$

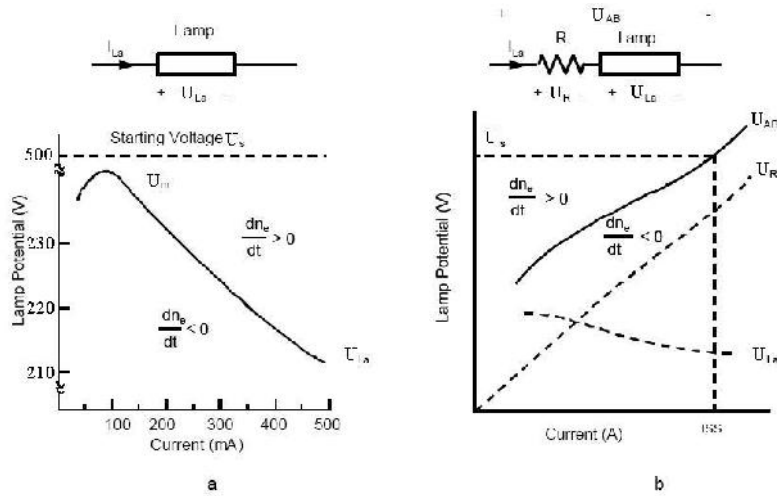


Fig.2. U-I lamp characteristics for d.c. power supply: a. without ballast; b. with ballast

The operating point of the lamp is the domain of positive dn_e/dt increase the current until it reaches the point (I_{ss}, U_s) . The resistor R helps to establish the stable operating point of the lamp and acts as the ballast.

The resistor R increases power loss and the system efficacy reduces.

For a.c. voltage supply, the ballast is inductive or capacitance impedance can be used to provide current limitation and reduce wearing of the two electrodes and maintains a longer lamp life.

The gas discharge lamps require an auxiliary apparatus called magnetic ballast and glow starter.

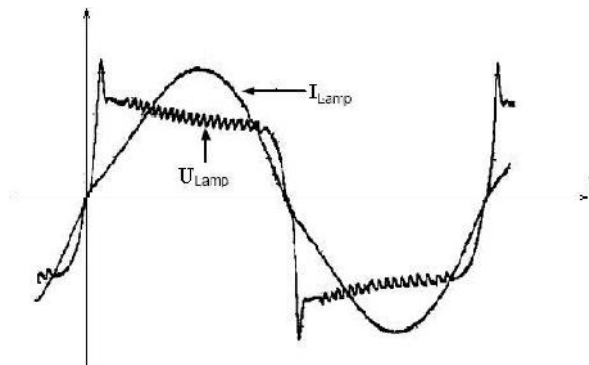


Fig.3. Voltage and current lamp when operate at 220 V, 50 Hz

The magnetic ballasts operate in 50 Hz line frequency (fig.3). Every half cycle (10 ms) they re-ignite the lamp and limit the lamp current. The magnetic ballasts are large and heavy. The time constant of the lamp is around 1 ms, the arc extinguishes when the voltage is zero and then re-ignited. From these reasons, the lamp voltage waveform has a voltage spike that causes the lamp electrode wearing and the flickering of the lamp.

3. EXPERIMENTAL RESULT

The electric circuit used in experiments is presented in fig.4. In fig.4: AT – autotransformer, A_1 , A_2 , V - MY 64 digital multimeter, W - EL 21 wattmeter, $C_1 = 3.75 \mu\text{F}$, $C_2 = 5 \mu\text{F}$, $C_3 = 8.75 \mu\text{F}$, H fluorescent lamp 2x20 W with magnetic ballast L.

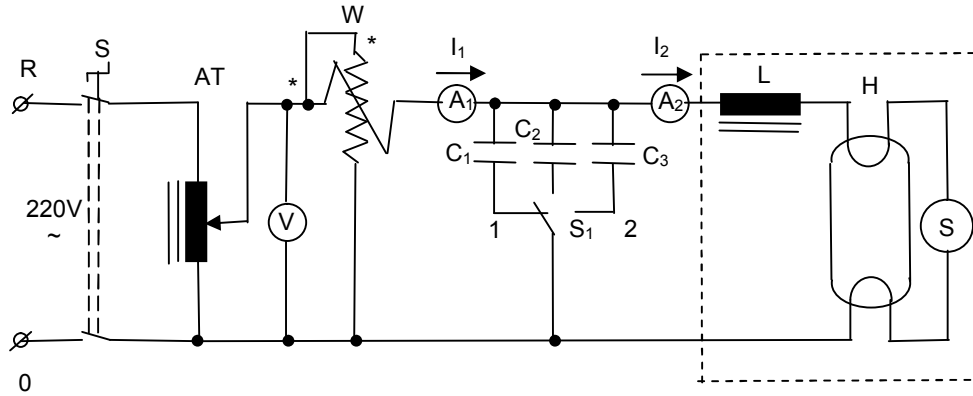


Fig.4. Experimental circuit

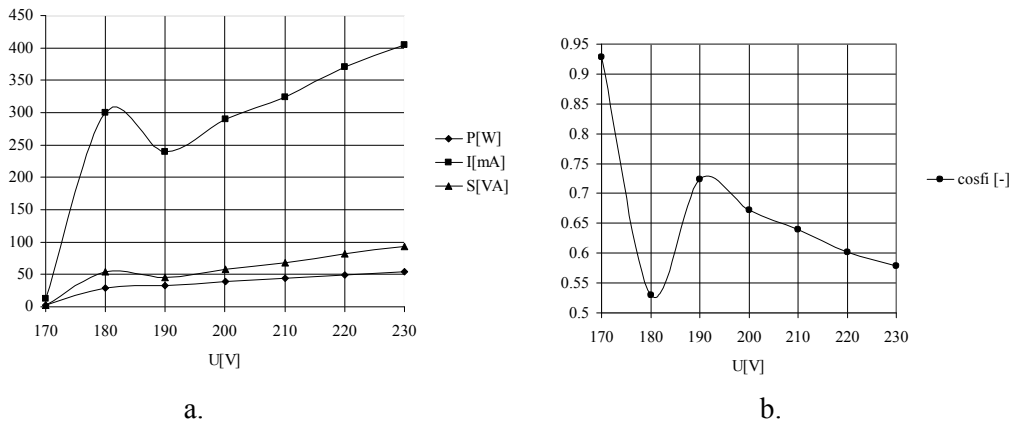


Fig.5. Results for 2x20 W fluorescent lamp with magnetic ballast; $U_{\text{extinction}}=150 \text{ V}$, $I_{\text{extinction}}=50 \text{ mA}$

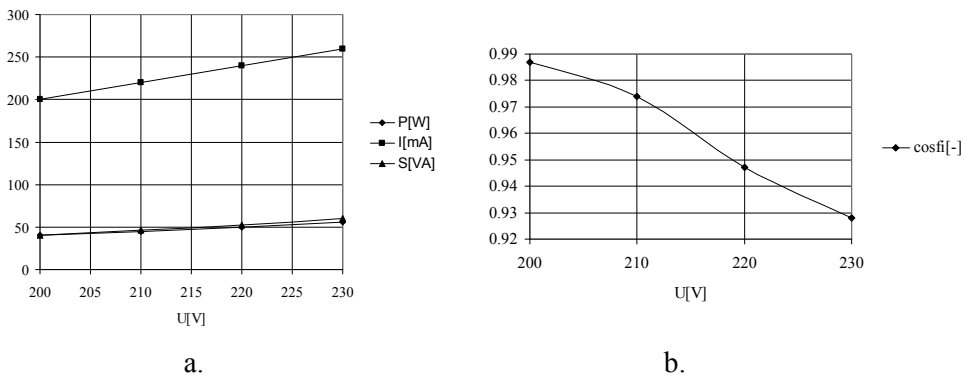


Fig.6. Results for 2x20 W fluorescent lamp with magnetic ballast with $C = 3.75 \mu\text{F}$

Phase between current and voltage, before power factor compensation is:

$$\operatorname{tg} \varphi_1 = \frac{X_L}{R} = \frac{2 \cdot \pi \cdot f \cdot L}{R} \quad (3)$$

Phase after power factor compensation must be:

$$\operatorname{tg} \varphi_2 = \frac{\sqrt{1 - \cos^2 \varphi_2}}{\cos \varphi_2}; \cos \varphi_2 = 0,92 \quad (4)$$

Capacitance that must be connected to the lamp, to obtain $\cos \varphi_2 = 0,92$ is:

$$C = \frac{P}{2 \cdot \pi \cdot f \cdot U_a^2} (\operatorname{tg} \varphi_1 - \operatorname{tg} \varphi_2) \quad (5)$$

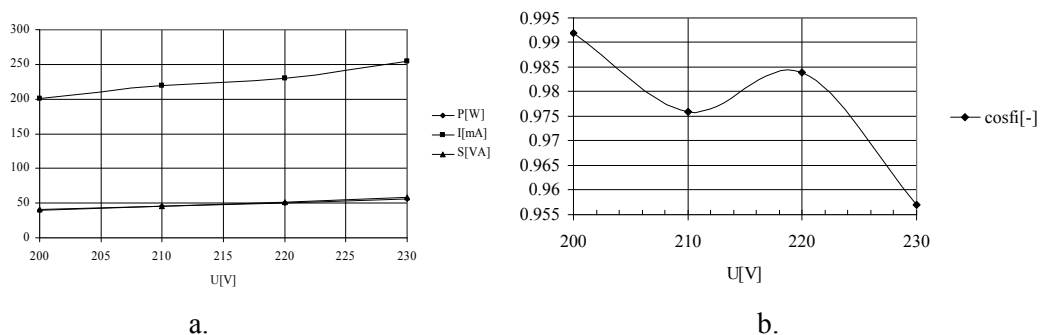


Fig.7. Results for 2x20 W fluorescent lamp with magnetic ballast with $C = 5 \mu\text{F}$

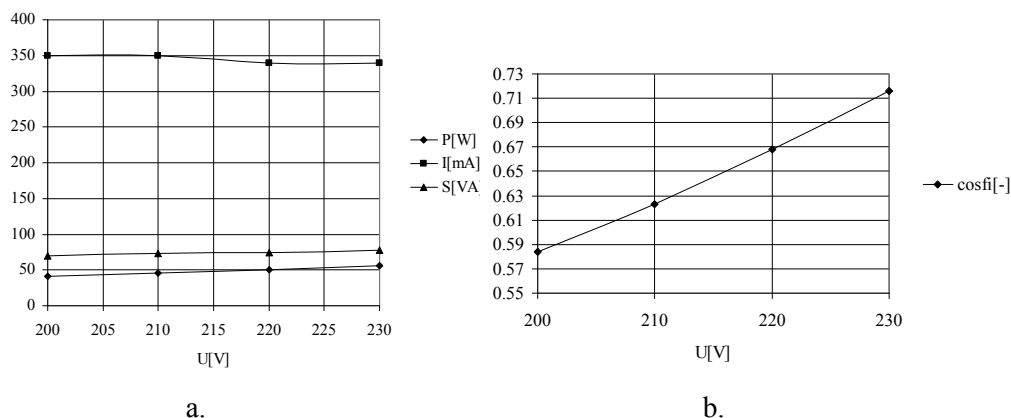


Fig.8. Results for 2x20 W fluorescent lamp with magnetic ballast with $C = 8.75 \mu\text{F}$

The current lamp is not sinusoidal and from this reason the current and active power measure (normal measuring devices) are made with error. In fig.6 the lamp is inductive ($X_L > X_C$) and in fig.8 the lamp is capacitive ($X_L < X_C$).

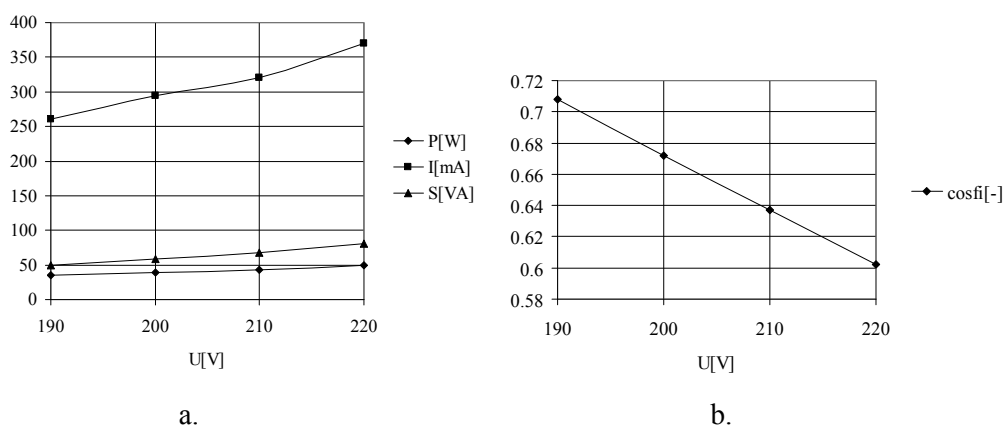


Fig.9. Results for 2x20 W fluorescent lamp with magnetic ballast supply through variable alternating voltage (600W/220 V/50 Hz)

If capacitance for improving power factor is too big (5 or 8,75 μF , fig.7,8) the current slow down with the increase the voltage and cause lamp unstable. The improving power factor with capacitance cause a lot of current harmonics and the lamp performance decrease. From this reason, before improving power factor the current must be filtered with pasive or active filters, and then connect the capacitance. If the fluorescent lamp with magnetic ballast supply through variable alternating voltage (with triac), because of current harmonic, the lamp does not work with capacitance.

4. CONCLUSIONS

The fluorescent lamps operate most efficiency and economically at their rated voltages. Operating outside their normal operating range is undesirable. The undervoltage and overvoltage conditions have negative effects on the life, efficiency and economy of he life sources.

For fluorescent lamps, line voltages greater than the nominal voltages will shorten lamp and ballast life. Line voltages less than the nominal voltages will also shorten lamp life, reduce illumination and may cause uncertain starting. Frequent starting will shorten lamp life.

Fluorescent lamp high frequency operation (with electronic ballast, instead of magnetic ballast and glow starter) results in significant ballast volume and weight reduction and improves the performance of the discharge lamp (save energy and long life).

REFERENCES

- [1] Arsenie D., *Iluminat*, Litografia Universității Tehnice Timișoara, 1995;
- [2] Gendre M., *Two Century of Electric Light Source Innovations*, Eindhoven University of Technology, Holland, 2005;
- [3] Popa G.N., Popa I., *Instalații electrice*, Editura Mirton, Timișoara, 2005.

COAL/PETCOKE CONVERSION LIKE AUXILIARY FUEL AT S.C. CARPATCEMENT HOLDING S.A DEVA BRANCH

ARAD SUSANA ^{*}, VICTOR ARAD ^{**}, BOBORA BOGDAN ^{***},
MIHAELA BOBORA ^{***}

Abstract: One of the most important cost driver for cement production price is clinker cost and implicit fuel cost. Due to the fact that the price of traditional fuels has greatly increased at world level, we need to identify and use other types of fuel. These new identified fuels could be used to replace, completely or partially, the traditional fuels natural gas and fuel oil. In the paper it will be presented the use in the future of the coal or petcoke like auxiliary fuel and the grinding in a mill of coal designed will be researched. In this paper, different scenario the use in the future coal or petcoke will be researched.

Keywords: cement plant, auxiliary fuel, coal mill, energy balance,

1. INTRODUCTION

The cement plant situated near Deva town is one of the three cement plants that belong to the HeidelbergCement Group in Romania. Since 2004, this cement plant, along with the cement plants of Fieni and Bicaz form together the company called Carpatcement Holding S.A. HeidelbergCement has been present in Romania since 1998. They are the market leader in Romania and one of the largest German investors in this country.

The Deva Cement Plant was built among 1972 – 1978 and it was commissioned in 1977 – 1978. It was projected to have two production lines of 1.9 millions tones/year capacity. In 1990 The Cement Plant changed its name and became a joint stock company called S.C. CASIAL S.A. DEVA. In 2000 HeidelbergCement became the main shareholder and started an important investment and restructuring program, aiming at:

^{*} *Assoc. professor at University of Petrosani*

^{**} *ProfessorPhD at University of Petrosani*

^{***} *Engineer at S.C. CARPATCEMENT HOLDING S.A -Sucursala Deva*

- productivity increase
- improvement of products quality
- modernization of the technological flow
- improvement of environmental quality

The company's development policy is materialized by reinvestment of the profit in modernization and technology. During the last years at Deva Cement Plant there were invested much money in replacement and modernization of the equipments on one side, and in environmental protection also.

2. GENERAL PROBLEMS

The cement is produced through the following steps: (i) extraction, processing and storage of the raw materials; (ii) grinding of the meal (limestone, clay and pyrite) in the raw mill where the mixture is proportioned according to the fabrication recipe (75-79% limestone, 20-22% clay and 1-3% pyrite); (iii) clinker fabrication, by burning the raw meal in the clinker kiln; (iv) cement fabrication, by grinding of the clinker in the cement mills together with the grinding additives (slag, gypsum, fly ash) according to the cement type we want to obtain; (v) storage of the cement; (vi) dispatching.

The forecast for the cement market is to increase the cement sales and the clinker production from 377 ths t/y to 550 ths t/y for the next 15 years. The production cost must be the lowest possible according to the raw material and energy costs.

One of the most important cost' driver for cement production price is clinker cost and implicit the fuel cost. For clinker fabrication, the rotary kiln uses at this time the natural gas as main fuel. The clinker kiln burner can use both gaseous fuel, and liquid and solid. The used alternative fuels are old tyre and SAF replacing about 12% from the natural gas.

The electrical energy consumed in the cement making process from the total

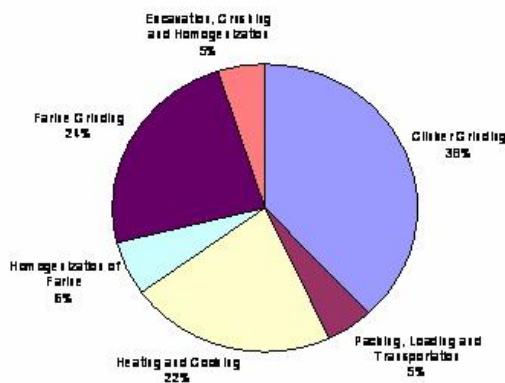


Fig.1. The electrical energy consumption graph

used, is presented in Figure 1, where 5% is used in the excavation crushing and homogenization of raw material, 38% kWh/t is the energy consumption for clinker grinding, 22% for heating and cooking, 24% for farine grinding and the rest for other operations.

Due to the fact that the price of traditional fuels has greatly increased at word level, we need to identify and use other types of fuel. These new identified fuels could be used to replace, completely or partially, the traditional fuels natural gas and fuel oil. The possible

auxiliary fuels to be used at this time can only substitute up, to about 20% of the basic fuel-assumption for further calculation.

3. THE TECHNICAL AND THEORETICAL ASPECTS

The savings achieved through the replacement of natural gas, which is at this time the basic fuel, by coal have been calculated considering replacement of natural gas in proportion of 99%. The alternative fuel equipment for the burning of the solid alternative fuels (ECO-Fuel) will be designed like in Figure 2.

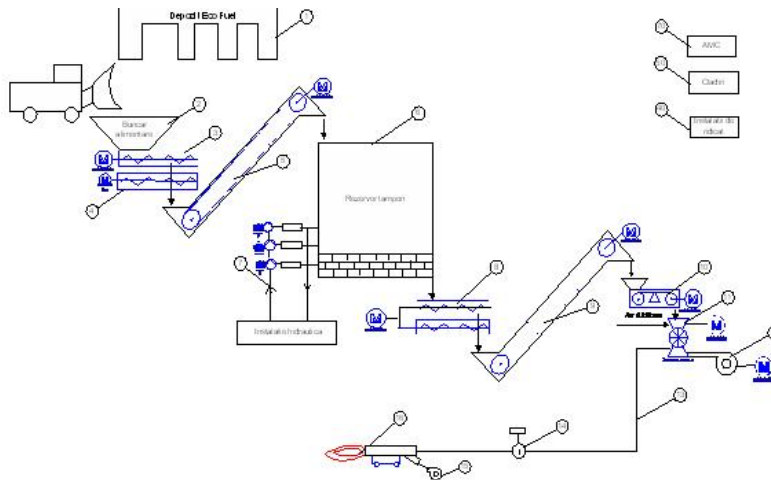


Fig.2. Technological system of the Eco Fuel equipment

In this technological system the most important equipments are: vertical mill for grinding coal, transport and storage system, electrical equipment, dust silos, dosing system, deducting unit, air compressor plant, hot gas fan and inertization system. The flow chart of technological system is shown in Figure 3.

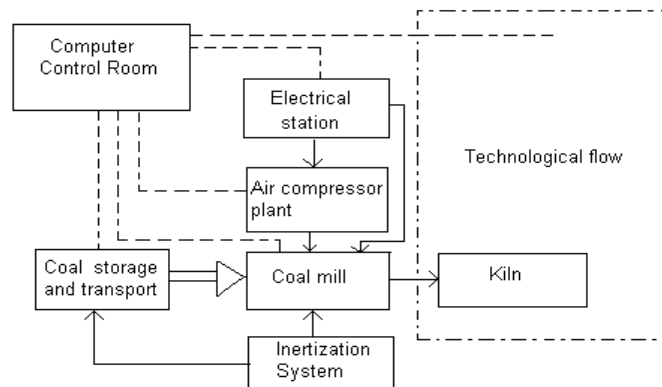


Fig.3. The coal mill flow chart

The coal mill flow sheet is illustrated in principles in Fig. 4. The coal is fed to the coal mill through the inlet pipe. The coal is pulverized on the rotating grinding table by the rollers. The coal mill is a new type medium speed mill, adopting advanced grinding technology and basing on technology of vertical mill. This equipment is consist of main engine, speed reducer, casing, grinding device, separator, output, powder-falling pipe, piping device, loading device, controlling box, sealing device, etc. The peripheral equipments are bucket elevator, feeder, storage bin, coal mill filter, electric control cabinet, etc

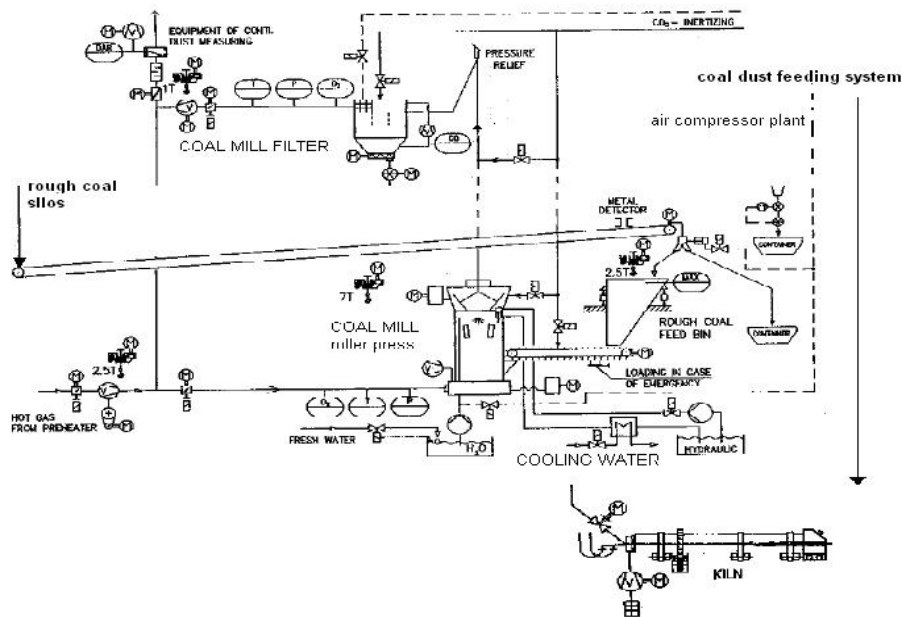


Fig.4. Coal mill flow sheet

The temperature of the primary air is used to control the temperature in the coal mill at the classifier. The temperature controller is often required to keep temperature constant at 100°C in order to evaporate the moisture content in the coal. A coal mill is a harsh environment in which it is difficult to perform measurements; this means that all the variables are not measurable. E.g. the actual coal flows in and out of the coal mill are not measurable. However, the primary air flow and temperature are, as well as the temperature at

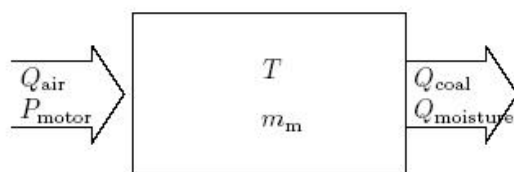


Fig.5. An illustration of energy balance in the coal mill

the classifier.

A simple energy balance model of the coal mill is illustrated in Fig. 5. In this model the coal mill is seen as one body with the mass m_m , in which T is the temperature in the mill, Q_{air} is the energy in the primary air flow, P_{motor} denotes the power delivered by the grinding table, Q_{coal} is the energy in the coal flow, and $Q_{moisture}$ is the energy in the coal moisture.

The energy balance is given by (1).

$$m \cdot C_m \cdot \dot{T}(t) = Q_{air}(t) - Q_{coal}(t) - Q_{moisture}(t) + P_{motor}(t) \quad (1)$$

Electrical equipment is the major factor in the powering and control of cement plants. The feeding system of the kiln with conventional fuel and the alternative fuel are also monitored. The CemScanner system checks the kiln (shield) temperatures. The regulation of temperature is done in real time and in the same time the safe operation of the equipment is assured.

We ensure good quality and durability of the whole machine, small size, light weight, small space, low energy consumption, long life of worn out parts, etc.

4. CONCLUSIONS

According to the specific situation of the Deva cement plant, the following issues have been considered:

- fuel proportion; natural gas 1%, old tyre 10%, SAF 9% and coal 80%,
- imported coal through Constanta port,
- calorific power assumed; gas 33.7Gj/000 m³ and coal 25.08 Gj/t,
- utilization of existing rail road discharge area for rough coal.

At the coal mill, the grinding capacity of 18t/h is enough for the new burning capacity of plant used.

Target intention:

- reduction of the specific cost for clinker production
- emission under the accepted level of the European law
- minimum invested amount
- high level of work safety
- high level of technology

In the analyses done to now, there have been considered various versions regarding the storage and grinding of the raw coal. There have also been analyzed versions of grinding in ball mills or vertical mills. There has been chosen as optimum version the vertical mill, considering the following:

- Arrangement of a large-size raw coal silo,
- Creation of higher capacities for grinded coal storage and implicitly of loading and unloading equipments for this,
- Increase of explosion or fire this,
- Establishing a dependency on the transport system,
- Additional transport costs,
- Impossibility of providing the drying air from the hot air recovered.

Considering the above mentioned, the version with a vertical mill of 15t/h in each of two cement plants has been chosen.

The vertical mill of 15t/h proposed has the following advantages:

- low grinding specific energy consumption,
- possibility of using heat exchanger waste gases for heat recovery
- reduction of explosion hazard due to the low O₂ content in these gases
- independence of plants operation
- low grinded coal transport costs.

REFERENCES

[1] **Arad, S., Arad, V., Bobora, B.** *Cement Production at Deva Cement Factory from Romania*, 23 nd ISARC2006 Tokio, Japan, Proceedings CD, C8 Plant and Dismantling IAARC Publ. Int. Assoc. Aut. Rob. Constr., pg. 806- 809 ISBN 4-9902717-1-8, http://www.iaarc.org/external/isarc_proceedings, 2006

[2] **Arad, S.** *Tehnologii pentru "cărbune curat" clean coal technology, o provocare pentru cercetare în context european. Revista Minelor*, 2/2007, ISSN 1220-2053, 2007

[3] **Arad, S.**, *Assesment Environmental Impact from S C Casial SA Deva*, M.Sc Dissertation Thesis, University of Petroșani, Petrosani; 2001

[4] **Rees, N.W. and F.Q. Fan.** *Modelling and control of pulverised fuel coal mills. In: Thermal power plant simulation and control* (D. Flynn, Ed.). first ed. Institution of Electrical Engineers, 2003

[5] *Conversie pe carbune/cocs de petrol la S.C. CARPATCEMENT HOLDING S.A.*, Contract cercetare C665/2006, CEPROCIM S.A. Consulting and Engineering Devision, 2006

COAL-MAIN BASIC RESOURCE IN THE ENERGY PRODUCTION

LIVIU BLANARU *, SORIN CURELEANU *,
ANGHEL STOICHITOIU **

Abstract. This study is analyzing the trend of the electric energy production on coal-based power plants.

Key words: lignite, energy, power

1. INTRODUCTION

Nowadays a modern industry, in evolution, cannot survive without an efficient energetic sector able to provide and sustain with energy various economical branches and the social development. Due to the economical, political, social and ecological impact the energy problem has become the major imperative of the global economy, preoccupation of all nations being targeted on this matter on the higher degree.

Increasing of population and the diminishing of the economical difference between the developed and third world countries is generating the global ascending request of primary energy. In this situation, more, not less energy can solve the global problems, especially the social ones, as true as today, about two billions peoples has no access at the so called – commercial energy. Under economical and environment purpose, there is a continuous and sustained request for the improvement of energetic efficiency, by researching and development of some new energetic technologies because the generation and consumption of energy is a significant indicator of civilization degree of any nation, being seldom used in the world hierarchy.

* *Ph D. Student Eng.*

** *Professor PhD .eng. University of Petrosani*

2. COAL – MAIN PRIMARY RESOURCE ON THE WORLD'S ENERGY GENERATION

Demographical prognosis are showing an increase from 6 billions to about 8 billions by the year 2010. The Energy World Council is estimating that the energy needs will be 50% higher until 2020. Assuming this prognosis with precaution, we are considering that all countries will reach the developed countries energetically high efficiency level.

So in the future, fossil oil and energetic coal together with natural gas will remain the most important energetic resource. The contribution of non-conventional resources – wind, sun, water and biomass – will increase in absolute value, but it will play a minor role in the future.

A major shift that will overcome the fossil resources, according to the last World Energy Council will be possible not sooner than the second half of this century and only if the necessary actions will start on the nearby future.

In the mean time, the prognosis implies the fact that all the energetic policy options are requesting the assurance of the global energetic resources.

Therefore, the coal and nuclear fuel together with the water will form the base of electric power generation and the future increase of energy request will lead to a global increase of coal production. The coal will contribute with over 50% on the power generation process and will still be the primordial energetic resource all over the world.

The coal market will run through some structural changes in the future in the same measure that the third world countries developing rates will overcome the economically advanced countries.

For all the countries, the coal represents an attractive economic resource, especially the lignite. Nowadays the European mining industry capacity has a decreasing trend. Asian, Australian, and Latin American mining industry has a sensitive growth. In these circumstances, is explained the higher quantity of European coal import especially by the continuous decline of the pit coal production in U. E. countries, from 105 Mt. in 2000, to 70 Mt. in 2020.

The situation of global consumption of fuel has the following structure (fig. 1):

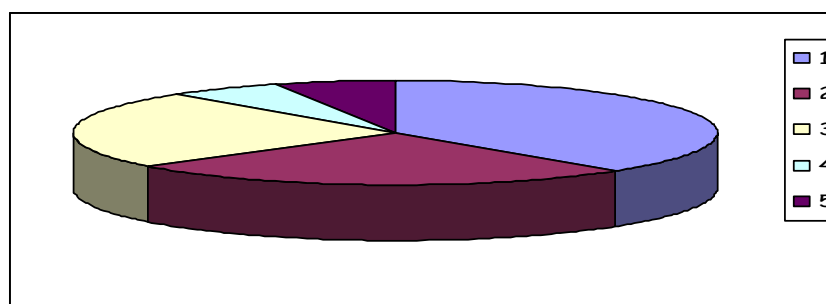


Fig.1

1 – Oil 38%; 2 – coal 26%; 3 – natural gas 24%; 4 – nuclear 6%; 5 - regenerative 6%.

In the European Union, we have the consumption as shown (fig. 2):

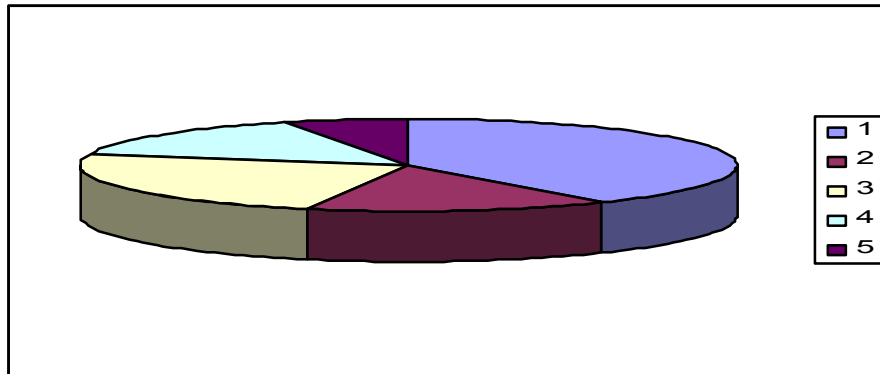


Fig. 2

1 - Oil 40%; 2 – coal 15%; 3 – natural gas 24%; 4 – nuclear 15%; 5 – regenerative 6%.

The enlargement of the European Union is bringing the “coal issue” in political debates about redefining of the solid fuel as a long – term energy primary resource.

For implementing the 1997 Kyoto Protocol Resolutions, is necessary to develop the environment protection policies, but without discrimination against the coal.

On the Lignite and Pit Coal European Association, where Romania is also affiliated, the coal power generation Clean Technologies debates has a huge innovation potential. Today, coal –based power plants can touch efficiency levels of 40% for lignite and 45% for pit coal, so the priority is to create the best conditions for improvement of the power generating process, especially reducing the CO2 emissions by investing in modern technologies.

3. CONCLUSIONS

Therefore, it is obvious that the coal will have a great influence on power generation and any country development. In the future, will be enforced an active power saving policy, by revising all technologies implying high-energy consumption.

REFERENCES

- [1] *European AQUIS Requests;*
- [2] *CESCO Consulting Committee Declaration about the role of coal in the XXI century Europe (July 1999);*
- [3] **EUROCOAL Report** – PATROMIN Magazine;
- [4] **LEGEA 3 / 2001** – Kyoto Protocol ratification on the United Nation Convention about Environment and Climate Altering.

COMPARATIVE STUDY ON THE TYPES OF PROTECTION FOR THE ELECTRIC APPARATUS INTENDED FOR USE IN EXPLOSIVE ATMOSPHERES

SORIN BURIAN^{*}, JEANA IONESCU^{**}, MARIUS DARIE^{**},
LUCIAN MOLDOVAN^{*}

Abstract: This paper shows the important conditions involved in the selection of a protective solution on the apparatus intended for use in areas with hazard of explosive atmospheres. Then, in relation to the operation of the apparatus, one can derive the economically eligible variants for the protection of the apparatus intended for use in areas with hazard of explosive atmospheres.

Consequently, this paper intends to be the precursor of a practical guide for the selection and implementation of different types of protection on the apparatus intended for use in areas with hazard of explosive atmospheres, both for designers and manufactures.

Key words: types of protection, comparison

1. INTRODUCTION

Generally speaking, designing and manufacturing of electrical apparatus benefits lately of special advantages, offered by the appearance of new components (integrated) and technologies, which makes the time that passes from enouncing the idea until physical achievement of the apparatus to be relatively short, and the process involved by that to be a monotonous one.

But, when the problem of adapting this apparatus to the particularities of use them in atmospheres with explosion hazard, the above mentioned process is considerably slowed, not by the missing of consecrated components for such processes, but especially by the leak of experience and knowledge regarding the standard

^{*} *PhD.Student Eng. at the INSEMEX Petroșani*

^{**} *Ph.D.Eng. at the INSEMEX Petroșani*

requirements, referring to construction and using of electrical apparatus in areas with hazard of explosive atmosphere.

This state of fact is negatively more emphatic because, lately, the groups of standards from this field in the world, Europe and Romania have a peculiar dynamic caused especially by the homogenisation and generalisation process opened and maintained by IEC.

Considering the above mentioned, this paper proposes to help the designers and manufacturers of electric apparatus designed to be used in areas with hazard of explosive atmosphere by displaying a comparative study regarding definitive aspects for applicable types of protection.

2. CLASSIFICATION OF EXPLOSIVE ATMOSPHERES. HAZARD OF EXPLOSION

To have an explosion three factors must exist at the same time and in the same space. These factors form the triangle of explosion hazard (fig. .1):

Presence of flammable substances in form of gases, vapours, mists;

Presence of oxidant substance, air or oxygen, as support for violent combustion (explosion);

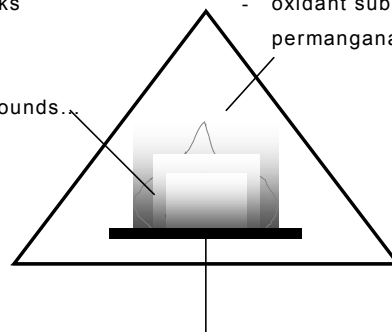
Presence of ignition source in form of sparks and hot surfaces.

Ignition sources:

- Hot surfaces
- Flames and hot gases
- Mechanical sparks
- Electrical wiring
- Static electricity
- Lightning, ultrasounds.

Oxygen sources:

- air (21% oxygen)
- pure oxygen
- oxidant substances (potassium permanganate etc)



Flammable substances:

"flammable gases and powders and which are in critical concentration"

Fig.1 Ignition triangle

3. TYPES OF PROTECTION – SHORT DESCRIPTION

The type of protection represents a technical solution by which at least one of the factors represented in the ignition triangle is removed or limited below the critical values.

Flameproof enclosure

Represents a type of protection that permits to have an explosion inside equipment, but which by the characteristic elements for this type of protection (flameproof joints) makes that explosion not to be transmitted to the explosive atmosphere that surrounds the enclosure. Generally, it is used for power apparatus, but can also be used for other kinds of apparatus.

Increased safety

A type of protection which consists in applying some supplementary measures to avoid producing electric arcs, sparks, or excessive temperatures on any part of electrical apparatus (internal or external). These phenomena are not produced even in normal operation.

Non-incendive

Represents a type of protection which is based on the other types of protection principles, but it contains less rigorous prescriptions than those contained in the standards for types of protection eligible in zone 1. This type of protection is only eligible for zone 2.

Intrinsic safety

Represents a type of protection by which electrical parameters are safely limited so than the ignition source to be limited to a non hazardous value. This is also a consecrated type of protection for “low currents” applications.

Encapsulation

It is a type of protection by which the small kind apparatus is separated from hazardous atmosphere by moulding / enclosing in compound.

Pressurization

It's a type of protection by which the apparatus (often) in normal construction is placed inside an enclosure in which a protective gas is circulated so as in the inner space the explosive gas concentration is much lower than the lower explosive limit (LEL). Pressurization remains the only available solution for high frame sizes apparatus.

4. COMPARATIVE STUDY FOR THE TYPES OF PROTECTION

Age

The types of protection showed up like technical punctual solutions of protect the electrical equipment for use in surface or underground areas which involves the occurrence of explosive atmospheres.

The oldest types of protection are flameproof enclosure “d”, which appeared at the end of the 19th century, oil immersion “o”, sand filling “q”, pressurization “p” and intrinsic safety “i” which appeared around 1930, their use and standards occurrence for them being noticed even from the first half of the 20th century.

Then after the second half of the past century started to be use the types of protection increased safety “e” (standardized in 1969) and encapsulation “m” (standardized in 1988).

At the end of the 20th century the types of protection oil immersion (o) and sand (powder) filling (q) were less and less used and leaved the place for a composite

type of protection which has some “soften” requirements regarding the type of protection. This type of protection was called non-incendive (n) and has a few subtypes like nA, nL, nC, nR.

Incidence on equipments

Regarding the usage frequency, it is relatively hard to do a documented (objective) study especially because the information regarding this subject are disparate and the study of certified / tested articles in INSEMEX Petroșani offers a unilateral image of this issue.

Based on authors experience the following conclusions can be exposed:

- The type of protection flameproof enclosure (d) is one of the most used types of protection for electrical apparatus operating in areas with hazard of explosive atmosphere as well for the power part and low current part. The tendency remarked regarding the use of this type of protection it’s a low decreasing one especially because the appearance and use of other types of protection.

- Increased safety (e), pressurization (p), non-incendive (nA and nL) shows an increasing tendency regarding the usage owned especially to the less rigorous requirements comparative with the type of protection flameproof enclosure “d” and intrinsic safety.

- Intrinsic safety (i) keeps and consolidates its position being the direct applicable solution for low currents apparatus and systems.

- Encapsulation (m) has a low incidence, but the tendency is to slowly increase.

- Oil immersion (o) and powder (sand) filling (q) are types of protection practically unused.

Eligibility for hazardous zones

All types of protection are eligible for Zone 1, except the type of protection non-incendive (n) which is eligible only for Zone 2.

Zone 0 necessitates special considerations, and intrinsic safety – level of protection ia, and encapsulation level of protection ma are (for the moment) the only types of protection eligible to use in such areas.

Requirements regarding mechanical protection

The requirements regarding normal degree of protection of enclosures varies from minimum to medium as a function of the types of protection.

Type of protection (symbol)	Degree of protection
Intrinsic safety (i)	IP 20
Pressurization (p)	IP 40
Increased safety (e)	IP 44 (insulated conductive live parts) IP 54 (bare conductive live parts) IP 20 (rotating electrical machines installed in clean environments and regularly supervised by trained personnel)
Non-incendiv	IP 54 IP 20 (rotating electrical machines installed in clean environments and regularly supervised by trained personnel)

Creepage distances and clearances

For the comparative study of those distances the clearance was chosen having as reference the value imposed by the type of protection increased safety (e).

For accomplishing the comparison the downgrade of the regression line was used.

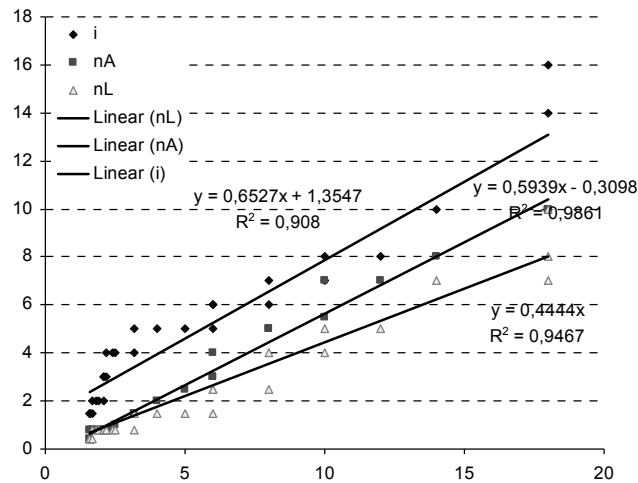


Fig.2 Clearance (mm) at different voltages for the types of protection i, nA, nL function of the clearance (mm) imposed by the type of protection increased safety (e)

Taking into account the above mentioned criteria it can say that the type of protection increased safety prescribes the largest clearances, being followed by the type of protection intrinsic safety, non-incendive nA and respectively nL, at approximately half values.

Maximum voltage

The maximum admitted voltage values for the types of protection are given in the bellow table.

Type of protection (symbol)	Maximum voltage [kV]
Intrinsic safety (i)	1,575
Non-incendive (nL)	15,6
Encapsulation (m)	11
Pressurization (p)	11
Increased safety (e)	11
Flameproof enclosure (d)	-
Non-incendive (nA)	15,6

Technical protection solution

Taking into account the protection strategy mentioned in the beginning of the paper four technical solution of protection can be stated, like this:

- segregation – separates the ignition source (apparatus) from the explosive atmosphere. The types of protection pressurization (p), encapsulation (m),

oil immersion (o), powder filling (q) are based on this technical protection solution;

- eliminates the source of ignition. The types of protection increased safety (e) and non-incendive (nA) are based on this technical protection solution;
- limitates the energy of ignition source. The types of protection intrinsic safety (i) and non-incendive (nL) are based on this technical protection solution;
- limitates the deflagration expansion zone. The type of protection flameproof enclosure (d) is based on this technical protection solution.

5. CONCLUSIONS

By the study made, in this paper were brought out the aspects that recommends various types of protection for one specific application (apparatus).

REFERENCES

- [1]. **SR EN 60079-14:2004**, *Electrical apparatus for explosive gas atmospheres. Part 14: Electrical installations in hazardous areas (other than mines)*
- [2]. **SR EN 60079-0:2005**, *Electrical apparatus for explosive gas atmospheres. Part 0: General requirements*
- [3]. **R EN 60079-1:2005**, *Electrical apparatus for explosive gas atmospheres. Part 1: Flameproof enclosures "d"*
- [4]. **SR EN 60079-2:2005**, *Electrical apparatus for explosive gas atmospheres. Part 2: Pressurized enclosures "p"*
- [5]. **SR EN 50017:2003**, *Electrical apparatus for potentially explosive atmospheres. Powder-filling "q"*
- [6]. **SR EN 50015:2003**, *Electrical apparatus for potentially explosive atmospheres. Part 6: Oil-immersion "o"*
- [7]. **SR EN 60079-7:2004**, *Electrical apparatus for explosive gas atmospheres. Part 7: Increased safety "e"*
- [8]. **SR EN 60079-10:2004**, *Electrical apparatus for explosive gas atmospheres. Part 10: Classification of hazardous areas*
- [9]. **SR EN 50020:2003**, *Electrical apparatus for potentially explosive atmospheres. Intrinsic safety "i"*
- [10]. **SR EN 60079-15:2004**, *Electrical apparatus for explosive gas atmospheres. Part 15: Type of protection "n"*
- [11]. **SR EN 60079-18:2004**, *Electrical apparatus for explosive gas atmospheres. Part 18: Encapsulation "m"*
- [12]. **SR EN 60079-26:2005**, *Electrical apparatus for explosive gas atmospheres. Part 26: Special requirements for construction and test of electrical apparatus for use in zone "0"*
- [13]. **S. Burian, J. Ionescu, M. Darie, L. Moldovan, ș.a.**, *Aparatură tehnică pentru medii potențial explozive. Grupa II, Ediția a II-a revizuită, Ed. Europrint Oradea, 2006, ISBN 973-7735-32-3*
- [14]. **R.STAHL Schaltgeräte GmbH**, *Ex-Magazine 32/2006-00-en-08/2006, ID-Nr. 00 006 24 76 0 S, ISSN 0176-0920, pg. 60-69*

CONDITIONS FOR INTERCONNECTING INTRINSIC SAFETY CIRCUITS SUPPLIED BY LINEAR AND NON-LINEAR SOURCES INTENDED FOR USE IN POTENTIALLY EXPLOSIVE ATMOSPHERES

TIBERIU CSASZAR^{*}, SORIN BURIAN^{*}, MARIUS DARIE^{}**

Abstract: The design and use of non-linear sources need solid knowledge and a rich experience gained in the use of electric apparatus intended for use in potentially explosive atmospheres. Consequently, after a test house checks the safety level that corresponds to a supply source with intrinsic safety type of protection, the design of a system with intrinsic safety type of protection is then allowed, but any special condition regarding this type of system shall be considered.

When analyzing the safety level for a combination of supply sources with non-linear outputs, then the interaction of the two circuits may lead to a significant increase of energy dissipation on the regulating components of the circuit, aspect that shall be considered during the evaluation.

Key words: intrinsic safety, non-linear sources

1. INTRODUCTION

This topic has been under analysis for a long period of time and it is still under study. This paper represents the common opinion of several test houses expert in testing of equipment intended for use in potentially explosive atmospheres and covers the latest information in this field.

The design and use of non-linear sources need solid knowledge and access to suitable testing facilities. After the test laboratory checks out the safety level of a system with intrinsic safety type of protection, it is allowed to design a system with intrinsic safety type of protection but all special conditions with respect to such a system shall be clearly stated and valued.

** Ph.D. Student Eng at the INSEMEX PETROȘANI*

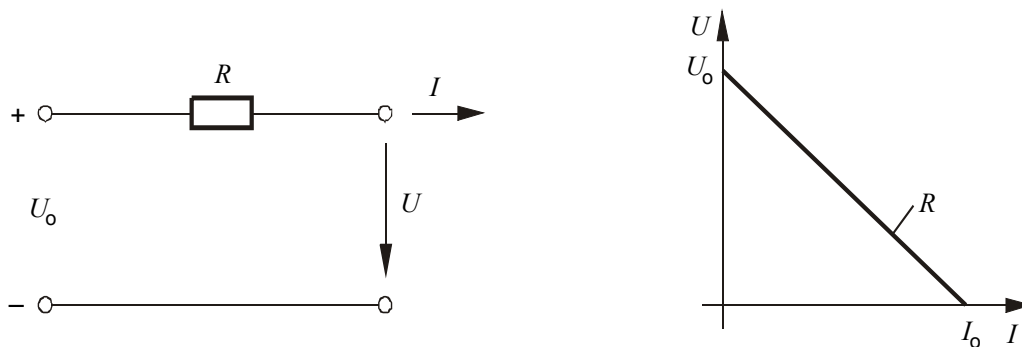
*** Ph.D.Eng. at the INSEMEX PETROȘANI*

When analyzing the safety level for a combination of supply sources with non-linear outputs, then the interaction of the two circuits may lead to a significant increase of energy dissipation on the regulating components of the circuit, aspect that shall be considered during the evaluation.

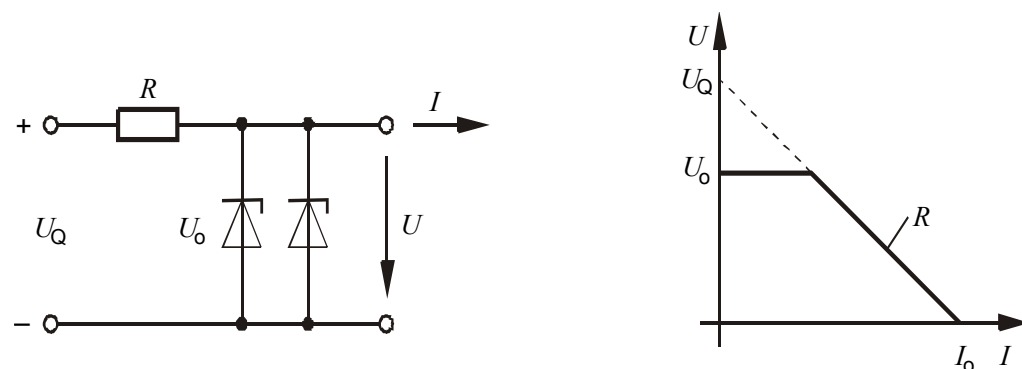
The installation regulations stated by the specific standards allow that the operator in charge with the hazardous area combines by interconnecting several circuits with intrinsic safety. This aspect also includes the situation when there are used several “associated apparatus” (i.e. active in normal operation or in state of failure). When this thing is done, it is no longer necessary to involve a test house whether the intrinsic safety of the interconnection is checked out by calculation or by tests.

It is easy to evaluate interconnection of resistive circuits by means of calculation whether the involved sources have an internal linear resistance as shown in Fig. 1 Hence the limit ignition curves from the specific standard are being used for this situation for the intrinsic safety circuits (SR EN 50020).

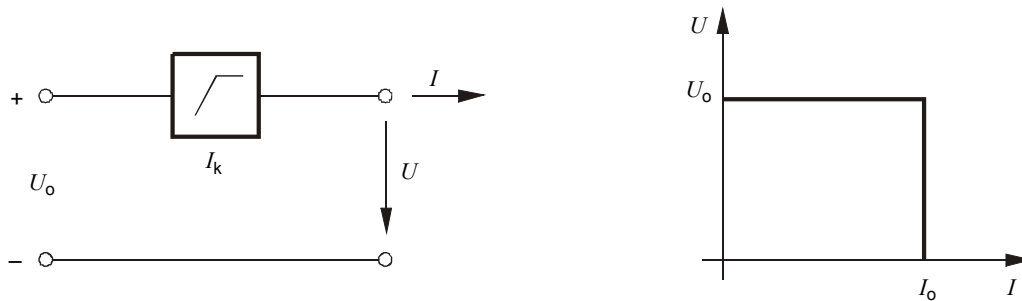
But the problem gets complicated when the technical equipment is supplied by two or several sources. In this case the evaluation should consider the possibility of an accidental connection of the two sources. The first stage involves the evaluation of the view maximum values for current and voltage, which represent the result of the combination of the associated apparatus.



a) Circuit with linear characteristics



b) Circuit with trapezoidal characteristics

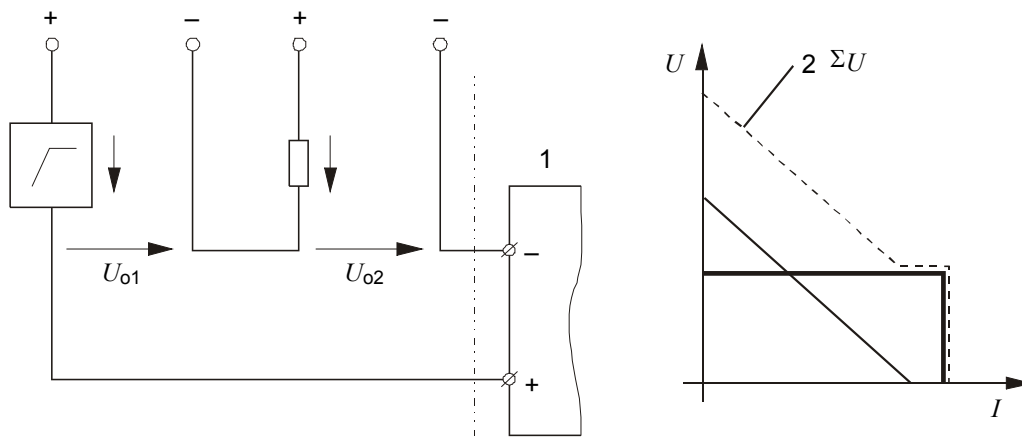


c) Circuit with rectangular characteristics

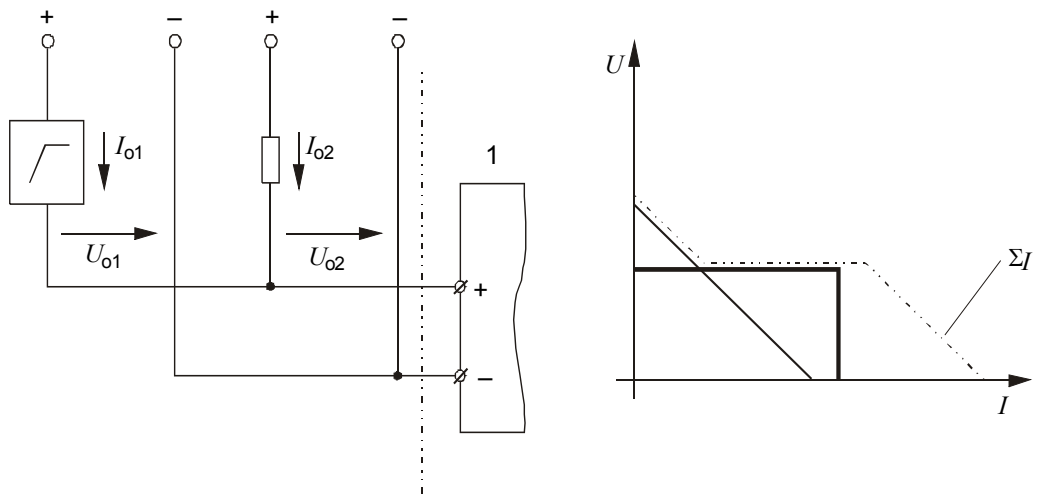
Fig. 1 Equivalent circuit and the output characteristics of resistive circuits

Whether the associated apparatus is combined as shown in Fig. 2 case a), it results a serial connection. In this situation the maximum values of idle voltages, U_0 , of each subassembly are summed up and there shall be selected the maximum value of the short-circuit currents, I_0 , of subassemblies. If the layout is case c) (Fig.2), then we have a parallel connection, it results a summation of the short-circuit currents and there shall be selected the highest value of the idle voltage.

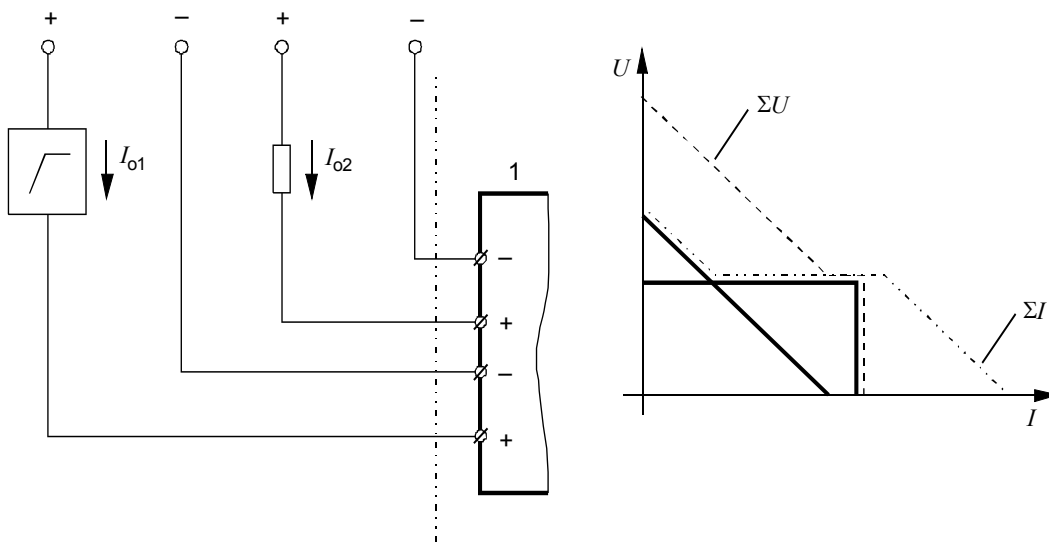
Even if it is not clearly defined the connecting manner of apparatus with respect to polarity (Fig. 2, case c)), then we may have a serial or a parallel connection depending on the fault condition considered, for this situation both the summation of voltage and of current shall be considered for both cases, but separately. The calculation shall consider the most unfavourable values.



a) Serial connection with the summation of voltages



b) Parallel connection with the summation of currents



c) Serial or parallel connection with the summation of voltage and current

Fig. 2 Summation of the current and /or voltage for different interconnections

After determining the new maximum values for current and voltage, the intrinsic safety of the mixed circuits shall be checked out with the help of the ignition limit curves stated by SR EN 50020; there shall also be considered the safety coefficient for the resistive circuit and it is compulsory to determine the new maximum admitted values of the external inductance L_0 and the external capacitance C_0 . Nevertheless, such an approach cannot cover all the situations possible with respect to

safeness, such as when two or several active sources from inside a circuit display non-linear characteristics, so the evaluation based only on the idle voltages and short-circuit currents is not enough.

Practical applications use mostly “trapezoidal sources” (see Fig. 1, case b)), often with rectangular output characteristics (see Fig. 1, case c)) if one uses current limitation electronic devices. The ignition limit curves (SR EN 50020) cannot be used for such circuits; the circuit has to be considered vs. one of the above-mentioned patterns for defining the intrinsic safety parameters of individual circuits or of the associated apparatus.

For the evaluation of intrinsic safe active circuits, both the internal resistance and the voltage of the source shall have to be known. For the simplest situation, the source can be characterized by two electrical values (constants), either voltage U_0 or the internal resistance R_1 or U_0 and the short-circuit current I_0 (see Fig. 1, case a)). U_0 and I_0 are the maximum values which can occur in the fault condition stated by the specific standard for the evaluation of intrinsic safe circuits (SR EN 50020). Consequently, we can take into consideration, for example, a battery equipped with an external resistor for current limitation with no constant internal resistance. Similarly, the voltage of the source shall change depending on the charging level. For studying the behaviour of these circuits in practical applications, they are being represented by their simplest equivalent circuits which obviously shall have to be the least capable to ignite compared to the real circuit. For the above said battery, the maximum value corresponding to the open circuit shall be considered for U_0 .

Also, the non-linear circuits can be divided into two basic types shown in Fig 1-case b) and case c). Thus, the source with the trapezoidal characteristic (Fig. 1, case b)) is made of a voltage supply source, a resistance and additional components for limitation of voltage (for ex. Zenner diodes) and terminals. For the situation shown in Fig. 1, case c), the rectangular characteristics has the current limited by an electronic current regulator.

In compliance with the aspect said above, one may say that the available maximum power of a voltage supply source with the characteristics as the one shown in Fig. 1- case a) is:

$$P_{max} = \frac{1}{4} U_0 \times I_0 \quad (1)$$

And for the trapezoidal characteristics (according to Fig. 1, case b), is:

$$P_{max} = \frac{1}{4} U_Q \times I_0 \text{ (for } U_0 > \frac{1}{2} \times U_Q), \text{ or} \quad (2)$$

$$P_{max} = U_0 \times (U_Q - U_0)/R \text{ (for } U_0 \leq \frac{1}{2} \times U_Q) \quad (3)$$

But for a full electrical type description of the source there are necessary two parameters for the linear and rectangular characteristics and three parameters for the trapezoidal characteristics (Table 1).

Table 1 Necessary parameters for describing the output characteristics

Characteristic	Necessary parameters
Linear, Fig. 1 a)	U_0, I_0 or U_0, R
Trapezoidal, Fig. 1 b)	U_0, U_Q, R or U_0, R, I_0 or U_0, U_Q, I_0
Rectangular, Fig. 1 c)	U_0, I_0

Usually, the stated values are as it follows: idle voltage (hereinwith called U_0), the short-circuit current (hereinwith called I_0) and the maximum available power P_0 . There is sometimes possible to determine the type of the characteristics even from these values.

Nevertheless, in certain circumstances even if the values of power, current and voltage are given, these data are not concluded for a test house because the maxim power is given for the stationary regime (the heating effect of the components that have been subsequently connected) and the values of current and voltage for the dynamic regime (ignition by sparks). Whether there are doubts, it is necessary to check out which of the characteristics shall be taken as basis for interconnection, with respect to the evaluation to ignition by spark. Consequently, for the trapezoidal characteristics, the information given by the manufacturer is not enough to determine the characteristics because the third parameter is missing (see Table 1), i.e. either U_Q or R .

At the end, one can conclude that a certification documentation shall also have to state the characteristics of non-linear circuits involved in the construction of a intrinsic safety system.

REFERENCES

- [1] SR EN 50020:2003, *Electrical apparatus for potentially explosive atmospheres. Intrinsic safety "i"*
 [2] SR EN 60079-25:2006, *Electrical apparatus for potentially explosive atmospheres. Systems with intrinsic safety.*

CONSIDERATION VIEWING THE OPTIMAL DIMENSIONING OF THE MAINTENANCE TEAM FROM THERMO-ELECTRIC POWER PLANTS

MILTIADE CÂRLAN*, HORIA GOIA*, SIMONA DZIȚAC**

Abstract: Viewing the optimal structure of the maintenance team, the problem of its dimensioning is very important; in the paper, the proposed optimal criterion is the “maximal engaged degree” of the members. The paper contains general considerations viewing the optimal component of the maintenance team, presentation of a statistical method – the least squares method, adapted to maximize the engage rate of the team, accompanied with a case analyze.

Key words: maintenance, engaged degree, work team, thermoelectric plant, statistic sample

1. CONSIDERATIONS VIEWING THE STABILIZING THE OPTIMAL COMPONENT OF OPERATIONAL EQUIPMENT IN MAINTENANCE ACTIVITIES

The optimal structure of the maintenance team follows a double scope: it must dimension for the optimal dimensioning of the work, and on the other part, founds its optimal number. For both aspects of the problem, the decisional factor must have criteria of optimal performance, in the selection of mathematical model but in the obtained efficiency too.

The proposed optimal criteria for the solution of the problems are *the maximal engage degree of the team's member*. The engaged degree of a member from the team (maintenance team) is expressed by the relation:

* *Professor PhD University of Oradea*

** *Eng. PhD Student University of Oradea*

$$G_o = \frac{\overline{M}_e}{M} \cdot 100 \quad (1) \text{ where:}$$

G_o - engaged grade of the team's members [-]%;

\overline{M}_e - average number of effective producing staffs (from the production process analyst);

$$\overline{M}_e = \frac{\sum_J M_{e_j}}{m}, \quad J = \overline{1, m} \quad (2)$$

where: M_{e_j} - is the number of executants, observed by the analyst in the m moments of the days,

M - is the number of available staffs from the team

To stabilize of the moments and days when the measurements are performed is used the technique of the Monte Carlo simulation method.

Relation (1) has sense only when the executant's qualification level, the workplaces logistic for all period of the information collection matches with the requirements of the work.

Under these conditions, stabilization of a function of dependence $G_{op} = f(M)$ imposes the fulfilling of the following restrictions:

$$\begin{cases} a / \lim_{m \rightarrow 0} G_o = 0 \\ b / \lim_{M \rightarrow \infty} G_o = 0 \end{cases} \quad (3)$$

To evaluate of the staffs engaged grade is proposed the following relation:

$$G_o = A e^{-cM} (1 - e^{-M}) \quad (4)$$

where: A, C represents the regressions coefficients of the function $G_{op} = f(M)$.

Expression (4) satisfies the restriction (3) and represents a point of extreme (the abscissa of it's the optimal number of staff).

$$\frac{dG_o}{dM} = 0 \Rightarrow M_{optim} = \ln \frac{c+1}{c} \quad (5)$$

Also, the grade of staff engage offers a modality to structure optimal the equipment of the maintenance - fig.1. In this fig Z_o signs the optimal number of staffs:

$$Z_o = [M_o^{\inf}, M_o^{\sup}] \quad (6)$$

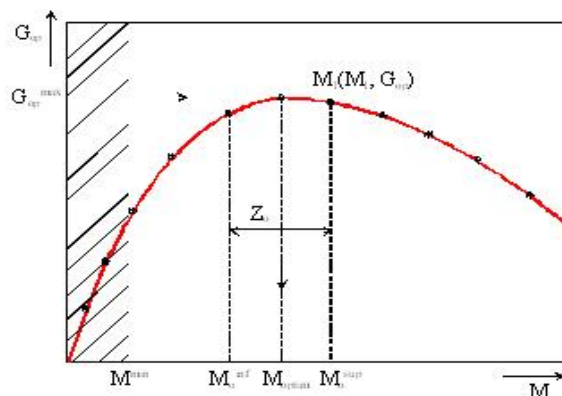


Fig. 1. - $G_0 = f(M)$ function graph

To determine the regression coefficient A , c (from relation 4) may be realized through many methods, but in this paper we will use the least square method.

2. THE METHOD OF THE LEAST SQUARE METHOD

Let it be M_i the component number of a little group and G_{0_i} the values of engaged grade of the group components, table 1.

Table 1. Number of components and the engaged values of the components of group

M_i - executants	M_1	M_2	M_k	M_n
G_{0_i} [%]	G_{01}	G_{02}	G_{0k}	G_{0n}

In the figure 1 are presented the points and results that there is a tendency to form a “group” for a certain shape, the **geometrical position** of the points.

In concordance with the least square method, the sum of the deviation points resulted from the observation, viewing the points located on the regression curve, must be minim.

This criterion, leads to the regression coefficients evaluation of the function of the graph.

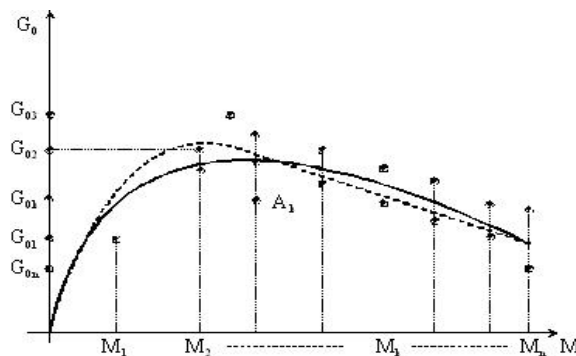


Fig. 2 - Function $G_0=f(M)$; „positioning” of the couples $A_K (M_K, G_{0_K})$

The proposed relation 4 for the applying of this method satisfies the following restriction set:

$$\left. \begin{array}{l} a - \lim_{M=0} G_0 = 0 \\ b - \lim_{M \rightarrow \infty} G_0 = 0 \\ c - M_{optim} \Rightarrow G_0^{\max} \end{array} \right\} \quad (7)$$

Results that for dimensioning of a work team, the optimal criterion is the maximal **engaged grade**:

$$M_{optim} \Rightarrow G_0^{\max} \quad (8)$$

From the condition: $\frac{dG_0}{dM} = 0$ is deduced:

$$M_{optim} = \ln \frac{c+1}{c} \quad (9)$$

To calculate the regression coefficient, it must take into account the criterion:

$$S \Rightarrow \sum_i (G_{0_i} - \tilde{G}_{0_i})^2 \Rightarrow \text{minim}, \quad S \Rightarrow \sum_i \{G_{0_i} - [Ae^{-cM}(1 - e^{-M_i})]\}^2 \Rightarrow \text{minim} \quad (10)$$

with: G_{0_i} - are the observed values of the engaged grade of a person M_i ;

\tilde{G}_{0_i} - values of the engaged grade established by the regression relations.

Linearizing the relation, results:

$$\ln A - cM + \ln(1 - e^{-M}) = \ln G_0 \quad (11)$$

With the conditions (12)

$$\frac{\partial S}{\partial A} = 0, \quad \frac{\partial S}{\partial c} = 0 \quad (12)$$

There is obtaining the following system of linear equation (13):

$$\left. \begin{array}{l} n \ln A - c \sum_i M_i = \sum_i \ln G_{0_i} - \sum_i \ln(1 - e^{-M_i}) \\ \ln A \sum_i M_i - c \sum_i M_i^2 = \sum_i M_i \ln G_{0_i} - \sum_i M_i \ln(1 - e^{-M_i}) \end{array} \right\} \quad (13)$$

Where (n) is the statistic sample volume.

A case study: staff for change of the caoutchouc belt rollers support.

Let be the elements of calculus in the table 2.

Table 2. Elements of calculus

i	M _i	G _{0_i} [%]
1.	5	70
2.	7	72
3.	5	70
4.	6	70
5.	7	75
6.	6	75
7.	5	65
8.	7	65

To calculate:

- to determine the optimal number of the executants;
- maximal engaged grade realized by this team.

In table 3 is presented the synthesis of the regression grade coefficients.

Table 3. Calculus of the regression coefficients

i	M _i	G _{0_i} (%)	M _i ²	ln G _{0_i}	1 - e ^{-M_i}	ln(1 - e ^{-M_i})	M _i ln G _{0_i}	M _i ln(1 - e ^{-M_i})
1.	5	70	25	4,24849	0,99326	-0,00676	21,24245	-0,03380
2.	7	72	49	4,27667	0,99909	-0,00091	29,93670	-0,00637
3.	5	70	25	4,24849	0,99326	-0,00676	21,24245	-0,03380
4.	6	70	36	4,24849	0,99752	-0,00248	25,49094	-0,01488
5.	7	75	49	4,31749	0,99909	-0,00091	30,22243	-0,00637
6.	6	75	36	4,31749	0,99752	-0,00248	25,90494	-0,01488
7.	5	65	25	4,17439	0,99326	-0,00676	20,87195	-0,03380
8.	7	65	49	4,17439	0,99909	-0,00091	29,22073	-0,00637
\sum_i	48	*	294	34,00540	*	-0,02797	204,13259	-0,15027

Starting from the equation system (13) results the coefficients values of the regressions: $c \cong 0,03$; $A \cong 85$.

There is reduced the optimal number of the staff: $M_{optim} \in \{3;4\}$ executants.

In some situations the optimal zone is greater.

The correlation rate (coefficient of Pearson) evidences the linear links intensity but of the curvilinear too (relation adopted for G₀).

$$\eta = \sqrt{\frac{\sum_i (\tilde{G}_{0i} - \bar{G}_0)^2}{\sum_i (G_{0i} - \bar{G}_0)^2}} \quad (15)$$

where: G_{0_i} - calculus data;

\bar{G}_0 - medium value of "the engaged grade";

\tilde{G}_{0_i} - the computed values through the regression relation:

$$\Delta G_{0_i} = G_{0_i} - \bar{G}_0 \text{ și } \Delta \tilde{G}_{0_i} = \tilde{G}_{0_i} - \bar{G}_0$$

The correlation rate is: $\eta = 0,6$

Due to the reduced volume of the statistic sample, results a medium intensity correlation rate.

3. CONCLUSIONS

The optimal components of a work team that makes all activities of maintenance are stabilized in concordance with the strategy and the maintenance works, using the criteria of "maximal engaged degree of the teams' components". From the expression of engaged degree the regression coefficients are established by using one from the following methods: least squares method, the method of double point and the method of interpolation; in this paper we will use the least squares method.

The problem of rational dimensioning of executants team resolves: the efficient utilize of the works time, stabilizing the necessary number of staffs, realizing a complete concordance between the work's complexity and medium level of qualifying of the members of the team, squandering the human resources of high quality, realizing a synergy contribution of high level as effect of a cooperation in works of high productivity of the executant's team.

REFERENCES:

- [1]. Carabulea A., ș.a.- *Managementul sistemelor industriale. Probleme, studii de caz și aplicații*- E.T.P.București, 1995.
- [2]. Cârlan M. – *Mentenanța și disponibilitatea instalațiilor electrice*, Revista *Producerea, transportul și distribuția energiei electrice și termice* – nr.12/1994.
- [3]. Cârlan M., Goia H. Ștei M. - *Posibilități privind utilizarea metodei expertonilor cu fundamentarea strategiei de mentenanță a morilor de cărbune ale unui generator de aburi de 420t/h-*, Sesiunea anuală de comunicări științifice, Universitatea din Oradea, 2001.
- [4]. Goia H. C., Cârlan M., Goia E., Dzițac S.- *Determinarea numărului optim al personalului din activitatea de mentenanță la repararea și întreținerea STPCS CET I Oradea*, C.I.E., Universitatea din Oradea, Facultatea de Energetică, 2006.
- [5]. Ivas D.- *Modele de calcul a structurii optime pentru instalații energetice și domeniu de aplicare a acestora* – C.I.E., București, 1983.
- [6]. Kaufmann A.- *Metode și modele ale cercetării operaționale*-Traducere din limba franceză, E.Ș., București, 1968.

CONTRIBUTIONS TO IMPLEMENT THE RELIABILITY CENTERED MAINTENANCE AT THE THERMO- ELECTRIC PLANTS

IOAN FELEA*, HORIA GOIA*, SIMONA DZIȚAC**

Abstract: The paper is structured in three parts. In the first part is presented the methodological considerations viewing the reliability centered maintenance. The second part contains a synthesis of appliance opportunities of reliability centered maintenance referring on thermo electric plants. There are presented the appliance directions, the approach mode, mathematic models, and the appliance algorithm. The last part of the paper contains two case studies result and conclusions.

Key words: maintenance, reliability, thermo-electric plants, optimization

1. PRELIMINARIES

A general classification imparts the maintenance politics in two great categories: the corrective maintenance (CM), and the preventive maintenance (PM) [1]. The combine of the two modalities is named as mixed maintenance. In last few years it was developed a new direction of preventive maintenance, the proactive maintenance [1,2].

The changing politics (after the age, in blocks, opportunity, stage, and mixed) [1,2] are modalities of PM strategies application. A significant example on scientific management is the reliability centered maintenance (RCM). [2] In RCM concept an efficient maintenance program, plans only that procedures that are necessary to attain the proposed objective for all operation of the system. The actual practice justifies the following definition for this maintenance strategy: evaluations and actions that leads to the maintenance works achieve in correlation with a certain reliability level (previsional) or certifiable (operational). To an analytical approach of RCM, is

* *Professor, Ph.D. at the University of Oradea*

** *Eng. PhD Student at the University of Oradea*

necessary to know the real operational reliability level that is obtained from studies, having a good outlined space- temporal localization. For the equipment from the power engineering systems, the main aspects that are approached and treat and represents RCM actions [1 ÷ 6] are: establishing the optimal testing frequency, to minimize the time unavailability, applying the substituting politics after the testing, optimal management of the structures of “k from n” type, optimal, structural and temporal weight, of the works from the two categories (PM+CM), optimizing the stocks level of the equipment, materials and subunits.

2. RCM STRATEGIES APPLICATION MODELS IN TERMO - ELECTRIC PLANTS (TEP)

The RCM strategy is utilized to all equipment from the TEP (electric, heating, electro-mechanic). The application with success of RCM strategy implies the continuous evaluation and actualization of the operational reliability indicators of the equipment, following the common algorithm [1, 3, 5]. The detailed analysis [7], allowed the application models selection, referring on TEP equipment. The direction of the application and the models are synthesized in the followings.

2.1. Substitution politic by stage

This politic supposes the restrictive criterion application [1]:

$$\text{Prob}(t \geq T) \geq R_L \quad (1)$$

where: R_L – is a pre-established limit of the probability of good operating
Enjoining the MP works periodicity is obtained:

- Exponential distribution

$$T_{LM} = -\frac{1}{\lambda} \ln R_L \quad (2)$$

- Weibull distribution

$$T_{LM} = \gamma + \eta \left(\ln \frac{1}{R_L} \right)^{\frac{1}{\beta}} \quad (3)$$

where $\lambda, \beta, \gamma, \eta$ - parameters of the distribution [1,3,6]

2.2. Selection the maintenance strategy basing on operational availability level

Hypothesis:

H_{P1} : The equipment comes under only action of CM actions;

H_{p2} : The equipment comes under the action of PM action;

H_{p3} : The equipment comes under action of predictive maintenance action (PRM), the period of testing is 1 year, and the duration of the testing is 1 day.

In case of H_{p1} the time availability of the system may be write as:

$$D_c = \frac{T_c}{T_c + T_{CM}} \quad (4)$$

where, T_c - time between two replacements [1],

T_{MC} - total period of corrective interventions [1].

In case of a preventive maintenance politics H_{p2} , the availability of the system is:

$$D_p = \frac{T_p}{T_p + \Pi_T} \quad (5)$$

where, T_p – continuous operating average time

Π_T the non operating average time for a duration of $(0, T)$:

$$\Pi_T = T_{PM} \cdot R(t) + T_{CM} \cdot [1 - R(t)] \quad (6)$$

The availability of the equipment in condition of H_{p3} for the duration of “n” inspection:

$$D_{T_{1 \rightarrow n}} = \frac{T_{p_{1 \rightarrow n}}}{T_{p_{1 \rightarrow n}} + \Pi_{T_{1 \rightarrow n}}} \quad (7)$$

where, $T_{p_{1 \rightarrow n}}$ - continuous operating average time for “n” inspection

$\Pi_{T_{1 \rightarrow n}}$ - non operating average time for “n” inspection

2.3. The maintenance of the structure of “k din n”

The structures of „k din n” type, are frequently utilized in thermal heat plants. There are researches and applications that studies the structural optimization (at the design) and functional (exploitation) of „k din n” type system [5].

The criteria that is the base of stabilization of the actions moment releasing of the PM, is the maximal reliability gain, that justifies the including of such type of procedure in category of RCM options. After the release of the PM actions, these will achieve, successively for “n” elements from the investigated structure. The diagram of equivalent reliability block diagram (RBM) is presented in fig.1.

The time safety of the system with “n” and with “n-j” elements in operating is explained as:

$$R_n = \sum_{i=k}^n C_n^i R^i (1 - R)^{n-i} \quad (8)$$

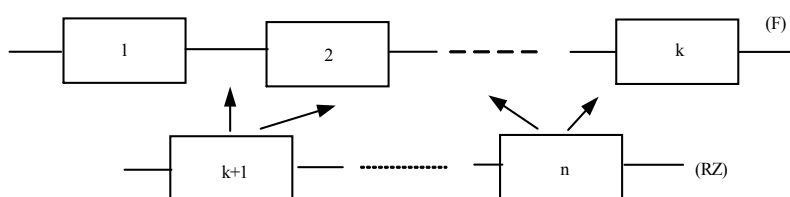


Fig 1. – RBM of the system „k din n” type

The time safety of the system with “n-j” elements in operating is explained similarly:

$$R_{n-j} = \sum_{i=k}^{n-j} C_{n-j}^i R^i (1 - R)^{n-j-i}; j \leq n - k \tag{9}$$

The reliability gain between the two stages is explained as:

$$\Delta R = R_n - R_{n-j} \tag{10}$$

To determine the maximal value of the „ΔR” indicator and of T_s indicator value, it is derivate in function with “t” variable of ΔR.

3. THE RESULTS OF THE CASE

For a perfect cooperation between the three entities it were made operational and previsional reliability, and was established the characteristics of RCM strategy for the equipment of the transport system structure and for the preparation of solid fuels (STPCS) from CET I Oradea and CTE Mintia.

The complete results of the studies are in [7] and offer for two entities the necessary dates for the maintenance program.

The obtained results referring on the presented models in chapter 2, applied at certain equipment from the two plants.

Table 1. The values of T_{LM} parameter for equipment from structure STPCS, al CET I Oradea and CTE Mintia

Equipment	Reliability impose (R _L)	0,98	0,96	0,94	0,92	0,90
	Values of parameters (T _{LM}) [h]					
Rotating arms feeder, bands		51	114	117	258	337
Machines of delivery – storing of coal		293	426	529	617	714
Coal crusher		868	1070	1207	1316	1428
Coal mill feeder, CET I		855	1117	1298	1450	1608
Coal mill feeder, CTE Mintia		1096	1352	1586	1667	1809
Mill grind coal (MV)		974	1230	1410	1553	1701
Mill grind coal (MC)		1113	1372	1151	1692	1836

Table 2. The availabilities of time for equipment from STPCS structure that are supposed to actions

Nr. crt.	Equipment	CM actions (H_{p1})	PM actions (H_{p2})		Predictive maintenance actions (H_{p3})
			RK	RT	
1.	Feeder with rotating arms (CET I Oradea)	0,9991	0,9455	0,9234	0,9234
2.	Machines of delivery – storing (CTE Mintia)	0,9931	0,9877	0,9543	0,9543
3.	Transmission bands (CTE Mintia)	0,9940	0,9754	0,9678	0,9678
4.	Crushers (CET I Oradea)	0,9982	0,9865	0,9245	0,9245
5.	Crushers CTE Mintia)	0,9947	0,9890	0,9851	0,9851
6.	Coal Feeder (CET I Oradea)	0,9724	0,9923	0,9678	0,9678
7.	Coal feeder (CTE Mintia)	0,9737	0,9898	0,9489	0,9489
8.	Fan mills (CET I Oradea)	0,9666	0,9843	0,9324	0,9324
9.	Hammer mills, with ball crusher (CTE Mintia)	0,9970	0,9264	0,9421	0,9421

The maintenance program

There were analyzed the structures of „2 from 5” type, for the transmission bands from CET I Oradea, „4 from 5” for the fan mills from CET I Oradea, „2 from 4” for the machines of coal delivery and store from CTE Minita (the old stage) and „3 from 5” for the transmission bands from CTE Mintia (new stage). Similarly, may be treated other structures with a concrete number of reserve elements from the structure of STPCS.

Structure	R	$R(T_s)$	T_s
„2 din 5”	0,99768	0,4	3806
„4 din 5”	0,8521	0,8	3910
„2 din 4”	0,999984	0,5	3080
„3 din 5”	0,99943	0,6	1667

For the compute it was utilized the Weibull distribution function, that offers the best approximation of empirical distribution by the analyzed equipment.

4. CONCLUSIONS

The equipment and transport systems maintenance strategies adequacy as well the solid fuels preparation is a solution of action through that are obtained major financial economize by CET and CTE.

The RCM strategy application is the most efficient path with actuality for implementation of a modern and efficient maintenance system of the equipment from the structure of STPCS.

RCM strategy operationalization, from STPCS structure, in principal, is made through: the application of substituting politics viewing the stage, the comparatively evaluation and the availability maximization of the equipment, optimizing the testing frequency, the maintenance program adequacy by the structures with „k from n” type.

The substituting politic application viewing the stage of the analyzed equipment, that are made with Weibull distribution of TBF variable, and for the values of the reliability function that are in interval of $[0,9;0,94]$.

The obtained values for indicator of "time availability" of the equipment from the STPCS structure, reflects the opportunity of mixed maintenance strategy (PM + CM), with the time interval activation between two works of PM in function with the operational reliability level of each type of equipment.

The application of the testing optimal frequency optimization model is made by grouping of the analyzed equipment in "basic installations" category, which implies the assurance of characteristic risk level exponential distribution of operating and leads to conclusion of opportunity of mixed maintenance strategy application by the equipment from structure of STPCS of CET I Oradea and CTE Mintia.

The major of the subsystems from STPCS structure are of „k from n” type. An essential management aspect of maintenance of structures „k from n” type, is the moment of releasing the maintenance actions, so that, the gain of reliability is maximum.

Such an approach takes part of strategy of reliability centered maintenance. The indices with interest for management of maintenance systems of „k from n” type, are: the time interval value, after the reliability gain attains the maximal value (T_s), the time safety $[R(T_s)]$ and the reliability gain $[\Delta R(T_s)]$ at T_s moment.

The numerical evaluation of T_s parameter (interval of time between two actions of preventive maintenance) for equipment from STPCS that are of „k from n”, reflects, the main dependency of this parameter from the distribution type and the operational reliability's indicator values.

REFERENCES

- [1]. Felea, I., Coroiu N.- *Fiabilitatea și mentenanța echipamentelor electrice*, Editura Tehnică, București, 2001.
- [2]. Monbray I. – *Reliability Centered Maintenance*, Butterworth, Heinemann, 1991.
- [3]. Lyonnet P.- *La maintenance Mathematiques et Methodes*, Technique Documentation, Paris, 1992.
- [4]. Cârlan M. – *Probleme de optim în ingineria sistemelor tehnice*, E.A.Române, București, 1994;
- [5]. Felea I., Coroiu N.,- *Recurs la mentenanța bazată pe fiabilitate în rețeaua de repartiție și distribuție*, Revista Energetica, nr. 3, 2005.
- [6]. Nitu V. I. – *Fiabilitate, disponibilitate, mentenanță în energetică*, E.T. București, 1987.
- [7].Goia H. C.- *Contribuții privind implementarea strategiei de mentenanță RBM la echipamentele din structura STPCS*, teză de doctorat, 2006

DIAGNOSTIC TESTING FOR ASINCRONOUS MOTORS

TABACARU-BARBU TEODOR*

Abstract. Nondestructive diagnostic tests are used to determine the condition of the insulation and the rate of electrical aging. The description of the recommended diagnostic tests for the insulation system of motors and the conditions they are designed to detect are discussed. Methods to test stators and rotors of asynchronous motors are presented and their advantages.

Keywords: asynchronous motors, the insulation system

1. INTRODUCTION

The following factors affect the insulation systems in motors:

- High temperature
- Environment
- Mechanical effects such as thermal expansion and contraction, vibration, electromagnetic bar forces, and motor start-up forces in the end turns
- Voltage stresses during operating and transient conditions

All these factors contribute to loss of insulation integrity and reliability.

These aging factors interact frequently to reinforce one another's effects. Nondestructive diagnostic tests are used to determine the condition of the insulation and the rate of electrical aging. The description of the recommended diagnostic tests for the insulation system of motors and the conditions they are designed to detect are discussed.

2. STATOR INSULATION TESTS

An electrical test is best suited to determine the condition of electrical insulation. The tests on insulation systems in electrical equipment can be divided into two categories:

* *Asoc.Prof.Dr.Eng., University of Petroșani*

- High-potential (hipot), or voltage-withstand tests
- Tests that measure some specific insulation property, such as resistance or dissipation factor.

Tests in the first category are performed at some elevated a.c. or d.c. voltage to confirm that the equipment is not in imminent danger of failure if operated at its rated voltage. Various standards give the test voltages that are appropriate to various types and classes of equipment. They confirm that the insulation has not deteriorated below a predetermined level and that the equipment will most likely survive in service for a few more years. However, they do not give a clear indication about the condition of the insulation.

The second category of electrical tests indicates the moisture content; presence of dirt; development of flaws, cracks, and delamination and other damage to the insulation.

A third category of tests includes the use of electrical or ultrasonic probes that can determine the specific location of damage in a stator winding. These tests require access to the air gap and energization of the winding from an external source. These tests are considered an aid to visual inspection.

3. DC TESTS FOR STATOR AND ROTOR WINDINGS

These tests are sensitive indicators to the presence of dirt, moisture, and cracks. They must be performed off-line with the winding isolated from ground, as shown in **fig. 1**.

Suitable safety precautions should be taken when performing all high-potential tests.

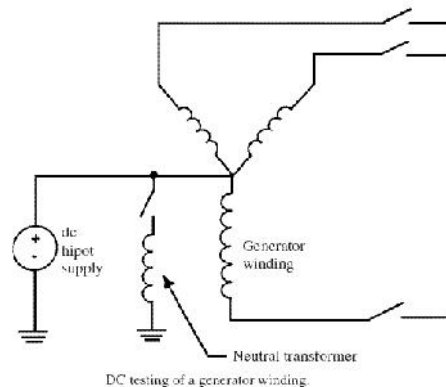
When high-voltage d.c. tests are performed on water-cooled windings, the tubes or manifolds should be dried thoroughly, to remove current leakage paths to ground and to avoid the possibility of damage by arcing between moist patches inside the insulating water tubes. For greater sensitivity, these tests can be performed on parts of the windings (phases) isolated from one another.

The charge will be retained in the insulation system for up to several hours after application of high d.c. voltages. Hence, the windings should be kept grounded for several hours after a high-voltage d.c. test to protect personnel from a shock.

Tests using d.c. voltages have been preferred over the ones using a.c. voltages for routine evaluation of large machines for two reasons:

- The high d.c. voltage applied to the insulation during a test is far less damaging than high a.c. voltages due to the absence of partial discharges;
- The size and weight of the d.c. test equipment are far less than those of the a.c. test equipment needed to supply the reactive power of a large winding.

3.1. Insulation Resistance and Polarization Index



The *polarization index* (PI) and insulation resistance tests indicate the presence of cracks, contamination, and moisture in the insulation. They are commonly performed on any motor and generator winding. They are suitable for stator and insulated rotor windings.

The insulation resistance is the ratio of the d.c. voltage applied between the winding and ground to the resultant current. When the d.c. voltage is applied, the following current components flow:

- The charging current into the capacitance of the windings;
- A polarization or absorption current due to the various molecular mechanisms in the insulation;
- A “leakage” current between the conductors and ground. This component is highly dependent on the dryness of the windings.

The first two components of the current are lowering in time. The third component is mainly determined by the presence of moisture or a ground fault. However, it is relatively constant. Moisture is usually absorbed in the insulation and/or condensed on the end winding surfaces. If the leakage current is larger than the first two current components, then the total charging current (or insulation resistance) will not vary significantly with time. Therefore, the dryness and cleanliness of the insulation can be determined by measuring the insulation resistance after 1 min, and after 10 min. The polarization index is the ratio of the 10-min to the 1-min reading.

3.2. Test Setup and Performance

Several suppliers offer insulation resistance meters that can determine the insulation resistance accurately by providing test voltages of 500 to 5000 V d.c. For motors and generators rated 4 kV and higher, 1 kV is usually used for testing the windings of a rotor, and 5 kV is used for testing the stator windings.

To perform the test on a stator winding, the phase leads and the neutral lead (if accessible) must be isolated. The water must be drained from any water-cooled winding, and any hoses removed or dried thoroughly by establishing a vacuum.

The test instrument is connected between the neutral lead or one of the phase leads and the machine frame (fig. 1). To test a rotor winding, the instrument should be connected between a lead from a rotor winding and the rotor steel. During the test, the test leads should be clean and dry.

Interpretation

If there is a fault or the insulation is punctured, the resistance of the insulation will approach zero. The IEEE standard recommends a resistance in excess of $V_{L-L} + 1$ M Ω . If the winding is 13.8 kV, the minimum acceptable insulation resistance is 15 M Ω . This value must be considered the absolute minimum since modern machine insulation is on the order of 100 to 1000 M Ω . If the air around the machine had high humidity, the insulation resistance would be on the order of 10 M Ω .

The insulation resistance depends highly on the temperature and humidity of the winding. To monitor the changes of insulation resistance over time, it is essential to

perform the test under the same humidity and temperature conditions. The insulation resistance can be corrected for changes in winding temperature. If the corrected values of the insulation resistance are decreasing over time, then there is deterioration in the insulation.

However, it is more likely that the changes in insulation resistance are caused by changes in humidity. If the windings were moist and dirty, the leakage component of the current, which is relatively constant, will predominate over the time-varying components. Hence, the total current will reach a steady value rapidly.

Therefore, the polarization index is a direct measure of the dryness and cleanliness of the insulation. The PI is high (>2) for a clean and dry winding. However, it approaches unity for a wet and dirty winding.

The insulation resistance test is a very popular diagnostic test due to its simplicity and low cost. It should be done to confirm that the winding is not wet and dirty enough to cause a failure that could have been averted by a cleaning and drying procedure. The resistance testing has a pass/fail criterion. It cannot be relied upon to predict the insulation condition, except when there is a fault in the insulation.

The high-potential tests, whether d.c. or a.c., are destructive ones. They are not generally recommended as maintenance-type tests.

For stator windings rated 5 kV or higher, a partial discharge (PD) test, which in the past has been referred to as *corona*, should be done. The level of partial discharge should be determined because it can erode the insulation and lead to insulation aging.

4. D.C. HIGH-POTENTIAL TESTING

The d.c. high-potential test is a nondestructive test used to evaluate the dielectric strength of the groundwall insulation. The voltage applied across the windings is given by

$$V_{\text{dc-hipot}} = 2V_0 + 1000 \quad [\text{V}]$$

where V_0 is the operating voltage and $V_{\text{dc-hipot}}$ is the voltage applied across the windings during the d.c. hipot test. The casing of the motor is maintained at ground voltage. The leakage current between the windings and the core is measured. The insulation resistance is obtained by dividing the voltage imposed across the windings by the leakage current. The test indicates that the groundwall insulation is able to withstand high voltage without being damaged.

Note that this test is different from the destructive a.c. and d.c. high-potential tests performed by the manufacturer of the motor. These tests are performed to determine the maximum voltage that the insulation of the motor can withstand. The voltage reached during these tests is much higher than the voltage recommended for the nondestructive d.c. high-potential test. They are performed by a qualified operator to prevent the destruction of the motor.

4.1. Surge Testing

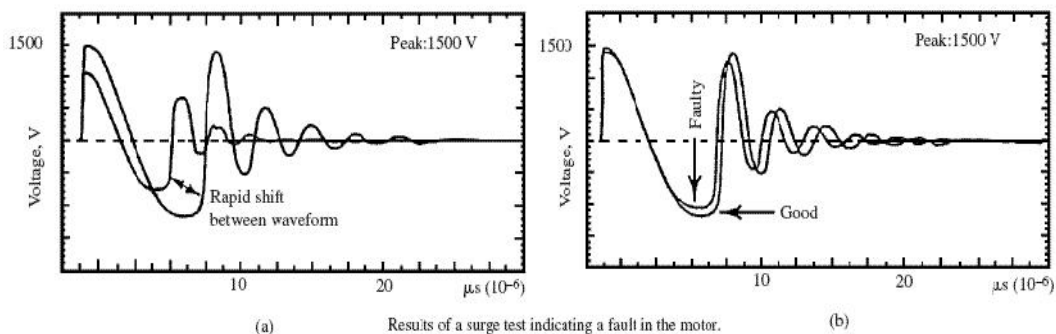
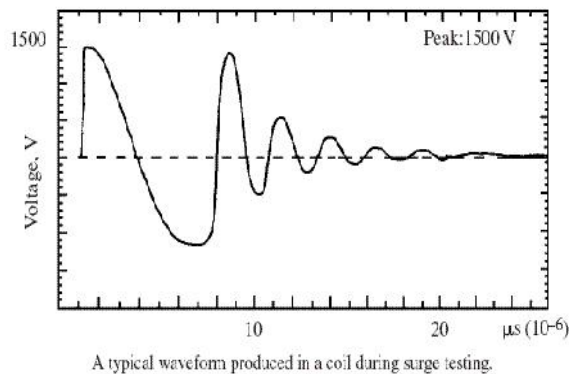
The d.c. high-potential test confirms the integrity of the insulation. However, it does not indicate a failure of the insulation between the turns of the windings (interturn fault). The surge test is used to detect the early stages of insulation failures in the

windings such as coil-to-coil failures, short circuits, ground, and misconnections. During the surge test, brief voltage surges (pulses) are applied across the coil. These pulses produce a momentary voltage stress between the turns of the coil. **Fig. 2** illustrates a typical response of a coil.

Each coil has a unique signature waveform, which can be displayed on the screen of the equipment during the test. The waveform obtained during the surge test is directly related to the inductance of the coil.

A surge test can detect an interturn fault due to weak insulation. If the voltage spike is greater than the dielectric strength of the interturn insulation, one or more turns could be shorted out of the circuit. The number of turns in the coil will drop, leading to a reduction in the inductance of the coil and an increase in the frequency of the waveform produced by the surge test. If the coil has an interturn fault or a phase-to-phase fault, the waveform produced during the test could become unstable. It could shift rapidly to the left and right and back to its original position (**fig. 3 a**).

A comparison is done between the surge tests performed on each of the phases. A healthy three-phase motor should have three identical phases. Therefore, the results of the surge tests performed on each of the phases should be identical. Any differences found between the three results indicate that there is a fault in the motor (**fig. 3 a** and **b**).



4.2. Winding Resistances

This test involves measuring the resistance of each of the three phases. The resistance unbalance is given by

Resistance unbalance = (Maximum resistance – Minimum resistance)/Average resistance

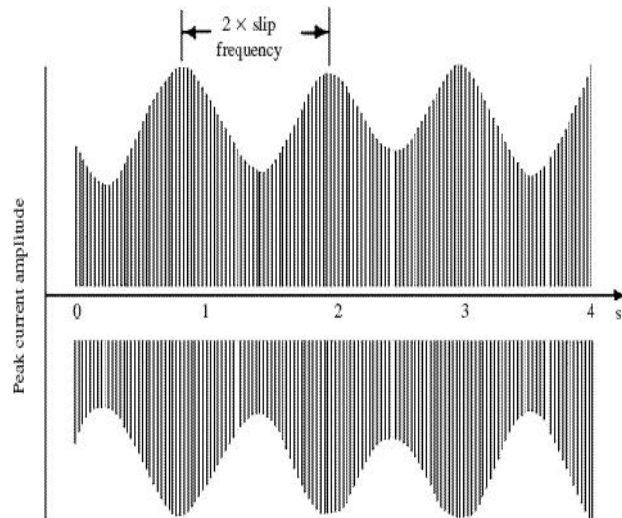
For a healthy motor, the resistance unbalance should be less than 10 % if the test is performed from the motor control center. It should be less than 5 % if the test is

performed at the motor. The larger resistance unbalance (10 % instead of 5 %) is allowed when the test is performed from the motor control center due to the long cables between the motor control center and the motor.

The voltage and current used during the test for 4-kV and 575-V motors are 5 V d.c. and 6 A, respectively. This test is used to detect short circuits, ground faults, phase-to-phase faults, loose connections, open circuits, dirt accumulation at connections, etc.

5. STATOR CURRENT FLUCTUATION TEST

The stator current fluctuation test is performed on an operating and loaded motor. The current in one of the phases is monitored for fluctuations at twice the slip frequency (fig.4). An ammeter is observed, or a current transformer output is monitored on a strip chart recorder or oscilloscope. The results should be interpreted by an experienced operator.



Two times slip frequency stator current modulation is induced by cage winding open circuit.

6. MANUAL ROTATION TEST

The motor is disconnected from its normal three-phase power supply for its off-line test. The driven equipment should be uncoupled unless it can be manually rotated with the motor. A single-phase a.c. supply is connected across two motor terminals. It has voltage rating of 10 to 25% of rated line-to-line volts and a kVA rating of 5 to 25% of rated kVA. The rotor is manually turned for one-half revolution while monitoring the variations in the current. A broken rotor cage winding is indicated by current fluctuations in excess of 10%. The current fluctuations can also be monitored on a strip chart recorder connected to the output of a current transformer.

It is important that the test time should not exceed 1 min. due to rapid heating in the stator and rotor windings. The main limitation of this test is that it can only be conducted off-line. Therefore, breaks in cage windings may not be detected if they close up, giving low-resistance connections when centrifugal forces are removed.

REFERENCES

- [1]. L. R. Higgins, *Maintenance Engineering*, 5th ed., McGraw-Hill, New York, 1995.
- [2]. A. S. Nasar, *Handbook of Electric Machines*, McGraw-Hill, New York, 1987.
- [3]. *** , *Electrical Equipment Handbook – Troubleshooting and Maintenance*, McGraw-Hill, New York, 2004.

ELECTRIC FRAMES WITH LINEAR INDUCTION MOTOR PROPULSION SYSTEMS. ELECTRIC TRACTION SCHEME

DRAGOS PASCULESCU*, CONSTANTIN BRINDUSA**

Abstract: In the case of the electric drive systems which are based on the static converters and on the traction linear induction motors (LIM), specific to the urban electric frame of subway type, it is necessary to establish the traction electric schemes. Their analysis is made on the basis of some criteria, among the most important is the travelling transport safety.

Keywords: electric frames, electric traction

1. INTRODUCTION

The subway frames electric drives impose a series of specific conditions and, particularly, a great operation safety and the compulsory introduction of the energy recovery brake. The mechanico-pneumatic brake has the drawbacks of the clogs wear and the mechanical dust appearance during the friction.

The traction scheme imposed on the urban electric frames of type VM+VM, with the feeding from the d.c. network contents, mainly, the following equipments:

- the intermediary circuit, known as network filter FLC
- the voltage and frequency static converter CTF;
- the braking chopper + the braking resistance + the shunt;
- the current captor + the axle contact;
- loading contactor + loading resistance;
- ultra-rapid automat breaker;
- wagons electric couple;
- traction motor.

The traction scheme as figure:

- the electric energy captation, from:
 - the catenary, by the pantograph, inside the depots where it is not allowed the rail

* *Assistent Drd.Eng., University of Petrosani*

** *Professor Dr.Eng., University of Petrosani*

III assembling;

-the rail III, by the captors, on the travelling paths; this kind of feeding it is met to the subway or overhead metro urban transport.

- the voltage and current waves level under a admissible level, meaning:

$$\Delta U_{\max} < (0,1 - 0,2) U_{d \min}$$

$$\Delta I_{\max} < (0,1 - 0,15) I_{s \max}$$

- the conversion d.c. - a.c., by a voltage and frequency static converter CTF, which are supplying the traction motors, at variable voltage and frequency, in concordance with the adjustment requirements imposed by the assembly CTF-LIM;

- the transformation of the electric energy into the mechanical energy by the traction linear induction motors (LIM), which are electric connected on the bars RST of the CTF; The vehicle propulsion force (the traction force) appears due to the linear induction motors.

2. ELECTRIC TRACTION SCHEMES. POSSIBLE VARIANTS

The vehicle is an electric frame VM+VM type, meaning that it is formed by two motor wagons which are elastic coupled. On each motor wagon there are installed traction linear induction motors (LIM).

An exemplu of the traction linear induction motors (LIM), made in Romania, is LIM 02.

The linear induction motors LIM 02, with the technical characteristics presented in Table 1, it is made by S.C. ELECTROPUTERE CRAIOVA S.A., for the urban electric vehicul, class ROM-U-LIM-01.

Table 1

Nr.	Tip	Symbol	ML- 02
1	Rated power (kW)	P_n	140
2	Rated voltage on fase(V)	U_n	225
3	Rated current (A)	I_n	180
4	Starting current (A)	I_p	420
5	Rated frequency (Hz)	f_n	60
6	Nominal speed (m/s)	v	20
7	L. primar (m)	$2a$	0,27
8	Poles number	$2p+1$	11

The traction electric frame scheme can be presented in the following variants:

- V1 - defined by the coefficient $k=1/4$ (Fig.1), meaning that on the vehicle it exists a voltage and frequency static converter which, are supplying the four (4) LIM;

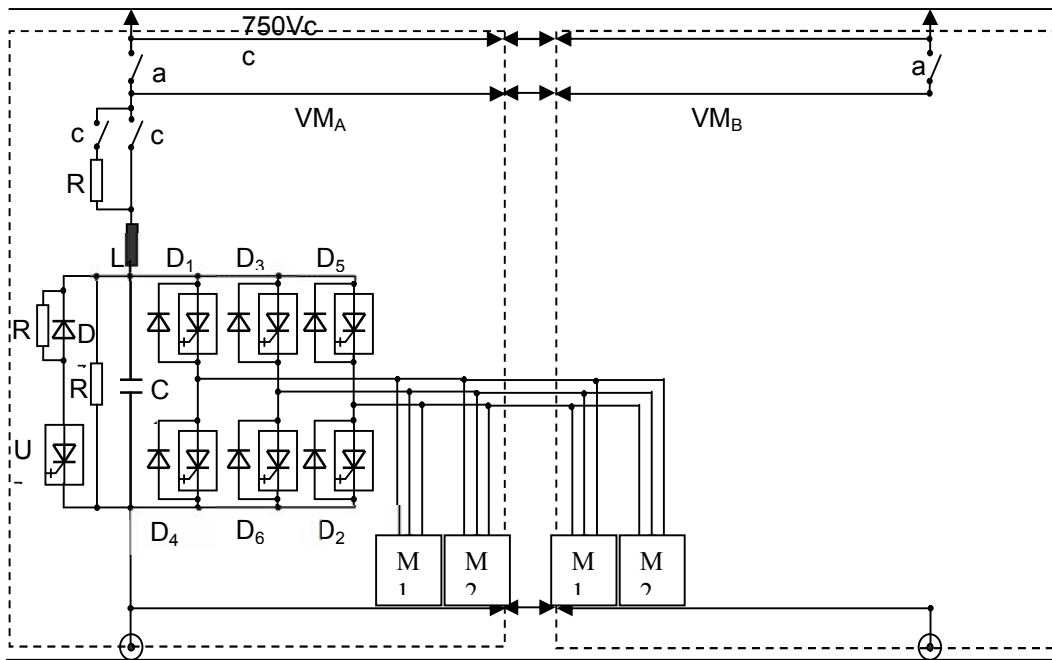


Fig.1 Principle traction scheme; $k=1/4$

- V2 - defined by the coefficient $k=2/2$ (Fig.2), meaning that on the vehicle there exist two voltage and frequency static converters, each of them supplying two (2) LIM;

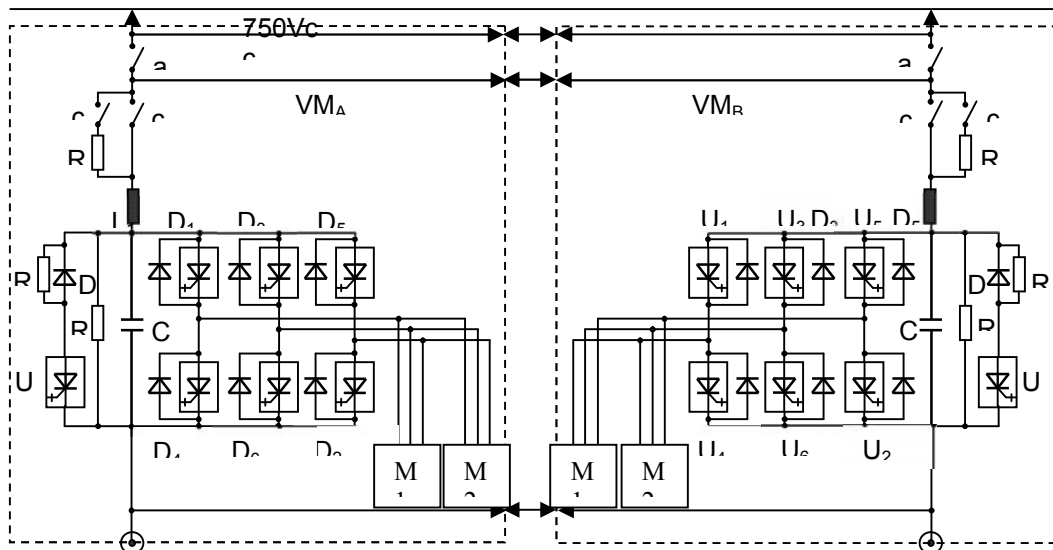


Fig.2 Principle traction scheme; $k=2/2$

In the Table1 there are presented (grouped) the main elements, which are defining the urban subway traction electric frames schemes, with the structure VM+VM.

Table 1 The urban subway traction electric frames

Nr.	Traction scheme variant code:	Coefficient K	Nr. CS / Frame	Nr. LIM / CS
1	V1	1 / 4	1	4
2	V2	2 / 2	2	2

The operation mode of the main traction scheme (Fig.2) for the electric frames it is following:

- the coupling of the captors U_1/VM_A and U_1/VM_B at the rail III. This way it is allowed the feeding of the auxiliary services of the urban electric frame, meaning:
 - the main compressor feeding at 750 Vd.c., which are supplying the pneumatic energy to:
 - the mechanical brake system;
 - pneumatic damping system of the frame wagon mechanic waves;
 - electric-pneumatic line switchers;
 - the auxiliary services converter feeding, which can be either a rotating converter or a static one, with power electronic devices (750V/ 3*220V;50Hz; $S_n=10KVA$);
- the closing of the ultra-rapid breaker a_1/VM_A , respectively a_1/VM_B , in function of the frame control cabin: A or B. This way it is allowed the vehicle traction supplying;
- the closing of the contactors c_1/VM_A and c_1/VM_B . This way it is allowed the condensator battery loading C_1/VM_A and C_1/VM_B under a controlled current slope, under $(di/dt)_{cr}$, by the loading resistors battery R_1/VM_A and R_1/VM_B . The loading time is of *1s order.
- the closing of the contactors c_2/VM_A and c_2/VM_B . This thing it is automatically realized by the control scheme, in the moment when the intermediary circuit voltage it is reaching the $0,85*U_{dmin}$ value;
- the operation starting command of the inverter on the VM_A and of the inverter on the VM_B (composed: U_i+D , where $i=1,...,6$, with the intermediary circuit L_1+C_1);
- the feeding of the linear induction motors (LIM), (in concordance with V2 defined by the coefficient $k=2/2$) in the three-phase voltage system with frequency and voltage variable with modulation PWM.

This is the moment when the frame is able to travel; thus, at the minimum chosen frequency $f_{min}=s_n*f_n$ (in concordance with the technical literature), the traction asynchronous motors M_1 and M_2 / VM_A , respectively M_1 and M_2 / VM_B are stacked, and when this value it is exceeded the motor it is starting on the linear part of the artificial mechanical characteristic corresponding to the supply minimum frequency. The urban electric frame it is accelerating, at the constant traction torque, on the artificial characteristics U_1/f_1 up to f_{sn} , when $U_1=U_{1n}$ and then, at the constant power, over f_{sn} .

With a view to the frame electric braking, the traction linear induction motors (LIM) are passing into the generator regime, by the decrease command of the voltage

frequency applied to the motors. The traction electric machines are modifying the operation points on the mechanical characteristics in the dial II, passing into the generator regime.

In that situation, which is complex from the powers circulation view point, the inverter (by U_i , where $i=1,\dots,6$) it is ensuring the reactive energy necessary to the generator regime, by the recovery diodes group (by D_i , where $i=1,\dots,6$) the machine supplying the voltage intermediary circuit, as asynchronous generator.

This energy it is taken through recovery by other electric frames situated in travel on the network portion considered or, if the voltage on the intermediary circuit it is increasing over $1,2 U_d$ (meaning over $1,2 \cdot 750=900V$), it is commanded the automatically operation of the braking chopper U_7 / VM_A and U_7 / VM_B , which are realizing an electric brake on the braking resistors R_2 and D_7 / VM_A , respectively R_2 and D_7 / VM_B .

The frame disconnection from the network it is realized into the reverse order to the start, with the exception that at beginning there are disconnected the ultra-rapid breakers a_1 / VM_A , respectively a_1 / VM_B .

3. CONCLUSIONS

The analysis of the variants V1 and V2 must be made taking into account a criteria series, such as:

-the vehicle travelling safety criterium. In concordance with this criterium, the variant V2 it is advantageous, because even after the failure of a CTF, meaning a supplying unit, the vehicle it is able to arrive into a garage point on the travelling path, with 2/4 of the installed power;

-the traction scheme reliability criterium. In concordance with this criterium, the scheme realized with the variant V1 it is the most reliable, taking into account the fact that the traction scheme operation safety it is decreasing with the number of the power electronic devices;

-the traction scheme complexity criterium. The force scheme CTF simplifying it had been realized by using the electronic devices with gate stack, meaning the thyristors with blocking on gate GTO or bipolar transistor with insulated gate IGBT.

From the analysis of the variants of the traction schemes, taking into account the criteria enunciate as before, it had imposed the variant V2 defined by the coefficient $k=2/2$, meaning that on the vehicle there are two voltage and frequency static converters (namely, one on each motor wagon), each of them supplying 2 traction bimotors.

REFERENCES

[1] Krause P.C., Wasynczuk O., Sudhoff S.D., *Analysis of Electric Machinery*, IEEE, 1995.

[2] Brîndușa, C., ș.a., *Sisteme electrice de transport neconvenționale (A23)*; Rama de metrou acționată cu motoare asincrone; Execuție și experimentare modele (Faza 23.1), Contract cercetare 606C- Anexa A, Institutul național de cercetare și proiectare pentru mașini electrice, echipament electric și tracțiune, ICMET, Craiova, 1992

ELECTROMAGNETIC DEVICE DESIGN SYNTHESIS

ANDREI CECLAN*, DAN DORU MICU**, DAN MICU***, EMIL
SIMION***

Abstract: We approach the synthesis of a winding configuration with a numerical regularization method. The mathematical model leads to an ill-posed inverse electromagnetic problem. Uniformly textile bands painting use this application for a homogeneous magnetic flux density.

Key words: coil, homogeneous, ill-posed, regularization

1. INTRODUCTION

Shape design synthesis of magnetic coils is of great importance in manufacturing some electromagnetic devices. In this paper we focus on setting the configuration of a magnetic device to be used in the efficient painting treatment of textile bands. We start from imposed performances of the coil and through synthesis reach those magnetic/electric values, or geometrical dimensions that lead to the desired characteristics. [1]

Generally, the synthesis process may be regarded as an inverse and ill-posed electromagnetic problem. That is, the solution is not unique and very unstable. [2] The approach of the problem shall be taken from a special Tikhonov regularization numerical procedure. Argues about the numerical results and the method validity conclude the paper.

2. DESIGN PARAMETERS

* *Engineer, Ms.C. at the Technical University of Cluj-Napoca*

** *Lecturer Ph. D. at the Technical University of Cluj-Napoca*

*** *Professor Ph.D. at the Technical University of Cluj-Napoca*

Let us consider the configuration given in fig. 1, and assume the magnetic circuit to be of very high permeability. Also consider the air gap between the poles of this electromagnet as a linear, homogeneous and isotropic medium, of permeability $\mu = \mu_0$. The objective is to obtain a constant and homogeneous magnetic field density B_0 , generated by an unknown configuration of windings located on the ferromagnetic circuit. By rafting across the textile band through this homogeneous field density, the painting process is assumed to be uniform and economical.

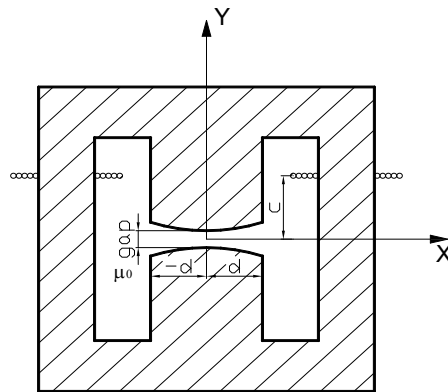


Fig. 1 General design of the magnetic device

3. TIKHONOV REGULARIZATION SYNTHESIS

Accounting the symmetry of the device, let us reconsider the winding as located only on the main pole. To accomplish the desired homogeneous magnetic field density B_0 in the air gap, we have to synthesize a certain configuration of the coil. In this situation B_0 has to be created by a number of windings z_k , all feed with a constant current I , as figure 2, and shows.

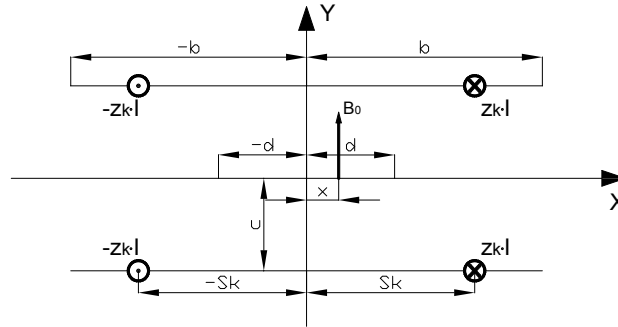


Fig. 2 Windings and magnetic images method

If we assume that the magnetic permeability of the medium is almost infinitely, then the magnetic images method can be applied. The four conducting wires, from the above fig. 2, will generate on the Ox axis a magnetic flux density of:

$$B_k(x) = \frac{z_k \cdot I \cdot \mu_0}{\pi} \cdot \left[\frac{s_k - x}{c^2 + (s_k - x)^2} + \frac{s_k + x}{c^2 + (s_k + x)^2} \right] \quad (1)$$

The total magnetic flux density:

$$B(x) = \sum_{k=1}^n B_k(x) \quad (2)$$

And pass to the integral form:

$$\frac{b \cdot \pi}{\mu_0 \cdot n \cdot I} \cdot B(x) = \int_0^b \left[\frac{s - x}{c^2 + (s - x)^2} + \frac{s + x}{c^2 + (s + x)^2} \right] \cdot z(s) ds \quad (3)$$

which is a Fredholm integral equation of the first kind. Generally, this represents an ill-posed mathematical model, with non-unique and unstable solutions. [3]

$$\int_0^b K(x, s) \cdot z(s) ds = u(x) \quad (4)$$

If we mesh the x and s domains, the model may be written in a matrix form: $M \cdot z = u$, which has a very ill-conditioned coefficient matrix. Therefore, a Tikhonov regularization procedure has to be applied. On the matrix expression the following transformation occurs [4]:

$$\left(M^T \cdot M + \alpha \cdot I \right) \cdot z = M^T \cdot u \quad (5)$$

The regularization parameter α , gives the ratio between the stability and the precision of the solution. Its values are chosen according to the L-curve criterion [5].

Physical achievability and precision of the solution are next to be appreciated. The error evaluation formula relates to the attainment of the imposed magnetic flux density:

$$\varepsilon = \max \left[\sum_{i=1}^m (u_i - B_0)^2 \right] \quad (6)$$

4. NUMERICAL RESULTS

The initial values for the given geometrical configuration were as below:

Table 1

b [m]	c [m]	d [m]	gap[m]	B ₀ [mT]	I [A]
0.8	0.1	0.4	0.02	0.5	1

A high level of the precision is attained for $\alpha = 3 \cdot 10^{-16}$ in Table 2, but the physical achievability of the current surface density appears to be impossible. See in Table 3 some of the calculated values:

Table 2

B [mT] Numerical method $\alpha = 3 \cdot 10^{-16}$	0.5000004	0.499997	0.499994	0.499999
--	-----------	----------	----------	----------

Table 3

J [A/mm] Numerical method $\alpha = 3 \cdot 10^{-16}$	0.0249	- 0.6688	$9.089 \cdot 10^4$	$4.12 \cdot 10^4$
--	--------	-------------	--------------------	-------------------

Thus, we use a compromise and modify the parameter to $\alpha = 10^{-7}$ so as to reach more appropriate values:

Table 4

B [mT] Numerical method $\alpha = 10^{-7}$	0.499	0.503	0.504	0.497
---	-------	-------	-------	-------

Of course, the picked number of values may be extended to an enlarged domain of meshing. [6] Numerical validation of the achieved solutions is also tested with a FEM procedure. [7]

5. CONCLUSIONS

Synthesis design of an electromagnetic industrial coil has been proposed. An optimal approach from which uses a numerical regularization method, leads to achievable and precise results. Special attention had to be given to the choice of the regularization parameter for Tikhonov regularization numerical method.

REFERENCES

- [1]. **Micu D., Micu Adriana**, *Electromagnetic field synthesis (in Romanian)*, Mediamira, Cluj-Napoca, 2005.
- [2]. **Tikhonov A. N., Arsenin V. I.**, *Methodes de resolution de problemes mal poses*, Edition MIR, Moscou, 1974.
- [3]. **Micu D. D., Ceclan A., Micu D., Simion E.**, *Synthesis Method of an Inductive Sensor using Tikhonov Regularization Procedure*, OIPE'06, Sorrento, 2006, pp. 177 – 178.
- [4]. **Ceclan A., Micu D. D., Micu D., Simion E.**, *Tikhonov Regularization for Electric Field Synthesis*, Numelec'06, Lille, 2006, pp. 175-177.
- [5]. **Hansen C.**, *Analysis of Discrete Ill-posed Problems by Means of the L-curve*, SIAM Review, Vol. 34, No. 4, 1992, pp. 561 – 580.
- [6]. **Micu D. D., Ceclan A.**, *Numerical Methods, Electrical Engineering Applications (in Romanian)*, Mediamira, Cluj-Napoca, 2007.
- [7]. **Țopa V.**, *Optimal Design of electromagnetic Devices*, Casa Cartii de Stiinta, Cluj-Napoca, 1998.

ELECTRONIC TIME RELAYS WITH DIFFERENT FUNCTIONS WITH T.T.L. INTEGRATED CIRCUITS

IOSIF POPA* , GABRIEL NICOLAE POPA , SORIN DEACONU***

Abstract. The paper introduces the configurations of electronic devices with T.T.L. integrated circuits performing mains timing functions. These can be used in command installations with T.T.L. static switching elements. In order to be used in command installations with contact, the analogical time circuits have as an operation element an electro-magnetic relay, whose coil is charge of a logic amplifier. The main element of the electronic time devices is a T.T.L. monostable, whose work time can be modified with a resistance. The maxim value of the work time of those devices is 27,5 s. These circuits perform the main functions: drive timing, recovery timing and drive and recovery timing, and also used logical NOT, OR and NOR circuits.

Keywords: control relays, protection relays, electronic time relays.

1. INTRODUCTION

The timing circuits used in the command installations using T.T.L. integrated circuits have as a basic element the CDB 4121 E monostable circuit (CBM) [1], [2], [3]. The T.T.L. monostable multivibrator has the circuit diagram given in fig.1.a, where we also gave the arrangement used to check its functioning. With this arrangement structure we achieved the timing function, specific to a photographic time-relay. The command part of the monostable multivibrator is made of the logical circuits I and II. Signal D, obtained as output of AND circuit II depends on signals A_1 , A_2 and B, according to function:

* *Ph.D. Associate professor Eng., Electrotechnical Department, Faculty of Engineering Hunedoara, "POLITEHNICA" University of Timișoara, Romania*

** *Ph.D. Lecturer Eng., Electrotechnical Department, Faculty of Engineering Hunedoara, "POLITEHNICA" University of Timișoara, Romania*

$$D = A \cdot B; D = (\overline{A_1} + \overline{A_2}) \cdot B; D = \overline{A_1} \cdot A_2 \cdot B \quad (1)$$

These values of the output signals are maintained along the period of time:

$$t_1 = R \cdot C \cdot \ln 2; t_1 = 0.693 \cdot R \cdot C \quad (2)$$

The time circuit works normally if $R = (1.4, \dots, 40) \text{ k}\Omega$ and $C = (0.1, \dots, 1000) \mu\text{F}$. For the maximal values of the parameters of these elements ($R_{\max} = 40 \text{ k}\Omega$, $C_{\max} = 1000 \mu\text{F}$) a maximal work time is obtained: $t_{1\max} = 0.693 \cdot R_{\max} \cdot C_{\max}$; $t_{1\max} = 27,5 \text{ s}$.

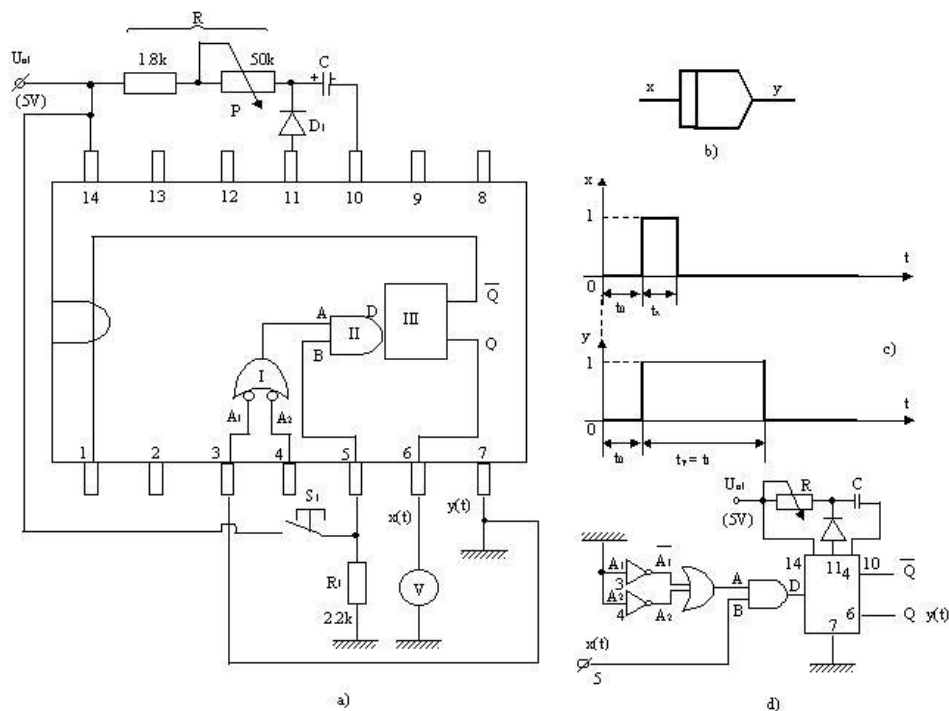


Fig.1.a. The block diagram using the CDB 4121 E monostable circuit, achieving the function of a photographic time-relay; **b.** the block diagram; **c.** the diagrams of the signals $x = f_1(t)$ and $y = f_2(t)$; **d.** The simplified diagram.

Using the CDB 4121 E monostable as a basic element, one can create electronic drive-timing circuits, recovery-timing circuits of with timing for both driving and recovery.

If signal y at the output of the electronic circuit given in fig.1.a attacks a logic amplifier having as charge an electro-magnetic relay, we obtain a photo-type time electronic relay, which can be used in command installations with contacts [2], [4], [5].

2. DRIVE TIMING ELECTRONIC CIRCUITS

The functional diagram of this circuit is given in fig.2.a. For the initial state, when $x = 0$, $E = 1$ and $F = 1$, y will therefore be 0. When, after time t_0 the value of

signal x ($x = 1$) has changed, $E = 0$, but F keeps its logical value 1 for a very short time, depending on the time constant.

$$T_I = R_I \cdot C_I \tag{3}$$

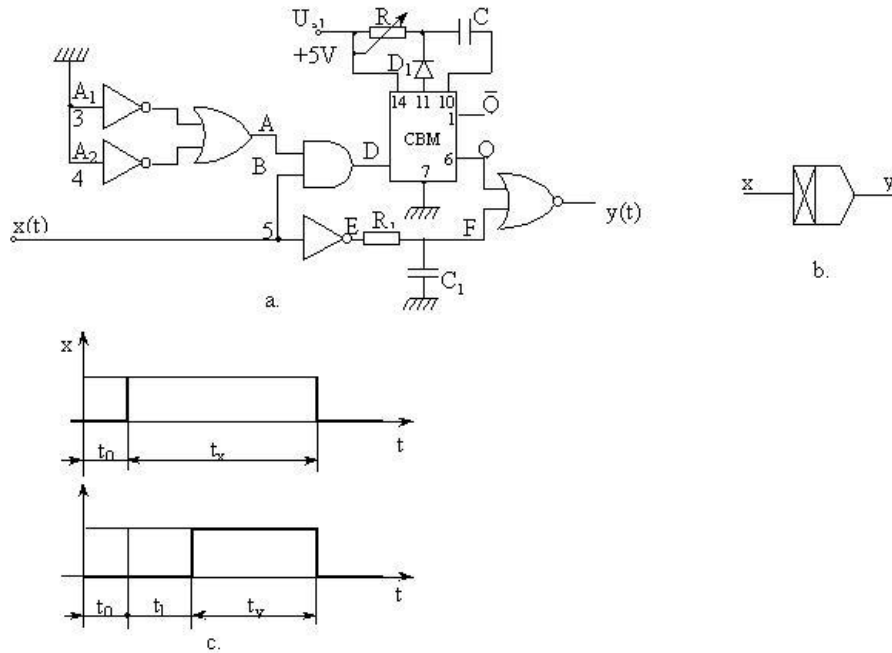


Fig.2.a. The functional diagram of the drive timing electronic circuit; **b.** the block diagram [5]; **c.** the diagrams of the input ($x(t)$) and output ($y(t)$) signals.

Along this very short interval of time, CMB switches and $Q = 1$, so $y = 0$ even after signal F changes its value ($F = 0$). Signal Q preserves its logic value 1 all along the time period t_i , calculated by means of (2) and controlled by modifying resistor R . According to the corrected time t_i , $Q = 0$. As signal $F = 0$ also, it thereby results $y = 1$. Signal x is kept at the logic value 1 all along the period t_x (fig.2.c.). After the value of signal x ($x = 0$) has changed, $E = 1$, but signal F keeps its logic value 0 for a short period of time, determined by time constant T_I , after which $F = 1$ and $y = 0$.

3. RECOVERY TIMING ELECTRONIC CIRCUIT

The functional diagram of this circuit is given in fig.3.a. In its initial state, signal $x(t)$ has the logic value 0, therefore $A = 0$, $E = 1$, $F = 0$, $B = 0$, $D = 0$, $Q = 0$, $y_1(t) = 0$ and $y_2(t) = Q = 0$. Changing the value of signal $x(t)$ ($x(t) = 1$) after time t_0 (fig.3.d.), $A = 0$, $E = 0$, $F = 1$, $B = 1$ only after condenser C_1 is charged – in a short period of time ($R_1 \cdot C_1 \ll R \cdot C$), therefore $D = 0$, $Q = 0$ ($y_2(t) = 0$) and $y_1(t) = 1$ (at the same time with $B = 1$). These values of the signals are maintained all along time t_x . After this period of time, $x(t)$ passes from logic value 1 to logic value 0 ($x(t) = 1 \downarrow 0$) and the other signals have the values $A = 1$, $E = 1$, $F = 0$, condenser C_1 starts to

discharge, but for a short period of time $B = 1$. As $A = 1$ also, $D = 1$ and the monostable switches. It results that $Q = 1$ ($y_2(t) = 1$), and maintains this value along the period t_b , given by relation (2). $y_1(t) = 1$ also and therefore $y_1(t) = 1$ in the time interval $t_x + t_b$. Using output $y_1(t)$, the circuit performs the function of recovery timing, variant I (the block diagram is given in fig.3.b.) and using output $y_2(t)$, the circuit performs the function of recovery timing, variant II (fig. 3.c.).

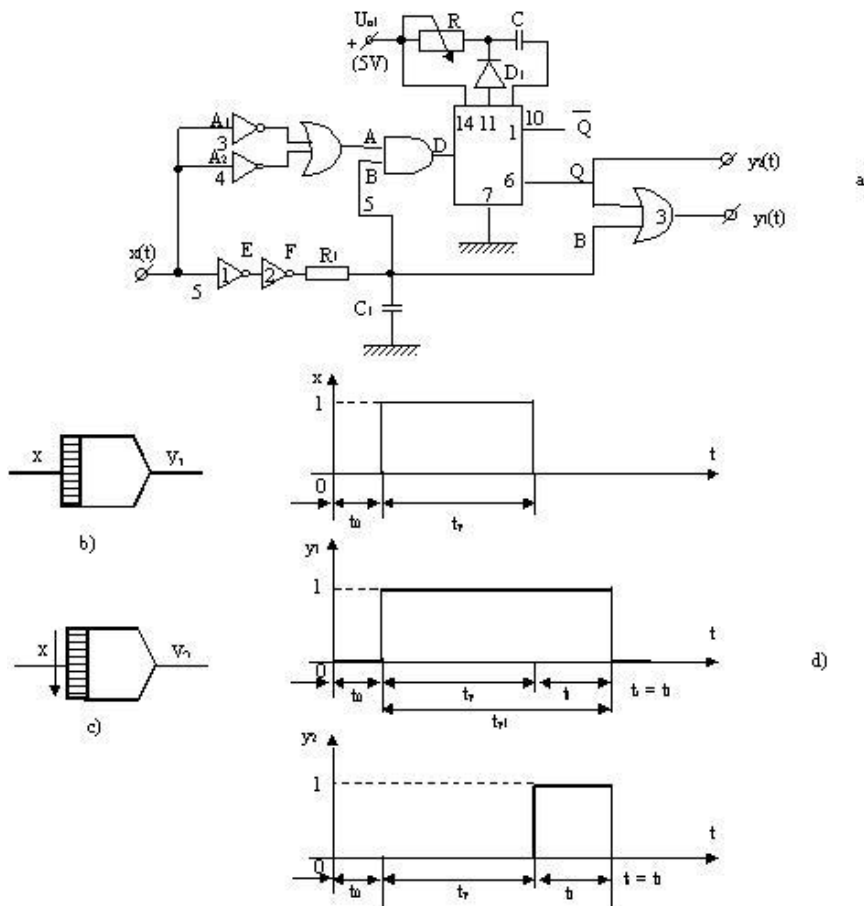


Fig.3.a. The functional diagram of the recovery-timing electronic circuit; **b.** The block diagram of the recovery-timing electronic circuit, variant I; **c.** The block diagram of the recovery-timing electronic circuit, variant II [5]; **d.** The time modifications of the input output signals.

4. DRIVE AND RECOVERY TIMING ELECTRONIC

The electronic time circuit used in drive and recovery timing (fig.4.a.) is made of the ensemble of circuits performing the drive timing (fig.2.a.) and recovery timing (fig.3.a.).

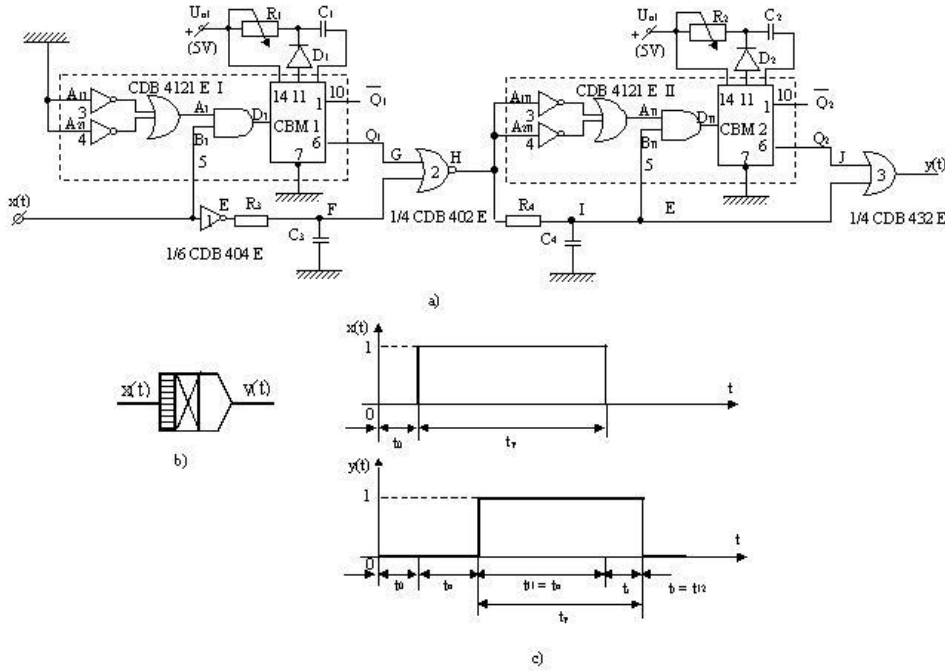


Fig.4.a. The functional diagram of the drive and recovery timing electric circuit; **b.** the block diagram [5]; **c.** the variation of the input ($x(t)$) and output signals ($y(t)$).

In order to perform this function, the output of the drive timing circuit is connected to the input of the recovery timing circuit.

The CBM 1 monostable multivibrator has the work time:

$$t_a = t_{l1} = 0.693 \cdot R_1 \cdot C_1 \quad (4)$$

The CBM 2 monostable multivibrator has the work time:

$$t_r = t_{l2} = 0.693 \cdot R_2 \cdot C_2 \quad (5)$$

5. CONCLUSIONS

The paper establishes the configurations of the main time electronic circuits based on the CDB 4121 E monostable and using TTL integrated circuits. These circuits perform the functions: drive timing, recovery timing and drive and recovery timing, within work times of up to 27,5 s. In order to eliminate a random functioning of these time electronic circuits, we used R-C type integrated circuits with low time constants, which do not have a significant influence upon the work time of the time electronic circuits, as given in relations (2), (4) and (5). These circuits can be used in command installations, which TTL static switching elements, in cable logic.

REFERENCES

- [1] **Morris R.L., Miller J.R.**, *Designing with T.T.L. Integrated Circuits*, Texas Instruments Incorporated, U.S.A., 1971.
- [2] **Pop E.**, *Automatizări în industria minieră*, Editura Didactică și Pedagogică, București, Romania, 1983.
- [3] **Pop V., Popovici V.**, *Circuite de comutare aplicate în calculatoarele electronice*, Editura Facla, Timișoara, Romania, 1976.
- [4] Popa I., Nekula Fr., Maksay Șt., *Releu electronic de timp cu structură variabilă*, Invention Patent, RO 106044/30.01.1993, Romania.
- [5] **Popa I., Popa G.N.**, *Dispozitive electronice cu structură cablată și programată, de protecție a motoarelor asincrone trifazate de joasă tensiune*, Editura Mirton, Timișoara, Romania, 2000.

ESTABLISHING OF THE EFFECTS PRODUCED BY THE PASSIVE FILTERS OF RC TYPE ON THE SINUSOIDAL VOLTAGE SOURCE

CORINA CUNȚAN *, IOAN BACIU **

Abstract: This work is analysing the influence of the passive filters upon the parameters of the single-phase supply line of a resistive consumer using the Lab VIEW program. The filter's model is represented by the mathematical function related to each harmonic in part, expression which is introduced based on a previously established law. It's aiming the possibility to modify the filter's expression depending on the power supply line's parameters.

Keywords: RC filters, power, current, voltage

1. WORK'S PRESENTATION

In order to compensate the harmonics of the currents absorbed from the distribution networks by different consumers of which supply is made by commutation elements are used passive and/or active power filters of high performance. In the usual case, the passive filters are influenced by the modification of the own resonance frequency of the power supply network. This present survey is analyzing the situation when the own filter's frequency is modifying by a sinusoidal law and the network's frequency remains unmodified. The operation is emphasized by showing on the same graphic the input voltage, the current and signal's power on the load resistance, as well as by showing the related frequency spectrum, determined with the Fourier

It's used a signal generator which allows to obtain two dephased output signals, with a phase displacement imposed depending on the capacitor's and coil's values, which is the one introduced by the two elements in the circuit. The two elements are modeled by a mathematical law and which takes into account the sinusoidal shape we want to have the filter's impedance module.

* *Ph. D. eng University from Timișoara, Faculty of Engineering from Hunedoara.*

** *Dipl. Eng. University from Timișoara, Faculty of Engineering from Hunedoara*

$$R = K$$

$$X_C = \frac{1}{\frac{C}{10^n} \sin x}$$

where: R and C are values to be imposed for the resistance, respectively capacitor.

K is a constant value;

n is a weighting factor of capacitor's value;

$\sin x$ signal generated by a sinusoidal signal generator.

Considering the two ideal elements, without loss resistance, is obtaining the RC circuit's impedance:

$$Z = R + \frac{10^n}{C} \sin x = R + \frac{10^n}{C} \sin x$$

Having the impedance value, will be obtained the current through the RC circuit:

$$I_F = \frac{\sqrt{2}U}{Z} \sin t = \frac{\sqrt{2}U}{|Z| \sin x} \sin(t - t_1); \quad t_1 = \frac{\varphi}{\omega}$$

where: φ represents the phase displacement introduced by RC for the signal generator's function from the input circuit on the load circuit R_S , and ω is the generator's pulsation.

$$\varphi = \arctg \frac{X_C}{R + R_S}$$

Is obtained: - the energy stored in the RC filter by the relation:

$$E_n = \frac{1}{2} C U^2 = \frac{1}{2} C (I \cdot X_C)^2 = \frac{1}{2} I^2 \frac{10^n}{C \cdot \sin x}$$

- input signal U_{in}

$$U_{in} = \sqrt{2} U \sin t$$

- signal's power on the filtration circuit

$$P = \frac{\sqrt{2}U}{Z} \sin(t - t_1) \cdot \sqrt{2} \cdot U \sin t$$

- current through the filtration circuit

$$I = \frac{\sqrt{2} \cdot U}{Z} \sin t = \frac{\sqrt{2} \cdot U}{|Z| \sin x} \sin(t - t_1)$$

Is applied the Fourier Transformation upon the current and is obtained the spectrum's module for a sampling sequence of 250Hz.

The circuit's operation diagram (fig. 1) drawned in LabView allows the visualization of the connexions between the elements which intervene, as well as the modality to implement the mathematical relations.

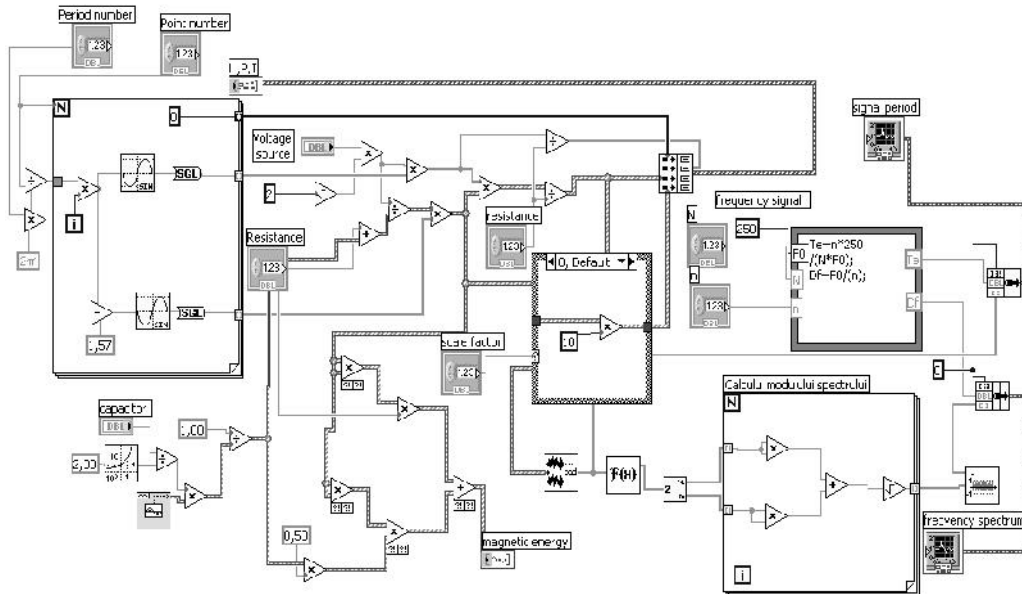


Fig.1

Thus are obtained the wave shapes of the voltage, current and power (fig. 2), the frequency spectrum (fig. 3) and the energy stored in the RC filter (fig. 4).

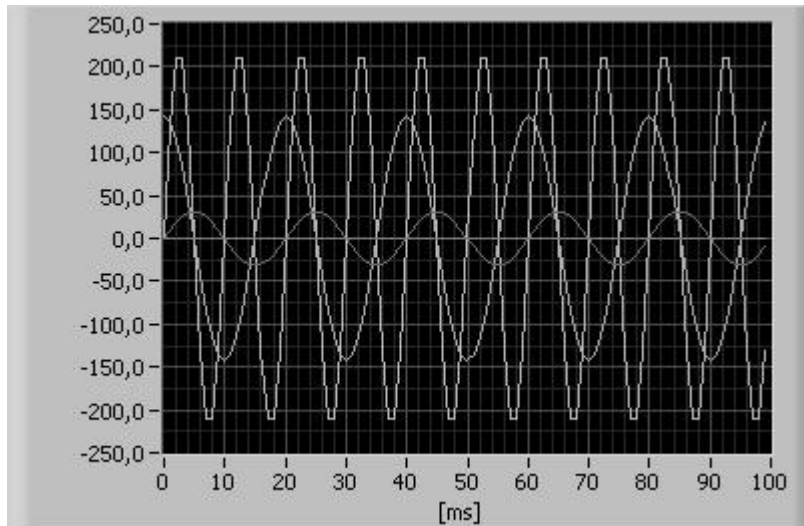


Fig.2

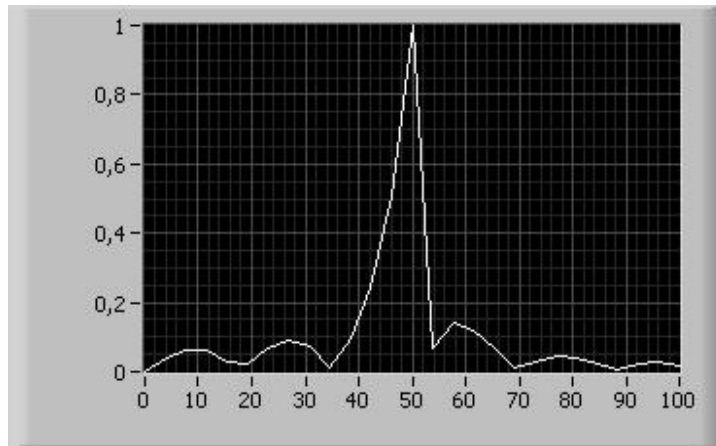


Fig.3 Frequency spectrum

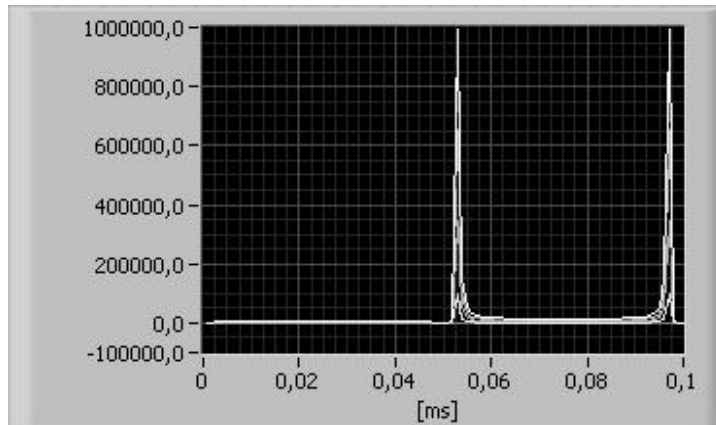


Fig.4 Magnetic energy

2. CONCLUSIONS

The harmonics spectrum emphasizes the existence of the harmonics in the form of the current through the filter, harmonics which have a large spectrum and relatively small values against the fundamental.

For the signal power on the filter is found its double variation frequency, as well as a shape distortion at maximum values. Also, one can observe the phase displacement imposed between voltage and current.

Interesting is how it's presenting the shape of the energy stored in the RC filter, being obtained more simultaneous values, which leads to more sinusoids of different amplitudes and identical frequency.

REFERENCES

- [1] Pop E., Naforniță I., Tîponuț V., Toma L., Mihăescu A., - *Metode în prelucrarea numerică a semnalelor*, Editura Facla, Timișoara 1986;
- [2] Cottet F., Ciobanu O., - *Bazele programării în LabVIEW*, Editura Matrix Rom, București 1998.

IMPROVEMENT METHODS AND TECHNICAL TESTS FOR TECHNICAL EQUIPMENT INTENDED FOR USE IN AREA WITH COMBUSTIBLE DUSTS

LEONARD LUPU^{*}, NICULINA VĂTAVU^{**}, FLORIN PĂUN^{***}

Abstract: In many industrial branches, the technological processes are closely related to manufacturing, processing, handling, transportation and storage of the combustible dusts that give rise to fire hazards and, in air mixtures, in certain concentrations, and in the presence of a ignition source, give rise to explosion hazards.

In the paperwork was carried out a study regarding the explosion and/or fire risk - factors that determine explosion risk occurrence; the safety requirements in order to prevent that risk; and technical solutions proposed for the electrical apparatus used in explosive atmospheres with combustible dusts, taking into account especially the maximum admissible temperature of the apparatus surfaces, temperature that should be lesser than the ignition temperature of the dust or layer cloud, so as the normal protection degree IP5X or IP6X is ensured.

Key words: combustible dusts, ignition source, explosion hazard, explosion risk , normal protection degree

1. GENERALITIES

Many types of dust that are generated, processed, handled and stored, are combustible. When ignited they can burn rapidly and with considerable explosive force if mixed with air in the appropriate proportions. It is often necessary to use electrical apparatus in locations where such combustible materials are present, and suitable precautions must therefore be taken to ensure that all such apparatus is adequately protected so as to reduce the likelihood of ignition of the external explosive atmosphere. In electrical apparatus, potential ignition sources include electrical arcs and sparks, hot surfaces and frictional sparks.

^{*} *D.Eng, research assistant at INSEMEX Petroșani*

^{**} *D.Eng, senior scientific researcher III at INSEMEX Petroșani*

^{***} *D.Eng, scientific researcher at INSEMEX Petroșani*

Areas where dust, flyings and fibres in air occur in dangerous quantities are classified as hazardous and are divided into three zones according to the level of risk.

Generally, electrical safety is ensured by the implementation of one of two considerations, i.e. that electrical apparatus be located where reasonably practicable outside hazardous areas, and that electrical apparatus be designed, installed and maintained in accordance with measures recommended for the area in which the apparatus is located.

Combustible dust can be ignited by electrical apparatus in several ways:

- by surfaces of the apparatus that are above the minimum ignition temperature of the dust concerned. The temperature at which a type of dust ignites is a function of the properties of the dust, whether the dust is in a cloud or layer, the thickness of the layer and the geometry of the heat source;
- by arcing or sparking of electrical parts such as switches, contacts, commutators, brushes, or the like;
- by discharge of an accumulated electrostatic charge;
- by radiated energy (e.g. electromagnetic radiation);
- by mechanical sparking or frictional sparking associated with the apparatus.

In order to avoid ignition hazards it is necessary that:

- the temperature of surfaces on which dust can be deposited, or which would be in contact with a dust cloud, is kept below the temperature limitation specified.
- any electrical sparking parts, or parts having a temperature above the temperature limit specified.
 - are contained in an enclosure which adequately prevents the ingress of dust, or
 - the energy of electrical circuits is limited so as to avoid arcs, sparks or temperatures capable of igniting combustible dust;
- any other ignition sources are avoided.

2. ELECTRICAL APPARATUS FOR USE IN THE PRESENCE OF COMBUSTIBLE DUST

In order to select appropriate electrical apparatus for use in a zone 20, 21 and 22 hazardous area, the following information is required:

- a) The classification of the area, i.e. the zone.

The layer ignition temperature of the combustible dust involved or the lowest layer ignition temperature if more than one combustible material might be present. If the installation is likely to be subjected to excess layers, then the layer ignition temperature for the maximum layer depth of the combustible dust(s) will be required.
- b) The cloud ignition temperature of the combustible dust involved or the lowest value of cloud ignition temperature if more than one combustible material might be present.
- c) Where applicable, the minimum cloud ignition energy of the dust involved or the lowest minimum ignition energy if more than one combustible material might be present (see 6.3.3).
- d) Electrical resistivity (conductivity).

Electrical apparatus selected for use in a combustible dust hazardous area shall be protected by one or a combination of the following types of explosion protection to ensure the safety of electrical apparatus:

- a) dust excluding, ignition-proof enclosures (Ex tD); enclosures complying with IEC 61241-1;
- b) encapsulated apparatus (Ex mD); encapsulated apparatus complying with IEC 61241-18;
- c) intrinsically safe apparatus (Ex iD) complying with IEC 61241-11;
- d) pressurized enclosures (Ex pD); pressurized enclosures complying with the requirements for dust hazardous areas, specified in IEC 61241-2.

Electrical apparatus for zones 20, 21 and 22 is intended for use in an ambient temperature within the range $-20\text{ }^{\circ}\text{C}$ to $+40\text{ }^{\circ}\text{C}$, unless marked accordingly. Where apparatus is installed in an area where the local ambient temperature is likely to be outside the specified range $-20\text{ }^{\circ}\text{C}$ to $+40\text{ }^{\circ}\text{C}$, precautions shall be taken to ensure that the apparatus operates within its specified range. Examples of such sources might include solar heating, an electric heater or a boiler.

When apparatus is to be located where its ambient temperature is not within its specified range, then the justification for this decision shall be documented. This decision should take into account the rating of components and the possible deterioration of enclosures and insulation and any other factors which adversely affect the method of protection. Consultation with the manufacturer and, where appropriate, the certifying authority for the apparatus so as to make an informed decision, will normally be necessary

Dust layers exhibit two properties as layer thickness increases: a reduction in minimum ignition temperature and an increase in thermal insulation.

The maximum permissible surface temperature for apparatus is determined by the deduction of a safety margin from the minimum ignition temperature of the dust concerned, when tested in accordance with the methods specified in IEC 61241-20-1 for both dust clouds and layer thickness of up to 5 mm for type of protection “tD”, practice A and all other types of protection, and 12,5 mm for type of protection “tD” practice B.

The maximum surface temperature of the apparatus shall not exceed two-thirds of the minimum ignition temperature in degrees Celsius of the dust/air mixture concerned:

$$T_{\max} = 2/3 T_{\text{CL}}$$

where T_{CL} is the minimum ignition temperature of the cloud of dust.

3. IMPROVEMENT METHODS AND TECHNICAL TESTS FOR TECHNICAL EQUIPMENT

Enclosures with the degree of protection IP 5X “Dust protected” do not have to prevent ingress of dust totally. However, dust should not penetrate in an amount sufficient to interfere with the satisfactory operation of the equipment enclosed or to impair safety. In the case of enclosures with degree of protection IP6X “Dust tight” it is necessary to prove that no dust can penetrate into the inside of the enclosure. The

talcum powder must be prepared in such a manner that it will pass through a sieve with a mesh size of 0,075mm. The quantity of talcum given in the regulation is 2 kg per cubic of test cabinet volume. The enclosure under test, in the following called specimen, is suspended in the test cabinet and – if prescribed – connected to a vacuum pump. This produces inside the specimen a depression of maximum 2 kPa = 20mbar (=approx. 200 mm water column) bellow atmospheric pressure. The test is completed after 2 hour, if within 2 hours 80 to 120 times the air volume of the specimen has been drawn through.

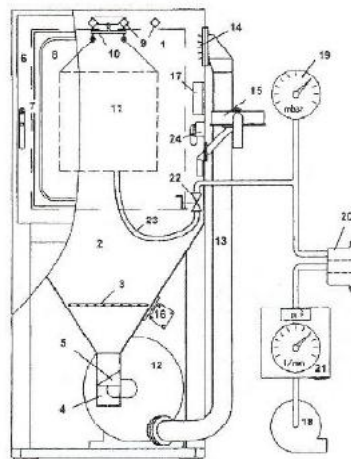


Fig.1 Dust test Chamber

1 to 3 dust circulation pumps (12) with transfer pipes (13) and dust distribution out-lets (14); 1 pressure equalizing air filter (15); 1 to 3 electric vibrators (16) at the funnels, to remove dust deposition from the walls; 1 to 3 electric heating elements (17) inside of the test cabinet to keep the talcum powder dry; 1 vacuum pump (18) to cause a depression inside of the specimen; 1 depression indicator (19); 1 dust filter (20) with removable insert, to collect the dust, which has been exhausted out of the specimen; 1 air volume meter (21) with pointer and counter; 1 vacuum connecting fitting with shut-off valve (22) in the test cabinet behind the door, with hose (23), 2m long, to connect the specimen; 1 socket outlet (24) inside of the test cabinet for energizing the specimen, two-pole with side earthing contacts.

4. CONCLUSIONS

As a consequence of these improvements, the assessment and testing level of the technical equipment intended for use in area with combustible dusts has increased.

REFERENCES

- [1] SR CEI 61241 *Aparatură electrică destinată utilizării prezența prafului combustibil*
- [2] SR EN 60529 *Grade de protecție asigurate prin carcase (Cod IP)*
- [3] [www. Product SafeT.com](http://www.ProductSafeT.com) – *Educated, Design and Development Inc.*

INCREASE OF ENERGETIC EFFICIENCY AT S.E. PAROSENİ PLANT CONCERNING OF ENVIRONMENTAL EUROPEAN RULES

DORU VISAN*, DANIELA MARDARE**, ADRIANA BUSONIU**,
ILEANA MARCU**

Abstract: The paper present the rehabilitation work at SC Termoelectrica SA – Paroseni Branch, by development the 4th energetic group, which include the setting of a new generator and steam boiler, designed and made by Japanese companies.

Keywords: S.E. Paroseni, energetic efficiency, environment, electric and thermal energy

1. INTRODUCTION

The SC Termoelectrica SA – Paroseni Branch is the first thermoelectric power plant from Romania. During the activity our plant had the following development stages:

- 1979 – opened the founding to pass from the urban heating to the central heating, with the unique source at the CET Paroseni.
- 1980-1983 - accomplish the development 3x50 MW turbine engine from compression turbine to the heating turbine with controller setting (1,5-2,5 ata)
- 1999 – putting into service of CAF –100 Gcal/h to assure the peak heating values.

The heating system of Jiu Valey is assured by two transport base-lines which supply 24 consumers, four of them supply urban consumers from Petroșani, Vulcan, Aninoasa, Lupeni (fig.1). The monitoring of the parameters are made directly from the plant, with some dedicated systems, and the data transmission is made through GSM systems.

* *Eng., manager, SC Termoelectrica SA – Paroseni Branch*

** *Eng, SC Termoelectrica SA – Paroseni Branch*

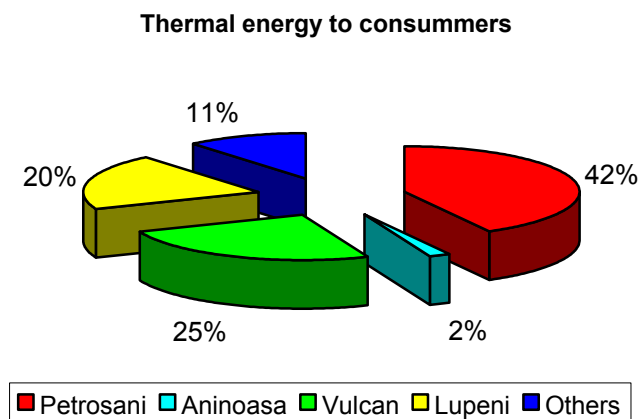


Fig.1.

Taking into account that the most important factors for the durable development in Romania are the growth of economy, security of electric and thermal energy distribution, decrease of pollution due to the energy generation, the present attention of SC Termoelectrica SA plant (fig.2) is to integrate to the European environmental policy and to be a real competitor to the energy market.



Fig.2.

These are possible only with development of technology and equipments, taking into account that the existing equipments are appreciatively 50 years old. After 1998, we began negotiations with a Japanese corporation (ITOCHU – HITACHI – TOSHIBA CORPORATION) to start a rehabilitation works to the 4th energetic group, which include the setting of a new generator and steam boiler, designed and made by Japanese companies.

The rehabilitation of 4th energetic group from CET Paroseni is now the biggest invest in energetic area, after 1989, the amount of this invest is around 191 million EUR, and founding are around 80% from the Japanese bank credit.

2. REHABILITATION OF THE 4TH ENERGETIC GROUP

With rehabilitation of the 4th energetic group are followed the next targets:

- decrease of polluting emission, monitoring, evaluation and report of polluting emission levels in accord with 2001/80/CE;
- increase of work length of energetic group with about 150.000 h.;
- increase of main equipments reliability;
- operating performance of energetic group will be at the same level like the best groups of SEN ;

The 4th energetic group (fig.3) will be equipped with reduced NO_x burners with a 400 mg/Nm³ maximum emission of nitrogen oxide, and the electro filters will be updating to be in the European rule of 100 mg/Nm³.



Fig.3.

The rehabilitation of the 4th energetic group consists in:

➤ **BABCOK HITACHI BOILER**

Performances:

- Efficiency – 90,7%

- Availability - 91%
- Flow – 540 t/h
- Pressure – 138,2 bar
- Temperature – 540 °C
- The boiler has 4 roll mills, with capacity of 43,1 t/h each, located on +0,00 height on the lateral side of the boiler. Work in good parameters is assured with three mills.
- The boiler has 16 reduced NO_x burners with a 400 mg/Nm³ maximum emission of nitrogen oxide, installed on the front and back side of the boiler, burners which pulverize the coal from the mills according with BAT techniques.

➤ **K-160-130-2ÖP2 TURBINE**

- Supplier: the company TURBOATOM Ucraina.
- The turbine is especially built for operating in co-generation (BAT technology) with the possibility to extract maximum thermal energy, sacrificing the electrical energy..

The turbine performances are:

- Electric and thermal energy produced in co-generation - 146 MW și 150 Gcal/h.
- Heat specific consumption - 282 grcc/kwh
- Turbine availability – 96%
- Unit availability - 87%
- Flow – 540 t/h
- Pressure – 130 bar
- Temperature – 535 °C.

➤ **TAKS GENERATOR**

- Supplier – Toshiba Company Japan
- The only one air cooling generator in Europe with following parameters:
- Voltage – 18 kV
- Rated power - 176,5 MVA
- Efficiency - 98,5%

➤ **P320TGC ELECTRO-HYDRAULIC CONTROLLER**

- Supplier - ALSTOM France
- To connect at the UCTE and in order to respect the constraint, will be used a new controller, electro-hydraulic instead of the existing one which is mechanic-hydraulic.
- The special measurements (vibrations, axial movements, displacements, expansion) will be performed on-line with high quality devices.

➤ **DIGITAL DISTRIBUTED CONTROL SYSTEM MAIN AUTOMATION SYSTEM (DCS)**

- Unit IV is endowed with a distributed control system, type TOSMAP DS provide by Toshiba Company (fig.4).

- This system can lead by means of control loops the entire unit as follows:
 - boiler following
 - turbine following
 - Boiler +turbine operate independently.
- The unit can work without operator interference between 50% and 100% of load.

DCS system record the events, the operating parameters and compute on-line the main technical and economical parameters.

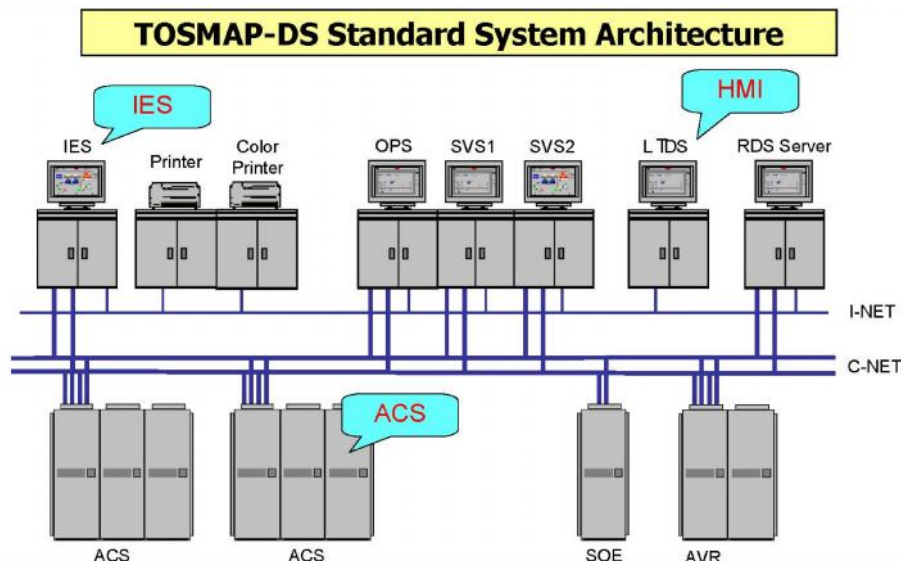


Fig.4.

➤ **110 kV Substation (fig.5)**

- 5 related bays will be rehabilitated
- Overhead Electric Line Baru Mare II
- Auxiliary transformers 51
- Bay for Generator 4
- Transversal coupling bay and measurement group
- Transformer bay of 110&220 kV

For operating security the protection installation of each bay are provided with numerical protections segregated in two main and spare groups.



Fig.5.

REFERENCES

- [1] *Studiul de fezabilitate pentru reabilitarea blocului numărul 4 de la CET Paroșeni* – ISPE București, 2000;
- [2] **Directiva 2001/80/CE** – *Limitarea emisiilor în aer a unor poluanți din instalațiile mari de ardere;*

INTEGRATED STARTER-GENERATOR MACHINES FOR HYBRID AUTOMOTIVE VEHICLES

DAN STOIA* , MIHAI CERNAT*

Abstract - The advent of higher voltages in automobiles constitutes an opportunity for new electrical features and systems. In that regard, an integrated starter/generator (ISG) also called integrated starter/alternator (ISA) would have several important benefits, most notably, it would enable the turning off the engine at idle and provide efficient high power generation, both resulting in improved fuel economy. The objective of this paper is to provide a guideline to ISG engineers and other automotive engineers as well as people who are interested in mild-hybrid electric vehicles.

Keywords: integrated starter/generator (ISG), integrated starter/alternator (ISA), mild-hybrid electric vehicles,

1. INTRODUCTION

Internal combustion engines are generally paired with two electrical rotating machines. One is a motor, optimised for overload operation at low speed and high torque, functioning as starter. The other machine is optimised for continuous operation at high speed, at much lower torque, functioning as generator. Commonly available commercial starters are brush commutated dc machines, while typical generators are claw pole synchronous machines (Lundell alternators) with rectified output.

Implementations of starter/generators (ISG) for automotive use are quite attractive, and have been explored for some time. Some have reached production in current hybrid vehicle systems from Toyota, Honda, and others. However, starter/generator is not in wide use on conventional ICE vehicles, and hybrids only account for approximately 1% of new car sales. There are several reasons for this. The first could be termed the “installed base” effect: systems become cheap and well known because they are in common use; the same systems are then used elsewhere because they are cheap and well known. The second reason is interface: the starter is generally connected to the engine via gear teeth on the flywheel, while the alternator is

* *Professor PhD , “Transilvania” University of Brasov, Romania,*

connected using a belt system. The gear ratios are generally different, and the operational life is designed differently. Finally, the use of starter/generator introduces new control issues.

In common use, the starter is a dc motor connected “across the line” to the battery via a contactor, and the alternator is directly connected to the dc bus via simple rectifiers. Control of the alternator output is via control of alternator field, usually through a wound field coil on the claw pole rotor. These are extremely simple, robust, and inexpensive controls. A starter/generator requires a more complex control mechanism; one that can transition the machine between starting and generating operations.

A reasonable sized starter/generator would be sufficient to handle the kinds of overloads required in order to start the engine. While operation in overload means that the motor would heat rapidly, the thermal mass of a motor the size of the current starter motor is usually more than adequate to handle the start duration of an engine start. But the alternator is optimised for high-speed operation, and the starting loads are at low speeds. This means that the power electronic control system must be capable of providing extremely high current at low voltage for the low speed, high torque operation, while the same time being capable of providing normal voltage and current for high speed generation operation. With three-phase and brushless technologies, this means that the drive has to be greatly oversized in order to provide the necessary current for the starting loads.

The power ratings of starters and alternators often hide a significant pitfall. An inverter is normally rated in terms of horsepower or kilowatts. But if one looks at the detailed ratings, both voltage and current are separately limited, and full power is only available when full voltage is combined with full current. Because of the voltage/frequency ratio of most controlled motors, full power is only available at full speed. When conventional inverter is paired with a conventional motor, capable of providing the starting overload current at low speed and low voltage and running current, the result is a greatly oversized inverter.

In automotive engineering, the development of secondary aggregates is on the verge of a huge tap forward which reduce the average fuel consumption by approximately 0.7-1.7 l/100 km. The extent of the reduction will depend on which partial or secondary aggregates are “electrified” or newly added. The following electric aggregates are primarily included: electromagnetic valve timing; electric water pump; pump for cooling; electro-mechanical brake; electric air conditioning compressor; crankshaft starter-alternator. These aggregates of which some are innovative require a safe and balanced energy management system made up of battery storage and electromechanical energy traducer (alternator) with the maximum efficiency. Whereas batteries with are in use today already have a high level of energy development, this does not necessarily apply to the alternators, which are referred to as claw-pole generators. Its efficiency is at about 20-50% within the full-load range, which is restricted to about 2 kW power output at present with no further substantial increases to be expected. The most obvious conclusion would be to use reliable and sturdy electromechanical energy converters, which are highly efficient for future electrification in automotive engineering. Otherwise a significant reduction of fuel consumption would hardly be possible.

In order to reach such goals, highly-efficient alternators must be able to transmit their rated output to a broad speed range. With reference to the crankshaft speed of combustion engine, its speed range would be between 100 r/min and 7000 r/min.

Therefore, contemplations on other constructive solutions were made at an early stage and consisted of coupling the alternator and starter as an integrated system directly to the crankshaft. According to this integrated solution, which consisted of one electric machine, only the latter was operated both as a starter motor and as an alternator.

At the moment it can be noted that the following constructive alternative is appearing to be a highly integrative solution. The flywheel of the combustion engine, which is directly connected to the crankshaft, serves additionally as a rotor of the starter-alternator and also includes clutch. Depending on the type of electrical machine there is also an active engine vibration control, control of the driving mechanism. The bearings are already available and are therefore not part of the starter-alternator, which is a further advantage of this highly integrative solution. The starter is “simply built around the flywheel of the combustion engine” by means of which further friction loss prevented in the ISG (efficiency improvement).

The electric machine with a short end-turn is valuable because a thick, short machine package is required in the available space. The machine rotor replaces the flywheel and takes over its available mechanical damping function so rotor inertia is not so critical.

A histogram of vehicle propulsion energy as a percentage of drive cycle versus power shows that most energy is consumed where the internal combustion engine is least efficient, conversely, only a small fraction of total propulsion energy is consumed at loads points at and above the peak internal combustion engine efficiency region.

2 ISG SYSTEM CONFIGURATIONS

A conventional power-train system is composed of a gasoline/diesel engine, energy storage battery/batteries, mechanical transmission, and power-train control. If an ISG system is added to the power-train subsystem, a conventional power-train becomes a hybrid power-train system. The ISG electric drive subsystem consists of an electric machine and a power electronic box.

If a new electric machine is mounted directly on the crankshaft, the conventional alternator and starter as well as the mass damper and flywheel, including the ring gear, can be eliminated and the new electric machine can replace their functions. This is the concept of the crankshaft-mounted integrated starter-generator (ISG).

The electric machine with a short end-turn is valuable because a thick, short machine package is required in the available space. The machine rotor replaces the flywheel and takes over its mechanical damping function so rotor inertia is not so critical. The ISG machine is located at the place where the conventional alternator is removed. It can be driven by either a separate belt or included in the existing belt system. The belt transfer ratio accelerates the ISG machine speed; so low rotor inertia and high structure strength are preferred. A typical ISG system consists of an electric machine, a power electronic inverter/rectifier, a dc-dc converter, and an optional

additional starter for initial cold cranking. A dual-voltage system can avoid reforming all vehicle 12 V loads.

3 ISG CAPABILITY REQUIREMENTS

In practice, the available 30-36 V battery voltage at motoring and the required 36-42 V charging voltage at generating are the main challenge during electric machine design. The requirement of a wide speed range and the high temperature of cooling media bring several new critical issues to the electric machine in the ISG system. The ambient temperature ranges from -40°C to 125°C , which is a typical requirement for an air-cooled ISG machine. The speed of the electric machine runs from zero to 6000 r/min for crankshaft-mounted ISG system, which is the same as the engine speed. The maximum operation speed of a electric machine runs as high as 13,800 -19,200 r/min with the belt-transfer ratio 2.3-3.2.

In the 42 V dc electrical systems, the motoring performance specifications should be met even at a lower voltage level of 30-33 V dc and the maximum available battery voltage at dc input of electric machine drive is 36 V. If a 14 V dc electrical system is used, the motoring operations of the machine have to be fully functional at 10-11 V dc voltage in spite of the battery voltage of 12 V.

Under motoring operation state, for a belt-driven ISG system, the duration of a cranking cycle is normally up to 1.3 s.

Full engine cranking torque is required up to 250 r/min after which it is allowed to decrease to zero above engine idle speed.

For quick response and frequent stop/starts, the moment of inertia of the ISG machine rotor should be as low as possible. Although cranking time can be as short as 0.08-0.35 s, the cranking torque at the required higher speed is still a big challenge to machine designers due to low available battery voltage at low temperature, such as -30°C .

The normal generating operation is required for the ISG machine from the idle speed up to the red line speed of the engine.

The torque curve for sustaining generator output required to capture vehicle a short term, intermittent high generator output required to capture vehicle breaking energy through regeneration into the high voltage battery. Over the interval from low engine idle (600 r/min) to approximately 2000 r/min, the ISG may also be operated as a driveline damper for torsion oscillations.

All electric power required by electric loads on or off vehicle board is supplied by ISG machine under the generating condition, so the regenerating performances of the machine, including power output and efficiency, are critical specifications. Generally, the output power at idle engine speed shall be larger than 35-60% of the maximum continuous output. Within a short time, such as 1-3 min, about 1.3-1.4 per unit power is required for a rush charge.

In practice, the available 30-36 V battery voltage at motoring and the required 36-42 V charging voltage at generating are the main challenge during electric machine design. Besides the dilemma from voltage specifications, the requirement of a wide speed range (from idle 600 r/min to redline 6000 r/min) and the high temperature and temperature of cooling media bring several new critical issues to the electric machine in the

ISG system. The ambient temperature ranges from -40°C to 125°C , which is a typical requirement for an air-cooled ISG machine.

Starter operation at low temperatures (-30°C) makes the greatest demands on the battery, power electronics (starter currents) and electrical motor, as the torque required of the starter-alternator by the combustion engine is quite considerable at the given unit volume. This torque ranges between 200 Nm and 240 Nm for medium class cars and an estimate value of 300 Nm for high class. It is to be concluded that the torque requirement would have to be known precisely when starting the combustion engine, in particular at low temperatures and depending on “the most inappropriate” lubrication oil. For initial cold engine cranking, the machine has to provide a breakaway torque that is 1.5-1.8 times the nominal cranking torque to overcome the engine static torque and rotates the engine from 0 to 10–20 r/min at -30°C . Depending on the design of the electrical motor/generator a starter current of 1,000 A to 1,200 A flowing over the semiconductors would have to be expected for a 42 V on-board system. The speed/voltage requirement for the ISG system rules out the machine with low weakening capability unless a costly extra dc/dc converter is added the dc bus voltage-charging and as current reducing solution for the semiconductors.

These requirements of the combustion engine and the starter alternator would have to be reliably met by the electrical battery at low temperatures i.e. the battery will be extremely strained at such low temperature with regard to high starter current and the starting performance. Also there would have to be a sufficiently large start torque at a low temperature (motor operation). For an ideal design of the starter-alternator it is indispensable that the interval resistance of the battery is well known.

As a rule it would be possible to use the decoupling capacitor in the dc link of the converter as an additional energy source during start-up operation and consequently relieving the battery. On account of the small energy storage capacity in the electric field, very large capacities would be essential for a sufficient energy supply during the start. The alternator is not quite as critical from the view of electronic power components as the currents are approximately 100 A. During such an operation care must be taken that the iron loss as a result of the alternator frequency at high crankshaft speed (6000 r/min) does not increase to such to large extend so that alternator efficiency drops to value on the level of the claw-pole alternator.

Starter-generator, as others automotive applications, is very constrained. These constraints create specific behaviours (high magnetic saturation) and limitations (current, voltage, power, energy). Moreover, terminal voltage, equal to the battery voltage, varies with the state of charge and the consumed power. All these machines must respect very strong rules and specifications (low size, high torque, speed and efficiency). Constraint function is of various types: torque-speed characteristics; efficiency characteristics; thermal characteristics; geometric constraints; supply constraints

Torque-speed characteristics [5]

- starter mode (M1): 215 Nm from 0 to 110 r/min
- generator mode (G1) $P_{elc}=1500$ W at 850 r/min
- generator mode (G2) $P_{elc}=2500$ W at 2000 r/min
- generator mode (G3) $P_{elc}=1000$ W at 6000 r/min

Efficiency characteristics

- 80% (including power converter efficiency) for G1, G2, G3
 - For M1 no minimum efficiency is required. Nevertheless, the battery current has to be limited to a maximal value.

Thermal characteristics: Thermal constraints have been taken into account by the limitation of the current density in the windings:

- 50 A/mm² max for starter mode (M1)
- 10 A/mm² max for generator mode (G1, G2, G3)

Geometric constraints

- The maximal external diameter is 255 mm². The value of the laminated core would be approximately 2,500 cm².

A typical ISG system consists of an electric machine, a power electronic inverter/rectifier, a dc/dc converter, and an optimal starter for initial cold cranking. A dual-voltage system can avoid reforming all vehicle 12 V leads. On account of the considerable electric power increase in the vehicle, the installation of a “two-battery on-board system” with both voltages 14 V and 42 V would appear to be most likely, also being favoured by automobile manufacturers and suppliers.

The electrical machines to be taken in consideration for use in ISG system are, as a rule, brushless machines: induction machines; permanent-magnet synchronous machines (non salient pole or salient pole); reluctance machines.

Although the number of pole pairs can be chosen relatively freely. The torque is not determined by the number of pole pairs at the given geometrical conditions of the combustion engine. In order to reduce the iron loss in dynamo sheet (0,5 mm), it is important for the frequency, the number of pole pairs and speed, it would be best to choose the number of pole pairs as small as possible (minimum $p=1$). This solution is opposed by the overhang of the stator winding and the large height of the yoke. The tests revealed that the unreal number of pole pairs ranges between $p=3$ and $p=6$ under consideration of diverging influences.

From the viewpoint of an electrical motor or generator constructor this new voltage level of 42 V for the ISG is not the best option, as the high starter currents which also flow at this voltage require a large number of parallel connected semiconductors in the difficulties known. From the viewpoint of an electrical machine constructor it would be advisable to set the second voltage as high as safety requirements permit. Therefore, a battery voltage of 100 V to 120 V would be considered which is a voltage level corresponding to the maximum electromotive force in low-voltage supply systems.

4. SELECTION AND COMPARISON OF ISG ELECTRIC MACHINES

4.1 Machine Sizing and Winding

The D^2L electromagnetic torque scaling was employed as the first step in designing the ISG machine given the engine cranking requirement and constraints on stator OD to fit into the transmission bell housing and on rotor ID to accommodate the coaxial clutch. Three machine technologies (induction machine, PMDC machine, and PMAC machine) can be evaluated by varying the machine stator ID (as independent

variable) and calculating machine OD and torque for each machine type given a fixed stack length. The sizing equation machine is [3]:

$$T = \frac{\pi}{2} \left(\frac{K_e K_i K_p}{1 + K_\Phi} \right) B_g A_x D_g^2 L \quad (1)$$

where the following notations have been used:

- K_e - the voltage waveform factor;
- K_i - the current waveform factor;
- K_p - power factor estimate;
- K_Φ - ratio of the rotor/stator electric loading;
- D_g - the machine air gap diameter, a variable;
- L - the machine stack length, a variable;
- B_g - midgap magnetic flux density;
- A_x - stator electric loading.

During this stage of machine sizing, the decision was made in function of magnetic material of laminations. During the second phase of the design, magnitudes A_x and B_g in relation (1) were coupled.

The voltage of a rotating machine is determined by the winding configuration. The voltage across a coil in alternating magnetic field is given by the rate change of flux coupling this coil. The voltage of the entire machine is set by the interconnection of these coils. The voltage developed in coil coupling a sinusoidal ac magnetic field is determined by the known relation $U_e = N \Phi \omega / \sqrt{2}$, where the following notations were been used: U_e - rms voltage; Φ - peak flux; N - number of turns; ω - angular frequency.

Given the same motor frame, with fixed geometry and magnetic steel arrangement, different windings design result in different voltage and current relationships for a given mechanical output state. Motors, which may be reconnected for one of two different voltage stages, are in common use. For example, reconnecting a 23 V motor as a 46 V motor would double the voltage required but the current required for any given torque is halved. The net result is that on the same frame, the same electrical power input is required to produce the same mechanical power output. But voltage can be traded for current by selecting the proper winding. By selecting a motor with a high turns count, high voltage would be required at low speed, but very little current is required to produce high torque. A motor with a low turn count would match the output capabilities of the inverter to high speed and low torque requirements for alternating operation.

4.2 Induction Machines

Most induction machines in ISG applications are three-phase machines and connected to the dc bus through a power electronic inverter/rectifier.

Most important for the design are the curves of torque versus rotor speed when the induction machine runs for an ISG application: the curve represents the electric power generation from weakening, and the curve represents the electric power

generation from the idle through the maximum speed.

At the beginning of engine cranking, the induction machine produces 1,5-1,6 times of cranking torque reaching or exceeding the breakaway torque at the lowest start frequency f_{min} of the stator current. At the given f_{min} , the stator voltage required to drive the engine from static state can be derived from $U_e/f = \text{constant}$ or even higher than this, and voltage is higher than that from $U_{ph}/f = \text{constant}$ during conventional constant torque/flux control because at low frequency, the stator resistance has more effect than start circuit reactance. The induction machine is allowed to run at slip values corresponding to the maximum torque with frequency variation during cranking procedure because this is very short (0.2-0.3 s), although the slip at the maximum torque causes a low power factor and high machine losses at low-speed range.

At each individual frequency point, the maximum torque decreases with the stator resistance while the slip corresponding to the maximum torque, s_m , is proportional to the rotor resistance. This means that the low-stator resistance benefits torque capability while low rotor resistance helps the thermal capability of the ISG induction motor. This is the reason why rectangular stator windings and more expensive copper rotor benefit ISG machine. The maximum torque is proportional to the square of the ratio of voltage to frequency at the high-frequency range. Therefore, the power capability of the induction machine decreases with speed increase at constant voltage operation by flux weakening (especially for ISG electric power generation), and the constant power operation can only be valid within the speed variable ratio of 3-5. Fortunately, it is not necessary for the ISG machine to run at redline speed without compromising the power output.

4.3 Permanent Magnet Machines

The main advantage of PM machines is their high efficiency due to the absence of field coil losses. From the efficiency and package point of view, the PMAC machine with 6-12 poles is preferable for belt-driven ISG applications while the PM machine with concentrated no-overlap fractional slot winding is suitable for crankshaft-mounted ISG.

Based on the structure of PMAC machines, they can be categorized as the surface-mounted PM type or the interior-mounted PM type. The surface-mounted PM machine combined with concentrated windings and fractional windings has been developed for variable speed application; its speed-variable ratio has relatively low while its no-load EMF is very high.

Surface PM can be designed to achieve wide speed ranges of constant-power operation. The key of the new-found capability is the fractional-slot concentrated windings.

The adoption of fractional-slot concentrated windings makes it possible to significantly increase the machine's characteristic current, defined as $I_{ch} = \Psi_m / L_d$, where Ψ_m is the rms flux linkage and L_d is the d-axis stator inductance. More specifically, the conditions for optimal flux weakening operation can be achieved by designing the machine so that its characteristic current equal the rated current value (i.e. $I_{ch} = I_r$ where I_r is the rated current of the machine). The use of conventional

distributed windings in such machines with integral value of slot/pole/phase makes it difficult to meet the conditions for optimal flux weakening. More specifically, the machine phase inductance of machine with distributed windings tends to be low, leading to characteristic current values that significantly exceed the machines rated current. The low magnetic permeability of the permanent magnets in the machine's air gap is a major contributing factor that causes the low inductance. High values of characteristic current lead to rapid drops in the machine's torque and power production capabilities when the machine spins at speed above its rated speed.

In contrast, the introduction of fractional-slot concentrated windings makes it possible to significantly increase the machines phase inductance. With proper design, the value of the characteristic current can be lowered and tuned to match the machine's rated current achieving the conditions for optimal flux weakening. By introducing appropriate control for the flux-weakening regime, such a machine can achieve very wide speed ranges of constant power operation.

The current limitation circle in the sinusoidal-IPM machine is similar to that in the surface-mounted PM machine. The stator current phasor must be inside the current limit circle to prevent damaging the inverter and overheating the machine, whichever has limitations, i.e. $i_s < I_{max}$. Unlike the surface mounted PM machine, the reluctance torque in the IPM machine adds one more limitation to the operation area in d - q plane. The current i_d has to meet the torque limitation of $[\Psi_f + I_d (L_d - L_q) \geq 0]$ if motoring operation with $i_q > 0$ or a generating operation with $i_q < 0$. The torque limit area can be further expressed by half-plane equation $i_d \geq \Psi_f / (L_d - L_q)$.

That is, if adjusting $i_q > 0$ for motoring and $i_q < 0$ for generating, the equation displays the right-half plane at the critical torque line of $i_d = \Psi_f / (L_d - L_q)$. The voltage limitation ellipse in IPM machines have the centre located on the d -axis, and its distance from d - q plan origin is approximately equal to three-phase short-circuit current ($I_{sc} = -\Psi_f / L_d$). The machine with p pole pairs can run for constant power by flux weakening if $\Psi_f / L_d < I_{max}$. The risk for this design consideration is a possible demagnetisation of the PM when the d -component of the stator current is higher than short-circuit current I_{sc} but is still within the current limit circle at the deep-flux weakening operation. The PM materials, such as NdFeB or SmCo, with a property curve extending to the third quadrant in B - H plane become necessary.

In general, the operation during flux weakening must be limited within the intersection of the current limit circle and the voltage-limitation ellipse as well as the torque-limit plane for each given speed.

The no-load EMF of the IPM machine at its highest speed and the lowest temperature should be controlled within a reasonable range to keep the power electronics inverter in the ISG system from being damaged.

The rectangular PMDC (dc brushless) machines with surface-mounted PM does not meet the voltage requirements at generating and the wide-flux weakening specifications at motoring of the ISG machine, unless a dc/dc converter is added between the electronic inverter bridge and the battery. The speed-variable ratio is still relatively low while its no-load EME is very high.

5. CONCLUSIONS

Integrated starter/generator (ISG) is a solution for mild hybrid vehicles. High efficiencies, low cost and easy implementation are required. Various types of electric machines have to be considered and lead comparisons between behaviour of different machines structure: induction machine and PM machine, in ISG system configuration and specifications. A qualitative analysis of the practical characteristics for these machines is given in Table 1.

By preliminary tests resulted advantages for the induction machine due to its being sturdy and reliable which provided good experimental results with the use of modern electronics. Of course, special attention must be paid to construction (air gap). The PM machine has the disadvantage that the good magnetic characteristics are “undetermined” on purpose in order to control the voltage and that the thermo-stability of the permanent magnets is not very high. In case of an intern short circuit the PM alternators would brake the car unexpectedly (important question off security).

Table 1: A qualitative analysis of practical characteristics of ISG machines

Electric Machine Type	PMDC	PMAC	IM
Efficiency and compactness	X	X	X
Low torque ripple and noise		X	X
Easy closed-loop control	X		
Fewer control sensors	X		
Wide speed range		X	X
High power applications	X	X	X

With ISG applications, the technology and experience will benefit to not only the ISG developers and customers, but also the entire generation of hybrid electric vehicles, especially the full-hybrid vehicle.

REFERENCES

- [1] **W. Cai**, “Starting Engines and Powering Electric Loads with One Machine,” in IEEE Industry Applications Magazine, Nov./Dec. 2006, pp. 29-38.
- [2] **S. Chen, R.R. Henry, and Y. Xue**, “Design and testing of a belt-driven induction starter-generator,” IEEE Trans. Ind. Applications, vol.38, no 6, Nov./Dec. 2002, pp. 1525-1533.
- [3] **D.D. Stoia**, “Induction motor and dc brushless in integrated inverter-electrical machine design,” “Transilvania” University Publisher, Brasov, 2006 (in Romanian).
- [4] **T.M. Jahns**, “Flux weakening regime operation of interior PM synchronous motor drive,” IEEE Trans. Ind. Applications, vol.23, no 4, July/Aug. 2000, pp. 681-689.
- [5] **G. Friedrich, L. Chédât**, “Need of an optimal design and control approach,” EMD’05, Madison, WI, 2005, pp. 1529-1534
- [6] **I.A.Viorel** “Special electrical machines for ISA systems” Revista de politica stiintei, raport, Cluj-Napoca, 2005 (in Romanian).
- [7] **V. Hajek, M. Travnicek, B. Kysely**, “Integrated Starter-Generator,” ACEMP 2004, Istanbul, Turkey, 26-28 May 2004.

MODERN SYSTEM FOR MONITORING AND DIAGNOSIS OF THE MECHANICAL AND ELECTRICAL DEFECTS FOR HIGH CAPACITY INDUCTION MOTORS

SORIN DEACONU^{*}, GABRIEL NICOLAE POPA^{}, IOSIF POPA^{*},
IOAN RODEAN^{***}**

Abstract: This paper presents a modern system for monitoring and recording the vibrations of the high capacity induction electric motors, for the purpose of predictive diagnosis of electrical or mechanical defects. Thus, technical and logistic actions can be taken in due time to minimize the costs incurred by a failure occurrence.

Keywords: monitoring, recording, diagnosis, vibrations of high capacity induction electric motors, minimum costs per defect.

1. INTRODUCTION

The high power asynchronous machines are vital elements of the production lines or even of a factory. Their accidental, unpredicted failure can lead to production outages which could last as long as several weeks or even months (if the respective machine is not available on stock at the manufacturer factory, or if it is a singular product), causing lost which could be tens times higher than in case of using an integrated defects monitoring and diagnosis system.

These systems become indispensable for all major equipment, and especially for the electric motors larger than 200 kW.

^{} Assistant Professor Ph D. Eng., University Timisoara*

*^{**} Lecturer Ph D. Eng., University Timisoara*

*^{***} Eng., Kronosphan S.A. Sebes, Romania*

2. THE METHOD CONCEPT

Vibrations monitoring for the bearings of an induction motor – working machine train is a component of the modern predictive maintenance systems, which is based on sensors, controllers and state of the art analysis techniques.

The sensors are speed transducers or acceleration transducers type. The speed transducers provide a high measurement accuracy of the absolute vibrations in the narrow frequency range ($0 \div 2500$ Hz), with the advantage of easy installation and connecting. The acceleration transducers enable recording within a wider frequency range ($0 \div 20$ kHz). Thus all the relevant vibration frequencies can be precisely measured, and based on these measurements, the defect type can be correctly diagnosed.

Figure 1 shows the block diagram for a monitoring, alarm, recording and diagnosis system for the vibrations caused by the occurrence of a mechanical or electrical defect in a system with electric motor.

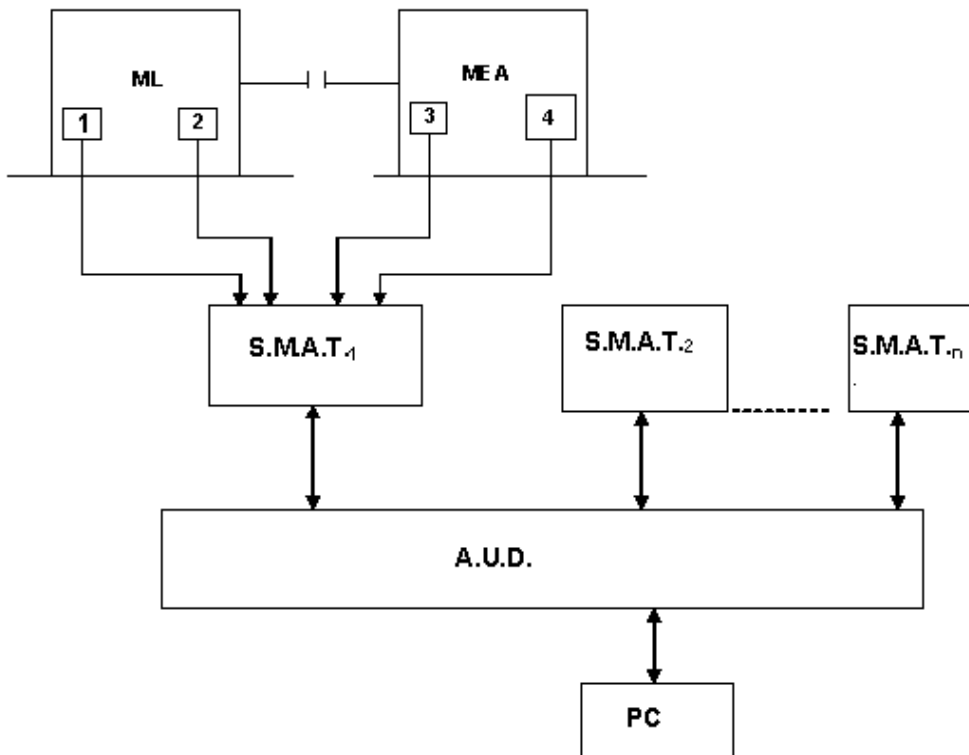


Fig.1 The block diagram for a monitoring, alarm

Legend:

- ML - driven equipment;
- MEA - electric motor;
- 1, 2, 3, 4 – vibrations transmitters installed on bearings area;
- S.M.A.T – monitoring, alarm and data communication system;
- A.U.D. – programmable automation for defects monitoring and recording;
- PC - process computer.

At the AUD block level the decisions are taken in terms of alarming, and recording the vibrations which overpass the allowable limits, which are sent to the process computer for further data processing. Based on the recorded vibration spectrum and on the vibrations amplitude, the defect type can be diagnosed with a precision of over 95 %, either on motor or on driven equipment area.

3. EXPERIMENTAL RESULTS

In this chapter we will present the case of an induction motor from wood pulp grinding equipment operating in the plastic-faced agglomerated wooden board factory S.C. Kronosphan S.A. Sebes. The motor rated technical data are:

- Rated voltage 6000 V;
- Rated power 7000 kW;
- Rated frequency 50 Hz;
- Type: AMB 630 L4L BAM;
- Producer: ABB Industria, Italia.
- Rated speed 1492 rpm;
- Rated efficiency $\eta_N = 0.95$
- Rated power factor $\cos \varphi = 0.92$;

The speed transducers installed on motor bearings read the overpassing of the allowable vibration level and recorded the vibrations trend during idle run as well as in load operation.

The Figure 2 below presents the recorded vibration spectrum with their corresponding amplitudes.

Figure 3 presents the diagram of the vibration speed versus motor speed in idle run mode and in normal load mode, based on the data listed in Table 1.

Table 1 Data listed

Operation mode	Idle run	n [rpm]	750	850	950	1050	1150	1250	1350	1490
		v [mm/s]	0.28	0.29	0.3	0.37	0.43	0.95	0.78	0.9
	Rated load	n [rpm]	760	845	962	1075	1132	1286	1345	1472
		v [mm/s]	0.3	0.31	0.33	0.4	0.45	1.1	0.9	1.07

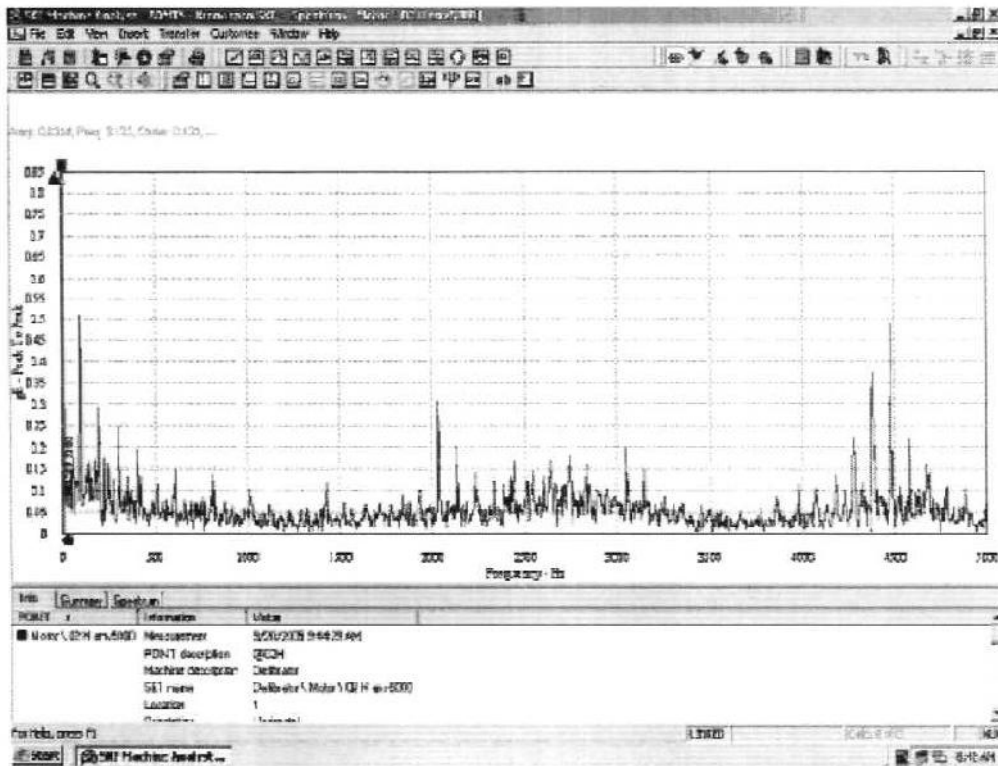


Fig.2 The recorded vibration spectrum with their corresponding amplitudes

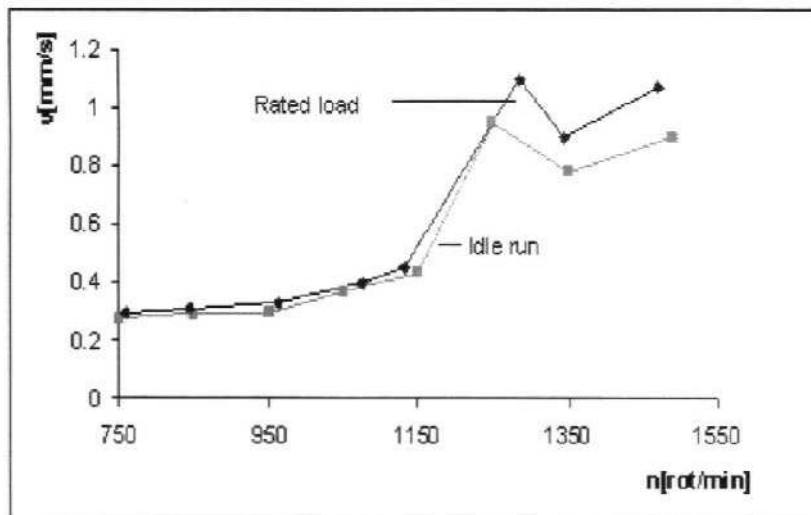


Fig.3 The diagram of the vibration speed versus motor speed

Based on the diagrams in Figure 2 we have reached the conclusion that the vibration level is generated by the interruption of few stator bars. A decision was made

to replace the motor with a spare motor, and this work was prepared in 10 days. The works for replacing the motor took 30 hours. Considering the factory production level on a daily basis, identifying the defect in advance enabled a reduction of losses by 1200000 EUR, which means the cost of purchasing six new motors.

4. CONCLUSIONS

The predictive maintenance concept is gaining a crucial importance in the frame of reliable operation of a modern enterprise. This concept aims to minimize the losses caused by the occurrence of a defect.

REFERENCES

- [1]. **J.A. Antonino, P.Jover, ș.a.**, *Wavelet analysis for the detection of inter – turn shortcircuits and broken rotor bars in induction machines*, ICEM 2006, Chania, September 2 ÷ 5, Crete Island, Greece, PMM 4 – 3.
- [2]. **K., Dabala**, *Modified method to determine rotor bar-iron rezistance in three-Phase copper squirrelcage induction motor*, ICEM 2006, Chania, September 2 ÷ 5, Crete Island, Greece, PMM 4 – 6.
- [3]. **Gerling, D., Hildebrand, H., ș.a.**, *Test – bench for high – speed high – power electrical drives*, ICEM 2006, Chania, September 2 ÷ 5, Crete Island, Greece, PMM 4 – 8.
- [4]. **Fiser, R., Bugeza, M., ș.a.**, *Detection of broken rotor bars in induction motor drives using run-up test*, ICEM 2006, Chania, September 2 ÷ 5, Crete Island, Greece, PMM 4 – 17.
- [5]. **Liese, M.**, *Vibration sparking, an unrecognized damage mechanism of high voltage windings*, ICEM 2006, Chania, September 2 ÷ 5, Crete Island, Greece, PMM 4 – 12.
- [6]. **Balan, H., Tîrnovan, R., Karaissas, P.**, *Vibroacoustic methods in the diagnosis of electric machines*, ICEM 2006, Chania, September 2 ÷ 5, Crete Island, Greece, PMM 4 – 28.
- [7]. **Deaconu, S., Popa, G.N., ș.a.**, *Diagram for artificial charge loading of asynchronous machine and the study of the influence of the frequency change on the charge loading*, EPE 2002, Tom XLVIII (LII), fascicola 5, Iași, 2002.
- [8]. **Deaconu, S., Tutulea, L.**, *Experimental identification of the ideal regime at the induction machine*, Annals of the Faculty of Engineering Hunedoara, Tom III, fascicola 2, ISSN 1454 – 6531, pag. 173 ÷ 178, 2005.
- [9]. **Deaconu, S., Popa, G.N., Popa, I.**, *Wind power station with induction generator and static frequency converter*, UNIVERSITARIA SIMPRO 2006, ISSN 1842 – 4449, pag. 31 ÷ 33, Petroșani, 2006.
- [10]. **Popa, G.N., Popa, I., Deaconu, S.**, *Automate programabile în aplicații*, Editura Mirton, Timișoara, 2006.
- [11]. **Deaconu, S.**, *Mașini electrice*. Culegere de probleme, Editura Politehnica, Timișoara, 2005.

NEW APPROACH IN MEASUREMENT-BASED POWER NETWORK MODELING BY USING SMART SENSORS

MIRCEA RISTEIU*, ADRIAN TULBURE**, MOISE ACHIM***,
COSMIN COVACIU****

Abstract: The paper is part of an energetic dispatching system project and is focused on interfacing the local parametric measuring system to the remote processing step. For measuring procedure in high power networks the data safety is the main issue. We have implemented a Zigbee- based smart sensor system which consists of full- function (FFD) and reduced-function devices (RFD). The FFD system is programmed for measuring and routing functions. Selections of transmission parameters are based on side information that is obtained from the demodulation and decoding processes within the receiving radio for EMC compatibility. Such a change in transmission parameters also reduces the interference that the transmission causes to unintended receivers. For this strong demand we have modified sensor hardbit header by integrating a Zigbee ping-pong data packet for the transmission rate evaluation. In this stage, we have tested the sensors for temperature, light and voltage input data.

Keywords: Zigbee, smart sensor, measurements-based modeling, stack development, 802.15, TCP/IP, adaptive-transmission protocol, wireless network protocols, mobile communications

1. INTRODUCTION ON SEMICONDUCTOR DEVICES FOR LOW POWER WIRELESS NETWORKS

Comprehensive monitoring and control of industrial processes and equipment is crucial to achieving efficient production, minimizing cost, and ensuring safety of staff and public. However, providing enough wired sensors – perhaps thousands -

* Associate prof., PhD. at University of Alba Iulia

** Senior lect., PhD. at University of Petrosani

*** Professor, PhD. at University of Alba Iulia

**** Eng. at CARPSIT SRL Alba Iulia

tomonitor and control an average industrial process is costly and complex business. Applications range from meter reading, through pipeline flow measurement, to machine control. Apart from being cheaper and more flexible, wireless sensors can also be used in hazardous environments inaccessible to normal wired systems.

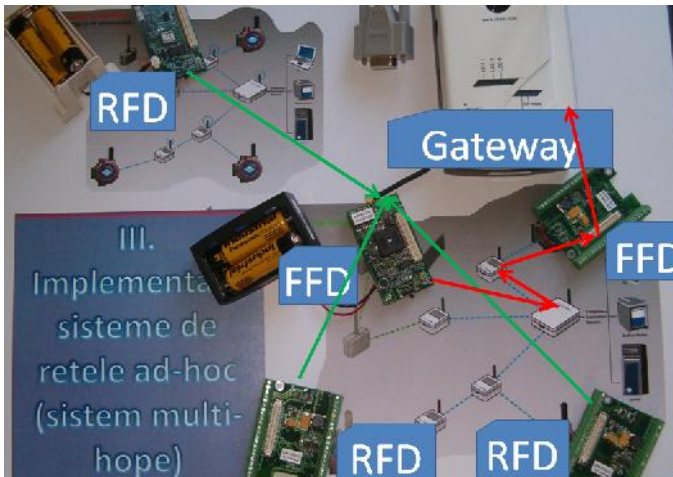


Fig.1 Typical measurement implementation

at 2.4 GHz. IEEE 802.15 uses a FHSS (Frequency Hopping Spread Spectrum) scheme, while IEEE In this paper, we present a coexistence mechanism based on a simple traffic shaping technique. The proposed mechanism is to be performed at the WLAN stations in presence of a 802.15 voice link. It does not require a centralized traffic scheduler and can be implemented in non-collaborative mode, thus allowing for interference mitigation between co-located and non co-located 802.11 and 802.15 devices. Performance, as well as advantages and disadvantages, of the presented algorithm are compared with those of the so called MEHTA scheme, which is a collaborative algorithm proposed within the IEEE 802.15 Working Group.

IEEE 802.11 and IEEE 802.15.3 target at designing PHY and MAC specifications for wireless local area network (WLAN) and wireless personal area network (WPAN), respectively. They adopt different philosophies for MAC design, namely CSMA/CA in 802.11 and TDMA in 802.15.3. An interesting problem is the performance of each MAC working on the same physical layer, e.g., ultra wideband (UWB). The results show that the newly added mechanisms of 802.11e, such as transmission opportunity (TXOP) and Block Ack, improve its throughput greatly, making it comparable to that of 802.15.3. In addition, 802.15.3 MAC has easier power management by utilizing its TDMA access method. ZigBee fills yet another niche. It is a PAN technology based on the IEEE 802.15.4 standard. Unlike Bluetooth or wireless USB devices, ZigBee devices have the ability to form a mesh network between nodes. Meshing is a type of daisy chaining from one device to another. This technique allows the short range of an individual node to be expanded and multiplied, covering a much larger area.

In this paper, we deal with the problem of mutual understanding the differences between IEEE 802.11 WLANs (Wireless Local Area Networks) and short-range radio systems based on the Zigbee technology, or equivalently, IEEE 802.15 WPANs (Wireless Personal Area Networks). These systems will operate in the ISM (Industrial, Medical and

Scientific) frequency bands, i.e., the unlicensed spectrum

The chipset and the stack are incomplete without a profile, which defines the module application. As mentioned previously, there are public profiles and private profiles. For public profiles, ZigBee Logo Certification is available; private profiles are not intended to interoperate and therefore cannot be certified. Implementing profiles, either public or private, is no small undertaking. In addition to the need to license development tools from the stack providers and attending a training class, we have to be prepared to spend a fair amount of time studying the various firmware components that constitute the ZigBee stack. Also we have to make sure that the firmware engineers are familiar with the microcontroller used in the platform. While none of these items is insurmountable, they do add to development costs and time to market.

2. ZIGBEE TECHNOLOGY IMPLEMENTATION FOR IN-SITU MEASUREMENTS

In our approach we used smart sensor system and it is based on 8-bit single-chip microcontroller 78K0/KF1+ (μ PD78F0148HGK) 128KB Flash, 512KB serial Flash, 8KB RAM, A/D converter, with 2420 radio transceiver. For our purpose we built up a client application packet for using Object Oriented approach around a Xmesh server. Before running real time measurements we have built up a virtual sender (local emulator) (figure 4) where we have programmed fixed packets, for comparison and errors checking.



Fig.2 Sensors position in situ

Before running real time measurements we have built up a virtual sender (local emulator) (figure 4) where we have programmed fixed packets, for comparison and errors checking.

(local emulator) (figure 4) where we have programmed fixed packets, for comparison and errors checking.

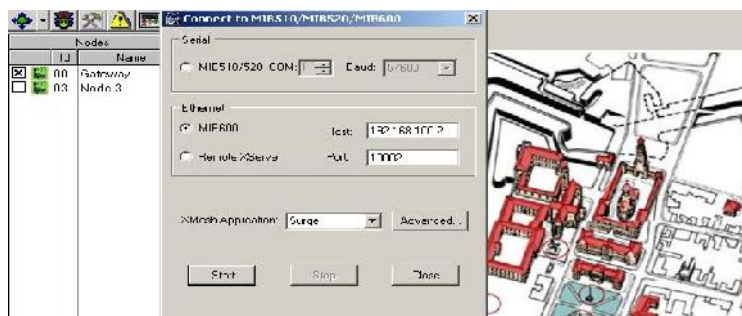


Figure 3 Configuration interface of the real-time measurement application

On the other hand we have executed device control center for real measurements. This OEM application is designed to be an interface (“client tier”) between a user and a deployed network of wireless sensors. It provides users the tools to simplify deployment and monitoring (figure 5). It also makes it easy to connect to a database, to analyze, and to graph sensor readings. The associated server protocol is a multihop mesh networking protocol that has various options including low-power listening, time synchronization, sleep modes, any-to-base and base-to-any routing. All of our sensor and data acquisition boards are supported with these enabled applications. The installation of database environment (*PostgreSQL*) will automatically install and configure a local *PostgreSQL 8.0* database on the machine when that option is checked. The installation requires administrative privileges on the system, including the ability to create a new user called *postgres*. The Data tab on the application interface displays the latest sensor readings received for each node in the network. Any column of data can be sorted by left clicking the top. This allows you to sort by node ID, parent, temperature, voltage, last result time, or any other sensor reading. For configuring the communication protocol between gateway (FFD) and measurement station some extra facilities have been developed.

Gateways, together with their related system software, are a key component of WSNs. Their duties include protocol conversion; acting as proxy servers (thus eliminating the need to poll every node from an application or management tool); and performing sensor management functions such as network definition, monitoring, deployment, and configuration. Additional duties may include alert and alarm processing; sensor logging and database management; application programming interfaces (APIs); security key management; traffic analysis and optimization; application integration; and routing management. Gateway TCP/IP application programming interfaces enable developers to leverage WSN technology using familiar Internet programming paradigms. Protocol conversion will break down barriers between WSNs and other types of networks. Gateway standards such as Universal Plug and Play (UPnP) and OPC support integration of diverse devices, including computers, electronics, security and automation components, and other networked devices spanning wireless and wired networks.

2. WIRELESS MEASUREMENT- BASED SETUP

By implementing this setup, we have started measurement analysis. The data packets are framed (at the start and end) by 0x7e (126) (SYNC_BYTE) bytes. Each packet has the form: <packet type><data bytes 1...n><16-bit CRC>.

Each packet is framed on either end by a SYNC_BYTE. The value of the SYNC_BYTE is 0x7E. The type field indicates the type of packet sent. There are five packet frame types:

- *P_PACKET_NO_ACK* = 0x42(66): A user-packet with no acknowledgement required.
- *P_PACKET_ACK* = 0x41: A user-packet that requires acknowledgement.

- *P_ACK* = 0x40: Required response for P_PACKET_ACK packet.
- *P_UNKNOWN*: Unknown packet type received. Requires response of type P_UNKNOWN

Data is the packet payload. If the packet payload contains the special SYNC_BYTE, it is escaped out. The escaping algorithm is described below.

The 2-byte CRC is a redundancy check on the packet type and the data bytes. It is used by the receiving application to verify the packet is not been corrupted during transport. The CRC calculation includes the type byte through the end of the data payload. If the SYNC_BYTE is sent in data portion of the application it would confuse the receiving application by making prematurely end the packet. To avoid this, if a SYNC_BYTE is in the data portion of the packet, the byte is escaped out. Escape bytes are proceeded with 0x7d (ESC_BYTE), then the byte value XOR (exclusive or) with 0x20. For example, 0x7e is converted to 0x7d5e; 0x7d and 0x7e bytes must be escaped; 0x00 to 0x1f and 0x80 to 0x9f can be optionally escaped. By following XServe User's Manual (XServe_Users_Manual_7430-0111-01_B.pdf , pag 188) we have access to the programming environment of TinyOS as:

Bin	126,66,125,94,0,17,125,93,22,0,0,0,0,0,0,0,0,125,94,0,180,1,0,194,100,110,0,0,82,109,66,143,126
Hex	7E 42 7D 5E 00 11 7D 5D 16 00 00 00 00 00 00 00 00 00 00 7D 5E 00 B4 01 00 C2 64 6E 00 00 52 6D 42 8F 7E

After processing:

Bin	126,66,125,94,0,17,125,93,22,0,0,0,0,0,0,0,0,125,94,0,180,1,0,194,100,110,0,0,82,109,66,143,126
Hex	7E 00 11 7D 16 00 00 00 00 00 00 00 00 00 00 00 7E 00 B4 01 00 C2 64 6E 00 00 52 6D

Because the header of TinyOS is:

7E 00 11 7D 16 00 00 00 00 00 00 00 00 00 00 00 7E 00 B4 01 00 C2 64 6E 00 00 52 6D

With the associated commands:

- *dest_address* - Single hop destination address: 7E 00 (126, 0) => bytearray="0" length="2" type="uint16"
- *am_type* - Active message type: 11 (17) => bytearray="2" length="1" type="uint8"
- *group* - Active message group ID: 7D (125) => bytearray="3" length="1" type="uint8"
- *length* - Length of entire message: 16(22) => bytearray="4" length="1" type="uint8"

And the associated chain header:

00 00 00 00 00 00 00 00 00 00 00 7E 00 B4 01 00 C2 64 6E 00 00 52 6D.

The XMesh header is:

00 00 00 00 00 00 00 00 00 00 7E 00 B4 01 00 C2 64 6E 00 00 52 6D

With the main associated commands:

- sourceaddr - Single hop sender address: 00 00 (0,0)=> bytearray="5" length="2" type="uint16"
- originaddr - Node ID of originator of message: 00 00 (0,0)=> bytearray="7" length="2" type="uint16"
- seqno - Sequence number for link estimation: 00 00 (0,0)=> bytearray="9" length="2" type="int16"
- Socket - Application ID: 00 (0)=> bytearray="11" length="1" type="uint8"

And, the associated chain header is: 00 00 00 7E 00 B4 01 00 C2 64 6E 00 00 52 6D

The associated combined commands are:

- XSensor Header: 00 00 00 7E 00 B4 01 00 C2 64 6E 00 00 52 6D
- board_id - Sensor Board ID: 00 (0)=> bytearray="12" length="1" type="uint8"
- packet_id - Sensor Packet ID: 00 (0)=> bytearray="13" length="1" type="uint8"
- Parent - Sensor Parent: 00 7E (0,126)=> bytearray="14" length="2" type="uint16"

The main conclusion related to sensor analysis is that each sensor has own packet structure. The packet ends with a CRC that is calculated on the entire packet excluding the packet header and the CRC field itself. A CRC is calculated by XORing the current byte with a shifted CRC accumulator. The CRC Is always 2 bytes. (XServe_Users_Manual_7430-0111-01_B.pdf , pag 68).So, by extracting the specofoc code from 7E 00 11 7D 16 00 00 00 00 00 00 00 00 00 00 7E 00 06 00 00 BE C0 7A 60 79 8E 74, result: 00 7E – parent; 00 06 – epoch; C0 – Light; 7A – Thermistor; 60 – magX; 79 – magY; 8E – accelX; 74 – accelY. Measured data (case study) exported into datasheet is shown in next figure:

id	Sample #	Time	parent	light	temp [C]	voltage [V]	mag_x [mgauss]	mag_y [mgauss]	accel_x [g]	accel_y [g]
2	890	3/15/2007 11:48	0	218	-273.15	2.9467	16.206	19.582	-1.7259	-1.7716
0	915	3/15/2007 11:48	126	100	-14.441	3.2277	0	0	-1.8883	-1.797
2	891	3/15/2007 11:48	0	218	-273.15	2.9467	16.206	19.582	-1.7259	-1.7716
0	916	3/15/2007 11:48	126	101	-14.949	3.2277	0	0	-1.9442	-1.8274
2	892	3/15/2007 11:49	0	218	-273.15	2.9537	16.206	19.582	-1.7259	-1.7716
0	917	3/15/2007 11:49	126	101	-14.949	3.2277	0	0	-1.9543	-1.8274

Fig.4 Measured data, exported into datasheet

4. SELF- HEALTHING NETWORK. MULTI-HOPE PROTOCOL

In order to fit this requirement, the main components of the setup are:

- **End Devices**, also called Nodes, Edge Nodes, Devices, or Reduced Function Devices (RFDs), are battery-powered devices that wake up periodically and send data to a host..

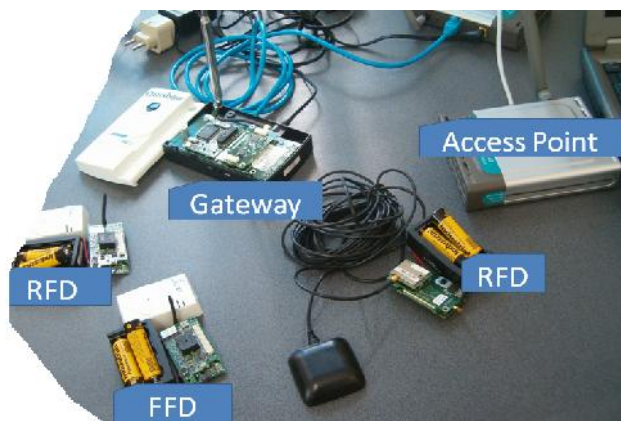


Fig.5 Integrating smart sensors into TCP/IP configuration

- **Routers**, also called Mesh Nodes, Coordinators, or Full Function Devices (FFDs), form a wireless backbone that ferries messages in a multi-hop fashion across the network. Routers allow messages to flow in various directions on demand and buffer messages for nearby End Devices that are currently sleeping.
- **Gateways**, also called Bridges, Controllers, Internet Interfaces, or PAN Coordinators, are usually envisioned as Internet appliances that provide an interface between the WSN and the Internet. Gateways control and monitor the WSN, consolidate data from various nodes, execute business logic, and provide a TCP/IP interface to the outside world.

5. CONCLUSION. ENSURING MULTI-HOPE PROTOCOL

It is a goal at some point to add mesh routing support to this stack. The figure 6 shows the diagram form multi-hope and self-healthing situation.

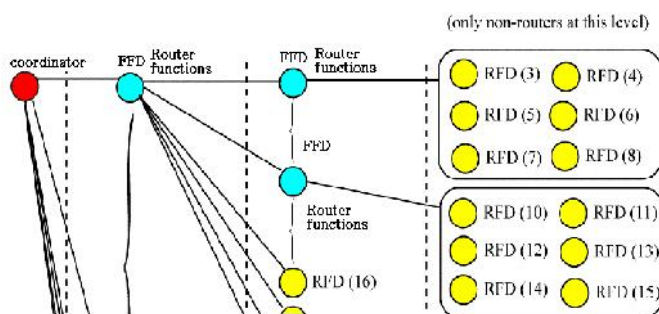


Fig.6 Multi-hope and self-healthing configuration for a study case

In this approach, wireless sensor networks offer numerous benefits over previous networking solutions for many applications, including lowered costs, the

ability to leverage infrastructure for multiple applications, and the capacity to restructure the network quickly and easily, as well as security, scalability, and ease of administration.

The catch-all phrase for low power, low data rate sensor networks targeted at condition monitoring, lighting and climate control as well as safety and security. The goal is to provide a standard, yet extensible, protocol stack for use with 802.15.4 radios with enough flexibility for use in limited power environments for low latency, single hop networks as well as longer distance, multi-hop mesh network configurations. There are also noteworthy proprietary options for similar technology. So, the main pros are: standards based sensor networking allows multi-sourcing, interoperability; multi-path mesh architecture can overcome difficult RF environments.

REFERENCES

- [1] **Xin Wang, Yong Ren, Jun Zhao, Zihua Guo, Yao, R.** Comparison of IEEE 802.11e and IEEE 802.15.3 MAC, Emerging Technologies: Frontiers of Mobile and Wireless Communication, 2004. Proceedings of the IEEE 6th Circuits and Systems Symposium on Volume 2, Issue , 31 May-2 June 2004 Page(s): 675 - 680 Vol.2
- [2] **xxx** A Zigbee -subset/IEEE 802.15.4, Multi-platform Protocol Stack, IEEE 802.xx, 2006
- [3] **xxx** IEEE Std. 802.15.4, Part 15.4: Wireless Medium Access Control (MAC) and Physical Layer (PHY) Specifications for Low-Rate Wireless Personal Area Networks (LR-WPANs), pp. 679.
- [4] **xxx** Zigbee Alliance, Zigbee SPecification Version 1.0, pp. 376. Available online at www.zigbee.org

POSSIBILITIES TO PROTECT AGAINST EXPLOSION THE LOW CURRENT CIRCUITS MADE OF MICRO-DRIVINGS

SORIN BURIAN* , JEANA IONESCU* , MARIUS DARIE*

Abstract: The low current circuits represent an ever-growing trend in the industrial applications, which involve the occurrence of explosive atmospheres. This paper intends to underline the conditions and the limits required for using micro-drivings on low currents circuits protected by intrinsic safety.

Key words: intrinsic safety, micro-drivings

1. INTRODUCTION

It is widely recognized the fact that the intrinsic safety type of protection is suitable and recommended for the protection of low currents apparatus/electric systems which operate in areas with hazards of explosive atmospheres. But the use of the intrinsic safety type of protection on low current circuits which enclose mini/micro-drivings is a domain which has been less approached. This paper intends to identify and present the parameters specific for the intrinsic safety type of protection applicable to low currents apparatus / systems.

2. SPECIFIC PARAMETERS – GENERAL PRESENTATION

The technical solution selected for the protection of equipment with the intrinsic safety type of protection involves a limitation of the conveyed energy and of the one stored in the protected circuits to non-hazardous values, with the consideration of the predictable failures with cumulative effects.

Consequently, it is natural that the specific standard for this type of protection regulates the maximum admitted values for the parameters: maximum admitted values

* *Ph D.Eng. at the INSEMEX PETROȘANI*

for the parameters: maximum voltage (U_0), maximum current (I_0), maximum power of the source (P_0), maximum equivalent capacity allowed for connection to the intrinsic safety output of the source (C_0), maximum equivalent inductance allowed for connection to the intrinsic safety output of the source (L_0).

For the purpose of this paper the “source” shall be any circuit which may generate/transfer energy to that part of the apparatus/system located in the hazardous area.

Since the specific standard defines a safety factor of 1.5 and 1, depending on the number of failures and on the protection level (ia or ib), the following lines shall focus on the stricter values (with the safety factor of 1.5).

3. LIMITATION FOR INDUCTIVE MICRO / MINI-DRIVINGS

There follows a presentation of tables with values and of charts for the maximum admitted inductance in relation to the maximum voltage of the source (U_0), gas / vapours subgroup and to the source type (linear / non-linear).

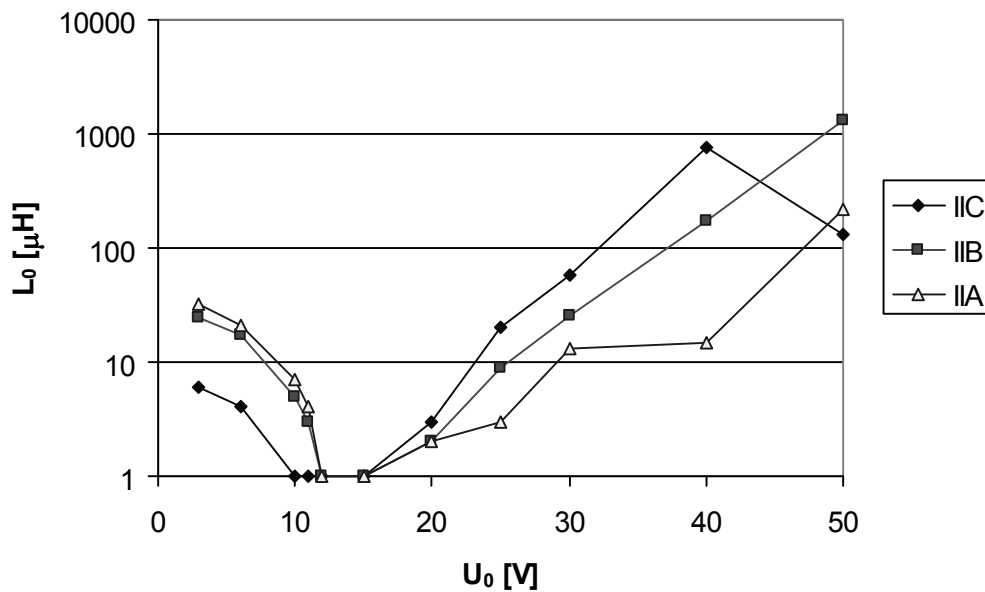


Fig. 1 – Value of the maximum admitted inductance which can be connected to the output of a non-linear source in relation to the idle voltage of the source

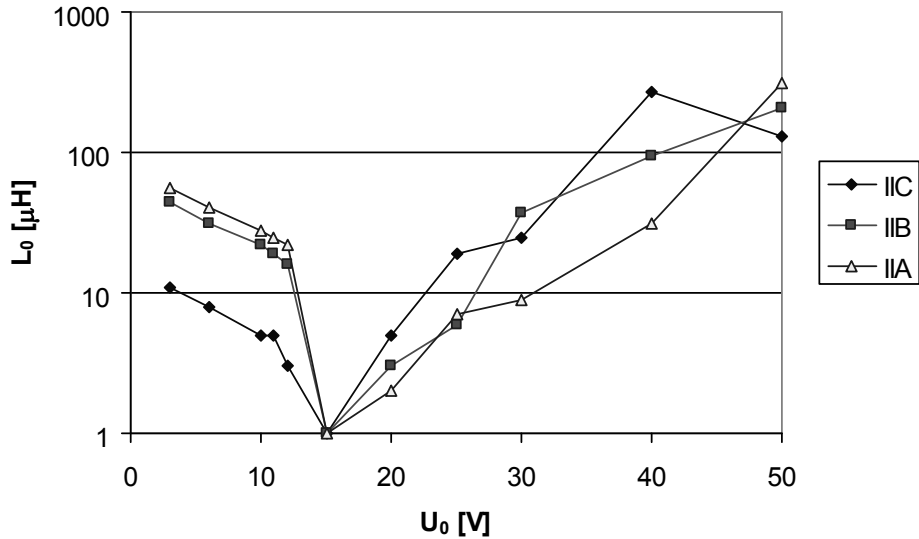


Fig. 2 – Value of the maximum admitted inductance which can be connected to the output of a linear source in relation to the idle voltage of the source

Table 1 Value of the maximum admitted inductance, which can be connected to the output of a source in relation to the idle voltage of the source

U ₀ [V]	L ₀ [μH]					
	Non-linear source			Linear source		
	IIC	IIB	IIA	IIC	IIB	IIA
3	6	25	32	11	44	56
6	4	17	21	8	31	40
10	1	5	7	1	22	28
11	1	3	4	5	19	25
12	1	1	1	3	16	22
15	1	1	1	1	1	1
20	3	2	2	5	3	1
25	20	9	3	19	6	7
30	57	26	13	25	37	9
40	770	170	15	270	95	31
50	130	1300	220	130	210	310

4. LIMITATIONS FOR CAPACITIVE MICRO/MINI-DRIVINGS

There follows a presentation of tables with values and of charts for the maximum admitted capacitance in relation to the maximum voltage of the source (U₀), gas / vapours subgroup and to the source type.

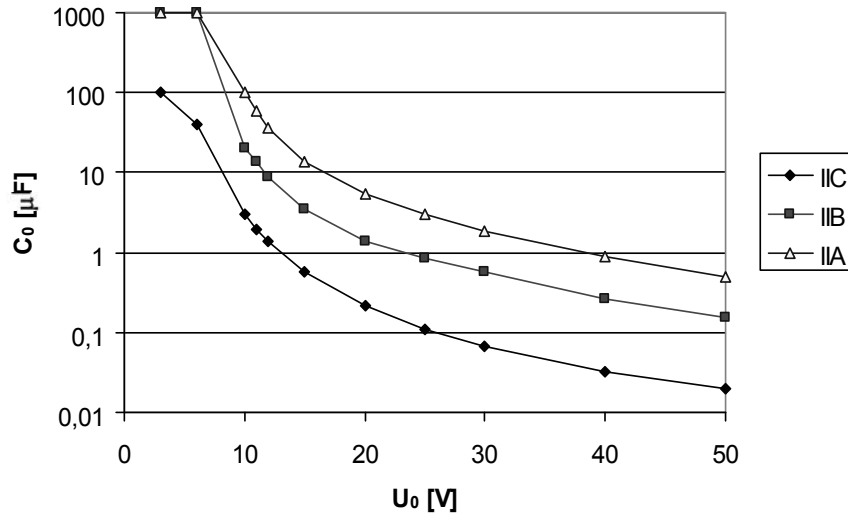


Fig. 3 – Value of the maximum admitted capacitance which can be connected to the output of a source in relation to the idle voltage of the source

Table 2 - Value of the maximum admitted capacitance which can be connected to the output of a source in relation to the idle voltage of the source

U ₀ [V]	C ₀ [μF]		
	IIC	IIB	IIA
3	100	1000	1000
6	40	1000	1000
10	3	20	100
11	1,97	13,8	60
12	1,41	9	36
15	0,58	3,55	14
20	0,22	1,4	5,5
25	0,11	0,84	2,97
30	0,066	0,56	1,82
40	0,033	0,26	0,88
50	0,02	0,15	0,49

5. LIMITATIONS OF POWER FOR SOURCES THAT SUPPLY MICRO/MINI-DRIVINGS

There follows a presentation of tables and of charts for the maximum admitted capacitances in relation to the maximum voltage of the source (U₀), gas / vapours subgroups and the source type.

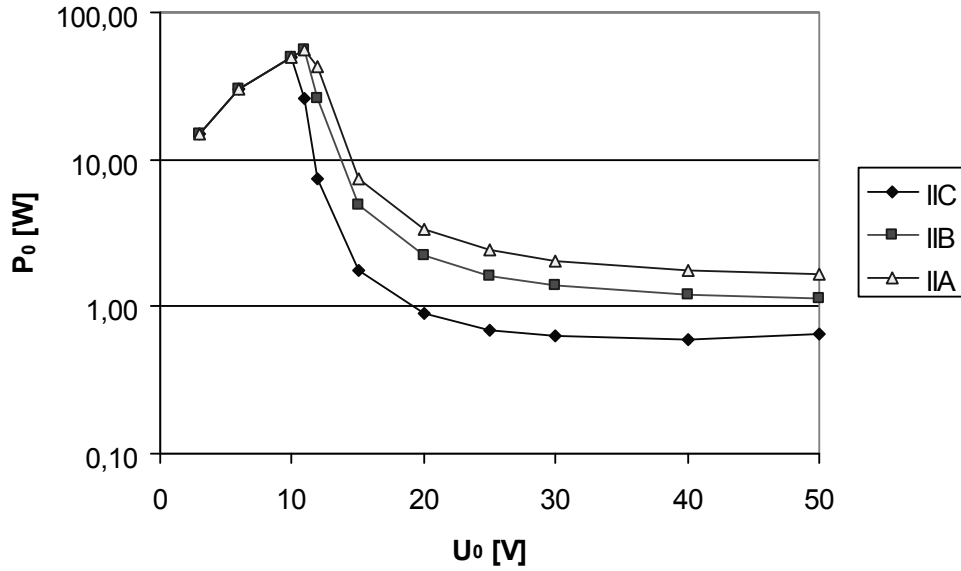


Fig. 4 – Value of the maximum admitted power that can be delivered by a non-linear source to the apparatus located in hazardous area

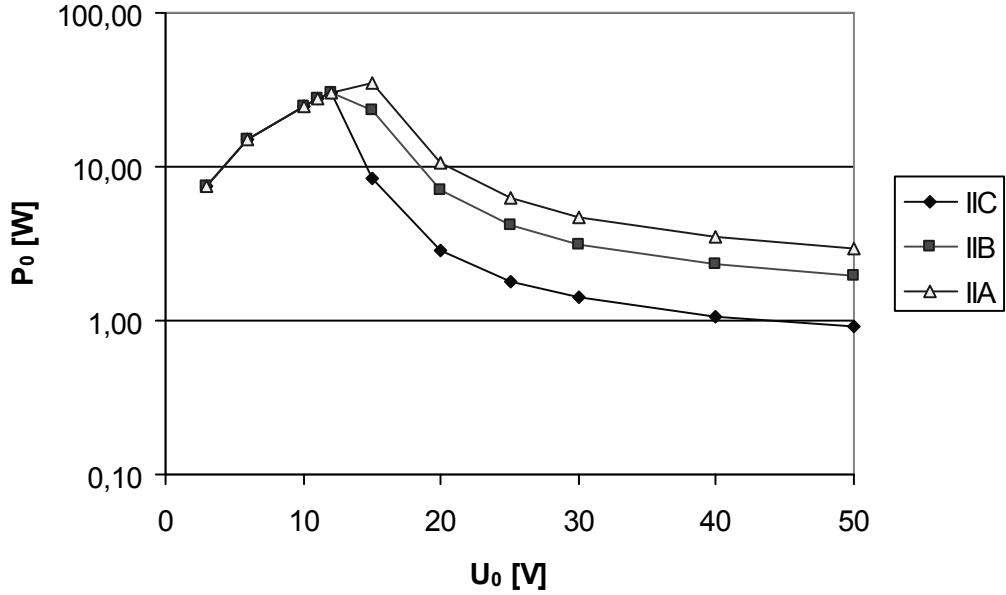


Fig. 5 – Value of the maximum admitted power that can be delivered by a linear source to the apparatus located in hazardous area

Table 3 – Values of the maximum admitted power that can be delivered by a source to the apparatus located in a hazardous area

U ₀ [V]	P ₀ [W]					
	Non-linear source			Linear source		
	IIC	IIB	IIA	IIC	IIB	IIA
3	15,00	15,00	15,00	7,50	7,50	7,50
6	30,00	30,00	30,00	15,00	15,00	15,00
10	50,00	50,00	50,00	25,00	25,00	25,00
11	26,40	55,00	55,00	27,50	27,50	27,50
12	7,42	26,05	42,18	30,00	30,00	30,00
15	1,77	4,97	7,43	8,47	23,27	35,35
20	0,90	2,24	3,34	2,86	6,97	10,49
25	0,70	1,63	2,43	1,81	4,19	6,29
30	0,63	1,38	2,04	1,41	3,14	4,73
40	0,60	1,20	1,76	1,06	2,30	3,46
50	0,65	1,15	1,65	0,93	1,95	2,90

6. CONCLUSIONS

Since the specific standards contain the maximum admitted values for inductances and capacitances valid for linear sources only, we have used an expert software for simulating such types of circuits within the range 0-5A, 0-50V.

As a result of this study, we have noticed that approximately above 12V, the admitted inductance that can be connected to the output of a source shall rise a lot and the admitted capacitance that can be connected to the output of a source and the maximum admitted power delivered by a source shall diminish to a great extent when the value of the idle voltage increases.

Under 12V for the idle voltage of the source, the variation of the parameters L₀, C₀ and P₀ is being smoothed mainly because of the range limitation for currents (0-5A) required by the software.

The analysis in this paper makes reference only to strict capacitive and strict inductive apparatus.

REFERENCES

- [1] SR EN 50020:2003, *Electrical apparatus for potentially explosive atmospheres. Intrinsic safety "i"*

POWER SUPPLY AND DESIGN PROBLEMS OF LONGWALL INSTALLATIONS OF RATED VOLTAGE ABOVE 1 kV IN UNDERGROUND COAL MINES

PIOTR GAWOR*, **SERGIUSZ BORON****,

Abstract: The power requirements of modern longwall systems in underground coal mines have increased to over 2,5 MW of total demanded power. The article presents selected problems of supplying such installations from existing power networks in coal mines. Problems of assuring the required quality of energy and safety of operation as well as some problems related to the starting of face conveyors have been presented.

Keywords: underground mining, electrical safety, power systems, longwall electrical installations.

1. INTRODUCTION

The tendency to increase the effectiveness of coal extraction process in Polish coal mines and the evolution of electrical equipment resulted (in recent years) in significant increase of power demand in longwalls. The rated power of particular motors reached 500 kW while total power of electrical equipment in longwall (coal shearer, face conveyor, stage loader, crusher, pumps etc.) can exceed 2,5 MW. Supplying such a network with 1000 V (voltage usually used in conventional longwalls) is impractical or even impossible, mainly because of excessive voltage drops, requirements for short circuit protection and limited conductor size of cables. The main method of improving supply quality is to increase supply voltage.

* *Ph. D., D.Sc. Department of Electrical Engineering and Process Control in Mining Faculty of Mining and Geology, Silesian University of Technology, Gliwice, Poland*

** *Ph. D., Department of Electrical Engineering and Process Control in Mining Faculty of Mining and Geology, Silesian University of Technology, Gliwice, Poland*

2. CHARACTERISTICS OF MIDDLE VOLTAGE LONGWALL NETWORK

Utilization of middle voltage (in Poland usually 3,3 kV) to supply longwall equipment gives following advantages:

- lower currents at start-up and during normal operation of motors, lower voltage drops and lower energy losses in longwall installation,
- possibility of decreasing cable sizes,
- possibility of increasing the distance between the power station (supplying transformer) and the coal face even to 3000 m, what eliminates the necessity of moving the transformer station during exploitation of longwall and eliminates the heat emanated by the transformer from the air ventilating the face.

However, the decision to use higher voltage, must be preceded by the analysis of technical and economical aspects, taking into account, among others, the following factors:

- high cost of electrical equipment, motors and cables rated 3,3 kV, justified only in high-capacity longwalls,
- suitable parameters of mining power system, especially short circuit power,
- increase of electrical hazards.

As far as the safety is concerned, Polish mining regulations introduce some specific (in comparison to low voltage networks) requirements for MV longwall installations:

- increased to 2,0 sensitivity coefficient of short circuit protection devices (additionally, the short circuit protection in the transformer station should work as a backup for protection in the starter with sensitivity coefficient 1,5),
- limited to 2,5 μF phase-to-earth capacitance of cables in the network,
- necessity to use special double-screened flexible cables.

One of the tasks of the designer of longwall installation is to determine the maximum rated power of motors that can be supplied from given MV network and to calculate the longest possible distance between the power station and the coal face. The most important factors limiting these quantities are:

- the voltage drop under normal condition; the supply voltage of motor shouldn't be lower than $0,95 \cdot U_n$, the problem is that the actual value of this voltage depends not only on voltage drops in designed installation, but also on the voltage at the bus-system of the switchgear supplying the longwall, which sometimes is difficult to estimate,
- requirements for the sensitivity coefficient (defined as a ratio of minimum short circuit current to the setting of short circuit protection); to fulfill this requirement the minimum short circuit current has to be at least 2,4 times greater than the maximum operating current (during the start-up of the motor),
- voltage drop at the motor start-up; the mechanical torque produced by the motor is approximately proportional to the square of the voltage and for some of longwall drives, which require relatively high torque at the start-up (especially face conveyor), it may be difficult or even impossible to start a loaded motor.

3. PROBLEMS OF FACE CONVEYORS SUPPLY

The biggest problem in longwall installations design is to provide satisfactory supply conditions for face conveyors. The extremely high friction forces associated with conveying system require big torque that has to be produced by electrical motors. A typical drive consist of 2÷3 induction squirrel-cage motors of total rated power often exceeding 1 MW. With the exception of systems with fluid coupling (described below), these motors are simultaneously started what results in very big voltage drop.

The situation is complicated by the fact, that the nominal in-rush current of some types of motors exceeds $7 \cdot I_n$. In the traditional drive system all the motors of face conveyor are started by the contactor starter. The main disadvantage of this system is that, due to excessive voltage drops, it's sometimes impossible to provide required starting torque and low voltage level at the starter may be a reason of contactor dropout. Furthermore, the in-rush current of 2 or 3 motors supplied from one transformer outlet can be too high to provide required sensitivity of short circuit protection in the power station.

The maximum power rating of a single motor that can be supplied in the longwall depends (apart from rated voltage of the motor) mainly on the parameters of supplying network (short circuit power), the cables length and size and the nominal parameters of the motor (in-rush current and starting torque). The simplified scheme of one motor supply is shown on fig. 1.

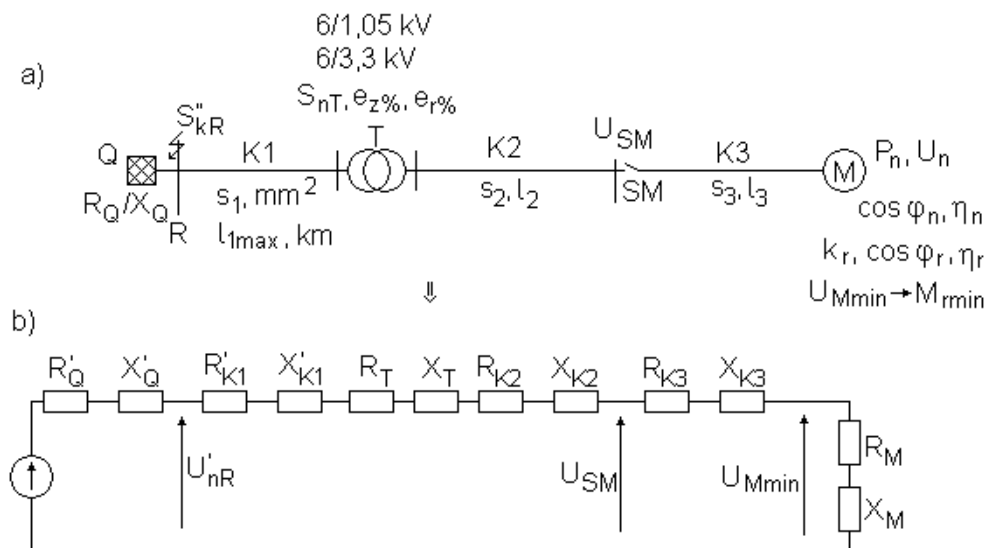


Fig. 1. Simplified scheme of motor supply

The most important elements of the scheme are: power system Q characterized by the short circuit power S_{kr}'' , switchgear R , power station T , starter SM , motor M and cables $K1$ to the power station, $K2$ to the starter and $K3$ to the motor.

One can derive the equation that helps to predict the dependence between the short circuit power of the distribution network and the maximum rated power of a motor [1]:

$$S_{kR}^n = \frac{1,1 \cdot U_{nR}^2 \cdot \beta}{\Theta^2 \cdot \sqrt{k_s^2 + 1} \cdot \left[\frac{U_n^2 \cdot (U_{SM} - U_{M \min})}{c \cdot U_{M \min} \cdot P_n} \cdot 10^3 - \alpha \right]} \quad (1)$$

Where:

U_n – rated voltage of the motor, kV

U_{nR} – rated voltage of the distribution network, kV

U_{SM} – operating voltage at the starter before start-up of the motor, kV

$U_{M \min}$ – minimum required voltage on the motor at the start-up, kV

P_n – maximum rated power of the motor in the longwall, kW

$k_s = R_Q/X_Q$ – ratio of supplementary resistance to reactance of the distribution network ,

Θ - ratio of primary to secondary rated voltage of the transformer,

c, β - coefficients characterizing the properties of motor during the start-up and properties of supply network:

$$c = \frac{k_r \cdot I_n}{I_n \cdot \cos \varphi_n \cdot \eta_n} \quad \beta = k_s \cdot \cos \varphi_r + \sin \varphi_r$$

I_n – nominal current,

I_r – in-rush current,

$k_r = I_r/I_n$,

$\cos \varphi_n, \cos \varphi_r$ – power coefficients of the motor: nominal and at the start-up,

η_n – nominal efficiency factor of the motor,

α - coefficient depending on the parameters of the network:

$$\alpha = (R_{K1}' + R_T + R_{K2} + R_{K3}) \cdot \cos \varphi_r + (X_{K1}' + X_T + X_{K2} + X_{K3}) \cdot \sin \varphi_r$$

For the typical parameters of the distribution network and longwall installation the exemplary dependence of $P_{n \max}$ on the S_z for different required voltage levels during the start-up of the motor is shown in the fig. 2 [1].

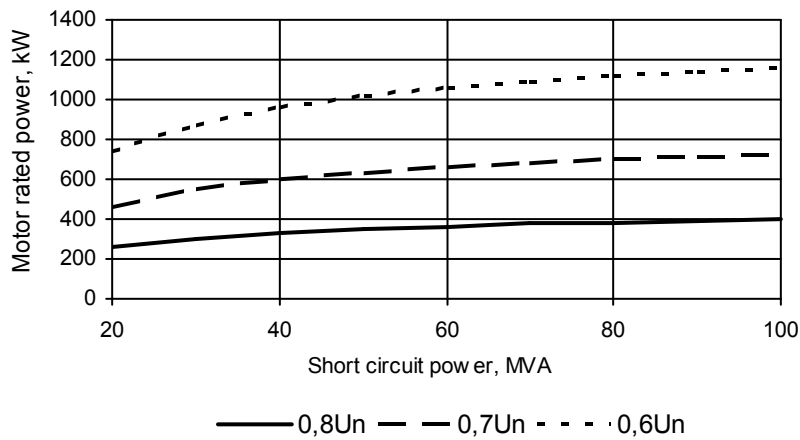


Fig. 2. Maximum power rating of the 3,3 kV motor as a function of short circuit power of MV distribution network

Typical values of short circuit power in the underground distribution networks of coal mines vary between 40÷100 MVA, so, as can be seen in the fig. 2, it may be difficult or impossible to start a motor rated 400 kW or more (one should remember that the face conveyor drive consists of more than one motor). To avoid problems with the low voltage level, in recent years another elements of face conveyor drive system are introduced: two-speed motors, thyristor starters (so called soft-start devices) and fluid coupling.

3.1. Two-speed motors

Two-speed motors used in face conveyor drives are built for a constant torque with RPM ratio 1:3 or 1:2. The full analysis of starting conditions, especially of phenomena during switching the speeds is difficult, because it requires the knowledge of actual motor load, switching time etc. The main advantages of two-speed motor drives are:

- lower in-rush current on the slow speed (practically two times lower than of single-speed motor) which helps to keep the voltage drop within acceptable limits and makes possible to fulfill the requirement of protection sensitivity coefficient,
- high starting torque on the slow speed which makes possible to start and unload even overloaded conveyor.

To take the full advantage of two-speed motors the controller has to be able to switch from slow speed to fast in very short time.

3.2. Thyristor starters

Utilizing thyristor starters makes possible to increase the voltage and the torque gradually during the start of the motor. Controller can keep the current at the

previously set level (so called current start) or just increase the voltage from the initial value (voltage start). The main advantage of thyristor starters is limiting mechanical stresses to shafts, clutches, chains of face conveyor etc. However, the designer of the network has to consider the most disadvantageous conditions, so, when calculating voltage drop or sensitivity of protection, one must assume that the load torque of the motor is maximum. The voltage level, at which the motor starts to rotate, depends on the mechanical load of driven machine, which means that, if the conveyor is overloaded, the starter won't limit the current (the motor will start only when the voltage is at its maximum). In fact, from the designer of electrical installation point of view, there could be no difference in the results of the calculations between contactor and thyristor starter.

In some applications thyristor starter works with two-speed motor, usually with the slow speed started by the contactor and fast speed by the thyristor starter. The most important benefits of this system is the possibility of unloading overloaded face conveyor (high torque on slow speed) and after that soft start of fast speed with limited stresses to the mechanical elements and limited in-rush current.

3.3. Drives with fluid coupling

In this system the torque is transferred from the motor to the reduction gearbox of a drive through a fluid coupling. The amount of transferred torque can be changed by adjusting fluid level in the coupling. The advantage of this system comes from the fact, that the motor starts practically unloaded, so there is no problem with the voltage level at the motor. During the start of the face conveyor even the critical moment of the motor can be utilized. Motors designed to work with fluid coupling have low starting torque (e.g. $1,2 \cdot M_n$) and high critical torque (e.g. $3,2 \cdot M_n$). The nominal in-rush current of these motors is usually relatively high (e.g. $7,8 \cdot I_n$), what can cause too low voltage level at the starter, but on the other hand, motors don't need to be started simultaneously, which limits the voltage drops and problems with sensitivity of short circuit protection.

4. CONCLUSIONS

1. The possibility of supplying high power electrical equipment from existing power system in underground coal mine is conditioned mainly by:
 - short circuit power of distribution network,
 - method of starting the motors.
2. Proper start of face conveyor supplied from power system with short circuit power not greater than 60 MVA may require using two-speed motors or fluid couplings.
3. The maximum distance between the transformer station and the coal face can be limited by:
 - excessive voltage drops during normal operation,
 - too low starting torque of the motor due to low voltage level caused by high in-rush currents,

- required sensitivity coefficient of short circuit protections in the transformer station or in the starter,
- too low voltage at the contactor of the starter during start-up of the motors.

REFERENCES

[1]. **Gawor P.:** *Prognosis of possibilities of feeding the high-efficiency wall complexes in the existing distribution network of coal-mine.* International Conference “Balanced Development in Mining”, Gliwice, Poland 2005 r.

[2]. **Boron S.:** *Designing of medium voltage mining networks in longwall faces – selected problems.* International Conference “Balanced Development in Mining”, Gliwice, Poland 2005 r.

PROBLEM VIEWING THE DRIVE OF LARGE POWER MACHINES FROM COAL EXTRACTION INDUSTRY

ORBAN MARIA*, POPESCU CRISTINEL**, CURELEANU SORIN***,
BLANARU LIVIU***

Abstract: In the exploitation process, the technological lines contain bucket wheel excavators (BWE), belt conveyers (BC) and dumping machines (MH) for having a large productivity and the other machines which are driving using asynchronous motors (630 kW, 6kV, 71A, 980 ro/min, $k=0,92$). It is recommended to reduce the electrical energy consumption through choosing a transmission raport in dependence with the structure of the electrical system drive.

Key words: energetically ground, technological flux, lignite, electrical energy consumption

1. INTRODUCTION

Taking into account the competition on the energetically market, energetically grounds as Rovinari, Turceni, Isalnita, etc. was developed from 2004. The basic source is the lignite which is extracted in the lignite open pits from Oltenia coal basin.

The price of solid fuel, gases and oil increases from day tot day due to the ecological restrictions which are against of mining activities. The achievement costs are bigger and bigger as the lignite open pits from energetically grounds become 'center of cost' and gives the price of RON/tonne utile or Ron/kWh.

It is necessary that each of economic agent has to take technological and technical measurements of restructure, to reduce the electrical energy consumption.

The Energetical Grounds (CE) Rovinari and Turceni, Isalnita-Craiova represents the reorganization and restructure result of electrical energy activity. The lignite open pits are integrated as the cost parts of energy production in the energetical

* *PhD Associate Professor University of Petrosani*

** *PhD Lecturer University of Petrosani*

*** *PhD Student Eng. University of Petrosani*

grounds. The lignite production is not subsidized in Romania. The lignite consumption will be about 30 mil.tone/year in 2005 as well as in 2010.

The asynchronous motors in schortcut or induction motors are frequently used in electrical drives for open pits machines. The motor 's power are from 100 to 630 kW and the open pits costumers are supplied from transformer stations about 2x4MVA, 20/6 kV using different electrical cables.

The lignite open pits from Oltenia are equipped with technologies in continous flux characterized by: the lignite deposits are excavated by bucket wheel excavators (BWE) with the following capacities 470 l, 1300 l, 1400 l, 2000 l and productivity about 1680 m³/h - 6500 m³/h; the belt conveyer has the productivity about 1400 - 12500 m³/h ; the laying down machines have capacity about 2500 -12500 m³/h.

2. THOROUGHGOING STUDY OF PROBLEM

For avoiding the construction of some asynchronous motors with reduced speed for to drive mechanisms of mining tools it is necessary to accustom oneself the power of motor to the gauge of tools. To fulfill this reason, the transmission of power from motor to work mechanism is made through the transmission mechanism as shown in the picture no. one. In the dynamic stage the drive motor develops un torque necessary to accelerate the own masses and to win the total torque (static and dynamic) reported to the motor shaft.

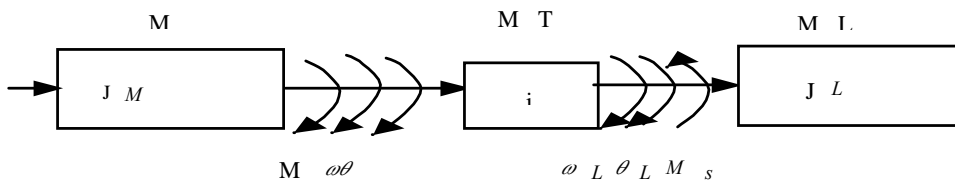


Fig.1 The drive structure

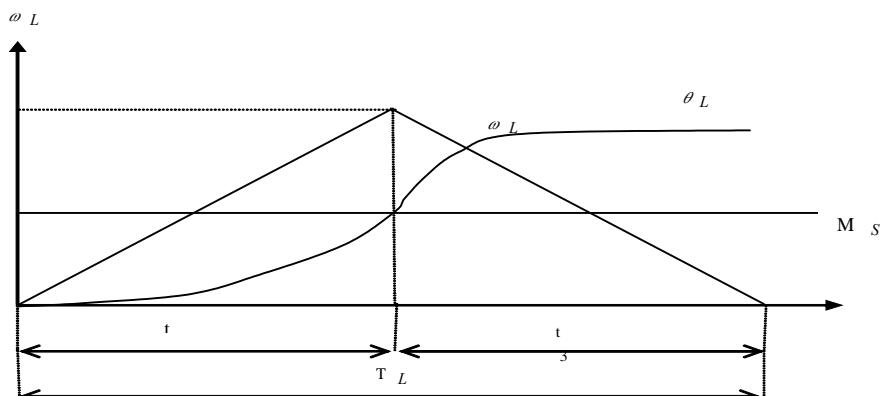


Fig.2 Triangle diagram

The transitory stage duration it is as so short as the energetically transfer of shaft is large. This transfer is depending by the transmission rapport of the mechanism and it is maximum when the transmission rapport is optimal, the rapport leads to a minimum time of starting, of stopping and change the sense from some mining tools as BWEs, BCs and MHs resulting from obtaining the biggest accelerations on the motor's shaft.

The moving equation is:

$$M = M_s + J \frac{d\omega}{dt} \quad (1.1)$$

The transmission mechanism as transformer of moving (M – motor; MT – transmission mechanism; ML – work mechanism) is characterized by the transmission rapport:

$$i = \frac{\omega}{\omega_L} = \frac{\theta}{\theta_L} \quad (1.2)$$

In case of driving with transmission mechanism and trapezium diagram (this is the most useful case used in site) it is necessary that the starting (acceleration till the stage speed) and breaking (reduction from the stage speed to zero) to be made in the shortest time and have an energy consumption as small as is possible. For simplification it is takes into account that the acceleration is made using a triangle diagram (fig.2) described by the speed and moving integral:

$$\omega_L = \int \dot{\omega}_L dt, \theta_L = \int \omega_L dt \quad (1.3)$$

The global displace made by the mechanism on the entire cycle of diagram is:

$$\theta_L = \int_0^{t_1} \omega_L dt + \int_0^{t_2} \omega_L dt = \frac{1}{2}(t_1 + t_2)\omega_L \quad (1.4)$$

If the transmission mechanism has an unitar efficiency (as BWE, BC, etc) and rapping all the parameters to the mechanism shaft and taking into account the conservation power and cinetical energy rule, results:

$$M_{red}\omega_L = M\omega, \quad M_{red} = M \frac{\omega}{\omega_L} = Mi, \quad \frac{1}{2}J_{red}\omega_L^2 = \frac{1}{2}J_M\omega^2 + \frac{1}{2}J_L\omega_L^2,$$

$$\text{Or} \quad J_{red} = J_M i^2 + J_L \quad (1.5)$$

From the equation no.1-1 and for starting and breaking periods of mechanism shaft we can obtain the acceleration express for these period:

$$\varepsilon_p = \frac{d\omega_L}{dt} = \frac{iM_p - M_s}{i^2 J_M + J_L}, \quad \varepsilon_f = \frac{d\omega_L}{dt} = \frac{iM_f + M_s}{i^2 J_M + J_L} \quad (1.6)$$

The above expressis show the acceleration and deceleration evolution in dependence with the driving system strucure and by the optimal transmission rapport.

If we take into account the inertial moments $J_M, J_L = \text{constant}$ and the torques $M, M_s = \text{constant}$, integrating rel (1.6) we determine the acceleration time t_1 and deceleration time t_3 and total time t_L which depend by transmission rapport and it is possible to be esteem the optimization criteria for transmission mechanism:

$$t_L = \sqrt{2\theta_L} \cdot \sqrt{(i^2 J_M + J_L) \cdot \left(\frac{1}{iM_p - M_s} + \frac{1}{iM_f + M_s} \right)} \quad (1.7)$$

3. DETERMINING THE OPTIMAL RAPPORT OF TRANSMISSION

We have to determine that transmission rapport which assure maximum values for acceleration and deceleration (rel.1.6), or to assure the maximum change of energy to the work mechanism shaft, or to minimize the work time (1.7) for a given value of work mechanism displace (rel.1.4).

In this case the minimum necessary condition of work results through make the derivate, of criteria function in dependence with transmission rapport, to be zero:

$$\frac{M_p}{M_s} = p, \quad \frac{M_f}{M_s} = f, \quad \frac{J_M}{J_L} = m_j \quad (1.8)$$

If the drive function is supposing to be without load $M_s = 0, p \rightarrow \infty, f \rightarrow \infty$, the above condition becomes:

$$i^2 m_j - 1 = 0 \Rightarrow i_{opt} = \sqrt{\frac{1}{m_j}} = \sqrt{\frac{J_L}{J_M}} \quad (1.9)$$

The acceleration in the starting time is limited by the restrictions of the developed torque of motor while the deceleration of breaking can be increase through the static breaking couple and/or working with a supplementary break, but the maximum acceleration (minimal time) problem appears for the starting period.

Canceling the derivate from (1.6) we can obtain the maximum acceleration condition (1.10) and the optimal transmission rapport(1.11):

$$i_{opt}^2 - 2i_{opt} \frac{M_s}{M_p} - \frac{J_L}{J_M} = 0 \quad (1.10)$$

$$i_{opt} = \frac{1}{p} \left(1 + \sqrt{1 + \frac{p^2}{m_j}} \right) = \frac{M_s}{M_p} + \sqrt{\left(\frac{M_s}{M_p} \right)^2 + \frac{J_L}{J_M}} \quad (1.11)$$

The maximum value of acceleration results through replace the transmission rapport with its optimal rapport in (1.6):

$$\varepsilon_{p \max} = \frac{M_p}{J_M} \cdot \frac{i_{opt} - \frac{M_s}{M_p}}{i_{opt}^2 + \frac{J_L}{J_M}}$$

(1.12)

If we consider (1.11) and replace in (1.12) we obtain:

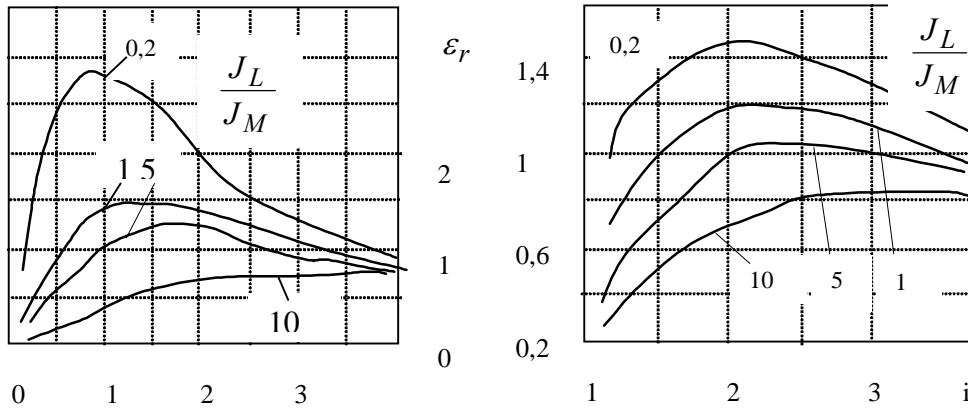
$$\varepsilon_{\max} = \dot{\omega}_{l \max} = \frac{M_p}{J_M} \cdot \frac{\sqrt{\frac{M_p^2}{M_s} + \frac{J_L}{J_M}}}{\left(\frac{M_p}{M_s}\right)^2 + \frac{J_L}{J_M} + \sqrt{\left(\frac{M_p}{M_s}\right)^2 + \frac{J_L}{J_M}}}$$

(1.13)

Making an rapport with (1.6) to its maximum value (1.13) result:

$$\varepsilon_r = \frac{\dot{\omega}_L}{\dot{\omega}_{L \max}} = 2i_{opt} \frac{J_M}{J_p} \cdot \frac{iM_p - M_s}{i^2 J_M + J_L} =$$

$$2 \left(\frac{M_s}{M_p} \right) + \sqrt{\left(\frac{M_s}{M_p} \right)^2 + \frac{J_L}{J_M}} \cdot \frac{i - \frac{M_s}{M_p}}{i^2 + \frac{J_L}{J_M}} \quad (1.14)$$



a) for $\frac{M_s}{M_p} = 0,5$

b) for $\frac{M_s}{M_p} = 2$

Fig.3 The relative acceleration in dependence with transmission rapport

4. CONCLUSIONS

From picture no.3 we can draw some conclusions:

- the optimal values of transmission rapport increase in the same time with increasing of $\frac{J_L}{J_M}, \frac{M_s}{M_p}$ so at the driving of work mechanisms with large static and

inertial torques (as belt conveyers) is necessary to use a reduction while driving of work mechanisms with small static and inertial torques the direct coupling is enough.

- at the starting the acceleration increase to maximum value and then it decrease in short spets with the increasing of transmission rapport so in the site the transmission rapport is equal with the optimal rapport.

- the maximum values of acceleration are as bigger as the rappers $\frac{J_L}{J_M}, \frac{M_s}{M_p}$ are smaller.

-the obtained results are available as for trapesium diagram as the triangle diagram and for changing sense too, both of them has a acceleration period and a deceleration period.

It is requiring to put a corelation between the driving motor, the transmission mechanism and work mechanism to assure the maximum power transfer (an optimal transmission rapport of reductor) when the component elements of driving system are choosing.

REFERENCES

- [1.] Ghita Constantin Elemente fundamentale de masini electrice, E. Printech, Bucuresti 2002
- [2.] Orban M. Daniela Modernizarea actionarilor electrice la excavatoarele din carierele de lignit in vederea cresterii eficientei lor, teza de doctorat , Petrosani, 1999
- [3.] Manolea Ghe., s.a. Actionari electromecanice, Reprografia Univ. din Craiova, Craiova 2000

REFLECTIONS ON THE QUALIFICATION OF THE GENERATION UNITS FOR PROVIDING THE SERVICE CONSISTING IN REACTIVE POWER WITHIN THE VOLTAGE SECONDARY CONTROL RANGE

VICTOR VAIDA*

Abstract: Qualifying the generation units for providing the reactive power within the secondary control range is an approach in increasing the efficiency and operation reliability of the power plants as well as of the power system. The synchronous generator P/Q diagram plotting by testing is needed in order to have the generation unit qualified for the secondary control. At Deva-Mintia Power Plant, P/Q diagrams have been plotted for 5 generation units, which will be declared fully qualified.

Keywords: system services, voltage secondary control range, P/Q diagram

1. INTRODUCTION

The qualification of the power generation units for providing the system service consisting in reactive power within the voltage secondary control range is achieved in accordance with the provisions of the operation procedure for qualifying the internal producers as system services providers, elaborated by Transelectrica (TEL - 07 VOS – DN/154).

Qualification criteria in this case are:

The excitation control system should ensure the variation of the reactive power supplied/absorbed by the Transmission Network or by the distribution network, in view of a quick and stable offset of the

- voltage variations that occur during normal operation;
- The Automatic Voltage Regulator should act continuously, free of any instability, on the entire operation range of the generator;
- The Generator should be able to repeatedly sweep the reactive power range, within the limits of the P/Q diagram for which it was designed;

* *Prof. Dr. Eng. S.C. Electrocentrale Deva S.A.*

- The generator should be able to provide the rated active power at any operation point between $\cos \phi = 0.85$ inductive and $\cos \phi = 0.95$ capacitive;
- The value of the reactive power delivered in stable operation should be fully available for voltage variations of $\pm 5\%$ in the 400 kV network and of $\pm 10\%$ in the 220 and 10 kV networks;
- There should exist means of measurement and control of the reactive energy generated/absorbed within the voltage secondary control ranges;
- The generator P/Q diagram should be plotted.

The ANRE procedure, code 35.1.432.1.01, defines the terms and conditions of payment for the voltage control service by generating/absorbing reactive energy, in accordance with the operation P/Q diagram of the unit.

The above mentioned procedure has defined the voltage secondary control ranges on the P/Q diagram: Q_1 – inductive area and Q_2 – capacitive area, situated between the maximum operation limit and a limit jointly agreed by the grid operator and the system service provider.

To practically implement the ANRE regulations regarding the voltage secondary control, the real operation P/Q diagrams of the synchronous generator need to be accurately determined by tests and measurements.

The operation in inductive mode is conditioned by the limit of the excitation current and by the stator current limit, both determined without exceeding the allowable temperatures.

The operation in capacitive mode is conditioned by the warming up at the front end of the generator stator, i.e. at the stator front teeth (the last laminated plate bundle with recesses).

2. THE P/Q DIAGRAM OF SYNCHRONOUS GENERATORS

The P/Q diagrams of the synchronous generators are needed also for making planning, operation and operation analysis more effective

The P/Q diagrams allow the dispatcher of the National Power System to load and unload the synchronous generator reactive power according to the system's needs and the reactive power resulting from the balancing market.

The theoretical P/Q diagrams and those plotted by testing are used for calculating static and transient stability, operational planning and implementation of the normal operation configurations of the National Power System.

In accordance with the Transmission Grid Code (TGC), the power plants shall submit the Transmission System Operator (TSO) the theoretical P/Q diagrams for the new and rehabilitated units when they obtain the permit to connect to the grid, while for the units already in operation they shall submit actual P/Q diagrams plotted by testing.

In accordance with the TGC, the TSO may request the electricity producers to perform some tests to prove that the respective generators are able to generate reactive power according to the submitted data. Thus the TSO dispatcher may order the loading/unloading of the tested unit to $P_{\min \text{ stable}}$ and $P_{\max \text{ stable}}$ and shall create all the grid

conditions necessary for such loading/unloading with the needed maximum/minimum reactive power.

3. DETERMINING THE P/Q DIAGRAM OF THE SYNCHRONOUS GENERATORS OF DEVA-MINTIA POWER PLANT BY TESTING

P/Q diagram plotting by testing was performed at Deva-Mintia Power Plant, together with ICEMENERG, for 5 synchronous generators (no. 2, 3, 4, 5 and 6). We will present here the plotting method and the results thus obtained for the rehabilitated unit no. 3.

The synchronous generator no. 3

The Generator no. 3 is provided with stator winding direct cooling by distilled water, whilst the rotor windings and the active stator core are cooled by hydrogen in closed circuit inside the generator. The distilled water is circulated through the stator windings by means of pumps (water inlet pressure is 2.8 bar and the nominal temperature is 40 °C) and is cooled by means of heat exchangers installed inside the generator. The cooling hydrogen is circulated inside the generator by means of fans (of 3 bar rated pressure), installed on the rotor shaft and is cooled in gas coolers installed inside the generator body (hydrogen nominal temperature is 32°C).

The stator windings are three-phased, short-pitched, in two layers, made of copper bars with elementary conductors through which distilled water is circulated for cooling.

The stator cooling water pressure at the winding inlet should be lower (by approximately 0.2 bar) than the hydrogen pressure inside the generator to avoid hydrogen entering the distilled water system.

Before rehabilitation and upgrading, the rotor winding was provided with radial cooling using the hydrogen inside the generator and a system of cooling channels. When the rotor was upgraded, it was equipped with a more effective cooling system, with increased heat dissipation in the winding area, and new insulation materials of class F were provided, allowing the increase in the generator power, better operation in transient modes and a more effective cooling of the winding due to the subslot cooling system.

The generator has the following allowed operation modes:

- a) Normal operation at rated voltage, of 15.75 kV. When voltage variations are within 5% of the rated voltage, the generator provides the rated output with the nominal power factor ($\cos \phi = 0.95$), while the stator current varies by 5% from the rated current.
- b) The operation at asymmetric loads creates a rotating magnetic field of negative sequence, counter to the rotor magnetic field, therefore crossing the rotor field at double sequence. The effect of the asymmetric operation is the dangerous heating of the rotor, even if the current does not exceed the allowable values. The allowable negative sequence current should not exceed 8% of the stator rated current. The load and phases instability is obviously different for a period of time.

In case of an unbalanced short circuit, the duration of the short circuit should be so that the result of multiplying the inverse current square root by its duration (in seconds) does not exceed the number 8 [4].

c) If frequency varies within a range of 2% of the nominal value, the generator output does not change. However if the frequency variation is between 2% and 5% of the nominal value, the generator voltage and current do not change. The generator is not allowed to operate with a frequency exceeding the nominal value by more than 5%.

d) The generator output cannot be increased, if the water temperature at the gas cooler inlet decreases below 24°C. If the gas temperature increases over 33°C or the water temperature increases over 40°C, the generator output should be reduced (by 7.5% at an increase by 5°C, by 17.5% at an increase by 10°C, and by 52.5% at an increase by 15°C). Water maximum temperature at stator winding outlet is 75°C. If the cooled gas temperature exceeds 45°C, the generator output needs to be reduced, and if that is not enough then the generator should be disconnected from the grid.

e) From the process point of view, the following issues need to be followed:

- If stator winding temperature exceeds 75°C, the generator should must be decreased;
- If cooling water flow decreases to 18 m³/h (the rated flow is 30 m³/h), an alarm is generated, and the generator trips when the flow is 13 m³/h, with a 2-minute delay.
- The cooling water conductivity must not exceed 13 μS/cm (the normal value is 2.5 μS/cm).
- The generator is not allowed to operate if there are water leakages in the stator windings.
- The generator is not allowed to operate with a hydrogen pressure that is 10% less than the 3 bar nominal pressure or with purity less than 95%.

f) The operation of the generator with underexcitation is limited by the heating of the generator front ends and by the stability limit. The loading in capacitive mode can be determined on the P/Q diagram of the generator.

g) When operating in asynchronous mode, the loading of the generator must not exceed 40% of the nominal load during more than 5 minutes.

During the first 30 seconds of asynchronous operation, the generator load should be decreased to 60%, and during the following 90 seconds, down to 40% of the nominal load. During the asynchronous operation, the stator current must not exceed, on any phase, 110% of the nominal current.

However, according to the PE 130 regulations, it is forbidden to operate the generator in the asynchronous mode.

4. DETERMINING THE P/Q DIAGRAM OF THE UNIT 3 GENERATOR AT DEVA-MINTIA POWER PLANT

The methodology for determining the operation limits of a generator consists of determining the maximum heating in the generator's active parts: stator copper, stator core, rotor winding and generator stator front laminated plate bundles.

The following allowable temperature values are provided for our Unit 3 generator:

- Stator winding: $T_{Cu \max} = 105^{\circ}\text{C}$;

- Rotor winding: $T_{Cu\ ex}=115^{\circ}C$;
- Active core: $T_{Fe}=105^{\circ}C$;
- Hot distillate at stator winding outlet: $T_{DC}=85^{\circ}C$;
- Hot H_2 in the generator: $T_{Hc}=75^{\circ}C$;
- H_2 nominal temperature: $T_{Hn}=32^{\circ}C$;
- Cold distilled water nominal temperature: $T_{Dn}=40^{\circ}C \pm 5^{\circ}C$;

Maximum allowable heating of the generator active parts, relative to the cooling medium at the inlet are:

$$D_{T_{Cu\ max}} = T_{Cu\ max} - T_{Dn} = 60^{\circ}C$$

$$D_{T_{Fe\ max}} = T_{Fe\ max} - T_{Hn} = 73^{\circ}C$$

$$D_{T_{ex\ max}} = T_{ex\ max} - T_{Hn} = 83^{\circ}C$$

In view of plotting the P/Q diagram, the temperatures of these active parts of the generator are measured, as follows:

- For the stator winding bars, by means of RTD's installed between bars in the same slot;
- For the stator core, by RTD's installed between the bar at the bottom of the slot and the bottom of the slot;
- For the front teeth, by means of RTD's installed in the first stator radial groove and towards the outside of the first stator plate bundle;
- For the cold distillate temperature, local readings are used.

For the long-term inductive operation, the generator operation limits are determined by defining the maximum heating that can occur in the stator winding copper bars, in the stator magnetic core and the excitation rotor winding.

For the long-term capacitive operation, some thermal and electromagnetic phenomena occur, that affect only the front end of the stator, without having any impact on the central part of the stator, by greatly heating the stator teeth at the end of the generator stator. Therefore, the operation limits of a generator for long-time capacitive operation (underexcited) are related to the determination of the maximum heating occurring in the teeth area of the front laminated plate bundle, which, if exceeding the allowable values, may damage the insulation between stator plates and may cause local melting spots and ageing of the stator winding insulation.

During generator no. 3 testing, the following issues were observed:

- Verifying the generator nominal operation point in inductive mode at the maximum possible active power, $P=P_n$; $Q=Q_n$;
- Determining the maximum capacitive operation at the maximum active power $P=P_n$; $Q=Q_{cap\ max}$;
- Verifying the minimum active power operation point in inductive mode when operating with two boilers, $P=P_{min}$, $Q=Q_{ind\ max}$;
- Verifying the minimum active power operation point in capacitive mode when operating with two boilers, $P=P_{min}$, $Q=Q_{cap\ max}$;

Based on the performed tests and measurements, the actual P/Q diagrams were plotted, having sections determined by the maximum stator current, by the minimum rotor current and by other thermal aspects.

The static stability curves determine the generator capacitive operation.

Some tests were performed with the unit in operation with one or two boilers.

Reflections on the qualification of the generation units for providing the service consisting in reactive power within the voltage secondary control range

-144-

secondary control range

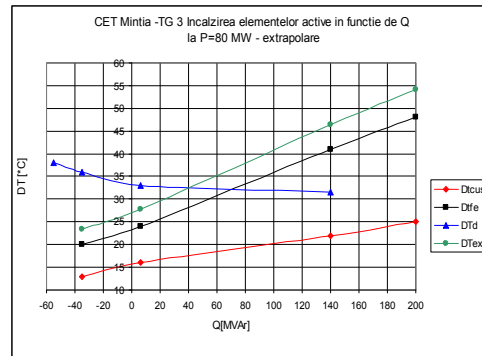
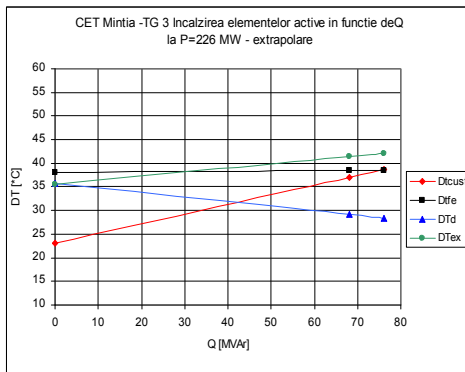
Further to the tests and the P/Q diagram plotting the following conclusions were reached:

The temperatures of the stator copper, stator core, stator front teeth and of the rotor excitation windings did not reach the maximum allowable values in any of the testing operation modes (Fig.1, 2, 3, 4, 5, 6).

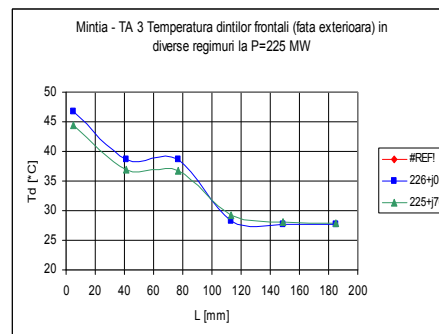
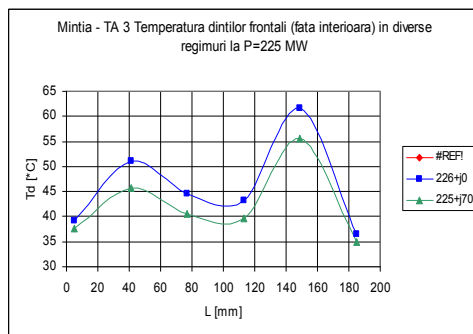
The curves extrapolated over the entire inductive operation range of the turbogenerator in accordance with the theoretical P-Q diagram, which represents the maximum operation range, do not generate limit values for the heating of the generator active parts (stator copper and core, and rotor copper) and they do not restrict the P/Q capacity diagram.

The capacitive operation is limited only by the static stability curve.

The charts in Figures 1 and 2 below present the heating of the active parts of the generator as a function of the reactive power Q, at P=226 MW and P=80 MW, corresponding to the operation of the unit with one or two boilers.



The charts in Figures 3 and 4 present the temperature of the front teeth, on the inner and outer side, at P=225 MW.



The charts in Figures 5 and 6 present the temperature of the front teeth, on the inner and outer side, at P=80MW.

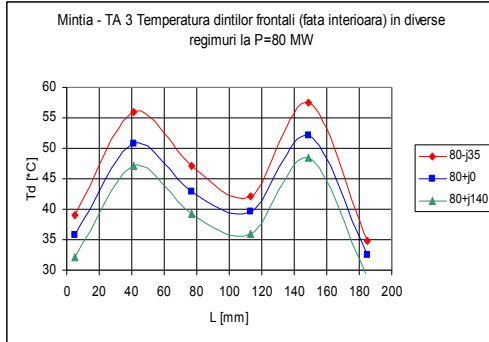


Fig. 5 Temperature of the front teeth (inner side) at P = 80 MW

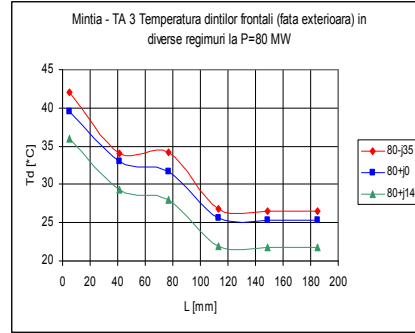


Fig. 6 Temperature of the front teeth (outer side) at P = 80 MW

5 – practical static stability curve (10% reserve) and the capacitive operation limit; For the rehabilitated generator no. 3, having the rated capacity of 234.8 MW (210 MW before rehabilitation), the nominal power factor of 0.95 (0.85 before rehabilitation), the nominal excitation current of 2164 A ($I_{exn}=2600A$ before rehabilitation), ALSTOM company had submitted a theoretical P/Q diagram.

By trials and testing the actual P/Q diagram was plotted, which confirmed the theoretical diagram (Fig.7).

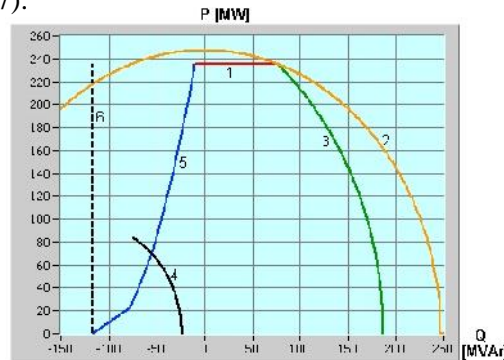


Fig. 7 Theoretical and actual P/Q at $U=U_n$, for Unit 3 generator

- 1 – turbine power limit;
- 2 – stator current limit;
- 3 – nominal rotor current limit;
- 4 – minimum rotor current limit;
- 6 – natural static stability curve.

The P-Q diagrams were plotted also for the operation with the generator terminal voltages of $0.95 U_n$, $0.9 U_n$, $1.05 U_n$, $1.1 U_n$.

The operation range of the generator within the P/Q diagram is given by the minimum area delimited by the curves of the diagram (Fig.8).

- 1 – turbine power limit;
- 2 – stator current limit;

- 3 – maximum rotor current limit;
- 4 – minimum rotor current limit;
- 5 – practical static stability curve (10% reserve) and the capacitive operation limit;
- 6 – natural static stability curve.

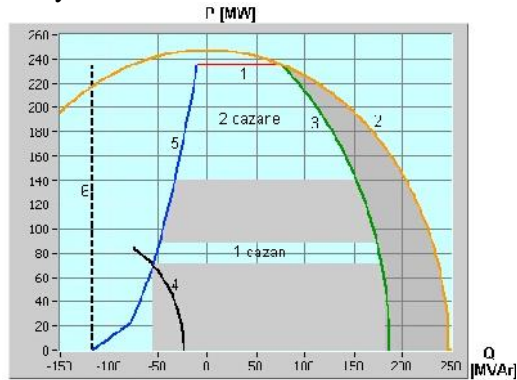


Fig. 8 Practical operation areas of the Unit 3 generator at $U=U_n$

The minimum excitation current of 658 A, was determined by calculation so that the generator should be able to operate with $P_{\min}=70\text{MW}$ and $Q=-56\text{MVA}_r$ at U_n .

When operating with two boilers, there are areas on the P/Q diagram where the generator cannot operate as the maximum and minimum power is defined from thermal point of view, $P_{\max}=234.8\text{MW}$, $P_{\min}=140\text{MW}$, and when operating with one boiler, $P_{\max}=90\text{MW}$; $P_{\min}=70\text{MW}$. The Unit cannot operate over the shadowed areas in Figure 8.

5. THE VOLTAGE SECONDARY CONTROL RANGES

The ANRE methodology for determining the prices for the power system services defines the procedure for calculating the qualified suppliers' rate for providing the reactive power needed for voltage control.

The voltage secondary control range is defined by those areas on the P/Q diagram of the synchronous generator where the generation/absorption of the reactive energy is costly and stressful for the generator and where the generated reactive power is paid for.

The primary voltage control range is defined by that area on the P/Q diagram of the synchronous generator where the reactive energy generated/absorbed is not paid for. The secondary voltage control ranges for the qualified generators are jointly agreed by the interested parties, the TSO and operators. The issue of the reactive power market emerged in Europe in 1996, and is not homogeneously regulated, each country having its own regulations in that respect. Using the same methodology as for the other generators of Deva-Mintia Power Plant, the diagram presented in Figure 7 is used for the Unit 3 generator, and the primary and secondary control ranges have been defined on this diagram. (Fig.9), when $U=U_n$ and the cooling media at the nominal temperatures.

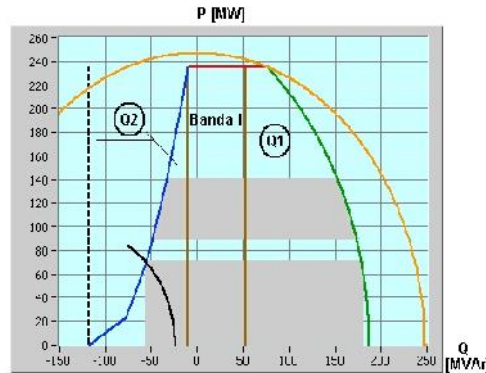


Fig. 9 Determinarea benzilor de reglaj al tensiunii pe diagrama P/Q.

For the inductive operation mode, the control ranges are defined by a straight line, $Q = 53 \text{ MVA}_r$, and for the capacitive operation mode by a straight line $Q = -10 \text{ MVA}_r$ (at the point where the nominal power line crosses the practical static stability curve). The secondary voltage control ranges are noted Q_1 and Q_2 .

From the presented facts it can be concluded that Unit no. 3, like the Units 2, 4, 5 and 6 for which the P/Q actual diagrams were plotted, is able to provide the system service consisting in the secondary voltage control, being capable of generating-absorbing reactive power.

6. CONCLUSIONS

1. The qualification of the generation units to provide system services is a feasible solution for improving the operation reliability and efficiency of the generation units as well as the power system as a whole.

2. The power units of Deva-Mintia Power Plant are capable of providing the system service that is the secondary voltage control, as they are able to generate/absorb reactive energy and can therefore be qualified finally and fully for providing this system service.

REFERENCES

[1]. **SC Tranelectrica.** *Operational Procedure for qualifying the internal producers as system services providers – Tel – 07VUS – DN/154.*

[2]. **ANRE.** *The ANRE procedure, Code 35.1.432.1.01./1999, regarding terms and conditions of payment for the services of voltage control by generating/absorbing reactive electricity.*

[3]. **SC Tranelectrica.** *Operational Procedure – The operation modes of the power generators within the National Power System. Code Tel. 07 III RS – DN/196.*

[4]. **ICEMENERG – SC Electrocentrale Deva.** *The determination by testing of the thermal limitations of the P/Q diagram in view of qualifying the Unit 3 Turbogenerator of Deva-Mintia Power Plant for providing the voltage control system service in accordance with the ANRE regulations – 2006.*

RESEARCHES ON THE RISK FACTORS WHEN USING ELECTRO-INSULATING MATERIALS IN CONSTRUCTION OF TECHNICAL EQUIPMENT INTENDED FOR USE IN AREAS WITH EXPLOSION HAZARDS

NICULINA VĂTAVU*, ADRIAN JURCA**, FLORINA MUNTEAN
BERZAN***

Abstract: The use of electro-insulating materials in construction of technical equipment intended for use in areas with explosion hazards give rise to many problems because of the microclimate which contributes to insulation impairing (ageing), thus leading to an increased risk of technical equipment malfunction and generating faults and/or explosions.

In order to prevention the faults (the risk factors) in technical equipment used in areas with explosion hazard, a basic measure is considered to be the requirement of improving their construction, having in view the use of electro-insulating materials with superior characteristics related to their behavior to surface currents leakage in wet conditions, to electric arc, to inflammability and to high temperatures.

The proof and the comparative tracking indices represent an important parameter to assess the performances of electro-insulating materials used in construction of technical equipment intended for use in potentially explosive atmospheres. The testing method simulates the specific requirements for the electric arc or creepage or clearance through the electro-insulating materials, and the results are being used for a proper adequate selection of the materials.

Keywords: explosion hazard, explosion risk, explosion protection, explosive atmosphere, comparative tracking indices

*D:Eng, senior scientific researcher III at INSEMEX Petroşani

**D:Eng, scientific researcher at INSEMEX Petroşani

***D:Eng, research assisstant at INSEMEX Petroşani

1. INTRODUCTION

Using of electro-insulating materials in construction of apparatus designed to be used in potentially explosive atmospheres raises important issues due to the microclimate conditions that have a decisive influence on their quality, regarding insulation degradation (ageing), so leading to an increased fault hazard in electric apparatus and, also, possible damages and/or explosions.

It has been ascertained that the main cause of insulation ageing is represented by the physical-chemical irreversible alterations within the electro-insulating material, due to exploitation stresses and mainly due to thermal stresses. Related to this, it has been found that the thermal breakdown voltage, respectively the dielectric rigidity of material may be increased by choosing materials with high thermal conductivity and lower electric conductivity and thermal coefficients; by decreasing the work environment temperatures (especially in the case of thick insulations, where inner layers show a slower cooling process); by diminishing the stress periods.

It is of a great importance that selection of electro-insulating materials to be made on a full knowledge of the electric, mechanic and thermal functions which must be fulfilled in operation conditions.

2. TECHNICAL CONDITIONS AND SAFETY REQUIREMENTS FOR THE ELECTRO-INSULATING MATERIALS

The electro-insulating materials used in construction of electrical equipment for potentially explosive atmospheres shall conform the safety requirements in the product standards, in the technical equipment general standards (with the specific types of protection) SR EN 60947/1-2001; SR EN 60079-0; SR EN 50018-2003; SR EN 50019-2003 and in the general standard of the electro-insulating materials used in construction of electrical equipment STAS 6790-1989 and also in the specific standards prescribing the test methods.

According to STAS 6790-1989, the electro-insulating materials, in form of test samples (specific to each test) shall have the following mechanical, electrical and thermal properties, and the test and check methods shall conform to the product standards, with the following completions:

- *Resistance to static bending* checked according to SR ISO 178 (bend stress at maximum load): minimum 50 MPa;
- *Resistance to Charpy shock* determined on samples without notch checked according to SR EN ISO 179-1, 2: minimum 2 kJ/m²;
- *Resistance to compression* checked according to SR EN ISO 604 (STAS 587 clause 3; 4; 6) : minimum 10 MPa ;
- *Volume resistivity*:
 - minimum 10⁸ Ωcm for equipment having $U_n \leq 127$ V;
 - minimum 10¹⁰ Ωcm for equipment having $U_n > 127$ V;
- *Surface resistivity*:
 - minimum 10⁸ Ω for equipment having $U_n \leq 127$ V;
 - minimum 10¹⁰ Ω for equipment having $U_n > 127$ V;

The surface and volume resistivity is verified according to the DECISION no. 27/2004 tat replaced partially STAS 6107 clauses 3; 4; 5; 6; 7; 8 ; 10, after

conditioning of 120 h at a temperature of $(40 \pm 2)^\circ\text{C}$ and a relative humidity of $(50 \pm 2)\%$, respectively SR HD 429 S1 and SR HD 568 S1.

- *The proof and comparative tracking indices in humidity conditions CTI and PTI:* minimum 175 V at 50 drops. The proof and comparative tracking indices are checked according to SR EN 60112-2004 (which replaced STAS 6205-1986). If an encapsulation or a part of an encapsulation serves directly to support uninsulated live parts, the resistance to leaking currents and the clearance distances on the inner walls surfaces of the encapsulation shall correspond to the comparative and proof tracking indices minimum 250 V at 50 drops;

In the flameproof capsulations of Group I, the electro-insulating materials subject to electric stresses that may produce electric arc in air as result of nominal currents higher than 16 A (in commutation apparatus as switches, contactors, separators) shall have an comparative tracking index to surface leaking currents equal or greater than IRC 400M, according to SR EN 60112.

When the electro-insulating materials above mentioned do not correspond to this verification, they may be used though, if their volume is limited to 1% of the total empty enclosure, or if an adequate detection device allows power disconnection of the enclosure on the inlet side before the electro-insulating material possible decomposition may lead to dangerous situations. The testing station shall verify the presence and efficiency of those devices.

The lengths prescribed for the clearance distances depend upon the working voltage, the resistance to leaking currents on the electro-insulating materials surface and also upon the configuration of the electro-insulating parts of the equipment.

The inorganic insulating materials, e.g. glass and ceramics are not subjected to the above verification, they are conventionally classified into Group I.

This classification applies to electro-insulating materials without ribs or notches. If the electro-insulating parts do have notches or ribs, then the minimum value of the clearance distance for the working voltage over 1100 V shall be taken as the one in the next superior group.

According to comparative tracking indices to surface leaking currents, the electro-insulating materials (without ribs or notches) are divided into 3 groups:

- group I of materials: $\text{IRC} \geq 600$;
- group II of materials: $400 \leq \text{IRC} < 600$;
- group III of materials: $175 \leq \text{IRC} < 400$.

- *The dielectric rigidity:* determined according to SR EN 60243/1,2,3 and it represents the ratio between the breakdown voltage and the distance between the electrodes on which the voltage is applied. The test voltage can be applied in 3 ways:

- control test - voltage is raised at the prescribed value and maintained constant for 1 min. or 5 min;
- short time test - voltage is raised from 0 with an even increasing rate, so as the breakdown will occur after 10...20 s (quick apply)
- the test in steps of 20 s - it begins from the value of 40% of the probable breakdown voltage. The step value is chosen among a row of successive pre-established values (in kV).

- *The resistance to electric arc* checked according to STAS 6415/1, 2:

- as a minimum, the steps 2 and 3 for materials intended for manufacture of items that shall withstand to low voltage electric arcs;
- the resistance step prescribed in the product standard, for materials intended for manufacture of items that shall withstand to high voltage and low currents electric arcs.

The condition of resistance to electric arc is not mandatory when:

- the items are manufactured of plastic materials immersed in an encapsulation mass (e.g. epoxy resins);
 - the electro-insulating materials are used in electric equipment having U_n maximum of 60 V, regardless the power;
 - the electro-insulating materials are used in electric equipment having a maximum power of 50 VA, regardless the voltage;
 - the electro-insulating materials are used in electric equipment having a maximum voltage of 127 V and a maximum power of 250 VA and where there is no danger or sparks and electric arcs occurrence.
- *The resistance to glowing* checked according to STAS 6174 clauses 3; 4; 5, it shall be: minimum burn class 2
 - *The thermal stability Martens* checked according to STAS 6174 clauses 3; 4; 5, it shall be minimum 100°C
 - *The temperature indices "IT"* corresponding to the point of 20.000 h of the thermal endurance graph, without losing more than 50% of the resistance to bending (determined according to SR EN 60216/1, 2): at least 20 K higher than the hottest point on encapsulation or part of encapsulation taking into account the maximum service temperature but a minimum of 80°C for electro-insulating materials and 120°C ceramics.
 - *The resistance to flammability* checked according to SR ISO 1210 clauses 6; 7; 8; 9, combustion time shall be less than 15 sec. and degradation shall not reach the 75 mm marking.

3. ELECTRO-INSULATING MATERIALS BEHAVIOUR IN OPERATION

In operation conditions, insulation of electric apparatus, especially of those of high voltage, is subjected to various stresses by separate or combined actions of magnetic, electric, thermal, electro-dynamic or mechanic fields. These stresses act directly or indirectly towards insulation degradation (ageing) or even damaging by insulation breakdown or creepage.

The physic phenomenon of impairing the electric apparatus insulation differs to a certain extent if it takes place outside (breakdown or creepage of outer insulation) or inside (breakdown or creepage of inner insulation), if it takes place inside the longitudinal or transverse (main) insulation, between the apparatus phases.

The disruptive discharge phenomenon is based on ionization processes development and on their diffusion in form of avalanche of electrons.

Breakdown is accompanied by luminescent and acoustic phenomena, especially under operation conditions, where, due to the high short-circuit power of the

source, the initial discharge transforms in electric arc, with all its unwanted consequences.

In some reactions, the grater molecules decompose into smaller molecules, where new ions are generated and they diminish the dielectric rigidity and decrease the insulation resistance of the electro-insulating material.

Generally, those chemical reactions have an action of ageing on the insulation, with different speeds related to regime temperatures (permanently or intermittently) and related to the insulation particularities. For example, the inorganic insulation practically does not age at the operation temperature of the high voltage electric apparatus.

When choosing the electro-insulating materials, a great importance have their behavior when an electric arc may occur in an encapsulation as a result of to overvoltages produced in the commutation moment, of surpassing the rupturing capacity or different mechanical damages in the commutation apparatus.

The value of explosion pressure produced in the case of an short-circuit with effect of electric arc depends upon the electric current intensity and upon the duration of electric arc. When an electric arc occurs in an enclosure, in the presence of electro-insulating materials, especially organic materials on basis of phenolic resins with organic materials filling, due to high temperatures, these become current conductive fact which leads to their decomposition.

In case where the quantity of hot decomposition gases is greater than the one that may be evacuated outside, a pressure rise within the enclosure will occur leading to its deterioration. If the quantity of gas is lesser or equal to the one evacuated on the outside, then there will be no inner pressure rise but flame jets on outside may occur.

From this point of view, the electro-insulating materials are divided into three groups. In the first group are included the electro-insulating materials on which decomposition continues even after the quenching of the electric arc. This group includes plastic materials on basis of phenolic resins with organic filling materials. In the second group are included the electro-insulating materials for which decomposition continues as long as the electric arc persists. This group comprises electro-insulating inorganic materials on basis of polyester resins filling. In the third group are included the electro-insulating materials that do not decompose under an electric arc influence, as the ceramic materials.

As a result, the short-circuits with electric arc within the encapsulations are dangerous, they may provoke damage to the enclosures either as a result of high pressures, or as a result of electric arc creepage to the enclosure walls and then its breakthrough.

As a remark, the regulations in force both in our country and abroad do not include provisions to ensure the required measures to reduce or diminish these hazards. Thus, no norm regulates the minimum thickness of enclosure walls made of different materials, according to the pressure that may occur, in order to prevent a short-circuit with electric arc, or according to the ways of breakthrough the enclosure walls in the case of creepage of these short-circuits.

4. CONCLUSIONS

In order to prevent the damages to electric equipment intended for use in environments endangered by explosive atmospheres, it is considered as necessary to improve their construction by using in encapsulations of electro-insulating materials having superior characteristics regarding resistance to electric arc, leaking currents on surface in humidity conditions, flammability and temperature. Having this in view, it is considered necessary to remove from utilization the electro-insulating materials on basis of bakelite, textolite, pertinax etc., and to replace them with materials that are resistant to electric arc and surface leakage currents.

The laboratory tests that reproduce the most the stresses specific to electric arc and creepage in operation (that alter and show the ageing phenomenon in materials) are the ones of flammability and comparative tracking and proofing indices on surface on humidity conditions. This is the reason of imposing for the electro-insulating materials (in the case of group I flameproof enclosures) which are subject to electric stresses that may lead to electric arc at a current higher than 16 A (in the commutation apparatus as switches, separators, contactors) an surface proof and comparative tracking indices that is equal or above 400 V at 50 drops (determined according to SR EN 60112) and a combustion maximum time of 15 seconds (determined according SR ISO 1210).

REFERENCES

- [1] Ifrim A., *Materiale electrotehnice*, Editura Didactic și Pedagogic , 1979
- [2] Lică, V., *Materiale electroizolante*, vol. 1+2, Editura tehnic 1992
- [3] STAS 6790-86, *Materiale electroizolante utilizate în echipamentele electrice pentru atmosfere potențial explozive*
- [4] SR EN 60079-0:2005, *Aparatură electrică pentru atmosfere potențial explozive. Cerințe generale*
- [5] SR EN 60079-1:2005, *Aparatură electrică pentru atmosfere potențial explozive. Capsulare antideflagrantă 'd'*
- [6] SR EN 60079-7:2004, *Aparatură electrică pentru atmosfere potențial explozive. Securitate mărită 'e'*
- [7] SR EN 60112:2004, *Metodă de determinare a indicilor de rezistență și de ținere la formarea de căi conductoare a materialelor electroizolante solide*

SIMULATION SOFTWARE FOR STATIC SWITCH CONTROLLERS

MARIUS MARCU*, ILIE UTU*, FLORIN POPESCU**, PANA LEON***

Abstract: This paper present a simulation software for d.c. and ac static switch controller function, made like a Windows independent application helping with Visual Basic's software packages. The simulation windows is dynamically modifying in accord with static converter working regime.

Keywords: a.c. switch controller, d.c. switch controller, static converter, simulation software.

1. INTRODUCTION

The development of industrial automation led by default also to the improvement of electrical actuating systems, a fortiori such kind of the systems represent the most spread conversion format to electrical energy in mechanical energy.

The static converter (CS) had become an important element in alimentation systems with electrical energy to every kind of consumers. The most frequently, the static converters are used in adjusting systems to the static action, in this case the assignment being an electrical engine. Hereby, by an adequate command given by a controller in to a close circuit, the static converters adjust the output electrical energy parameters, to the necessity demand by electrical engine.

The simulation software for static converter function it is realized like a Windows independent application helping with Visual Basic's software package. Once one of the simulation software is launched one window is opened, allowing choosing the simulation type to be run, using radio buttons. The window also contains two buttons, one for continuing the simulation (*Continua*), the other for exit the application (*Iesire*).

* Associate professor, dr. eng., University of Petrosani

** Assistant, eng., University of Petrosani

*** Lecturer, dr.eng., University of Petrosani

Following the simulation start-up, the simulation window is opened, containing three main parts:

- A part which contains simulation scheme. Simulation scheme is dynamically modifying its margin colors which are in conduction at a certain moment.
- Another part it is dedicated to information zone. This zone presenting the text type information as regards to function mode to the converter analyzed (semiconductor elements which are in conduction, semiconductor elements directly polarized, etc.). Inside of this zone it is also find buttons for command angle modification, for choosing the function dial, etc.
- The third part it is the zone where is dynamically getting up the wave forms characteristic to the static converter analyzed.

Beside this zones, one of simulation windows also containing a pull-down menu type, for modification of some parameters or for choosing of different type of assignment. Moreover the window have two command buttons, one for starting up the simulation (*Simulare*), who then it is transforming in button for hold up the simulation (*Stop*) and a button for the exit of the window (*Iesire*).

2. STATIC SWITCH CONTROLLER SIMULATION

The static switch controllers are converters were the exit size have the same form with the entry size, after modifying the command angle α of thyristors obtaining the converter out put of voltage variation.

Figure 1 shows the application of main window of static switch controllers simulation software application, it allows selection for a. c. switch controllers, single-phase or three-phase, respectively the simulation for d.c. switch controllers.

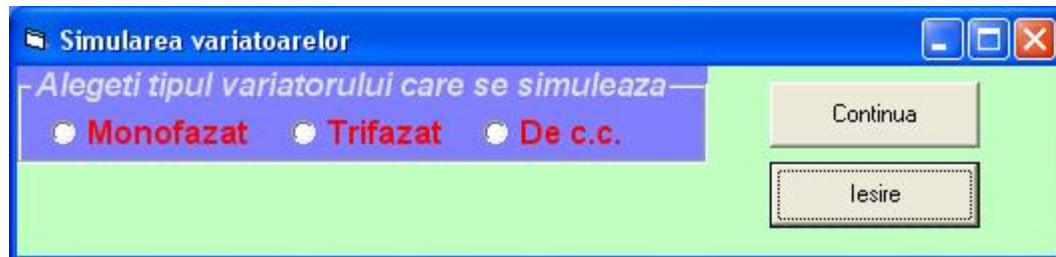


Fig.1. The application of main window of static variators simulation software application

2.1. A.c. switch controllers

Figure 2 shows the simulation window for a single-phase switch controller with resistive charge. It can be seen the main menu to choose the type of switch controller (with two thyristors, with one thyristor or with a thyristor across a diode bypass), and also the charging type. The charge may be resistive, inductive or resistive-inductive type.

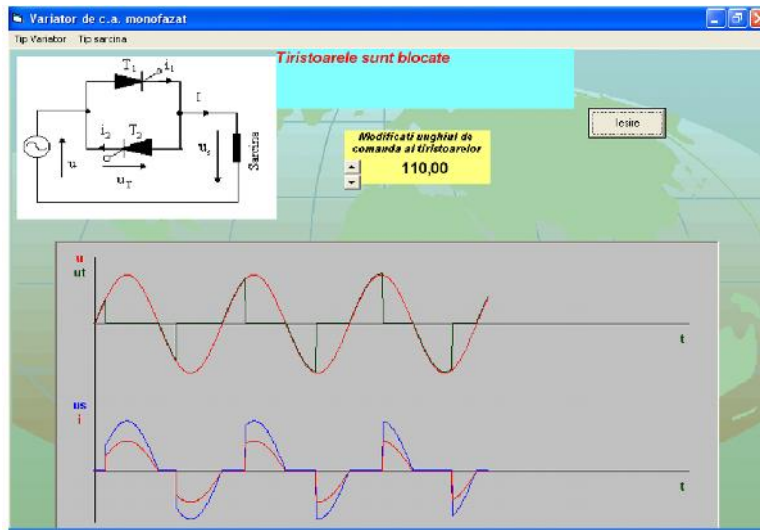


Fig.2. The simulation window for a single/phase switch controller with resistive charge

Along the simulation, it has been modified the command angle of the switch controller, in order to evidence also the way of voltage modification, respectively of the current through charge. The command angle may be modified using up/down arrows, being shown their values.

Figure 3 shows the simulation windows for single-phase switch controller with resistive-inductive charge. In case of resistive-inductive charge the software request by an additional window the input of power factor value.

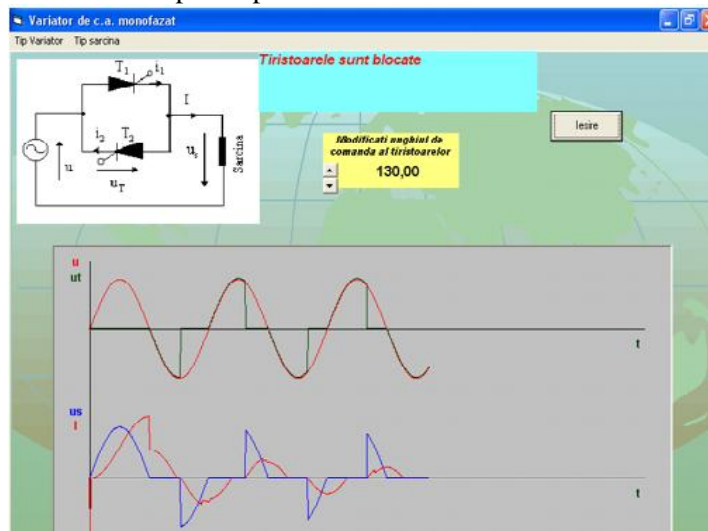


Fig. 3. The simulation windows for single/phase switch controller with resistive-inductive charge.

For the three-phase a.c. switch controller, the simulation window it is showed in figure 4 for a resistive charge. The simulation has been performed by modifying command angle.

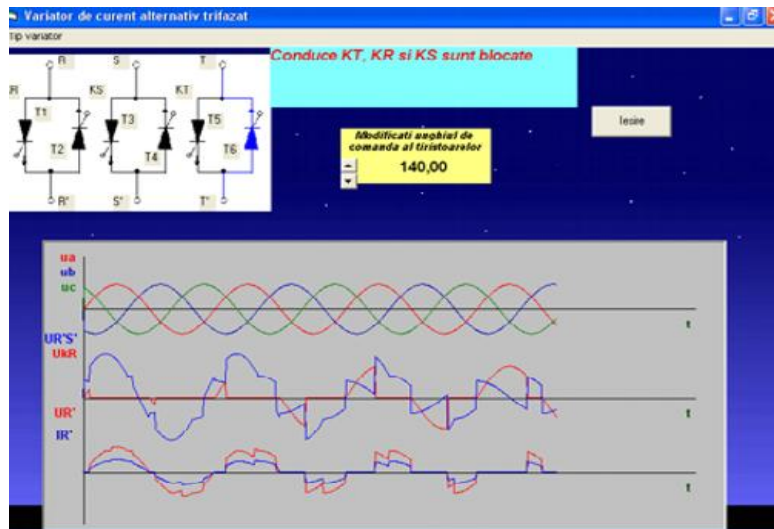


Fig.4. The simulation windows for three-phase switch controller with resistive charge.

2.2. D.c. switch controller

The d.c. switch controller, the chopper, it is the static converter who transform the entry continue voltage into a orthogonal voltage impulses. The exit voltage medium value its may be modified between 0 and entry value of voltage, in function with the rapport between the period when the chopper is controlling and the period when this is blocked.

Figure 5 shows simulation window for function simulation of one of static variator by a quadrant realized with thyristor, being represented the wave forms characteristic to the charge, the main thyristor and the switch off circuit.

Entering command in the main thyristor conductivity is to be done by pushing the related command button and to switch off the main thyristor, its related push button is pressed.

Figure 6 shows the simulation window related with the d.c. switch controller, in four quadrants from the same window, it is possible to be modified the operation quadrant (using the four radio buttons) and also the period for the switch controller or conductivity period.

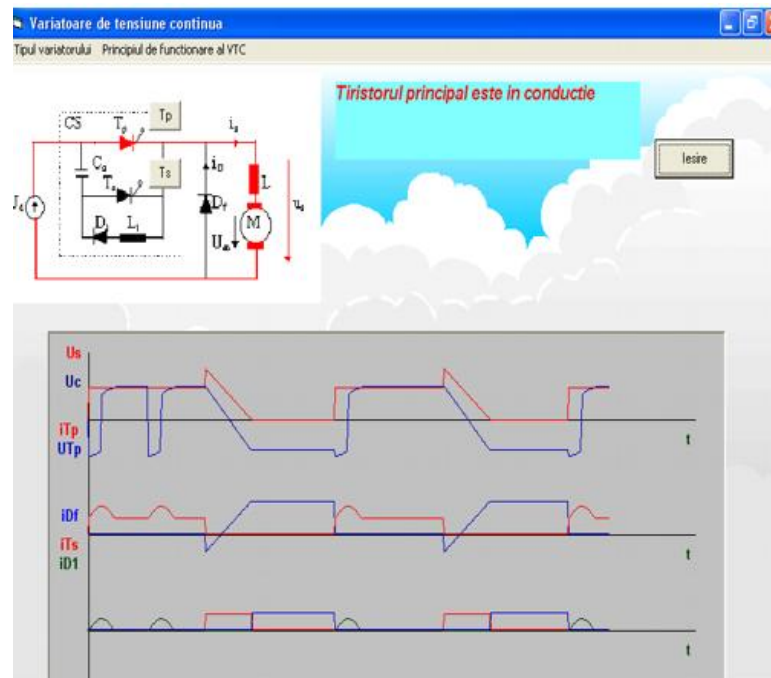


Fig. 5. Simulation window for function simulation of d.c. switch controller by a quadrant realized with thyristors.

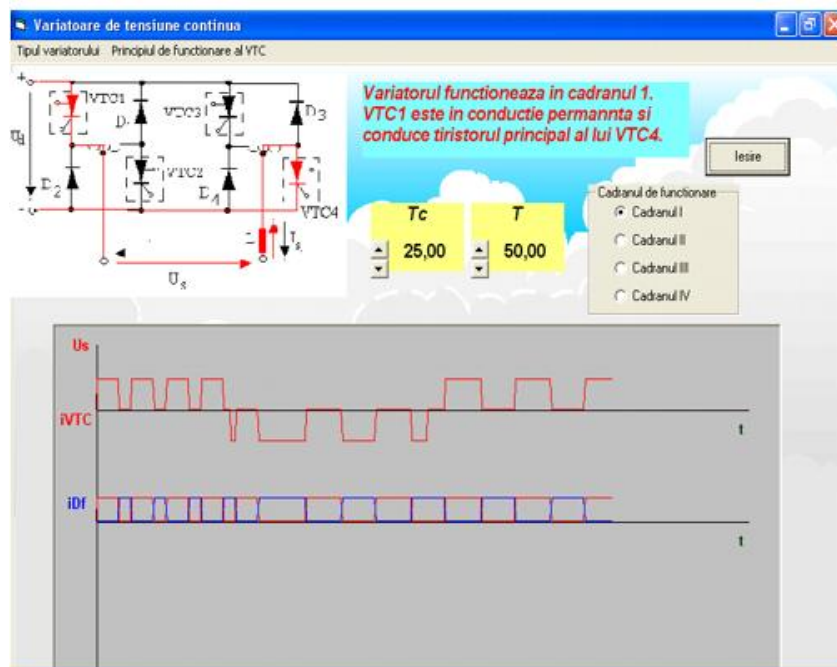


Fig.6. The simulation window related with the d.c. switch controller, in four quadrants

3. CONCLUSIONS

This documentation describes a Windows application, useful for understanding the functioning of the static variators, converters, trying to cover all the needed aspects. This application has an teaching purpose, being useful for the students studying static converters.

REFERENCES

- [1]. **Marcu, M., Borca, D.** *Convertoare statice în acționări electrice*. Editura TOPOEXIM, Bucure ti, 1999
- [2]. **Tunsoiu, Ghe.,** *Acționări electrice*. Editura Tehnic , Bucure ti, 1981.

SOME RESULTS IN SOLVING FIELD ENGINEERING PROBLEMS USING FINITE ELEMENT METHOD

NICOLAE DAN*, VISALON DAN**

Abstract Finite Element Method (FEM) is one of the most reliable numerical methods in solving complex engineering problems in real-life applications. This method is extensively used in the field of structural mechanics, civil engineering and fluid mechanics; however the method is applied with the same success in other areas of engineering such as electrical and magnetic. The similarities are discussed on practical examples to better illustrate the analogy.

Keywords: finite element method (FEM), numerical examples, heat transfer, magnetic and electrostatic fields, incompressible fluid flow.

1. INTRODUCTION

The finite element package ABAQUS is used next to solve the field problems mentioned above. ABAQUS is an advanced FEM package dedicated for solving non-linear stress analysis, mechanical contact, and heat transfer problems. To better illustrate the analogies between the engineering fields, it will be shown that using the heat conduction capability in ABAQUS all four classes of problems mentioned in literature [1] can be solved. In fact if a finite element algorithm is available for any of the areas presented in literature [1], the same finite element algorithm can be easily adapted to solve the other classes of problems.

2. NUMERICAL EXAMPLES

a) Heat Transfer

First the heat transfer field in an electrical machine will be investigated. Due to problem's symmetry, only a part of the cross-section is considered in the analysis. The

* *PhD, ABAQUS Inc., USA*

** *Assoc. Prof. PhD, University of Petrosani, Romania*

heat sources in Eq. 1.1 (literature [1]) are the Joule losses in the rotor’s armature slot and the core losses in the ferromagnetic material. Equivalent thermal conductivities were considered for the air-gap and for the slot region [3]. On the sides the boundary conditions are natural (Neumann), and Dirichlet boundary conditions on the bottom edge. Convective boundary conditions are specified on the upper (external) surface.

$$k_x \frac{\partial T}{\partial x} + k_y \frac{\partial T}{\partial y} + h(T - T_e) = 0 \quad (1)$$

Where:

h = heat transfer coefficient

T_e = surrounding air temperature

The thermal results are presented in Figure 2; NT11 in the legend indicates the nodal temperatures.

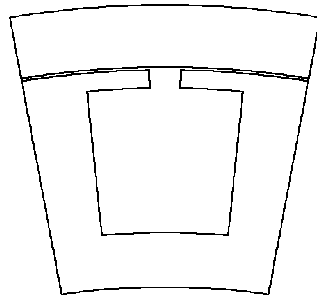


Fig. 7. Electrical machine cross-section

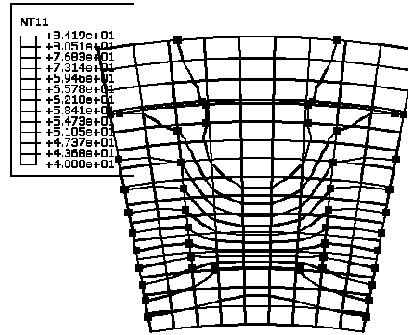


Fig.2. The mesh and the isothermal lines

b) Magnetic Field Problem

The magnetic field example is performed on the same configuration shown in Figure 1. The heat transfer capability is used again to solve the magnetic vector potential problem (Eq.1.2, literature [1]). The thermal conductivity is replaced by the magnetic reluctivity, and the temperature is the two-dimensional magnetic vector potential. The boundary conditions are homogeneous on all edges. The magnetic flux distribution (constant vector potential) is shown in Figure 3.

To obtain the magnetic flux density (in the air-gap for example), from the heat transfer variables, we rely on the analogy with elemental heat flux. The heat flux components and the heat flux magnitude for the isotropic material (at the element integration points) are given by:

$$\Phi_x = -k \frac{\partial T}{\partial x}; \Phi_y = -k \frac{\partial T}{\partial y}; \Phi = \sqrt{(\Phi_x^2 + \Phi_y^2)} \quad (2)$$

The magnetic flux density components, and the magnitude, are given by:

$$B_x = \frac{\partial A_z}{\partial y}; B_y = -\frac{\partial A_z}{\partial x}; B = \sqrt{(B_x^2 + B_y^2)} \quad (3)$$

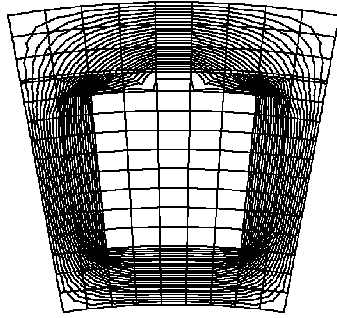


Fig.3. Magnetic flux distribution.

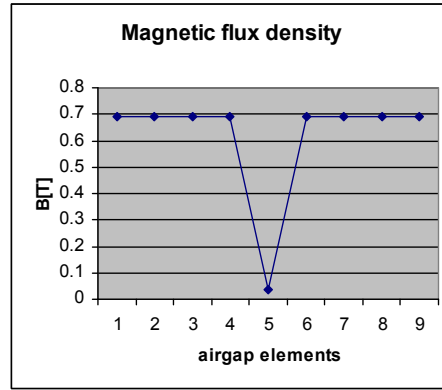


Fig.4. Magnetic flux density in the air-gap.

Therefore the magnetic flux density magnitude can be easily obtained from the heat flux magnitude by dividing by the thermal conductivity. Similar calculations are also valid for orthotropic materials. The magnetic flux density in the air-gap, calculated using the above observations, is presented in Figure 4.

c) Electric Field Problem

The study domain represents an electrical capacitor (Figure 5). Following the same analogy, the temperature in this case is replaced by the electric scalar potential (Eq.1.3, literature [1]).

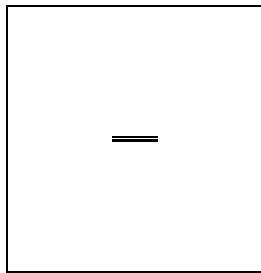


Fig.5. Electrical capacitor.

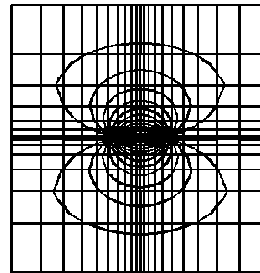


Fig.6. Equipotential line distribution.

The thermal conductivity becomes the electric permittivity for this case. The boundary conditions are homogeneous on the external edges; non-zero Dirichlet conditions (opposite sign) are prescribed on the capacitor's armatures. The FEM mesh is intentionally more refined in the area of high electric potential.

The contours of the constant electric potential are presented in Figure 6. Again the electric field intensity $\vec{E} = -\nabla V$ can be calculated similar as in Eq. (2-3, literature [1]).

d) Incompressible Fluid Flow Problem

The study domain is a water pool in which the fluid is pushed diagonally by a solid structure, Figure 7. The problem is solved in terms of velocity potential function Φ presented in Eq. 1.4 (literature [1]). The boundary conditions are Dirichlet on the top surface and on the impinging structure, and homogeneous Neumann on the sides. The velocity field was computed based on the analogy used presented in the previous applications (Eq. 2-3, literature [1]).

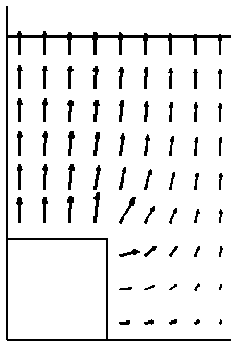


Fig.7. The fluid domain and the velocity field.

3. CONCLUSIONS

The similarities between the engineering field problems were presented on practical examples. The heat transfer capability in ABAQUS FEM dedicated package was used to solve four other classes of engineering problems.

Note: the “License Student” package was presented by ABAQUS to the Faculty of Electromechanics on the occasion of celebrating 50 years since this branch of the University of Petrosani was founded. The package offers us the possibility of implementing numerous finite element algorithms in the process of solving other classes of engineering problems.

REFERENCES

- [1] Dan, V., Dan N., “Theoretical Aspects in Solving Field Engineering Problems Using Finite Element Method”, Annals of the University of Petrosani, 2007.
- [2] ABAQUS User’s Manual, Version 6.5, 2005.
- [3] Dan, N, Ledezma, G.A., Craiu, O., “An improved Algorithm for Coupled Thermal and Magnetic Problems in Electromagnetic Devices”, HTD-Vol. 348, Volume 10, ASME 1997.
- [4] Sivester, P.P., Ferrari, R.L, 1996, “Finite Elements for Electrical Engineers, Cambridge University Press

STANDARDISATION TEST METHODS USED AT ASSESSMENT OF PRODUCT CONFORMITY WITH THE REQUIREMENTS OF PREVENTING THE EXPLOSIVE ATMOSPHERE IGNITION BY ELECTROSTATIC DISCHARGES

FLORIN ADRIAN PĂUN^{*}, LEONARD LUPU^{}, FLORINA MUNTEAN
BERZAN^{***}**

Abstract: It is very important to take adequate protection measures to prevent the electrostatic discharges from persons or their clothing for ensure a suitable level of security against explosions in dangerous Ex areas. Preventing the electrostatic charging of men, of clothes or on the surrounding objects suppose an ensemble of complex means and measures, hardly to supervise even in the present conditions of scientific knowledge.

Having in view this matter, it resorts to using of some standardized testing methods which allow further risk assessment of explosive atmospheres by the electrostatic discharges from clothing. Also a standardized testing method is to determination the dissipation capacity of charges. The principle of this test method supposes the charging by induction of the specimen test and then the determination the dissipation capacity of charges accumulated on this.

Taking into account the assessment criteria for materials/products from the ignition risk point of view of the explosive atmosphere by electrostatic discharges, the main criteria is the electric conductivity (see SR EN 13463 -1, (SR EN 50014:2004) substitute with SR EN 60079-0, SR EN ISO 20344, STAS 11 004-88, SR EN 61340-4-1, SR EN 1149-1:2002, SR EN 1149-2:2003). The newest assessment criteria are based on the charge determination (SR EN 61340-4-1) and the electrostatic discharge time determination (SR EN 1149-3:2004).

Key words: electrostatics, explosive atmosphere, explosion protection, electrostatic discharges, corona discharges.

^{*} *Scientific researcher, Ph D.Eng. at the INSEMEX-Petroșani*

^{**} *Assistant researcher, Ph D.Eng. at the INSEMEX-Petroșani*

1. INTRODUCTION

It is well known that the ignition risk of the explosive atmosphere occurs when two conditions are simultaneously fulfilled:

- an explosive atmosphere which could be a mixture of the gases, vapors, dusts, powders, lints and air with concentration within the upper and lower explosive limits and an ignition source of adequate energy to initiate the atmosphere are present.

If one of these conditions but preferably both of them are avoided, the ignition risk of the explosive atmosphere is diminished and even eliminated.

2. STATIC ELECTRICITY - POTENTIAL IGNITION SOURCE FOR AN EXPLOSIVE ATMOSPHERE

The static electricity is a phenomenon that frequently occurs in industrial activities. Sometimes it represents a part of technological process as painting in the electrostatic field, substances separation, deducting a.s.o., but many times it occurs accidentally and could represent a risk source, causing technological damages, fires and explosions.

The essential risk is that of fires and explosions due to discharges of electrostatic nature in explosion hazard areas respectively with explosive atmosphere or explosive substances. Also through the electrostatic discharges from all surrounding objects or from the operating personnel, the sensitive operation and control apparatus could be unexpectedly switched on. In some activities which imply manual work, the static electricity has an undesirable action on the human body having a negative influence over his mental. Also, electrostatic discharges from persons represent a shock risk which may lead to accidents at personnel implied in the different activities such as: work in a processing machine, or carrying out operations at a certain height, as a result of miss handling caused by scared personnel.

Considering the risks presented by static electricity, it is necessary to take protection measures against them. Prevention of electrostatic charge formation, accumulation and discharge from metallic elements is carried out by bounding to earth.

Frequent use, on a larger and larger scale, in the industrial activities, of non-metallic materials susceptible to major electric charging, produces problems regarding methods and means of protection against static electricity. Because their electric charge degree is influenced by many factors that are difficult to control in practice, in the some situations the risk of the static electricity formation cannot be prevented entirely, being necessary to take an assembly of measures for the purpose of their limitation within non-dangerous values according to endangered system influence.

Another technical solution for diminishing the dangers generated by static electricity could be employment of conductive and dissipative materials instead of non-conductive materials. Many materials were once entirely non-conductive, such as rubbers or plastic materials, now available in the dissipative category.

3. METHODS AND TECHNIQUES FOR ASSESSMENT OF PRODUCT CONFORMITY WITH THE SAFETY REQUIREMENTS FOR PREVENTION OF IGNITION SOURCES BY ELECTROSTATIC DISCHARGES

Taking into account the assessment criteria for materials/products from the ignition risk point of view of the explosive atmosphere by electrostatic discharges, the main criteria is the electric conductivity (see SR EN 13463 -1, (SR EN 50014:2004) substitute with SR EN 60079-0, SR EN ISO 20344, STAS 11 004-88, SR EN 61340-4-1, SR EN 1149-1:2002, SR EN 1149-2:2003). The newest assessment criteria are based on the charge determination (SR EN 61340-4-1) and the electrostatic discharge time determination (SR EN 1149-3:2004).

3.1 Test method for measurement of charge decay

The principle of the methods supposed charging by induction of a test specimen. In the few seconds under test specimen, which is placed on horizontal line is placed an electrode field without to have contact with the test specimen. Then on the electrode field is applied a high voltage. If the specimen test is conductive or held conductive elements a charge with opposite polarity at the electrode field is induced by the test specimen.

The field from the field electrode which is struck on the conductive elements, it's not cross by the test specimen and the effective field reduced in the same manner so that is characteristic to the material supposed at test method. This effect is measured

and recorded in the specimen past with a suitable electrical sounder field measuring.

In the time what inducing charges sum in the test specimen increase the effective field recorded by measuring electrical sounder decrease.

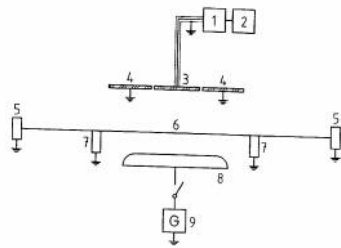
This decrease of the field is used to determination of the half time decay charge and a shield factor. The test method is

made to twelve specimens with dimensions (50 ± 2) mm x (300 ± 2) mm, which is cutting up

Fig. 1 Arrangement of equipment for induction charging test method

Key: 1 charge amplifier; 2 recording device; ; 3 field measuring probe; 4 guard ring; 5 specimen clamping ring; 6 test specimen; 7 support ring; 8 field electrode; 9 voltage generator

from a fabric sample or clothes; is cutting up six specimens test in the warp sense and six specimens test in the filing sense or in width. Three test specimens cutting up in the warp sense respectively three test specimens cutting up in the filing sense will be used with stems (rods) type HDPE and three test specimens cutting up in the warp sense respectively three test specimens cutting up in the filing sense will be used with stems (rods) of aluminum. The samples shall not comprise seams. Handling of the test specimens will be done only on their edges to avoid their contamination.



The test apparatus is composed by following:

- a field electrode (a rustless steel plate with diameter 70 ± 1 mm fixed on insulating support);
- guard ring;
- specimen clamping ring;
- voltage generator capable to produced a voltage of (1200 ± 50) V;
- electrical sounder field measuring;
- recording device.

REFERENCES

- [1]. **SR EN 1127-1 : 2003** *Atmosfere explozive - prevenirea exploziilor și protecția contra exploziilor. Partea 1. Concepte de bază și metodologie*
- [2]. **SR EN 13463 - 1:2003** *Echipamente neelectrice pentru atmosfere potențial explozive Partea 1: Metode și cerințe de bază*
- [3]. **SR EN 50014:2004** *Aparatură electrică pentru atmosfere potențial explozive. Cerințe generale înlocuit cu SR EN 60079-0:2005 Aparatură electrică pentru atmosfere explozive gazoase. Partea 0: Condiții generale*
- [4]. **SR EN ISO 20344:2004** *Echipament individual de protecție. Metode de încercare pentru încălțăminte.*
- [5]. **STAS 11 004-88** *Pardoseli pentru încăperi cu pericol de explozie; Determinarea rezistenței de descărcare și a rezistenței de scurgere a sarcinilor electrostatice*
- [6]. **SR EN 61340-4-1** *Electrostatică Partea 4-1: Metode de încercare standardizate pentru aplicații specifice. Rezistența electrică a pardoselilor și a straturilor de acoperire*
- [7]. **SR EN 1149-1:2006** *Îmbrăcăminte de protecție. Proprietăți electrostatice. Partea 1. Metodă de încercare pentru măsurarea rezistivității de suprafață.*
- [8]. **SR EN 1149-2:2003** *Îmbrăcăminte de protecție. Proprietăți electrostatice. Partea 2. Metodă de încercare pentru măsurarea rezistenței electrice la traversarea materialelor (rezistență verticală)*
- [9]. **SR EN 1149-3:2004** *Îmbrăcăminte de protecție. Proprietăți electrostatice. Partea 3. Metodă de încercare pentru măsurarea capacității de disipare a sarcinilor.*
- [10]. **BS 5958: Part 1:1991** *Cod of practice for Control of undesirable static electricity. General considerations*
- [11]. **Ulrich von Pidoll** *Determining the incendivity of electrostatic discharges without explosive gas mixtures, PTB Germany*
- [12]. **CLC/TR 50404 June 2003** *Electrostatics - Code of practice for the avoidance of hazards due to static electricity*

STOCHASTIC MODELS FOR RELIABILITY ANALYSIS OF PROTECTION SYSTEMS

LEON PĂNĂ*, ION FOTĂU***, HORIA ȘERBAN**

Abstract: A small part of power system, including one or more protection systems, is modeled by using mathematical techniques: Markov theory, renewal theory, Petri nets and Monte Carlo simulation. In this paper the Markov models from protection systems are discussed and analyzed.

Keywords: reliability, protection system, failure to operate, mal-trip

1. INTRODUCTION

An industrial supply network system consists of a combination of lines or cables, power transformers and incoming power sources including co generators. The power cables, overhead lines and transformer form the main supply network, which provides a reliable power transmission from sources to loads.

A protection system protects the power system from the harmful effect or faults. a fault is an abnormal system condition, which is in most cases a short circuit and occurs as a random event . In general, protection systems do not prevent damage to the power system, they operate after some detectable damage has already occurred.

In this section an overview of protection models used in reliability analysis and the stochastic models of the protection systems used in other area will be presented. The models are not discussed in full detail, only the main characteristics are presented. For more information, references are included.

Of the qualities required of the protection systems [1, 2, 4, 5] the two of main interest to us here are:

<i>Selectivity or discrimination</i>	The protection system is effectiveness in isolating only the faulty part of the system.
<i>Stability</i>	The property of remaining in operation with faults occurring outside the protected zone.

* *PhD. Lecturer Eng. at the University of Petrosani*

** *PhD. Student at the University of Petrosani*

In other words, the power system protection should isolate the fault and refrain from action for the rest. These two aspects of the protection lead to two aspects of the reliability of the protection as defined by the IEC [1].

Reliability of protection The probability that a protection can perform a required function under given conditions for a given time interval.

Dependability The probability for a protection of not heaving a failure to operate under given conditions for a given time interval.

Security The probability for a protection of not having an unwanted operation under given conditions for a given time interval.

Reliability is generally defined as a measure of certainly that a piece of equipment or system will perform as installed.

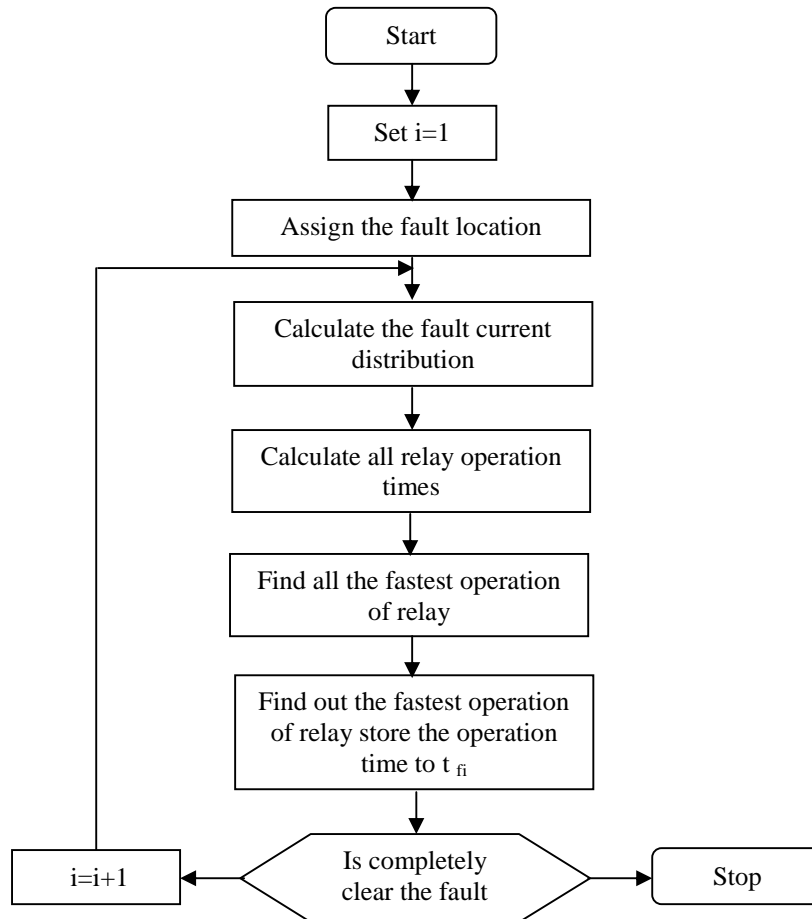


Figure 1 The flow chart for the reliability algorithm to clear one simulated faults

In figure 1 is illustrated the flow chart for the reliability algorithm to clear one simulated faults.

Here the two principal failure modes of the protection appear, namely, failure to operate and unwanted operation. These two terms will reappear further on, but there is more to failure of the protection than this. For example, the unwanted operation can be spontaneous, or due to an event in the power system (often a fault outside the zone to be protected, i.e. an external fault). The failure can be due to a relay failure, a circuit breaker failure, a current transformer failure or even due to an error in the calculation of the setting. The first aspect of the protection to be modeled in a stochastic way was the fault clearance time [1, 2]. Once the probability density function of the fault clearance time is known, of the fault clearance time is known, the required time-grading can be calculated for any given value of the acceptable chance of unwanted operation. A similar concept is used for stochastic assessment of transient stability [2, 3, 4, 5].

2. SYSTEM PROTECTION MODEL AND RELIABILITY ALGORITHM

At the occurrence of fault on a power system, the current is almost always greater than the pre-fault load current in the components in the vicinity of the fault. The operational time of an overcurrent relay depends on its operating characteristics. Figure 2 shows the operational time of an overcurrent relay with definite-time characteristic. Such a relay does not operate (operating time is infinite) as long as the current magnitude is less than I_p . If the current magnitude exceeds I_p the relay operate after T_s seconds.

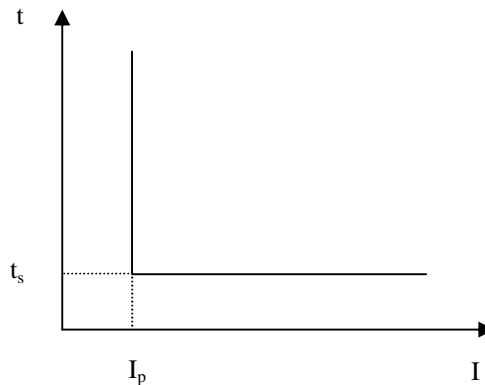


Figure 2 Overcurrent relay with definite-time characteristic

In order to design a protection system, one must be able to represent and evaluate the performance of protection systems. Thus, methods of representing the performance of relays alone and in relation to other relays of the protection system are required. In this section, the *relay-unit* that has the simplest operating characteristic is introduced. The operating characteristic of any relay can be represented by a set of relay-units. Moreover, this section presents a method for representing the performance of a protection system.

A relay-unit (denote by r) is the relay that has a simplest operating characteristic, as shown in figure 3. Such a relay operates after a pre-set delay times t_s , in case of any fault for which operating quantity q is above the pick-up value q_p . In general, the operating quantity of a relay-unit can be any function of the currents and voltages of the component being protected.

As overcurrent relay with a definite time characteristic is an example of a relay-unit with the component current at the operating quantity. Such a relay operates for all currents above the pick-up setting of the relay. It is possible to set up a relay-unit that operates for values smaller than the pick-up value and take no action for values above the pickup. Under-voltage and one step impedance or distance relays are examples of such a relay.

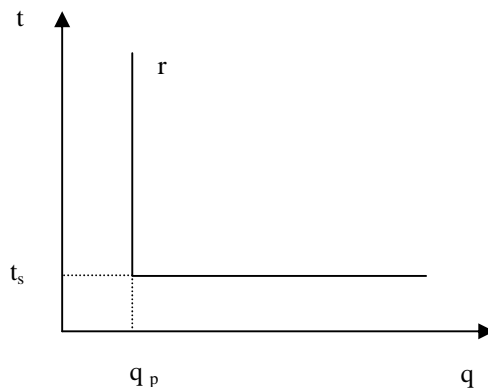


Figure 3 Unit-relay is operating characteristic

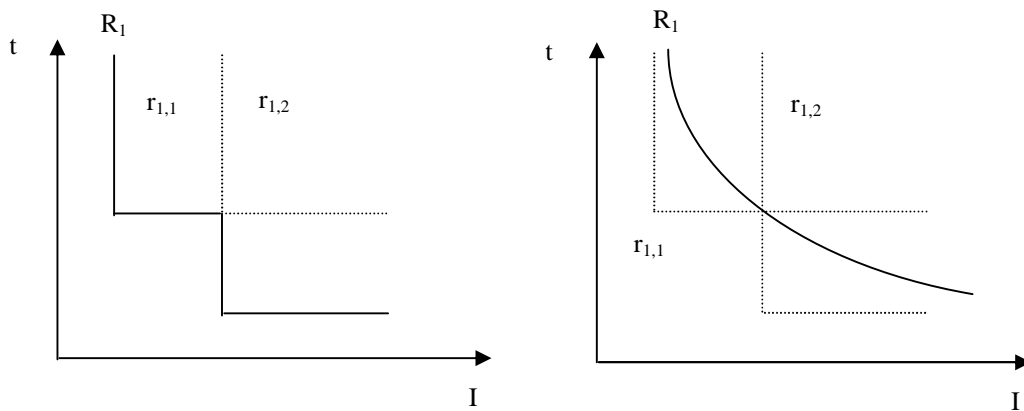


Figure 4 Complex characteristics by combining relay-units

Due to simplicity of the operating characteristics of relay-units, every relay-operating characteristic can be represented by a combination of a set of relay-units.

In figure 4 two steps and an inverse characteristic are represented by a combination of two relay-units. In this paragraph, a small letter “r” denotes each relay-unit (e.g. r_1, r_2) and each protective relay that consist of one or more relay-units is denoted by a capital “R”.

The dynamic equation for the OC relay operation time calculation is defined by IEEE standard C37.112-1996 as shown in equation (1):

$$\int_0^{T_0} \frac{1}{t(I)} dt = 1 \quad (1)$$

where:

$t(I)$ Is the relay disc traveling time from 0 to operating distance at fault current I

For the three consecutive fault currents, I_1, I_2, I_3 the t_{actual} is calculated as follows:

$$\begin{aligned} \int_0^{t_{f1}} \frac{1}{t_1} dt + \int_{t_{f1}}^{t_{f1}+t_{f2}} \frac{1}{t_2} dt + \int_{t_{f1}+t_{f2}}^{t_{\text{actual}}} \frac{1}{t_3} dt &= 1 \\ \frac{t_{f1}}{t_1} + \frac{t_{f2}}{t_2} + \frac{1}{t_3} (t_{\text{actual}} - t_{f1} - t_{f2}) &= 1 \quad (2) \\ t_{\text{actual}} &= \sum_{i=1}^2 t_{fi} + t_3 \left(1 - \sum_{i=1}^2 \frac{t_{fi}}{t_i} \right) \end{aligned}$$

where:

t_1, t_2, t_3 are the relay operating times at fault current I_1, I_2, I_3 respectively.

The inverse definite minimum time lag (IDMTL) over current relay (OC) operating time for “n” steps of fault currents with n consecutive fault currents is shown in following equation:

$$t_{\text{actual}} = \sum_{i=1}^{n-1} t_{fi} + t_n \left(1 - \sum_{i=1}^{n-1} \frac{t_{fi}}{t_i} \right) \quad (3)$$

The protection is here considered to consist of four parts:

- Main protection
- Backup protection
- Breaker failure protection

- Circuit breaker

A protection system has two alternative ways in which it can be unreliable it may fail to operate when it is expected to (referred to as *fail-to-trip*), or it may operate when it is not expected to (referred to as mal-trip). This leads to a two-pronged definition of the reliability of protection systems.

3. ASSUMPTION AND SITUATION DESCRIPTION

The following assumptions are used in modeling the system:

- After a failure to operate, which is followed by a repair, and after maintenance the relay is working properly.
- The times to failure of a relay (TTF) are independent and exponentially distributed with parameter p . This means that if a relay is last seen healthy at time t_h , than the chance the relay is dormant at time t is equal to:

$$P(T < t) = 1 - e^{-p(t-t_h)} \quad \text{for } t > t_h \quad (4)$$

Here T is the moment at which the relay becomes dormant.

- Times between short circuits (TBSC) are independent and exponentially distributed with parameter δ . Since short circuits are cleared immediately in the model, the chance that a short circuit will happen in the next interval of time t is equal to:

$$P(T_{sh} < t) = 1 - e^{-\delta t} \quad (5)$$

Here T_{sh} denote the time to the next short circuit.

- The time between two successive maintenance (TBM) is independent and in a protection system with “ n ” relay, the TBM is exponentially distributed with parameter μ/n . All “ n ” relays are maintained at the same time. The average number of relays maintained in one unit of time then equals:

Due to characteristics of matrix T , the changes in $P_i(t)$ will diminish in $t \rightarrow \infty$. With this, the set of differential equations reduces to set of linear equations having the form:

$$T \cdot P = O \quad (6)$$

where

P a column vector whose i^{th} term is steady-state probability of residing in state i

Since the elements in each columns of matrix A add up to zero, the determinant of T in zero and, therefore, the equations in (9) are not linearly independent.

Each equation is linear combinations of others. To provide an additional equation, the simple fact is recognized that the state probabilities must add up to 1 at time t , and therefore:

$$\sum_{k=1}^n P_k = 1 \tag{7}$$

For this reason, the steady-state probabilities can be obtained by solving the following matrix equation:

$$T' \cdot P = C \tag{8}$$

where:

- T' a matrix obtained from matrix A by replacing the elements of an arbitrarily selected row p by ones
- P a column vector whose i^{th} term is the probability of residing in state I
- C a column vector with the p^{th} element equal to one and other elements set to zero

In figure 5 the standard graphical representation of the Markov model is shown. The model contains two relays. Short circuit lead to the fail-to-trip if both relays are dormant at the time of occurrence at the short circuit. Maintenance is performed simultaneously at both relays. The times between maintenance are exponentially distributed with parameter $\frac{\mu}{2}$.

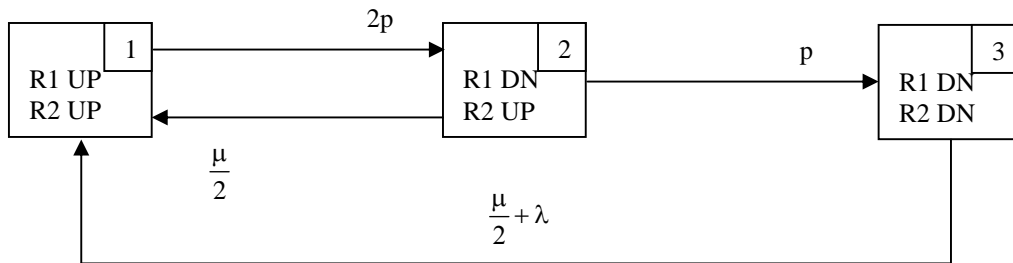


Figure 5 State-space diagram for a system comprising two protective

The three states of this model are defined as follows:

- State 1:* In this state both relays are healthy. The short circuit and the maintenance do not cause a transition when the system is in this state. Both relays can fail with rate p. this cause a total transition rate out of state one, equal to 2p.
- State 2:* In this state one of the relays is dormant. In this case short circuits do not have any influence on the state of the model because the relay that is healthy will work properly. Maintenance with rate $\frac{\mu}{2}$ will cause a

transition to state 1 while the failure of the healthy relay with rate p , will cause a transition to state 3.

State 3: In this state both relays are dormant. Maintenance with rate $\frac{\mu}{2}$ will cause a transition to state 1. Short circuits with rate λ , while the system is in a state 3 will cause a failure to operate and the repair of both relays that is represented by a transition to state 1.

The matrix T is:

$$T = \begin{pmatrix} T_{11} & T_{21} & T_{31} \\ T_{12} & T_{22} & T_{32} \\ T_{13} & T_{23} & T_{33} \end{pmatrix} = \begin{pmatrix} -2p & \frac{\mu}{2} & \frac{\mu}{2} + \lambda \\ 2p & -\frac{\mu}{2} - p & 0 \\ 0 & p & -\frac{\mu}{2} - \lambda \end{pmatrix} \quad (9)$$

The matrices T' and C is:

$$T' = \begin{pmatrix} -2p & \frac{\mu}{2} & \frac{\mu}{2} + \lambda \\ 2p & -\frac{\mu}{2} - p & 0 \\ 1 & 1 & 1 \end{pmatrix}, \quad C = \begin{pmatrix} 0 \\ 0 \\ 1 \end{pmatrix} \quad (10)$$

Solving equation (8) results in:

$$P = T'^{-1} \cdot C = \begin{pmatrix} P_1 \\ P_2 \\ P_3 \end{pmatrix} = \frac{1}{12\lambda p + 8p^2 + 2\lambda\mu + 6p\mu + \mu^2} \begin{pmatrix} (2\lambda + \mu)(2p + \mu) \\ 4p(2\lambda + \mu) \\ 8p^2 \end{pmatrix} \quad (11)$$

REFERENCES

- [1]. International Electrotechnical Vocubular. Chapter 448: *Power System Protection*. IEC 50(448): 1987. Geneve: IEC, 1987
- [2]. **Anderson P.M.**, *Reliability modeling of protective systems*, IEEE Transactions on Power Apparatus and Systems, vol.103 (1984), p.2207-2214
- [3]. **Anderson P.M. and Agarwal S.K.**, *An improved model for protective systems reliability*, IEEE Transactions on Reliability, vol. 41 (1992), p. 422-426
- [4]. **Anders G.J.**, *Probabilistic concepts in electric power systems*, New York: John Wiley & Sons, 1990
- [5]. **Billinton R. and Allan R.N.**, *Reliability evaluation of power systems*, London: Pitman, 1984

STUDY DYNAMIC OF A SYNCHRONOUS GENERATOR WITH ELECTRONIC LOAD

JENICA ILEANA CORCĂU*

Abstract: In this paper is present study dynamic and analysis of a system consisting of a variable-speed synchronous generator that supplies an active load (inverter) through a three-phase diode rectifier. A particularity of the described system is strong non-ideal operation of the diode rectifier, a consequence of the large value of generator's synchronous impedance. This paper presents a new average model of the system. The average model accounts, in a detailed manner, for dynamics of generator and load, and for effects of the non-ideal operation of diode rectifier. In particular, the systems control-loop, responsible for stability and proper impedance matching between generator and load, an difficult to design without an accurate small-signal model.

Keywords: variable-speed synchronous generator, electronic load, control-loop, stability, small-signal model.

1. INTRODUCTION

This paper presents study dynamics of the system whose block diagram is shown in figure 1. It is a 150kW generator with inverter output, in which a natural gas engine drives a synchronous generator. Field voltage is provided to main generator by means of a separate, smaller synchronous machine, an exciter.

In order to make engine operation as efficient as possible, speed is varied from 1800 rpm to 4000rpm according to a load-versus-speed relationship considered optimal for the engine. Such variable speed operation affects generator design in several ways, of which the most important for study is the effect it has on the value of main generator's synchronous inductance [1].

* *Lecteur Ph D., University of Craiova, Faculty of Electrotechnics, Division Avionics, jcorcau@elth.ucv.ro*

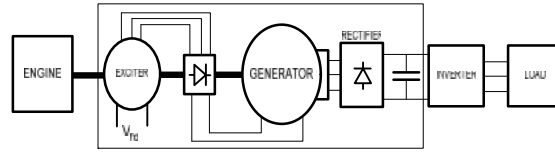


Fig.1. Block diagram of the studied system

The system shown in figure 1 cannot work in open loop: dc link voltage v_{dc} , needs to be regulated at a constant value 800V for the inverter to operate properly [1]. Since diode rectification provides no means of regulation, constant dc-link voltage can be achieved only by adjusting the exciter's field voltage v_{fd} . That can be done by closing the dc-link voltage feedback control-loop, as shown in figure 2.

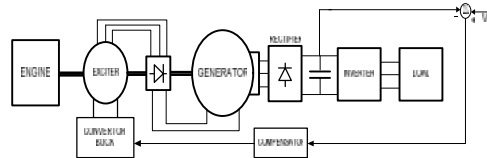


Fig.2. Block diagram of studied system in closed loop

2. AVERAGE MODEL EQUATIONS

In figure 3 is presents implement the average generator/rectifier model [2].

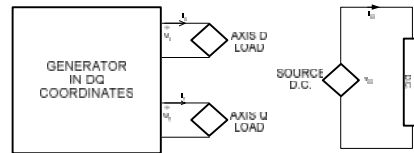


Fig.3. Block diagram of the average model

The dc source can be either a voltage or a current source; the d and q axis load can be given by either's current or voltage sources.

The equations of average model are [2]

$$\hat{v}_{dc} = k_v(\hat{v}_d \sin \delta + \hat{v}_q \cos \delta), \quad (1)$$

$$\hat{i}_d = \frac{\hat{i}_{dc}}{k_i} \sin(\delta + \phi), \quad (2)$$

$$\hat{i}_q = \frac{\hat{i}_{dc}}{k_i} \cos(\delta + \phi), \quad (3)$$

$$\delta = \arctg \frac{\hat{v}_d}{\hat{v}_q}. \quad (4)$$

$$\hat{i}_{dc} = k_i[\hat{i}_d \sin(\delta + \phi) + \hat{i}_q \cos(\delta + \phi)], \quad (5)$$

$$\widehat{v}_d = \frac{\widehat{v}_{dc}}{k_v} \sin \delta, \quad (6)$$

$$\widehat{v}_q = \frac{\widehat{v}_{dc}}{k_v} \cos \delta, \quad (7)$$

$$\delta = \arctg \frac{\widehat{v}_d}{\widehat{v}_q}. \quad (8)$$

It can be seen that the average model's equations establish a "transformer-like" relationship between the generator's output in the dq reference frame and the rectifier's dc output.

2.1. Linearized average model

The average model's equations, presented in relationships 1 to 8 are non-linear because they contain products of variables, as well as trigonometric functions. For some purposes such as control-loop design, it is necessary to study the linearized system. In many causes, software used for simulation of the average model is capable of linearizing system equations, after it determines the steady-state operating point. An example using software Matlab/Simulink, is procedure "linmod" obtained linearized system equations. However, it is useful to find analytically the linearized version of average model equations. That makes it possible to easily simulate cases that would cause numerical problems in determining the steady-state operating point, as well as to find the linearized state space representation of the system. In this model the steady-state value of an average variable \hat{x} will be denote X , while \tilde{x} represents small perturbation of same variable. The scope is to find a linear state space representation of the system consisting of the exciter, main generator and dc load. This is obtained by combining the machine's equations with the linearized generator/rectifier average model's equations, and equations describing the dc load [3]. This is algebraically tedious process that does not introduce any new concepts. If the generator's speed is constant and treated as a parameter of the system; are linear differential equations, and they can be rewritten for small perturbation by simply adding a tilde to all currents and voltages. Since both the exciter's and main generator's equations will be treated in this paper, index "e" will be added to all parameters and variables relative to the exciter; and index "a" to those entire relative to the main generators.

3. STATE-SPACE REPRESENTATION OF THE SYSTEM

State-space representation of the system is

$$\dot{x} = Ax + Bu, \quad (9)$$

Where

$$x = \begin{bmatrix} \tilde{i}_{ed} \\ \tilde{i}_{eq} \\ \tilde{i}_{efd} \\ \tilde{i}_{ad} \\ \tilde{i}_{aq} \\ \tilde{i}_{akd} \\ \tilde{i}_{akq} \\ \tilde{v}_{adc} \end{bmatrix} \quad (10)$$

Is the vector of state variables, and

$$u = \begin{bmatrix} \tilde{v}_{efd} \\ \tilde{i}_{sarcina} \end{bmatrix} \quad (11)$$

Is the vector of system's inputs.

In order to find matrices A and B from (9), the system's equations will be written in the form

$$E\dot{x} = Fx + Gu \quad (12)$$

After that, matrices A and B can be calculated as

$$A = E^{-1}F, \quad (13)$$

$$B = E^{-1}G. \quad (14)$$

The matrices E and F are [3]

$$E = \begin{bmatrix} -(L_{eis} + L_{emd} + L_{edd}) & -L_{edq} & L_{emd} & \alpha_{f_{ae}} & 0 & -\alpha_{f_{ae}} & 0 & 0 \\ -L_{eqd} & -(L_{eis} + L_{emq} + L_{eqq}) & 0 & -\alpha_{f_{ae}} & 0 & \alpha_{f_{ae}} & 0 & 0 \\ L_{emd} & 0 & L_{eifd} + L_{emd} & 0 & 0 & 0 & 0 & 0 \\ L_{amd} f_{aed} & L_{amd} f_{aeq} & 0 & -(L_{uis} + L_{umd}) & 0 & L_{umd} & 0 & -b_{addc} \\ 0 & 0 & 0 & 0 & -(L_{uis} + L_{umq}) & 0 & L_{umq} & -b_{aqdc} \\ L_{umd} f_{aed} & L_{umd} f_{aeq} & 0 & -L_{umd} & 0 & (L_{ulkd} + L_{umd}) & 0 & 0 \\ 0 & 0 & 0 & 0 & -L_{umq} & 0 & L_{ulkq} + L_{umq} & 0 \\ 0 & 0 & 0 & 0 & 0 & 0 & 0 & e_{88} \end{bmatrix} \quad (15)$$

$$e_{88} = -(b_1 b_{addc} + b_2 b_{aqdc}),$$

$$F = \begin{bmatrix} R_{es} + r_{edd} & f_{12} & 0 & 0 & 0 & 0 & 0 & 0 \\ f_{21} & R_{es} + r_{eqq} & -\omega_c L_{emd} & 0 & 0 & 0 & 0 & 0 \\ 0 & 0 & -R_{efd} & 0 & 0 & 0 & 0 & 0 \\ 0 & 0 & 0 & R_{us} + r_{add} & f_{45} & 0 & \omega_c L_{umq} & f_{addc} \\ -\omega_c L_{umd} f_{aed} & -\omega_c L_{umd} f_{aeq} & 0 & f_{54} & R_{us} + r_{aqq} & -\omega_c L_{umd} & 0 & f_{aqdc} \\ 0 & 0 & 0 & 0 & 0 & -R_{ukd} & 0 & 0 \\ 0 & 0 & 0 & 0 & 0 & 0 & -R_{ukq} & 0 \\ 0 & 0 & 0 & f_{84} & f_{85} & 0 & 0 & f_{88} \end{bmatrix} \quad (16)$$

$$\begin{aligned}
f_{21} &= r_{eqd} + \omega_e(L_{els} + L_{emd}), \quad f_{12} = r_{edq} - \omega_e(L_{els} + L_{emq}), \quad f_{45} = r_{adq} - \omega_a(L_{als} + L_{amq}), \\
f_{54} &= r_{aqd} + \omega_a(L_{als} + L_{amd}), \quad f_{84} = b_1 r_{add} + b_2 r_{aqd}, \quad f_{85} = b_1 r_{adq} + b_2 r_{aqq}, \\
f_{88} &= b_1 f_{addc} + b_2 f_{aqdc} - 1.
\end{aligned}$$

$$G = \begin{bmatrix} 0 & 0 \\ 0 & 0 \\ 1 & 0 \\ 0 & r_{adl} \\ 0 & r_{aql} \\ 0 & 0 \\ 0 & 0 \\ 0 & g_{82} \end{bmatrix}, \quad (17)$$

$$g_{82} = b_1 r_{adl} + b_2 r_{aql}.$$

If a resistive load were connected to the dc-link, equations which allow us to determine matrices E , F and G can easily be modified by substituting

$$\tilde{i}_{sarcina} = \frac{\tilde{v}_{adc}}{R_l}, \quad (18)$$

Where R_l is the load resistance. In that case, the only input to the system is represented by exciter's field voltage (\tilde{v}_{efd}). If the dc-link voltage is considered to be system's output, the output equation can be written in the form

$$\tilde{v}_{adc} = Cx + Du, \quad (19)$$

$$C = [0 \ 0 \ 0 \ 0 \ 0 \ 0 \ 0 \ 1], \quad (20)$$

$$D = [0]. \quad (21)$$

4. TRANSFER FUNCTIONS

A linearized representation of the system allows finding system's transfer functions. For dc-link voltage controller design, it is necessary to have Bode plots of function transfer control-to-output. This transfer function can be found from linearized state space representation as

$$\frac{\tilde{v}_{adc}}{\tilde{v}_{efd}} = C(sI - A)^{-1}B + D. \quad (22)$$

In table 1 are listed the transfer function's poles and zeros numerically for the operating point characterized by: 3340rot/min, 105kW current source load and field voltage 33V. In table 2 consists the transfer function's poles and zeros numerically for the operating point characterized by: 3340rot/min, 105kW resistive load and field voltage 33V and table 3 are listed the transfer function's poles and zeros numerically

for the operating point characterized by: 2240rot/min, 15kW resistive load and field voltage 26V.

Table 1

Zeros(rad/s)	Poles (rad/s)	Gain
1074,4	-1721,6+3008,2j	1832,4
338,6+745,2j	-1721,6-3008,2j	
338,6-745,2j	-2111,6	
-731,7	11,8+62j	
-615,9	11,8-62j	
11,7	15,3	
	-27,6	
	Poles (rad/s)	

Table 2

Zeros (rad/s)	Poles (rad/s)	Gain
1074,4	-1662,7+2524,3j	1832,4
338,6+745,2j	-1662,7-2524,3j	
338,6-745,2j	-2111,6	
-731,7	89,3+119,5j	
-615,9	89,3-119,5j	
11,7	15,1	
	-27,3	
	-43,7	

Table 3

Zeros (rad/s)	Poles (rad/s)	Gain
5372,1	-13879	1832,4
4642,3	-1489+7301j	
649	-1498-7301j	
-815,9	4012	
-731,7	-40	
-4,5	20	
Zeros (rad/s)	-8	
	2	

In figure 4 is presented the block scheme of simulation for two constants input.

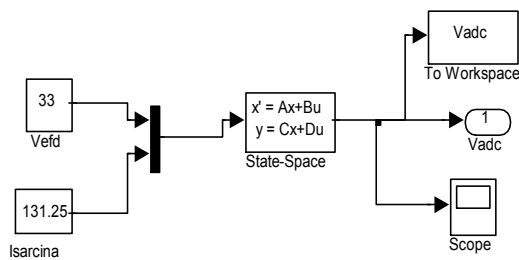


Fig.4 The block scheme in Simulink

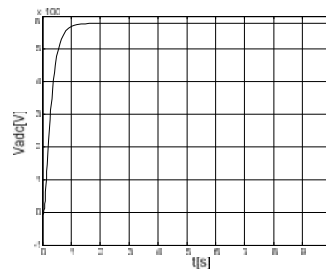


Fig.5. The variation in time of the output voltage

In figure 5 is presented the variation in time of the output voltage V_{adc} .

It can be seen that current source load, as opposed to resistive load, makes the system more difficult to stabilize in closed loop.

5. CONCLUSIONS

In this paper is presented a study dynamic of synchronous generator with electronic load. It presents a new average model of the system studied. This model accounts in a detailed manner, for the dynamics of the generator and load, and for the effects of the non-ideal operation of the diode rectifier. A linearized representation of the system allows finding the system's transfer functions. For the dc-link voltage controller design, it is necessary to have plots of the transfer functions control-to-output, which represent the system's control-to-output transfer function. The dependence of these transfer functions on the operating point and the nature of the dc load was discussed from the point of view of the dc-link voltage control-loop design.

REFERENCES

- [1]. **Jadric I., Borojevic D., Jadric, M.** *Modeling and control of a synchronous generator with an active dc load.* IEEE Trans., Power Electronics, vol. 15, no.2, march 2000.
- [2]. **Corcau, J.** *Three-phase synchronous generator modeling as subsystem of a PDS (Power Distribution System).* 7th International Conference of Applied and Theoretical Electricity ICATE 2004, 14-15 octomber, Baile Herculane, pp. 543-546.
- [3]. **Corcau J.** *Sisteme evaluate de comanda si control al proceselor din instalatiile electrice ale avioanelor.* Teza de doctorat, Universitatea " Politehnica", Bucuresti, aprilie, 2006.
- [4]. **Louganski K. P.** *Modeling and analysis of a DC power distribution system for in 21st century airlifters.* Doctoral dissertation, Virginia, 1990.
- [5]. **Elbuluk, M. E., Kankam, M.D.** *Potential starter/generator Technologies for Future Aerospace applications.* IEEE AES Magazine, vol.11, no.10, 1996, pp. 1724.

TENSIONS INVERTORS WITH COMMUTATION ON THREE LEVELS. MATHEMATICAL MODELING; STRUCTURAL DIAGRAM

CONSTANTIN BRÎNDUŞA^{*}, MIHAI PĂSCULESCU^{**}, DRAGOŞ
PĂSCULESCU^{***}

Abstract: The tension inverter with commutation on three levels is applied in electric action systems specific to electric urban traction. Based on commutation functions the tension invertors with commutation on three levels it can mathematical modeled. Beginning from the mathematical model it can be made a structural diagram of the tension inverter with commutation on three levels.

Keywords: tension inverter, three levels, urban frame, mathematical model, structural diagram.

1. INTRODUCTION

The working hypothesis for the modelling of the semi-conductor power devices considered are: commutation as working regime, with the neglect of the commutation times and the voltage failures for the conduction in direct sense, from here resulting the fat that the converter is consider without losses.

Every converter type has construction and functioning particularities that impose certain restrictions when passing to the mathematical modelling process. The mathematical modelling of the voltage invertors, thus of the static power converters without the intermediary circuit, can be done in many ways, and they are:

- throughout the state equations that most of the analysis packages of the electronic power circuits are based on;
- through the use of the Laplace transformant;

^{*} *PhD Student. Eng. University of Petrosani*

^{**} *Professor PhD .eng. University of Petrosani*

^{***} *Assistant PhD Student Eng. University of Petrosani*

- through the analysis of the spatial phasor;
- on the basis of the discrete samples, method which can be applied to the semi-conductor power devices which work in commutation regime, etc..

The chosen modelling method is based upon the commutation functions, taking into account also the MATLAB utilitarian.

2. MATHEMATICAL MODELING; STRUCTURAL DIAGRAM

On the basis of the electronic scheme of principle assembly inverter of voltage with commutation on 3 levels and asynchronous engine, (figure 1), we will obtain the mathematic level and the structural scheme.

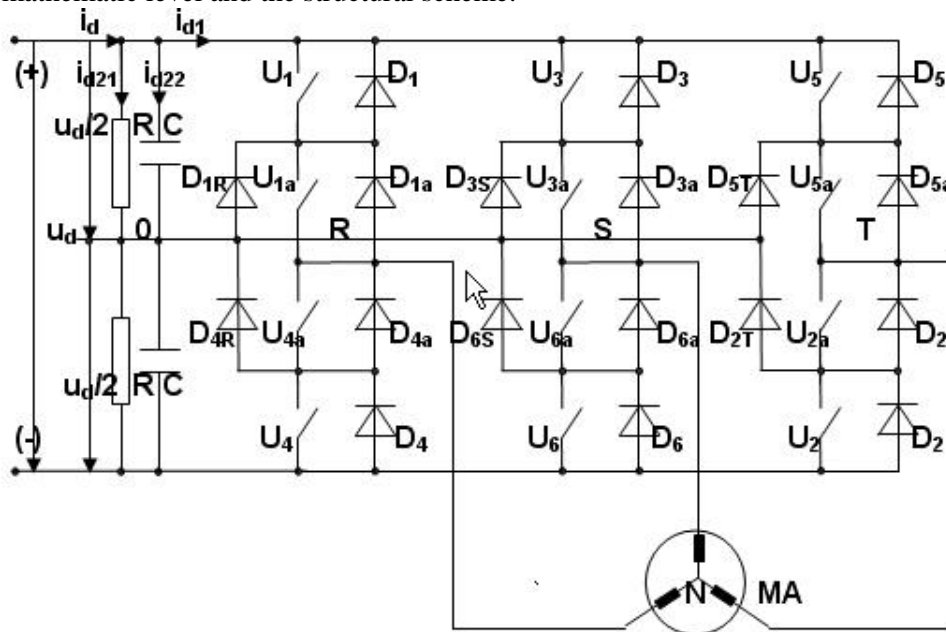


Fig. 1 The electronic scheme on principle assembly inverter of voltage with commutation on 3 levels and asynchronous engine

For shaping the inverter of voltage with commutation on 3 levels (to see fig.1), is been considered the ideal case in which the two groups RC divide in equal way the U_d tension. For shaping the inverter of voltage with commutation on 3 levels it is used the function with commutation on three levels f_{3C} , (Tab.1):

Table 1

Nr. crt.	Tip inverter of voltage	Commutation function	Values function	Variable: tiristor s ext.	Variable: tiristor j ext.	Variable: tiristor m int.
1	Inverter with commutation on 3 levels	f_{3C}	1	1;3;5		$1_a;3_a;5_a$
			0			$1_a;3_a;5_a;4_a;6_a;2_a$
			-1		4;6;2	$4_a;6_a;2_a$

By utilizing the f_{3C} function result's table 2:

Table 2

Type circuit force	Voltage fase R	Voltage fase S	Voltage fase T
Inverter of voltage	$u_{R0} = \frac{u_d}{2} \cdot f_{3CR}$	$u_{S0} = \frac{u_d}{2} \cdot f_{3CS}$	$u_{T0} = \frac{u_d}{2} \cdot f_{3CT}$
Motor asinc.	$u_{RN} = u_{R0} - u_{N0}$	$u_{SN} = u_{S0} - u_{N0}$	$u_{TN} = u_{T0} - u_{N0}$

In case we have a connection Y asynchronous engine, we have the relation:

$$u_{N0} = (u_{R0} + u_{S0} + u_{T0})/3 \tag{1}$$

Taking into account the relations previously presented it results the structural scheme three phase inverter of voltage with commutation on 3 levels, (fig.2).

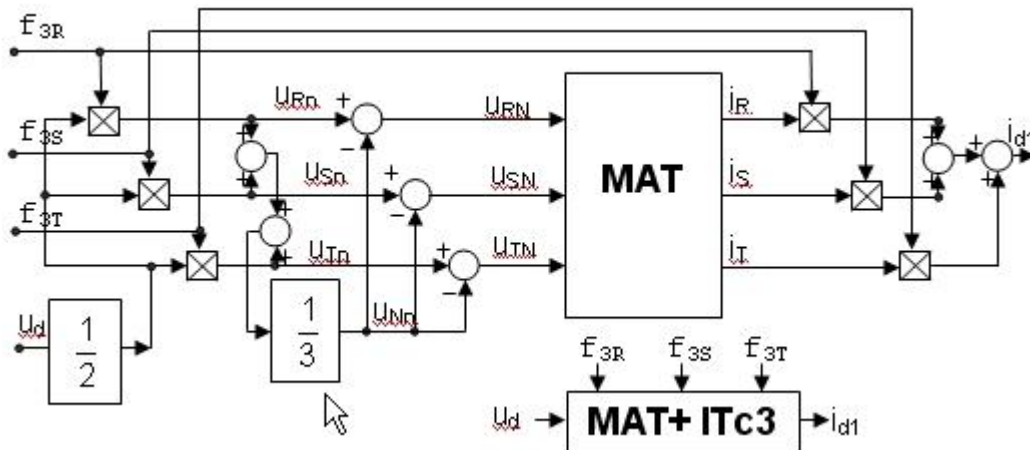


Fig 2 The structural scheme and the mask block, three phases voltage inverter with commutation on 3 levels

Afte rit was expected the models and the structural scheme corresponding with the two invertors of voltage are similar, indifferent of the commutation functions which stand at the base of modelation.

This thing allows the introduction of a mathematical drives λ , and obtaining a unitary structural scheme and the corresponding mask block., (fig.3).

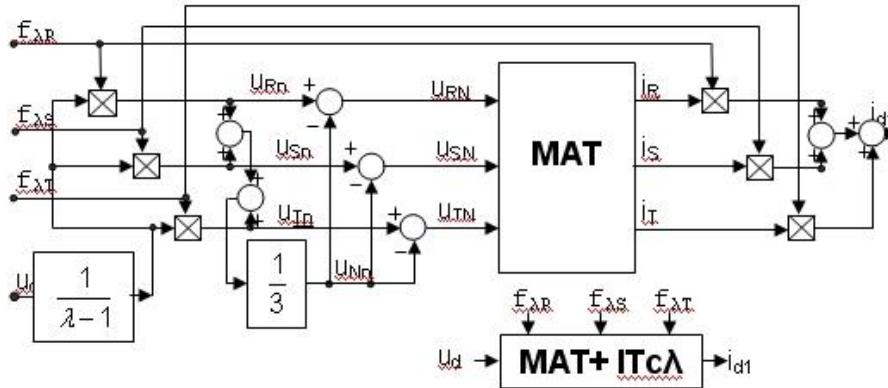


Fig 3 The structural scheme and the mask block, three phases voltage inverter with commutation on 3 levels

The λ driver is defined in N multitude and has the value according to table 3.

Table 3 The value for λ driver

Nr.	Type circuit force	Type comut.	Values op.	Commut. function $f_{\lambda C}$
1	Inverter of voltage	2 levels	2	f_{2C}
2	Inverter of voltage	3 levels	3	f_{3C}

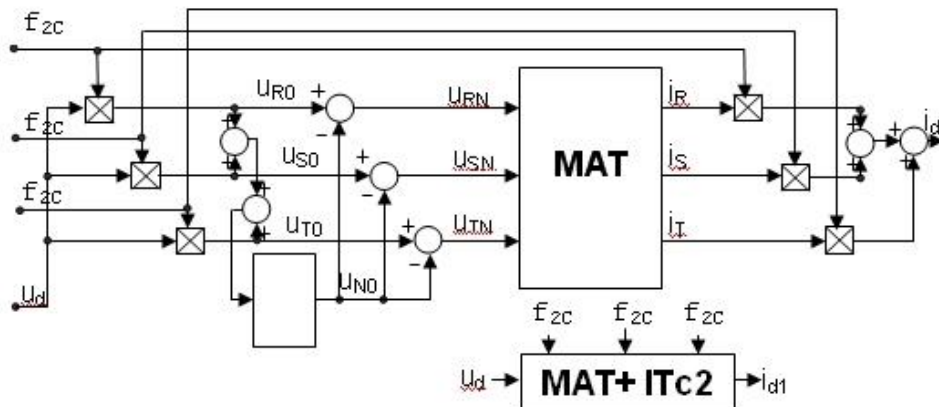


Fig 4 The structural scheme and the mask block, three phases voltage inverter with commutation on 2 levels

It can be observed that through allocating value 2 to λ driver we have the case of the inverter of voltage with commutation on two levels and the f_{2C} commutation function, (fig.4).

So the structural scheme and the generalized mask block, (fig.3), it transform in structural scheme and mask block inverter of voltage with commutation on two

levels.

By allocating value 3 to λ driver we have the case of inverter of voltage with commutation on 3 levels and the f_{3C} commutation function. So the structural scheme and the generalized mask block (fig.3), it transform in structural scheme and mask block inverter of voltage with commutation on three levels, (fig.2).

The two models have included in their structure the model of the asynchronous engine of traction MAT, the bundle with this is been made through tension and the stator current. The commutation function generated by the control system of traction allow the control of the ensemble tension inverter – asynchronous engine.

3. CONCLUSIONS

Se pot trage urmatoarele concluzii:

- The mathematic modelling of the voltage inverter with commutation on 2 levels, on the basis of the electronic scheme of the principle assembly voltage inverter with commutation on 3 levels - asynchronous engine can be made through the use of the commutation function with 3 levels;

- The structural scheme and the mask block assembly voltage inverter with commutation on 3 levels - asynchronous engine is obtained on the basis of the mathematical model;

- Is been established a structural, unitary scheme, no matter the voltage inverter type, (commutation on 2 or 3 levels);

- The necessity of establishing an unitary voltage inverter model, indifferently of the number of inverter commutation levels

REFERENCES

[1]. Brîndușă, C., ș.a., *Sisteme electrice de transport neconvenționale (A23); Rama de metrou acționată cu motoare asincrone*; Execu ie i experimentare modele (Faza 23.1), Contract cercetare 606C- Anexa A, Institutul na ional de cercetare i proiectare pentru ma ini electrice, echipament electric i trac iune, Craiova, 1992.

[2]. Brîndușă, C., Păsculescu, M., Popescu, L., *Drive systems behavior analysis in urban electric traction with Matlab software extensions*, Simpozion Interna ional Multidisciplinar „UNIVERSITARIA SIMPRO” ,2006, Petro ani, Editura Universitas Petrosani, 2006.

[3]. Nicola, D.A., Cismaru, D.C., *Mathematical models for control simulation of traction induction motors*, ICATE'98, Craiova, 1998.

TENSIONS INVERTORS WITH COMMUTATION ON TWO LEVELS. MATHEMATICAL MODELING; STRUCTURAL DIAGRAM

CONSTANTIN BRÎNDUȘA*, MIHAI PĂSCULESCU**
DRAGOȘ PĂSCULESCU ***

Abstract: The tension inverter with commutation on two levels is applied in electric action systems specific to electric urban traction. Based on commutation functions the tension invertors with commutation on two levels it can mathematical modelade. Beginning from the mathematical model it can be made a structural diagram of the tension inverter with commutation on two levels.

Keywords: tension inverter, two levels, urban frame, mathematical model, structural diagram.

1. INTRODUCTION

Every converter type has construction and functioning particularities that impose certain restrictions when passing to the mathematical modelling process. The mathematical modelling of the voltage invertors, thus of the static power converters without the intermediary circuit, can be done in many ways, and they are:

- throughout the state equations that most of the analysis packages of the electronic power circuits are based on;
- through the use of the Laplace transformant;
- through the analysis of the spatial phasor;
- on the basis of the discrete samples, method which can be applied to the semi-conductor power devices which work in commutation regime, etc..

The chosen modelling method is based upon the commutation functions, taking into account also the MATLAB utilitarian.

* *PhD Student.Eng., University of Petrosani*

** *Professor PhD Eng. University of Petrosani*

*** *Assistant PhD Student University of Petrosani*

Taking into account the voltage inverters type used in the electric action with static converters and asynchronous traction engines namely voltage converters with commutation on 2, in their modelling we will define through tables the commutation function, (table 1).

Table 1

Nr. crt.	Tip inverter of voltage	Commutation function	Values function	Fase inverter
1	Inverter with commutation on 2 levels	f_{2C}	1	R;S;T
			0	R;S;T
3	Inverter with commutation on 3 levels	f_{3C}	1	R;S;T
			0	R;S;T
			-1	R;S;T

The working hypothesis for the modelling of the semi-conductor power devices considered are: commutation as working regime, with the neglect of the commutation times and the voltage failures for the conduction in direct sense, from here resulting the fact that the converter is consider without losses.

2. MATHEMATICAL MODELING; STRUCTURAL DIAGRAM

On the basis of the electronic scheme of principle assembly inverter of voltage with commutation on 2 levels and asynchronous engine, (figure 1), we will obtain the mathematic level and the structural scheme.

For the modelling of the voltage inverter with commutation on 2 levels is used the commutation function in 2 levels, f_{2C} , (Tab.2):

Table 2

Nr. crt.	Tip inverter of voltage	Commutation function	Values function	Variable Tiristor s	Variable Tiristor j
1	Inverter with commutation on 2 levels	f_{2C}	1	1; 3; 5	
			0		4; 6; 2

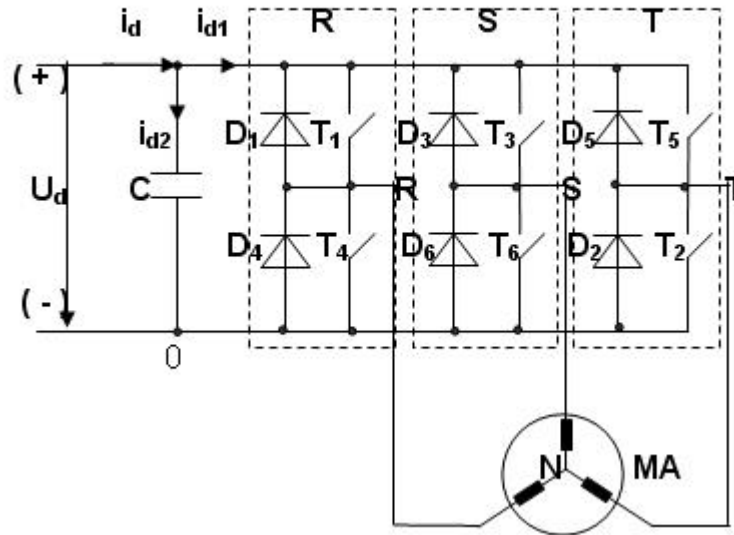


Fig 1 The electronic scheme on principle assembly inverter of voltage with commutation on 2 levels and asynchronous engine

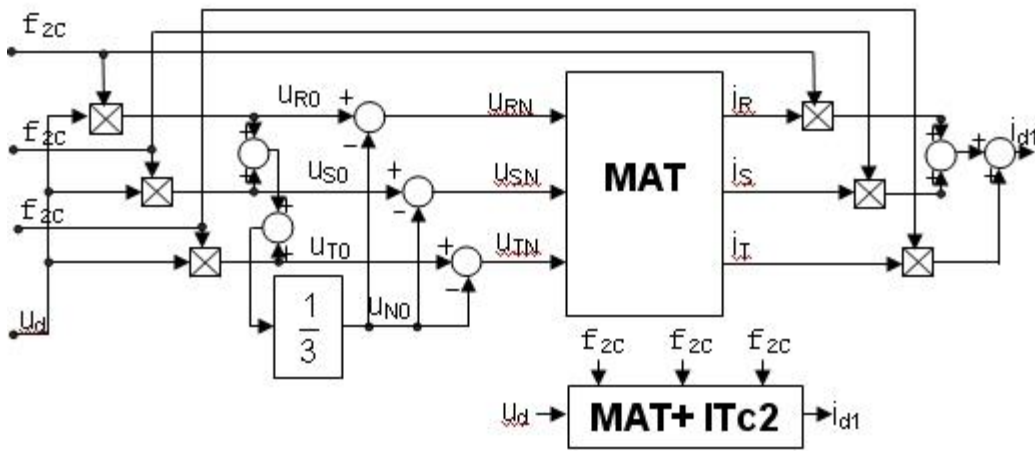


Fig 2 The structural scheme and the mask block, three phases voltage inverter with commutation on 2 levels

By utilizing the f_{2c} function it results table 3:

Table 3

Type circuit force	Voltage fase R	Voltage fase S	Voltage fase T
Inverter of voltage	$u_{R0} = U_d f_{2CR}$	$u_{S0} = U_d f_{2CS}$	$u_{T0} = U_d f_{2CT}$
Motor asinc.	$u_{RN} = u_{R0} - u_{N0}$	$u_{SN} = u_{S0} - u_{N0}$	$u_{TN} = u_{T0} - u_{N0}$

In case we have a connection Y asynchronous engine, we have the relation:

$$u_{N0} = (u_{R0} + u_{S0} + u_{T0})/3 \quad (1)$$

Taking into account the relations previously presented it results the structural scheme three phase inverter of voltage with commutation on 2 levels, (fig.2).

3. CONCLUSIONS

We can draw the following conclusions:

- The mathematic modelling of the voltage inverter with commutation on 2 levels, on the basis of the electronic scheme of the principle assembly voltage inverter with commutation on 2 levels - asynchronous engine can be made through the use of the commutation function with 2 levels;
- The structural scheme and the mask block assembly voltage inverter with commutation on 2 levels - asynchronous engine is obtained on the basis of the mathematical model;
- The necessity of establishing a structural, unitary scheme, no matter the voltage inverter type, (commutation on 2 or 3 levels);
- The necessity of establishing an unitary voltage inverter model, indifferently of the number of inverter commutation levels.

REFERENCES

- [1]. Brîndușă, C., ș.a., *Sisteme electrice de transport neconvenționale (A23); Rama de metrou acționată cu motoare asincrone*; Execu ie i experimentare modele (Faza 23.1), Contract cercetare 606C- Anexa A, Institutul na ional de cercetare i proiectare pentru ma ini electrice, echipament electric i trac iune, Craiova, 1992.
- [2]. Brîndușă, C., Păsculescu, M., Popescu, L., *Drive systems behavior analysis in urban electric traction with Matlab software extensions*, Simpozion Interna ional Multidisciplinar „UNIVERSITARIA SIMPRO” ,2006, Petro ani, Editura Universitas Petrosani, 2006.
- [3]. Nicola, D.A., Cismaru, D.C., *Mathematical models for control simulation of traction induction motors*, ICATE'98, Craiova, 1998.

THE ANALYSIS OF THE LC-TYPE PASSIVE FILTERS' INFLUENCE UPON THE POWER SUPPLY NETWORK OF A REZISTIVE CONSUMER USING THE LABVIEW PROGRAM

IOAN BACIU*, **CORINA CUNȚAN****

ABSTRACT. This work is analysing the influence of the passive filters upon the parameters of the single-phase power supply line of a rezistive consumer using the LabVIEW program. The filter's model is represented by the mathematical function related to each harmonic in part, expression which is introduced based on a previously established law. It's aiming the possibility to modify the filter's expression depending on the power supply line's parameters.

Key words: LC filters, power, current, voltage

1. WORK'S PRESENTATION

In order to compensate the harmonics of the currents absorbed from the distribution networks by different consumers of which supply is made by commutation elements are used passive and/or active power filters of high performance.

In the usual case, the passive filters are influenced by the modification of the own resonance frequency of the power supply network. This present survey is analyzing the situation when the own filter's frequency is modifying by a sinusoidal law and the network's frequency remains unmodified. The operation is emphasized by showing on the same graphic the input voltage, the current and signal's power on the load resistance, as well as by showing the related frequency spectrum, determined with the Fourier Transformation of the current from the circuit by connecting the LC filter. It's used a signal generator which allows to obtain two dephased output signals, with a phase displacement imposed depending on the capacitor's and coil's values, which is the one introduced by the two elements in the circuit. The two

* *Dipl. Eng University from Timișoara, Faculty of Engineering from Hunedoara*

** *Ph. D. Eng University from Timișoara, Faculty of Engineering from Hunedoara*

elements are modeled by a mathematical law and which takes into account the sinusoidal shape we want to have the filter's impedance module.

$$X_L = \frac{L}{N} \sin x$$

$$X_C = \frac{1}{\frac{C}{10^n} \sin x}$$

where: L and C are values to be imposed for the coil, respectively capacitor.

N is a weighting factor of inductance's value

n is a weighting factor of capacitor's value

$\sin x$ signal generated by a sinusoidal signal generator

Considering the two ideal elements, without loss resistance, is obtaining the LC circuit's impedance:

$$Z = \frac{L}{N} \sin x + \frac{10^n}{C} \sin x = \left(\frac{L}{N} + \frac{10^n}{C} \right) \sin x$$

Having the impedance value, will be obtained the current through the LC circuit:

$$I_F = \frac{\sqrt{2}U}{Z} \sin t = \frac{\sqrt{2}U}{|Z| \sin x} \sin(t - t_1); \quad t_1 = \frac{\varphi}{\omega}$$

where: φ represents the phase displacement introduced by LC for the signal generator's function from the input circuit on the load circuit R_S , and ω is the generator's pulsation.

$$\varphi = \text{arctg} \frac{X_L - X_C}{R_S}$$

Is obtained: - the energy stored in the LC filter by the relation:

$$E_n = \frac{1}{2} LI^2 + \frac{1}{2} CU^2 = \frac{1}{2} L \sin x I^2 + \frac{1}{2} C (I \cdot X_C)^2 = \frac{1}{2} I^2 \left(\frac{L}{N} \sin x + \frac{10^n}{C \cdot \sin x} \right)$$

- input signal U_{in}

$$U_{in} = \sqrt{2}U \sin t$$

- signal's power on the filtration circuit

$$P = \frac{\sqrt{2}U}{Z} \sin(t - t_1) \cdot \sqrt{2} \cdot U \sin t$$

- current through the filtration circuit

$$I = \frac{\sqrt{2} \cdot U}{Z} \sin t = \frac{\sqrt{2} \cdot U}{|Z| \sin x} \sin(t - t_1)$$

Is applied the Fourier Transformation upon the current and is obtained the spectrum's module for a sampling sequence of 250Hz.

The circuit's operation diagram (fig. 1) drawn in LabView allows the visualization of the connexions between the elements which intervene, as well as the modality to implement the mathematical relations.

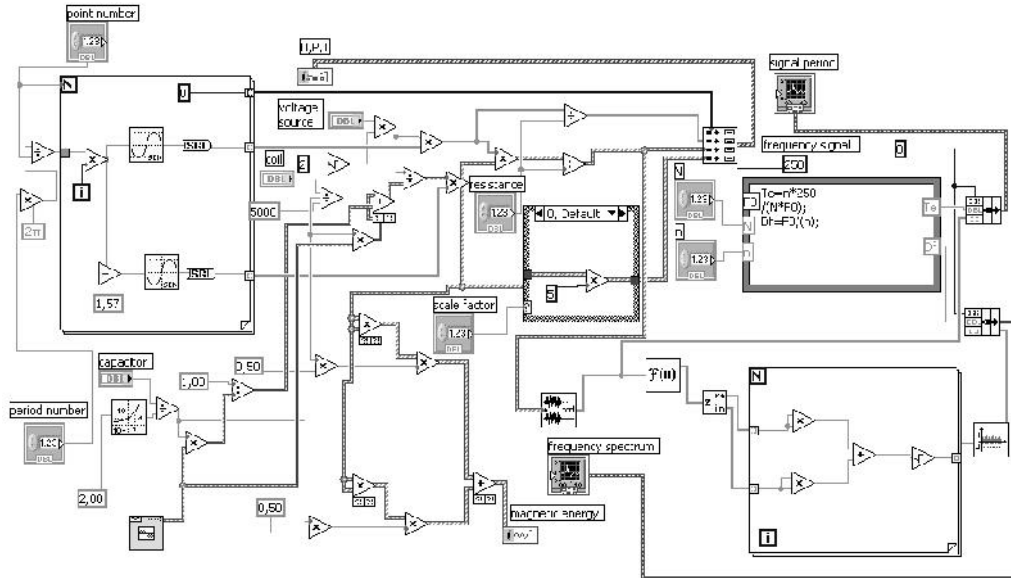


Fig.1

Thus are obtained the wave shapes of the voltage, current and power (fig. 2), the frequency spectrum (fig. 3) and the energy stored in the LC filter (fig. 4).

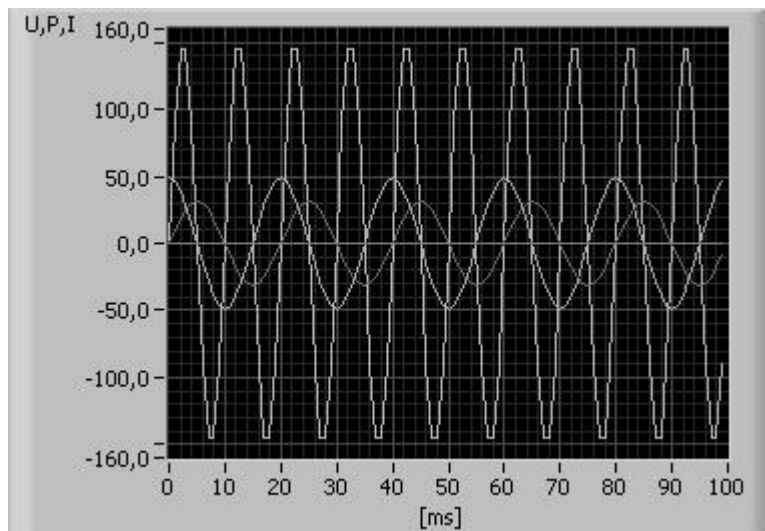


Fig.2

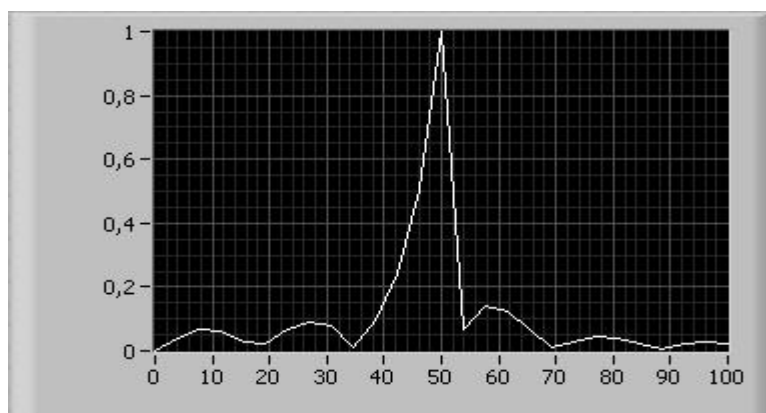


Fig.3 Frequency spectrum

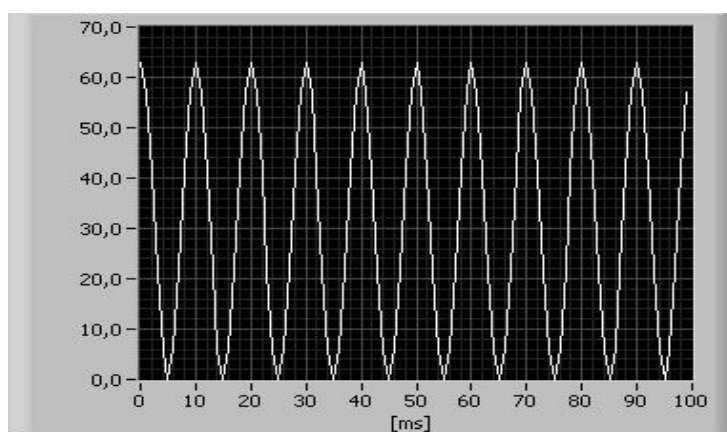


Fig.4 Time domain

2. CONCLUSIONS

The harmonics spectrum emphasizes the existence of the harmonics in the form of the current through the filter, harmonics which have a large spectrum and relatively small values against the fundamental. For the signal power on the filter is found its double variation frequency, as well as a shape distortion at maximum values. Also, one can observe the phase displacement imposed between voltage and current.

Interesting is how it's presenting the shape of the energy stored in the LC filter, being obtained more simultaneous values, which leads to more sinusoids of different amplitudes and identical frequency.

REFERENCES

- [1] Pop E., Nafornită I., Tiponuş V., Toma L., Mihăescu A., - *Metode în prelucrarea numerică a semnalelor*, Editura Facla, Timișoara 1986;
- [2] Cottet F., Ciobanu O., - *Bazele programării în LabVIEW*, Editura Matrix Rom, București 1998

THE LIGNITE ROLE AS THE PRIMARY SOURCE IN THE ELECTRICAL ENERGY SUPPLY IN ROMANIA

CURELEANU SORIN*, BLANARU LIVIU*, STOICHITOIU ANGHEL**

Abstract. This study is analyzing the odds of coal production industry after the integration of our country into the European Community

Key words: lignite, energy, power

1. INTRODUCTION

The investments concerning the National Energetic System (S.E.N.) have permitted our country to become energetically since 2004 a full-rights member in the European Union.

2. THE ROLE OF THE LIGNITE IN POWER GENERATION

Recently the reorganization of the coal-based power generation was accomplished by founding the Energetic Complex in Rovinari, Turceni and Craiova. In this system, the open pit coal mines are integrated like cost-centre of the power producer. In the following table is illustrated the Romanian energy production prognosis in the interval 2005 – 2010:

Table 1 [GWh]

	2005-	2010-	2015-	2020-
Total production	76000	88000	102000	112000
Coal-based power plants	31000	33000	35000	35000
Hydro-centrals	13700	14200	14600	15000
Fuel-oil and nuclear power plants	29800	39100	50400	60000

* *PhD Student. University of Petrosani*

** *Professor PhD .Eng. University of Petrosani*

The considerations about the internal energetic resources in the biggest Romanian burning power plants are as follows: the existing coal (lignite and brown coal) is used by the big thermo-electrical power plants (CTE) of the national energetic system endowed with high performance energy generation installations and natural gas (imported and indigene) are imposing the expansion and the development of the transport and distribution network. Heavy fuel oil importing is an important issue on a non-predictable market.

Based on the analyses of the Romanian extracting industry recovery trend, the significant aspects are as follows:

- the natural resource (coal) is ensuring a large amount of the primary resources for the energetic sector, presenting on the internal market a large absorption capacity;
- there is an important capacitive potential partially worn-out physically and morally, only partly used, with a structure not enough adapted to the new competitively standards from the European Union and other developed countries;
- the equipment and technology's performances can be substantially improved by an accelerated and selective modernizing effort of the production capacities with viability real chances;
- it is still available qualified personnel with technical capacity comparable with the one from the developed countries, etc.

For a large time interval the coal is the base energetic resource for Romania. The situation of the energetic fuel consumption is as follows: (fig. 1)

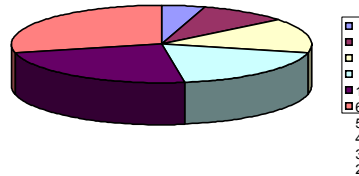


Fig. 1 Romanian fuel consumption situation:

1. heavy oil – 3%;
2. other conventional resources – 4%;
3. nuclear – 11%;
4. natural gas – 16%;
5. regenerative – 28%;
6. coal – 38%;

In the present tight competition situation in the energetic market, when the ecological restrictions are derogatory for the Energetic Complex Structures, where the basic fuel is the lignite and the price of the solid fuel, oil and natural gas is increasing as well, the marketing compartments are looking for improved organization methods by technical and technological restructuring. The target of these measures is to reduce the specific energy cost price especially by reducing the extracting cost of the lignite.

Our lignite has an average lower caloric capacity compared with other European zones, having higher ash content, and the outturn of the lignite power plants (CTE) is less than the ones using the brown coal or hydrocarbons.

Lignite-based power generation has the following benefits:

- production costs closer than oil;
- ensuring the use of the internal resources and diminishing of the hydrocarbons fuel import;
- the primary investments are lower than nuclear power plants and hydro centrals with the same installed power;
- ensuring a higher zonal number of employment, thus resolving an important social aspect;
- thermal energy is produced in co-generation with electric power;
- environmental problems are solved by the present technologies.

The adapting process of the open pit mining to the free market conditions, when there are still some technical endowment pending problems, can be accomplished by adopting a complex reorganization system aiming managing components, as well as mining and environmental components.

3. EUROPEAN DIRECTIONS FOR MINING INDUSTRY

The principal instruments for implementing the European legislation consist of the European directions with a large impact over the Romanian mining industry. We are mentioning the 94/22/EC direction regarding the licensing and the license use for hydrocarbons exploit, 92/91/EC direction regarding the minimal requirements for the mining extraction personnel safety and the proposed instruction for waste materials disposal management in the extraction industry.

4. CONCLUSIONS

In the future, the coal will take an important share in power generation as well as in the economical development of the society.

An energy saving active policy will be applied in parallel with the energy production cost savings. The available internal lignite reserves is about 55 years of about 35 millions tons per year in the open pit mines and for the brown coal is about 3.5 million tones.

REFERENCES

- [1] **European AQUIS Requests;**
- [2] **CESCO Consulting Committee Declaration about the role of coal in the XXI century Europe** (July 1999);
- [3] **EUROCOAL Report – PATROMIN Magazine;**
- [4] **LEGEA 3 / 2001 – Kyoto Protocol ratification on the United Nation Convention about Environment and Climate Altering.**

THE NEW EUROPEAN CONCEPT OF EXPLOSION PROTECTION FOR THE NON-ELECTRICAL EQUIPMENT INTENDED FOR USE IN EXPLOSIVE ATMOSPHERES

ADRIAN MARIUS JURCA*, MIHAELA PĂRĂIAN**, EMILIAN GHICIOI***, NICULINA VĂTAVU***

Abstract: Non-electrical equipment has been used for over one hundred years in industry branches with environments having potentially explosive atmospheres generated by gas, vapor, mist and/or combustible dust. Thus, a great deal of experience has been gained in the application of protective measures to reduce the risk of ignition to an acceptably safe level. With the introduction of the ATEX Directive 94/9/EC and the inclusion of non-electrical equipment in its scope, it became necessary to produce standards which have to include: ignition protection concepts, protective measures clearly defined and, nevertheless, the benefit of the extensive experience gained over the years. In the case of non-electrical equipment, the reference standard is SR EN 13463-1:2003, Non-electrical equipment for potentially explosive atmospheres Part 1: Basic method and requirements, that specifies the basic method and requirements for design, construction, testing and marking of the non-electrical equipment intended for use in potentially explosive atmospheres in air of gas, vapor, mist and/or combustible dusts. This standard must be applied together with the European standards regarding the specific types of ignition protection, part of those in courses of harmonization.

Keywords: non-electrical equipment, explosion prevention, explosion protection, ignition sources, explosive atmosphere

1. GENERALITIES

Explosion protection is of particular importance to safety; since explosions endanger the lives and health of workers as a result of the uncontrolled effects of flame and pressure, the presence of noxious reaction products, and consumption of the oxygen in the ambient air, which workers breathe.

* *PhD.Eng, scientific researcher at INSEMEX Petroșani*

** *Ph.D:Eng, senior scientific researcher I at INSEMEX Petroșani*

*** *Ph.D:Eng, senior scientific researcher II at INSEMEX Petroșani*

For this reason, the establishment of a coherent strategy for the prevention of explosions requires that technical and organisational measures be taken at the workplace, that shall be decided individually for each case.

Technical measures for explosion protection means all measures that:

- prevent the formation of hazardous explosive atmospheres,
- avoid the ignition of hazardous explosive atmospheres or
- mitigate the effects of explosions so as to ensure the health and safety of

workers.

As general rule: preventing the formation of *hazardous explosive atmospheres* must always be given priority.

If it is not possible to prevent the formation of a *hazardous explosive atmosphere*, its ignition must be avoided. This can be achieved by protective measures which avoid or reduce the probability of *ignition sources*. To lay down effective precautions, one must know the various types of ignition source and the ways in which they operate. The probability that a *hazardous explosive atmosphere* and a *source of ignition* will be present at the same time and place is estimated and the extent of the measures required is determined accordingly. This is done on the basis of the zone system described below, from which the necessary precautions are derived.

In many cases, it is not possible to avoid explosive atmospheres and sources of ignition with a sufficient degree of certainty. Measures must then be taken to limit the effects of an *explosion* to an acceptable extent. Such measures are

- explosion-resistant design;
- explosion relief;
- explosion suppression; prevention of flame and explosion propagation.

Requirements for work equipment

The employer must ensure that *work equipment* and all *installation materials* are suitable for use in *hazardous places*. In doing so, he must take account of the possible ambient conditions at the workplace in question. The work equipment must be so assembled, installed and operated that it cannot cause an *explosion*.

In order to facilitate the selection of appropriate apparatus and the design of suitable installations, hazardous areas are divided into zones 0, 1 and 2 according to **SR EN 60079-10**, and equipment is divided into categories, according to European Directive 94/9/CE.

In most practical situations where flammable materials are used, it is difficult to ensure that an explosive gas atmosphere will never occur. It may also be difficult to ensure that apparatus will never give rise to a source of ignition. Therefore, in situations where an explosive gas atmosphere has a high likelihood of occurring, reliance is placed on using apparatus which has a low likelihood of creating a source of ignition. Conversely, where the likelihood of an explosive gas atmosphere occurring is reduced, apparatus constructed to a less rigorous standard may be used.

Extent of protective measures

Levels of protection required for group IIG equipment

Zone	Presence of explosive atmospheres (explosion hazard)	Avoidance of effective ignition sources (ignition hazard)	Level of protection required	Group II category
------	---	---	------------------------------------	----------------------

2	Infrequently and for a short period only	During normal operation	Normal	3
1	Likely to occur	Also during foreseeable malfunctions (single fault)	High	2
0	Continuously, for long periods or frequently	Also during rare malfunctions (two independent faults)	Very high	1

Levels of protection for Group I equipment(mining)

Group I comprises equipment intended for use in the underground parts of mines, and to those parts of surface installations of such mines, likely to become endangered by **firedamp and/or combustible dust**.

Group I category M1 (very high protection level): Products of this category are required to remain functional for safety reasons when an explosive atmosphere is present and is characterised by integrated explosion protection measures (two means of protection or safe against two faults).

Group I category M2 (high protection level): These products are intended to be de-energised in the event of an explosive atmosphere (safe in normal operation and for severe operating conditions).

Essential requirements

The essential requirements include all those requirements necessary in order to attain the objective of a directive. Essential requirements are of **mandatory application**. Only products complying with the relevant essential requirements can be placed on the market. Essential requirements must be applied depending on the hazards inherent to a given product. But the directives do not contain information on how the essential requirements could or should be met. Thus, manufacturers need to carry out hazard analysis to determine whether a product complies with the essential requirements. This analysis should be documented and included in the technical documentation of the product.

2. HARMONISED STANDARDS

There are different ways of demonstrating conformity either directly to essential requirements or to harmonised standards. Harmonised standards provide detailed specifications in terms of objectives with regard to the practical fulfilment of essential requirements. Harmonised standards are of **voluntary application**.

One standard does not necessarily cover all essential requirements of one directive. It might be that only one, or selected, essential requirements are addressed by the harmonised standards.

The application of harmonised standards may drastically simplify and speed up the procedure for conformity assessment.

A number of harmonised standards is available in the field of **explosion protection**. For electrical equipment, these standards are published by CENELEC. For non-electrical equipment explosion protected equipment and protective systems these standards are prepared by CEN/TC 305.

The main standards prepared for non-electric equipment intended for use in potentially explosive atmospheres are: the main standard that establishes the basic

method and requirements for design, manufacture, test and marking for non-electric equipment intended for use in potentially explosive atmospheres of gas, vapor, mists and dusts (SR EN 13463-1) and then the specific standards comprising the types of explosion protection:

- “fr” : Protection by flow restricting enclosure (SR EN 13463-2)
- “d” : Protection by flameproof enclosure (SR EN 13463-3)
- “g” : Protection by inherent safety (pr EN 13463-4)
- “c” : Protection by constructional safety (SR EN 16463-5)
- “b” : Protection by control of ignition source (SR EN 16463-6)
- “p” : Protection by pressurisation (pr EN 16463-7)
- “k” : Protection by liquid immersion (SR EN 16463-8)

Up to the present there were harmonized as SR, the general standard and the standards with the types of protection: flow restricting enclosure “fr”, flameproof enclosure “d”, constructional safety “c”, control of ignition source „b” and liquid immersion „k”.

3. ASSESSMENT OF IGNITION HAZARDS

All equipment and all parts of it shall be subjected to a formal documented hazard analysis and lists all of the potential sources of ignition by the equipment and the measures to be applied to prevent them becoming effective. Examples of such sources include hot surfaces, naked flames, hot gases/liquides, mechanically generated sparks, adiabatic compression, shock waves, exothermic chemical reaction, thermite reactions, self ignition of dust, electrical arcing and static electricity discharge.

Protective measures /types of protection shall be considered and/or applied in the following order:

- ensure that ignition sources cannot arise;
- ensure that ignition sources cannot become effective ;
- prevent explosive atmosphere reaching the ignition source;
- contain the explosion and prevent flame propagation.

Protective measures/types of protection provided in the non-electric equipment standards are the following:

Protective measure	Type of protection
ensure that ignition sources cannot arise	“c” : Protection by constructional safety
	“g” : Protection by inherent safety
ensure that ignition sources cannot become effective	“b” : Protection by control of ignition source
prevent explosive atmosphere reaching the ignition source	“fr” : Protection by flow restricting enclosure
	“p” : Protection by pressurisation
	“k” : Protection by liquid immersion
contain the explosion and prevent flame propagation	“d” : Protection by flameproof enclosure

4. ASSESSMENT FOR THE GROUP II EQUIPMENT

In the case of category 1 equipment, the list shall include all potential ignition sources that are effective or may become effective during expected malfunction and rare malfunction. It shall also indicate the measures to prevent the ignition used according to this standard and the ignition protection standards listed in the scope of this standard which have been applied. Category 1 equipment shall not have and ignition source that is effective or may become effective in normal operation.

In the case of category 2 equipment, the list shall include all potential ignition sources that are effective or may become effective during normal operation and expected malfunction. It shall also indicate the measures to prevent the ignition used according to this standard and to the ignition protection standards listed in the scope of this standard which have been applied.

In the case of category 3 equipment, the list shall include all potential ignition sources that are effective or may become effective during normal operation. It shall also indicate the measures to prevent the ignition used according to this standard and to the ignition protection standards listed in the scope of this standard which have been applied.

5. CONFORMITY ASSESSMENT/ PROCEDURES

Before being placed on the market, products that are covered by the New Approach directives must be submitted to a conformity assessment procedure. The appropriate conformity assessment procedure in accordance with the levels of possible hazards and with the necessary levels of protection and confidence required is defined in the Directive 94/9/CE.

6. MARKING

Marking example for non-electrical equipment



Marking according to Directive 94/9/EC:

- name and address of the manufacturer,
- designation of series or type,
- serial number, if any,

- year of construction
 - CE marking (first line; but **not on components**),
 - identification number of the Notified Body involved in the production surveillance,
 - the (well-known) Epsilon-X in a hexagon,
 - the symbol of the equipment-group and category,
 - for equipment group II, the type of hazard, gas (G) or dust (D)
 - additional marking required by standards or due to certification

BIBLIOGRAPHY

[1] **Directive 1999/92/EC of the European Parliament and of the Council of 16 December 1999 on minimum requirements for improving the safety and health protection of workers potentially at risk from explosive atmospheres.** Official Journal No. L 023, 2000-01-28, 57-64,

[2] **Directive 94/9/EC of the European Parliament and the Council of 23 March 1994 on the approximation of the laws of the Member States concerning equipment and protective systems intended for use in potentially explosive atmospheres.** Official Journal No. L 100, 1994-04-19,

[3] **Non-binding Guide of Good Practice for implementing of the European Parliament and Council Directive 1999/92/EC on minimum requirements for improving the safety and health protection of workers potentially at risk from explosive atmospheres,** European Commission, DG Employment and Social Affairs, Brussels, April 2003

[4] **ATEX-Guidelines: Guidelines on the Application of Council Directive 94/9/EC of 23 March 1994 on the approximation of the laws of the Member States concerning equipment and protective systems intended for use in potentially explosive atmospheres.** European Commission, Second edition, July 2005

[5] **Heino Bothe** *ATEX 94/9/EC - Identification and treatment of non-electrical ignition hazard in standards*

[6] **Beyer Michael** *European New Approach Directive Structure and ATEX Directive 94/9/EC*

[7] **SR EN 13463-1** *Non-electrical equipment for potentially explosive atmospheres. Part 1 : Basic method and requirements*

[8] **SR EN 13463-2** *Non-electrical equipment for use in potentially explosive atmospheres. Part 2: Protection by flow restricting enclosure “fr”*

[9] **SR EN 13463-3** *Non-electrical equipment for use in potentially explosive atmospheres. Part 3: Protection by flameproof enclosure “d”*

[10] **prEN 13463-4** *Non-electrical equipment for use in potentially explosive atmospheres. Part 4: Protection by inherent safety “g”*

[11] **SR EN 13463-5** *Non-electrical equipment for use in potentially explosive atmospheres. Part 5: Protection by constructional safety “c”*

[12] **SR EN 13463-6** *Non-electrical equipment for use in potentially explosive atmospheres. Part 6: Protection by control of ignition source “b”*

[13] **prEN 16463-7** *Non-electrical equipment for use in potentially explosive atmospheres. Part 7: Protection by pressurisation “p”*

[14] **SR EN 13463-8** *Non-electrical equipment for use in potentially explosive atmospheres. Part 8: Protection by liquid immersion “k”*

THE OPTIMAL OPERATING RANGES OF THE STEAM GENERATORS WITH NATURAL CIRCULATION WORKING ON POWDRED COAL IN THE ROMANIAN POWER PLANTS

IOAN VASIU *

Abstract: The work presents some conclusions of the author's research carried out with the aim of increasing the energetic efficiency of the steam generators with natural circulation, running on coal in pulverized state in the Romanian thermal power plants.

The exergetic analysis of the thermodynamic processes, which take place in these thermal installations, made possible the identification of an optimal operating range, characterised by an increased overall efficiency and lower fuel consumption.

An optimal range of the air-powdered coal mixture temperature, flue gas outlet temperature and consumed fuel flow was established, while maximum values of exergetic efficiency are registered.

Keywords:: powdered coal combustion, high exergetic efficiency, low consumed fuel.

1. INTRODUCTION

The fossil fuels are now in a dominant position in the structure of the primary energy resources used in order to produce heat and electric energy in the thermal power plants. An important part of the energetic processes in the thermal cycle of the power plants are achieved inside the equipments of the steam generators, when there occurs a conversion of the chemical energy of the fuels in thermal energy contained in the live steam produced by the installation.

At present, the energetic steam generators working with coal pulverization have a low overall efficiency due to the important thermal losses which are registered in the actual stage of development of this installations, [2].

Taking into account the actual Romanian energy conditions, the steam generators with pulverized coal burning will be utilized in thermal power plants in the future. Therefore, the increase of the overall performances of this type of installations

* *Lecturer, Ph.D. at the University of Oradea, Faculty of Energy Engineering*

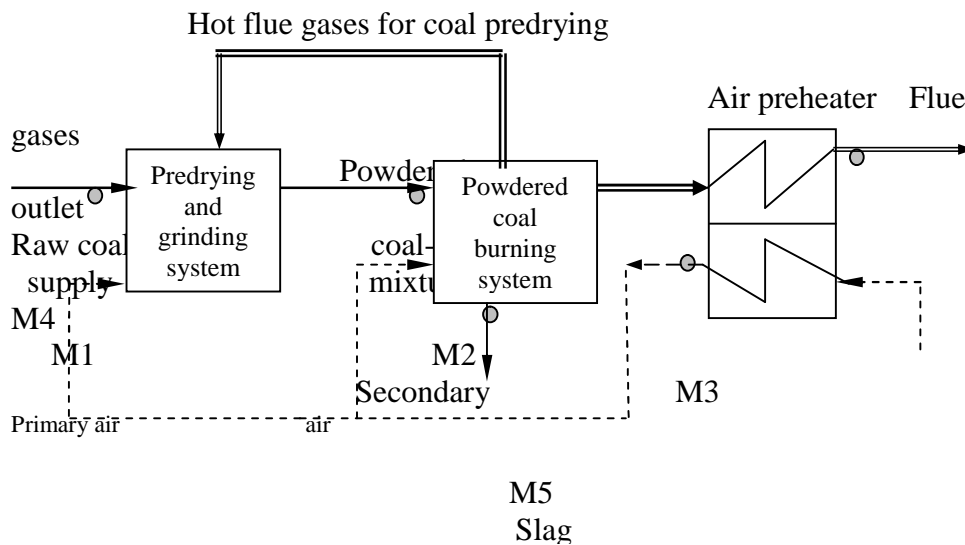
during operation became a requirement in order to diminish the fuel consumption, to reduce the electricity and heat cost, to protect the primary sources of energy of the country.

The qualitative analysis of the thermodynamic processes developed in the energetic steam boilers with natural circulation running on pulverized coal, through an exergetic efficiency, made it possible to identify the optimal ranges of the some operating parameters inside which the global efficiency reaches maximum values, [2].

The exergy represents the maximum useable fraction of an energy form, which could be obtained by a reversible transformation in another energy form, taking into consideration the state of the ambient.

2. EXPERIMENTAL RESEARCH

The experimental research has been achieved in the installation of a steam generator with natural circulation delivering 400 ton/hour (111.1 kg/s). The furnace is fully screened with membrane walls consisting of tubes of low diameters having 60x5 mm.



The main technical characteristics of the experimental steam generator at nominal load are: steam flow $D_n = 111.1 \text{ kg/s}$; thermal capacity $P_{tn} = 340 \text{ MW}_t$; superheated steam temperature $T_n = 823 \text{ K}$; steam pressure $p_n = 13.7 \text{ MPa}$; feed water temperature $T_{aa} = 503 \text{ K}$; combustion air temperature $T_{ac} = 513 \text{ K}$; flue gases temperature after heater $T_{gev} = 413 \text{ K}$, [2].

The processes of preparing and burning coal powder achieved in the thermal power plants are indicated in figure 1. The coal grinding equipment is composed of 6 mills having 30 ton/hour, of which 4 – 5 mills were maintained in operating state in order to assure the thermal load of the steam generator, required inside the power plant

at a certain point. The powdered coal fineness was in range of $R_{0,09} = 40 - 60 \%$, in accordance with the fan mills grinding elements wear cycle. Coal pre-drying is achieved using hot flue gases, extracted from the final part of the furnace at a temperature of 950°C . The air for the process of combustion was preheated at $190 - 220^\circ\text{C}$ in a regenerative equipment using the recovered heat of the outlet flue gases. For the burning of powdered coal a technology of preparation with coal dust concentrator and direct blowing sketch in furnace of the flow mixture of air – coal has been used, [2].

The values of the sizes for the fuel supply, the combustion air, the flue gases, the slag and ash discharge circuits used in the exergetic analysis have been measured in the following points, indicated in figure 1: M1-flow and characteristics of the consumed coal; M2- primary air-coal dust mixture parameters; M3-preheated air combustion temperature; M4-flue gases outlet temperature; M5-incompletely burnt

Table 1-Average characteristics of the equivalent fuel

Chemical elementary analysis at initial state	Symbol	Unit	Average values
Carbon	$C_{m,e}^i$	%	23.74
Hydrogen	$H_{m,e}^i$	%	1.86
Sulphur (combustible)	$S_{cm,e}^i$	%	1.16
Nitrogen	$N_{m,e}^i$	%	0.61
Oxygen	$O_{m,e}^i$	%	9.22
Total humidity	$W_{tm,e}^i$	%	34.24
Ash	$A_{m,e}^i$	%	29.17

content from slag and ash.

The chemical and energetic properties of the coal are variable in a wide range during the operation of the steam generator. For this reason it was necessary to define a fuel having middle properties. The average properties of the equivalent burnt fuel, which is a mixture between coal and oil, are indicated in table 1, [2].

The main fuel used for the steam generator running was

low-grade coal, characterised by high humidity and ash content, having a reduced heating power. The flame support of the powdered coal burner was assured by using oil with low sulphur content.

3. MATHEMATICAL EQUATIONS OF THE EXERGETIC ANALYSIS

The exergetic efficiency of the steam generator η_e can be expressed in the following form [1], [2] :

$$\eta_e = \frac{E_u}{E_t} \cdot 100 = 1 - \frac{\Pi_e}{E_t} \cdot 100 \quad [\%] \quad (1)$$

where : E_u [kW] - useful exergy output flow produced by steam generator,
 E_t [kW] - total exergy input flow of the analysed thermal system,
 Π_e [kW] - sum of the exergy flows lost from installation.
 Total exergy input flow results from the balanced equation :

$$E_t = E_{ch} + E_{fce} + E_{fa} + E_{aa} = E_u + \Pi_e, \text{ [kW]} \quad (2)$$

in which : E_{ch} [kW] - chemical exergy input flow of the equivalent fuel,
 E_{fce}, E_{fa}, E_{aa} [kW] - physical exergy of the equivalent fuel, combustion
 air and feed water input flows.

The components of the total exergetic input flow E_t , are defined as follows,
 [2], [3]:

$$E_{ch} = B_e \cdot e_{ne}, \text{ [kW]} \quad (3)$$

$$E_{fce} = \left(1 - \frac{T_o}{T_c}\right) \cdot B_c \cdot c_{pc} \cdot t_c + \left(1 - \frac{T_o}{T_p}\right) \cdot B_p \cdot c_{pp} \cdot t_p, \text{ [kW]} \quad (4)$$

$$E_{fa} = \left(1 - \frac{T_o}{T_{aci}}\right) \cdot B_e \cdot \lambda_f \cdot V_{ae}^o \cdot i_{aci}, \text{ [kW]} \quad (5)$$

$$E_{aa} = \left(1 - \frac{T_o}{T_{aai}}\right) \cdot D_{aai} \cdot i_{aai}, \text{ [kW]} \quad (6)$$

The useful exergy output flow E_u is defined by equation :

$$E_u = [D_{ab} \cdot e_{ab} - D_{aai} \cdot e_{aai}] + B_e \cdot \lambda_f \cdot V_{ae}^o \cdot \left[\left(1 - \frac{T_o}{T_{ace}}\right) \cdot i_{ace} - \left(1 - \frac{T_o}{T_{aci}}\right) \cdot i_{aci} \right], \text{ [kW]} \quad (7)$$

The sizes mentioned in the relations (3) – (7) represent: B_e, B_c, B_p [kg/s] -
 equivalent fuel flow, coal, fuel oil flow; e_{ne} [kJ/kg] - specific exergy of the equivalent
 fuel; c_{pc}, c_{pp} - medium value of specific heat at constant pressure of the coal, fuel
 oil; λ_f - air ratio in the furnace; V_{ae}^o [m_N^3 /kg] - theoretical air volume for the equivalent
 fuel burning; t_c, t_p [°C] - coal, fuel oil temperature; i_{aci}, i_{ace} [kJ/kg] - specific
 enthalpie of combustion air before and after preheater; T_{aci}, T_{ace} [K] - temperature of
 combustion air before and after preheater; D_{aai}, D_{ab} [kg/s] - feed water input flow,
 delivered steam flow; T_{aai} [K], i_{aai} [kJ/kg] - feed water input temperature and specific
 enthalpie; e_{aai}, e_{ab} [kJ/kg] - feed water input and delivered steam specific exergy.

4. RESULTS AND CONCLUSIONS

The behaviour of the steam generator working with coal in pulverised state was analysed in 6 operating regimes characterised by delivered steam flow inside the range of 66.1 kg steam/s – 108.6 kg steam/s (238 ton steam/hour – 391 ton steam/hour).

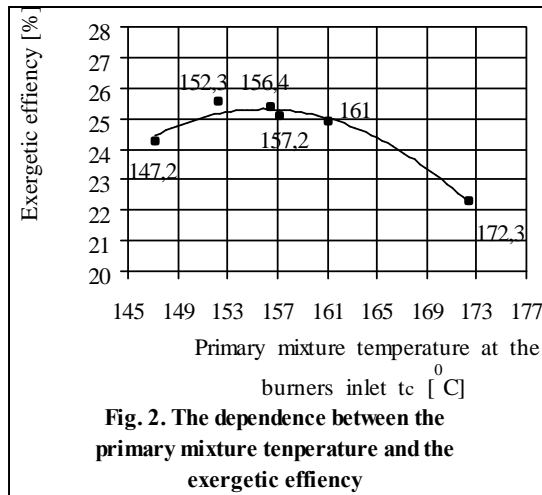


Fig. 2. The dependence between the primary mixture temperature and the exergetic efficiency

Based on experimental measures, the calculations achieved according to the relations (1) – (7) indicated in chapter 3, have permitted to establish the total exergy input flow E_t , the useful exergy output flow E_u and, finally, the values of the exergetic efficiency η_e of the analysed steam generator.

The graphic correlation established by experimental research, based on exergetic analysis, between the operating parameters measured in coal preparation and flue gases circuits, on the one hand, and the exergetic output, on the other hand, takes into evidence optimal ranges of the steam generator running on coal pulverisation, characterised by maximum efficiency and lower fuel consumption.

The admission of air-powdered coal mixture in the burning space at optimal temperatures, which results from the proper increase of the preheated combustion air temperature, led to the improved ignition and burning conditions of coal particles, due to the higher level of the combustion temperature achieved inside the furnace. The high intensity of the abstracted heat in the combustion space was obtained through a good carbon oxidation. At the same time, the process of heat transfer to the screened walls placed in the radiation zone becomes stronger due to the uniform thermal load of the furnace.

All these thermal processes have a remarkable contribution to the decrease of the main exergy losses which left the steam generator furnace, consist in the exergy lost flows by irreversibility of the burning and heat transfer processes, as parts of the total exergy losses Π_e .

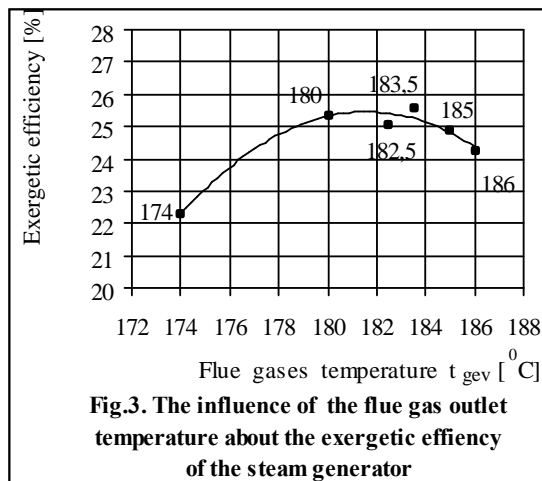


Fig. 3. The influence of the flue gas outlet temperature about the exergetic efficiency of the steam generator

The influence of the air-powdered coal temperature, measured at the outlet from mills separators, about the exergetic efficiency is shown in the figure 2. A range

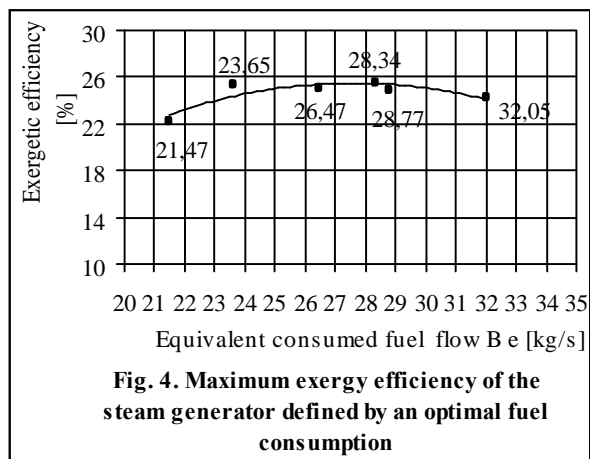


Fig. 4. Maximum exergy efficiency of the steam generator defined by an optimal fuel consumption

of the primary mixture temperature at the burners inlet $t_c = 154 - 158^\circ C$ can be observed, while the exergetic overall output reaching the highest values, [2].

By increasing the heat flow delivered to the combustion air in the preheater, the temperature of the flue gases was reduced after this thermal equipment and, in this way, an important diminishing of the exergy losses by the flue gasses exhausted from the

steam generator, was achieved.

A zone of the flue gasses temperature's at the outlet of the steam generator, $t_{gev} = 181 - 182^\circ C$, was established in a graphical way, in which the maximum value of the exergetic output can be registered, (figure 3), [2].

The increase of the efficiency of the steam generators, by operating in an optimal range of the technological parameters, had an important effect on the reducing of the consumed fuel flow. The correlation between the equivalent fuel flow consumption and the exergetic output of the steam generator is shown in figure 4. In a range of the burnt fuel, maximum values of the exergetic efficiency can be observed. In the case of the analysed steam generator, between $B_e = 27 - 28$ kg coal/s, the highest values of the exergetic output $\eta_e = 25.5$ % are obtained, [2].

This experimental research has a practical importance for the specialists in the field of thermoenergetics working in the power plants equipped with steam generators with natural circulation burning pulverised coal, in order to define the fuel consumption required for running with high performances.

REFERENCES

- [1]. Mădărășan, T., *Bazele termotehnicii*, Editura Sincron, Cluj-Napoca, 1998.
- [2]. Vasii, I., *Performanțele generatoarelor de abur energetice pe cărbune pulverizat*, Editura Universității din Oradea, 2003.
- [3]. Bejan, A., *Thermal design and optimization*, Ed. Wiley, Interscience, New-York, 1996.

THEORETICAL ASPECTS IN SOLVING FIELD ENGINEERING PROBLEMS USING FINITE ELEMENT METHOD

VISALON DAN*, NICOLAE DAN**

Abstract: In this paper we present a more unified view on FEM applied to field problems. A short introduction to the equations governing heat transfer, magnetic, electric, and irrotational fluid flow problems is presented first. The finite element algorithm is shortly outlined. Although the similarities between different engineering fields are mentioned in the literature [1], [2], there is still a strong tendency to separate the formulation of FEM from area to another.

Keywords: finite element method (FEM), heat transfer, magnetic and electrostatic fields, algorithm, numerical examples.

1. INTRODUCTION

Let's consider first the governing equations for some common two-dimensional boundary-values problems.

a) Heat transfer problem.

The heat transfer differential equation for the steady state two-dimensional conduction problem and orthotropic materials is:

$$\frac{\partial}{\partial x}\left(k_x \frac{\partial T}{\partial x}\right) + \frac{\partial}{\partial y}\left(k_y \frac{\partial T}{\partial y}\right) + \dot{q} = 0 \quad (1.1)$$

where:

k_x, k_y = thermal conductivity in x and y directions

T = temperature, and

\dot{q} = heat source rate per unit volume

b) Magnetic field problem.

* Assoc. Prof. PhD, University of Petrosani, Romania

** PhD, ABAQUS Inc., USA

The two-dimensional magnetic field problem in terms of magnetic vector potential:

$$\frac{\partial}{\partial x}(\nu_x \frac{\partial A_z}{\partial x}) + \frac{\partial}{\partial y}(\nu_y \frac{\partial A_z}{\partial y}) = -J_z \quad (1.2)$$

where:

ν_x, ν_y = magnetic reluctivity in x and y directions

A_z = magnetic vector potential, and

J_z = current density

The domain was assumed infinitely long in the axial direction and therefore the magnetic vector potential has only one component (e.g. it becomes a scalar quantity).

c) Electrostatic field problem.

The Maxwell's equation that governs electrostatics written in terms of electric scalar potential is:

$$-\nabla(\epsilon \nabla V) = \rho \quad (1.3)$$

with:

ϵ = electric permittivity

V = electric scalar potential, and

ρ = charge density

d) Incompressible inviscid flow.

The Navier-Stokes equations under irrotational and incompressible two-dimensional flow condition:

$$\frac{\partial^2 \Phi}{\partial x^2} + \frac{\partial^2 \Phi}{\partial y^2} = 0 \quad (1.4)$$

Where Φ denotes the velocity potential. The flow velocities are given by:

$$u = \frac{\partial \Phi}{\partial x}; v = \frac{\partial \Phi}{\partial y} \quad (1.5)$$

It is sometimes convenient to describe this type of flow in terms of stream function equation

$$\frac{\partial^2 \Psi}{\partial x^2} + \frac{\partial^2 \Psi}{\partial y^2} = 0 \quad (1.6)$$

Where Ψ denotes the stream function. The flow velocities can be calculated in this case as:

$$u = \frac{\partial \Psi}{\partial y}; v = -\frac{\partial \Psi}{\partial x} \quad (1.7)$$

The equations (1) to (7) are similar partial differential equation in terms of a field variable. Other similar physical problems may include seepage flow, torsion of shafts, fluid film lubrication. This class of engineering problems is usually called field problems.

As a result, having implemented the FEM equations for one of these problems all other problems could be solved by re-interpreting the field variable, the derived variables, and the field constants.

2. ALGORITHM OF THE FINITE ELEMENT METHOD

The basic idea in the finite element method is to find the solution of a complex problem by replacing it by simpler ones. The solution region is considered as build of many smaller interconnected subdivisions, called finite elements. In each subregion, or finite element, an approximate solution is assumed. These elements are interconnected at specified points called nodes. The actual variation of the field variables (such as temperature, potential function) inside elements is assumed to be defined by the values of the field variable at the nodes. The approximating function is called interpolation function or shape function.

There are two classes of variational methods, which are used to obtain the specific finite element equations: pure variational methods and energy functional methods. The energy functional methods assume that there is an energy functional associated with field distribution, while the pure variational method is more general. Although both of these methods can be used for solving the field problems presented in chapter 1, we present here the Galerkin variational method (also called the method of weighted residuals).

By multiplying any of the field equations by a set of weighting functions w , and integrating over the study domain we have:

$$\int_D w \left(\frac{\partial}{\partial x} \left(k_x \frac{\partial T}{\partial x} \right) + \frac{\partial}{\partial y} \left(k_y \frac{\partial T}{\partial y} \right) + \dot{q} \right) = 0 \quad (2.1)$$

where we considered the field problem as being the heat conduction equation. Integrating by parts, the following equation can be easily obtained:

$$\int_D \left(\frac{\partial T}{\partial x} k_x \frac{\partial w}{\partial x} + \frac{\partial T}{\partial y} k_y \frac{\partial w}{\partial y} \right) dD = \int_D w \dot{q} dD + \int_S w \frac{\partial T}{\partial n} dS \quad (2.2)$$

where S represents the part of the domain's surface where the derivative is known.

Equation 2.2 is called the weak form of the finite element problem. The application of the above Galerkin variation approach to the finite element method can be described in the following steps:

1. Divide the study domain D in N finite elements (quadrilateral elements for the application considered here)
2. Assume the variation of the field variable (temperature in this particular case), in each element as bi-linear:

$$T^e(x, y) = \sum_{a=1}^4 N_a(x, y) T_a^e \quad (2.3)$$

where: T^e represents the temperature variation inside each element, $N_a(x, y)$ are the interpolation (or shape) functions, and T_a^e are the nodal temperature values. Note

that in the Galerkin approach the shape functions N_a have the same form as the weighting functions w .

3. Assemble the elemental equations to obtain the overall system of equations. Therefore the equation (2.2) in finite element form becomes:

$$\sum_{e=1}^M \left\{ \int_{D^e} \left(\frac{\partial T^e}{\partial x} k_x^e \frac{\partial w^e}{\partial x} + \frac{\partial T^e}{\partial y} k_y^e \frac{\partial w^e}{\partial y} \right) dD^e + \int_{S^e} w^e \frac{\partial T^e}{\partial n} dS^e \right\} \quad (2.4)$$

where M represents the total number of finite elements covering the domain D .

4. Solve the resulting general system of equations.

The elemental temperature variation inside one element (Eq. 2.3) can be written:

$$T^e(x, y) = \alpha_1 + \alpha_2 x + \alpha_3 y + \alpha_4 xy \quad (2.5)$$

where the coefficients in the above can be determined by enforcing the temperatures at the four nodes of the element:

$$\begin{aligned} T_1 &= \alpha_1 + \alpha_2 x_1 + \alpha_3 y_1 + \alpha_4 x_1 y_1 \\ T_2 &= \alpha_1 + \alpha_2 x_2 + \alpha_3 y_2 + \alpha_4 x_2 y_2 \\ T_3 &= \alpha_1 + \alpha_2 x_3 + \alpha_3 y_3 + \alpha_4 x_3 y_3 \\ T_4 &= \alpha_1 + \alpha_2 x_4 + \alpha_3 y_4 + \alpha_4 x_4 y_4 \end{aligned} \quad (2.6)$$

The evaluation of the coefficients in the above (Eq. 2.6) is usually greatly simplified by using the natural (local) coordinates of the element, which will both vary between (-1, +1). The relationship between the natural and actual Cartesian coordinates is obtained by well-known coordinate transformations, which can be found in any finite element literature.

3. FINAL NOTES

The similarities could be extended to the three dimensional analyses. For this case the magnetic vector potential reduces to three scalar equations, however the divergence of the magnetic potential needs also to be determined to completely define the magnetic field (gauge condition)

REFERENCES

- [1] Rao, S.S., 1982, "The Finite Element Method in Engineering", Pergamon Press, NY.
- [2] Bathe, K.J., 1982, "Finite Element Procedures in Engineering Analysis", Prentice Hall, NJ.
- [3] Dan, N, Ledezma, G.A., Craiu, O., "An improved Algorithm for Coupled Thermal and Magnetic Problems in Electromagnetic Devices", HTD-Vol. 348, Volume 10, ASME 1997.
- [4] Sivester, P.P., Ferrari, R.L., 1996, "Finite Elements for Electrical Engineers", Cambridge University Press

THERMOENERGETIC BLOCK ON COAL POLLUTION VECTOR: WATER HYDROCONVEYER FOR ASHES

ANDREEA BRÎNDUȘA*, IOSIF KOVACS, ADRIANA BOCIAT***

Abstract: In the energetic industry the evacuation of the ashes specific to the burning process in the thermo energetic blocks is made hydraulic based on the pollution vectors water hydro conveyer in the ashes and slag warehouses. The main problem concerning the returning of water in the hydro conveyer circuit consists in making a suitable decantation so that the load with suspensions is diminished.

Keywords: water hydro conveyer, coal, thermo energetic block, pollution vector

1. INTRODUCTION

The energetic blocks, with installed powers of great values from our country, have as basis turbo- generators of an apparent power of 388 MVA, an active power of 330MW, the THA330-2 type and the steam turbine of the FIC 330 MW type.

The steam turbine of the FIC 330 MW type has the following technical characteristics:

- the maximum cont. power:330MW
- the power of overcharge: 345MW
- the revolution: 3000rpm
- the pressure in. IP: 186atm
- the temperature in. IP:535C
- the debit in. IP: 1035t/h
- the pressure ot.IP: 49,8atm
- the temperature ot. IP:344C
- the debit ot. IP: 1023t/h

This are to be found at the level of the Energetic Complexes Oltenia (CE Turceni, CE Rovinari, Ce Craiova).

The evacuation of the ashes specific to the burning process in the thermoenergetic blocks is made hydraulic based on the pollution vectors water

* *PhD Student. Ec. University of Petrosani*

** *PhD Professor.eng. University of Petrosani*

hydroconveyer in the ashes and slag warehouses.

The main problem concerning the returning of water in the hydroconveyer circuit consists in making a suitable decantation so that the load with suspensions is diminished.

As a rule industrial water that supply the thermoenergetic blocks are surface water which temperature varies depending on the season and geographical areas in the 0- 30°C interval.

In the case of the thermoenergetic blocks from the Craiova Energetic Complex Turceni and Rovinari we have a common characteristic that they bot huse the same source of industrial water, river Jiu. The collected and evacuated water in and from river Jiu is made throu the collecting and evacuating points and the Evacuation and Collection Channels. The volumerical debit industrial water, collected from Jiu, is provided through some big capacity pumps and through modifying the level of the upstream dam point.

2. WATER HYDROCONVEYER FOR ASHES TO THE ENERGETIC BLOCKS

The energetic blocks with great values impose in their function big volumes of collected and evacuated industrial water. Some of that collected water is used to evacuate the ashes obtained through burning solid fuel, in this case with lignit a type of coal.

Hydro conveyer water is recalculated in proportion of 70-80%.

The main problem concerning the returning of water in the hydroconveyer circuit, consists in making a suitable decantation so that the load with suspensions is diminished.

A flooded moist waste dump can contain up to 30% moisture between the ashes particle.

This paper presented the washing tests in cascade on ashes type Craiova Energetic Complex– SE Isalnita. In table 1 is presented the granulometrical analysis on ashes of the Craiova Energetic Complex– SE Isalnita, and in table 2 is presented the ashes chemical composition base don oxide

Table 1

Nr. crt.	Grain Diameter [mm]	Sample [%]
1	> 0,5	0
2	> 0,25	10
3	> 0,09	50
4	> 0,045	94

Table 2

Nr. crt.	Components	Composition [%]
1	Fe ₂ O ₃	10,58
2	Al ₂ O ₃	20,38
3	CaO	8,83
4	MgO	7,45
5	SiO ₂	47,11

The washing agent was demineralized water, and the used proportion was 1 part ashes at 10 parts water.

The mixture water-ashes have been agitated for 24h, and the washing water has

been analyzed and stained. It has been done PH and conductivity measurements and have been determined the SO_4^{2-} , Na^+ , Ca^{2+} ions concentration.

The determination results are presented in table 3.

Table 3

The analysed parameter	UM	Sample		
		I	II	III
pH		10,42	7,82	8,53
Conductivitate	$\mu\text{S}/\text{cm}$	1984	1161	918
Ca^{2+}	mg/l	400	252	192
Na^+	mg/l	22	27	23,2
SO_4^{2-}	mg/l	764,5	592	438

3. CONCLUSIONS

The evaluation of the environment performance of the industrial branch-Energetic industry- is absolutely necessary in an open and interconnected society specific to the XXI century, where the globalization phenomenon is present all over.

The biggest consumption of industrial water from the surface area leads to:

- the necessity of introducing solutions and technical methods which can stop the growth slope of the consumption of industrial water
- the necessity of permanent monitorisation of the physical-chemical parameters, water collected and evacuated from the industrial giants, Energetic Complex.

Based on the type of the tests presented we can make the conclusions:

- we have a important mobilization of ions SO_4^{2-} , cca. 31%;
- we have a mobilization of ions Ca^{2+} , cca. 7%.
- the Ph value covers the 7,5-10 interval;
- the conductivity evolution presented a growth of washing saline water

REFERENCES

- [1]. Brîndușă, A., Kovacs, I., *Physical-chemical parameters water collected and evacuated at the energetic blocks*, Simpozion internațional multidisciplinar "UNIVERSITARIA SIMPRO 2006", Universitatea din Petroani, Petroani, 13-14 octombrie 2006.
- [2]. Brîndușă, A., Bulucea, A., *Considerations upon industrial wastewater purifying equipments*, Simpozion național "Ingineria mecanică în mediul", Universitatea din Craiova, Craiova, 6-7 octombrie 2006.
- [3]. Brîndușă, A., *The factors of degradation of the environment and of the tourist potential specific to the autochthon relief*, Simpozion internațional multidisciplinar "UNIVERSITARIA SIMPRO 2006", Universitatea din Petroani, Petroani, 13-14 octombrie 2006.

THERMOENERGETIC BLOCK ON COAL POLLUTION VECTOR: BURNING GAS

ANDREEA BRÎNDUȘA *, IOSIF KOVACS**

Abstract: Burning gas is one of the pollution vectors specific to the thermoenergetic blocks and they are the result of the proces of burning the coal. The main problem concerning the return of burned gas in the environment is making a suitable filtration so that the load with suspensions is diminshad and disseminated on big areas.

Keywords: burned gas, coal, thermoenergetic block, pollution vector

1. INTRODUCTION

At the level of the Energetic Complex from Oltenia (CE Turceni, CE Rovinari, CE Craiova) we have thermo energetic blocks with installed power of great values which have as base turbo generators of 388 MVA apparent power, 330 MW active power, of THA 330-2 type and the steam turbine of FIC 330 MW type.

The steam production is made in steam boilers in which takes place the burning of the solid fuel of lignite type. It has developed varied technologies which combines the diversity of the firebox with the way of putting the radiant pipes of special steel, through which circulates the production water, the heated steam and is a way of evacuating the slag made from burning the coal.

In the firebox takes place the process of reaction between the burning air and the combustibile with the forming of burning gas at high temperature. The evacuation of burning gas in the atmosphere is made through the evacuation pipes (gas channels, gas fan, evacuation chimney).

The pollution source for air is the emission of the effluent from burning gas resulted from burning combustibile in fireboxes of burning boiler as: NO_x, SO₂, CO₂, CO, dust, (table1).

* *PhD. Ec. University of Petrosani*

** *Professor PhD .eng. University of Petrosani*

Table1

Nr. crt.	Poluant	Valoare
1	NO _x [mg/Nm ³]	200-500
2	SO ₂ [mg/Nm ³]	2000-4500
3	Pulberi [mg/Nm ³]	40-50
4	CO ₂ [%]	8-10
5	CO [mg/Nm ³]	40-120

The main problem concerning the returning of burned gas in the environment consists in making a suitable filtration so that the load with suspensions is diminished on big areas of land.

2. BURNED GAS, ENERGETIC GROUPS. EFFLUENTS EMITTED

If some fireboxes make together an exploitation unit, the thermic power of the exploitation assemble (total thermal power) is determined for the limitation of the emissions of every firebox. The application of this foresight (Ord. 462/1993 mod.) makes obligatory the reduction of the emissions at all boilers, indifferent of the thermal power, if the power station, has a thermal power bigger than 150 MW. There are no derogations from the norms bound to the age of the boilers, and the period of life.

A calculation of emissions is presented in table 2 and it refers to this case: The Energetic Complex Craiova-SA Craiova II, the chimney of evacuated burned gas nr.1.

Table 2

boiler/ cos	2						
Inalt. cos[m]	160						
Diam. virf [m]	9						
month	Ian	Feb	Mar	Apr	Mai	Iun	Iul
Debit g.a. [miiNm ³ /luna]	10,1*10 ⁸	14,2*10 ⁸	15,5*10 ⁸	9*10 ⁸	5,9*10 ⁸	6*10 ⁸	9,6*10 ⁸
Debit g.a. [mim ³ /luna]	16,1*10 ⁸	22,5*10 ⁸	24,3*10 ⁸	18,5*10 ⁸	9,3*10 ⁸	9*10 ⁸	16*10 ⁸
Cons. coal[t/luna]	217811	299427	318940	185387	116700	10 ⁵	2*10 ⁵
Cons. pacura [t/luna]	3160	4074	5095	2908	1915	1366	2303
Emission SO ₂ [t/luna]	3685	5055	5415	3145	1983	2175	3455
Emission NO _x [t/ month]	411	566	619	354	207	247	397
Emission dust[t/month]	71	97	104	60	38	42	66
Conc. SO ₂ [mg /Nm ³]-6%O ₂	4445	4473	4478	4479	4521	4538	4486
Conc. NO _x [mg	495	501	512	503	472	516	515

/Nm ³]-6%O ₂							
Conc. Pub [mg /Nm ³]-6%O ₂	85	86	86	86	87	87	86
Month	Aug	Sep	Oct	Nov	Dec		Total
Debit g.a. [mii Nm ³ / month]	6,9*10 ⁸	6,6*10 ⁸	12,2*10 ⁸	12,9*10 ⁸	12,6*10 ⁸		121*10 ⁸
Debit g.a. [mii m ³ / month]	11,2*10 ⁸	10,7*10 ⁸	19,5*10 ⁸	20,7*10 ⁸	19,8*10 ⁸		194*10 ⁸
Cons. coal[t/ month]	153357	142892	254589	275676	261150		2,6*10 ⁶
Cons. pacura [t/ month]	1480	1888	3083	3047	3931		34250
Emisie SO ₂ [t/luna]	2564	2410	4282	4625	4424		43217
Emisie NO _x [t/ month]	294	274	481	602	490		4941
Emisie dust[t/ month]	49	46	82	88	85		826
Conc. SO ₂ [mg /Nm ³]-6%O ₂	4473	4463	4497	4492	4481		53826
Conc. NO _x [mg /Nm ³]-6%O ₂	512	508	506	585	496		6122
Conc. Pulb[mg /Nm ³]-6%O ₂	85	85	86	86	86		1031

3. CONCLUSIONS

The evaluation of the environment performance of the industrial branch-Energetic industry- is absolutely necessary in an open and interconnected society specific to the XXI century, where the globalization phenomenon is present all over.

The biggest consumption of industrial water from the surface area lead to:

- the necessity of introducing solutions and technical methods which can stop the growth slope of effluents in the atmosphere;
- the necessity of permanent monitorisation of the physical-chemical parameters, pollution vectors: burned gas from the industrial giants, Energetic Complex.

Thouse Energetic Complex have in common four big characteristics:

- big power installed: of order *1000MW;
- they are situated in the same hydrographic basin, the river Jiu basin, which is situated in the neighborhood of the river;
- there are Energetic Complex which use as prime substance inferior coal of lignite type from the Oltenia miner basin;
- it polluted a commune region definite so ,such from the commune geographical elements and the specific elements of activity (technological processes of production and socio-economical services) very close.

REFERENCES

[1]. **Brîndușă, A., Kovacs, I.**, *Physical-chemical parameters water collected and evacuated at the energetic blocks*, Simpozion internațional multidisciplinar “UNIVERSITARIA SIMPRO 2006”, Universitatea din Petroani, Petroani, 13-14 octombrie 2006.

[2]. **Brîndușă, A., Bulucea, A.**, *Considerations upon industrial wastewater purifying equipments*, Simpozion național “Ingineria mecanică și mediul”, Universitatea din Craiova, Craiova, 6-7 octombrie 2006.

[3]. **Brîndușă, A.**, *The factors of degradation of the environment and of the tourist potential specific to the autochthon relief*, Simpozion internațional multidisciplinar “UNIVERSITARIA SIMPRO 2006”, Universitatea din Petroani, Petroani, 13-14 octombrie 2006.

URBAN FRAME WITH STATIC CONVERTER AND ASYNCHRONOUS MOTORS. DIRECT FIELD OREINTATION

CONSTANTIN BRÎNDUȘA*, MIHAI PĂSCULESCU**, MARIUS
POPESCU***

Abstract: Direct Field Oreintation DFO is perfectly possible to be implemented in the case of electric urban frames. This can be made with the help of the electrical control frame computer system. The structural diagram in the case of Direct Field Oreintation DFO is based on mathematical models of asynchronous motors and static converter.

Keywords: vector control, urban frame, asynchronous motor, static converter.

1. INTRODUCTION

In defining a computerized control system for the urban train having in the computers electrical frames with modern action (CTF+MA), we start from an electrical scheme of traction of the vehicle. Thus considering the fact that we are dealing with an electrical frame with the VM+VM composition the computerized control system is distributed and will operate in real time, similar to the one used in the case of the automated production lines.

The important characteristic of such a computerized control system is the integrated network of data buses which, in order to reduce to minimum the cables volume, it is necessary to be made with optical fibres. This assures the synchronized functioning of the electrical frames which compose the urban train, includes a diagnosis system and a services system of information and advertisement for passengers.

* *PhD Student. University of Petrosani*

** *Professor PhD .eng. University of Petrosani*

*** *Associat Professor PhD .eng. University of Craiova*

1	R1	R1	1	2	R2	R2	2	3	R3	R3	3
C	MT	SL	C	C	SL	SL	C	C	SL	SL	C
A	V _{A1}	V _{B1}	B	A	V _{A2}	V _{B2}	B	A	V _{A3}	V _{B3}	B

Fig 1 Structure urban train (VM_{A1}+ VM_{B1}+ VM_{A2}+ VM_{B2}+ VM_{A3}+ VM_{B3})

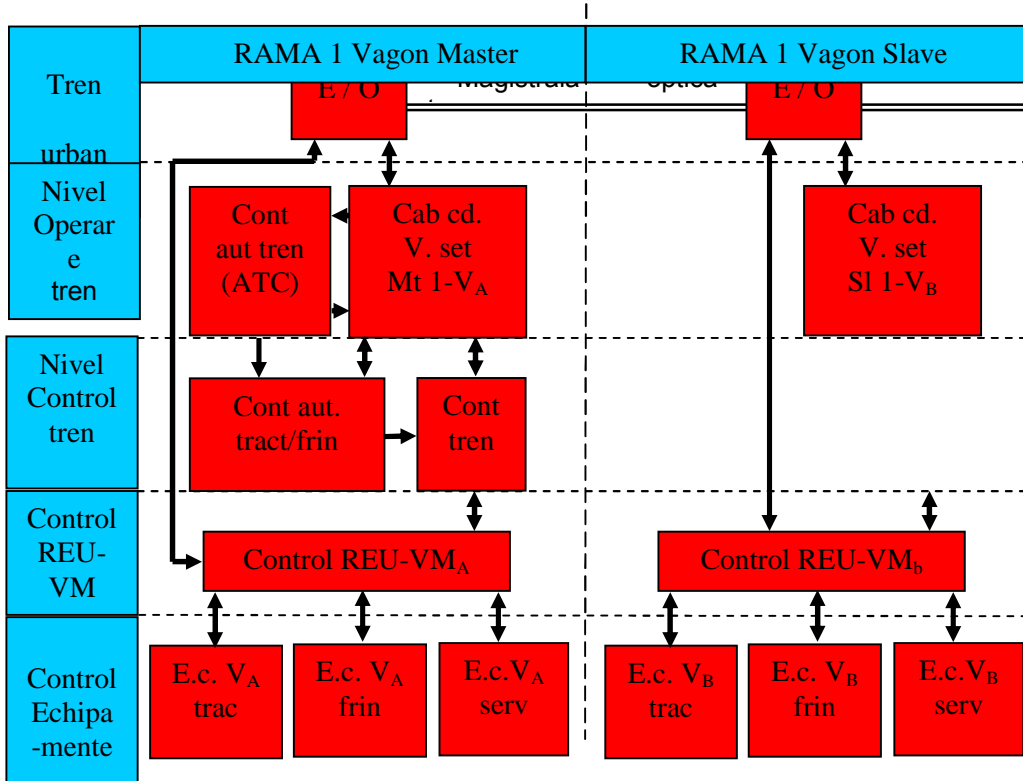


Fig 2 The system structure computerized urban electrical train control

The control system is earmarked on 4 levels:

- the urban electrical frames train operation system;
- the urban electrical frames train control level;
- engine wagons, electrical frame control level;
- equipments control level.

2. URBAN FRAME; DIRECT FIELD OREINTATION

The regulation of the asynchronous engine's speed can be done at the same performances with the regulation from the continuum power engine, through the separate control of the flux. However in this case, the one of the asynchronous engine, we are facing a series of problems connected to the identification of the position of the rotor flux's phasor $\underline{\psi}_r$ in the referential (,), the making of all the operations especially in the coordinates transformations, obtaining the values of the currents

resulted from the control scheme through the adequate command of the voltage inverter which fuels the asynchronous traction engine and which has a restrictive commutation frequency.

In the case of the work speeds, of relatively medium values, the rotor flux can be determined, through calculation, on the basis of the voltages and the traction asynchronous engine measured in real time. We are dealing with the control method called direct (Direct Field Orientation- DFO), the developed method, in the beginning, by Blaschke and which is encountered in a series of applications, in the electrical actions with static converters and asynchronous traction engines.

The structural scheme is presented in fig.3.

As in the case of every PI regulator we find input parameters the prescribed value and the reaction one. Thus we have:

- for Reg Ψ_r : entering size Ψ_r^* , Ψ_r ; exit size i_{sx}^* ;
- for Reg i_{sx} : entering size i_{sx}^* , i_{sx} ; exit size u_{sx} ;
- for Reg i_{sy} : entering size i_{sy}^* , i_{sy} ; exit size u_{sy} .

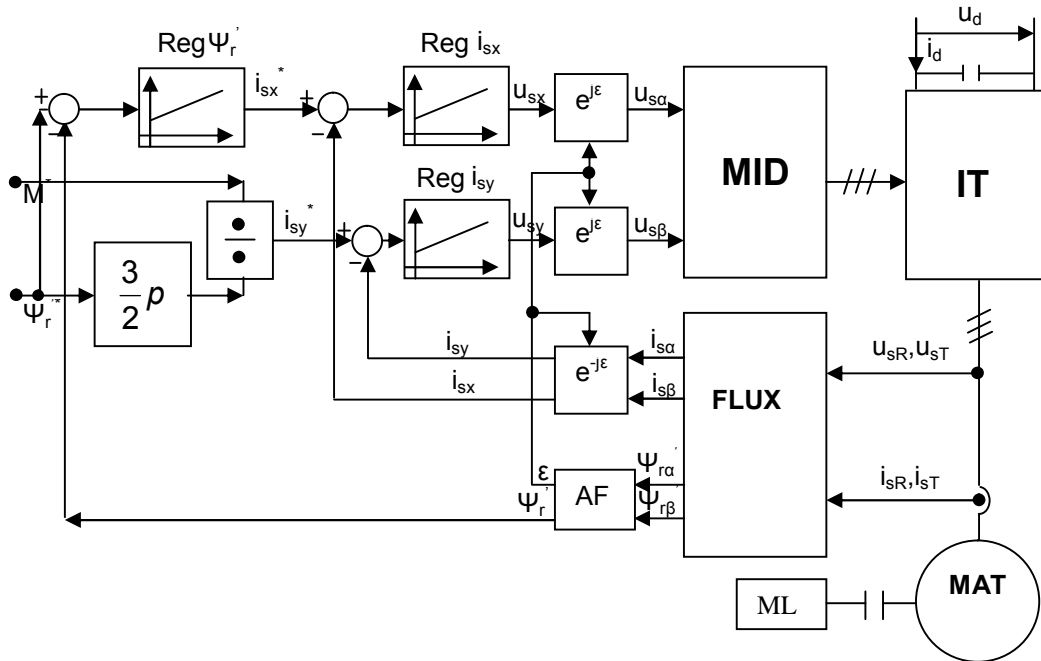


Fig 3 Structural scheme direct vectorial control (DFO)

The current i_{sy}^* is obtained from the prescribed values M couple and rotor flux

$$i_{sy}^* \text{ base on the relation: } i_{sy}^* = \frac{M^*}{\frac{3}{2} p \Psi_r^*} \quad (1)$$

In their turn the two components u_s and u_s , of the stator voltage \underline{u}_s 's phasor in the referential (α, β) that the asynchronous traction engine must be fuelled with, are obtained on the basis of voltages u_{sx} and u_{sy} after the coordinates transformation through the $e^{j\theta}$ factor. The asynchronous engine is fuelled by a modulation in duration

voltage inverter MID (PWM), the modulation being achieved on the basis of the two components u_s and u_s .

The structure of the FLUX block allows the calculation of the components of the stator current i_s and i_s and those of the rotor flux ψ_r and ψ_r , in the referential (d, j) .

The AF block's structure allows the calculation of the ψ_r phasor's module, on the basis of the $e^{j\theta}$ factor, which allows the coordinates transformation from the (d, j) referential into the (x, y) referential.

3. CONCLUSIONS

We can draw the following conclusions:

- In the earmarking of the urban electrical frames train control system on 4 levels we take into account the electrical traction scheme of the vehicle, evenly distributed on the entire urban train, including the traction function, braking;
- Direct vectorial control (DFO), at electrical frames with modern acting (CTF + MA), it allows the regulation of the asynchronous engine's speed at the same performances as in the case of the continuum current engine, through the separate control of the flux.
- It has been established the structural scheme direct vectorial control (DFO).

REFERENCES

- [1]. Brîndușă, C., ș.a., *Sisteme electrice de transport neconvenționale (A23); Rama de metrou acționată cu motoare asincrone; Execu ie și experimentare modele (Faza 23.1), Contract cercetare 606C- Anexa A, Institutul național de cercetare și proiectare pentru mașini electrice, echipament electric și trac iune, Craiova, 1992.*
- [2]. Brîndușă, C., Păsculescu, M., Popescu, L., *Drive systems behavior analysis in urban electric traction with Matlab software extensions, Simpozion Internațional Multidisciplinar „UNIVERSITARIA SIMPRO” ,2006, Petroani, Editura Universitas Petrosani, 2006.*
- [3]. Nicola, D.A., Cismaru, D.C., *Mathematical models for control simulation of traction induction motors, ICATE'98, Craiova, 1998.*

USING GRAPHICAL PROGRAMMING VEE Pro 6 SOFTWARE FOR FUNCTION SIMULATION OF THE GRINDING AGGREGATES TO MAINTAIN OPTIMUM SPECIFIC ENERGY CONSUMPTION

VISALON DAN* , CAROL ZOLLER**

Abstract: Between the absorbed power and the ore fill of the aggregate there is proved an extremal connection, [1]. So, we propose to use the information from the filling transducer to command the input flow, obtaining a PC working system within which productivity is at its best. A specific graphical software, for simulation of the optimum command of the ore grinding aggregates, interfaced with the PC by a data acquisition board for input-output proces control was developed. With some adjustments, the software can be implemented for real time driving to optimum of the ore grinding aggregates.

Key words: grinding aggregates, productivity, VEE Pro 6 software.

1. INTRODUCTION

The specific consumption of energy in copper ore grinding and separation process, using high capacity autogenous aggregates, in primary phase and ball mills in the second stage, (figure 1), is about 35 kWh/t. That specific consumption can be decreases with 5 to 10% by introducing a control system. As the aggregates drive is accomplished with 4 MW synchronous motors, to decrease the specific consumption is a desiderate of high actuality.

* Associate professor, PhD University of Petrosani,

** Professor, PhD University of Petrosani

It's impossible to decrease the consumption maintaining constant ore feed flow rate and water - ore ratio, because of the continuous variation of the physical and mechanical properties (which can be expressed by grinding ability). It is usual to command the feed flow rate depending on the absorbed power (figure 2) together with electrical energy measured, but aggregates can be overloaded or underloaded because of the non-linear character of the dependence between power and filling.

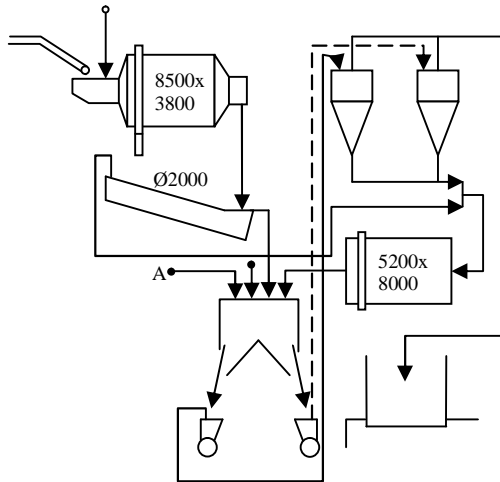


Fig.1. Block diagram of the grinding process

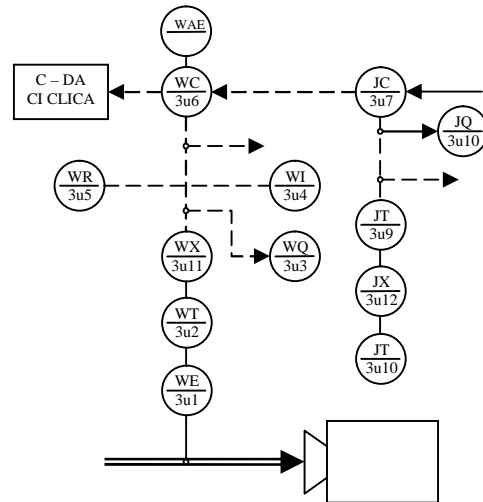


Fig. 2. Feed flow the absorbed power

2. FEED FLOW CONTROL

Knowing that this dependence has an extremal character, we propose a feed flow rate control system that uses, besides the information concerning the power absorbed by the driving motor, the information about the load (filling) with ore. The load information is given by a transducer of oil pressure in the bearing or a weight transducer.

This solution is based on the following considerations:

- The grinding aggregates productivity is mainly determined by the quantity of material in the aggregate (by its filling degree). Between the productivity and the material reserve (filling degree) there is an extremal dependence (figure 3), which is expressed by:

$$y = y_{\max} - k(x - x^*)^2$$

where:

y_{\max} – maximum productivity;

x^* - ore reserve for which the productivity is maximum;

k – constant, aggregate characteristic.

It is unanimously recognized that, between the driving power and the productivity, there is the following dependence: *the maximum productivity is obtained at the maximum consumed power.*

It is justified to use process control methods based on power control as long as it is difficult to appreciate the grinding capacity and power information is more accessible.

If y_1 is the driving power and m the grinding ability (a high m meaning easy grinding), we assume that:

- y_1 increases monotonously with y_2 and m (figure 4.a);
- y_1 decreases monotonously with the increment of the ore density ρ ;
- y_2 (the pressure in the bearing) is linearly dependent on the reserve (x) and density (ρ) (figure 4.b).

The system we have conceived aims to maintain the aggregate load at the value x^* , corresponding to the nominal power. As practically x^* is not known because of the stochastic variation of the ore characteristics, in order to determine x^* (for $dy_1/dx=0$), the procedure is the following:

- for a certain $x=x_1$, $y_1(x_1)$ is read and memorized;
- $x_1+\Delta x$ is read and $x_1+2\Delta x$ is commanded;
- if $y_1(x_1+\Delta x) > y_1(x_1)$, $x_1+2\Delta x$ is commanded;
- if $y_1(x_1+\Delta x) < y_1(x_1)$, $x_1-\Delta x$ is commanded;
- $y_1(x_1-\Delta x)$ is read and memorized, and so on.

So, if x belongs to the domain for which $y_1 < y_{1max}$, we command the increment of the load x by increasing the feed rate u . As the point y_{1max} moves continuously, it is necessary that the system follows permanently the algorithm above. In order to be sure that the variation of the power (y_1) is caused by the load (x), the system needs to use another information (y_2), which is the pressure in the bearing, depending linearly on x (figure 4.b). It is necessary to use two transducers: one of active power and another one of weight on the bearing, in order to provide information from the technological process. Using just some information (absorbed active power, filling degree and re-circuited flow), we achieved the control by discrete steps of the feed flow rate in a view to obtain maximum processing capacity.

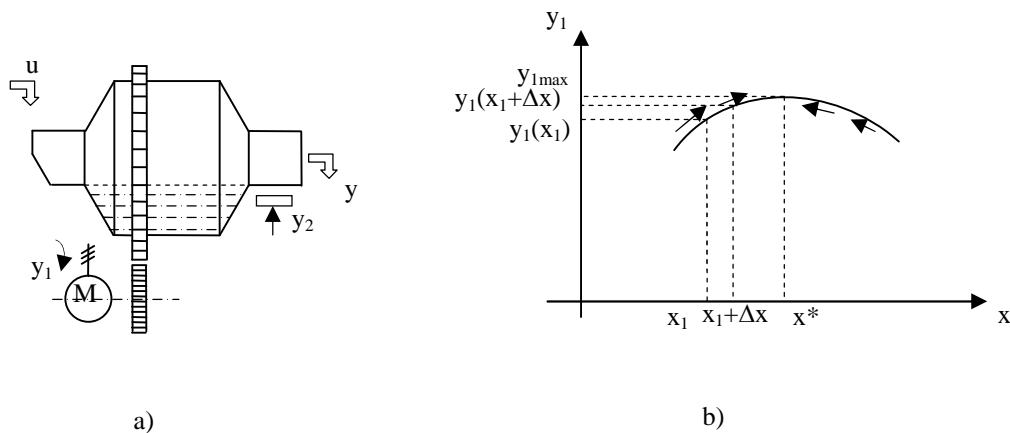


Figure 3

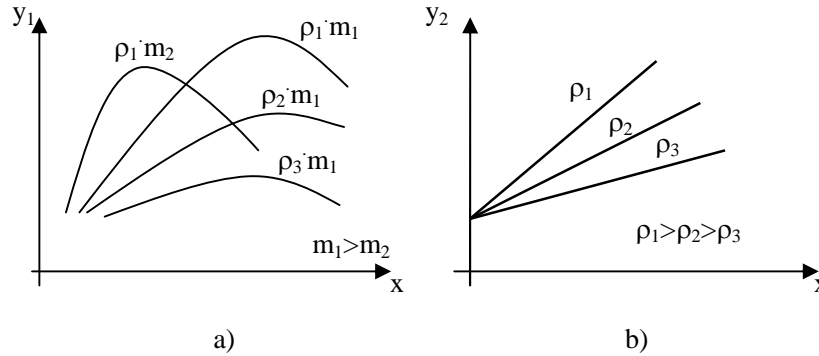


Figure 4

3. CONTROL ALGORITHM

The control algorithm, developed initially for a microprocessor control, is going through the following stages:

- a) It checks whether the starting conditions are fulfilled; if they are, the conveyor for feeding the aggregate with ore is started; if not, the restrictions are signaled optically and acoustically;
- b) It operates, on different stages, SUB_i:
 - transfers the active power value to M₁ and the pressure in the bearings value to M₃;
 - resets the active power integrator;
 - transfers the content of the M₁ memory to M₂, with a delay of τ seconds; transfers the content of the M₃ memory to M₄; transfers the value of the active power to M₁; transfers the value of the pressure in the bearings to M₃.
- c) It evaluates the variation of the power value that is measured at the beginning and at the end of the period τ . If $\Delta P > 0$, it commands a new step of ore feed increment and if $\Delta P < 0$, it commands the decrement of the feed flow by a step.
 - c1) If $\Delta P > 0$, after incrementing the feed flow by $+\Delta Q_{al}$, SUB.1 is run again and if ΔP and ΔP_1 is logically determined. If ΔP and $\Delta P_1 > 0$, Q_{ret} (return flow) is checked. If ΔP and $\Delta P_1 < 0$, the decrement $-\Delta Q_{al}$ is commanded and the program returns to ET.2. Depending on the correlation of the return flow Q_{ret} , it will take the decision: if $Q_{ret} < Q_{ret\ max}$, it is commanded again $+\Delta Q_{al}$; otherwise, it jumps to ET.4 checks whether the absorbed power is between its limits: $P_{min} \leq P \leq P_{max}$. If this condition is accomplished, the algorithm goes on with the pressure (P_1) check in the bearing. If $P_{1min} \leq P_{1max}$, the program jumps to ET.2 and the process is restarted following the algorithm. If one of the conditions is not fulfilled, this situation is signaled optically and acoustically and, after a period of $(4 - 5)T$ when the technological process gets stabilized, the control is restarted beginning with ET.1.
 - c2) If $\Delta P < 0$, it results the necessity of decrementing the feed flow and, starting with ET.5, it is checked whether the conditions $\Delta P > 0$ and $\Delta P_1 < 0$ are fulfilled simultaneously

with the condition $Q_{ret} < Q_{ret\ min}$. After checking whether P and P₁ are included within the admissible interval, the algorithm continues cyclically until the process stabilizes itself without needing to reduce Q_{al}.

This procedure lasts until the maximum of the function $P=f(Q_{al})$ is reached. From this moment on, the aggregate works on the stable characteristic as long as $\Delta P < 0$ and $\Delta P_1 < 0$. Afterwards, $+\Delta Q_{al}$ is commanded and, after running SUB.2, the program ET.5 is restarted.

If the curve maximum is moving to the right, that is $\Delta P < 0$ and $\Delta P_1 > 0$, $-\Delta Q_{al}$ is commanded if $Q_{ret} > Q_{ret\ max}$. The cycle continues with SUB.2 and it restarts with ET.5. If these conditions are not true, it restarts with ET.1.

The above described algorithm was developed using a graphical programming software, HP VEE Pro6, for simulation of the described proces, in the first stage, (figure 5) and for future optimum control of the ore gridding aggregates, using PC and data acquisition interfaces, in the second stages.

In figure 6 is presented the panel interface of the simulator, that presenting the graphical instruments to be set up by operator as:

- measured parameters, (pressure, absorbed active power, etc.,)
- prescriptions for limiting parameters evolutions, between minimum and maximum;
- delay between data acquisitions times, etc.

Time evolution of the controlled parameters and regulated parameters are presented also in to graphical panel as data recorder charts and bargraphs.

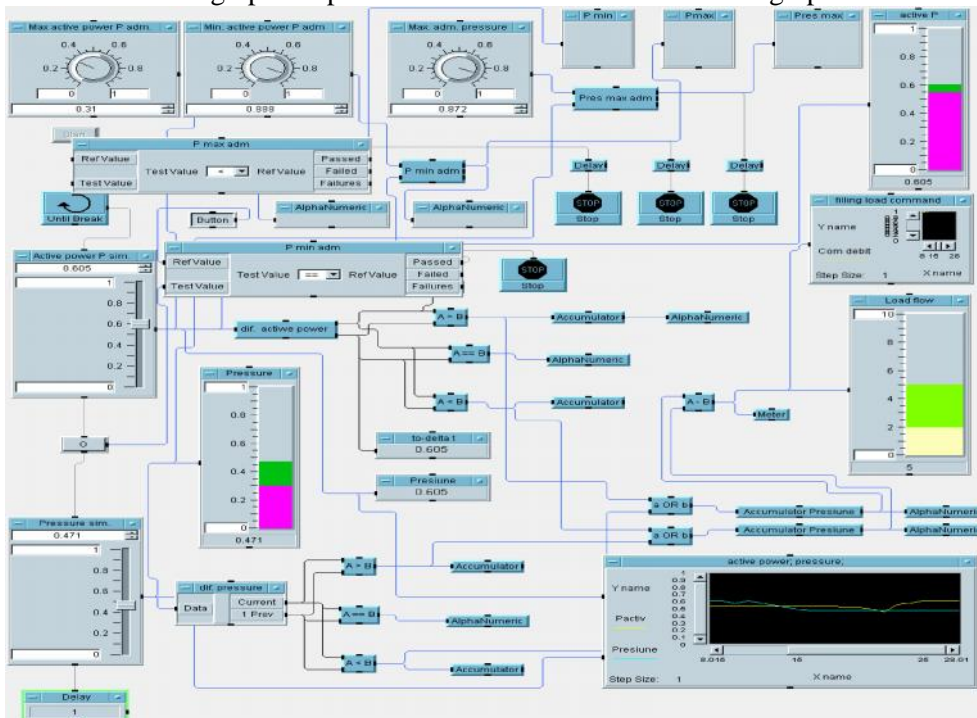


Fig. 5 Graphical programming software

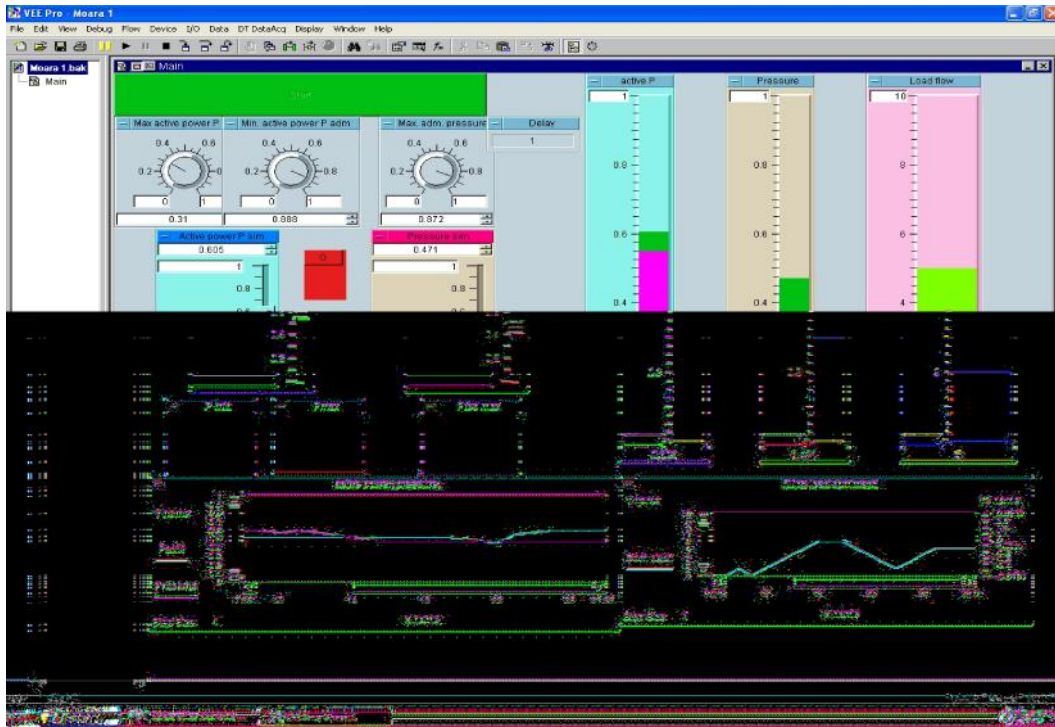


Fig 7 The panel interface of the simulator

4. CONCLUSIONS

For huge girding aggregates the working regime at nominal power and maximum grinding capacity means, energetically speaking, to reduce the specific electric energy consumption.

Between the absorbed active power and the ore fill of the aggregate there is an extremely connection, we propose to use the information from the filling transducer to command the input flow, obtaining a PC working system within which productivity is at its best.

A specific program for simulation of the optimum command of the ore girding aggregates, using HP VEE Pro 6 software was developed in the paper.

REFERENCES

[1] Dan Visalon, Carol Zoller - *Metodă pentru reglarea automată optimală a puterii agregatelor de măcinare autogenă a minereurilor complexe*. Brevet de invenție nr RO 121061, 2006, OSIM București;

[2] *** **Agilent Technologies**: VEE Pro user's guide. Agilent Technologies, Inc, E2110-90062. USA, 2000.

VOLTAGE ELECTRONIC REGULATOR FOR AIRCRAFT

JENICA ILEANA CORCĂU*

Abstract: In this paper is presenting a study about one electronic regulator of voltage afferent of one starter/generator who equipped the IAR-99 aircraft; it is regulating the voltage supplied by the generator D.C. of 9kW who discharges in bus of IAR 99 aircraft 28,5 V_{dc} voltage, simultaneous with the loads equaling in case of connecting of two groups of generates in parallel. Also, the voltage regulator protected the generator at overvoltage. The principle of working if this regulator consists in modulating in time of one impulse group with frequency $f=400\text{Hz} \pm 50\text{Hz}$ applied winding to exciting of generator. It is presenting the block scheme of this regulator and electronic scheme, the waveform of generators voltage, making the amplitude and frequency of ripple.

Keywords: electronic regulator of voltage, starter/generator, ripple, modulating in time of impulse.

1. INTRODUCTION

The voltage regulator for starter/generator is designated for: 1) the governing voltage supplied by generator D.C. who has ensuring at the way out a voltage equal with 28,5V_{dc} value at 300A, simultaneous with the equaling of loads, in case of connecting in parallel of two groups of generators; 2) the protection of 9kW generator at overvoltage simultaneous with the discrimination of defect sewer with a view to connect in parallel two groups of generators, the blocked of this would be ensured through the agency of excitation relay.

The principal of working of regulator is based on modulating in time of continuous group of impulses with the 400 ± 50 Hz frequency applicated coiling generator excitation. Mean value of power through excitation coiling so, will depends on value of filling factor of waveform, from behind this would be approximate 50% for voltage value of way-out +28,5 V_{dc} generator.

* *Lecteuur Ph D., University of Craiova, Faculty of Electrotechnics, Division Avionics, Romania, jcorcau@elth.ucv.ro*

The filling factor modification, respectively the modification of equated value of the power through excitation coiling has compensated through the feedback is provided for this purpose the voltage variations at the way out of generator.

Thus, the growth tendency of voltage value of way out is quiding at a subtraction on value of filling factor of waveform, respectively of mean value of power through excitation coiling, and each-other, the growth tendency of voltage value of way out is quiding at one growth of value of filling factor of waveform, respectively of mean value of power through excitation coiling.

Eliminated the parts of protection of voltage regulator block scheme of one electronic voltage regulator destined to work completely with the board generator D.C. with powers until 9KW is presenting in figure1.

In figure 2 are presenting the diagrams of variation of factor for 3 cases; $U_g = U_{ref}$; $U_g > U_{ref}$; $U_g < U_{ref}$. The principle scheme of electronic regulator voltage who worked completely with board generators D.C. of power until at 9KW is presenting in figure 3 [4].

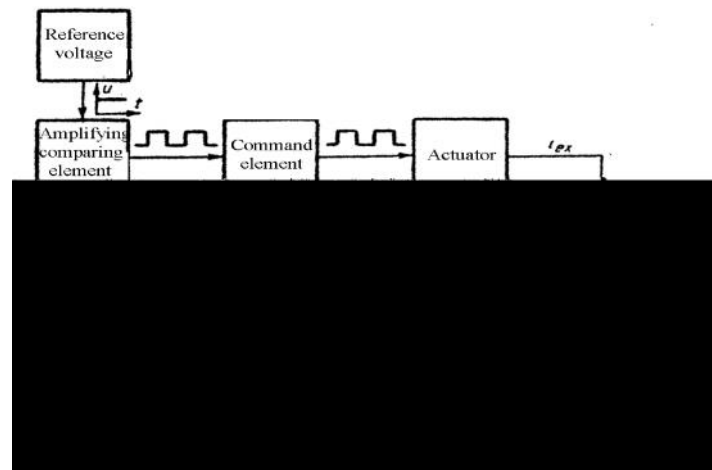


Fig.1. Block scheme of voltage electronic regulator

The voltage of the terminal generator tacked from agency of voltage factor is totaling with a slow variable supplied by the tooth-saw voltage generator. Voltage resulting is comparing from comparator-amplifier with reference voltage.



Fig.2. Command impulse modulation diagram

When the voltage from the summator is signal-bigger then reference voltage, comparator is opening, and when this is signal-smaller comparator has blocked. At way-out of comparator will have rectangular impulses between 0 and 1, after have the generator tendency is bigger or smaller than the reference voltage.

The voltage regulator for starter generator noticed the way-out voltage generator has applied a part of this voltage for first time non-invertor on 3 terminal, of CI1 (LM101AH) operational amplifier of other way-out invertor (2 terminal) has been applied a reference voltage tacked from a Zener diode.

Over the reaction voltage applied of CI1 operational amplifier is near a signal with waveform tooth saw with 400 ÷ 50Hz frequency, so that the CI1 operational amplifier is working like a switching comparator, his way-out has been a rectangular signal with the same frequency, but is variable filling factor.

Filling factor [3]

$$\theta = \frac{t_i}{T}, \tag{1}$$

where $t_i \ll T$, t_i - impulse duration e, T - period.

This filling factor is a different function between feedback voltage applied non-inverter for entry of operational amplifier and reference stabilized voltage applied for entry non-inverter of the same operational amplifier (the 2 terminal).

The way-out of operational amplifier is amplifying with stage of amplifier power realized by T7 transistor; the signal obtained like had been used then for transistors command that is working in switching regime T1 and T2 that feeded the excitation coil of generator assured in this way the regulating of voltage at way-out of generator.

2. THE IMPULSE MODULATING IN TIME

The impulses modulations in time consist in transferring characteristic of $x(t)$ base signal over the carrying un presented by a series of rectangular impulses [3].

$$\tau(t) = \tau_p + \Delta\tau(t). \quad (2)$$

$$\Delta\tau(t) = kx(t). \quad (3)$$

$$x_{MD}(t) \cong \frac{1 + k_D x(t)}{2} + \frac{2}{\pi} \sum_{n=1}^{\infty} \frac{\sin[n\pi(1 + k_D x(t))]}{n} \cos n\Omega t, \quad (4)$$

where τ_p - duration carrier, $\Omega = \frac{2\pi}{T}$, T - period.

It is remarking that this signal contains the base signal and a double infinity of componentd with armoning carrng modulated in stage. After the filtration type low pass filter obtain base signal. The blocks through block scheme that has realized the modulation in time are: block reference voltage, block divizor voltage, block comparator and block amplifier.

3. THE LINEARIZATION WAVEFORM VOLTAGE

In figure 4 are presenting the waveforms voltage of terminals generator [1], where t_d - the time that transistor is opening (conduction) and t_i - the time that transistor is closing (blocked).

$$t_c = t_d + t_i. \quad (5)$$

The relative during time of opening and closing are

$$\tau_d = \frac{t_d}{t_c}, \quad \tau_c = \frac{t_i}{t_c}, \quad \tau_d + \tau_c = 1. \quad (6)$$

$$tg\alpha_1 = \frac{2\Delta U}{t_d}, \quad tg\alpha_2 = \frac{2\Delta U}{t_i}, \quad 2\Delta U = \left(\frac{dU}{dt}\right)_d \cdot t_d = -\left(\frac{dU}{dt}\right)_i \cdot t_i, \quad (7)$$

where $\left(\frac{dU}{dt}\right)_d, \left(\frac{dU}{dt}\right)_i$ the equated velocity of various of voltage in two stare of transistor.

The repeater frequency of one cicle is

$$f_c = \frac{1}{t_c} = \frac{t_d}{(t_d + t_i)t_d} = \frac{\tau_d}{t_d} = \frac{\tau_i}{t_i}. \quad (8)$$

$$\Delta U = \frac{\left(\frac{dU}{dt}\right)_d \cdot t_d}{2} = \frac{\left(\frac{dU}{dt}\right)_d \cdot \tau_d}{2f_c} = -\frac{\left(\frac{dU}{dt}\right)_i \cdot \tau_i}{2f_c}. \quad (9)$$

Of equation (9) results

$$f = \frac{\left(\frac{dU}{dt}\right)_d \cdot \tau_d}{2\Delta U} = -\frac{\left(\frac{dU}{dt}\right)_i \cdot \tau_i}{2\Delta U}. \quad (10)$$

The ripple frequency of voltage depends even not by ripple amplitude, but even by growing and lawering velocity of excitation current respectively of voltage at terminals, so this velocity depends of circuit excitation [1].

For adjustable systems voltage who used the generator in impulses, the commutation frequency constituted a constant size, it has just modified the relative opening τ_d , who can have two limit values 0 and 1 of what the voltage ripple stopped and therefore ΔU is annulling.

4. CONCLUSIONS

In this work is presenting the block scheme and principle of electronic regulator voltage destined for regulating the voltage generator with 9KW power, of course are presenting the waveform of generator voltage and switching those, have determined the amplitude and ripple frequency.

REFERENCES

- [1]. **Aron, I., Paun, V.** *Echipamentul electric al aeronavelor*. Editura didactica si Pedagogica, Bucuresti 1980.
- [2]. **Barna, A.** *Amplificatoare operationale 222 exemple si probleme*. Editura Tehnica Bucuresti 1971.
- [3]. **Mateescu, Adelaida.** *Semnale, circuite si sisteme*. Editura Didactica si Pedagogica, Bucuresti, 1984.
- [4]. *** *Regulator electronic de tensiune pentru aeronava IAR-99*. Documentatie tehnica.

WEAR VALUATION OF BRAKING ACTIVE MATERIAL AT URBAN ELECTRIC FRAMES BRAKE REGIME

DRAGOS PASCULESCU* , CONSTANTIN BRINDUSA ,**

Abstract: In the case of subway electric frames operation it is necessary to estimate the environmental impact of the mechanical brake unrecovered energy. The amount of the material developed in the mechanical brake process (particularly, the clogs wear) it is depending on the mechanical brake unrecovered energy. Because this mechanical braking energy can be considered equal (like value) to the electrical energy (the active component) of the starting process, in the paper had been simulated a transient start regime, using MATLAB software and SIMULINK-Sim Power Systems Extensions. Consequently, it had evaluated the active braking material wear (the sabots wear) in the subway frames mechanical brake process, which has important environmental effects.

Keywords: transient start regime, MATLAB software and SIMULINK-Sim Power Systems Extensions

1. THEORETICAL CONSIDERATIONS

The modern subway urban electric frames are based on the driving systems with voltage and frequency static converters and traction asynchronous motors. These electrical driving systems allow to realize the vehicle electric brake, even with the energy recovery.

But, the vehicle brake regime can be also realized in a mechanical way, on the basis of the mechanical contact between the clog and the motor wheel rim. In this case, the environmental impact is important and it must be taken into account, because the subway frame it is operating into a closed (underground) space and the material amount developed into the mechanical brake process (particularly, the clogs wear) it is considerable, depending on the unrecovered energy which it is resulting in the mechanical brake regime.

For the quantitative evaluation of the unrecovered energy in the brake regime it can estimate that this energy is equal to the electrical energy absorbed by the driving

* *Assistant Ph.D. Eng. at University of Petrosani, Romania*

** *Ph.D. Student Eng. at University of Petrosani, Romania*

system in the transient starting regime of the vehicle. That is true in the most disadvantageous hypotheses of the drive system, meaning:

- only the mechanical brake it is taken into account; the electrical brake it is not applied in this case;
- the mechanical losses caused by the aerodynamic friction are insignificantly;
- the mechanical losses in the system of the mechanical movement transmission are not important, having been neglected;
- the electric losses in the driving system (electrical cables, power electronics elements etc.) are insignificantly.

Consequently, the mechanical braking energy will be considered equal (like amount) to the electric energy (the active component) received in the starting process. Therefore, in the paper will be simulated the transient starting regime of an electric subway urban frame, which is equipped with traction asynchronous motors, type MAB T₁.

2. SIMULATION MODEL AND MATLAB SOFTWARE

There is considered a traction asynchronous motor MAB T₁, which is an electric motor in a special construction, designed to operate in extremely heavy conditions. These motors are made to ensure the development of the traction torques, respectively, the traction forces at the electrical drive vehicles.

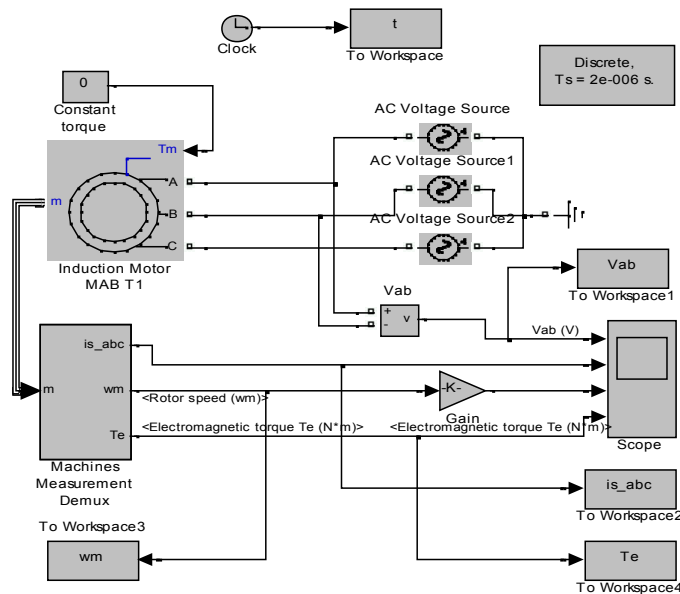


Fig.1. Simulation scheme for the vehicle behavior study in starting transient regime by direct network connection

For the simulation model from the Fig.1, there had been used the MATLAB software and the SIMULINK-Sim Power Systems Extensions. This model is based on the blocks specific to the electric drives, such as "Asynchronous Machine". "Machines

Measurement Demux", as well as on the blocks with general applications from Simulink library. In the technical literature there are presented technical data upon these, this paper emphasizing the potential of a such approach in the study of the traction electric motors. There are graphical drawn the time variation waves of the speed, the stator current and the electromagnetic torque developed by the motor in the transient starting regime of the subway electric frame. The traction motor MAB T₁, with the technical characteristics presented in Table 1, it is made by S.C. ELECTROPUTERE CRAIOVA S.A., for the urban electric frames, type subway, from the METROREX Bucuresti network.

Table 1 The traction motor MAB T₁, with the technical characteristics

Nr.	Tip	Simbol	MAB T ₁ (Y)
1	Rated power (kW)	P _n	70
2	Rated voltage (V)	U _n	560
3	Rated current (A)	I _n	96
4	Starting current (A)	I _p	720
5	Rated frequency (Hz)	f _n	60
6	Variation range of supply voltage frequency (%)	D	2
7	Rated power factor	cos _n	0,86
8	Poles pairs number	p	3
9	Rated speed (rpm)	n _n	1135
10	Rated efficiency (%)	_n	0,87
11	Rated torque (Nm)	M _n	589
12	Starting torque (Nm)	M _p	647,9
13	Stator resistance ()	R ₁	0,069

Starting from the data presented in Table 1, there had been determined/estimated the quantities values presented in Table 2.

Table 2

1	Z _p	0,4522	4	X ₁	0,2177
2	R ₂	0,0531	5	X ₂	0,2177
3	X ₁ +X ₂	0,4354	6	X _μ	4,5405

where:

- Z_p represents the starting impedance;
- R₂' represents the rotor resistance related to the stator;
- X₁ = X₂' represent the leakage reactances;
- X_μ represents the magnetizing reactance.

On the basis of the values presented in Table 1 and Table 2, there had resulted the characteristics from Fig.2, which are representing, in the MATLAB space, the wave forms for the main quantities which are characterizing the vehicle starting transient regime.

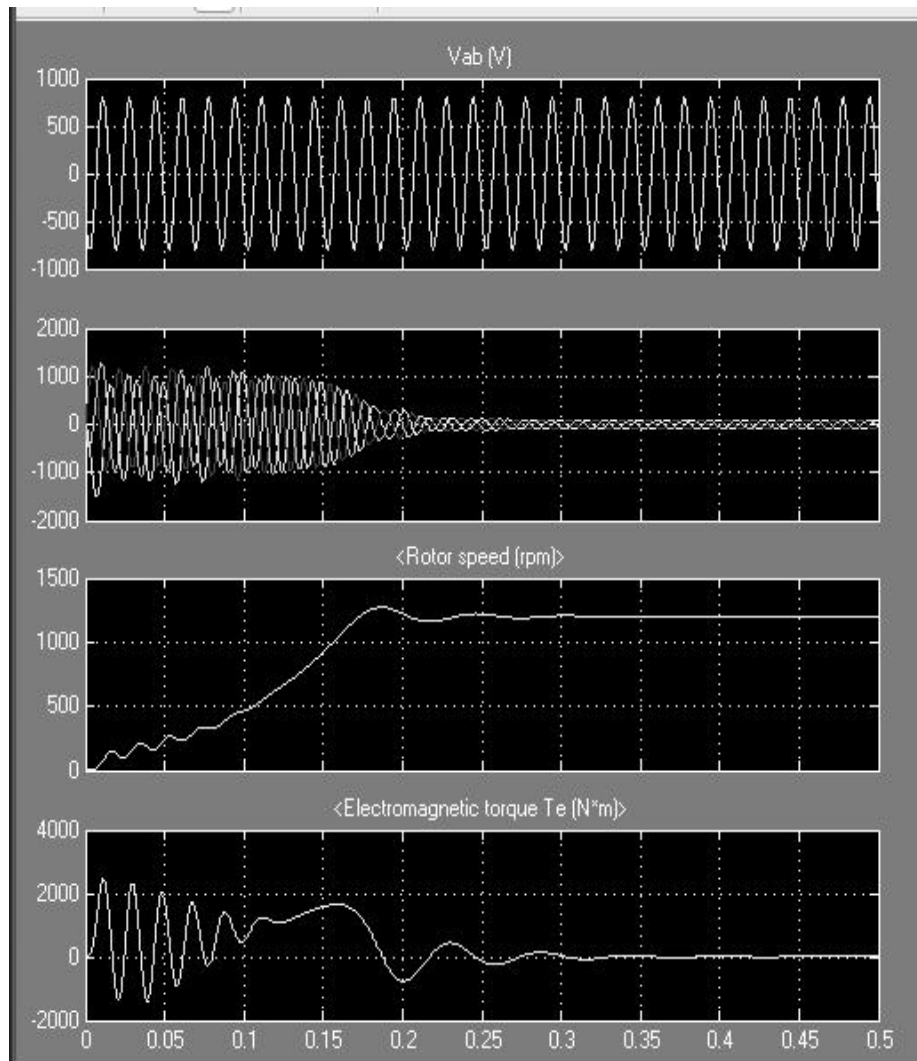


Fig.2. Electromechanical quantities definite for vehicle starting transient regime

Consequently, it can be determined the energy (the active component) absorbed by the system in the transient starting regime:

$$E_{aabs} = \sqrt{3}U_l I_l \cos \varphi \cdot t \cdot 10^{-3} (kWs) \quad (1)$$

Therefore, it will result:

$$E_{aabs} = \sqrt{3} \cdot 560 \cdot \frac{1000}{\sqrt{2}} \cdot 0,86 \cdot 0,25 \cdot 10^{-3} = 147,9kWs$$

Estimated, it can be considered that the amount of the material developed in the mechanical brake process (particularly, the clogs wear) it is proportional to the mechanical braking unrecovered energy. Taking into account the previous hypothesis, of the equality (like value) between the mechanical braking unrecovered energy and the electrical starting energy (the active component), on the basis of the relation (1) it can be determined the

wear rate of the braking active part, as below:

$$r_{Fe} = k_1 k_2 \lg a * E_{aabs} \tag{2}$$

where the coefficients a, k₁ and k₂ are experimentally determined and they are varying in function of some disturbing factors, like the material type, the contact pressure, the contact surface, the environment temperature and humidity and the local cooling.

Further on, considering a traffic with the frequency N₃, on a subway line (thoroughfare) of approximately 20 km, with an average of N₄ stations (equivalent to a tunnel with a complete aerating), it will result (as percentage) the active material wear amount, determined by the following relation:

$$R = 10^{-3} N_1 N_2 N_3 N_4 r_{Fe} (\%) \tag{3}$$

where: N₁ = number of days / year

N₂ = number of hours / day

N₃ = number of trains / hour

N₄ = number of stations / thoroughfare

Table 3 The resulted data

Q _{Fe}	80* 10 ⁻³	80* 10 ⁻³	80* 10 ⁻³	80* 10 ⁻³	80* 10 ⁻³	80* 10 ⁻³	80* 10 ⁻³	80* 10 ⁻³	80* 10 ⁻³	80* 10 ⁻³	80* 10 ⁻³	80* 10 ⁻³
N ₁	240	240	240	288	288	288	365	365	365	220	220	220
N ₂	20	20	24	20	20	24	20	20	24	20	20	24
N ₃	12	10	12	12	10	12	12	10	12	12	10	12
N ₄	20	20	20	20	20	20	20	20	20	20	20	20
R(%)	92	76	110	110	92	132	139	116	168	84	70	101

On the basis of the data of the table as before, it results that, in the hypothesis of an electrical brake absence, it would appear a wear of the mechanical braking equipment up to 100% during the entire year, leading, therefore, to its replacement.

3. CONCLUSIONS

The presented method represents a new approach in the study of the underground environmental impact of the travelling transport on the basis of the transport system realized with urban subway electric frames. The material amount released in the air and laid down into an underground (closed) space constitutes an important problem both for the environment and for the travelling transport safety, because the metals oxides can lead to serious perturbations in the centralized control system of the electric frames traffic.

REFERENCES

- [1] Krause P.C., Wasynczuk O., Sudhoff S.D., *Analysis of Electric Machinery*, IEEE, 1995.
- [2] Brîndușa, C., ș.a., *Sisteme electrice de transport neconvenționale (A23)*; Rama de metrou ac ionat cu motoare asincrone; Execu ie i experimentare modele (Faza 23.1), Contract cercetare 606C- Anexa A, Institutul na ional de cercetare i proiectare pentru ma ini electrice, echipament electric i trac iune, ICMET, Craiova, 1992

PC TO CY8C29466 MICROCONTROLLER SERIAL COMMUNICATION METHOD

DOBRA REMUS*

Abstract: This project shows how to connect the PSoC (Programmable System on Chip) mixed-signal array to a PC via an RS-232 serial interface. The scheme described in this paper consumes minimum current and works with applications that require low voltage. The aim of this project is to illustrate a data transfer between PC and PSoC and write the data bytes, which come from the PC (software) via RS232, to the PSoC device ROM (Flash) memory.

Keywords: CY8C29466 microcontroller, RS-232 serial interface

1. INTRODUCTION

To connect a PC to a CY8C29466 microcontroller via serial port, dedicated level translators, such as MAX232, are used. This paper demonstrates how to develop a simple, low supply current and low-cost level translator, which in many situations can replace a more expensive, dedicated level translator.

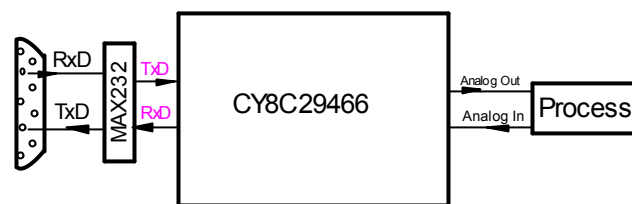


Fig.1 **Block diagram for serial communication PC - Microcontroller**

A level converter chip is required to connect a PC to a PSoC device with an RS-232 serial interface. Process

* *Assistant PhD student, University of Petrosani*

But there is a simpler solution that works well with the PSoC device. This solution is efficient with all PCs and has the standard UART interface for both stationary and portable devices.

The project provides efficient data exchange by using a supply voltage of 2.8 to 5 volts and it consumes very minimal current and supports data exchanges at a rate of at least 9600 bps.

Figure 2 illustrates communication protocol implementation.

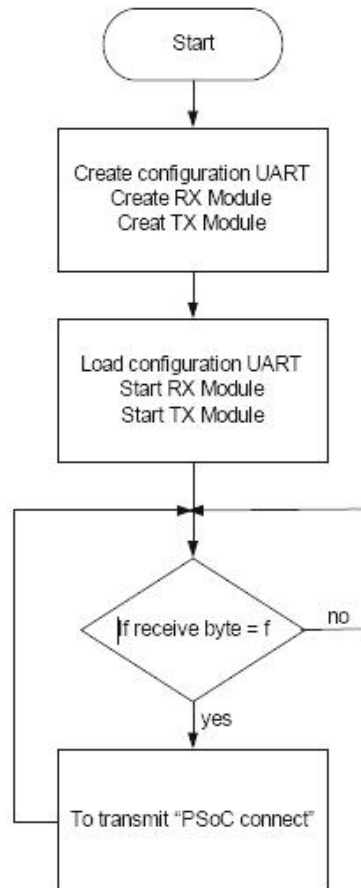


Fig.2 Communication algorithm

This algorithm has been written to get the information coming from the PC (software) via RS232 to the PSoC device and then write to the memory unit of ROM inside the device. The RX8 User Module checks the port continuously to interpret any data byte that has been sent from the PC. Then it waits for the receiving to complete. When data has completely been received, the RX8 checks for errors.

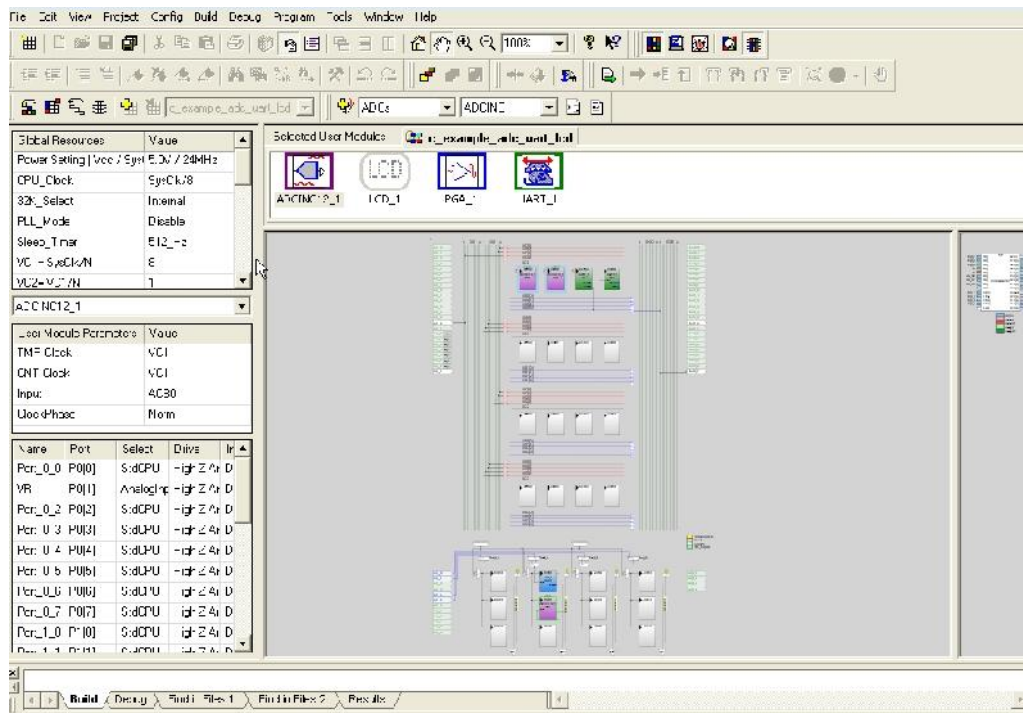


Fig.3 Graphical interface of the serial connection

3. MAIN PROGRAM

```

#include <m8c.h>
#include "PSoCAPI.h"
#define RESOLUTION 12
#define SCALE_BG (( 1 <<
RESOLUTION)/55)
int iResult;
void main()
{
    BYTE bgPos;

    UART_1_Start(UART_PARITY_NONE);
    UART_1_CPutString("Example
ADC_UART_LCD");
    UART_1_PutCRLF();

    PGA_1_Start(PGA_1_MEDPOWER);

    ADCINC12_1_Start(ADCINC12_1_MED
POWER);
    ADCINC12_1_GetSamples(0);
    LCD_1_Start();
    LCD_1_InitBG(LCD_1_SOLID_BG);

    LCD_1_Position(0,0);
    LCD_1_PrCString("PSoC LCD");
    M8C_EnableGInt;
    while (1)// Main loop
    {
        if (ADCINC12_1_fIsDataAvailable()
!= 0) {
            iResult = ADCINC12_1_iGetData()
+ 2048; and clear flag
            ADCINC12_1_ClearFlag();
            LCD_1_Position(1,0); //
display result on LCD in hex and as a bar
graph
            LCD_1_PrDecInt(iResult);
            bgPos =
            (BYTE)(iResult/SCALE_BG);
            LCD_1_DrawBG(1, 5, 11, bgPos);
        }
    }
}

```

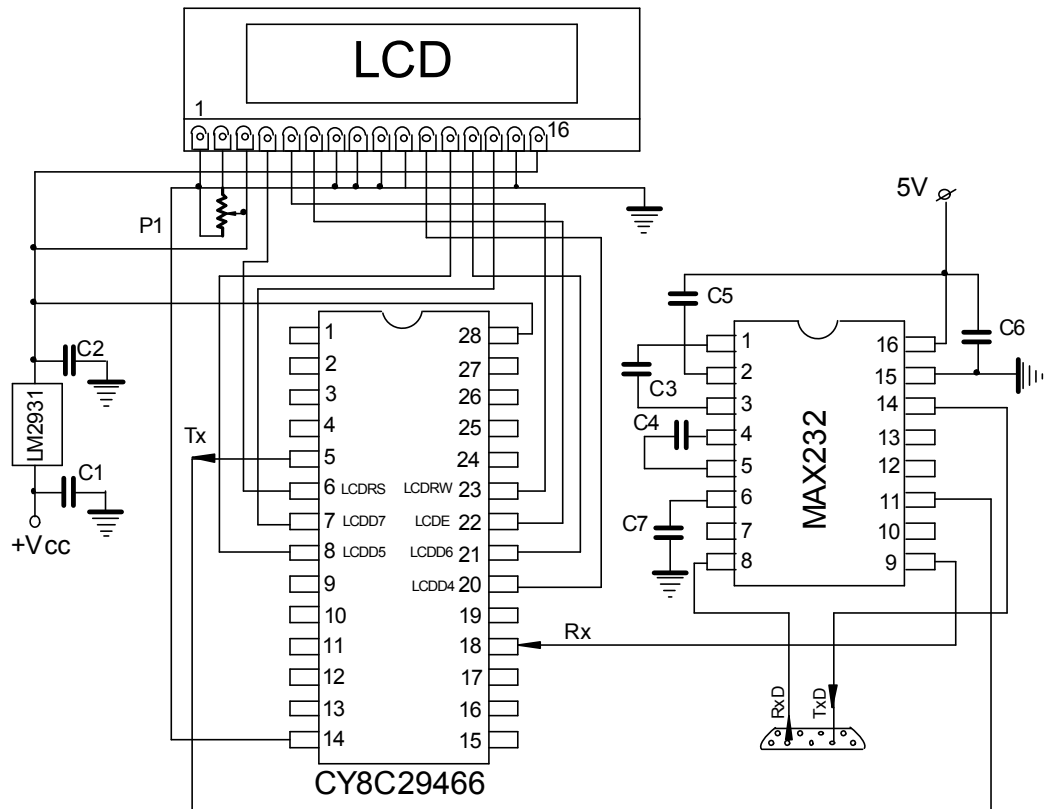



Fig.3. The connection between PC an CY8C29466

In the figure 3 is shown the low cost possibility to connect PC to a cypress microcontroller. This is possible with Max232 device, and if is necessary to realize real time measurement with an autonomic apparatus the microcontroller will be supplied trough a stabilizer device.

2. CONCLUSIONS

The design discussed in this paper is a model for several other data acquisition and control systems using PSoC Designer, which provides analog and digital migration required for any laboratory or industrial automation. This compact design can be mounted on the system under automation and interfaced with the PC through serial communication.

REFERENCES

- [1] *** Cypress 3210 MiniProg tehcnical documentation

ANALYSIS OF THE LUEMBERGER EXTENDED ESTIMATOR USED WITHIN A VECTORIAL-TYPE ELECTRICAL DRIVING SYSTEM WITH AN INDUCTION MOTOR

CORNELIU MÂNDRESCU*, OLIMPIU STOICUȚA**

Abstract: In this paper we present the analysis through simulation of the extended Luemberger estimator using the Matlab – Simulink platform. Within this analysis we emphasize the errors between real rotor flux and the estimated one as well as the error between real rotor speed and estimated one.

Keywords: Luemberger estimator, values rotation method, values moving method

1. IMPLEMENTATION OF THE INDUCTION MOTOR

In order to implement the induction motor in Matlab – Simulink we will use the S_Function blocks within Simulink. The structure of the simulation scheme of the induction motor is presented in Figure 1.

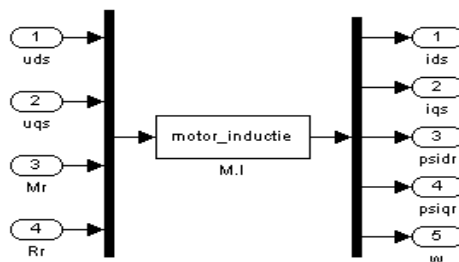


Fig. 1. Structure of the induction motor's scheme

* *Assoc.Prof.Eng.Ph.D., University of Petroșani*

** *Assist.Eng., University of Petroșani*

From this figure one may notice that the fourth entry variable is considered to be rotor resistance.

This is justified in the analysis phase of the extended Luemberger estimator, in order to emphasize the sensitivity of the extended Luemberger estimator when rotor resistance of the induction motor is changed.

In order to emphasize the source code, written in Matlab language, of the induction motor we will consider that the motor has the following electrical and mechanical parameters:

$$P_N = 500 \text{ [W]}; U_N = 127 \text{ [V]}; I_N = 2.9 \text{ [A]}; n_N = 1400 \text{ [rot/min]};$$

$$z_p = 2; M_N = 3.41 \text{ [Nm]}; R_s = 4.495 \text{ [\Omega]}; R_r = 5.365 \text{ [\Omega]};$$

$$L_s = 165 \text{ [mH]}; L_r = 162 \text{ [mH]}; L_m = 149 \text{ [mH]}; J = 0.00095 \text{ [Kg}\cdot\text{m}^2\text{]}.$$

Under these circumstances the source code in Matlab that is given to the S_Function block corresponding to the induction motor is:

```
function [sys,x0,str,ts] = motor_inductie(t,x,u,flag)
switch flag,
case 0,
[sys,x0,str,ts]=mdlInitializeSizes;
case 2,
sys = mdlUpdate(t,x,u);
case 3,
sys = mdlOutputs(t,x,u);
case 9,
sys = [];
otherwise
error(['unhandled flag = ',num2str(flag)]);
end
function [sys,x0,str,ts]=mdlInitializeSizes
sizes = simsizes;
sizes.NumContStates = 0;
sizes.NumDiscStates = 5;
sizes.NumOutputs = 5;
sizes.NumInputs = 3;
sizes.DirFeedthrough = 1;
sizes.NumSampleTimes = 1;
sys = simsizes(sizes);
x0 = [0;0;0;0;0];
str = [];
ts = [2000/(150e+6/2) 0];
function sys = mdlUpdate(t,x,u)
Rr=5.365;
Rs=4.495;
Ls=165e-3;
Lr=162e-3;
Lm=149e-3;
J=0.95e-3;
zp=2;
s=1-(Lm^2/(Ls*Lr));
```

```

Ts=Ls/Rs;
Tr=Lr/Rr;
T=2000/(150e+6/2);
B=[1/(s*Ls) 0 0;
0 1/(s*Ls) 0;
0 0 0;
0 0 0;
0 0 (zp*sign(x(5)))/J];
A=[-((1/(Ts*s))+((1-s)/(Tr*s))) 0 Lm/(Ls*Lr*Tr*s) (Lm/(Ls*Lr*s))*x(5) 0;
0 -((1/(Ts*s))+((1-s)/(Tr*s))) -(Lm/(Ls*Lr*s))*x(5) Lm/(Ls*Lr*Tr*s) 0;
Lm/Tr 0 -(1/Tr) -x(5) 0;
0 Lm/Tr x(5) -(1/Tr) 0;
-(3*zp^2*Lm)/(2*J*Lr))*x(4) ((3*zp^2*Lm)/(2*J*Lr))*x(3) 0 0 0];
F=eye(5)+A*T+(A^2)*(T^2/2);
H=B*T+A*B*(T^2/2);
sys=F*x+H*u;
function sys = mdlOutputs(t,x,u)
sys = x;

```

2. IMPLEMENTATION OF THE LUEMBERGER ESTIMATOR

The schematics of the Luemberger estimator used to estimate rotor fluxes and stator currents is presented in Figure 2.

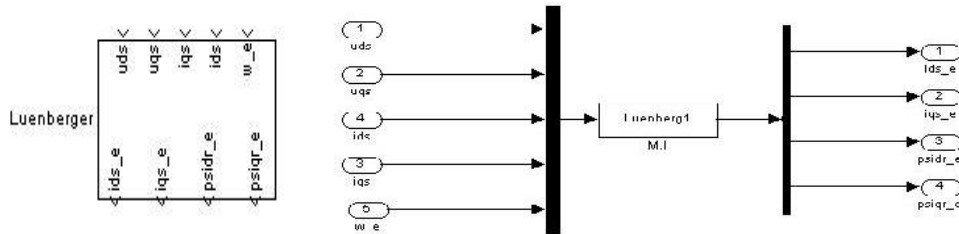


Fig. 2. Luemberger estimator schematics

Under these circumstances the Matlab source code given to the S_Function block corresponding to the Luemberger estimator is:

A. In case of projecting the estimator based on proportional self values method:

```

function [sys,x0,str,ts] =Luenberg1(t,x,u,flag)
switch flag,
case 0,
[sys,x0,str,ts]=mdlInitializeSizes;
case 2,
sys = mdlUpdate(t,x,u);

```

```

case 3,
    sys = mdlOutputs(t,x,u);
case 9,
    sys = [];
otherwise
    error(['unhandled flag = ',num2str(flag)]);
end
function [sys,x0,str,ts]=mdlInitializeSizes;
sizes = simsizes;
sizes.NumContStates = 0;
sizes.NumDiscStates = 4;
sizes.NumOutputs = 4;
sizes.NumInputs = 5;
sizes.DirFeedthrough = 1;
sizes.NumSampleTimes = 1;
sys = simsizes(sizes);
x0 = [0;0;0;0];
str = [];
ts = [2000/(150e+6/2) 0];
function sys = mdlUpdate(t,x,u)
Rr=5.365;
Rs=4.495;
Ls=165e-3;
Lr=162e-3;
Lm=149e-3;
J=0.95e-3;
zp=2;
s=1-(Lm^2/(Ls*Lr));
Ts=Ls/Rs;
Tr=Lr/Rr;
T=2000/(150e+6/2);
A=[-((1/(Ts*s))+((1-s)/(Tr*s))) 0 Lm/(Ls*Lr*Tr*s) (Lm/(Ls*Lr*s))*u(5);
    0 -((1/(Ts*s))+((1-s)/(Tr*s))) -(Lm/(Ls*Lr*s))*u(5) Lm/(Ls*Lr*Tr*s);
    Lm/Tr 0 -(1/Tr) -u(5);
    0 Lm/Tr u(5) -(1/Tr)];
B=[1/(s*Ls) 0;
    0 1/(s*Ls);
    0 0;
    0 0];
C=[1 0 0 0;
    0 1 0 0];
F=eye(4)+A*T+(A^2)*(T^2/2);
H=B*T+A*B*(T^2/2);
a1=-((1/(Ts*s))+((1-s)/(Tr*s)));
a2=-1/Tr;
a3=Lm/Tr;
c=Lm/(s*Ls*Lr);
k=1.3;
k11=(a1+a2)*(1-k);
k12=u(5)*(1-k);

```

```

k22=-k12/c;
k21=(a3+a1/c)*(1-k^2)-k11/c;
L=[k11 -k12;
        k12 k11;
        k21 -k22;
        k22 k21];
Ld=L*T+A*L*(T^2/2);
U=[u(1);u(2)];
Y=[u(3);u(4)];
x=F*x+H*U+Ld*(Y-C*x);
sys=x;
function sys = mdlOutputs(t,x,u)
sys=x;

```

B. In case of projecting the estimator based on self values rotation:

The program for this case is resembling the previous one, except that the lines in **bold** are to be replaced with the following ones:

```

c1=Lm/(s*Ls*Lr);
c=1/c1;
k=1.4;
teta_min=15*pi/180;
w_max=6000*pi/30;
ka1=teta_min/w_max;
teta=ka1*u(5);
kr=k*cos(teta);
ki=k*sin(teta);
k11=(1-kr)*(a1+a2)+ki*u(5);
k12=(1-kr)*u(5)-ki*(a1+a2);
k22=(1-kr^2+ki^2)*(a3+c*a1)-c*k11;
k21=-2*kr*ki*(a3+c*a1)-c*k12;
L=[k11 -k12;
        k12 k11;
        k21 -k22;
        k22 k21];
Ld=L*T+A*L*(T^2/2);

```

C. In case of projecting the estimator based on self values rotation:

The program for this case is resembling the first one, except that the lines in **bold** are to be replaced with the following ones:

```

c1=Lm/(s*Ls*Lr);
c=1/c1;
delta=-1;
k11=-2*delta;
k12=0;

```

```

k21=c*(a1+2*delta)-c*delta*((a2^2+u(5)^2)^-
1)*(a1*a2^2+a2*(a1+a2)*delta+a2*delta^2+(u(5))*(delta+a1));
k22=c*delta*u(5)*(a1+delta)*((a2^2+u(5)^2)^-1);
L=[k11 -k12;
   k12 k11;
   k21 -k22;
   k22 k21];
Ld=L*T+A*L*(T^2/2);
function sys = mdlOutputs(t,x,u)
sys=x;
    
```

3. IMPLEMENTATION OF THE EXTENDED LUENBERGER ESTIMATOR

Based on the things previously presented we can realize the simulation scheme of the extended Luemberger estimator. This will contain, as known, the speed adjusting mechanism or speed estimator. The simulation scheme realized in Simulink is presented in Figure 3.

Internal structure of the adjusting mechanism is in Figure 4.

As one may notice in Figure 4 we also emphasized the PI regulator used to estimate speed, implemented using trapeze digitization method (Tustin method).

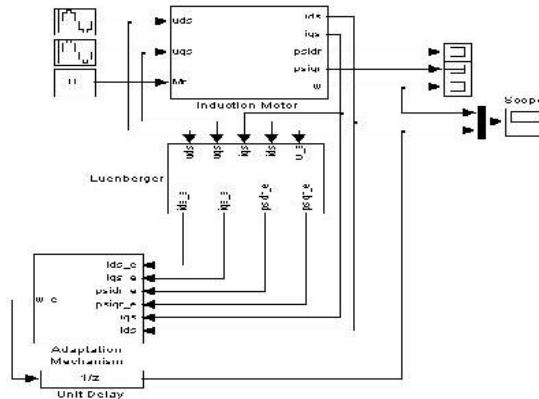


Fig. 3. Extended Luemberger estimator block schematics

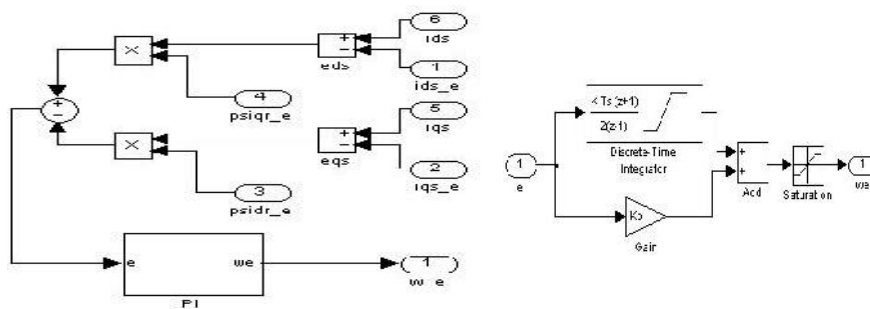


Fig. 4 Internal structure of the adjusting mechanism

4. ANALYSIS OF THE EXTENDED LUEMBERGER ESTIMATOR

In order to analyze the extended Luemberger estimator we considered the case in which the Luemberger estimator is projected based on self values proportionality method. Under these circumstances using a sampling time of $2000/(150e+6/2)$ and a nil resistant torque during the first 0.5 seconds and then a resistant torque. Equal to the nominal one, following the simulation we obtain the variations with time of the rotor flux in the dq coordinates as well as the variation of speed. Following the simulation we can realize a comparison between the real rotor flux and the estimated one as well as the real speed and the estimated one. These results are obtained after we power the motor with an amplitude tension of $U_N \cdot \sqrt{2}$. The graphs mentioned above are presented in Figure 5.

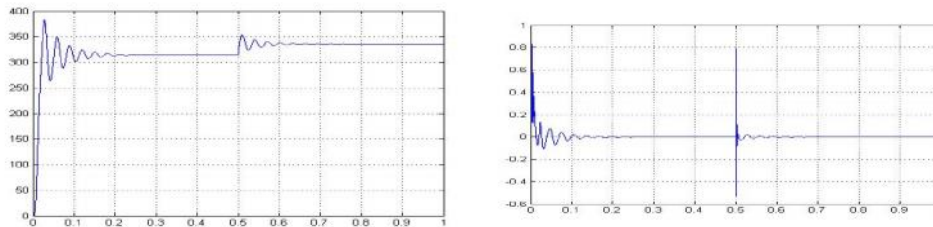


Fig. 5 Real and estimated speed with estimated and real speeds errors

One may notice that between the real and estimated speed big differences do not appear. In order to observe the small differences between the two speeds in the following we present the graph of errors for the two speeds.

In a resembling manner we will present the variation in time of the rotor flux, emphasizing both the variation with time and the error between them. In the graphs below we present the variations with time of the estimated flux on the d axis compared to the real flux on the d axis and the variation with time of the estimated flux on the q axis compared to the real flux on the q axis. The graphs mentioned are presented in Figure 6. One may notice, in this case also, that between the real and estimated rotor flux big differences do not appear. In order to observe the small differences between the two fluxes corresponding to the d axis we will present the graph of the error between the two fluxes.

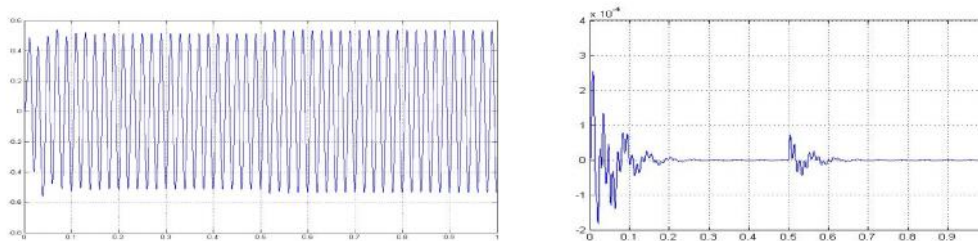


Fig. 6 Real and estimated rotor flux corresponding to the d axis with error

In a resembling manner the real rotor flux and the estimated one corresponding to the q axis is presented in Figure 7.

One may notice, in this case as in the preceding case that between real rotor flux and the estimated one big difference do not appear. In order to observe the small differences between the two fluxes corresponding to the q axis we will present the graph of error of the two fluxes.

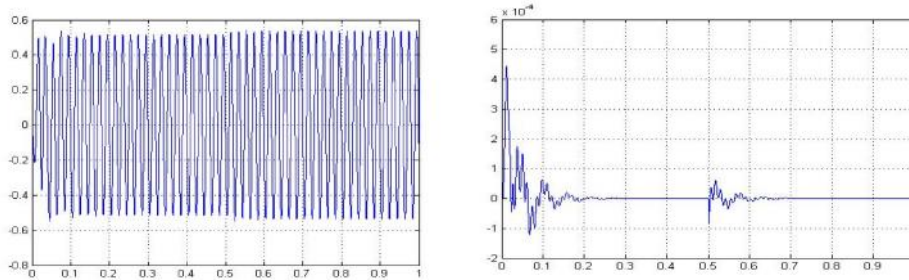


Fig. 7 Real and estimated rotor flux corresponding to the q axis with error

5. CONCLUSIONS

Based on the presented algorithms one can realize a real time simulation with hardware in the loop that will allow to obtain the self values of the estimator, motor and the regulating system in various working regimes of the motor, meaning a real time analysis of the motor- estimator ensemble stability.

The results presented above can constitute a reference point in projecting a sensorless vector regulating system.

Following the simulation one can conclude that the extended Luemberger estimator has a very good dynamics for low, medium or high speeds so that it is recommended to be used in sensorless vector regulating schemes.

REFERENCES

- [1] C.Ilas, V.Bostan, *Tehnici adaptive de control a motorului asincron: comanda vectoriala fara masurarea vitezei*, Litografia U.P.B. (2001)
- [2] M. Hilairret, C. Darengosse, F. Auger, P. Chevrel, *Synthesis and analysis of robust flux observers for induction machines*, IFAC Symp. on Robust Control Design, Prague. (2000)
- [3] O. Stoicuta, H. Campian, T. Pana, *The Comparative Study of the Stability of the Vector Control Systems that Contain in the Loop Luemberger and Kalman Type Estimators*, IEEE-ITTC International Conference on Automation, Quality & Testing, Robotics AQTR 2006 (THETA 15), Cluj-Napoca, (2006)

APPROACH ON DISTRIBUTIONS FOR CONTROL SYSTEMS WITH RELAY TYPE NONLINEARITIES

MONICA LEBA*, EMIL POP**, PETRE VAMVU***

Abstract: In this paper are presented distributions, their properties and applications in nonlinear system control. Using the definition of distributions, the mathematical formulas for relay type nonlinearity elements are determined. Based on distribution properties there can be easily designed flexible and reliable nonlinear systems with relay type nonlinearities. Using this theory there were designed, modeled and simulated the complex distributions that have many practical applications in nonlinear system control.

Keywords: distributions, relay, nonlinear systems

1. NONLINEAR SYSTEMS WITH SEVERE NONLINEARITIES OVERVIEW

One of the most developed theory, witch dominate the last century was Linear Dynamical System Control Theory. But linear systems represent only an approach of real systems and some time unacceptable approximation for others. In the real world, all the systems are nonlinear because the process and phenomena are always nonlinear. The nonlinear systems use nonlinear operators to describe their mathematical models. This approach is very exhaustive and is impossible to find general equations and methods for entire nonlinear systems class. There are only some methods to analyze several classes of nonlinear systems. The type of nonlinearities from the systems defines its classis. The nonlinearities can be classified in light and severe, according to the possibility of linearization. The light nonlinearities have good linear approximation, while for the severe nonlinearities the linear approximation has unacceptable errors.

The light nonlinearities are continuous and differentiable and the severe ones had discontinuities and are not differentiable.

* *PhD. Lecturer at the University of Petrosani*

** *PhD. Professor at the University of Petrosani*

*** *Assistant Eng. at the University of Petrosani*

The second category includes a wide range of switches like digital, relay and logic elements. A most used class of nonlinear systems is called relay type systems. In fig.1 are examples for these categories of nonlinearities: light and severe (relay types). For nonlinear systems with relay types nonlinearities elements is difficult to write a mathematical model, because there are equations with polymorph form, discontinuities and many non derivable points. This is a difficult barrier to avoid.

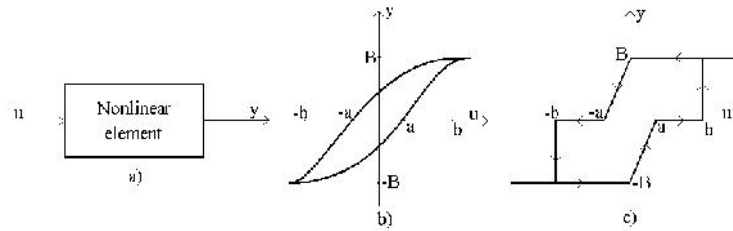


Fig.1. Nonlinear elements: a) Block diagram; b) Light; c) Severe (relay types)

If this element contains one light nonlinearity like in fig.1.b the equation can be written quite simple as follow:

$$y(u) = \begin{cases} B(1 - \exp(1 - abs(u - a))); \frac{d}{dt} u \geq 0 \\ B(\exp(-abs(u + a)) + 1); \frac{d}{dt} u \leq 0 \end{cases} \quad (1)$$

If this element contain severe nonlinearity like in fig.1.c the equation is more difficult to be written. The nonlinearity is discontinuous. The equations are as follows:

$$f(u) = \begin{cases} \left. \begin{array}{l} -B; u \leq 0 \\ \frac{B}{a} \cdot u - B; 0 \leq u \leq a \\ 0; a \leq u \leq b \\ B; u \geq b \end{array} \right\} \frac{du}{dt} > 0 \\ \left. \begin{array}{l} B; u \geq 0 \\ \frac{B}{a} \cdot u + B; -a \leq u \leq 0 \\ 0; -b \leq u \leq -a \\ -B; u \leq -b \end{array} \right\} \frac{du}{dt} < 0 \end{cases} \quad (2)$$

These model equations are difficult to use and many times become unacceptable for simulation. For this reason there are used generalized functions or distributions to avoid these difficulties.

2. MATHEMATICAL SUPPORT FOR APPLICATION OF DISTRIBUTIONS IN RELAY TYPE NONLINEAR SYSTEMS

Sever nonlinearities, like above, cannot be represented as closed mathematical formula because they present a lot of discontinuities, non-derivations, discrete transitions etc. In the classical theory this regions are avoided, eliminating the

discontinuities and never using the derivation operator in critical points. This approach has two disadvantages: first, the representation is complicated and unusual and second, just the discontinuities are eliminated where the systems work.

These difficulties can be eliminated by distribution theory extending the fundamental concepts, like derivability, to the whole domain, and can be easy to write the mathematical models and evaluate its qualitative properties, by simulation.

Now, in the next part the mathematical support for distributions will be considered. The distributions can be defined as the functional transformations between two linear spaces. We consider the n-dimensional Euclidian real space \mathbb{R}^n , organized as a vectors space. The elements of this space are n-coordinates vectors: $x = (x_1, x_2, \dots, x_n)$, $y = (y_1, y_2, \dots, y_n)$. On this space will be considered the applications $f : \mathbb{R}^n \rightarrow \mathbb{R}$.

From this applications will be selected $\varphi(x)$ which are continuous, derivable and the derivates are continuous with zero value out of their domain. The domain of these functions is compact. The space of $\varphi(x)$ functions continuous and derivable is K^n and has the properties:

- $\forall \varphi_1(x), \varphi_2(x) \in K^m, \alpha, \beta \in \mathbb{R}^n : \alpha \cdot \varphi_1(x) + \beta \cdot \varphi_2(x) \in K^m$;
- $\forall \varphi_k(x) \in K^m : \lim_{k \rightarrow \infty} |\varphi_k(x)| = 0$.

This is a fundamental space. In this space will define the functional applications:

$$f : K^m \rightarrow \mathbb{R} : f[\varphi(x)] \in \mathbb{R}.$$

Distributions are real, linear and continuous functional defined on fundamental space. The most important distributions in nonlinear systems are: pulse, step and ramp distributions.

The pulse distribution or Dirac pulse is defined as follows:

$$\delta : K^m \rightarrow \mathbb{R} : \delta[\varphi(x)] = \varphi(0); \forall \varphi(x) \in K^m \tag{3}$$

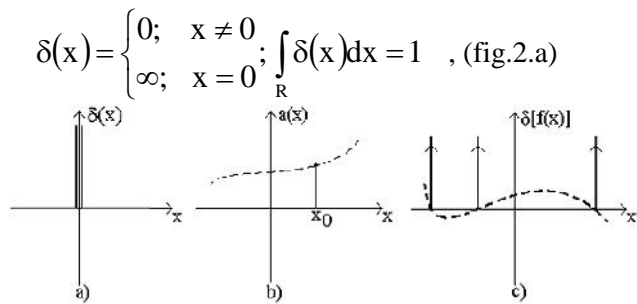


Fig.2. Distribution $\delta(x)$ and its properties

Proposition 1

The Dirac distribution has the following properties:

1. $a(x) \cdot \delta(x - x_0) = a(x_0) \cdot \delta(x - x_0)$, (fig.2.b)

2. $\delta(\alpha \cdot x + \beta) = \frac{1}{|\alpha|} \cdot \delta\left(x + \frac{\beta}{\alpha}\right); \delta(-x) = \delta(x)$
3. $\delta[f(x)] = \sum_{i=1}^p \frac{1}{|f'(x_i)|} \cdot \delta(x - x_i); x_i \text{ are simple solutions: } f(x) = 0, \text{ (fig.2.c)}$
4. $\frac{d[f(x)]}{dx} = f(x)' + \sum_{i=1}^p s_i \cdot \delta(x - x_i); s_i = f(x_i + 0) - f(x_i - 0)$

The step distribution or Heaviside distribution is defined bellow (fig.3.a):

$$\theta : K^m \rightarrow R; \quad \theta[\varphi(x)] = \begin{cases} 1; & x \geq 0 \\ 0; & x < 0 \end{cases}$$

Proposition 2

The Heaviside distribution has the following properties:

1. $\theta(-x) = 1 - \theta(x)$ (fig.3.b); $\theta(x) - \theta(-x) = \text{sign}(x)$ (fig.3.c)
2. $\theta(x^2 - a^2) = 1 - \theta(x + a) + \theta(x - a); f(x) \cdot \theta[f(x)] = f_+(x); \frac{d[\theta(x)]}{dx} = \delta(x)$

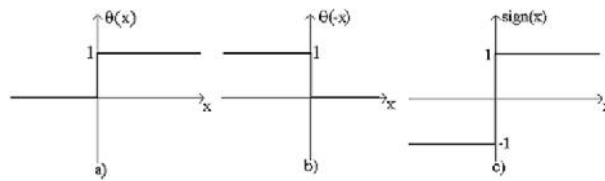


Fig.3. Heaviside distribution and its properties

The ramp distribution is defined as follows (fig.4.a):

$$r : K^m \rightarrow R; \quad r[\varphi(x)] = \begin{cases} x; & x \geq 0 \\ 0; & x < 0 \end{cases}$$

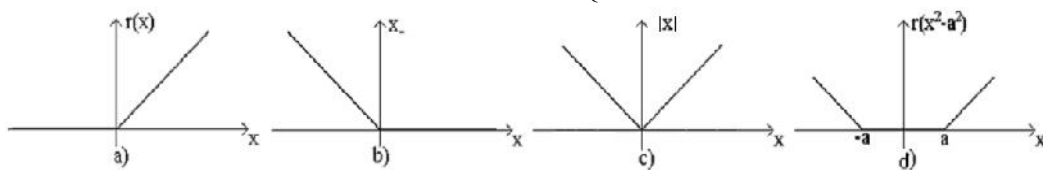


Fig.4. Ramp distribution and its properties

Proposition 3

The ramp distribution has the following properties:

1. $r(x) = x \cdot \theta(x) = x_+$ (positive ramp); $-x \cdot \theta(-x) = x_-$ (negative ramp) (fig.4.a,b)
2. $|x| = x \cdot \text{sign}(x) = x_+ + x_-; r(x^2 - a^2) = \theta(x - a) \cdot (x - a) + \theta(x + a) \cdot (x + a)$ (fig.4.c,d)
3. $[x_+] = \theta(x); [x_-] = -\theta(-x); x_+ - x_- = x; \frac{1}{2} \cdot (x + |x|) = x_+; \frac{1}{2} \cdot (|x| - x) = x_-$

Theorem of concatenation

Consider the $f_i(u)$, $i = 1, \dots, N$ a set of real functions defined on closed interval, μ_i step distribution, μ_i characteristic function of I_i and $f(u)$ the distribution obtained by $f_i(u)$ concatenation. There are relations:

$$\mu_i = \theta[-u^2 + (a_i + b_i) \cdot u - a_i \cdot b_i]; \text{ if } I_i = [a_i, b_i]$$

$$\mu_i = 1 - \theta(u - b_i); \text{ if } I_i = (-\infty, b_i]$$

$$\mu_i = \theta[u - a_i]; \text{ if } I_i = [a_i, +\infty)$$

$$f(u) = \sum_i [f_i(u) \cdot \mu_i \cdot \theta(\frac{du}{dt})]$$

The demonstration of this theorem result as a consequence of the last three propositions presented above. Based on the elementary distributions properties and using the theorem of concatenation, there can be obtained complex and polymorph distributions, like the examples shown in fig.5.

Mathematically these distributions have the following formula, respectively:

$$y(u) = B \cdot [\theta(u - a) - \theta(-u - a)] \tag{4}$$

$$y(u) = \begin{cases} B \cdot [\theta(u - a) - \theta(-u - b)]; \frac{du}{dt} > 0 \\ B \cdot [\theta(u - b) - \theta(-u - a)]; \frac{du}{dt} < 0 \end{cases} \tag{5}$$

$$y(u) = \begin{cases} B \cdot [\text{sign}(u - a)]; \frac{du}{dt} > 0 \\ B \cdot [\text{sign}(u + a)]; \frac{du}{dt} < 0 \end{cases} \tag{6}$$

$$f(u) = (u + 4) \cdot \theta(-u^2 - 7 \cdot u - 12) + (-u - 2) \cdot \theta(-u^2 - 5 \cdot u - 6) + (u + 2) \cdot \theta(-u^2 - 2 \cdot u) + (-u + 2) \cdot \theta(-u^2 + 2 \cdot u) + (u - 2) \cdot \theta(-u^2 + 5 \cdot u - 6) + (-u + 4) \cdot \theta(-u^2 + 7 \cdot u - 12) + \left[\left(\frac{u}{2}\right)^2 - 4\right] \cdot \theta(-u^2 + 16) \tag{7}$$

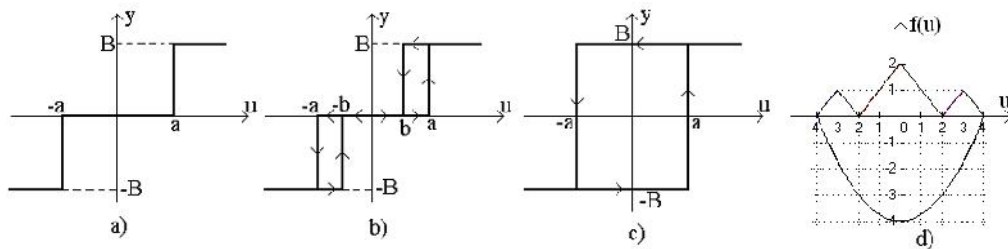


Fig.5. Complex and polymorph distributions: a) Tri-state; b) Tri-state with window; c) Two-state with window; d) Concatenation

3. MODELING AND SIMULATION OF DISTRIBUTIONS

In this section the elementary distributions and some properties will be simulated. In fig.6 the model of $\delta(t), \theta(t), r(t), \text{sign}(t)$ and $|t|$ were simulated.

In fig.7 there are presented the simulation model and results for several relay type complex distributions, like tri-state, window tri- and two- stare and concatenation.

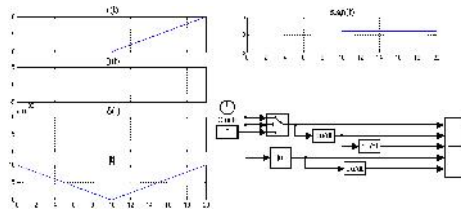


Fig.6. Simulation of elementary distributions

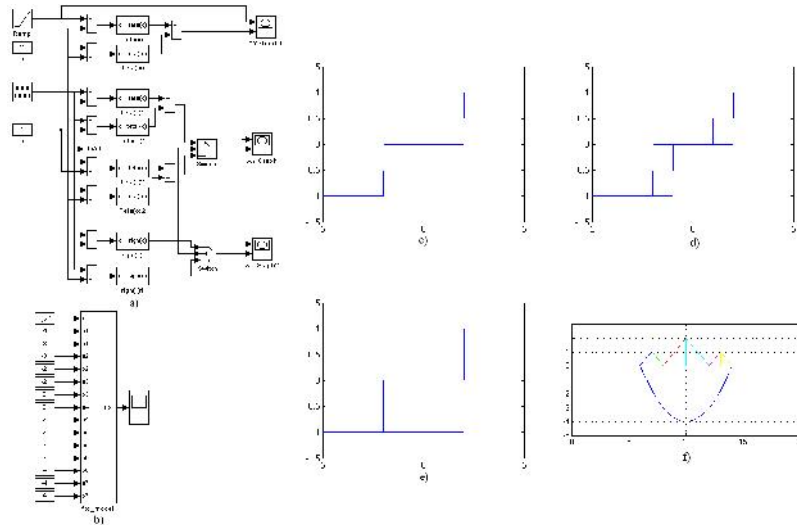


Fig.7. Simulation of complex distributions: a), b) Simulink models; c) Tri-state; d) Window Tri-state; e) Window Two-state; f) Concatenation

4. CONCLUSIONS

1. The distributions are very useful for nonlinear system elements approach.
2. For nonlinear systems with relay nonlinearity it is easy to write a distributions mathematical model. Using the concatenation theorem, it is possible to represent the mathematical model of complex polymorph distributions.
3. The modeling and simulation of relay type nonlinear systems using the distributions theory and properties is very easy to implement.

BIBLIOGRAPHY

- [1] KECS W.W.: *Teoria distributiilor si aplicatii*. Ed.Academiei, Bucuresti, 2003.
- [2] SCHWARTZ L.: *Theorie des distributions*. Paris, Hermann, 1951.
- [3] POP E., LEBA M.: *Contribution to sine delta pulse width modulation control of three-phase inverter*. Galati, Proceedings of 11th National Conference on Electric Drives, 2002.
- [4] POP E.: *Nonlinear systems. Introduction and applications in electrical drive control*. Jahresbericht des IEE nr.13, Clausthal, Germany, 2002.
- [5] LEBA M.: *A new PWM controller based on distributions properties*. microCAD 2006, Miskolc, Hungary, 2006

AUTOMATIC WIG WELDING CONTROL USING FEEDFORWARD NEURAL NETWORK

GABRIELA BUCUR*, LIVIU BUCUR**

Abstract: The paper presents the WIG arc welding industrial system control block diagram based on the correction of the trajectory welding torch through the welding seam. Welding trajectory is corrected using an automated control system in which the control function is realized with a feedforward neural network based on backpropagation algorithm. The reaction signal for the neural controller is obtained from the acquisition system of the voltage values of the arc-welding process.

Key words: neural network, backpropagation, welding process, robots.

1. INTRODUCTION

The final purpose of a welding operation is to achieve a welding seam that satisfies many imposed conditions. These conditions result from technological general system analysis, system which is composed by power source – welding source – arc welding system, welding seam, manipulation system and control system. The improvement of the welding quality is achieved by the trajectory correction, based on following the welding joint, processing the acquired signals in the command system and modifying, if necessary, the welding parameters. *The paper presents the way to process the welding-arc voltage with neural network [1].* That result can be applied in automated robotic welding based on the correction of the trajectory welding torch through the welding seam.

*Lecturer, Ph.D. at the “Petroleum-Gas” University of Ploiești, Department of Control Engineering and Computers, Romania

** Mathematician, Ph.D. Student, “Florin Comisel” School of Ploiesti, Romania

2. WIG WELDING MATHEMATICAL MODEL WITH NEURAL NETWORK

The paper presents the arc welding – power source model for the WIG welding process [4]. For this model, an input is the electrical arc external length l_{ae} , created by welding source. In 11 element, l_{ae} is added to the arc electrical arc internal length l_{ai} , created by penetration p and to the external perturbation of arc length l_a^* .

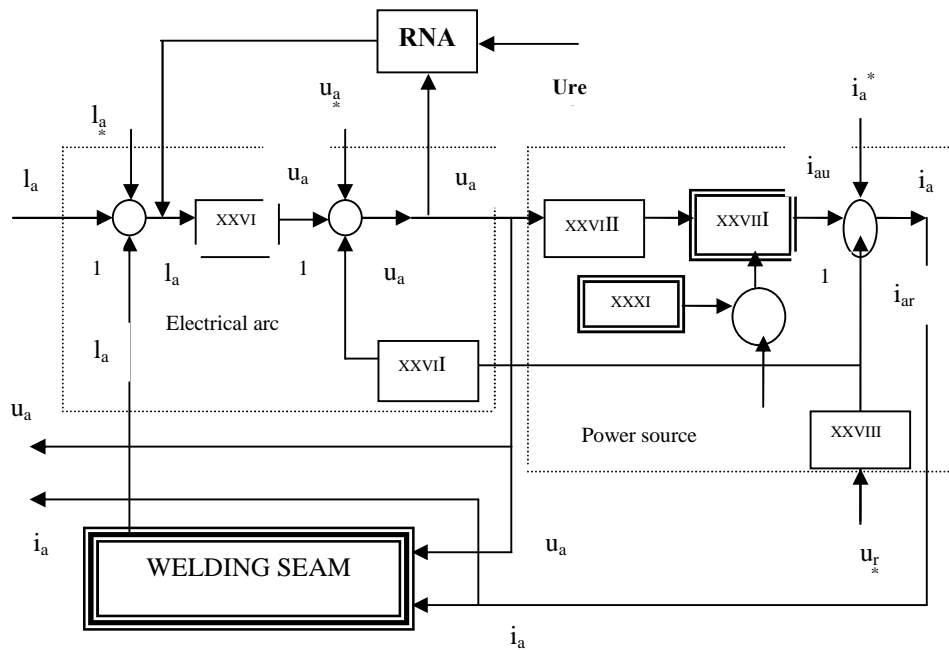


Fig. 1. WIG arc welding – power source model with neural network [4]

The output of 11 element is the welding arc total length l_a , which is transformed from XXVI transfer element in arc welding voltage u_{al} . In the same time, the XXVII transfer element has the arc welding power like input and the electrical arc voltage u_{ai} like output.

In 12 element, u_{ai} is added to the u_{al} and to the perturbation u_a^* . The result is the electrical arc voltage u_a which is transmit to power source. Figure 1 present the arc welding – power source model with a neural network.

The inputs of neural network are the signal u_a , means arc voltage, obtained from a real welding process and an arc voltage reference signal, u_a^{ref} [2], analytically computed. The output of neural network is used to command a robot engine for corection of trajectory welding torch through the welding seam.

3. NEURAL NETWORK STRUCTURE

The neural network structure is presented in figure 2. The input vector contain 310 neurons, the hidden layer contain 50 neurons and use the tan-sigmoid transfer

function and the output layer contain only one neuron and use the purelin transfer function.

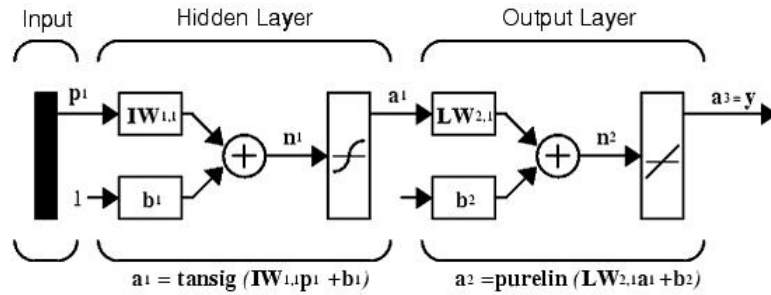


Fig. 2. Neural network designed structure

The reference signal $U_{ref} [V] = f(time)$ is analytically obtained using the model of WIG welding process [3]:

$$U_{arc}^{*ref} = -0.13 \sin(\pi t) - 0.07 \cos(2\pi t) + 3.62 [V]. \tag{1}$$

4. NEURAL NETWORK SIMULATION

Neural network simulation was realized with the MATLAB program:

```
time=0:0.1:30.9; time vector 31 seconds discretised by 100ms
x = - 0.13*sin(pi*time)-0.07*cos(2*pi*time)+3.62; reference signal (Figure 3)
plot(time,x,'b');
```

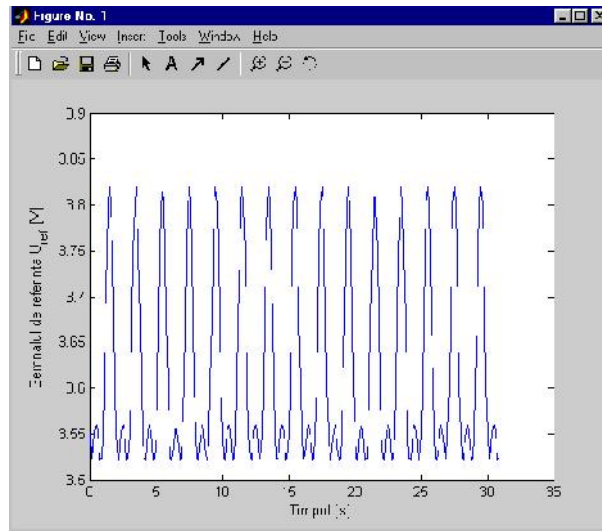


Fig. 3. Reference signal

```

xlabel('Timpul [s]');
ylabel('Semnalul de referință: U_r_e_f [V]');
p=dlmread('date_p.txt','\n'); process signal (Figure 4)
length(p);
plot(time,p,'m');
xlabel('Timpul [s]');
ylabel('Semnalul din proces: p [V]');

```

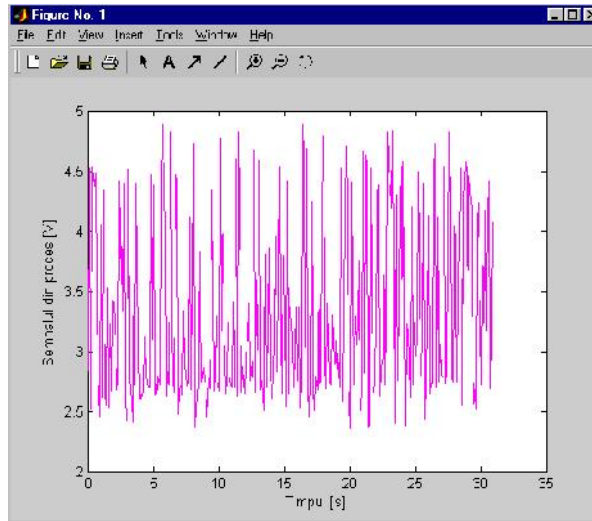


Fig. 4. Process signal

```

p=p';
net = newff (minmax(p), [310 50 1], { 'tansig' 'tansig' 'purelin' }, 'trainrp', 'learnkd',
'msereg' ); on create a backpropagation feedforward network
net = init(net);
net.trainParam.show = 10;
net.trainParam.epochs = 300;
net.trainParam.goal = 1e-2;
[net,tr]=train(net,p,x);
pause;
plotperf (tr)
a = sim(net,x); the output of the network (Figure 5)

```

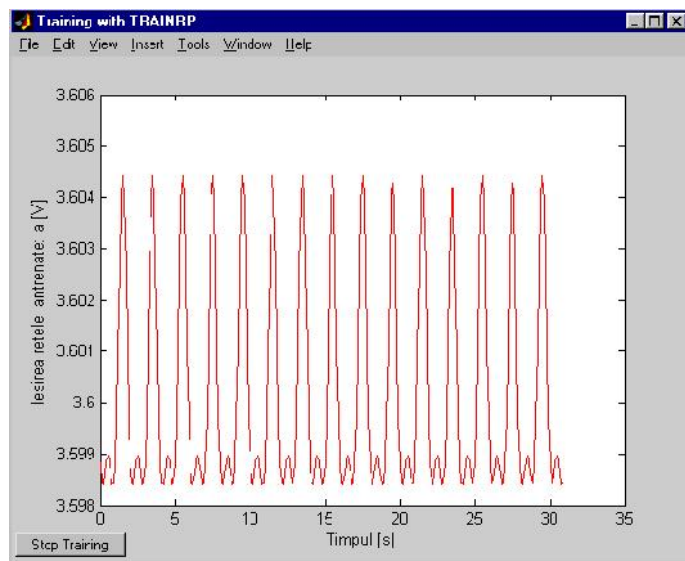


Fig. 5. Output signal

```

plot(time,a,'r');
xlabel('Timpul [s]');
ylabel('Ieșirea rețelei antrenate: a [V]');
pause;
e=x-a; error signal (Figure 6)
net.performParam.ratio=20/(20+1);
perf=msereg(e,net); network performance
plot(e,'g');
xlabel('Timpul [s]');
ylabel('Semnalul erorii: e [V]');

```

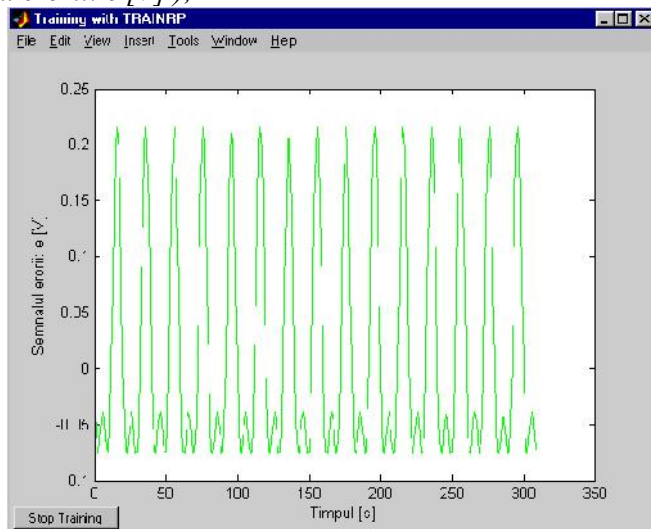


Fig. 6. Error signal

It was used the **trainrp** training algorithm for the neural network because the output and error signal is most appropriate for our purpose.

5. CONCLUSIONS

Theoretical and experimental background from this paper, means welding process control using analyze an arc welding parameter (electrical arc voltage) is a very good start point for another research in welding area. A substantial amount of research is being conducted with the goal of developing an intelligent, fully automatic welding system. These intelligent methods have been applied to control the behavioral characteristics of the welding process in order to improve quality and productivity in all industrial areas.

BIBLIOGRAPHY

- [1]. **Bucur, G.**, *Automated control system for robotic electrical arc welding*, Ph.D. Thesys, Ploiesti, 2002.
- [2]. **Bucur, G., Dumitrescu, St., Micloși, V.**, *Neural network control in robotic welding processes*. Journal of Symposium "35 de ani de activitate a Universit ii Petrol-Gaze la Ploie ti". Vol.LIV, 38-43, 2003.
- [3]. **Deheleanu, D.**, *Welding Technology.*, Editura Sudura, Cluj-Napoca, 1999.
- [4]. **Micloși, V.**, *Welding Equipments*, Editura Didactica si Pedagogica, Bucure ti, 1984.

ELECTRONIC GOVERNMENT–REFLECTIONS OVER THE DESIGN OF A REGIONAL DEVELOPMENT STRATEGY

IRIMIA ROXANA-ADINA *, **VLĂSCEANU ALINA NICOLETA ****

Abstract: E-Gov refers certainly to more use of IT, but more importantly to attempts to achieve more strategic use of IT in the public sector. It is about changes in the internal government operations that come about as IT is used for automation, cooperation, integration among government agencies and as tools assisting in decision processes. E-Government refers to government's use of information and communication technology (ICT) to exchange information and services with citizens, businesses, etc. E-Government may be applied by legislature, judiciary, or administration, in order to improve internal efficiency, the delivery of public services, or processes of democratic governance.

Keywords: E-government, digital economy, regional development strategy, Information Communications Technology, E-regional portals

1. INTRODUCTION-DIGITAL ECONOMY

Information Communications Technology (ICT) has been identified as a key enabler in the achievement of regional and rural success, particularly in terms of economic and business development. The potential for achieving equity of service through improved communications infrastructure and enhanced access to government, health, education and other services has been identified. ICT has also been linked to the aspiration of community empowerment where dimensions include revitalizing a sense of community, building regional capacity, enhancing democracy and increasing social capital.

With the proliferation of information and Web sites, it becomes increasingly difficult to find relevant information via the Internet. Web portals have developed to

* *university assistant Ph.D. candidate, The Christian University "Dimitrie Cantemir"-Bucharest- roxana_but@yahoo.com*

** *university assistant Ph.D. candidate, The Christian University "Dimitrie Cantemir"-Bucharest- alinab1973@yahoo.com*

facilitate the location of online information. Examples include: community portals, geographical or interest-based; business portals, internally or externally focused; and government portals, for particular groups such as businesses, young people, women or regional communities. In most cases, the objectives include providing efficient access to information, resources and services, reaching a larger audience, and providing "anytime, anywhere" service, 24 hours a day, seven days a week.

2. PERSPECTIVES ON ELECTRONIC GOVERNMENT

E-Government, also known as e-gov, digital government or online government refers to government's use of information and communication technology (ICT) to exchange information and services with citizens, businesses, and other arms of government. E-Government may be applied by legislature, judiciary, or administration, in order to improve internal efficiency, the delivery of public services, or processes of democratic governance. The primary delivery models are Government-to-Citizen or Government-to-Customer (G2C), Government-to-Business (G2B) and Government-to-Government (G2G). The most important anticipated benefits of e-government include improved efficiency, convenience, and better accessibility of public services. While e-government is often thought of as "online government" or "Internet-based government"—many non-Internet based "electronic government" technologies can be used in this context, including telephone, fax, PDA, SMS text messaging, MMS, and 3G, GPRS, WiFi, WiMAX and Bluetooth. There are many considerations and potential implications of implementing and designing e-government, including disintermediation of the government and its citizens, impacts on economic, social, and political factors, and disturbances to the status quo in these areas. In countries such as the United Kingdom, there is interest in using electronic government to re-engage citizens with the political process. In particular, this has taken the form of experiments with electronic voting, aiming to increase voter turnout by making voting easy. Economic and revenue-related concerns include e-government's effect on taxation, debt, Gross Domestic Product (GDP), commerce and trade, corporate governance, and its effect on non-e-government business practices, industry and trade, especially Internet Service Providers and Internet infrastructure.

The concept of electronic government (eGov) is about to emerge from a practitioners' concept to one that also attracts research. Conferences abound, and research scales up from individual researchers and projects to institutes, both those governed by industry, such as IBM's Institute for Electronic Government and those governed by universities, such as the Center for Technology in Government at Albany University. Research and development programs such as the EU Information Society Technologies and Government Online are focusing on developing strategic and transferable IT uses in government. Research institutes with the focus on policies and development focus increasingly on IT use, such as the Institute for Development Policy and Management at the University of Manchester. It is hard to estimate the amount of effort to implement eGov currently going on around the world. Many things relevant to the field come under different names.

3. BASIC ELEMENTS AND RELATIONSHIPS INTO AN E-GOVERNMENT SYSTEM

E-government communications procedures frequently require clear and unambiguous identification of the citizen and the public entity involved before the commencement of relations, otherwise the operation cannot be carried out. Without the relevant data, therefore, relations are restricted to the simple presentation of information to the citizen by public institutions.

To integrate the research from different disciplines and on different topics relevant to eGov, there is a need for defining a context in terms of the public sector model. In simple terms, and at a general level where national differences do not matter, a democratic government is organized as shown in figure 1:

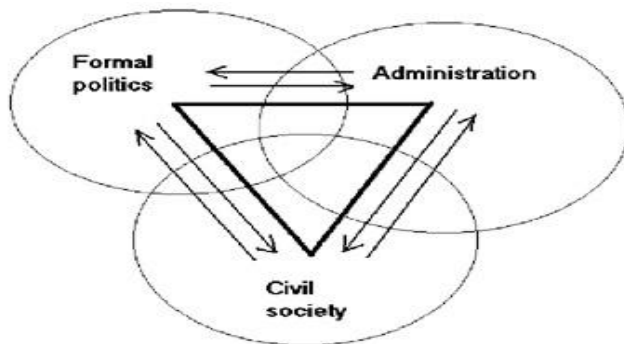


Fig.1 Basic elements and relations in a democratic government system.

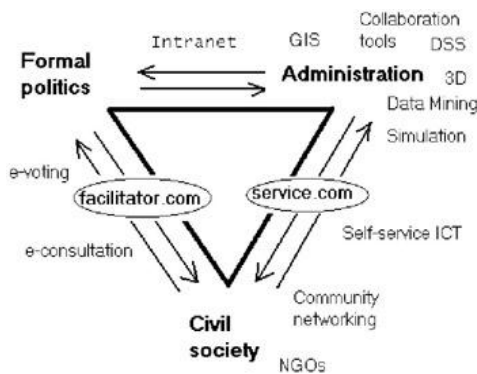


Fig. 2: Intermediaries in e-government processes

Currently, however, they are in a process of profound change in many countries, for several reasons including globalization, economic constraints, changing demographics and the availability of IT. This change can simplistically but effectively is described by two perspectives:

- Omnipresent IT
- Organizational change

In practice the system is of course much more complex, the political impact administrations can exert by having the expertise necessary to prepare

decisions in complicated matters is often acknowledged. The citizen act in many other ways than by casting votes, for example they organize in many ways, and they lobby. There are a number of relations, and that each node in the system influences both the others by a number of relationships— all nodes are interrelated in a complex pattern. The details of these relations are always under discussion and borders keep changing slightly.

In figure 2, is represented in a more complex manner the e-government process and the intermediaries involved in the process. They have appeared because the Internet in combination with government outsourcing policies has given rise to new business opportunities. They are currently working in a field where new relations are emerging, not just because of the emergence of e-business, but also because governments across the world are currently in a process of change for several other reasons. New actors will have a potentially important role because they bring to the field the important knowledge about how to use the Internet as a social medium, not just the technicalities of it. They will form the social practices that will guide the policies of electronic government.

The weaknesses of Internet use for e-government purposes comprise both problems inherent in the nature of the Net and the difficulties resulting from private ownership of telecommunications networks, as well as the initial adaptation of the infrastructure to the needs of e-commerce. This last limits the field for e-government, which is affected by a wider range of considerations than the optimization of profit.

In particular, this relates to:

- assignation of names and addresses,
- security of communications,
- respect for privacy and other legal principles,
- provision of access to the Internet and other communications networks, as well as telecommunications security services.

4. E-REGION DEVELOPMENT – VIRTUAL REGIONAL PLATFORMS

Studying the actual approach at the European level in the e-government area, it can be identified the preponderant existence of the traditional e-government services and the lack of the virtual design of the development strategy at the regional level. The new web technologies offer support for the efficient communication among main actors in the contemporary society, reduces the costs and increase the effective participation rate of the main regional entities and individuals (citizens and experts) in the democratic process of the regional development strategy design. It offers also the possibility of an iterative process for the refinement of the regional objectives and priorities. A realistic solution in this context is the design and development of virtual platforms, which ensures the possibility of a wider debate on a scientific and realistic base, offered by a set of detailed and relevant indicators and various analysis and scenarios, as embedded knowledge. The interactive regional platform facilitates the management of the regional intelligence capital and best practices, in the benefit of the region. It creates also the premises for a better supervision regarding the implementation of the regional strategies, and support the process of finding the best solutions for fulfilling the established goals. The main processes and interactions involved in the design of the regional development strategy are presented in the fig. 3.

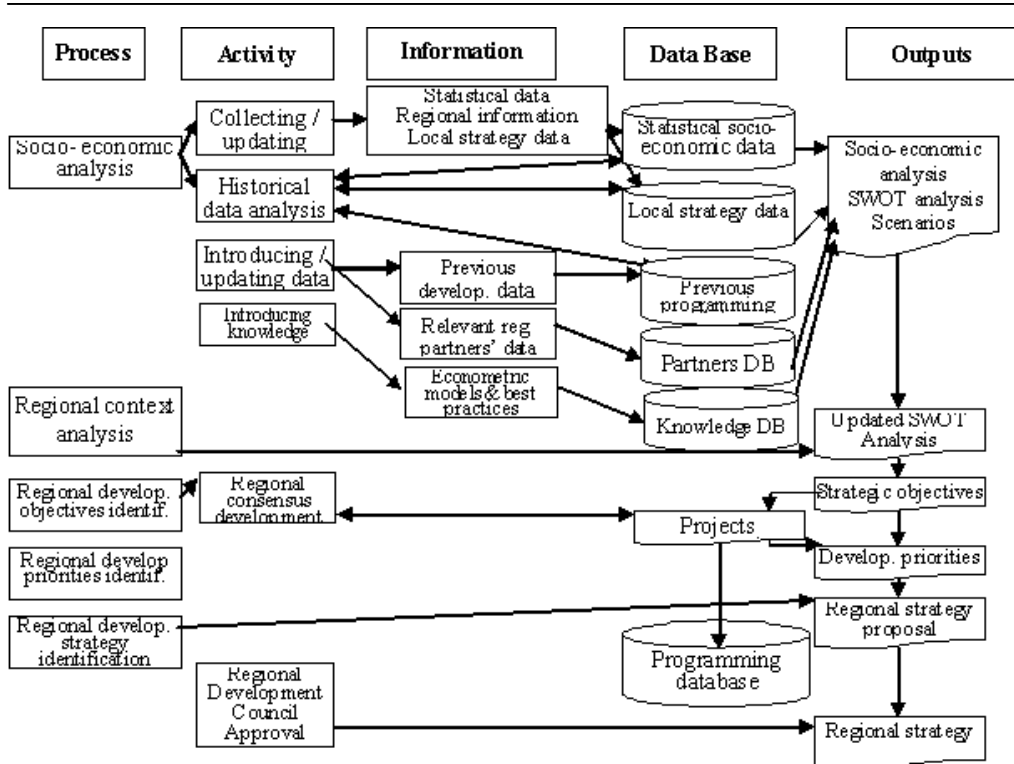


Figure – Main activities and interactions for the design of the regional strategy, as a knowledge based process

5. THE INFORMATION SOCIETY AND THE REGIONAL POLICIES

For Europe's regions and regional policy, the new technologies are both an opportunity and a challenge. An opportunity because these technologies create new prospects for development, especially in the more isolated regions, and a challenge because of the digital divides between rich and poor regions, urban and rural regions, and even within regions. Today, however, a region's competitiveness lies in its potential for innovation and the new technologies can be an instrument for social integration or a source of exclusion if not available to all. Regional development policies for 2000-2006 have consequently been steered towards the information society. Today, the information society is an integral part of the development programs being implemented under the Structural Funds and it's contribute to the development of the Europe of knowledge and know-how.

Two principles underpin interventions in support of the information society:

- the reorientation, allowing for exceptions of course, of structural assistance to the new technologies (human resources, innovation, etc.) rather than infrastructure, to help create the "digital reflex" that is sometimes lacking in Europe;
- the consistent and structured integration of the information society into the priority objectives of regional policy.

6. CONCLUSIONS

The mutations that appeared in the modern world in all the areas demonstrate that the implementation of new technologies does not represent only the assimilation of some concepts and techniques, but also it states the transition to a new economy, that of the informational society, along with a knowledge revolution. Although, in some specialists' opinions, the new technologies do not restructure the whole context of the socio-economic life, guarding its magic in Silicon Valley, it cannot be denied that the informational society made a spectacular debut, having a major impact over human society.

BIBLIOGRAPHY

- [1]. **Ake Gronlund**, *Electronic Government: Design, Applications and Management*, Idea Group Publishing, 2002.
- [2]. **Muresan, M.**, *European dimension of information society* , Tribuna Economica Magazine No. 2/2006, Bucharest, 11 jan 2006, pag 85-88, 2006
- [3]. *Guiding Principles for Sustainable Development of the European Continent*, CEMAT, Council of Europe, 2000
- [4]. *The Structural Funds and their co-ordination with the Cohesion Fund (Guidelines for 2000 – 2006)*, European Commission, Brussels, 1999
- [5]. *European Commission Regional Policy*
- [6]. *Centre for Urban and Regional Development Studies*
- [7]. *Tratatul de aderare a României la UE din aprilie 2005*

EMBEDDED-SYSTEM ZUR STEUERUNG LEISTUNGSELEKTRONISCHER MODULE

ADRIAN TULBURE*, MIRCEA RISTEIU**

Abstract: Die Tendenz für Schaltungszwecke in der Leistungselektronik ist heutzutage eine Kombination aus den Eigenschaften des MOSFET's und des Bipolartransistors immer mehr einzusetzen. Diese IGBT-Bauelemente sind in der Lage hohe Schaltleistungen bei guten Wandlungsgüten mit reduzierten Steuerleistungen zu realisieren. In wie weit sich die leistungselektronischen Wandler optimieren lassen, hängt auch vom eingesetzten Steuerungssystem ab. Für die Steuerungszwecke eignen sich aufgrund des Aufbaukonzeptes und schneller Leistungskern mit eingebauten Schnittstellen, die Microcontroller-Systeme. In diesem Zusammenhang wird in diesem Beitrag das am Lehrstuhl für Automatisierungstechnik der Universität Petrosani vorhandene Embedded-System vorgestellt. Das System besteht aus einem Microcontroller, Peripherie und leistungselektronischen Modulen und wurde für Steuerungszwecke entwickelt und im Labor getestet.

Keywords: Embedded-System, 16Bit-Mikrocontroller, Software-tools, Steuerleistung, Schaltung, PWM.

1. ANLEITUNG. DER 16-BIT MICROCONTROLLER.

Durch die Verfügbarkeit fortgeschrittener leistungselektronischer Komponenten: Power-IGBT, Hyper-MOSFET, Si-Cd-As Schottky Dioden ist es möglich heutzutage leistungsfähige elektronische Wandler aufzubauen, welche sogar unter Sonderbedingungen zuverlässig funktionieren können.

Für die zugehörigen Mess-, Steuer- und Regelungsaufgaben eignet sich die Familie von C166-Mikrocontrollern am besten. Die Einsatzfelder von Mikrocontrollern sind heutzutage: low-cost Anwendungen (Drucker, Scanner, Laufwerke), Standard-Anwendungen (Automotive, Motorsteuerungen, Messgeräte) und High-End-Anwendungen (A/D Wandler, PWM-Einheiten, CAN-Bus).

* *Lecturer at the University of Petrosani*

** *Ass.-Prof. at the "1 Dec.1918"-Univ. of Alba-Iulia*

Der Microcontroller C167 besteht aus folgenden Funktionseinheiten [1], [2]: 16-Bit CPU-Kern, interner Oszillator, interner Daten- bzw. Programmspeicher (bis 128 kB Flash ROM), peripheral Event bzw. Interrupt Controller, 9 Ports, 2 Timer Einheiten, 2 serielle Schnittstelle, A/D Wandler mit 16 Kanälen und 10 bit Auflösung, 4 PWM-Einheiten, 2 CAPCOM Einheiten mit mit 16 Kanälen und 4 Timer und den Watchdog-Modul.

Der 16-Bit Rechenkern besteht aus: Execution Unit mit Pipeline, 16 bit AL-Unit und folgende Systemregister: Processor Status Word (PSW), System Config (SYSCON), Adressenregister (IP, CSP u.a.) und Stack Register.

Eine Partikularität von Mikrokontroller ist bitadressierbare Speicherbereiche zuzulassen und zwar:

- im ESF-Register (0F100h bis zum 0F1FFh)
- im SF-Register (0FF00h bis zum 0FFFFh)
- im internen RAM (0FD00h bis zum 0FDFFh).

2. DAS EMBEDDED-SYSTEM

Das Minimalsystem besteht aus einem C167 CR zusammen mit einer Taktquelle und Stromversorgung. Ein erweitertes System beinhaltet je nach Bedarf sowohl ein externen Speicher als auch externe I/O Peripherie. Der Adressbereich kann bis zum maximal 16Mbyte für Daten, Programme und I/O-Konfiguration, gemäß von Neumann Architektur, erweitert werden.

Während des Programmablaufs holt der Prozessor die Instruktionen aus dem ROM und die Operanden/Daten aus dem RAM. Das Segmentation-Bit vom SYSCON soll festlegen, wie die Adresierungsart stattfindet: segmentiert oder unsegmentiert.

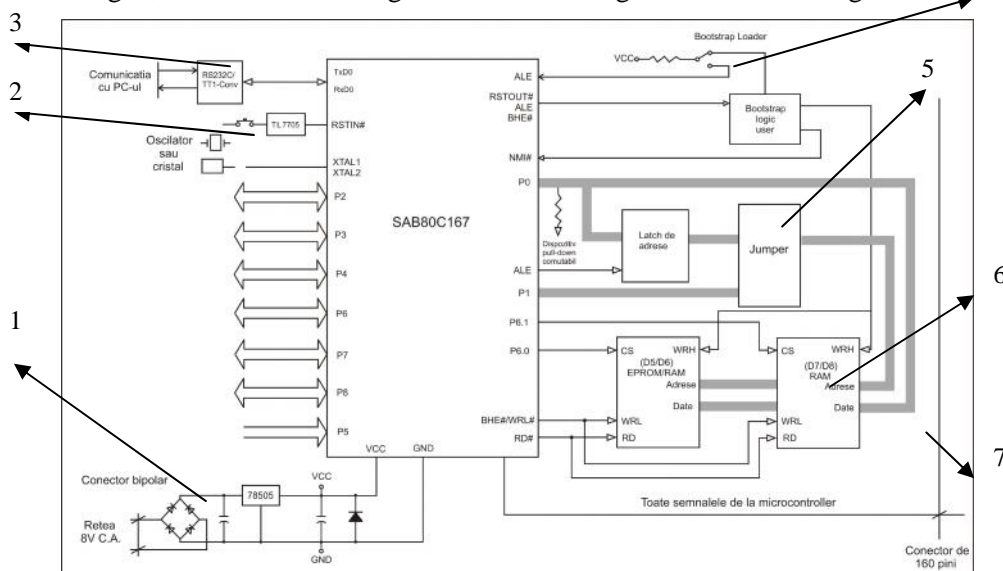


Abb.1 Ansicht der Entwicklungsboard

Das Entwicklungsboard (Abb.1) ist eine Platine (160mm x 100mm) gefertigt in Multi-Layer Technik. Folgende Hardwaregruppen ergänzen die Ausstattung:

Spannungs-versorgungskreis (Abb.1./1/), Schalter zum Bootstrap-Modus (Abb.1./4/), Steckerleisten zur externen Signale (Abb.1./7/), serielle RS232 Konverter (Abb.1./3/), Oszillator und Reset-Kreis (Abb.1./2/), externe Speicher (RAM oder EPROM (Abb.1./6/)) und Jumper zur Einstellung verschiedener Modus und Funktionen (Abb.1./5/).

Die Embedded Systemen bestehen aus dem Hardwareteil, welche schon beschrieben wurde und aus dem Softwareteil. Für die optimale Arbeit soll das Software-Packet die Entwicklungsumgebung und die dazugehörigen Hilfstoos/Werkzeuge beinhalten. Bei dem untersuchten System erfolgt die Mikrocontroller-Programmierung mit Hilfe folgender Soft-Werkzeuge (Abb.2) :

- *CodeWriter* – einfacher Texteditor (Textbearbeitungsprogramm)
- *cp166 / c166* – Ansi Compiler der den Zugriff auf alle μ C-Ressourcen hat.
- *m166* – Macropreprozessor-Software, der eine QuellCode in Asembler liefert
- *a166* – Cross-Assembler, geeignet für die untersuchte Mikrocontroller-Familie
- *l166* – Lokator und Linker, der Objekt-Dateien von *c166* oder *a166* oder aus Bibliotheken zu einem fertigen Programm bindet.

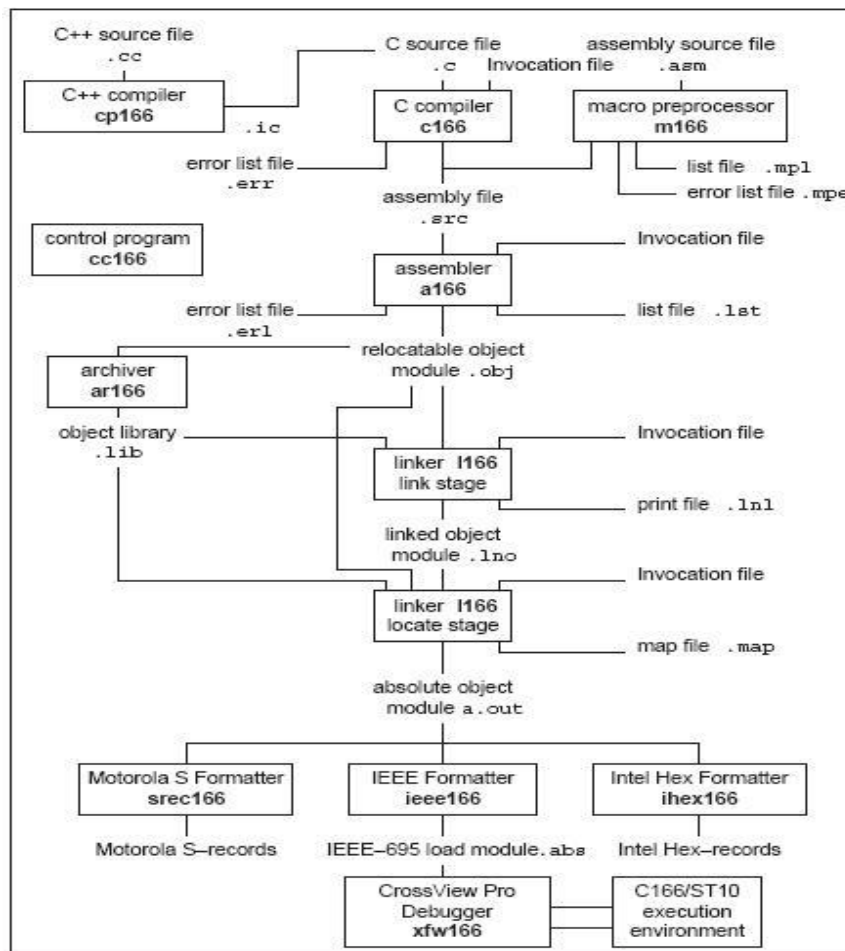


Abb.2 Kompilierung-Struktur

- *srec166/iee166/ihex166* – Code-Converter, der aus einer *.out Datei eine hardware-spezifische Datei zur Portierung auf einen PROM erstellt.

Die Entwicklungssoftware enthält noch ein Cross View Debugger (*xfw166*), der das Debuggen von den in C, C++ oder Assembler geschriebenen Quell-Dateien ermöglicht. Um die Peripherie nachzubilden sind unterschiedliche typsabhängige Treiber vorhanden. Um die Effizienz der Programmierungsarbeit zu erhöhen, sollen alle diese Soft-Werkzeuge zusammengefasst und per Maus-Click aufrufbar sein. So eine Umgebung mit freundlicher Bedienoberfläche steht dem Anwender unter der Namen *IDE (Integrated Development Environment)* zur Verfügung.

3. DER STEUERTEIL

Der Mikrokontroller besitzt vier *PWM (Puls-Weiten-Modulation)*-Einheiten, welche unabhängig von einander gesteuert werden können. Alle vier Einheiten werden via Oszillator (OSC/Abb.3) mit dem Systemtakt versorgt. Der Takt kann mittels des Bits (PTI_x) zusätzlich mit 64 geteilt werden.

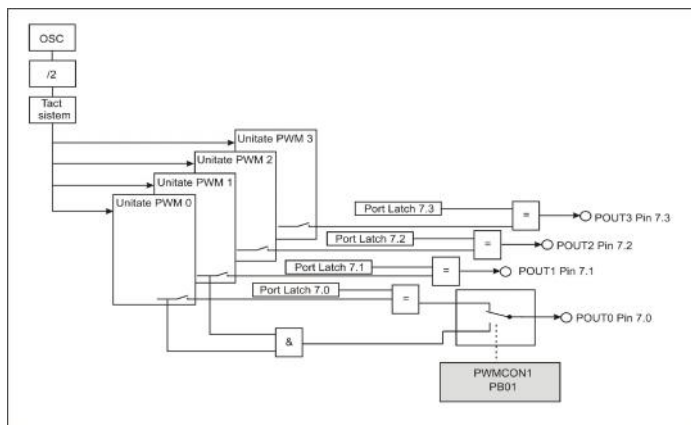


Abb.3 Aufbau der PWM-Einheit [3]

von seinem Zustand (Eins / Null) wird das reale PWM-Signal oder das invertierte Signal am Ausgang generiert.

Die Einheit ist mit einem Interrupt Control Register (PWMIC) ausgestattet, der vier IRQ-Bits beinhaltet, um identifizieren zu können, welche Kanal welche Interrupt ausgelöst hat.

Über das Bit PB01 vom Register PWMCON1 (Abb.3, unten) lassen sich die Steuersignale vom Kanal 0 bzw. 1 verknüpfen.

Über das PWM Channel-Mode-Control-Bit (PM_x) wird die Betriebsart festgelegt:

- Standard PWM (Edge Aligned PWM);
- Symmetrische PWM (Center Aligned PWM)
- Burst Mode
- Single Shot Mode

Durch Setzen eines entsprechenden Control-Bits wird der Takt weiter an einen Zähler mit zwei Komparatoren (Width und Period) geschaltet. Für die Ausgabe des Steuersignals auf einem I/O-Pin (POUT_i) ist das Bit PEN_x zuständig. Jeder Pin zwischen Pin7.0 bis zum Pin7.3 hat eine entsprechenden Ausgabe-Latch. In Abhängigkeit

4. DER LEISTUNGSTEIL

Die Auswahl des Treibers erfolgt nach dem Ansatz, dass der Treiber in der Lage sein muss, die notwendige Steuerleistung und den maximalen Gatestrom abzugeben. In dem Zusammenhang ist es üblich die Ansteuerschaltung abhängig vom erwünschten Schaltverhalten, Bauteilspezifikationen und Umgebungsbedingungen zu entwerfen bzw. dimensionieren. Dazu hat sich in letzter Zeit folgendes Vorgehen bewährt:

1. Messtechnische Bestimmung der Gateladung, Q_g (Abb.6)
2. Berechnung der Gatekapazität, C_g
3. Ermittlung der Ansteuerleistung, P_g
4. Berechnung des Gatestromes I_g / Gatewiderstandes R_g .

Das Applikations-Spektrum jeweiliges leistungselektronischen Bauteils lässt sich aus der unterstehenden Tabelle entnehmen.

Tab.1 *Eigenschaften der leistungselektronischen Bauteile.*

Eigenschaft	U_{max} [kV]	Strom-dichte	Steuer-param.	Steuer-block	Steuer-leistung	Schalt-geschwin-digkeit
Komponent	I_{max} [kA]	[A/cm ²]				
GTO	4,5 4	100-200	i_G	komplex	s.gross	langsam
BT	1,4 0,6	30-50	i_B	komplex	gross	mittel
IGBT	3,3 1,2	~50	u_G	einfach	s.klein	schnell
P-MOSFET	1-0,1 0,1-0,3	10-20	u_G	einfach	s.klein	s.schnell

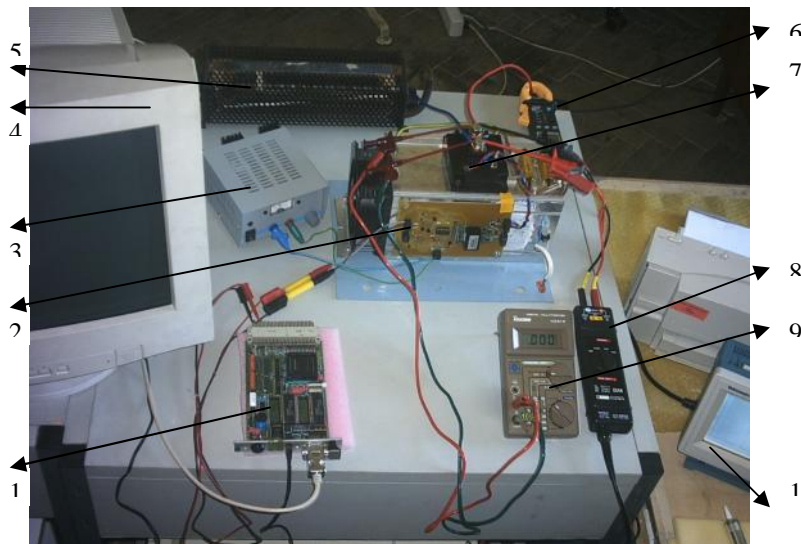


Abb.4 Aufbau des Prüfstandes für die Leistungshalbleiter

Die Hauptkomponenten des Leistungskreises sind: die externe Leistungsquelle (nicht im Bild), der IGBT-Schalter (7), auf dem Kühlkörper und die ohmische Last

(5). Der Steuerkreis besteht aus folgenden Komponenten: 16-Bit Mikrokontroller (1) und die Treiber-Platine (2), welche über die Gleichstrom-Spannungsquelle (3) versorgt wird. Die messtechnische Untersuchung wurde mit Hilfe von Stromzangen (6), Voltmeter (9) und Trennverstärker (8). Alle Messungen wurden mit dem Tektronix-Oszilloskop (10) aufgezeichnet und gespeichert.

5. MESSERGEBNISSE

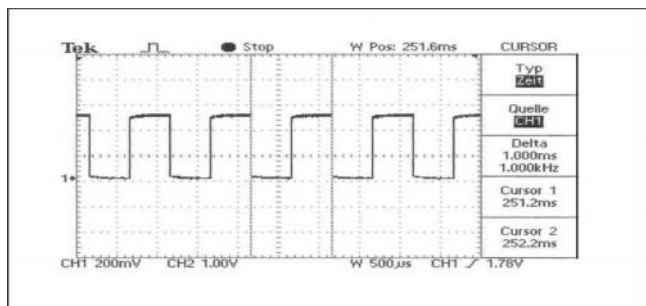


Abb.5 Oszilogramm des Steuersignals an der Ausgangsleiste

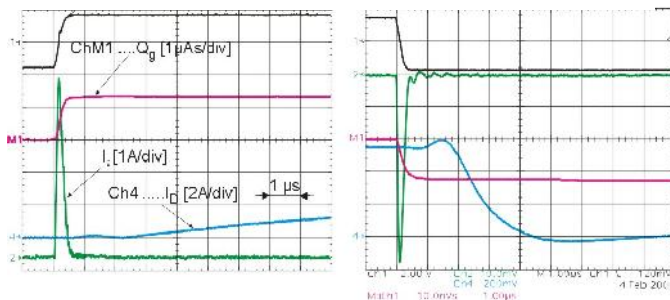


Abb.6 Zusammenhang zwischen dem Gate-Strom und Gate-Ladung).
Messergebnisse beim Ein-Ausschalten des Halbleiters [2]

LITERATUR

- [1] von Berg B., Groppe P.: *Das grosse C167-Mikrocontroller Praxisbuch*, pp.134-146, Editura Franzis. Poing 2001.
- [2] Tulbure, A: *Netzgespeiste ASM mit elektronischer Käfigumschaltung zur aktiven Schwingungsdämpfung*, pp. 54-64, Editura Papierflieger. Clausthal 2003
- [3] Klaus, Rolf.: *Der Mikrokontroller C167*, Hochschul Verlag der ETZ. Zürich 2000.

Die erhaltenen Messergebnisse an der Schnittstelle zwischen den Steuer- und Leistungsteil (am Ausgang des μC Abb.1 /7) sind in der Abb. 5 vorgestellt.

Die Abbildung 6 stellt den Einschaltvorgang mit unterschiedlichen Gateströmen dar. Zum Schalten muss eine bestimmte Gate-Ladung Q_g vorhanden sein, welche von sprungartigen (A) oder glätteren (B) Strömen aufgebracht werden kann. Die Einflussfaktoren für die Schaltzeiten des IGBTs sind die inneren Kapazitäten, die parasitären Induktivitäten und der Gatestrom.

EQUIPMENT USED IN PRIMING OF THE BLASTING CARTRIDGE WITH CYPRESS MICROCONTROLLER

ARON POANTA*, DAN DOJCSAR, BOGDAN SOCHIRCA*****

Abstract : In this paper is described a device used in the priming of the electrical blasting cartridge who supply the whole electrical priming energy. This device offers a much better security compare to the present similar devices because it eliminates the human factor errors. Also this device verifies and monitors the blasting line states and has the ability of blocking the blasting in improper functioning conditions. The system has the possibility of blasting line diagnosis with the state displaying. The device was conceived and tested, and satisfies the expectations in varied working conditions like underground with explosive gases or in quarries.

Keywords : blasting cartridge, programmable logic device, explosive areas, CYPRESS-PSoC microcontroller.

1. INTRODUCTION

The devices used for the priming of the electrical blasting cartridge must to supply, in the blasting network, the whole electrical priming energy. The device's power supply can be the electrical network, an electrical generator or a battery. The necessary energy for the blasting network is supplied from capacitors. The capacitors takes the necessary energy from a single power supply and delivers in a very short time (milliseconds) in the blasting network. Taking into consideration the consequences, with catastrophic effects, witch can appear in the improper working context for this devices, by standards are established the exactingness for the equipments. This exactingness refers, in function of the environment nature (on the ground, underground, dry or humid environment, explosive gases etc), to the level oh the delivered electrical impulse, the charged voltage, the current impulse duration for the

* *PhD. Professor at the University of Petrosani*

** *PhD. Lecturer at the University of Petrosani*

*** *Assistant Eng. at the University of Petrosani*

priming of all the cartridges from the network, an other standards referring to the environment conditions an priming control, the undesirable blasting avoidance etc.

The extant equipments achieves this standards by a series of mechanical blocks by keys or buttons witch involves a commands succession made by human operator. Besides the involve of the human factor the extant equipments not achieves an integrity control of blasting lives and not ensures a charged voltage according to the blasting circuit resistance. The charged voltage is pre established in function of the accepted maximum value for the blasting circuit resistance and can't be charged in function of the real resistance.

All this constituted the premises for this device synthesis witch removes the mentioned aspect and increases the safety level for the priming of the electrical blasting cartridge.

2. THE SELECTING OF THE PRIMING CIRCUIT PARAMETERS

The necessary energy for priming the electrical blasting cartridge is supplied from a capacitor, witch must to be charged with a voltage witch ensures a safe impulse level for priming. The estimate of the energy amount witch is delivered to the cartridges was made starting from the equivalent diagram (figure 1) witch contains the capacitor C charged an a voltage U (from a proper circuit) witch, at the starting blasting command, delivers the accumulated energy to the blasting network simulated by a equivalent resistance R.

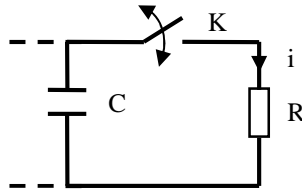


Fig. 1. The equivalent diagram of the priming circuit

The equivalent resistance R is given by the cartridge resistance R_C , the number of the connected cartridge N_C and coupling cable resistance R_{CABLE} in the following expression :

$$R = n_C * R_C + R_{CABLE} \quad (1)$$

The charged energy in the capacitor (E) depends on the capacity C and the charged voltage U :

$$E = \frac{CU^2}{2} \quad (2)$$

The delivered current over the blasting network is obtained from the next expression, obtained from the II Kirchhoff on the equivalent circuit.

$$R * i + \frac{1}{C} \int i dt = 0 \quad (3)$$

$$i = \frac{U}{R} * e^{-\frac{t}{RC}} \quad (4)$$

The delivered energy from the capacitor at the resistance unit (the specific energy W_s) in the blasting circuit at a complete capacitor's discharge will be:

$$W_s = \int_0^{\infty} i^2 dt = \int_0^{\infty} \frac{U^2}{R^2} * e^{-\frac{2t}{RC}} dt = \frac{CU^2}{2R} = \frac{E}{R} \left[\frac{W_s}{R} \right] \quad (5)$$

This equation indicates that the blasting circuit resistance can't exceed a certain limit value given by the necessary energy for a single priming.

The capacitor, with equivalent capacity $C=33 \mu\text{F}/1200\text{V}$, is achieved by connecting in series three capacitor with value $100\mu\text{F}/400\text{V}$. To not overloading the capacitors, the maximum charging voltage was limited to 1100V .

For the medium intensity cartridges the capacitor discharging time is limited to duration $t_1=4\text{ms}$, after this the line must to be setting in short-circuit.

The current delivered in circuit in this interval can not decrease under the admitted value:

$$I_A = 1,25 * I_s = 1,9\text{A} \quad (6)$$

where $I_s=1,5\text{A}$ is the current value for a certain priming.

The maximum value of the circuit resistance is founded from the expression (4) on condition that for $t=t_1=4\text{ms}$, the current in the circuit is equal to current I_A :

$$I_A = \frac{U}{R} e^{-\frac{t_1}{RC}} = \frac{U}{R} e^{-\frac{121,21}{R_{\max}}} \quad (7)$$

In this way was obtained the expression for calculation the maximum resistance

$$6,31 * R_{\max} - R_{\max} * \ln * R_{\max} = 121,21 \quad (8)$$

It was obtained the calculated value of $R_{\max} = 423$

By limiting the maximum resistance to the value $R=400$, the current I_0 , at the moment $t=0$, will be :

$$I_0 = \frac{U}{R} = 2,75\text{A} \quad (9)$$

But the resistance R depends on the number of the cartridges connected in circuit and, in function of this, must to computing the charging voltage. This dependence will be determined from the necessary energy at the resistance unit witch must to be, for the medium intensity cartridges at value $W_s=16\text{mWs/r}$, and for a certain priming at value:

$$W_c = 1,4 * W_s \quad (10)$$

This value was achieved from expression (5) for $t=t_1=4\text{ms}$. The capacitors energy is in the following form:

$$W_c = \int_0^{4*10^{-3}} i^2 dt = \frac{CU^2}{2R} \left(1 - e^{-\frac{8*10^{-3}}{R}} \right) \quad (11)$$

The charging voltage depending on the resistance is show in the following expression :

$$U = \sqrt{\frac{2 * R * W_C}{8 * 10^{-3} * C(1 - e^{-\frac{R}{C}})}} \quad (12)$$

The diagram of the function $U=f(R)$ traced in MATLAB is in the shape represented in figure 2:

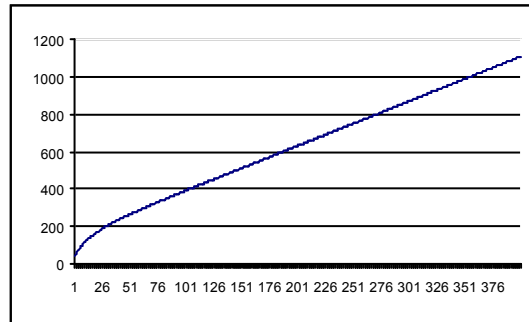


Fig. 2. The dependence $U = F(R)$

From the diagram can be noticed that the curve $U=f(R)$ is not linear for $R < 30$, but, for $R > 30$, the curve is almost linear and can be approximated by a straight line described by the equation:

$$U = 1100 + 2,4(R - 400) \quad (13)$$

If the voltage is computed with this equation (13) then the values are almost equal comparatively with the values computed with the exponential equation (12). The deviations are greater for $R < 30$, but the values are higher, even for this domain, than the exponential equation values, and this involves limit values lower than the specific energy. The linear equation approximation made possible the values computing by a microcontroller.

3. THE HARDWARE STRUCTURE.

For the synthesis of the device bloc diagram was identified the technical functional specifications. Besides the specifications stipulated by standards was taken into consideration, further functions like: diagnosis, safety running, displaying some interesting parameters and charging its bordering in the established limits. For the interface between device and user must be inserted a user control block, which ensures the device control by the user.

The start/stop key ensures : the connecting of the charging power supply, the power supply of the electronic control block and the block for the constant current injection in the charging network for measuring the blasting circuit resistance.

The dialogue key allows the starting of the diagnosis menu and finding the user command. The blasting key validates the blasting command, allows the transmission of the blasting command to the initiating explosion block and then

activates the line's short-circuit block (after 4 ms, time computed by the electronic block).

The device must ensure the measuring of the blasting line resistance, the checking of the limits bordering (maximum 400 Ω), the power supply checking (not more than 12 V), the computing of the charging voltage in function of the circuit resistance and displaying this values and/or some important messages (on an alphanumeric display). Beside this, the device must ensures the control of the constant current generator, the capacitors charging control, the initiating control and after 4 ms the line's short-circuit control.

On the ground of this specifications was synthesized the device's block diagram (fig.

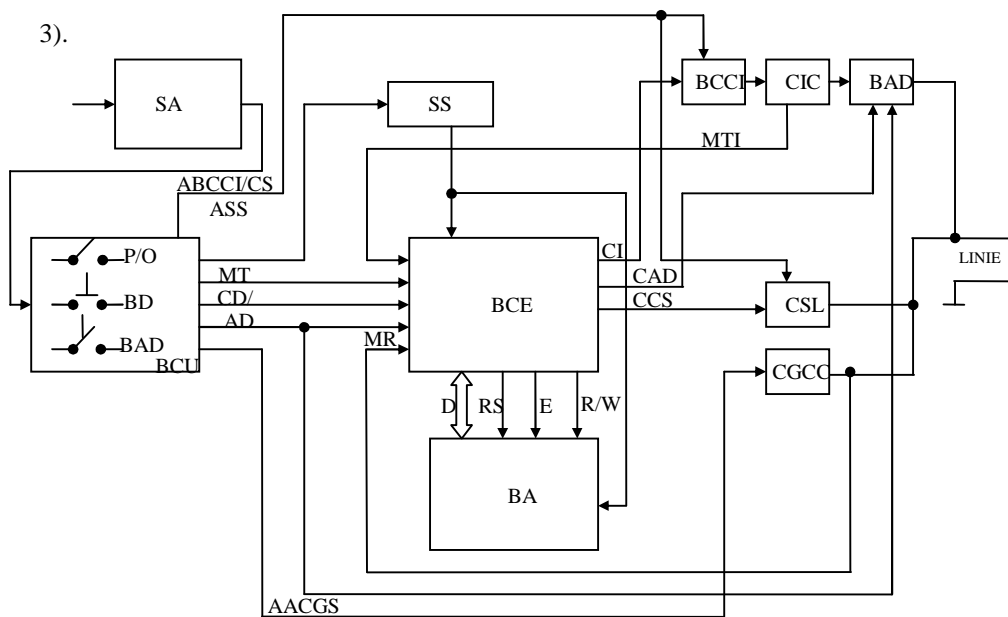


Fig. 3. The device's block diagram

The user's control block (BCU) ensures the interface between user and device. This block allows the user's equipment control by the start/stop button (P/O), the diagnosis button (BD) and the button for the blasting priming (BAD). The power supply (SA) lie in a 12 V storage battery and a circuit which allows to charge it from the electrical network. The electronic control block (BCE) administrates the whole device working and monitors it's proper running. This block lies on the CYPRESS CY8C29466 microcontroller and the auxiliary circuits.

The displaying of the measured parameters and the afferent messages is achieved by a displaying block (BA). The displaying block lie in the integrated circuit AC162B which contains in its structure the control circuit (KS0066), a driver and the LCD display with two symbol's lines and 16 symbols on the line. The measurement of the line resistance is achieved by injecting in the line a constant current, obtained from the generator circuit of constant current (CGCC). The capacitors charging with the proper voltage for cartridge priming is achieved by a capacitors charging circuit (CIC) controlled by a microcontroller using a control block for the charging circuit (BCCI).

The CIC back contains, in addition, a voltage divisor witch samples the capacitors charging voltage, applied on the analog input RAO/RNO of the microcontroller. The cartridge blasting is achieved by the priming blasting circuit (CAD), controlled by a microcontroller, but only in the case of the parameters bordering in the established domain and of the proper positioning of the blasting priming key (BAD). The line's short-circuit after 4 ms since the blasting command, is achieved by the line's short-circuit circuit (CSL). The two circuits have a similarly structure and contains the power circuit achieved with thyristors and the control circuit. On the ground of the block diagram was achieved the main electric diagram and then in ORCAD, the printed circuit board (PCB).

4. THE DEVICE'S SOFTWARE

For the software conceive afferent to this device was taken into consideration the technical and functional specifications and the device architecture. The working algorithm, based on the specification, is concise described by the logic diagram presented in figure 4.

The starting command is given from the P/O button witch through BCU generates the signals ASS (continuous power supply) and ABCCI/CSL (power supply of the BCCI/CSI block). Through the BD key can be selected either the diagnosis or the main running made witch transmitters to the microcontroller the CD/F signal (diagnosis/ main running command). In the diagnosing made appears on the display the afferent welcome message, following the displaying of the blasting commands number. Here is achieved the battery voltage measuring (MTA signal) and the measuring of the blasting line resistance (MR signal) using the A/D converter inputs from the microcontroller (RA2/AN2 input and RA1/AN1 input respectively). The measured values are displayed if they are in the pre-established domains or is displayed the error messages like: "DESCARGED BATTERY"; "BLASTING LINE BREAK"; "TO BIG RESISTENCE", etc. In the main warming mode is verified if the parameters are in the proper domain, is given the command for charging the capacitors (CI), is calculated the charging voltage and is verified the computed charging voltage, and, after this voltage attains the desired value, is displaying the message "WAIT FOR INITIATING" to inform the user that the priming command is ready. The priming command is given by the BAD block from the BCU block witch generates the AD signal (blasting initiating) witch evolves for the microcontroller to generate the command signal for blasting initiating CAD. This signal commands the BAD block to deliver in the line the capacitor's voltage. After 4 ms, the μc generates the CSSL command to the CSL circuit for the line short-circuit.

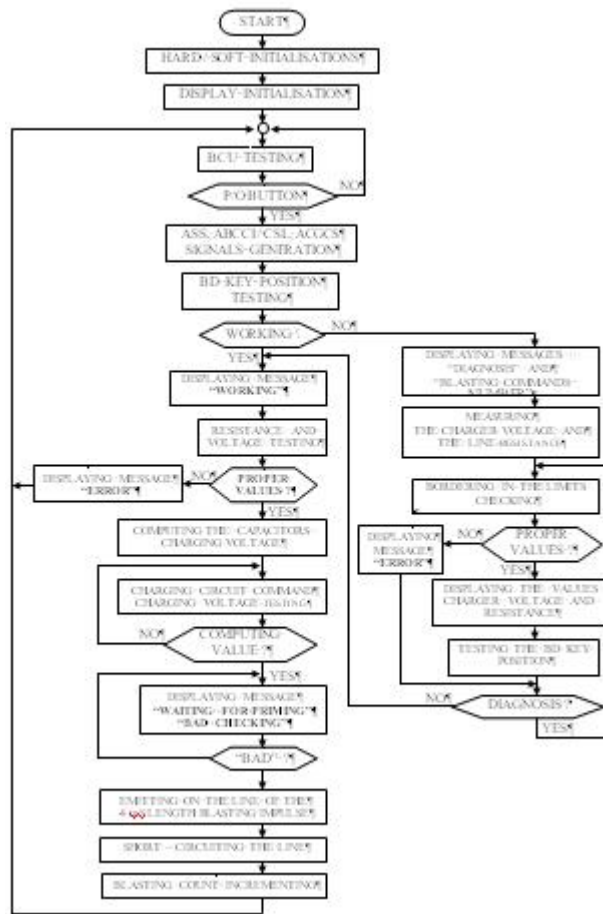


Fig. 4. The diagram of the working algorithm

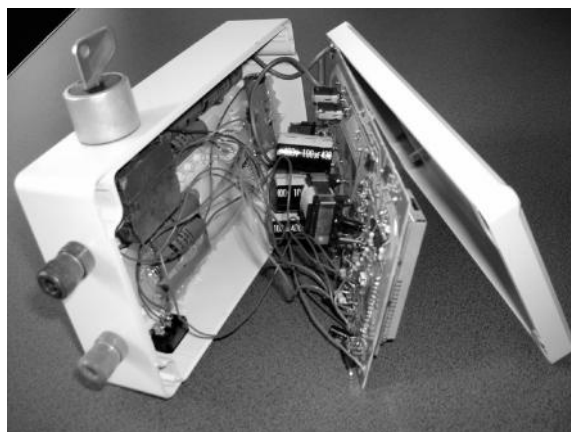


Fig. 5

For the undesirable blasting commands avoidance, the CAD command is inactive if the BAD key is not in the proper position. It was conceived the running algorithm and the programs written in the microcontroller's assembly language for the MPLAB software. In the next part of the paper is presented the main program and some relevant procedure used in the running algorithm. The MAIN program respects the algorithm presented in figure 4.

Of course, was conceived the others routines like : displaying the all messages, testing the BD key position, bordering in the limits testing, ASS, ABCCI/CSL, ACGCS signals generation, BCU testing, short-circuiting the line, blasting count incrementing etc. The equipment (device) was achieved and tested in the lab conditions.

5. CONCLUSIONS

The device avoids the improper blasting commands produced by the human operator. The capacitor's charging voltage hat not a pre-established value it is computed in function of the blasting circuit resistance. The blasting initiating command can not be started if the parameters of the blasting line, the voltage of the power supply, the charging voltage, etc, are not in the pre-established limits.

There are displayed continuously: messages witch informs about the equipment state, the values of the interesting parameters, etc. The device was achieved and tested in the lab condition and the results confirms the validity of the theoretical grounds. The achieved functions and the high safety level justifies the device's usefulness in the afferent industries.

BIBLIOGRAPHY

- [1] **Milonir B.** - *Bazele teoretice și practice ale sensibilității electrice a detonatoarelor comerciale și conceperea unor surse optime pentru detonare.*
- [2] **Pop E, Leba M.** - *Microcontrolere și PLC*, Ed Didactica si Pedagogica, Bucuresti, 2003
- [3] **Poanta A, Pătrășcoiu N.**- *Circuite și echipamente electronice în industria minieră*, Editura Didactica si Pedagogica, Bucuresti, 1997
- [4] **Tat S. Matei I. Fissgus K.** *Îndreptar de tehnica securității în minieră.*
- [5] **Thum W.** *Procedee moderne de împu care în cariere și probleme de securitate a muncii în diferite ri.*
- [6] xxx CYPRESS CY8C27xxx, CY8C29xxx Data sheets.
- [7] xxx Blaster hand book Cleveland, Ohio, ISEE USA 2000
- [8] xxx Die elektrische Zungung prosp Dynamit Nobel

EXPERIMENTAL MODEL FOR PREDICTIVE CONTROL OF THE PUMPING AGGREGATES USED FOR WATER DRAIN IN ROȘIA MINING PIT

POPESCU LUMINIȚA *, GROFU FLORIN**, POPESCU MARIAN**

Abstract: The preventive and predictive maintenance allows immediate tracking down, locating and identifying the fault or the broken piece. In this way, it is possible to plan the stop and minimally reduce the time needed for repairs. The costs for preventive and predictive maintenance recorded in the same time interval will be smaller.

Key word: preventive, predictive, vibration analysis, acquisition system

1. Introduction

The preventive and predictive maintenance allows immediate tracking down, locating and identifying the fault or the broken piece, also the calculus of the time of work in safety conditions of the machine. In this way, it is possible to plan the stop, to prepare the intervention team, to command necessary machine parts and to minimally reduce the time needed for repairs. The costs for preventive and predictive maintenance recorded in the same time interval will be smaller.

The main causes of the vibrations in the industrial equipments are:

- bearing damage;
- dynamic lack of balance of the wheels;
- wheels leave their center;
- damaged gearings;
- resonance because of the:
 - non corresponding rigidity;
 - not respected work technology;
 - wrong design;
- closing of the electric circuits through bearings;

* *PhD professor at the University Constantin Brancusi Tg-Jiu*

** *lecturer at the University Constantin Brancusi Tg-Jiu*

- transmitted vibrations;
- damaged couplings;
- increased temperature in bearings because of inefficient cooling systems;
- liquid flow through pipes.

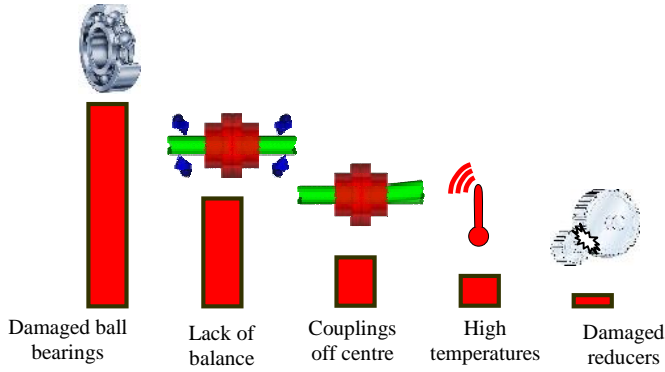
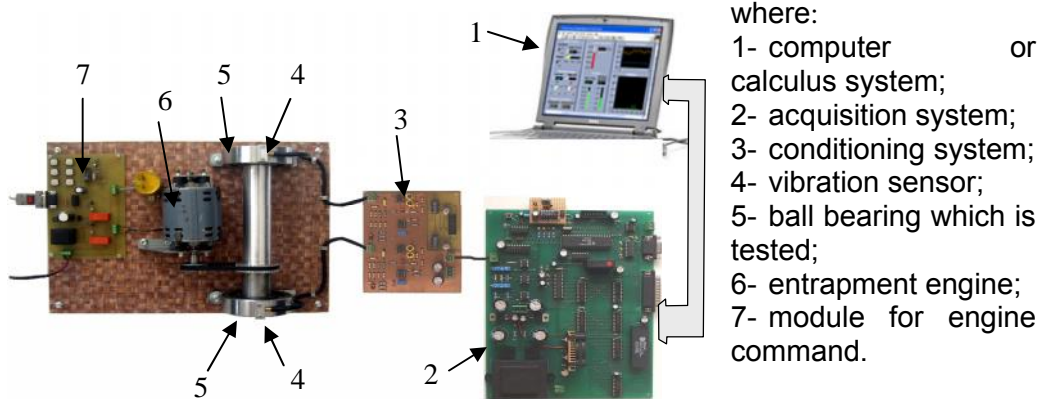


Fig.1 Fauts met at equipments

In figure 1 are the faults which appear most frequently to the industry dynamic equipments.

2. EXPERIMENTAL MODEL

Predictive detection of the faults in the pumping aggregates from the Ro ia de Jiu Mining Pit has been made through vibration analysis in the bearings of the entrainment engine and also in the pump's bearings. To build such a system, first an experimental model was built from an entrainment engine and an axel with two ball bearings, a new one and one with obvious damages. The vibrations are observed with piezo electric sensors whose output signal is applied to a signal conditioning circuit to be then transformed in digital signal using an acquisition system. The digital signal is transmitted after that to a calculus system to be processed in order to obtain information regarding the state of work of the observed system. The structure of the experimental model is the one presented below.



where:
 1- computer or calculus system;
 2- acquisition system;
 3- conditioning system;
 4- vibration sensor;
 5- ball bearing which is tested;
 6- entrainment engine;
 7- module for engine command.

Fig 2. Structure of the experimental model

Requirements for the system:

- In order to be able to analyze a high range of frequencies, first of all the vibration sensor must have a high range of working frequencies, which is found at piezoelectric sensors. Because the conditioning circuit is simple, this type of sensor is ideal for the system. When a wave is received, it is important to know that most of the times, high frequency information is more important. When an acceleration signal is integrated to obtain information about movement, the response in frequency decreases a lot as level, and lot of small variations of the signal cannot be analyzed. The study of the movement is difficult at high frequencies, because in most cases, that is the range where signals for damaged ball bearings appear.

That is why the acceleration is measured to determine different parameters.

-the signal conditioning circuit must be a simple circuit, but which allows initial processing, like adjustment, amplifying – which are necessary to the sensor's connection to the acquisition system, upon the signal received from the sensors.

-the acquisition system is the most pretentious part of the monitoring system. Because of the rough environmental conditions, and also the big distance between the sensors and calculus system (hundreds of meters) it is necessary that the acquisition system to be placed as close to the sensors as possible. And it also must be robust because it is an industrial environment.

It is necessary that a high frequency spectrum can be analyzed (of maximum a hundred kHz). To be able to do the Fourier analysis, a very high speed of acquisition is required (hundreds of thousands samples/second), and also a great number of samples.

For the experimental model two ball bearings were used on a single 6308C3 row, mounted at the heads of an axel activated through a belt by an alternative current engine, with the revolution of 1400 rotations/minute (figure 2). The vibration sensors are of MAQ36 type, one for each ball bearing.

For the experimental model, the signal conditioning circuit was mounted close to the mechanical part, and because of that, we took care that ground loops can't appear. The acceleration sensors can, for that reason, be mounted in direct contact with the exterior clothing of the bearing, without adding isolating materials which would have decreased the natural mounting frequency. To reduce the tribo-electric effect, the chosen signal cable was shielded and fixed so in doesn't vibrate due to the mechanical parts. After calculating the frequencies which may appear as a effect to damaged components of the bearings, the accelerometers and way of mounting them was chosen, taking into account the real working conditions of the system which will be used in Ro ia Mining Pit. Because in case of the real system the distance between the accelerometers and conditioning circuit is high, we used a charge amplifier for the signal received from the sensors. After planning this circuir, its simulation in Pspice, we effectively buit it.

For an exact analisys of the acquisitioned signals, a high acquisition speed was required, which implied high communication speed with the process computer. As the distance between the acquisition system and the process computer was over a hundred meters, a very complicated communication interface had to be planned and realized.

Because the analysis of the vibrations in the bearings of the pumping aggregates is neither continuous, nor in real time, we adopted the solution of a high conversion speed and the possibility of local saving of an important number of samples. The results of the conversions are then transmitted at demand to the process computer through the serial interface RS485, with a 38400 bits/second transfer rate.

After the studies regarding the analogical-digital converter types and of the available high speed microcontrollers, the acquisition system was completed. It is based on the high speed microcontroller, DS89C420, produced by Dallas, and also the analogical-digital converter MAX120, with a conversion speed of up to 500.000 samples/second.

In order to reach acquisition speeds of over 400.000 samples/second, we gave up generating the clock impulses needed for the converter, which was connected to a clock signal with a 6MHz frequency, from an external quartz oscillator. In this way, the conversions are continuously executed, the result of the previous conversion being available during current conversion. The microcontroller only saves the results of the conversions. For reception and visualization of the data, a graphical interface was made in LabView (figures 3 and 4):

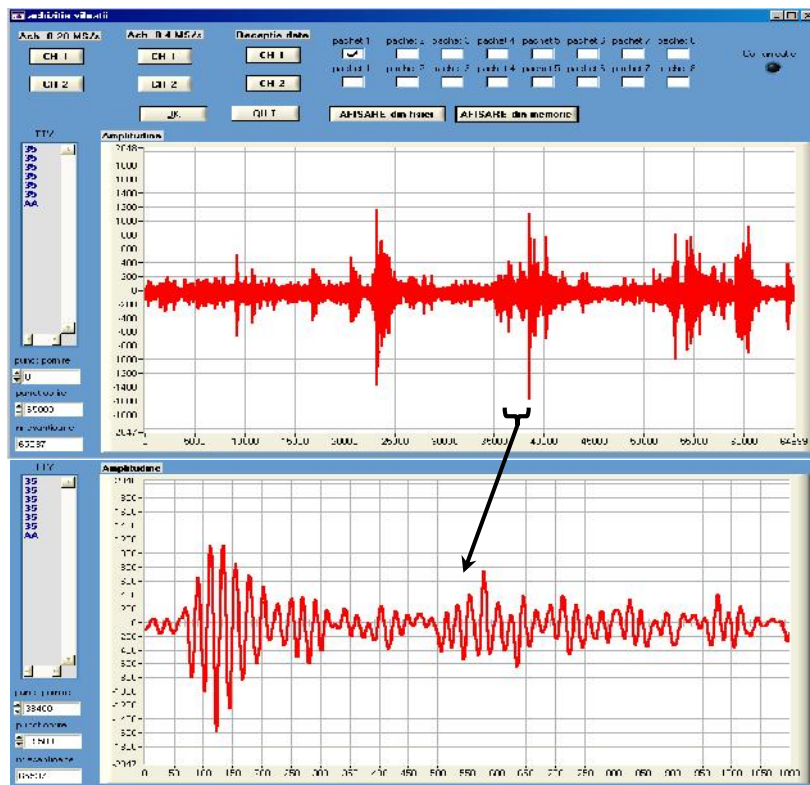


Fig. 3 The signal corresponding to a good ball bearing with the detail of a zone

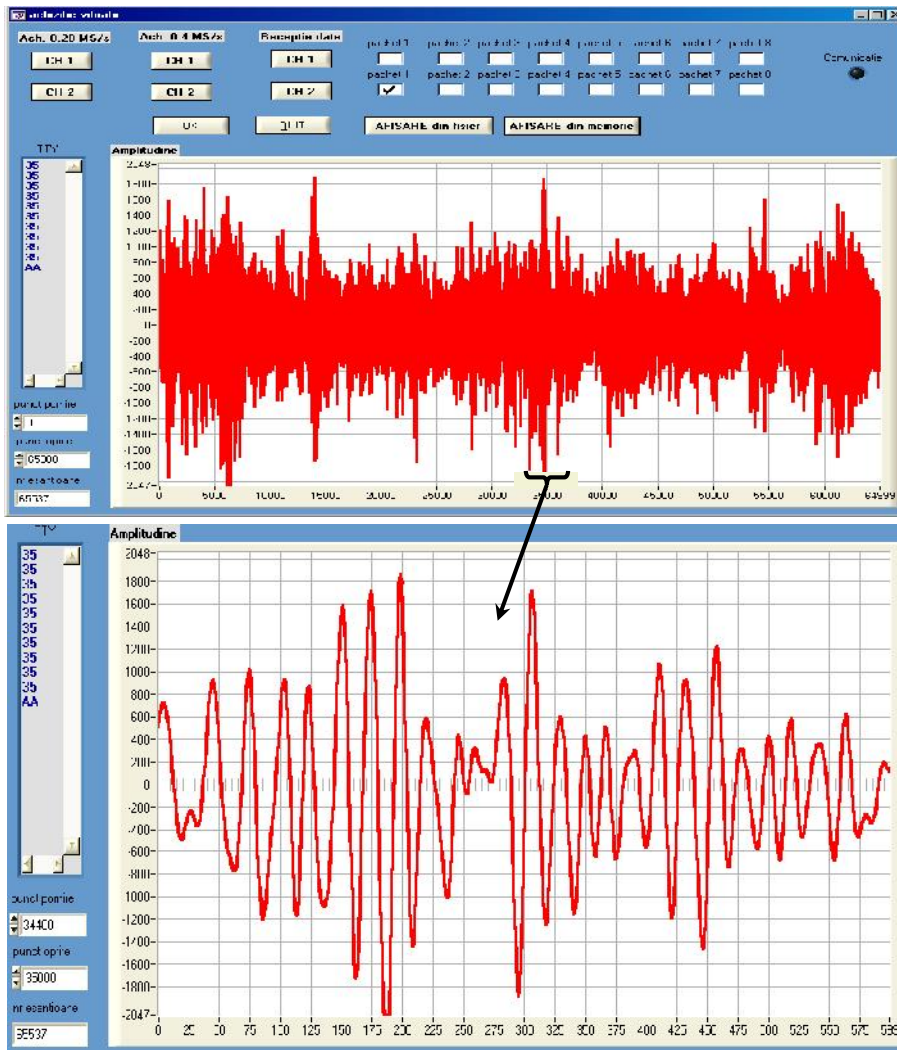


Fig. 4. The signal corresponding to a damaged ball bearing with the detail of a zone

After the acquisition, a number of over 500.000 samples resulted for each channel. To reduce the time for transmission in case of errors, the resulted samples were divided in 8 data packages, each package being separately transmitted and verified to be correct. After correct receiving of all data packages and creating a signal data package on the computer, the numerical analysis is performed upon the data.

3. CONCLUSIONS

After the numerical processing of the data through filtering and fast Fourier transform, the specters for power in figures 3 and 4 were obtained, corresponding to a good ball bearing and to a damaged one.

From the analysis of the two power specters, it results that we have a component given by the rotation frequency of the axel ($f_0=28$ Hz), which has approximately the same value for the two ball bearings. We observe that for the good bearing there are other spectral components, but smaller, and for the damaged bearing there are spectral components even higher than the fundamental component, f_0 . These spectral components appear at lower than f_0 frequencies and at higher ones.

Taking into account the information presented above about the causes of vibration appearance, after the calculus is made, we could say that in case of damages in ball bearings, there may appear spectral components at frequencies of 10 Hz (damaged cage), 26 Hz (axel rotation), 80 Hz (damaged ball), and also on other harmonics of the fundamental. Also, lower frequencies than f_0 appear in mechanical clearance in the gearing.

Analyzing figure 4, for the damaged ball bearing we observe the existence in the power spectrum of the components with very close frequencies to the ones calculated theoretically, but also of other spectral components. Only on the basis of the theoretical analysis of the observed data, the following conclusion can be drawn about the damaged ball bearing: has its cage very deteriorated (visible with the naked eye), has the exterior trajectory and one of the balls with faults and a powerful off centering and mechanical clearances in the gearing.

An exact diagnosis can be made through the practical study of a big number of ball bearings with only one fault, study of the resultant spectral components and creating a data base corresponding to that type of gearing and ball bearing.

BIBLIOGRAPHY

- [1]. *The automation and dispatching of the water evacuation process from the lignite mining pit EM Roşia*. Research Contract no. 276/C/2002, National Lignite Company of Oltenia.
- [2]. **Grofu Florin**. *Acquisition systems and numerical processing of the signals for the control of the industrial processes*. PhD thesis 2007.

EXPERIMENTAL MODEL FOR MONITORING A PUMPING AGGREGATE USED FOR WATER DRAIN IN ROȘIA MINING PIT

POPESCU LUMINIȚA*, OLARU ONISIFOR*, GROFU FLORIN**

Abstract: In mining pits coal basin appear different problems because water resulted from infiltrations and rain. To drain water there are used pumping aggregates. In order to reduce the electrical energy waste, we first need a correlation between the energetic parameters and the technological parameters. The functional correlation of the parameters can be realized through a complex informatics system, which assumes data acquisition, process control and elaboration of commands.

Keywords: electrical energy, informatics system, data acquisition, process control .

1. INTRODUCTION

In lignite mining pits from Oltenia's coal basin appear different problems because of the high amount of water resulted from infiltrations and rain.

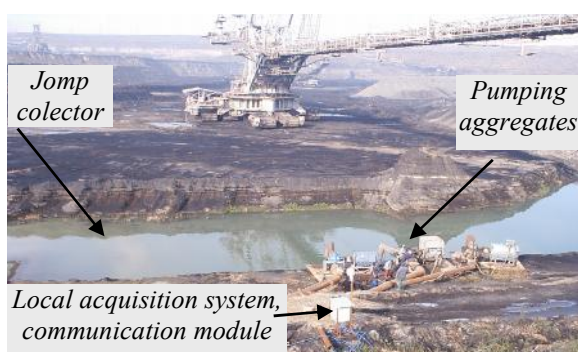


Fig. 1. Jomp collector (collector basin)

To drain these amount of water there are used pumping aggregates whose number depends on the area of the pit and of the estimated quantity of water from that pit. In figure 1 there is a view of a jomp (water collector basin).

In order to reduce the electrical energy waste, we first need a correlation between the energetic parameters (absorbed currents, power factor - \cos etc) which

* *PhD professor at the University Constantin Brancusi Tg-Jiu*

** *lecturer at the University Constantin Brancusi Tg-Jiu*

characterize the electrical engines which operate the evacuation (drain) pumps and the technological parameters (water level in the collector basin, warning level of the water in the basin, clogging level, depressurization from the breathe in column of the pumps, pressure from the breathe out column etc.).

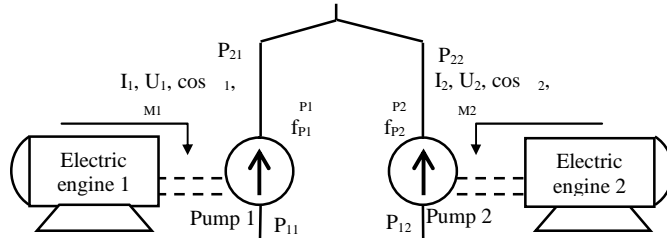


Fig. 2. Simplified representation of pumping aggregates

The functional correlation of the parameters above (and others) can be realized through a complex informatics system, which assumes data acquisition, process control and elaboration of commands. In figure 2 and 3 there are

presented the quantities which must be taken over by the acquisition system.

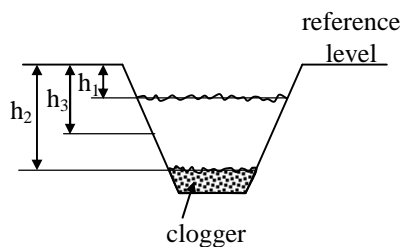


Fig. 3. Simplified representation of a jomp

With the data presented, this experimental model proposes the following objectives:

1. performance of the pumps in automated regime considering the quantity of water to be evacuated;
2. monitoring the energetic regime of functioning for the electrical engines which operate the pumps;
3. control of the technical state of the pumping aggregates.

1.1. Performance of the pumps in automated regime

At this point it has been followed the performance of the pumps with the water level in the collector basin. For this, we measured:

1. water level in the basin – h_1 [m], clogging level in the basin – h_2 [m];
2. warning level (defined as minimal level of the water in the basin at the breathe in of each pump) h_3 [m]
3. depressurization in the breathe in column of the pump 1 p_{11} [bar];
4. depressurization in the breathe in column of the pump 2 p_{12} [bar];
5. pressure in the breathe out column of pump 1 p_{21} [bar];
6. pressure in the breathe out column of pump 2 p_{21} [bar];
7. evacuated volume measured on the breathe out column of pump 1 Q_1 [mc/h];
8. evacuated volume measured on the breathe out column of pump 2 Q_2 [mc/h].

To realize these objectives we need a data acquisition system at the level of the pumping aggregates (electric box) and another acquisition system at the level of the electrical house, which takes over and processes the data and transmits them to the decisional units.

1.2. Monitoring the functioning regime

At this point we try to obtain a maximum energetic effective power at the pumping aggregates. For this, we measured:

1. absorbed current of the engines which operate the pumps, i_1 [A], i_2 [A].
2. supply voltage of the operating engines U [V].
3. phase difference between current and tension, $\cos \varphi$.

These parameters are measured, administrated and transmitted to the process computer by the acquisition and protection module SEPAM 1000. Also, we identified the state of the switching equipments: switches, separators, fuses, contractors:

- separators: general separator , interrupt separator, motive separators
- station general interrupt ,motor fuses: (at both operating engines)
- void contactor: C_{m1} , C_{m2} (at both operating engines).
- contact – tension presence, with logical „1” for presence and logical „0” for absence, state of protections.

Also there are monitored the environmental conditions with the following sensors:

1. temperature sensors inside electric box
2. temperature sensor for exterior temperature-initializes the anti freezing regime
3. sensor level for precipitations.

2. DATA ACQUISITION SYSTEM

The general presentation of the data acquisition system and the module in which the informatics application is structured is presented in figure 5.

The system for acquisition and control is based upon three levels:

Level 1 – Local panel (the cofret near the pumps)

At this level there are the field equipments responsible with the acquisition of the main analogical signals. So Real-Time Fieldpoint (RT FP2015) will take over the analogical signals (4..20mA) for flow, pressure, depressurization, level, signals which will be numerically converted on 12 bits and transmitted to the process computer from the electric house. Also, it has 16 digital output channels and 16 digital input channels used for different operations at the level of the pumping group. The digital inputs read the state of the off, on and other buttons, which will be used after in the data base to see the working profile of that pump.

In this panel is also positioned the vibration board, which takes over 4 signals of vibrations (2 pumps and 2 engines) in a buffer, with a frequency till 50kHz. These signals are memorized in the board memory and after that are transmitted at the process computer's (which is in the electric house) demand for processing. It was decided that the board to be placed close to the vibration sensors, because the vibration signal can be easily be perturbed through its analogical transmission at distance.

Level 2 – Electrical house

At this level, the process computer is positioned. It will communicate with the computer at the dispatcher through radio communication system, using the TCP/IP protocol.

The process computer from the electrical house is configured as master, which means that it must function continuously for process administration. In the situation that the computer does not work from various reasons, the process functions are realized manually. At this computer there are connected through a 5 channel switch the following equipments: the SEPAM, the radio antenna and the Fieldpoint (FP 2015 which is placed in the electric box near the pumps). At this computer is also connected through a RS485 port the 4 channel acquisition board of the vibrations which is placed in the electric box near the pumps. The process computer in the electrical house (NI PXI RT8187) is a product of the National Instruments, built especially for real time applications and so, besides the hardware configuration for the industrial environment it disposed of an operating systems with powerful real time facilities. It is not scheduled to operate with monitor within the application, but it has a video board and a monitor can be attached for testing.

At this computer there is another acquisition and control board, made with microcontroller, placed in the electrical house, and connected through a RS485 port which takes over the digital signals from the states of the fuses, states of the contactors, and also it controls the on and off states of the two engines of the pumps.

With the help of the screen, the good function of the whole assembly is tested and also, the sensors are calibrated through software, after the technological (electronic) calibration. All the data processing is made at this level with the purpose of having a smaller number of octets which must be sent to the dispatcher, and so the communication time to be reduced. In this way, the gained time is used for more complex processes at the level of the process computer and in the same time, the reliability of the communication with the dispatcher is increased.

Level 3- Dispatcher

This level is represented by the computer in the dispatcher room, the computer which is connected through radio communication system with the equipments in the electrical house of the pumps (level 2). At this computer are also connected directly through the RS232 serial port the acquisition board built as a core with microcontroller which takes over the signals from the precipitation transducer and the environment temperature transducer. These transducers have been placed at the dispatcher level to have valid global information in the whole pit. At the present moment, at the dispatcher, there are presented as a monitoring application, all the quantities measured at the level of the whole application.

The computer at the dispatcher is organized as client for the computer at level 2, which is the process computer in the electrical house. In this way, we give a higher importance to the process, and the dispatcher can connect asynchronously to the process computer to obtain data, but the controlled process is prior.

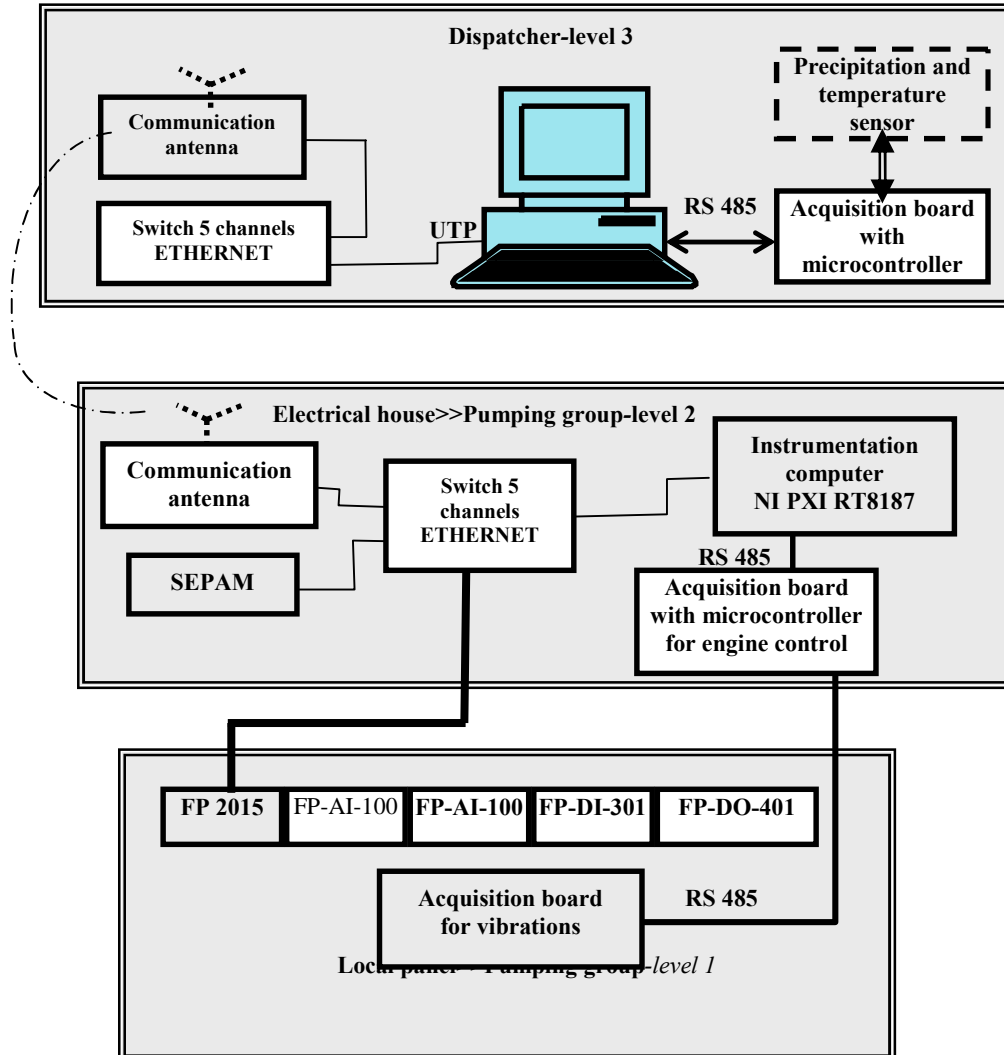


Fig. 4 The structure of the acquisition and control system

3. CONCLUSIONS

1. The main interaction of the operators with the automated process is through the computer from the dispatcher. There is a graphical interface organized under a very intuitive synoptic scheme. With the help of the interface is presented the whole information received from the sensors.

2. Through monitoring the value for the water flow for a pump by the dispatcher, conclusions may emerge about the increase of the pump's usage, or that pump 2 on the same column was started. Also, the decrease of water flow can be caused by the clogging in the pump.

3. In case that the pump is stopped and we have breathe out pressure, it means that the pump can be started only by the opening of the upstream vent. Otherwise, it must be started through manually input of water.

4. The level information is used by the operator to periodically calibrate. This thing is used because of the fact that the position of the level transducer isn't fixed (the architecture of the jump is modified, the height of the sorb is modified, the pumping system is moved into another jump) and the initial calibration is invalid. In this way, the dispatcher can periodically introduce a zero reference (reference valid only at that time) and after that to follow the increases and decreases of level comparing to that reference.

5. Using the information from the precipitation transducer, more pumps can be started with anticipation so that the increase of the level isn't waited and after that the pumps to start.

6. Using the information given by the temperature sensor from the cofret, the heating installation is started to maintain the temperature in the cofret at low values, for the components to function.

7. Using the information given by the environment temperature sensor from the dispatcher, the anti freezing regime for work can be started and it assumes starting the pumps at some time intervals, function of the temperature of the environment to avoid their freezing.

BIBLIOGRAPHY

[1].Popescu L., Olaru O., Vulpe I., Grofu F. *The automation of the water evacuation process from the lignite mining pit*. 5th European Conference of Young Research and Science Workers in Transport and Telecommunications, 23 – 25 June 2003, Zilina, Slovak Republic.

[2].Popescu L., Olaru O., Popescu M., Grofu F., Gidei G., *Pumps function and electrical motors monitoring with vibrations transducer*. Proceedings of 5th International Carpathian Control Conference ICC' 2004, Zakopane Poland May, 25-28, 2004, pag.641-646.

[3].*The automation and dispatching of the water evacuation process from the lignite mining pit EM Rosia*. Research Contract no. 276/C/2002 , National Lignite Company of Oltenia.

FCC MODEL PREDICTIVE CONTROL

CRISTINA POPA*, CRISTIAN PATRASCIOIU**

Abstract: The fluid catalytic cracking Unit (FCCU) has a major effect on profitability of on oil refinery. The FCCU is difficult to model well due significant nonlinearities and interactions. The purpose of this study is to develop a controller based on model predictive control algorithm. The paper is structured in four parts: the structure of the process, the mathematical model, the algorithm MPC for FCC and results.

In the first part of this paper is analyzed the catalytic cracking process where are identified the subsystems of process associated and the interaction between this subsystems. The model is essential element of an MPC Controller. The second part of this paper contains dynamic and steady state elements of modeling for each subsystem that was emphases within analysis process structure. The model predictive control was developed in Matlab using the MPC block from Predictive Control Toolbox. In last part of this paper the authors presents the results of the simulation. The simulation results reveal a superior behavior when the model predictive control is used on the FCC.

Keywords: kinetic, cracking, modeling, FCC, simulation.

1. INTRODUCTION

The fluid catalytic cracking (FCC) unit is one of the most important and complicated process in the petroleum refining industry. The complexity of the process from the point of view of modeling and control is determined by: i) strong interactions between the reactor and regenerator; ii) large degree of uncertainty in the kinetics of the cracking reactions and catalyst deactivation by coke deposited in the riser reactor; iii) uncertainty coke burning process in the regenerator.

Process structure of the catalytic cracking includes next subsystems: reactor, regenerator, preheating furnace (V. Marinoiu, 1992).

* *Assit.Eng. at the Petroleum – Gas University of Ploiesti*

** *Prof., Ph.D. at the Petroleum – Gas University of Ploiesti*

The reactor represents the principal element of the catalytic cracking plant. Because the modeling of the reactor is very difficult, the authors propose the decomposition in three subsystems (C. Popa, 2004).

This are:

- i) *The interfusion nod subsystem*, located at the de base of the riser, here the fresh gas oil is brought into contact with the hot regenerated catalyst, which leads to the vaporization of the gas oil. It assumed that the vaporization of the feed is instantaneous.
- ii) *The riser subsystem* is a vertical standpipe 25-40 m in length. All cracking reactions take place in riser over a short time 2.5 s. These reactions are primarily endothermic.
- iii) *The reactor-stripper subsystem*, located at the top of the reactor, a subsystem that realizes the catalyst separation from the feed stock vapors and the reaction products.

The regenerator is a large cylindrical vessel, where the coke deposited on the catalyst surface as result of the cracking reactions is burned off using air. Air enters the regenerator through an air distributor located at the bottom of the regenerator.

2. MATHEMATICAL MODEL OF THE FCC UNIT

In order to obtain the mathematical model of the reaction block, each subsystem was treated in a separate way (Patrascioiu C, Popa C., 2004).

The interfusion nod

The model of the interfusion node is represented by a heat balance in the steady state regime (Ali 1997). The temperature of the interfusion node T_{in} is calculated with the relation:

$$T_{in} = \frac{1}{Q_{cat}C_{pcat} + Q_{mp}C_{pmp}} \times (Q_{cat}C_{pcat}T_{reg} + Q_{mp}C_{pmp}T_{mp} - \Delta H_{vap}Q_{mp}). \quad (1)$$

The riser subsystem

The mathematical model of the riser subsystem is structured in the next components: *kinetic model, material and heat balance.*

- *Kinetic model.* The elaboration of mathematical model of riser required from the author's part an action for analytic and selection of kinetic models presented in literature. Taking into account the performance criterion, it was chosen the Weekman kinetic model, for the total description of the overall. The rates of the three reactions from kinetic diagram are definition on these relations:

$$\begin{cases} r_1 = -k_1 \cdot Y_A^2 \\ r_2 = -k_2 \cdot Y_B \\ r_3 = -k_3 \cdot Y_C^2 \end{cases} \quad (2)$$

Constant rates reaction k_1, k_2, k_3 are dependent for base material quality, riser temperature, activity equilibrium catalyst and condition operating.

• *Material balance.* The riser is considered a tube reactor with a total displacement operated in an adiabatic regime. The material balance equations have the form

$$\begin{cases} \frac{dY_A}{dz} = -\frac{1}{U_v} * (k_1 + k_3) * Y_A^2 \\ \frac{dY_B}{dz} = \frac{1}{U_v} * (k_1 * Y_A^2 - k_2 * Y_B) \\ \frac{dY_C}{dz} = \frac{1}{U_v} * (k_2 * Y_B + k_3 * Y_A^2) \end{cases} \quad (4)$$

where U_v represents vapor's rate.

• *Heat balance.* The heat balance lengthways riser is represented by differential equation

$$\frac{dT}{dz} = \frac{(-H_{r1}) * Q_{rA}}{Q_{mp} (Y_A C_{pA} + R_{abur} C_{pabur} + R_{cat} C_{pcat})} \quad (5)$$

where Q_A is raw material, Q_B - gasoline mass flow, Q_{cat} - catalyst mass flow, Q_{abur} - steam mass flow.

2.3. The reactor -stripper subsystem.

The mathematical model of the reactor stripper subsystem is based on the hypothesis of the perfect mixing. The dynamic model has two components: *the material balance* associated to the coke deposited on the catalyst and *the energy balance* in the strippers:

$$W_s \frac{dT_R}{dt} = Q_{cat1} T_r - Q_{cat2} T_R ; \quad (6)$$

$$W_s \cdot \frac{dC_{cocs2}}{dt} = Q_{cat1} C_{cocs1} - Q_{cat2} C_{cocs2} , \quad (7)$$

where C_{cocs1} mass fraction of coke on spent catalyst; C_{cocs2} mass fraction of coke on catalyst in separator; W_s - holdup catalyst in separator.

2.4. The regenerator model

The authors adapted the model developed by Erazu, model that treats the material balance associated to the coke, the material balance associated to the oxygen and the energy balance (Erazu ,1978).

The model is sufficiently complex to capture the major dynamic effects that occur in an actual FCCU system. It is multivariable, strongly interacting and highly nonlinear. The model is implemented in Matlab (SIMULINK) programming language and was used for the study of different operating regimes induced both by design

changes and by changing operation strategies but also for investigating which control strategies may be implemented.

3. MPC FOR THE FCC

The catalytic cracking process is complex both from modeling and from the control point of view. The FCCU is difficult to control due to the nonlinear behavior, the strong interactive feature coupled with the presence of equipment, and operating constraints. The complex dynamic behavior of the process was used in the MPC algorithm scheme based on nonlinear model.

The *controlled variables* have been selected to provide, through control, a safe and economic operation. The controller variables are regenerator temperature T_{reg} , and reactor temperature T_r . The regenerator temperature, T_{reg} has to be maintained at a certain value to allow a stable removal coke from the catalyst. Overriding a high temperature limit produces a permanent catalyst deactivation; a reduction under a lower limit leads to coke accumulation on the regenerated catalyst. The reactor temperature T_r , has to be maintained at certain level to a desired maximum conversion of the feed oil.

The *manipulated variables* are Q_{cat1} – regenerated catalyst flow rate; Q_{air} – mass flow rate of air to regenerator. The *disturbances variables* are Q_{mp} , T_{mp} – feed stock flow and temperature.

Process identification test. Elaboration an MPC controller Matlab(Simulink) suppose the linearized the model of the catalytic cracking, for the obtain the simplified model of the process. The model simplified is obtained used the process identification test.

The process identification test the methods presented by Coleman and Seborg in their papers. The scope of the process identification test was to capture the plant dynamic in the models to develop linear controller. The first step in this test is determination the inputs-outputs structure of the process, figure 1. The inputs variables of the process are Q_{mp} , T_{mp} – feed stock flow and temperature, Q_{cat1} – regenerated catalyst flow rate; Q_{air} – mass flow rate of air to regenerator. The outputs variables are regenerator temperature T_{reg} , and reactor temperature T_r .

Process identification tests were carried out variables by making step changes on each input variable. The magnitude of the steps was selected to ensure that a clear response of the outputs variables was observed. The transfer function models of the FCC process are given in table 1.

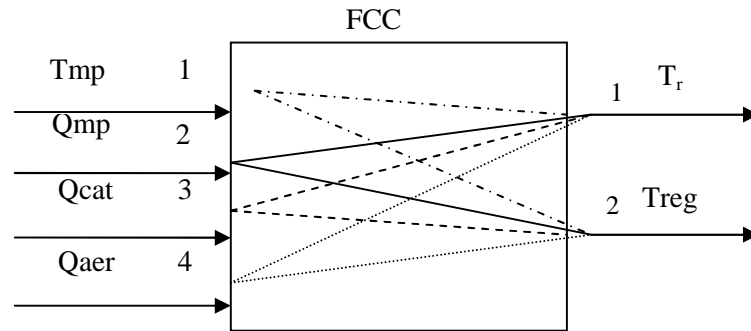


Fig. 2. Inputs –Outputs structures of the FCC.

4. SIMULATION RESULTS

The control objective is to maintain the controlled variables at predetermined set points in the presence of typical process disturbances while maintaining safe plant operation. The figure 2 presents the MPC controller response to 10% increases feed stock temperature. The figure 3 it can be observed the closed loop response of the system with MPC controller for 10% step increase the regenerated catalyst flow rate. Figure 4 show closed loop response of the system with MPC controller for 10 % step increase in the reactor temperature set point at 10s.

Table 1. The transfer function model of the FCC.

Inputs Outputs	T_{mp}	Q_{mp}	Q_{cat}	Q_{aer}
T_r	$\frac{0.1775}{0.03s + 1}$	$\frac{-0.0007913}{0.025s + 1}$	$\frac{0.0001751}{0.003s + 1}$	0
T_{reg}	$\frac{0.1655}{0.35s + 1}$	$\frac{-0.0007153}{0.35s + 1}$	$\frac{-0.00005791}{0.1s + 1}$	$\frac{0.002756}{0.2s + 1}$

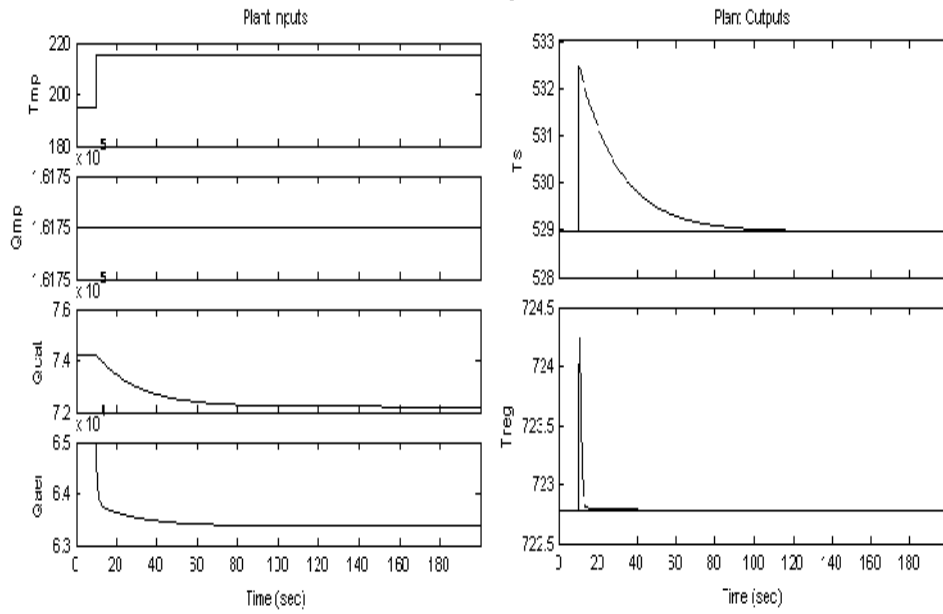


Fig 2. Closed loop response of the system with MPC controller for 10% step increase the feed stock temperature.

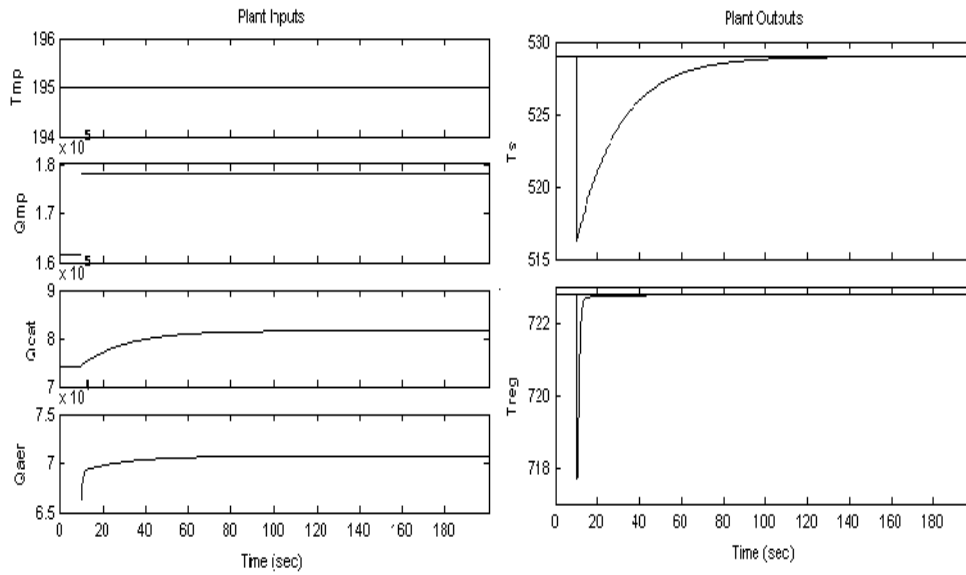


Fig . 3. Closed loop response of the system with MPC controller for 10% step increase the regenerated catalyst flow rate.

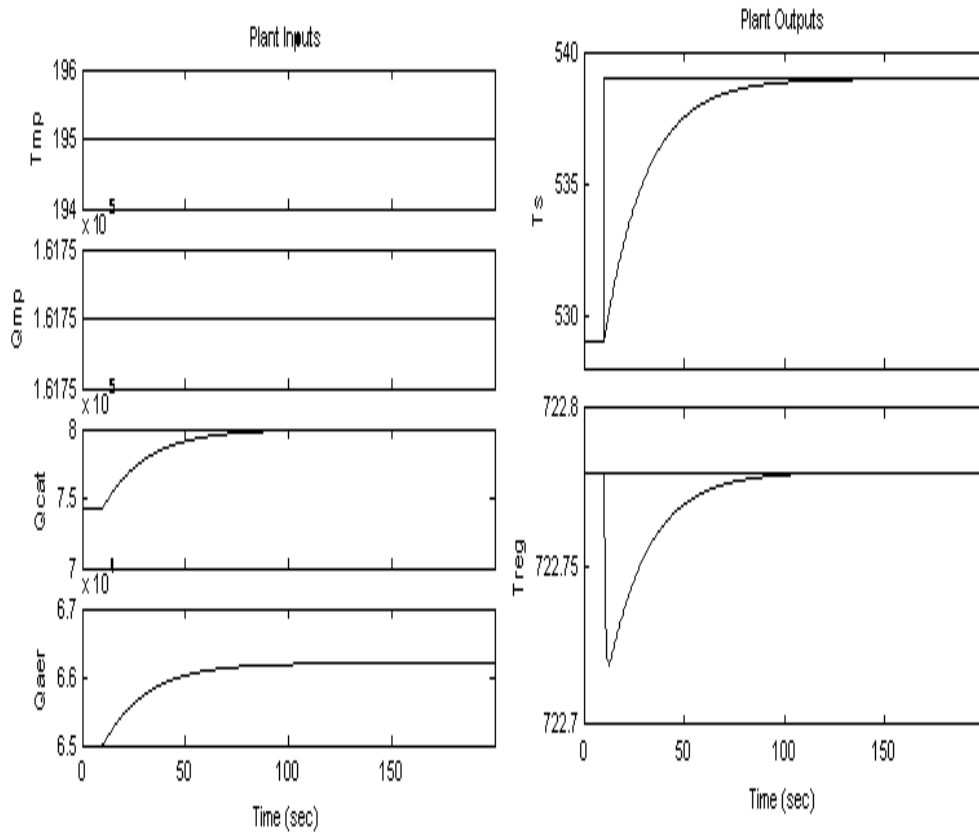


Fig 4. Closed loop response of the system with MPC controller for 10 % step increase in the reactor temperature set point at 10s.

From this graphs, it was observed that the MPC controller is powerful enough to bring the severe nonlinear, strong coupling, time varying process under control, making the operation smooth and stable, reducing products.

4. CONCLUSIONS

The linearized model was used to design an MPC controller, which was successfully, applied to original nonlinear model. From the graphs of the outputs and input variables, it is clear that MPC strategy is far more effective to handle the thorniest situations found in oil industrial. Based on the success of the MPC simulation on the FCC model, following objectives will be achieved in an industrial practice :

- i) improving the product quality- the MPC stabilizes the process operation, reducing the impact of control oscillations on the process;
- ii) minimizing energy consumption;
- iii) improving process economic performance;

- iv) improving the process operating stability, since the MPC reduces the process overshoot, it carries the process outputs to their set points in a smoother and faster manner in the presence of disturbances;
- v) maximizing the process throughput and desirable products yield. Traditional operation keeps the unit at some distance from the constraints (optimum conditions) to ensure equipment and unit safety.

The MPC technology minimizes the distance between operating points and the optimum, significantly increasing the processing capacity and desirable products yield.

BIBLIOGRAPHY

- [1] **Ali, H., and Rohani, S.**, *Dynamic modeling and simulation of a riser-type fluid catalytic cracking unit*. Chemical Engineering Technology, 20, 118, 1997;
- [2] **C. Popa, C. Pătrășcioiu** , *The adaptation of the control model for FCCU*, The 5th International symposion on process control, UPG, 2006;
- [3] **C.Pătrășcioiu Popa C** , *Modeling a riser-Type reactor of fluid catalytic cracking unit*, The International Symposium and Modeling, Simulation and System's Identification, Universitatea Dunarea de jos , 2004;
- [4] **Errazu A.F. , H. I. DeLasa and F. Sarti**, *A Fluidized bed catalytic Cracking Regenerator Model, Grid Effects*, Canadian Journal of Chemical Engineering, 57, 191-197, 1978;
- [5] **Coleman B., Babu J.**, *Techniques of Model Based Control*, Pentice Halll, 2004;
- [6] **Seborg D, Edgard T, Duncan M**, *Process Dynamic and Control*, John Wiley& Sons Inc, 2004.

GAS MONITORING SYSTEM BASED ON MODBUS PROTOCOL AND VIRTUAL INSTRUMENTATION

NICOLAE PĂTRĂȘCOIU*, ADRIAN MARIUS TOMUȘ**

Abstract: Major coal mine explosion disasters have always involved the combustion of coal dust, originally triggered by methane. So that is necessary to use monitoring and data logger systems to control the underground environmental methane concentration. In this paper we propose such system based on specific sensors to collect data from different measurement points, a serial data transmission based on Modbus protocol and a virtual instrumentation to data receiving, processing and visualization.

Keywords: methane sensor, modbus protocol, virtual instrumentation

1. METHANE GAS SENSORS SIGNAL TRANSMISSION

Many models of gas detectors are available to measure methane concentrations, as well as most of the other contaminant gases found in mines and tunnels. Most methane detectors used in mining use a catalytic heat of combustion sensor to detect methane and other combustible gases. These have been proven through many years of reliable operation.

To transmit sensors output signal from different systems like system gas monitor exists many methods and one of this is serial transmission based on the RS – 485 standard and the Modbus communication protocol.

Here are some gas sensors that are using catalytic heat of combustion or infrared absorption like operating method but the same the same signal transmission method namely serial transmission based on the RS – 485 standard and the Modbus communication protocol:

- S4100C Combustible Gas Addressable Transmitter from General Monitors designed to measure and display concentrations of combustible gases in the range of 0 – 100% LEL, but will continue to display concentrations up to

* *Assoc.Professor at the University of Petroșani*

** *Assist.univ. at the University of Petroșani*

- 120% LEL with the instrument addressed via the Dual Modbus RTU serial interface.
- Ultra 1000 Addressable Sensor for Combustible Gases from PEM – TECH, Inc. designed to provides a 4–20mA signal proportional to 0 – 100% of the detection range.
- 5100-02-IT Combustible Gas Sensor Module from Sierra Monitor that measure concentrations of combustible gases in the range of 0 – 100% LEL.
- Model D12-IR Gas Transmitter from AFC International, Inc that measure the methane in range 0 – 100 V/V.
- MC-4210-CH4 Modbus Addressable Sensor from American Mine Research (AMR). Inc.
- SEC 3000 Gas Detector from Sensor Electronics Corporation (SE).

2. GAS SENSOR S4100C MODBUS PROTOCOL

2.1. Modbus Protocol

The Modbus Serial Line protocol is a Master-Slaves protocol so that only one master (at the same time) is connected to the bus, and one or several (247 maximum number) slaves nodes are also connected to the same serial bus. A Modbus communication is always initiated by the master. The slave nodes will never transmit data without receiving a request from the master node. The slave nodes will never communicate with each other. The master node initiates only one Modbus transaction at the same time.

The master node issues a Modbus request to the slave nodes in two modes:

- In **unicast mode**, the master addresses an individual slave. After receiving and processing the request, the slave returns a message (a 'reply') to the master. In that mode, a Modbus transaction consists of 2 messages: a request from the master, and a reply from the slave. Each slave must have a unique address (from 1 to 247) so that it can be addressed independently from other nodes.
- In **broadcast mode**, the master can send a request to all slaves.

The drawing presented in fig.1 explains the master behavior:

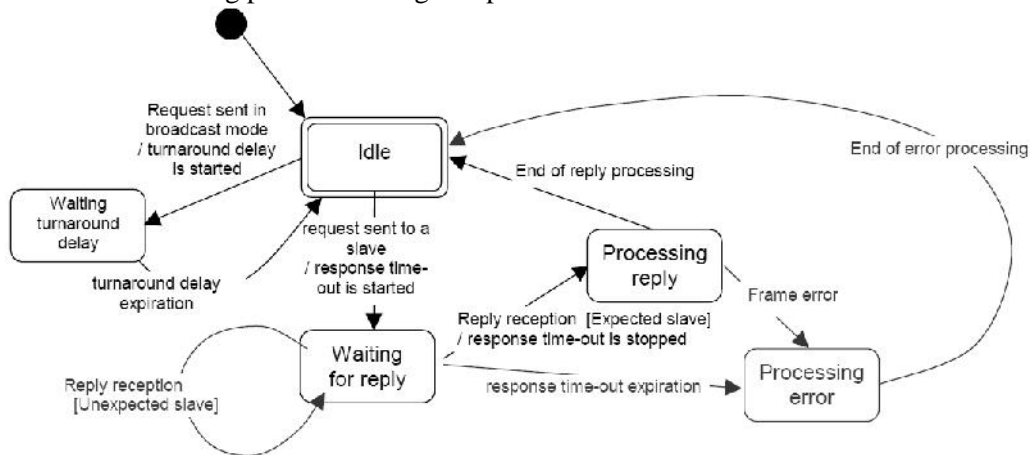


Fig.1. The Master state diagram

State "Idle" is the initial state after power-up. A request can only be sent in "Idle" state. After sending a request, the Master leaves the "Idle" state, and cannot send a second request at the same time. When a unicast request is sent to a slave, the master goes into "Waiting for reply" state, and a "Response Time-out" is started. It prevents the Master from staying indefinitely in "Waiting for reply" state. Value of the Response time-out is application dependant. When a reply is received, the Master checks the reply before starting the data processing. The checking may result in an error, for example a reply from an unexpected slave, or an error in the received frame. In case of a reply received from an unexpected slave, the Response time-out is kept running. In case of an error detected on the frame, a retry may be performed. If no reply is received, the Response time-out expires, and an error is generated. Then the Master goes into "Idle" state, enabling a retry of the request. The maximum number of retries depends on the master set-up.

In unicast mode the Response time out must be set long enough for any slave to process the request and return the response. Therefore the Turnaround delay should be shorter than the Response time-out. Typically the Response time-out is from 1s to several second at 9600 bps; and the Turnaround delay is from 100 ms to 200 ms.

The drawing presented in fig.2 explains the master behavior:

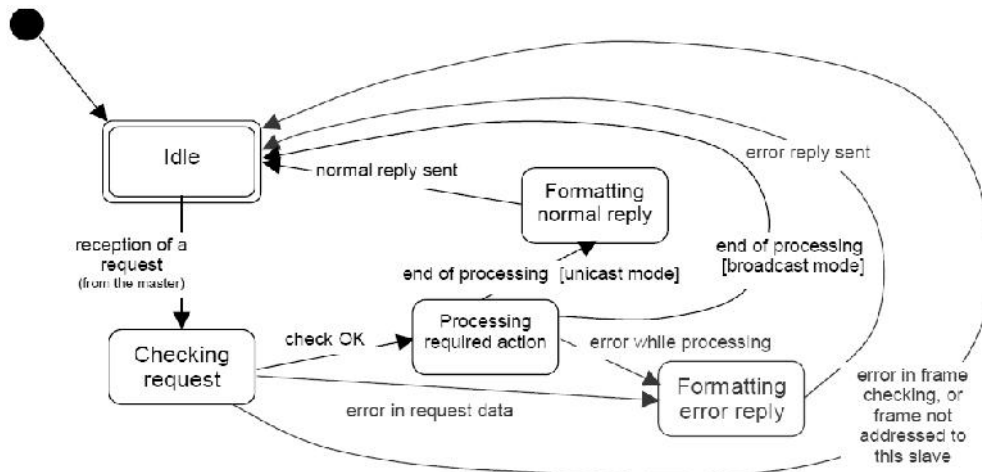


Fig.2. The Slave state diagram

State "Idle" is the initial state after power-up. When a request is received, the slave checks the packet before performing the action requested in the packet. Different errors may occur : format error in the request, invalid action, ... In case of error, a reply must be sent to the master. Once the required action has been completed, a unicast mode message requires that a reply must be formatted and sent to the master. If the slave detects an error in the received frame, no respond is returned to the master. Modbus diagnostics counters are defined and should be managed by any slave in order to provide diagnostic information.

2.2. Gas sensor S4100C

In this paper we deals with an application that use twelve S4100C sensors connected by an serial transmission line and from these the information is collected by an PC computer whereon run a program called virtual instrument (VI) written in LabVIEW.

The General Monitors Model S4100C Smart Transmitter is a highly reliable, self contained, microprocessor controlled, hydrocarbon gas monitor can be addressed via the Dual Modbus RTU serial interface. The Modbus communications interface is based on the RS485 standard, is implemented as a 2 wire, half-duplex, and conforms to the EIA-485 specification. The interface implements the RTU protocol that is an asynchronous NRZ format and the factory defaults are set to 19K2 baud, no parity and 1 stop bit.

For the S4100C sensor the Modbus register configuration is presented by following table 1

Table 1 The Modbus register configuration

Register	Function	Access Type	Hex address	Scaling
1	Analogue output current	Read	00	0mA =0x8000 20mA =0xFFFF
2	Sensor response at calibration in % of reference	Read	01	0% =0x8000 100% =0xFFFF
3	Alarm, fault and analogue output status	Read	02	NA
4	Calibration level setup	Read	03	0 =0x8000 100 =0xFFFF
5	A1 alarm trip level setup	Read/write	04	0 =0x8000 100 =0xFFFF
6	A2 alarm trip level setup	Read/write	05	0 =0x8000 100 =0xFFFF
7	Open collector outputs and analogue output current at calibration setup	Read/write	06	NA
8	Number of successful calibrations	Read/write	07	0 =0x0000 65535 =0xFFF
9	Modbus setup	Read/write	08	NA
10	Clear latched alarms and faults	Write	09	NA
11	Sensor response at calibration reference in mV	Read	10	0V =0x8000 10V =0xFFF

Here it can be observe that to collect information about gas concentration and about sensor status is necessary to read the registers #2 and respectively #3. To do this on the communication bus the master that is the PC computer must deliver the read command:

sensor address	function code	register address	number of registers to be read
1 byte	1 byte	2 byte	2 byte
01 ... 0C	03	0001	0002

The addressed sensor after receive the request and processing the required action sent a replay that has the format:

sensor address	function code	number of bytes	data
1 byte	1 byte	1 byte	4 byte
01 ... 0C	03	02	R _{2H} R _{2L} R _{3H} R _{3L}

3. VIRTUAL INSTRUMENT

To generate query for sensors and to receive and processing the sensor's answer is used a program written in graphical language LabVIEW named virtual instrument. This has two basic components: front panel that include the controls necessary to generate commands and indicators used to display measured values,

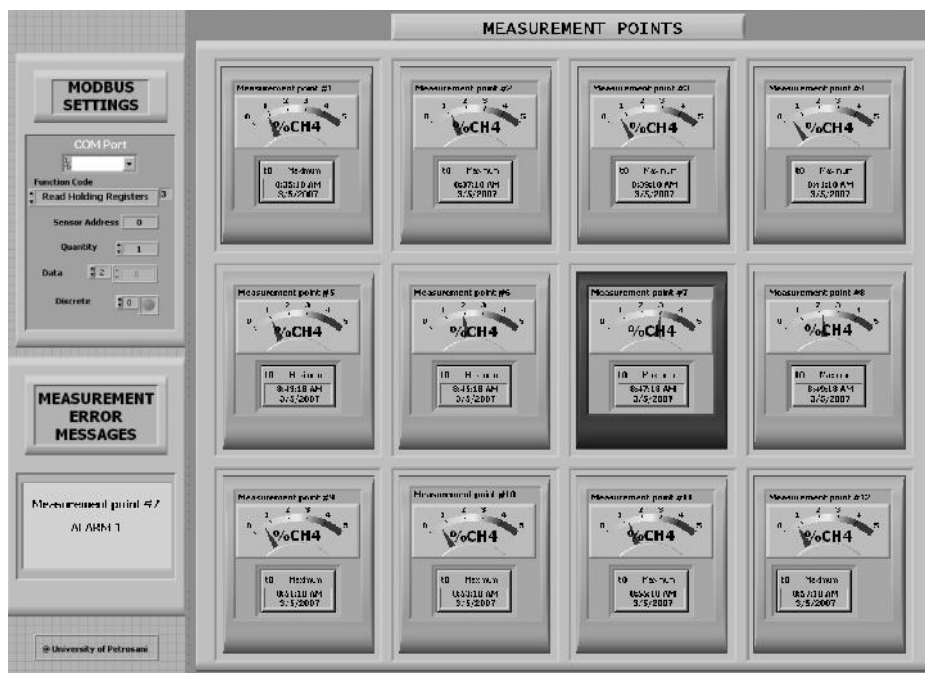


Fig. 3. Front panel of the virtual instrument

messages and others necessary information and block diagram.

On the front panel, figure 3, are dispose:

- in MODBUS SETTINGS section controls necessary to set the Modbus protocol parameters;
- in MEASUREMENT ERROR MESSAGES section a display area for miscellaneous messages generated for corresponding errors that can appear in measurement and data acquisition process like over limit gas concentration, sensor short circuit, sensor open circuit;
- in MEASUREMENT POINTS section, twelve indicators that display the gas concentration current value, the time for over limit gas concentration and for the nonce is changed the indicator color from green to red simultaneous with display the right message.

The block diagram, figure 4, represent the proper application program where are used the programming elements and one of these is Staked Sequence Structure by the medium of this are build the sequences for generate the queries and also for processing the answers.

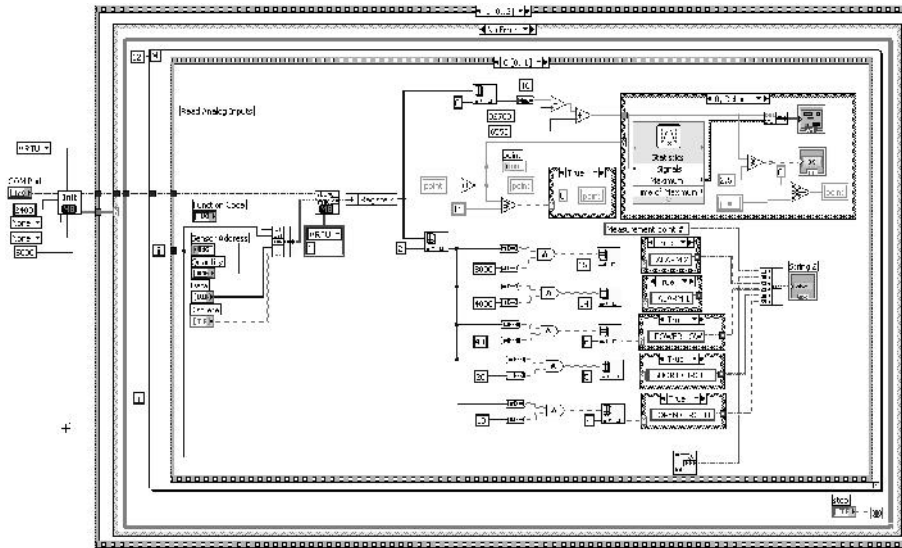


Fig. 4. Diagram block of the virtual instrument

The program starts with Modbus initialization (*INIT SubVI*), generate command and receive the answer (*abcWR SubVI*) followed by the function *Index Array* that extract from registers the gas concentration value (index 1) and sensor status (index 2). These information are represented by corresponding bytes with MSB first so that these hexa format bytes are converting into decimal number for display through the function *Cast Unit Bases*. From data extract by index 2 are forwards extract the bits through are generated the messages about sensor's status

BIBLIOGRAPHY

[1] **Pătrășcoiu, N.** *Sisteme de achizitie si prelucrare a datelor. Instrumentatie Virtuala.* Editura Didactica si Pedagogica, Bucuresti, 2004, pp 250-256, ISBN 973-30-2622-0
 [2] * * *. *MODEL S4100C Hydrocarbon Smart Transmitter.* Instruction Manual. Part No. MANS4100C-EU, Revision K08/05
 [3] * * *. *MODBUS over Serial Line.* Specification and Implementation Guide V1.01. Modbus.org. Aug. 30/2006
 [4] * * *. *LabVIEW™ 8.2. LabVIEW Fundamentals.* National Instruments August 2005 374029A-01

HYBRID NEURAL NETWORK FOR PREDICTION OF PROCESS PARAMETERS IN INJECTION MOULDING

POPESCU MARIUS-CONSTANTIN*

Abstract. In this paper, the attempts made by the authors to develop an artificial neural network system for prediction of injection moulding process parameters is presented. In this work, attempts have been made to determine the process parameters that could affect injection moulding process based on governing equations of the filling process.

Keywords: Hybrid neural networks; Injection moulding; Back propagation algorithm

1. INTRODUCTION

The industrial production process as practised in today's injection moulding industry is based on the interaction between regulation technology, industrial handling applications and computer science. Computer-integrated manufacturing has become a realistic prospect for injection moulding firms where maximum reproducibility and availability are necessary to guarantee the competitiveness. In injection moulding, the trial and error methods have always been as a practice to determine the optimum injection moulding process parameters. Experts of the trade often refer to previous mould design similar to the current design and use its successful moulding process parameters. Injection moulding is a cyclic process whereby a heat-softened plastic is injected into a mould from which it is ejected after it has set to the shape of the cavity. Thus, an injection moulding machine is one that discontinuously produces formed articles primarily from polymeric materials.

2. NEURAL NETWORKS

An artificial neural network is a massively parallel array of simple computational units that models some of the functionality of the human brain and attempts to capture some of its computational strength [1]. In other words, it is a

* *University of Craiova, Faculty of Electromechanics, Craiova, Romania*

system of interlinked but very simple data processors. Neural computing is defined as the study of networks of adaptable nodes which, through a process of learning from examples, store experimental knowledge and make it available for use.

Error-back-propagation is a particular example of a larger class of learning algorithms, which are classified as 'supervised learning', because at each step the network is comparing the actual output with the desired output [7]. Not only such algorithms are probably not implemented in biological neural networks, but also suffer because they are applicable only when the desired output is known in advance. Najmi and Lee [5] analysed the mould-filling process for injection moulding. Hung and Shen [2] believed that mechanical properties of fibre-reinforced polymer depend strongly on orientation patterns of fibres.

Liu and Manzione [4] developed a moulding technology that could deliver the micron-level precision in injection moulding process. Shelesh-Nezhad and Siores [13] developed an intelligent system for obtaining the magnitude of process parameters in plastic injection moulding operation. Rao and Yarlaga [12] developed a four-layer back-propagation network to acquire and apply knowledge from the flow-stress data obtained from experimentation. Popescu [6] also developed a similar artificial intelligence system for metal injection moulding. Yarlaga and Cheng [14] developed a network to predict the process parameters in pressure die-casting. It was based on the governing equations of the filling stage for the die-casting process and the network was trained with data collected from experts in this field. The trained neural network functions as a mapping mechanism and it is capable of predicting injection time when presented with unfamiliar data pair such as melt temperature, mould temperature, weight of casting and injection pressure. The Levenberg-Marquardt approximation algorithm was used as it reduced the sum-squared error to a very small value thus generating better accuracy of predictions. With the development of this network, a novice user can determine the injection time of the die-casting process. The range of the applications of neural networks is colossal ranging from speech recognition to flight control simulations. In the manufacturing field involving injection moulding, moulding parameters still remain an uncertainty without the assistance from experts. Hence, the neural network approach is used to overcome these uncertainties by predicting the injection moulding process parameters [10].

3. CONSIDERATION OF INJECTION MOULDING

Injection moulding is a high volume production process with high tooling and set-up cost. The four main moulding parameters that affect the properties of the moulded product are melt temperature, mould temperature, injection pressure and injection time. A successful moulding process is one, which optimises all the parameters to achieve mouldability. The characteristics of melt temperature are shown in Fig. 1 [11]. Fig. 2 shows the characteristic of mould temperature with injection time and characteristics of injection pressure. Injection pressure is the theoretical pressure due to the forces acting on the injection piston screw against the material, assuming no losses. In a rectangular channel, it is given by the expression

$$\Delta p = \frac{12\mu QL}{TH^3}, \tag{1}$$

where μ is the viscosity of the melt in poise, Q the volumetric filling rate in cubic centimetre per second, L the channel length in centimetres. As for the rectangular channel, T is the length of the slit in centimetres and H the thickness of the slit in centimetres. Fig. 3 shows the characteristics of injection pressure [3]. Injection time is the time required for the injection moulding machine to fill the part. The combined effect of high temperature and high shear rate (resulting from high flow rate) reduces the melt viscosity, and therefore offsets the pressure requirement. An estimation was based on the assumption that the mould be filled before half of the available gap has been taken up with solidified material. This results in the equation:

$$t = \frac{[d_w(P_t / P_{fr})]^3}{8C^3}, \tag{2}$$

where d_w is the minimum wall thickness of the moulding in millimetres, P_t the flow path in millimetres. P_{fr} is equal to the flow path ratio. The freeze-off constant, C , is proportional to the ratio given by:

$$C = \frac{T_x - T_m}{T_c - T_m}, \tag{3}$$

where T_x is the heat distortion of the material, T_m the mould temperature and T_c the cylinder temperature. Fig. 3 shows the relationship of injection time and pressure.

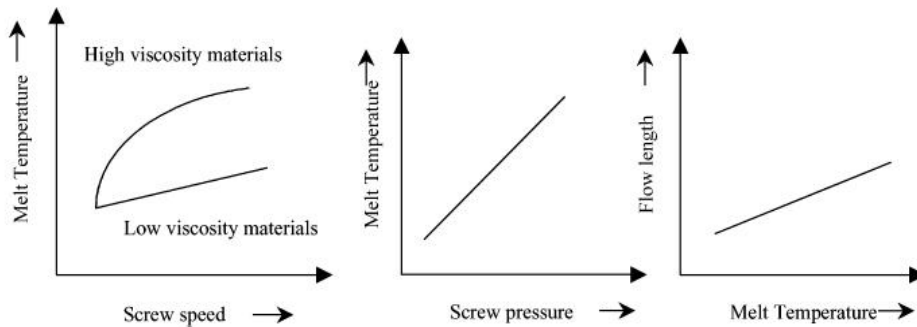


Fig. 1. Characteristics of melt temperature w.r.t screw speed, pressure and flow length.

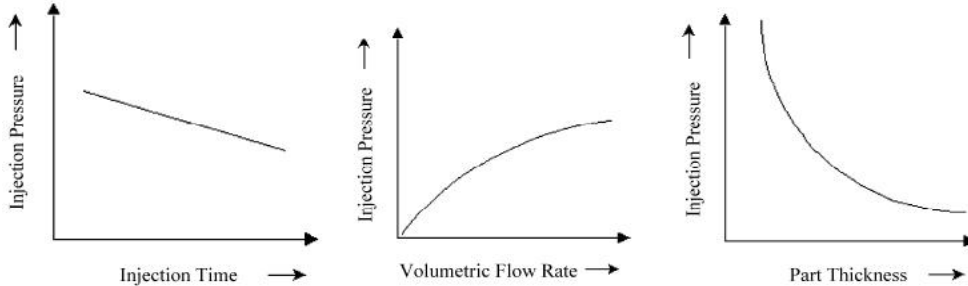


Fig. 2. Characteristics of mould temperature with injection time and injection pressure.

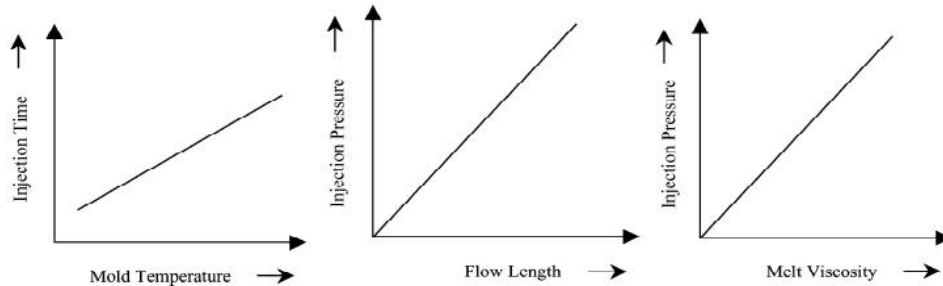


Fig. 3. Characteristics of injection pressure, flow rate and part thickness

4. CONFIGURATION OF THE NEURAL NETWORK

Neural networks are the family of artificial intelligence and can be defined as "massive parallel interconnected networks of simple (usually adaptive) elements and their hierarchical organisations which are intended to interact with objects of the real world in the same way as biological nervous systems do". Neural computation is performed by a dense mesh of computing nodes and connections. The neurons are often organised in layers and feedback connections both within the layer and toward adjacent layers are allowed. Each connection strength is expressed by a numerical

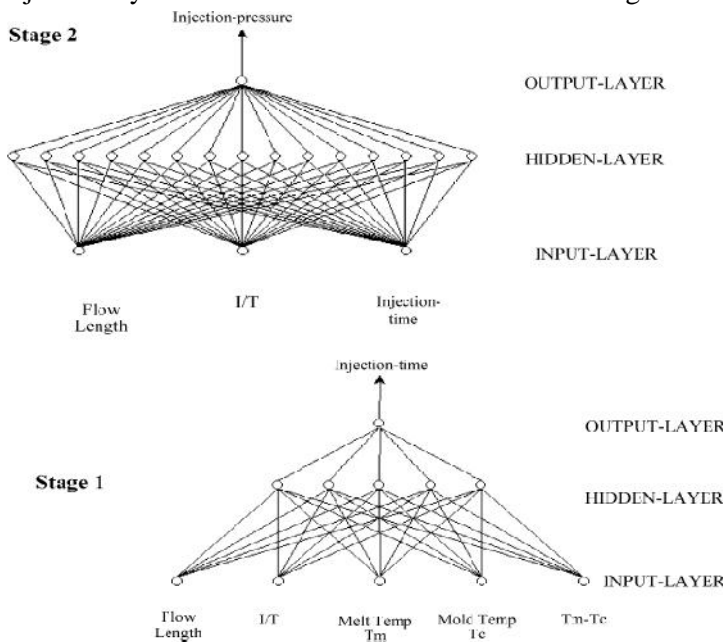


Fig. 4. Two-stage neural network system for prediction of injection time and pressure

value called a weight, which can be modified. These adjustable weights correspond to biological synapses. The weighted inputs to a neuron are accumulated and then passed to an activation function, which determines the neuron's response. One of the most attractive features of neural networks is the ability to produce an approximate solution rather than one, which is not correct when, presented with noisy or incomplete information or data.

When presented with such data, which lies within or outside the range of training data, the network will generally interpolate and degrade (properties of fuzzy logic) to

provide the best approximation [8]. The schematic representation of two-stage multi-layered feed-forward neural network for predicting injection time and injection pressure in injection moulding process is shown in Fig. 4.

In this work two specific neural network training algorithms namely, error-back-propagation, and Levenberg-Marquardt approximation (Gauss Newton) algorithm were used to train the network. The neural network in this work serves as a mapping function for injection time and injection pressure. Experts on the production floor often approximate these two parameters and with little trial and error, in order to determine the optimum operating parameters. However, the new designers rely on experts or use of simulation software for assistance. In this work, two networks were developed which were capable of approximating the function of the simulated data. The error-back-propagation and the Levenberg-Marquardt approximation algorithms were used during the training phase. However, the latter is often used due to its better convergence. The input parameters considered for the first network were melt temperature of the alloy, mould temperature, flow length, inverse function of part thickness, function of melt and mould temperatures and the output parameter predicted is injection pressure. The input parameters considered for the second network were the output of the first network, i.e. injection pressure, flow length and part thickness.

These input parameters are inter-dependent and are constantly in conflict in a very complex way. In practice, the process starts by setting up both the melt temperature and the mould temperature, then the expert will experimentally determine the injection time for the process based on the material characteristics and complexity of the part to be moulded. To eliminate the efforts of an expert, this work attempted to find the optimum injection time and injection pressure associated with a certain melt and mould temperatures by using a neural network approach. With the input parameters, the system predicts the injection time with an accuracy of 0.87% and a deviation of 3.52%, the injection pressure with an accuracy of 0.93% and a deviation of 3.93%. Fig. 5 shows a comparison of the simulated and the actual output. Initially the network was trained by considering flow length, part thickness, melt temperature and mould temperature as the input parameters and the injection time as the output parameter. After several attempts, it was found that the combination of flow length, the inverse of minimum part thickness, melt temperature, mould temperature, difference of melt and mould temperatures as the input parameters provide the best convergence. The training started with two sets of training data and finally increased to four sets of training data. Attempts to use more sets of training data and hidden-layers were made, but both did not yield better results. Instead, training cycles were longer than the initial configuration.

5. RESULTS

The initial process prior to training the network includes the analysis of governing equations of the filling stage. This is important in determining the input parameters to be collected for training the network. Training data could either be collected from experts from the industries or by simulation software packages. A total of 120 simulations were carried out, but only 114 were applicable, as six were found faulty due to incomplete filling. Out of the 114 data simulated, 94 were used for training and 20

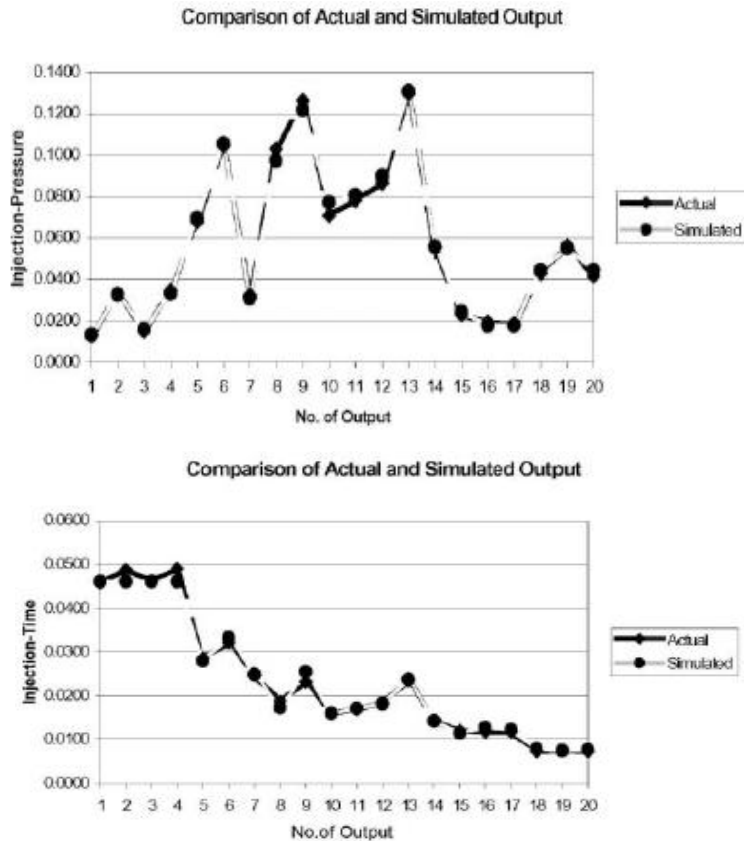


Fig. 5. Comparison of actual and simulated outputs or the injection time and pressure

The network was then changed to a two-stage neural network with the first network predicting injection time and the second network for injection pressure. How length, the inverse of minimum part thickness, melt temperature, mould temperature, the difference of melt and mould temperatures are the inputs for the first network. The output of the first network, injection time, together with flow length and the inverse of minimum part thickness are then carried over as inputs for the injection pressure network. Two algorithms were used during the training phase, namely the error-back-propagation algorithm and the Levenberg-Marquardt approximation algorithm [9]. Results show that the advanced algorithm Levenberg-Marquardt approximation was able to converge at a faster speed with lesser training cycles as compared to the error-

used to test the network. The initial intention was to develop a 5-input and 2-output network. With this proposed configuration, it was found that the network was able to predict the injection time to a certain level of accuracy, but it was giving some arbitrary numbers for the injection pressure output. This led to a revision of the structure of the entire network.

back-propagation algorithm. The Levenberg-Marquardt approximation algorithm could also achieve a lower sum-squared error. The scale of the input and output parameters is an important factor to consider when using the MATLAB [16]. Improperly-scaled values causing incompatibility may result in the network being inaccurate. During the training phase, the input and output parameters were converted to a smaller unit for compatibility. The number of repetitions for a set of data to be used during training was determined using the trial and error approach. In the case of the injection pressure network, the optimum solution was obtained by using the data set once, but randomly arranged in the matrix. On the other hand, the optimum result for the injection time network was obtained from using four repetitions of data. However, with eight repetitions of data, the results achieved were not as desirable as those obtained earlier. Table 1 shows the configuration of the network that was used in the training phases by using Levenberg-Marquardt algorithm. The optimum results were achieved by using the Levenberg-Marquardt approximation algorithm for both the networks. The first network was able to predict injection time to an accuracy of 0.91% with a deviation of 4.62% using four sets of training data and five neurons in the hidden-layer. The second was able to predict injection pressure to an accuracy of 0.93% with a deviation of 3.93% using two sets of data and 15 neurons in the hidden-layer. The graph below shows the proximity of the actual output and the simulated output of the injection time network and injection pressure network.

Table 1. Network configuration for training with Levenberg-Marquardt algorithm

2-Layer network	1st layer: hidden (Logsig), 2nd layer: output (Purelin)
Max. epochs	1000
Initial value for MU	0,001
Multiplier for increasing MU	10
Multiplier for decreasing MU	0,1
Maximum value for MU	1e10
Error goal	0,001
Number of neurons	05 input neurons, 05-20 neurons in hidden layer, 01 output neuron
Number of training data (94 data pairs per set)	2 and 4 sets

6. CONCLUSIONS

The application of artificial intelligence has assisted many operations in many fields. In this work, a neural network was developed to predict plastic injection moulding process parameters. Initially, the governing equations for mould-filling stage were analysed in order to identify the input parameters for the proposed network. The output parameters of the network developed are injection time and injection pressure. Based on the present work the following conclusions can be drawn. Moulding conditions such as melt temperature, die temperature, injection pressure and injection time dominate the quality of the part produced. The trained neural network functions as a mapping mechanism and it is capable of predicting injection time when presented with totally new operating conditions. The slow convergence and the tendency of the network to get stuck in local minima makes the gradient-descent method unsuitable for this kind of application. The Levenberg-Marquardt approximation, with its

sophisticated training algorithm, was found suitable for this application as it can reduce the sum-squared error to a very small value thus generating better accuracy of predictions. With the development of this network, any novice user without prior knowledge of the injection moulding process can carry out the selection of process parameters for injection moulding.

BIBLIOGRAPHY

- [1] **Bown J.**, *Injection Moulding of Plastic Components*, McGraw-Hill, Maidenhead, UK, 1979.
- [2] **Hung C.F., Shen Y.K.**, *Numerical simulation of fiber orientation in injection mold filling*, Int. Comm. Heat Mass Transfer 22, 1995.
- [3] **Johannber F.**, *Injection Moulding Machines, A User's Guide*, Hanser Publishing, 1985.
- [4] **Liu C., Manzione L.T.**, *Process Studies in Precision Injection Molding*, Polymer Engineering and Science, University of Massachusetts, 1996.
- [5] **Najmi L.A., Lee D.**, *Simulation of mould filling for powder injection molding processes*, Adv. Powder Metall. 3, 1990.
- [6] **Popescu M.C.**, *Rețele neuronale și algoritmi genetici utilizați în optimizarea proceselor*, Sesiunea Națională de Comunicări Tehnologice, Ediția a IX-a, Târgu-Jiu, 2001.
- [7] **Popescu M.C.**, *Optimizari în instalațiile de climatizare utilizate în incinte cu degajari de nocivități*, Ph.D. Thesis, University of Craiova, 2002.
- [8] **Popescu M.C.**, *Neuro-fuzzy control of induction driving*, 6th International Carpathian Control Congress, Miskolc-Lillafured, Budapesta, 2005.
- [9] **Popescu M.C.**, *Tracking Performance of a Quantized Adaptive Filter Equipped with the Sign Algorithm*, 7th International Carpathian Control Congress, Roznov pod Radhostem, Czech Republic, 2006.
- [10] **Popescu M.C.**, *Estimarea și identificarea proceselor*, Editura Sitech, Craiova, 2006.
- [11] **Rosato D.V.**, *Injection Moulding Handbook*, 2nd Edition, International Thomson Publishing, 1990.
- [12] **Rao K.P., Yarlagadda P.K.D.V.**, *Neural network approach to flow stress evaluation in hot deformation*, J. Mater. Process. Technol. 53, 1995.
- [13] **Shelesh-Nezhad K., Siores E.**, *An intelligent system for plastic injection moulding process design*, J. Mater. Process. Technol. 63, 1996.
- [14] **Yarlagadda P.K.D.V., Cheng W.C.**, *Artificial intelligent neural network system for pressure die-casting*, J. Mater. Process. Technol. 89-90, 1999.
- [15] **Zurada J.M.**, *Introduction to Artificial Neural Systems*, West Publishing Company, 1992.
- [16] *** User Guide Matlab for Simulink

INFORMATIC VIRUSES DETECTION USING HEURISTIC ALGORITHMS

OTILIA CANGEA*

Abstract: The paper deals with the problem of preventing electronic attacks against industrial systems, essentially referring to the problem of informatic viruses. The goal is understanding the concept of “informatic virus” and detecting the conventional informatic viruses using static and dynamic methods, as well as intelligent methods based on heuristic algorithms. A system designed for informatic viruses is software implemented in “Virus Inspector”, an original software product that verifies the characteristics of the program and estimates if that program is an informatic virus.

Keywords: informatic virus, heuristic algorithm, virus detection.

1. INTRODUCTION

In less than a generation, virtual introduction of computers has changed the way in which people and organizations obtain and exchange informations, allowing an increased efficiency, a greater operational control and a more efficient access to informations. Because computerized systems are essential for an adequate development of the majority of modern industrial activities, their security has to be an important concern for all the organizations dealing with them. Among the factors that may be considered responsible for the increase of the electronic attack risk are:

- inherent security difficulties;
- increased globalization;
- inadequate specific knowledge of the users of industrial systems [1], as well as ignoring the use of specific procedures.

Electronically stored information has a certain value. An incident that affects this information will consequently affect the industrial entity, the industrial system or the person that depends on or uses the respective informations. This is the reason why information is evaluated in relation with the possible impact of an incident that will

* Lecturer, Ph.D. at the “Petroleum-Gas” University of Ploiesti

negatively affect it. The threats, the vulnerabilities and the possible impact have to be combined in order to obtain an estimate of the risk the information is submitted to.

2. HEURISTIC ALGORITHMS FOR INFORMATIC VIRUSES DETECTION

The *informatic virus* represents [2] a program that has the ability to insert his own copies in other programmes and to cause varied effects, that range from harmless to very destructive ones. A program is considered to be a virus if :

- it modifies user programmes by inserting his own structures;
- the alterations caused refer not only to a programme, but to groups of programmes, as well;
- it recognizes an already infected program;
- if it finds an already infected programme, it forbids another modification;
- the infected programme has the same properties.

A virus is made of three components, namely the contamination part, the self-recognition part and the destructive part.

It is important to emphasize that the evolution of a virus is characterized by two stages:

- the *latent stage*, when the virus spreads itself in the system and may be detected and eliminated by specialized programmes;
- the *active stage*, when the virus is in action, fulfilling the tasks it was programmed to achieve.

Detection –or *scanning*- is finding viruses by means of checking every file.

There are two detection methods: *classic* and *heuristic*.

The *classic method* [3] generates a list of signatures -fingerprints- that define the known viruses. This list has to be daily modified, in order to recognize the new viruses. Classic detection means searching in every file of all known viruses fingerprints.

A *heuristic method* is a method that solves a problem using rules based on experience or intuition. The heuristic analysis is a small expert system that uses a set of rules that describe viruses and applies these rules to the analyzed programmes. Every analyzed file is being disassembled in order to search code sequences that may represent instructions specific to viruses, such as a request to remain memory resident or files searching. In the same time, there is a great probability that these may be false alarms –some programmes have to execute these operations, so that these are not informatic viruses.

Genetic algorithms are evolutive searching algorithms, designed in order to identify aproximative solutions of difficult problems, by means of principles derived from evolutive biology –mutation, heritage, natural selection, and crossing.

Genetic operators are those procedures that operate on the elements of the population array. There are two main genetic operators:

- a transforming *mi* operator, named *mutation*, that creates a new individual by means of a small change of a chosen individual ($mi:s \rightarrow s$);

- a more powerful operator cj , named *crossing*, that creates new individuals by combining two or more individuals ($cj:sxs...xs \rightarrow s$) (one usually uses two parents).

After a certain number of generations, the algorithm converges, that is the most promising individual reaches a value as close as possible to the optimum solution.

In order to describe the structure of a genetic algorithm one has to settle the following:

- the used chromosomes have a constant length;
- the population (generation) $P(t+1)$ is obtained by retaining all the descendants of the $P(t)$ population and by subsequently erasing of all the chromosomes of the precedent $P(t)$ population;
- the number of chromosomes is constant.

In these circumstances, the structure of the fundamental genetic algorithm is as follows:

1. $t \leftarrow 0$
2. the $P(t)$ population is randomly initialized
3. the chromosomes of the $P(t)$ population are evaluated
4. as long as the finish condition is not fulfilled, there are executed the next steps:
 - 4.1. one selects the $P(t)$ chromosomes that will contribute to forming the new generation; let them be $P1$
 - 4.2. the $P1$ chromosomes are submitted to the genetic operators (preponderant mutation and crossing operators) and the obtained population is $P2$
 - 4.3. one erases from $P1$ the parents of the obtained descendants and the chromosomes left in $P1$ are included in $P2$
 - 4.4. a new generation is built: $P(t+1) \leftarrow P2$; all chromosomes from $P(t)$ are erased; $t \leftarrow t+1$; one evaluates $P(t)$.

The finishing condition refers to obtaining the given number of generations. If the maximum admitted number of generations is N , then the condition is $t \geq N$. One considers that the algorithm result is given by the most promising individual from the last generation.

4. SOFTWARE PROGRAMS FOR INFORMATIC VIRUSES DETECTION

The software implementation of an informatic viruses detection system has been achieved using C++ *Builder*. „*Virus Inspector*” verifies the characteristics of the program and estimates if that program is an informatic virus.

In order to create an intelligent heuristic program, the genetic algorithms have been used, with the following characteristics:

- *genetic representation*: an individual representation is $(g_1, g_2, \dots, g_{10})$, where g_i may be 1, if i is a vulnerability, and 0, if i doesn't represent a risk;
- *individual representation*: the quality of an individual, C , is given by the value of the objective function that has to be maximized :

$$\sum_{i=1}^k (C_i * P_i), \quad k=10 \quad (1)$$

- *heuristic algorithm parameters*: dimension of the initial population ($n0$), maximum dimension of the population ($nmax$), maximum number of generations ($gmax$), crossing rate (cr) and mutation rate (mr).

The interface of the heuristic scanning module is presented in figure 1.

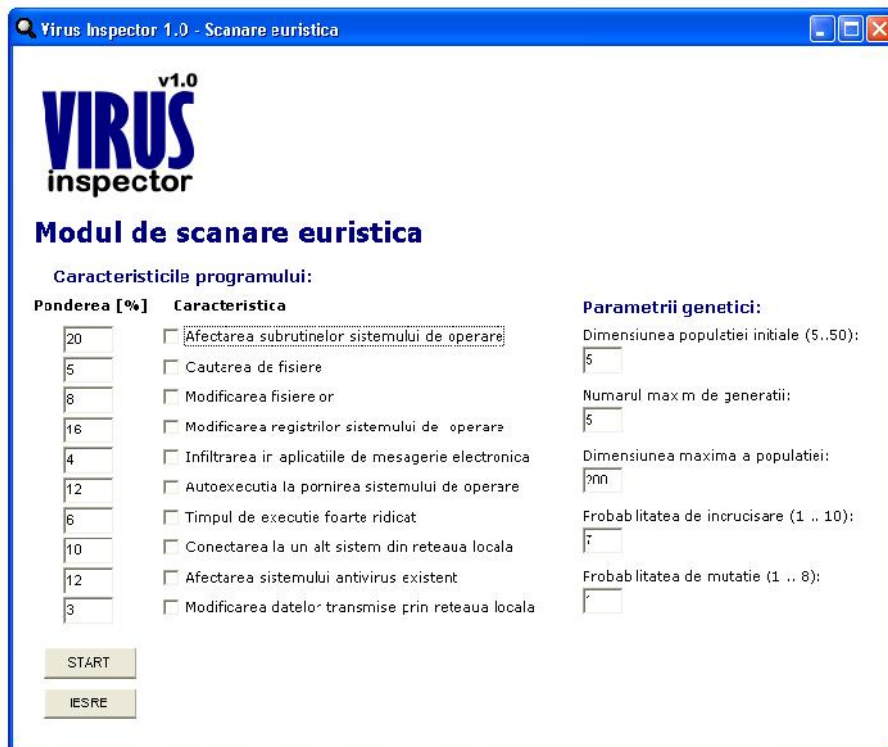


Fig. 1. Heuristic scanning interface module

The input data are the program characteristics, the weights associated to each characteristic, and the genetic parameters. One may choose the program characteristics, may modify the associated weights, as well as the parameters of the genetic algorithm.

Figure 2 presents an example for a virus program, having as input data the following characteristics:

- affecting the subroutines of the operating system
- modifying the registry of the operating system
- infiltration in the electronic mail applications



Fig. 2. An example for a virus program

In these circumstances, the scanned program is a virus. The obtained output file "c:\rezultate.txt." is presented below. Fitness is the value of the criterion function for each generated program, that reflects the performances of the respective program.

Population at 0 generation:

0 individual: (0010000111)

1st individual: (1010111001)

2nd individual: (1001000010)

3rd individual: (1110111011)

4th individual: (0010110000)

0 generation maximum fitness = 36

Population at 1st generation:

0 individual: (0010000111) fitness=0

1st individual: (1010111001) fitness=24

2nd individual: (1001000010) fitness=36

3rd individual: (1110111011) fitness=24

4th individual: (0010110000) fitness=4

1st generation maximum fitness = 36

Population at 3rd generation:

0 individual: (0010000111) fitness=0

1st individual: (1010111001) fitness=24

2nd individual: (1001000010) fitness=36

3rd individual: (1110111011) fitness=24

4th individual: (0010110000) fitness=4

3rd generation maximum fitness = 36

Population at 5th generation:

0 individual : (0010000111) fitness=0

1st individual : (1010111001) fitness=24

2nd individual : (1001000010) fitness=36

3rd individual : (1110111011) fitness=24

4th individual : (0010110000) fitness=4

5th generation maximum fitness = 36

5. CONCLUSIONS

Using "Virus Inspector", one may analyze the main problems of the heuristic algorithms. Some of the conclusions are presented below:

- the solution found by the heuristic algorithms it is not always the best one, but it is located in the proximity of the optimum solution;
- an efficient antivirus system has to be implemented in an assembling environment, that allows pursuing the effects and counteracts the disturbances that occur in the system as a result of the presence of the viruses;
- a multithreading or multitasking system may be implemented in order to significantly reduce the answer time.

BIBLIOGRAPHY

[1] Amor, D., *The E-Business (R)evolution: Living and Working in an Interconnected World*, Prentice Hall, 2001.

[2] Castano, S., Fugini, M., Martella, G., Samarati, P., *Database Security*, Addison-Wesley, 1995.

[3] Austin, R., Darby, C., *The Myth of Secure Computing*, Harvard Business Review, 2003.

[4] Dimitriu, G., *Programe antivirus*, Editura Teora, Bucuresti, 1997.

MODELING FOR INDUSTRIAL AND MANUFACTURING SYSTEMS

EGRI ANGELA*, SIRB VALI CHIVUȚA**

Abstract: Simulation modeling and analysis the process of creating and experimenting with a o computerized mathematical model of a physical system. For the purposes of this handbook, a system is defined as a collection tiled are traditional simulation and training simulators. In general, the distinction is as follows.. Examples of manufacturing systems include: machining operations, assembly operations, materials-handling equipment and warehousing. Machining operation simulations can include processes involving either manually or computer numerically controlled factory equipment for machining, turning, bending, cutting welding, and fabricating. Assembly operations can cover any type of assembly line or manufacturing operation that requires the assembly of multiple components into a single- piece of work. Material-handling simulations have included analysis of cranes, for klifts, and automatically guided vehicles, Warehousing simulations have involved the manual or automated storage and retrieval of raw materials or finished goods.

Keywords: manufacturing systems, Fishbone chart, Pareto chart.

1. OTHER TYPES OF SIMULATION MODELS

The types of simulation models previously discussed are not the only types of simulation model practitioner may encounter or have a need for. Another type of computer simulation mode computer simulator. Though the distinction between simulation models and computer simulate differ somewhat among practitioners, the following discussion may help differentiate these two simulation. Models of the systems are normally created with different resource or operating polis have been previously determined to be of interest. After the simulation runs, the output mea performance are compared between or among the models. Thus, the ultimate use or the mod make resource or operating policy decisions concerning the system. Simulators

* *Assoc.prof. univ. dr. Eng at the University of Petrosani*

** *Lecturer.ph at the University of Petrosani*

are also models of existing or proposed systems. In contrast to simulation models, and operating policy decisions are not made beforehand. These types of decisions are actual during the simulation run. Thus, the output measures are observed not only at the end of the more importantly, during the simulation run.

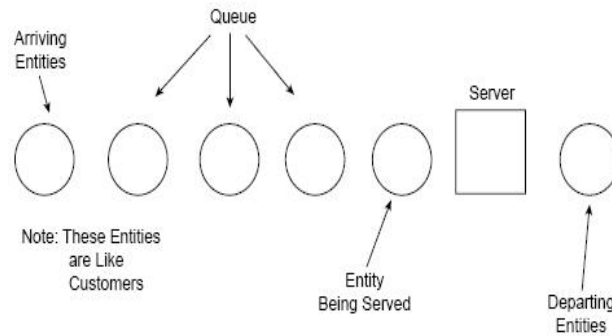


Fig. 1. Basil simulation model components

2. PURPOSES OF SIMULATION

The simulation modeling and analysis of different types of systems are conducted for the purposes of (Peden et al., 1995): Gaining insight into the operation of a system, Developing operating or resource policies to improve system performance, Testing new concepts and/or systems before implementation and Gaining information without disturbing, the actual system.

Advantages to simulation:

In addition to the capabilities previously described, simulation modeling has specific benefits. These include: Experimentation in compressed time, Reduced analytic requirements and Easily demonstrated models.

Disadvantages to Simulation:

Although simulation has many advantages, there are also some disadvantages of which the simulation practitioner should be aware. These disadvantages are not really directly associated with the modeling and analysis of a system but rather with, the expectations associated with simulation projects.

These disadvantages include the following:

- Simulation cannot give accurate results when the input data are inaccurate;
- Simulation cannot provide easy answers to complex problems;
- Simulation cannot solve problems by itself.

3. BASIC SIMULATION MODEL COMPONENTS

For demonstration purposes, consider the simplest possible system that may be of interest to the practitioner. Examples of this simple type of system would include, but not be

limited to: a customer service center with one representative, a barber shop with one barber, a mortgage loan officer in a bank, a piece of computer-controlled machine in a factory and an ATM machine. Each of these simple systems consists of three types of major components: Entities, Queues and Resources. The relationships among the components are illustrated in Figure 1.

3.1 Entities

The first type of component is an entity; something that changes the state of the system. In many cases, particularly those involving service systems, the entity may be a person. In the customer service center, the entities are the customers.

Entities do not necessarily have to be people; they can also be objects. The entities that the mortgage loan officer deals with are loan applications. Similarly, in the factory example, the entities are components waiting to be machined.

3.1.1. Entity Batches

The number of entities that arrive in the system at the same given time is known as the batch size. In some systems, the batch size is always one. In others, the entities may arrive in groups of different sizes. Examples of batch arrivals are families going to a movie theater. The batch sizes may be two, three, four, or more.

3.1.2. Entity Interarrival Times

The amount of time between batch arrivals is known as the interarrival time. It does not matter whether the normal batch size is one or more. We are interested only in the interval from when the last batch arrived to when the next batch arrives. The previous batch may have had only one entity, whereas the next batch has more than one. Interarrival time is also the reciprocal of the arrival rate. In collecting entity arrival data it is usually easier to collect the batch interarrival time.

3.1.2 Entity Attributes

Entities may also possess attributes. These are variables that have values unique to each entity in the system. Even though the entity attribute will have the same name, there could be as many different values as there are entities. An example of an attribute of this type involves the entity's arrival time. Each entity's attribute `ARRTIME` would store the simulation system time that the entity arrived in the system. So, unless a batch of entities arrived at the same time, each entity would have a unique value in its attribute `ARRTIME`. Some entity attributes may have the same value. In the case of airline passengers, the attribute `PASSTYPE` could hold a value corresponding to the type of passenger the entity represents. A value of 1 in `PASSTYPE` could represent a first-class passenger, and a value of 2 could represent a coach-class passenger. Simulation programs may also utilize global variables. Global variables are not to be confused with entity attributes. These variables differ from entity attributes in that each global variable can maintain only one value at a given time. A typical

use of a global variable in a simulation program is the variable that keeps track of the simulation run time.

4 TOOLS FOR DEVELOPING THE PROBLEM STATEMENT

There are two common tools available to the practitioner for assisting with the problem statement. These are not actually problem-solving tools but rather are problem identification tools. Although these tools were originally developed for the manufacturing environment, they can easily be adapted to other sectors of industry. These tools are:

- **Fishbone chart;**
- **Pareto chart.**

4.1 Fishbone Chart

The Fishbone chart is also known as the cause-and-effect diagram, man-machine-material chart, and as the Isikawa chart (Suzaki, 1987). The purpose of this chart is to identify the cause of the problem or effect of interest. The Fishbone chart looks similar to the bones of a fish. The head of the fish is labeled with the problem or effect. Each major bone coming out of the spine is a possible source or cause of the problem. For example, in a manufacturing process there are major bones for man, machine, material, and methods. This is illustrated in Figure 2.

Off each of the major bones the practitioner is to add additional subbones. For the man bone, this might include supervisors, shift 1, shift 2, etc. It may also include other people such as maintenance or engineering. For the materials bone, the fish would include subbones for all of the raw materials that are present in the process. For the machine bone, the fish would have a subbone for each major piece of equipment involved in the manufacturing process. Finally, the method bone would have subbones for the work methods for the different manufacturing processes.

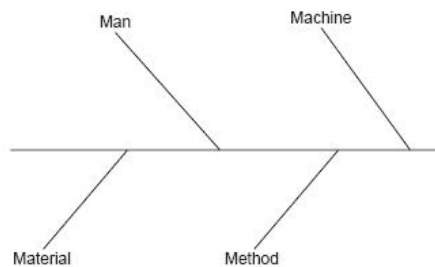


Fig. 2. Fishbone chart

4.2 Part-to Chart

The Pareto chart is a second technique to help the practitioner to develop the problem statement (Nahmias, 1987). Interested in increasing the quality of a manufacturing operation. By performing the wishbone diagram analysis, you have narrowed down the quality problem to a particular segment of the manufacturing process. Defects can be a result of variations in temperature, humidity, product age, or worker error. Depending on the severity of the defect, the product may be reworked or have to be scrapped. If the product is reworked, additional cost is entailed to disassemble the product and repeat the defective part of the process. If the product is scrapped, loss is associated with both the raw materials

particular segment of the manufacturing process. Defects can be a result of variations in temperature, humidity, product age, or worker error. Depending on the severity of the defect, the product may be reworked or have to be scrapped. If the product is reworked, additional cost is entailed to disassemble the product and repeat the defective part of the process. If the product is scrapped, loss is associated with both the raw materials

and the work invested in the part up to the tune that it is declared defective. To implement a Pareto chart, you would need to know the number of defects, from each source and the cost associated with the detect. If these are multiplied together, the true cost of each defect can be determined. It is possible to end up with four general combinations of true costs: Large number of inexpensive, easily repairable defects; Large number of expensive defects or a nonrepairable prouduct; Small number of inexpensive, easily repairable detects; Small number of expensive defects or a nonrepairable product.

5 SIMULATION PROJECT NETWORK EXAMPLES

We use tin AOA approach to illustrate one possible network for part of a simulation project (Fig. 3). In this network, the are correspond to the following first-level project tasks:

A = Problem statement; B = Protect planning; C = System definition;D = Input data;E = Model translation; F = Verification; G = Validation; H = Experimental design;

In this particular simulation project network model, we begin by simultaneously working on activity A, the problem formulation phase, and activity B, the project plan. We can begin the project planning before completing the problem formulation phase because we are already familiar with most of the simulation protect tasks However, before we can reach event node 3 to begin activity C, the system definition, we must complete both activity A. the problem formulation, and activity B, the protect plan. Once both of these are completed at node 3, we can proceed with activity C, the system definition, When we complete activity C, the system definition, we know what we need to model, and we know what data need to be collected. We can begin these tasks at the same time as represented by activity D, input data, and activity E, model translation. While we are building the model, we can use dummy or estimate input data until the actual data are ready. When both activity D input data, and activity E, model translation, are compete, we reach event node 6. With the initially complete, model, we are in the verification phase represented by activity F. On the completion of activity F, verification, we are at event node 7. With the verified model, we can begin the

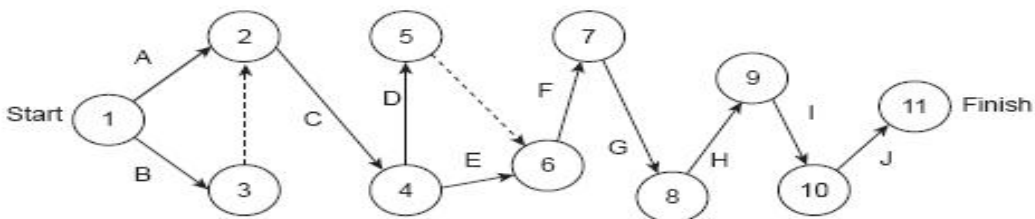


Fig. 3. Simulation project network

validation process represented by activity are G.

6. CALCULATING TIN- CRITICAL PATH

Once we have developed our AOA network and have estimated the duration of each activity arc in the network, we can consider calculating the critical path through the network. As we have previously defined, the critical path is the list of activities that, if delayed, will extend the overall length of time to complete the project. To compute the critical path, we will need to calculate the following values for each activity in the network: ES = Earliest start time, EF = Earliest finish time, LS = Latest starting time, LF = Latest finish time. For each of the activities in the network, we can easily calculate the earliest finish time as: $EF = ES + \text{task duration}$. Similarly the latest start time for each of the activities in the network can be calculated with the following equation: $LS = LF - \text{task duration}$. In the simplest implementation of calculating the critical path, we can use deterministic estimates of each of the activity durations (table nr. 1.). For our activities we can use:

Table 1. Activity duration

Activity	Task	Duration
A	Problem formulation	5
B	Project planning	2
C	System definition	5
D	Input data collection and analysis	25
E	Model translation	20
F	Verification	10
G	Validation	5
H	Experimental design	2
I	Analysis	10
J	Conclusion, report, presentation	10

We now begin our calculations with a chart with the following headings: Activity, Duration, Predecessor, ES and EF. The critical path can be identified by the activities with 0-day values in the slack column. This means that the critical path is: Activity A- Problem formulation, Activity C- System definition, Activity D - Input data collection and analysis, Activity F- Verification, Activity G –Validation, Activity H- Experimental design, Activity I- Analysis and Activity J- Report and presentation.

BIBLIOGRAPHY

- [1]. **Regh J.** *Introduction to robotics in CIM systems*. Prentice Hall, U.S.A, 2004.
- [2]. **Pop E.** *Microcontrollere si automate programabile*. E.D.P, Bucuresti, 2003.
- [3]. **Nolfi, S. Floreano, D.** *Evolutionary Robotics: The Biology, Intelligence, and Technology of Self-Organizing Machines*, MIT Press, 2000 .
- [4]. **Stout, B.** *The Basics of A* for Path Planning*. In: *Game Programming Gems*, 2000.
- [5]. **Calin S.** *Conducerea adaptiva si flexibila a proceselor industriale*. E.T, Bucuresti, 1998.
- [6]. **Levine, D.L.** - *Introduction to Neural and Cognitive Modeling*, 2nd Edition, Lawrence Erlbaum Associates, London, 2000

NEURAL NETWORK TECHNIQUES FOR MOBILE ROBOT NAVIGATION

CRISTINA POPESCU*

Abstract: To control a dynamic system it may be necessary to use some knowledge or model of the system to be controlled. The kinematics and dynamics of the robot may be complex and non-linear, and the interaction between the vehicle and the terrain may be hard to model in general. These problems determine to use neural network techniques for navigation. This paper presents some issues about neural network in general, and how these are used to control the mobile autonomous robot. The control architecture based on neural network enables the robot to perform several basic operations like obstacle avoidance, target following and local navigation in real world environments.

Key words: neural network, autonomous mobile robot, obstacle avoidance.

1. INTRODUCTION

One of the most important problems in the design of intelligent mobile robot is the navigation problem. This dwell in ability of a mobile robot to plan and execute motion without collision within its environment. This environment may be dynamical, unknown or non-structured and the robot must be able to understand the structure of this environment. For these capabilities it is necessary that the robots have perceptions, recognition, data processing, learning and action capacities. To achieve autonomy the robot must have an onboard system that deduce information about robot coresponding to the environment and a control system based on the algorithms that process this information in order to generate commands for robot. In this paper we give a brief overview of common artificial neural networks and their applications to mobile robots.

* *Lecturer, at the Petroleum – Gas University of Ploiesti*

2. NEURAL NETWORKS

Artificial Neural Networks are mathematical algorithms that are able to learn mappings between input and output states through supervised learning, or to cluster incoming information in an unsupervised manner.

Every neural network has two components: nodes, also known as neurons and connections between nodes, also known as synapses. The neurons are connected with each other via synapses. Each synapse has a weight attached. The output of a neuron is usually calculated with a function such as:

$$y_k = f\left(\sum_{j=0}^m w_{kj} * x_j\right) \quad (1)$$

where y_k is the output of the neuron, f is an activation (transfer) function, w_{kj} is the weight attached to synapse j for the neuron k , and x_j is the input signal of the neuron.

In [4] is presented the McCulloch and Pitts Neurons and the Perceptron learning rule and their implementation in obstacle avoidance behavior for mobile robot navigation.

McCulloch and Pitts Neurons

The McCulloch and Pitts neuron is shown in figure 1.

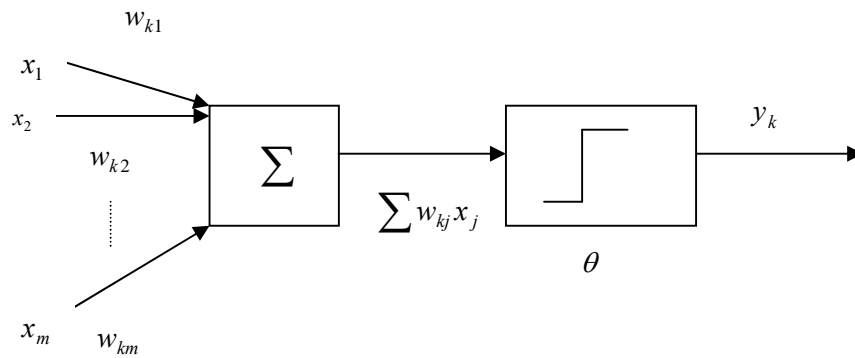
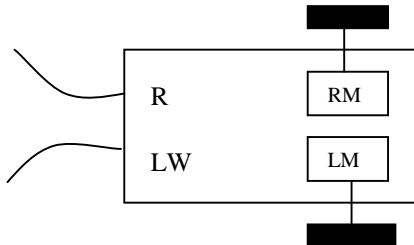


Fig.1. McCulloch and Pitts neuron.

The neuron computes the weighted sum $\sum w_{kj} x_j$ of all m inputs. This weighted sum is then compared with a fixed threshold θ to produce a final output y . If $\sum w_{kj} x_j$ exceeds θ , the neuron is “on” ($y=1$), if $\sum w_{kj} x_j$ is below the threshold, the neuron is “off” ($y=0$).

Obstacle avoidance using McCulloch and Pitts Neurons:

A robot as shown in figure 2 is to avoid obstacles when one or both of the whiskers trigger, and move forward otherwise.



Whiskers LW and RW signal “1” when they are triggered, “0” otherwise. The motors LM and RM move forward when they receive a “1” signal, and backwards when they receive a “-1” signal. The truth table for obstacle avoidance behaviour is shown in table 1.

Fig. 2. A simple robot.

Table 1

LW	RW	LM	RM
0	0	1	1
0	1	-1	1
1	0	1	-1
1	1	don't care	don't care

This function can be implemented using McCulloch and Pitts neuron for each motor, using neurons whose output is either “-1” or “+1”. In this example it will be determined the necessary weights w_{RW} and w_{LW} for the left motor neuron only. It was chosen for the threshold θ -0.01 value.

The first line of the truth table stipulates that both motor neurons must be “+1” if neither LW nor RW fire. Because it was chosen a threshold of $\theta = -0.01$ this is fulfilled.

Line two indicates that w_{RW} must be smaller than θ for the left motor neuron. It was chosen $w_{RW} = -0.3$.

Line three of the truth table indicates that w_{LW} must be greater than θ and it was chosen $w_{LW} = 0.3$.

These weights already implement the obstacle avoidance function for the left motor neuron. The functioning network is shown in figure 3.

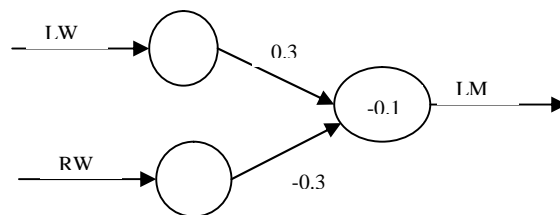


Fig.3. Left – motor node for obstacle avoidance

For more complicated functions determining weights is very hard and it is desirable to have a learning mechanism that would determine those required weights automatically.

The *Perceptron* is a network consisting of McCulloch and Pitts neurons that fulfils this requirement.

Perceptron

The Perceptron is a “single-layer” artificial neural network that is easy to implement, low in computational cost and fast in learning. It consists of two layers of units: the input layer (which simply passes signals on) and the output layer of McCulloch and Pitts neurons (which performs the actual computation).

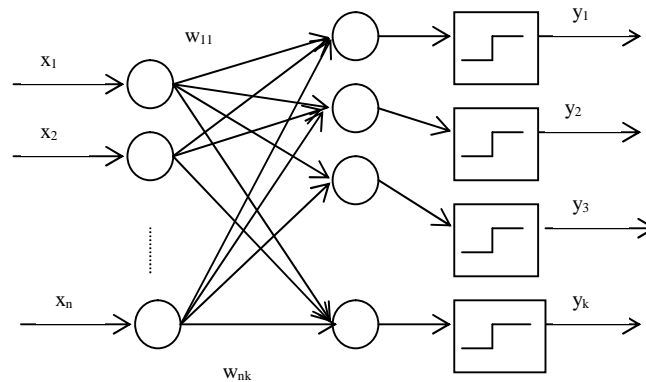


Fig. 4. Perceptron.

The perceptron learning rule

The rule for determining the necessary weights is very simple, it is given in equation (2).

$$\Delta \vec{w}(t) = \eta(t) \cdot (\tau_k - y_k) \cdot \vec{x} \quad (2)$$

$$\vec{w}_k(t+1) = \vec{w}_k(t) + \Delta \vec{w}_k \quad (3)$$

with τ_k being the target value for unit k (i.e. the desired output of output unit k), and y_k the actually obtained output of unit k . The speed of learning is determined by the learning rate $\eta(t)$. The learning rate η is usually chosen to be constant, but may be variable over time.

Obstacle avoidance using a perceptron

It will be consider the same example it has considered before: obstacle avoidance. The difference this time is that it will be use a Perceptron, and that will be determine the required weights using Perceptron learning rule (given in equations 2 and 3).

Let η be 0.3 and θ be -0.01 . The two weights of the left – motor node are zero to start with. This initial configuration is shown in figure 5.

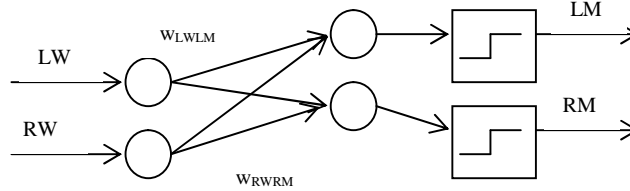


Fig. 5. Layout of a perceptron for obstacle avoidance.

It was applied equations (2) and (3) line by line through the truth table 1 and it was obtained:

Line one $w_{LWLM} = 0 + 0.3 \cdot (1 - 1) \cdot 0 = 0$
 $w_{LWRM} = 0 + 0.3 \cdot (1 - 1) \cdot 0 = 0$
 $w_{RWLM} = 0 + 0.3 \cdot (1 - 1) \cdot 0 = 0$
 $w_{RWRM} = 0 + 0.3 \cdot (1 - 1) \cdot 0 = 0$

Line two $w_{LWRM} = 0 + 0.3 \cdot (1 - 1) \cdot 1 = 0$
 $w_{RWLM} = 0 + 0.3 \cdot (-1 - 1) \cdot 1 = -0.6$
 $w_{RWRM} = 0 + 0.3 \cdot (1 - 1) \cdot 1 = 0$
 $w_{LWLM} = 0 + 0.3 \cdot (1 - 1) \cdot 1 = 0$

Line three $w_{LWRM} = 0 + 0.3 \cdot (-1 - 1) \cdot 1 = -0.6$
 $w_{RWLM} = -0.6 + 0.3 \cdot (1 - 1) \cdot 0 = -0.6$
 $w_{RWRM} = 0 + 0.3 \cdot (-1 - 1) \cdot 0 = 0$

The final network is shown in figure 6. A quick calculation shows that this network already performs the obstacle avoidance function.

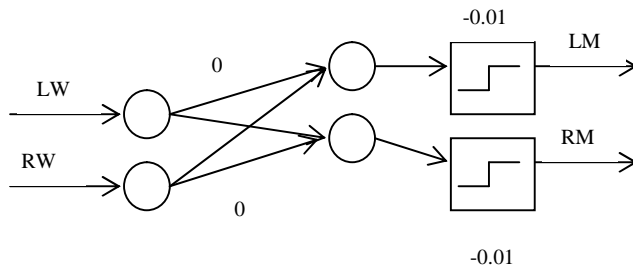


Fig. 6. Final network for obstacle avoidance.

3. CONCLUSIONS

Many functions robots have to learn are linearly separable, which means that the very fast learning Perceptron can be used for robot learning. In fact, its speed is the major advantage of the Perceptron over networks such as the Multilayer Perceptron or Backpropagation Network.

This paper presents a very simple ways to implement and use neural networks for the purpose of control a mobile robot for obstacle avoidance behavior. It is necessary to find a neural network which perform more behaviors, like wall following, or achieve a target and to test different parameters in neural network with the aim of reaching the optimal time for finding the safe path.

BIBLIOGRAPHY

- [1]. **Arkin, R.C.**, *Behavior –Based Robotics*, MIT Press, 1998.
- [2]. **Janglova, D.**, *Neural Networks in Mobile Robot Motion*, pp.15-22, International Journal of Advanced Robotic Systems, Volume 1, Number 1, 2004.
- [3]. **Martin, P., Nehmzow, U.**, *Programming by Teaching: Neural Networks Control in the Manchester Mobile Robot*, Intelligent Autonomous Vehicles 95, Helsinki, June1995.
- [4]. **Nehmzow, U. (2000)**. *Mobile Robotics: A Practical Introduction*, Springer Verlag London.

PROGRAM CONCEIVED IN THE VISUAL STUDIO.NET MEDIU, FOR A CAPITAL DEVALUATION CALCULATION AND DISPLAYING

VALENTIN CASAVELA*

Abstract: The program contains both a graphic interface, where the user may input the dates referring to the capital, which he possesses, and calculations for its devaluation. The formula may be modified, in accordance with the economical medium, in which you work and the program may use it in a adequate manner. We suppose that the Visual Studio.Net packet was installed on your computer.

Keywords. devaluation, deadtime, activevalue, percentage, textboxe

1. THE CONCEIVING OF THE PROGRAM

If we note with `ActiveValue` for the capital value to the initial moment, with `Percentage of devaluation` (abbreviated `P%`, being divided by 100) and `Deadtime` for the number of years, from the moment of the obtaining the capital, till its out of use (in the below formula it appears `nr_years`, but, in the program, `Deadtime` is the upper limit of a cyclic sequence), then the calculations for the dev devaluation formula is the next::

$$\text{dev} = \text{ActiveValue} * (\text{P}\%) * [(1 - (\text{P}\%))^{\text{nr_years} - 1}] \quad (1)$$

Execute double click on the icon with sign 8 overturned and you will obtain the main menu, and, after that, select **File...New...Project**, appearing another window, in which select **Project Types ...Visual C# Projects...Templates... Windows Application...Name....**and type **Capital_Devalorization**. Be continuing by selecting **Brows,...Location..C:\Documents and Settings\valy\My Documents\Visual Studio**

* *Lecturer, Ph.D. at the University of Petroșani*

Projects, or other convenient location. Execute click on **O.K.** It appears the window with the new project.

From the menu **Proprieties** select **Text**, in which write the name **Devaluation**, for the main form. Be continuing with **ToolBox**, where select and drag in the form four controls: **TextBox1**, **TextBox2**, **TextBox3**, **TextBox4**. Select all four with the combination **Ctrl+Click**, and, after that, from the menu **Format...Align..Right**, align right. For the **TextBox4** control you may select **Proprieties...Multiline...True**, obtaining the multi lines writing, inside this.

To be continuing, build other controls too. Three labels are obtained from: **ToolBox...label1...Text...Active Value** (the label name), then **label2...Text...Devaluation Percent** (the label name), respectively **label3,.. Dead Time** (name). We need still a **checkbox** control, which selection will permit to print to a printer. So, select **ToolBox...checkbox1..Text...Print to file** (name). The last control needed is a button, from where we shell command the calculation. So, select again **ToolBox...button1...Text...Calculation**.

Till now, we used the drag-and-drop technique and we achieved the figure below -**figure1**. But we will clean the names from the textboxes, because here the user will input the capital value, its percentage of devaluation and the number of years, while the capital is used, after which it is considered out of use (dead). It may be observed that we enlarged the forth textbox, because it will contain more text lines, having, otherwise, set the multi lines propriety, as we have shown.

After we achieved that, in the main menu, we select **View....Code** and it will appear at once the code, offered by the Visual Studio.NET programming medium., code which reflects all the operations, made till now. But we must added to this code some programming lines too, for performing the calculations, mentioned above. Under the figure1, it may be seen also the first added line code, highlighted with bold. It is the namespace IO, which allows the performing of a text file, with the calculation results.

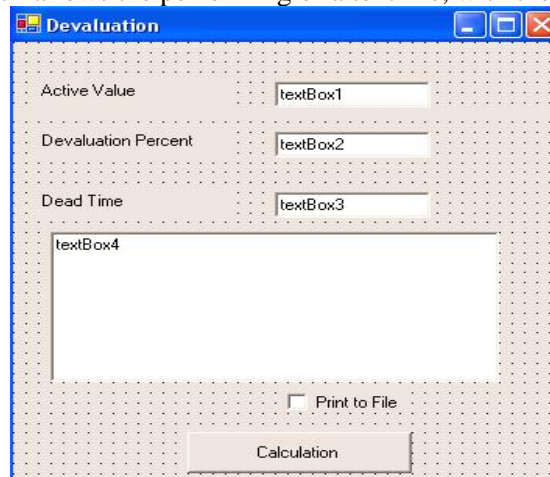


Fig.1

```
using System;
using System.Drawing;
using System.Collections;
```

```
using System.ComponentModel;
using System.Windows.Forms;
using System.Data;
using System.IO;
```

But come back to the previous window, executing double click on **Form1.cs[Design]**. Select **button1**, then, in **Proprieties**, the yellow light (that is the events icon), then double click on **Click**. It appears a program sequence, where it may be added the code:

```
private void button1_Click(object sender, System.EventArgs e)
    {
        double ActiveValue;
        double Percentage;
        double Deadtime;
        double temp;
        double dev;//variables in double precision, utilized sequel.
        string st1,st2;
        string str="";
        string lc="\r\n";//string significant a CR and a LF
        string forms;//string which will be used for concatenation of
```

the above
//strings.

```
        Double[]obj=new Double[1];//the double precision values array //definition, which array, in fact, contains a single one.
```

```
        ActiveValue=double.Parse(textBox1.Text);//it takes in the //ActiveValue capital, the value inputted by user in the first textbox. The text is "translated" //....Perse, in double value, called ActiveValue.
```

```
        Percentage=double.Parse(textBox2.Text);//analogous for the second //textbox.
```

```
        Deadtime=double.Parse(textBox3.Text);//...and for the third textbox.
```

```
        temp=Percentage/100;//in the temp variable is written the devaluation //value, inputted by user, but divided by 100, for representing the percentages
```

```
        for(int i=1; i <= Deadtime; i++)//in cyclic sequence are calculated the //yearly devaluations.
```

```
        {
            dev=ActiveValue * temp * Math.Pow(1-temp, i-1);
```

//expression in language of the formula enounced above.

```
            obj[0]=dev;//in the single array component is loaded the //devaluation from every year.
```

```
            forms="{0:#.00}";//a string which will served to the //devaluation will be printed with a single integer position and two decimals.
```

```
            st1=i.ToString();//the i variabila, that is the past years, becomes string of characters
```



```

st2=string.Format(forms,obj[0]);//also for the vector
//component.
str +=st1+"\t\t" + st2 + lc;//the string str will
compound the //characters for years, two pauses (tab), the string of numbers for
devaluation and the new line //with carry return , new line where the next year values
will be printed.
    }
textBox4.Text=str;//the complete characters string, obtained
above, is
// printed in the forth textbox.
if (checkBox1.Checked)//if the verifying box is selected too,
then...
    {
        FileStream afs=new
FileStream("Desktop:\\devaluation",
FileMode.Create, FileAccess.Write);//...a stream is
directed to
//a file location, file called devaluation, which is created on the Desktop, where...
StreamWriter sw=new StreamWriter(afs);
sw.WriteLine(str);//...the characters, printed above,
are written.
sw.Close();//it is closed the characters stream.
    }

```

For a 100\$ capital, with a devaluation of 10% per year, in 5 years, they are obtained 5 successive devaluations, as it is shown in the figure 2, above:

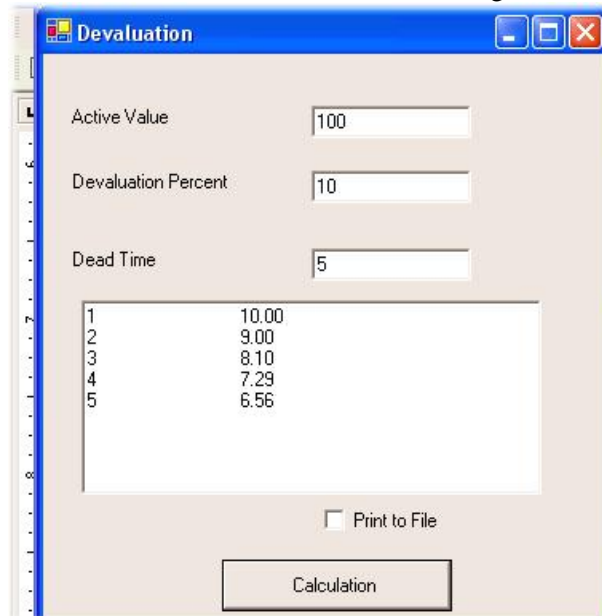


Fig. 2

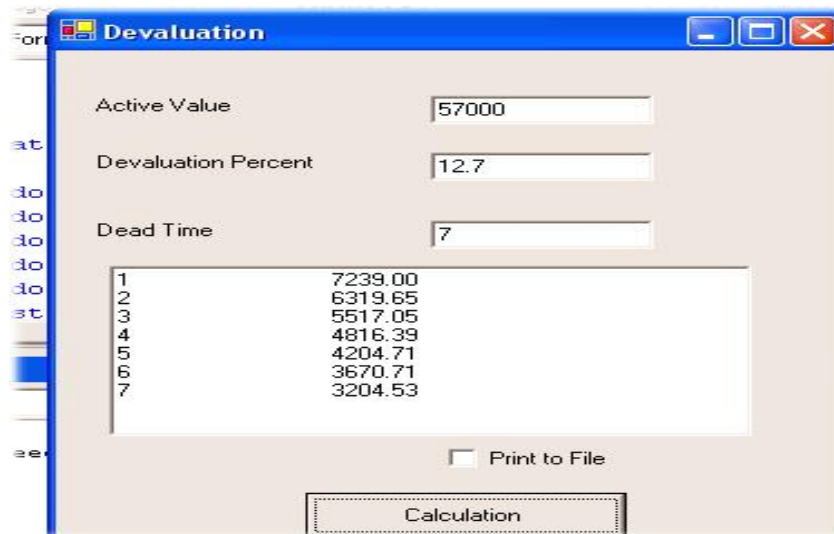


Fig.3

The greatest devaluation may be noted in the first year, and the smallest, in the last

In sequel, it goes off a 57,000 \$ capital, with a percentage devaluation of 12.7%, while 7 years. You may note that the program may be used in more complicated calculations

BIBLIOGRAPHY

[1] **Chris H. Pappas, William H. Murray**, *C# pentru programarea WEB*, Editura B.I.C. ALL-Timisoara, ISBN 973-571-472-8

[2] **Takatsuka, M and Gahegan, M.** : 2002 *GeoVISTA Studio: A Codeless Visual Programming Environment for Data Analysis and Visualization*. *Computers & Geosciences* 28(10): 1131-1144.

RENEWABLE ENERGY RESOURCES POSIBILITIES USE IN JIU VALLEY

EMIL POP*, IOANA CAMELIA TABACARU BARBU**, MARIA POP***

Abstract: In this paper are presented the main renewable energy resources. Based on these sources it is designed an integrated renewable and sustainable energetic park. The Jiu Valley is a properly place for implement an integrated renewable and sustainable energetic park and we present in this paper a real place where is possible to implement this park. The energetic park consists of wind turbines, hydro turbine, solar panels, and biomass power plant. We can reduce or eliminated the impact of greenhouse effect on Earth by using the renewable resources for producing electrical energy and by a good management of these resources.

Keywords: renewable resources, sustainable management, modeling and simulation, integrated renewable and sustainable energetic park.

1. THE POWER PLANT BASED ON RENEWABLE RESOURCES

Will be present the principles of clean energy power plant and its application. We insist on hydro, wind, solar and biomass installations, which should be applied to the local microclimate level and in the integrated systemic environment.

The hydropower plant

The possibilities to use hydro energy depend on the geographical and climate conditions. Several countries have a great potential in hydro electricity production, like: Norway – 99% from total electricity production, Austria – 76%, Switzerland – 62%, Sweden – 47%. The hydro-plants depend on the hydrological cycle, in which the water evaporated from the seas and oceans, due to solar energy, falls back on Earth as rain or snow.

The micro hydropower plants consist in the next components (fig.1):

- Source of water – an river or irrigation channel;

* *PhD. Professor Eng. at the University of Petrosani*

** *Assistant Eng. at the University of Petrosani*

*** *PhD. Professor Eng. at the University of Petrosani*

- Penstock – water flow from reservoir to the turbine through a long pipe named penstock;
- Turbine and generator – the turbine transform the hydraulic power in the mechanical power and the generator transform the mechanical power in the electrical power;

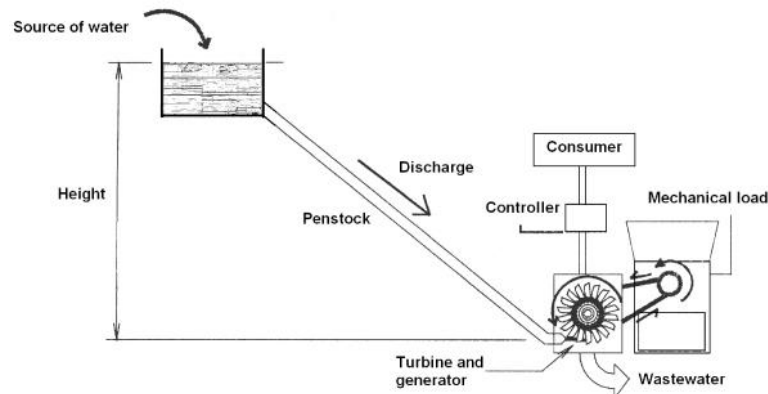


Fig.1. Hydropower plant

- Controller – make the produced energy matched with the needs of consumers;
- Mechanical load – a machine, like water mill connected at the turbine by the driving belt which used the mechanical power of the turbine;
- Consumers – any equipment which consume the electrical power.

The wind turbine power plant

The use of wind energy is very popular in electricity generation, this technology is non pollutant and the available potential is very high in many countries. This technology proved to be viable and economical. In most of the cases the production costs are comparable to conventional energy cost or even below it. In Germany, Denmark and Spain the wind energy is the main renewable energy source.

The major components of wind turbine power plant are given in fig.2.

- Wind energy is transformed into mechanical energy by means of a wind turbine that has one or several blades (three is the most usual number).
- The turbine coupled to the generator by means of a mechanical drive train. It usually includes a gearbox that matches the turbine low speed to the higher speed of the generator. New wind turbine designs use multi-pole, low speed generators, usually synchronous with field winding or permanent magnet excitation, in order to eliminate the gearbox. Some turbines include a blade pitch angle control for controlling the amount of power to be transformed. Stall-controlled turbines do not allow such control.
- Wind speed is measured by means of an anemometer.

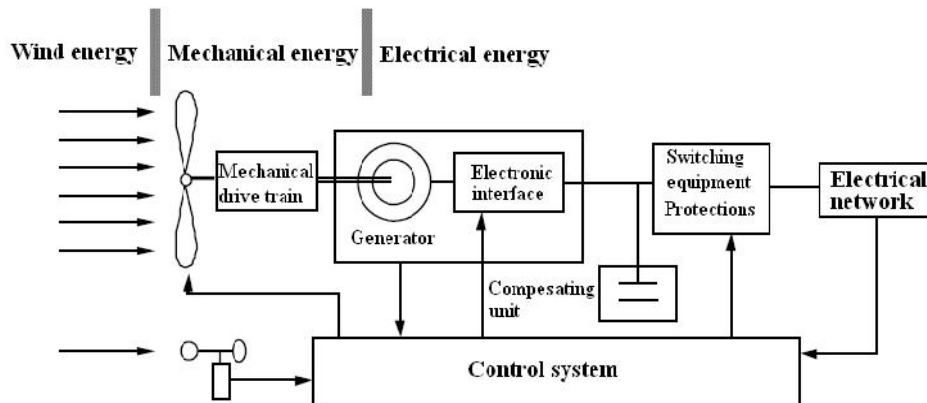


Fig.2. The wind turbine power plant

- The electrical generator transforms mechanical into electrical energy. The generator can be synchronous or asynchronous. In the first case, an excitation system is included or permanent magnets are used. Variable speed systems require the presence of a power electronic interface, which can adopt very different configurations.
- The compensating unit may include power factor correction devices (active or passive) and filters. The last ones may be necessary when there are electronic devices connected to the electrical network.
- The switching equipment should be designed to perform a smooth connection, a requirement usual in standards. Standards also specify some protections that, at least, must be present in the generating unit.
- Finally, the control system may have different degrees of complexity.

The solar cells power plant

The active use of solar energy by photovoltaic effect means the direct change of solar radiation in electricity. This is a completely new technology that was possible due to semiconductors technology improvements. The solar energy is used in Spain, Greece and Sweden.

The global solar radiation (fig.3.a) has three major components: the direct radiation, the reflected radiation and the diffused radiation. The direct radiation is the solar radiation received from the sun without being diffused by the atmosphere. The diffused radiation is the solar radiation diffused in all directions at the transit of the solar radiation through the atmosphere. The reflected radiation is the solar radiation reflected on the surface and absorbed by the solar panel.

The major components of the solar cells power plant (fig.3.b):

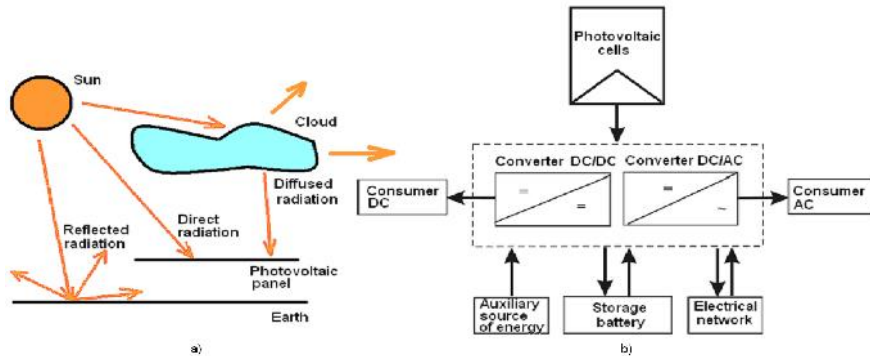


Fig.3 a) Solar radiation; b) The solar power plant

- The photovoltaic cells;
- Storage battery;
- Converter DC to DC/AC ;
- Auxiliary source of energy.

The biomass based power plant

The *biomass* is organic matter. It can be used directly as fuel for burning, indirectly by fermentation causing the change in alcohol or by extracting the fuel oils. The production of biomass does not represent only a renewable energy source but also an important opportunity for sustainable development of rural places. Now, in the European Union, 4% of the energy comes from biomass. The biomass based power plant is presented in fig.4.

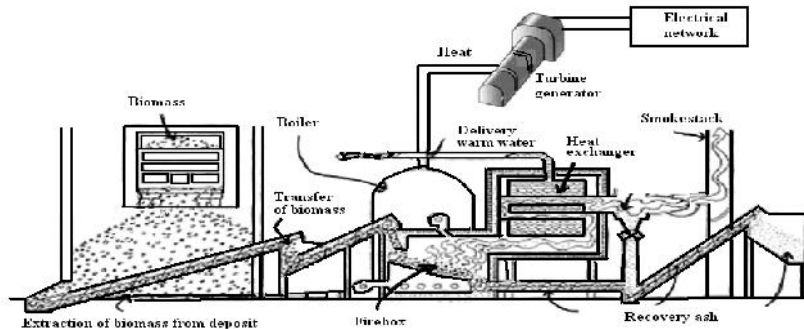


Fig.4. The biomass based power plant

2. RENEWABLE ENERGY RESOURCES POSIBILITIES USE IN JIU VALLEY

The Hunedoara district, where is placed Jiu's Valley, is located in south-west of Transilvania and contains parts of Mures and Jiu river basins.

The upper part of the Parang mountain could hold wind facilities because of strong winds almost all over the year, has the aspect of a high surface (1800-2000 m), dominated by several peaks over 2200 m.

From climacteric point of view, Hunedoara district is characterized by a mountain climate with 8 wet and cold months and 4 temperate ones in the upper zone, 5 wet and cold months and 7 temperate ones in the middle zone and a hill moderate continental climate in the rest of the district, with 4 wet and cold months and 8 temperate ones. Winters are relatively wet; summers are sunny, with a balanced rainfall regime.

The air wetness has a small gradient in the vertical scale: it rises from 74-75 %, at the mountain base, to 85-87 % on the peaks, with maximum values in May-June (90-92 %) and minimum ones in October (under 80 %). The air dryness phenomenon, caused by water vapor content lowering in the air, appears on the peaks mostly in autumn. The frequency of fuzzy days is 55-75 days at the mountain base and rise to 250 days at 1800 m and almost 300 days on the highest tops.

The dominant winds have a northern, northeastern component, their yearly frequency is growing with the altitude reaching 94-95% on the tops, where the calm weather is an exception; in the unexposed valleys the calm weather is 40-60 %. The wind speed also rising with the altitude, from 2-3 m/s at the mountain base to 10-11 m/s, even 14 m/s on tops.

The Jiu's Valley is a mountain zone, with strong winds, very well suited for wind farms to produce electric energy.

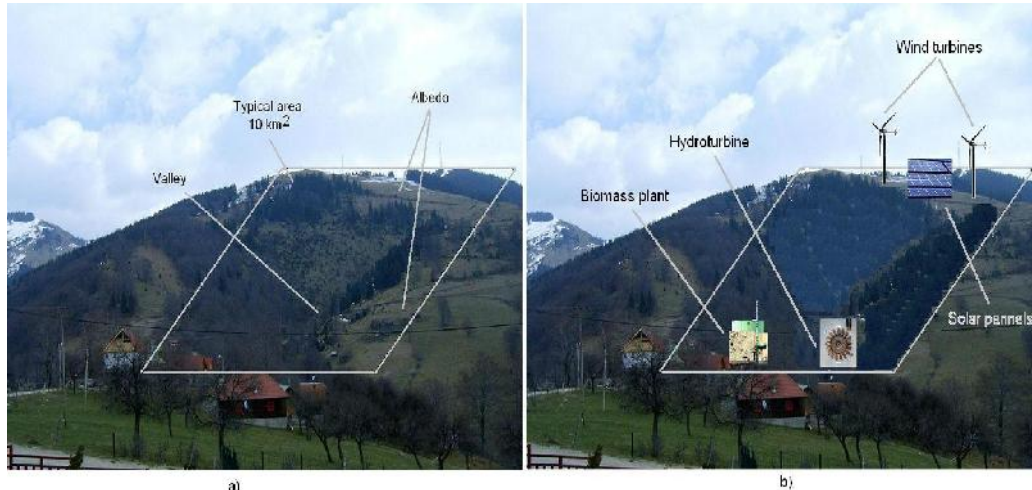


Fig.5. a) The real situation; b) The proposed situation

Also, because of the condition reached by almost all the Jiu's affluent and mountain ravines, a pico hydro-power plant may be installed on each of them, to generate electricity.

A very well suited place to implement an energetic system could be the place of ski lifting installation in Parang Mountain (fig.5.a). In this area may be implemented as well wind turbines, hydro turbines, solar panels or a biomass installation to produce

electric energy. Otherwise, this area is one of the more others from Jiu's Valley very well suited to implement an integrated, sustainable and renewable energetic system.

A solution is shown in fig.5.b; to reduce the albedo the area may be forested, with the wind turbines on the top of the hill (because there are conditions of wind almost all over the year), the hydro-turbine may be installed at the base of the hill; the biomass installation is quite necessary in a place like this, many wood wastes are present to ensure its function. So, we might say that an integrated, sustainable and renewable energetic system is on its way.

It is well known that to evaluate the energetic potential of the area actions have to be started for wind measuring along the year, solar intensity measurement, and hydrologic potential measurement.

The Jiu Valley is part of Central Carpathians Mountains, positioned in their western side. The medium air temperature is about 8-9° C in the space of the valley, up to 6° C at about 1000 m altitude and about 0° C on the mountain peaks (over 2000 m). In the summer time (July-Aug) the medium temperatures rise up to 15-16°C in the valley and in the winter time are lowering to -4°C. The region of Jiu Valley has temperate continental climate with wet and cold character, large amount of precipitation as rain and snow during a period of a year.

The hydrological net of the Jiu Valley contains 2 important rivers: Eastern and Western Jiu, gathering a lot of affluent such as: Jiet, Taia, Banita, Maleia, Slatioara, Salatruc, on the Eastern side and Buta, Valea de Pesti, Pilugul, Braia, Morisoara, Aninoasa on the Western side. The amount of water in the rivers is checked by the hydrometric station. This hydrometric station records the level of rivers and annual rainfall.

3. MODELING AND SIMULATION

The objective of the plant can be the maximum energy production in sustainable conditions. The integration plan mean to correlate the plants so that its work to fulfill the objective.

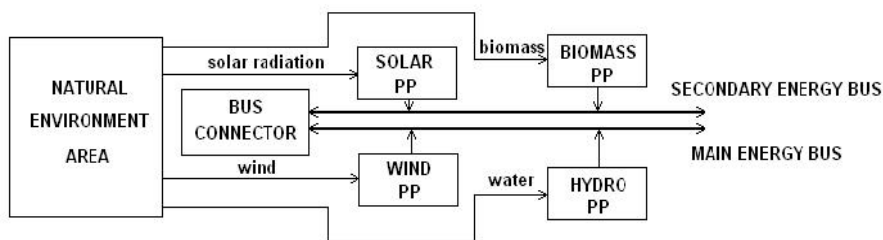


Fig.8. Systemic power plant interconnection

The solar power plant and biomass is intended to be used for secondary application as for internal equipment and local supply. The wind and the hydro are for main bus energy and are for all users. At the other hand the biomass energy can be used for heating the houses and power plant location. In general the main bus energy contain up to (80...90) % of total energy production. It is possible to interconnect the

busses if is necessary. All the input for the plant is from natural environment area (fig.8).

Very important is the modeling and simulation of integrated park. We begin to simulate first the environment which supplies the plants with primary energy (water, wind, solar radiation and biomass).

The rain energetic process is a complex phenomenon and in a simplified view can be represented as having two closed loops (fig.9). The first and main loop contains the following sub processes: water and micro particles, land micro particles, evaporation, condensation, clouds micro particles and rain. The second loop contains the following sub processes: land micro particles and clouds micro particles. The inputs and outputs of each sub process represent the relative transformation rates between water states: water, micro particles and steam, ice and rain droplets.

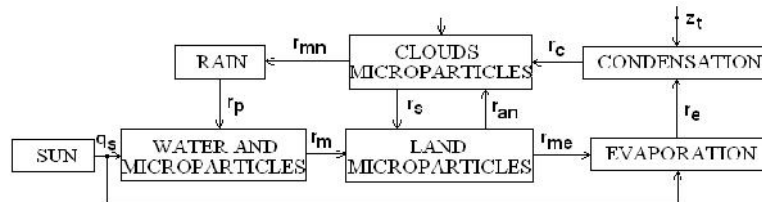


Fig.9. Simplified rain energetic process

For each sub process was written a linear mathematical model. Modeling and simulation of rain energetic process is presented in the next picture (fig.10):

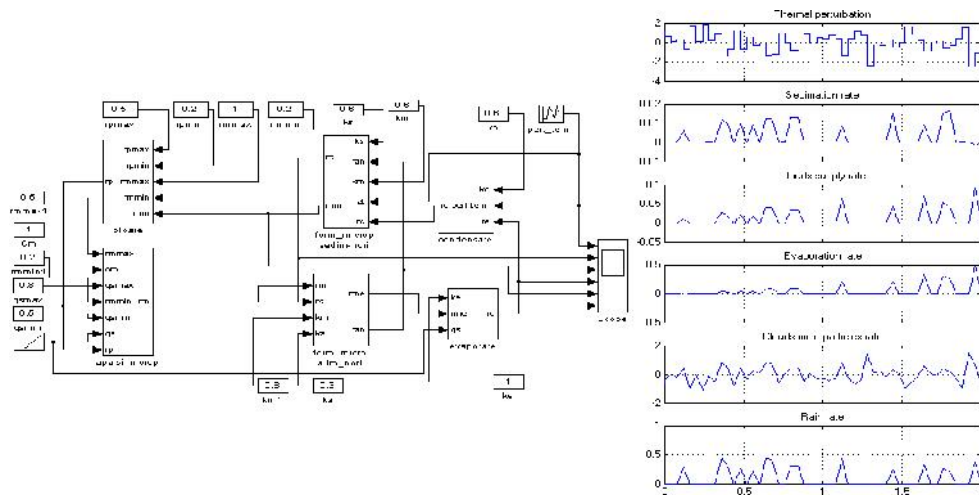


Fig.10. Model and simulation results

4. CONCLUSIONS

- In this paper is presented the structure of an integrated, renewable and sustainable energetic park, consisting of hydro power plant, wind turbine, solar cells and biomass.
- We present the possibilities of renewable energy resources use in Jiu Valley, in a properly place.
- At the end of the paper is achieved a simplified linear model of rain and clouds energetic process and simulated with expected results.

BIBLIOGRAPHY

- [1]. **Pop, E.**, *Automatizări în industria minieră*, EDP Bucuresti, 1983
- [2]. **Mukund, R. Patel**, *Wind and solar power systems*, CRC Press LLC, 1999
- [3]. **Maher, P., Smith, N.**, *Pico hydro for village power. A practical manual for scheme up to 5 kw in hilly areas*. Edition 2.0, UK, 2001
- [4]. *** - *Planning and installing bioenergy systems: a guide for installers, architects and engineers* / German Solar Energy Society (DGS) and Ecofys.
- [5]. *** - *Modeling new forms of generation and storage*, GIGRE Technical Brochure
- [6]. *** - *Layman's Handbook On How To Develop A Small Hydro Site*
- [7]. **Hau, E.**, *Wind turbines*, Springer-Verlag Berlin Heidelberg, 2006
- [8]. **Tabacaru Barbu I.C., Leba M.**, *The Study of the Opportunities to Implement the Pico Hydro in the Jiu Valley*, The VIIIth International Symposium „Young People and Multidisciplinary Research”, ACM-V, 2006, Timisoara, Romania, pag.472-479 , ISBN-10 973-8359-39-2 - ISBN-13 978-973-8359-39-0
- [9]. **Pop E., Tabacaru Barbu I.C., Leba M.**, *Modeling and simulation of integrated energetic parks in local climate context*, microCAD International Scientific Conference, 22-23 March 2007, Applied Information Engineering, Miskolc, Ungaria, pag. 213-218, ISBN 978-963-661-742-4, ISBN 978-963-661-754-7

RESISTIVE BRIDGE CONTROLLED BY VIRTUAL INSTRUMENTATION

NICOLAE PĂTRĂȘCOIU*, ADRIAN MARIUS TOMUȘ**

Abstract: A problem in wiring resistive sensors to the measurement circuits is the influences of the environment upon these connecting wires, influences depend on length of the connecting wires, length can be sometimes variable. We propose a system based on the data acquisition board PCI-1710 that control the operations of the measurement circuit used to connect more than one temperature sensor to the same measurement circuit.

Keywords: resistive bridge, RTD, PCI-1710, virtual instrument

1. CONNECTION OF MORE SENSITIVE ELEMENTS TO THE SAME BRIDGE

On data acquisition board PCI-1710 are connected 16 temperature sensors RTD through single resistive bridge and the sensors are connected through 3-wire connection, fig.1. The sensors are connected to the resistive bridge through 3 multiplexing circuits, one by one for every leads. The unbalanced bridge output tension U is acquired by one of the PCI-1710 analog differential inputs respectively AI_0 - AI_1 .

$$U_1 = \frac{R_4}{R_1 + R_4} \cdot U_a \quad (1)$$
$$U_2 = \frac{RTD^i + R_{w3}^i + R_{km3} + R_{k3}}{RTD^i + R_2 + R_{w3}^i + R_{km3} + R_{w1}^i + R_{k3} + R_{km1} + R_{k1}} U_a$$

The acquisition process consists in two steps, so that in first step the contacts k_1 , k_2 , k_3 , are considered closed. These represent the contacts of commutation of the unknown resistance in the active arm and the unbalanced tension is $U_1 = U_1 - U_2$.

* *Assoc.Professor at the University of Petroșani*

** *Assist.univ. at the University of Petroșani*

The tensions U_1 and U_2 are obtained in base of the diagram, fig.1, with the resistances of the connecting wires R_{w1} , R_{w2} , R_{w3} , the resistances of the multiplexing circuit R_{km1} , R_{km2} , R_{km3} and the resistances of the closed contacts R_{k1} , R_{k2} , R_{k3} :

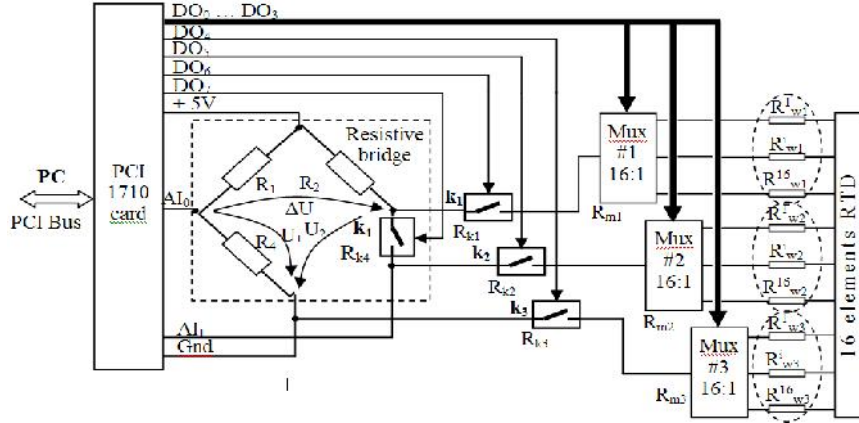


Fig.1. Programmable connection of more RTD to the same resistive bridge

Choosing $R_1=R_4$ and considering equal the resistances of the 3 leads for every sensor $R_{w1}=R_{w2}=R_{w3}=R_w$ and equal the closed resistances of the multiplexers, R_{kmi} and of the k contacts, R_{ki} namely $R_{km1}=R_{km2}=R_{km3}=R_{km}$ and $R_{k1}=R_{k2}=R_{k3}=R_k$ the unbalanced tension equation becomes:

$$\Delta U_1 = \frac{R_2 - RTD^i}{2 \cdot RTD^i + 2 \cdot R_2 + 4 \cdot (R_f + R_k + R_{km})} \cdot U_a \quad (2)$$

In second step the contacts k_1 , k_2 , k_3 are considered closed and using the same method it can obtain the same equation $U=U_1-U_2$ and here the tensions U_1 and U_2 are obtained in base of the theorem of resistive division where we can put the same condition for the resistance RTD:

$$U_1 = \frac{R_4}{R_1 + R_4} \cdot U$$

$$U_2 = \frac{R_{w3}^i + R_{km3} + R_{k3} + RTD^i + R_{w1}^i + R_{km1} + R_{k1}}{R_{w3}^i + R_{km3} + R_{k3} + RTD^i + R_{w1}^i + R_{km1} + R_{k1} + R_2} \cdot U_a \quad (3)$$

So that for this second case when the contacts k_1 , k_2 , k_3 are closed the unbalanced tension, becomes.

$$\Delta U_2 = \frac{R_2 - RTD^i - 2 \cdot (R_f + R_{km} + R_k)}{2 \cdot RTD^i + 2 \cdot R_2 + 4 \cdot (R_f + R_{km} + R_k)} \cdot U_a \quad (4)$$

With the equations (3) and (4), it can build a 2-equation system and by solving that provide:

$$RTD^i = \left(1 - \frac{4 \cdot \Delta U_1}{U_a + 2 \cdot \Delta U_2} \right) \cdot R_2$$

$$R^i_c = 2 \cdot \frac{R_2}{U_a + 2 \cdot \Delta U_2} \cdot (\Delta U_1 - \Delta U_2) \quad (5)$$

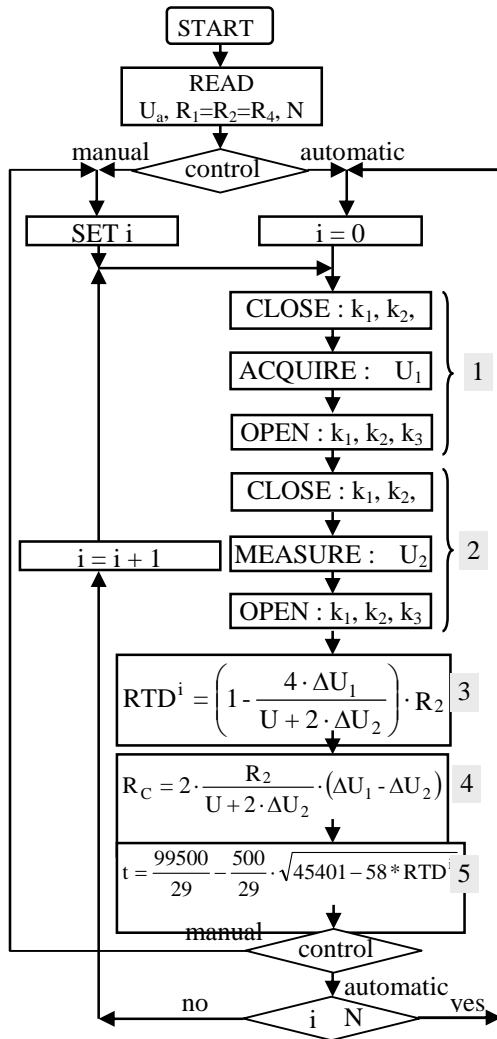


Fig.2. Main program algorithm

possible to compute RDT resistance and the measurement channel R_C resistance too. If it know the static characteristics of the RTD is possible to compute the corresponding temperature value and for platinum RTD, Pt100, it can use the relation from block (5).

3. VIRTUAL INSTRUMENT TO CONTROL RESISTIVE BRIDGE

The driver software is the programming interface to the hardware and is consistent across a wide range of platforms. Application software such as LabVIEW, LabWindows/CVI, deliver sophisticated display and analysis capabilities required for virtual instrumentation and the programs written in that application software are called Virtual Instruments (VI). It can use virtual instrumentation to create a customized

It can observe that measuring the unbalanced tensions U_1 and U_2 and maintaining constant the supply voltage U_a and the resistance R_2 , it can obtain the value of the resistance of the sensitive element RTD, and the resistance of the measurement channel ($R_f+R_{km}+R_k$) between the resistive bridge and the sensor.

2. FLOW CHART OF VIRTUAL INSTRUMENT

The virtual instrument controls the data acquisition process, fig.2, through acquisition board PCI-1710 which by its digital outputs control follows up static relays with contacts k_1, k_2, k_3 and k_4 . After its reads the measurement circuit parameters: bridge voltage supply U_a , bridge arm resistances $R_1=R_2=R_4$ and equal with unexcited sensor resistance in first step by data acquisition board are closed the contacts k_1, k_2, k_3 . After pre-set delay DELAY1 by analog input are gather the unbalanced voltage U_1 from the bridge and these contacts are opened after the pre-set delay DELAY2.

By the digital outputs of the same data acquisition card are closed contacts k_1, k_2, k_4 so that after the pre-set delay DELAY3 now can be gathered the unbalanced voltage U_2 from the bridge. With the two tensions gathered now is

$$RTD^i = \left(1 - \frac{4 \cdot \Delta U_1}{U + 2 \cdot \Delta U_2} \right) \cdot R_2 \quad 3$$

$$R_C = 2 \cdot \frac{R_2}{U + 2 \cdot \Delta U_2} \cdot (\Delta U_1 - \Delta U_2) \quad 4$$

$$t = \frac{99500}{29} - \frac{500}{29} \cdot \sqrt{45401 - 58 \cdot RTD} \quad 5$$

system for test, measurement, and industrial automation by combining different hardware and software components.

3.1. Front Panel Description

The front panels of the virtual instrument corresponding to the two operation modes MANUAL respectively AUTOMATIC are shown in fig.3.

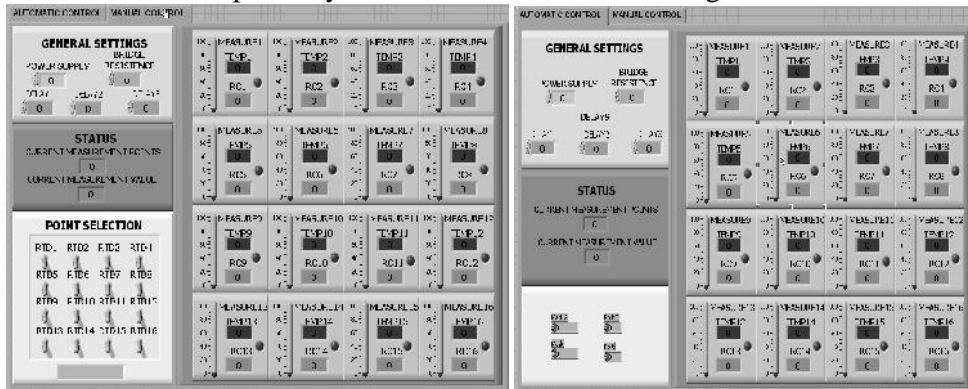


Fig.3. Front panels of the virtual instrument

AUTOMATIC CONTROL ensures measurement points read by pooling method end time spacing between two consecutively measurements points is set by delays mentioned before.

MANUAL CONTROL ensures possibility to select by toggle switches whichever measurement points must be read. This toggle switches corresponding to every measurement points and through this user can select measurement points.

All other sections are common and these are:

- **General settings** through user sets power supply, bridge resistance and delays mentioned above values;
- **Status** through user can make out the current measurement temperature value corresponding to the proper measurement point
- **Measurement panel** through user has a total view about all measurement points. This panel is divided into 16 areas corresponding to the right 16 measurement points. These areas contain numeric indicator to display in numeric and analogical form the values corresponding to the temperature (TEMP_i) and sensor resistance (RC_i) also LED indicator to indicate the current measurement point.

If are selected AUTOMATIC CONTROL these areas are simultaneous selected to the right measurement point so that user can observe the temperature in consecutive measurement points. If are selected MANUAL CONTROL these areas are selected by user on request through toggle switches.

3.2. Bloc Diagram Description

Block diagram represent properly working program also corresponding to the two operation mode are depicted in fig.4.

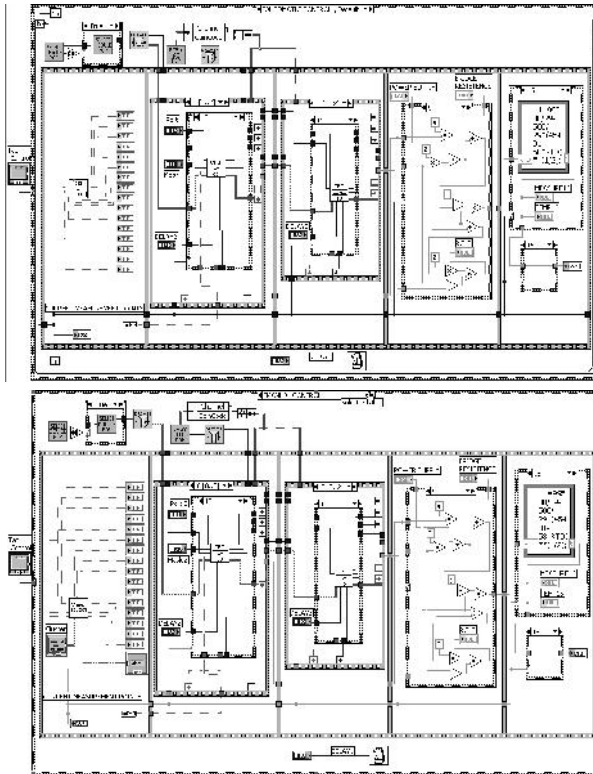


Fig.4. Block diagrams of the virtual instrument

The base element of the diagram bloc is **Case Structure** which has two subdiagrams exactly one of which executes when the structure executes. The value wired to the selector terminal is generating by **Tab Control** and that determines which case to execute respectively **AUTOMATIC CONTROL** and **MANUAL CONTROL**. **AUTOMATIC CONTROL** case includes a **For Loop** structure that executes its subdiagram 16 times, where n is the value wired to the count (**N**) terminal and represent measurement points. The iteration (**i**) terminal provides the current loop iteration count, which ranges from 0 to $n-1$ and this value, wired to proper selector are used to control the all subdiagrams used to realize the loop. A structure commune in either case

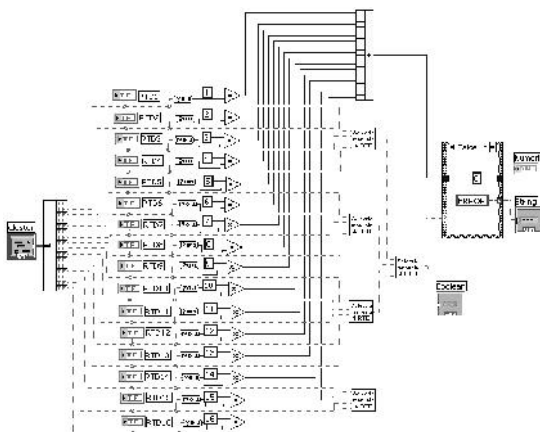


Fig.5. Manual selection diagram block

is **Flat Sequence Structure** that consists of five frames executed sequentially. We use the Flat Sequence structure to ensure those 5 subdiagram corresponding those 5 blocs in main program flow chart executes before or after another subdiagram. Frames in a Flat Sequence structure execute in order when all data wired to the frame are available.

Each subdiagram in this structure contain a **Case Structure** with 16 cases corresponding to the 16 measurement points and selection of these are execute by control of count terminal for automatic control respectively by control of SubVI **Manual_SELECT.vi**

terminal for automatic control respectively by control of SubVI **Manual_SELECT.vi**

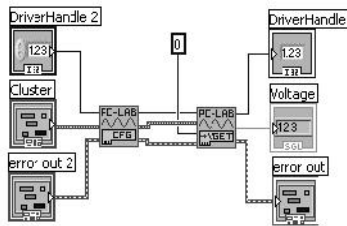


Fig.6. Acquire unbalanced voltage U diagram block

(fig.5) were the toggle switches are grouped into a cluster. The second subdiagram in **Flat Sequence** structure contains the logic necessary to contacts k_1 , k_2 , k_3 , k_4 control their diagram block is presented in fig.6. Here is used function **DIOWritePortByte** that write a byte of data to a digital output port of **DriverHandle** specified device. Also, here are acquired the first value for unbalanced voltage U with a SubVI with diagram bloc is presented in fig.6.

To do this is used function **AIVoltageIn** that read current value from differential analog input channel AI_0 - AI_1 of the PCI-1710 data acquisition board and return in converted voltage value from **DriverHandle** specified device. The third sequence is similarly with the second except for sequence of contacts that respect block 2 of main program data flow (fig.3). The forth sequence is used to compute value of the RTD^i accordance with block 3 of main program data flow, and finally the fifth sequence is used to compute the corresponding point temperature to the value of the RTD^i accordance with block 5 of main program data flow (fig.1).

4. CONCLUSIONS

Using this method is possible to compute simultaneous both sensor's resistance value and connection wires resistance value. Sensor's resistance values offer the information about temperature using the sensor characteristics. Connection wires resistance value offer the information that can be used to initial automating balancing of the bridge so that can obtain the maximum of the sensibility for measurement circuit.

BIBLIOGRAPHY

- [1] Bentley E. R. *Handbook of Temperature Measurement*. Springer-Verlag. 2001
- [2] Patrascioiu, N., *Sisteme de achizitie si prelucrare a datelor. Instrumentatie virtuala*. Ed.Didactica si Pedagogica, Bucuresti, 2004
- [3] Meza D., *Metode de masurare la distanta a termorezistentelor cu trei fire*. Automatic Control and Testing Conference. Cluj-Napoca.1994
- [4] * * * National Instruments (2003b) *LabVIEW. User Manual*. National Instruments, April 2003 Edition Part Number 320999E-01

STRATEGIES OF CONTROL FOR SOLAR PANELS POSITIONING SYSTEMS

LAURENȚIU ALBOTEANU*, GHEORGHE MANOLEA**, FLORIN
RAVIGAN*, ADRIAN NOUR***

Abstract: This paper presents some considerations concerning the positioning systems for solar panels as to obtain the maximum energy that these can furnish. There are also analyzed two versions of control for these positioning systems.

Keywords: solar panels, solar energy, solar motion, positioning system, fuzzy controller, PI controller.

1. INTRODUCTION

The photovoltaic (PV) modules work by converting sunlight directly into electricity. The sunlight is the necessary and efficient ingredient. The PV modules work at a maximum efficiency, when the incoming Sun rays are perpendicular to their cells. The adjusting of the static structure PV modules may have as a result more yearly power from 10% to 40%. Maintaining the module perpendicular to the incoming sunlight means that the module intercepts the maximum amount of sunlight.

The problem is that the Sun constantly moves being related to the static PV module. Actually, the apparent motion of the Sun is due, to the Earth's motion, but for our purpose here this celestial fact is mere trivia. Even if we place a module so that it may be perpendicular to the Sun at the solar noon, it is not perpendicular in the morning and in the evening. This daily motion from East to West is called the solar azimuth. The apparent height of the Sun in the sky also changes it self being related to the change of the season from winter to summer. This yearly North to South solar motion is called solar declination.

* *Assist., Eng. at the University of Craiova*

** *Prof., Ph.D. at the University of Craiova*

*** *Eng. at the Ministry of National Defense*

If the PV module is to be kept perpendicular to the daily motion of the Sun from East to West (azimuth), then a device called a tracker is used. A tracker follows the daily motion of the Sun and furnishes more power anywhere from 25% to 35% which is absorbed from the hitchhiking on its back.

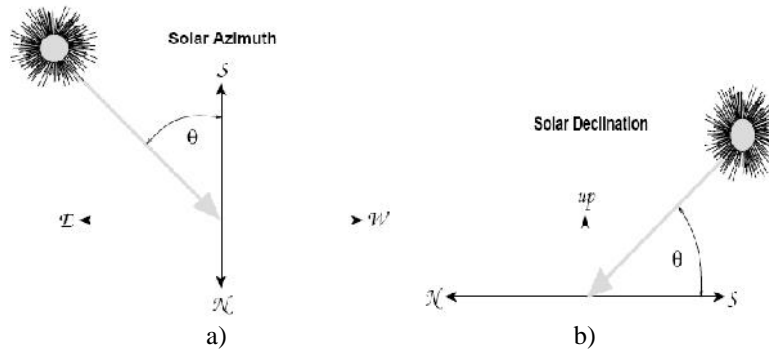


Fig.1. The angles for Sun; a) Solar Azimuth; b) Solar Declination

If one adjusts by manual the position of the PV panel accordingly to the North-South solar motion, the power broadcast by the PV modules increases whit 10%. The diagrams on the fig. 2 present all the necessary data for the achieving of the adjusting, North/South, PV panel position. The calculation of the panel angle (A) is based on the supposition that the panel will be perpendicular to the incoming Sun rays at solar noon. Solar noon (the local time) is the time when the Sun is highest in the sky. This is the time when the angle between the plane of the horizon and a line drawn from the site to the Sun is greatest.

This calculation involves two parameters. These parameters are the latitude of the site (L) and the declination of the Sun (D). The declination of the Sun is the latitude at which the Sun is directly overhead at solar noon. This varies from 23.5° North latitude on the summer solstice (June 21) to 23.5° South latitude on the winter solstice (December 21).

These latitudes are known as the Tropic of Cancer and the Tropic of Capricorn. During the equinoxes (March 21 and September 21) the declination of the Sun is 0°, so that it is directly over the Equator at solar noon.

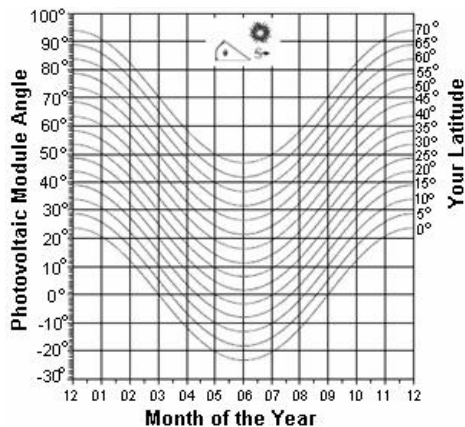


Fig. 2. Solar panel angle for various latitudes

The equation of the declination (D) for any day is:

$$D = 23.5^{\circ} \sin\left(\left(T / 365.25\right) * 360^{\circ}\right) \quad (1)$$

where T is the number of days to the day in question as measured from the spring equinox (March 21).

The panel angle (A), the angle between the panel and the horizontal plane, is then calculated from the equation:

$$A = L - D \quad (2)$$

2. POSITIONING SYSTEMS FOR SOLAR PANELS

Various positioning structures of the PV panels can be built from a variety of materials and in a variety of styles. Almost all designs can be made to be seasonally adjustable. All commercial produced PV panels have a virtual and difficult seasonally adjustment because they are made to work at a wide range of latitudes.

2.1 Single-axis positioning systems

These have a single axis for the rotation of the PV panel; the East-West motion. This system is a little complicated it need only a simple motor and a control system that turns the solar array from East to West each day. This maintains the panel in a close proximity to the Sun.

2.2 Dual-axis positioning systems

These use both East-West and South-North axes for positioning the solar panel. During a year, the dual axis system will produce the most amount of power, because one can follow the changing of the Sun trajectory every season. At the same time, this structure is more expensive, more complicated for being designed, constructed and maintained.

3. THE POSITIONING SYSTEM STRUCTURE WITH DC MOTOR

In the industrial applications it is more often necessary the accomplishment of a precise and accurate position in a very short time [5]. By the type of the used energy,

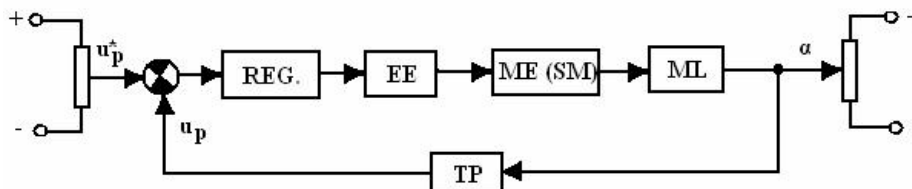


Fig. 3. The classical structure for positioning system

and a power element which assure motion of de charge, such a system may be: hydraulically, pneumatically and more often, electrical. For having a large view on such a positioning system let us consider a very short case, presented in fig. 3.

The analyzed system is composed from a transducer of position (T), a regulator (REG), machine (ME) and a charge machine represented an electrical by solar panel (ML).

The ideal equilibrium of system corresponds to the situation in which the position of the charges machine is the some with the one imposed, particularly, the output signal is identical with the command signal, situation in which the output tension of the position transducer, u_p , is zero, the supplying tension of the motor is null, and so, the whole structure remain static. At the arrival of a command signal at the output transducer of position appears a signal which is proportionally with the difference between the input size and the output size which, amplified and applied to the motor, it command to bring the charge a after a while in a new position of equilibrium [6].

4. THE ANALYZE OF CONTROL VARIANTS FOR SOLAR PANELS POSITIONING SYSTEMS

4.1 The control of positioning systems for solar panels with PI controller

The simulink model of the positioning system is presented in fig. 4. This model contain of the subsystem block for DC motor model and subsystem block for motor control model [8], [9], [10].

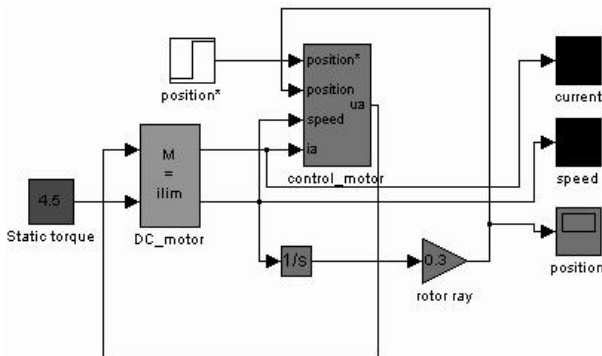


Fig. 4. Simulink model of the positioning system

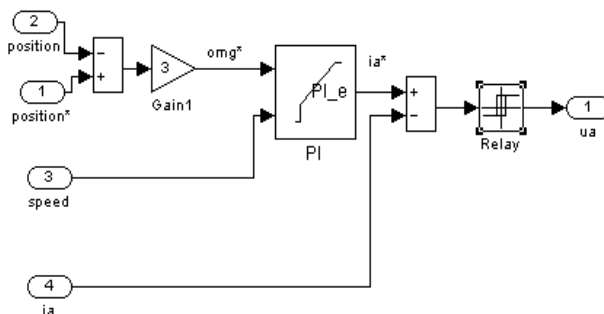


Fig. 5. The block mask for control motor

The control bloc for DC motor (fig. 5) it achieves with PI regulator which have of a the current limitation value to 15 Amperes, and the output Relay block having the signification of the static contactor command in inclusion of the chopper.

At the input of the control block the real position is compared with the set one and it is achieved the set speed.

The speed adjustment is made by a P regulator (proportionally) by comparison of the set speed with the real one. For the system position adjustment it is used a loop consisting of a regulator PI with

cancelling of the speed error (fig. 6).

In order to accomplish the current limiting function, the current regulator must sized so that its integration constant be smaller than the speed regulator constant (be faster).

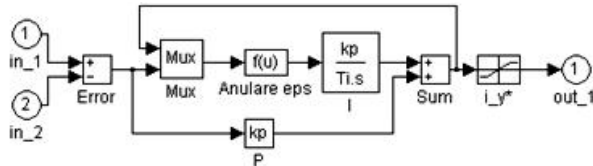


Fig. 6. The model of PI controller with remove of errors

The output of controller is:

$$c = \left(kp + \frac{ki}{s} \right) (i^* - i) \quad (3)$$

where:

c - output of controller;

kp - proportional constant;

ki - integral constant;

i^*, i - prescribed and measured values of input.

For the current regulator it is considered a easier type but very efficient, namely a bi-positioning regulator. In fact this regulator type is hysteresis comparator (fig. 7), changes being decided by the conditions:

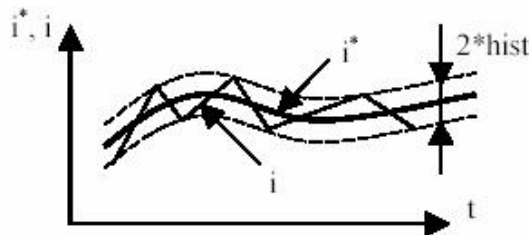


Fig. 7. Evolution of controlled condition for controller of current

$$c = \begin{cases} 1 \rightarrow 0; i = i^* + hist \\ 0 \rightarrow 1; i = i^* - hist \end{cases} \quad (4)$$

The current will be kept around the set value i^* , with an error given by the hysteresis band (fig. 7).

This regulator model has the advantage that the position error is removed and the set current is limited; the regulator parameters can be also changed.

The simulation results are shown in fig. 8.

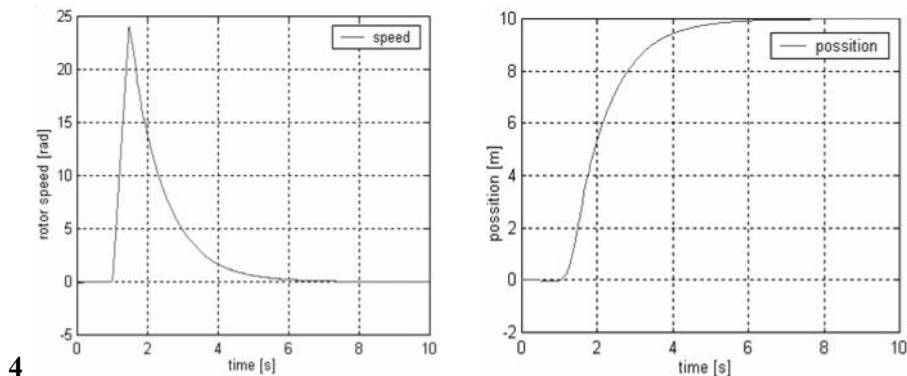


Fig. 8. Simulation results

The control of positioning systems for solar panels with fuzzy controller

The adjustment algorithm uses an external loop proportional to the position and an internal one of PI type for the speed. This is determined by the position information with the relation:

$$\omega_k \approx \frac{\alpha_k - \alpha_{k-1}}{T} = \frac{2\pi \cdot k_{div} \cdot \Delta N_k}{N_{i/r} \cdot T} = c_{vit} \cdot \Delta N_k \tag{5}$$

where:

k_{div} : coefficient of division / multiplication for encoder impulses

T : sampler period

ΔN_k : number of impulse for position meters on T period

c_{vit} : speed coefficient

The model SIMULINK for the position adjustment with a fuzzy regulator for the positioning system with DC current motor uses the block from FUZZY TOOLBOX, where it works with the variables:

- the position error $\varepsilon_{\alpha k}$ (at the sampling moment k);

- variation of the position error $\Delta\varepsilon_{\alpha k}$ is just the speed (with changed sign).

Taking into account relation (5) norming is made with the relations:

$$\varepsilon_{\alpha nk} = \varepsilon_{\alpha k} \cdot \frac{\varepsilon_{\alpha n max}}{N^*} \tag{6}$$

$$\Delta\varepsilon_{\alpha nk} = -\Delta N_k \cdot \frac{c_{vit} \cdot \Delta\varepsilon_{\alpha n max}}{\Omega_{max}} \tag{7}$$

The maximum norming values are usually 10. Fig. 9 shows the model of fuzzy position adjustment for the mentioned positioning system. The space image for rules table associate of fuzzy controller is show in fig. 10. It used interface min-max method.

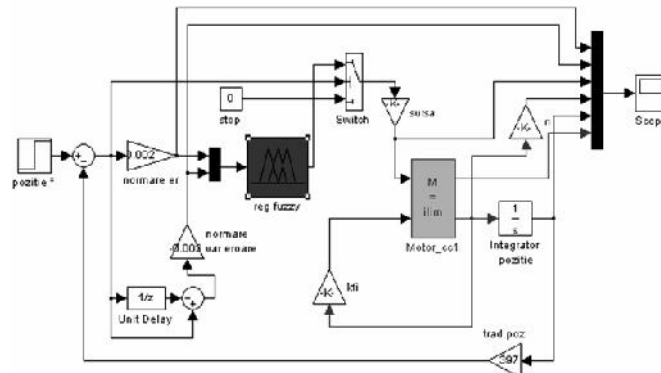


Fig. 9. Simulink model of the positioning system with fuzzy regulator

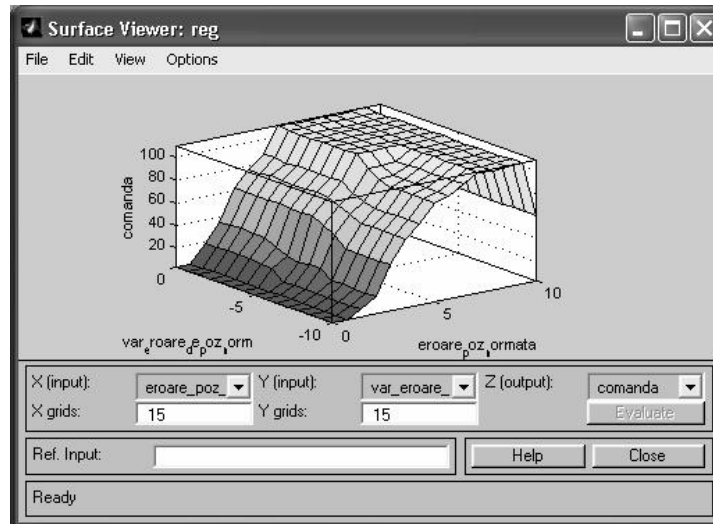


Fig. 10. Image of work for fuzzy controller

By rate set, the inputs are situating in standard ranges $[-10, +10]$. The fuzzy controller is a predefined block, configured with FUZZY TOOLBOX, the operation is determined of an associate file. It anticipation the control algorithm in real time trough by using the same sampling period at z^{-1} block of motor parameters from the real experiment and by eliminating the fuzzy command at the error of zero position. Also, the vague crowds for command are defined on integer numbers ranges with which should work the controller, hold on of the voltage power source characteristics and the connections

The simulation results are shown in fig. 11.

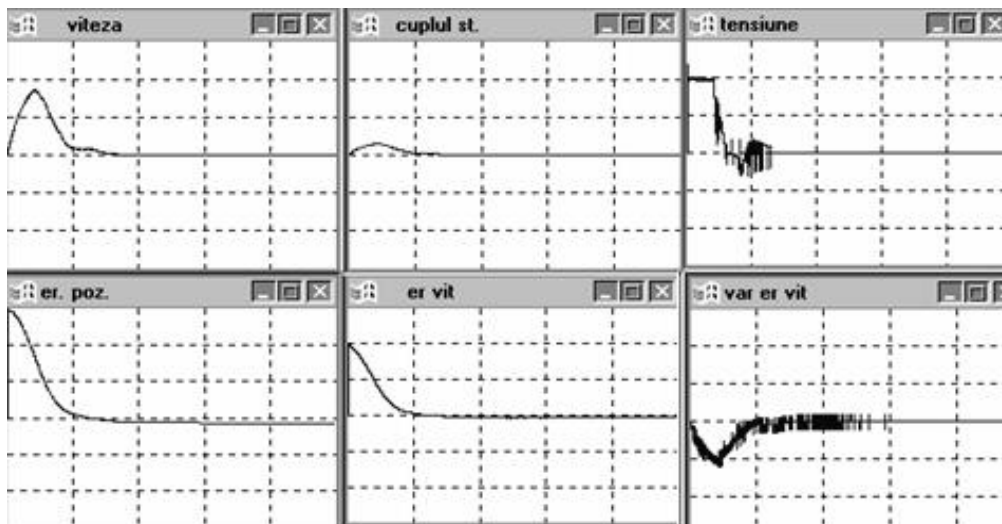


Fig. 11. Simulation results

5. CONCLUSIONS

The results of simulink model for control position with PI controller are relative good (see figure 8), for a linear position prescribed; the system had reached this position, without any oscillations.

The fuzzy controller provided positioning system records an over-adjustment leading to error of position. By simulation of other rules tables it has been achieved a positioning of the system closely to the reference point but it doesn't reach the point.

In order to avoid this error the following conclusions concerning some modifications to the servosystem behaviour, must be taken into account.

For a good answer of the servosystem the sampling period must be as little as possible.

A great influence has the check rules modification and the fuzzy set.

BIBLIOGRAPHY

[1]. **Perez Richard**, *To Track... or not to Track*, Home Power, no 101, June & July, 2004;

[2]. **L. Alboteanu, Gh. Manolea, Fl. Ravigan**, *Positioning systems for solar panels placed in isolated areas*, Annals of the University of Craiova, Ed. Universitaria, 2006, pp. 163-168;

[3]. **T. Ambros, V. Arion, A. Guțu, I. Sabor, P. Todos, D. Ungureanu**, *Surse regenerabile de energie*, Ed. Tehnica-Info, Chi in u, 1999;

[4]. **Zahari Zarkov, Vladimir Lazarov**, *Energy Balanced of a Hibrid Renewable Energy Sources System*, Proc. of the 7th International Conference of Applied and Theoretical Electricity, Ed. Universitaria 2004, pp. 291-297;

[5]. **Gh Manolea, M.A., Drighicu, Fl. Ravigan**, *The Optimal command for the Servosystem's Position in Minimal Time*. Conferinta Nationale de Actionari Electrice - CNAE 2002 -Galati 10-12 octombrie 2002;

[6]. **Gh. Manolea**, *Sisteme automate de acționare electromecanică*, Ed. Universitaria, Craiova, 2004;

[7]. **D. Mihai**, *Multicriterial Conditioning of a Digital Control Problem for a Positioning Electrical Drive System*, Annals of the University of Craiova, Ed. Universitaria, 1998, pp. 129-140;

[8]. **Mihaela Popescu, Al. Bitoleanu, M. Dobriceanu, O. Popescu**, *Reglage automate de la position par mode de glissement avec moteur a courant continu et hacheur*, Proc. of the International Conference of Applied and Theoretical Electricity, Ed. Universitaria 2002, pp.137-142;

[9]. **Gh. Manolea**, *Loss Function Optimal Control of the Positioning Servomotors with Static Torque Proportional to the Speed*, Advanced Motion Control AMC'02 Maribor, Slovenia, 3-5 iulie 2002;

[10]. **D. Mihai**, *Comenzi numerice pentru sisteme electromecanice*, Ed. Didactica Nova, Craiova, 1996.

SYNTHESIS OF THE LUEMBERGER EXTENDED ESTIMATOR USED WITHIN A VECTORIAL-TYPE ELECTRICAL DRIVING SYSTEM WITH AN INDUCTION MOTOR

CORNELIU MÂNDRESCU*, OLIMPIU STOICUȚA**

Abstract: In this paper we present the synthesis of the Extended Luemberger Estimator using the proportional self values method, self values rotation method and self values moving method. The speed estimator is projected based on the hyperstability theory of V.M. Popov.

Keywords: Luemberger estimator, values rotation method, values moving method

1. LUEMBERGER ESTIMATOR

The equations that define the discrete Luemberger estimator are:

$$\begin{cases} \hat{x}_{k+1} = F_d \cdot \hat{x}_k + H_d \cdot u + L_d \cdot (y_k - C \cdot \hat{x}_k) \\ w_k = \hat{x}_k \end{cases} \quad (1)$$

in which the F_d and H_d matrixes are obtained based on simplified digitization:

$$F_d = I + A \cdot T; H_d = B \cdot T$$

or complete digitization:

$$F_d = I + A \cdot T + A^2 \cdot \frac{T^2}{2}; H_d = B \cdot T + A \cdot B \cdot \frac{T^2}{2}$$

* *Assoc.Prof.Eng.Ph.D., University of Petroșani*

** *Assist.Eng., University of Petroșani*

and the entry, state and exit vectors is:

$$\begin{cases} u_k = [u_{dsk} \quad u_{qsk}]^T \\ \hat{x}_k = [\hat{i}_{dsk} \quad \hat{i}_{qsk} \quad \hat{\psi}_{drk} \quad \hat{\psi}_{qrk}]^T \\ y_k = [i_{dsk} \quad i_{qsk}]^T \end{cases} \quad (2)$$

Under these circumstances the C matrix is: $C = [I_2 \quad 0_2]$.

In the relations above the T variable is sampling time and the A and B matrixes have the following structure:

$$A = \begin{bmatrix} a_{11} & 0 & a_{13} & a_{14} \cdot \omega \\ 0 & a_{11} & a_{14} \cdot \omega & a_{13} \\ a_{31} & 0 & a_{33} & -\omega \\ 0 & a_{31} & \omega & a_{33} \end{bmatrix}; \quad B = \begin{bmatrix} b_{11} & 0 & 0 & 0 \\ 0 & b_{11} & 0 & 0 \end{bmatrix}^T \quad (3)$$

where: $a_{11} = -\left(\frac{1}{T_s \cdot \sigma} + \frac{1-\sigma}{T_r \cdot \sigma}\right)$; $a_{13} = \frac{L_m}{L_s \cdot L_r \cdot T_r \cdot \sigma}$; $a_{14} = \frac{L_m}{L_s \cdot L_r \cdot \sigma}$;

$a_{31} = \frac{L_m}{T_r}$; $a_{33} = -\frac{1}{T_r}$; $b_{11} = \frac{1}{L_s \cdot \sigma}$; $T_s = \frac{L_s}{R_s}$; $T_r = \frac{L_r}{R_r}$; $\sigma = 1 - \frac{L_m^2}{L_s \cdot L_r}$

The L matrix is determined in the continual case so that estimator's poles are located to the left of the Nyquist diagram. The most widely used solutions for on-line computing of the gain matrix L are:

- the formulas that ensure the proportionality between the machine poles and those of the estimator;
- self values rotation method;
- self values moving method;

PROPORTIONAL SELF VALUES METHOD

If we notate with λ_m the self values of the induction machine and with λ_e the self values of the estimator, the proportionality formula may be written like:

$$\lambda_e = k \cdot \lambda_m \quad (4)$$

The self values of the motor can be calculated by resolving the equation:

$$\det[(\lambda_m \cdot I_2 - A)] = 0 \quad (5)$$

in which I_2 is the second degree unit matrix and λ_m are the self values of the motor:

$$\lambda_m = \lambda_1 + j \cdot \lambda_2 \quad (6)$$

Alike, the self values of the estimator can be calculated as follows:

$$\det[\lambda_e \cdot I_2 - (A - L \cdot C)] = 0 \quad (7)$$

in which estimator's self values are:

$$\lambda_e = \lambda_1^* + j \cdot \lambda_2^* \quad (8)$$

and the L gain matrix is:

$$L = \begin{bmatrix} l_{11} & l_{12} & l_{21} & l_{22} \\ -l_{12} & l_{11} & -l_{22} & l_{21} \end{bmatrix}^T \quad (9)$$

where:

$$\begin{cases} l_{11} = (1-k) \cdot (a_1 + a_2) \\ l_{12} = \omega \cdot (1-k) \\ l_{22} = -\gamma \cdot l_{12} \\ l_{21} = (a_3 + \gamma \cdot a_1) \cdot (1-k^2) - \gamma \cdot l_{11} \end{cases} \quad (10)$$

in which:

$$a_1 = a_{11} ; a_2 = a_{33} ; a_3 = a_{31} ; c = \frac{L_m}{L_s \cdot L_r \cdot \sigma} ; \gamma = \frac{1}{c}$$

Digitization of the L matrix is done identically as with that of the B matrix by using simplified digitization:

$$L_d = L \cdot T \quad (11)$$

or by using complete digitization:

$$L_d = L \cdot T + \frac{A \cdot T^2}{2} \cdot L \quad (12)$$

Under these circumstances the discrete Luemberger rotor flux estimator is completely determined being defined by the equations in (1) in which the L_d gain matrix is given by (11) in case of simple digitization and by (12) in case of complete digitization.

SELF VALUES ROTATION METHOD

This method is identical with the proportional self values method with the exception that simultaneously with the amplification of the self values a self values rotation, with a θ angle is made. So that, if we notate with λ_m the self values of the induction machine and with λ_e the self values of the estimator, the formula that describes this method is:

$$\lambda_e = k \cdot e^{j\theta} \cdot \lambda_m \quad (13)$$

In order to obtain the L gain matrix an identical calculus is realised as with the case of proportional self values with the exception that in case that the self values of the motor are given as in (6) and those of the estimator as in (8) in (13) we get:

$$\lambda_1^* = k_r \cdot \lambda_1 - k_i \cdot \lambda_2; \quad \lambda_2^* = k_i \cdot \lambda_1 + k_r \cdot \lambda_2 \quad (14)$$

in which: $k_r = k \cdot \cos(\theta)$; $k_i = k \cdot \sin(\theta)$.

Based on the (14) relations we obtain that:

$$\lambda_1 = \frac{k_r \cdot \lambda_1^* + k_i \cdot \lambda_2^*}{k_r^2 + k_i^2}; \quad \lambda_2 = \frac{k_r \cdot \lambda_2^* - k_i \cdot \lambda_1^*}{k_r^2 + k_i^2} \quad (15)$$

Based on the relations (15) we obtain the L gain matrix coefficients. These coefficients are:

$$\begin{cases} l_{11} = (1 - k_r) \cdot (a_1 + a_2) + k_i \cdot \omega \\ l_{12} = (1 - k_r) \cdot \omega - k_i \cdot (a_1 + a_2) \\ l_{21} = (1 - k_r^2 + k_i^2) \cdot (a_3 + \gamma \cdot a_1) - \gamma \cdot l_{11} \\ l_{22} = -2 \cdot k_r \cdot k_i \cdot (a_3 + \gamma \cdot a_1) - \gamma \cdot l_{12} \end{cases} \quad (16)$$

Most of the time it is preferred that the θ angle by which the self values rotate does not remain constant for each sampling step. So, if we chose a θ angle as:

$$\theta = k \cdot \omega \quad (17)$$

in which $k = \theta_{\min} / \omega_{\max}$, then the self values will modify for each sampling step.

SELF VALUES MOVING METHOD

This method, too, is identical to the proportional self values method, with the exception that between the self values of the machine and those of the estimator a constant δ is kept. If we notate with λ_m the self values of the induction machine and with λ_e those of the estimator, the formula that describes this method is:

$$\lambda_e = \lambda_m + \delta \quad (18)$$

In order to obtain the L gain matrix an identical calculus is made as with the proportional self values, with the exception that the motor's self values are as in (6) and those of the estimator as (8) in (18) and we obtain:

$$\begin{cases} \lambda_1^* = \lambda_1 + \delta \\ \lambda_2^* = \lambda_2 \end{cases} \quad (19)$$

Based on the relations (19) we obtain the L gain matrix coefficients. These coefficients are:

$$\begin{cases} l_{11} = -2 \cdot \delta \\ l_{12} = 0 \\ l_{21} = \gamma \cdot (a_1 + 2\delta) - \gamma \cdot \delta (a_2^2 + \omega^2)^{-1} \left[a_1 \cdot a_2^2 + a_2 (a_1 + a_2) \cdot \delta + a_2 \cdot \delta^2 + \omega (\delta + a_1) \right] \\ l_{22} = \gamma \cdot \delta \cdot \omega \cdot (a_1 + \delta) \cdot (a_2^2 + \omega^2)^{-1} \end{cases} \quad (20)$$

2. CONSTRUCTION OF THE ADAPTIVE MECHANISM FOR THE GENERAL CASE

In this paragraph we will present a possibility for the deduction of the estimation law of one or more parameters, when the first solution of the problem is used in order to simultaneously identify the states and the parameters.

In order to realize the adaptive mechanism we presume that the equations of the two models are linear equations in which we suppose that only the A matrix contains the parameters that we need to estimate. This is the case of the induction motor regardless whether we identify speed or rotor resistance.

For calculus we will consider the most general case in which the reference model is really the induction machine and the adjustable motor is a Luemberger observer, whose outputs are the estimated values of the stator currents and rotor fluxes. In order to deduce the adaptive law we need to consider as outputs of the estimator only the estimated stator currents. Now we can write the equations of the two models like this:

$$\begin{cases} \frac{d}{dt} x = A \cdot x + B \cdot u \\ y = C \cdot x \end{cases} \quad (21)$$

$$\begin{cases} \frac{d}{dt} \hat{x} = \tilde{A} \cdot \hat{x} + B \cdot u + L \cdot (y - \hat{y}) \\ \hat{y} = C \cdot \hat{x} \end{cases} \quad (22)$$

in which the A,B and C are the matrixes of the stator currents model – rotor fluxes, and the gain matrix of the observer, L, is built according to the construction algorithm of the estimator presented in the preceding paragraph. In the case of the adjustable model the A matrix is noted with tilde (~) because is built on the estimated parameters. The generality of this case compared to the one in which both models are estimators results from the existence of the L and C matrixes.

In order to build the adaptive mechanism, for start we will calculate the estimation error given by the difference:

$$e_x = x - \hat{x} \quad (23)$$

Derivating the relation (23) in relation with time and by using the relations (21) and (22) the relation (23) becomes:

$$\frac{d}{dt}e_x = A \cdot x - \tilde{A} \cdot \hat{x} + L \cdot (C \cdot x - C \cdot \hat{x}) \quad (24)$$

Expression (31) can also be written as:

$$\frac{d}{dt}e_x = (A + L \cdot C) \cdot e_x + (A - \tilde{A}) \cdot \hat{x} \quad (25)$$

This equation describes a linear system in reversed connection with a non-linear system. The non-linear system receives at its entry the error between the outputs of the two models, and, as output, has the term $(A - \tilde{A}) \cdot \hat{x}$. If we consider the two systems connected in negative reaction we will note with:

$$\rho = -(A - \tilde{A}) \cdot \hat{x} \quad (26)$$

As one may notice, this problem is frequently treated in the literature of the non-linear systems, being exactly the configuration of the Lure problem, and of one of the problems treated by Popov.

Considering, according to the Popov terminology, the non-linear block described by $\Phi(e_y)$ the integral input- output index associated to it is:

$$\eta(t_0, t_1) = \text{Re} \left[\int_{t_0}^{t_1} e_y^T(t) \cdot \rho(t) dt \right] \quad (27)$$

in which we have introduced the following notation:

$$e_y^T = \begin{bmatrix} e_y^T & 0 & 0 \end{bmatrix} \quad (28)$$

in order to preserve the compatibility between the dimensions of the input and output.

In order for block to be hyper-stable a necessary condition is:

$$\eta(0, t_1) = \int_0^{t_1} e_y^T(t) \cdot \rho(t) dt \geq -\gamma^2(0) \quad (29)$$

for any input-output combination and where $\gamma(0)$ is a positive constant. Under these circumstances, using the relation (26) the expression (29) becomes:

$$\eta(0, t_1) = - \int_0^{t_1} e_y^T(t) \cdot (A - \tilde{A}) \cdot \hat{x} \cdot dt \geq -\gamma^2(0) \quad (30)$$

In the following we will presume that the error $A - \tilde{A}$ is determined by only one of the parameters of the electrical equations of the induction machine. In this case we may write:

$$A - \tilde{A} = (p - \tilde{p}) \cdot A_{er} \quad (31)$$

where p is the respective parameter (speed or rotor resistance), and A_{er} is a constant matrix, with elements depending on the place where p appears in A matrix's coefficients.

For any positive derivable f function we can demonstrate the following inequality:

$$K \cdot \int_0^{t_1} \frac{df}{dt} \cdot f \cdot dt \geq -\frac{K}{2} \cdot f^2(0) \quad (32)$$

On the other hand, using the relation (31), the expression (30) becomes:

$$\eta(0, t_1) = -\int_0^{t_1} e_y^T(t) \cdot (p - \tilde{p}) \cdot A_{er} \cdot \hat{x} \cdot dt \geq -\gamma^2(0) \quad (33)$$

By combining the relations (32) and (33) we can write the following relations:

$$f = p - \tilde{p} \quad (34)$$

$$-e_y^T \cdot A_{er} \cdot \hat{x} = K \cdot \frac{df}{dt} \quad (35)$$

From the relation (35) it immediately results that:

$$-k \cdot e_y^T \cdot A_{er} \cdot \hat{x} = \frac{d}{dt}(p - \tilde{p}) \quad (36)$$

Because K is a constant and then, in case of a slower p parameter variation related to the adaptive law, we can write:

$$\hat{p} = \tilde{p} = k \int e_y^T \cdot A_{er} \cdot \hat{x} \cdot dt \quad (37)$$

Relation (37) represents the general formula used to build an adaptive law. The “k” constant is chosen so that we get a good estimation regime.

Extended luemberger speed estimator

This estimator is a solution based on the use of an adaptive mechanism, in which the reference model is the induction motor, and the adjustable one is a Luemberger-type linear state estimator.

The output being both components of the stator currents in the unitary system of the stator measured for the first and estimated for the second. More than that, estimated rotor fluxes are used to realize the DFOC command.

The equations of the Luemberger estimator are those given by the relations (22) in which the matrixes A, B, L and C are those obtained within the preceding paragraph.

The adaptive mechanism is deduced from the general expression (37), considering that, in this case we have:

$$e_y = \begin{bmatrix} i_{ds} - \hat{i}_{ds} \\ i_{qs} - \hat{i}_{qs} \\ 0 \\ 0 \end{bmatrix} = \begin{bmatrix} e_{yds} \\ e_{yqs} \\ 0 \\ 0 \end{bmatrix}; \hat{x} = \begin{bmatrix} \hat{i}_{ds} \\ \hat{i}_{qs} \\ \hat{\psi}_{dr} \\ \hat{\psi}_{qr} \end{bmatrix} \quad (38)$$

and the A_{er} is:

$$A_{er} = \frac{1}{\omega - \tilde{\omega}} \cdot (A - \tilde{A}) = \begin{bmatrix} 0 & 0 & 0 & a_{14} \\ 0 & 0 & -a_{14} & 0 \\ 0 & 0 & 0 & -1 \\ 0 & 0 & 1 & 0 \end{bmatrix} \quad (39)$$

where:
$$a_{14} = \frac{L_m}{L_s \cdot L_r \cdot \sigma}$$

Under these circumstances, based on the relation (44) we obtain:

$$\hat{\omega} = k \int e_y^T \cdot A_{er} \cdot \hat{x} \cdot dt \quad (40)$$

Introducing in (40) the relations given by (38) and (39) we obtain:

$$\hat{\omega} = k \int \left[e_{yds} \cdot \hat{\psi}_{qr} - e_{yqs} \cdot \hat{\psi}_{dr} \right] \cdot dt \quad (41)$$

in which we considered the arbitrary character of the k constant.

Within numerical implementation of the ELO algorithm, the relation (41) is computed by using one of the methods for numerical evaluation of the integral.

Sometimes, instead of the adaptive law (41) a more complex form is used:

$$\hat{\omega} = k_p \cdot \left[e_{yds} \cdot \hat{\psi}_{qr} - e_{yqs} \cdot \hat{\psi}_{dr} \right] + k_i \int \left[e_{yds} \cdot \hat{\psi}_{qr} - e_{yqs} \cdot \hat{\psi}_{dr} \right] \cdot dt \quad (42)$$

in which appears a proportional component of the same expression that is integrated, from the need to have two coefficients to control the dynamic of the speed estimation. This thing is, in general, not necessary because good results are also obtained by using (41).

3. CONCLUSIONS

The three computing methods of the Luemberger matrix are the basis for the implementation of the Luemberger estimator as well as of the extended Luemberger estimator in various programming environments specific to implementing vector regulating systems for induction motors' speed. In this paper both, the relations that define the rotor flux estimator and the speed estimator are emphasized, the mathematical expressions being presented for both, continual and discrete cases. In case that the implementation of the extended Luemberger estimator is done on a numerical system, in this paper two implementing methods are emphasized: the first method is based on simplified digitization observing that the hardware resources are reduced, and the second method is based on complete digitization observing that the hardware resources are to be much bigger than the preceding case. We can say that the synthesis method of the extended Luemberger estimator is a complete synthesis method and can very easily be applied for a wide range of induction motors.

BIBLIOGRAPHY

- [1] **C.Ilas, V.Bostan**, "Tehnici adaptive de control a motorului asincron: comanda vectoriala fara masurarea vitezei", Litografia U.P.B. 2001
- [2] **T Pana**, *Controlul sistemelor de actionare vectoriala cu motoare de inductie*, Ed. Mediamira, Cluj-Napoca, 2001.
- [3] **A Kelemen, M. Imecs**, *Vector Control of Induction Machine Drives*, OMIKK Publisher, Budapest, 1992.

ZIGBEE DEVELOPMENT SETUP FOR MEASUREMENT-BASED WEB MODELING AND SIMULATION

MIRCEA RISTEIU*, ADRIAN TULBURE**

Abstract: The paper is part of an energetic dispatching system project and is focused on interfacing the local parametric measuring system to the remote processing step. This approach is called smart sensor system and it is based on 8-bit single-chip microcontroller 78K0/KF1+ (μ PD78F0148HGK) 128KB Flash, 512KB serial Flash, 8KB RAM, A/D converter, with 2420 radio transceiver. We have experienced the Zigbee stack for frequency hop method in temperature measurement on high voltage power system. Because the topology, propagation conditions, and interference are highly variable, adaptive protocols are essential for transmission on individual links and for routing packets through the network. For radios with only modest energy-storage capability, it is important that the protocols also conserve energy. The adaptive-transmission protocol allows a radio to change its power and code rate for the next transmission in response to changes in the link that were detected on the previous transmission. Selections of transmission parameters are based on side information that is obtained from the demodulation and decoding processes within the receiving radio for EMC compatibility. When the side information suggests that the interference has decreased, energy can be saved by decreasing the power or increasing the code rate for the next transmission. Such a change in transmission parameters also reduces the interference that the transmission causes to unintended receivers. For this strong demand we have modified sensor *hardbit* header by integrating a Zigbee ping-pong data packet for the transmission rate evaluation.

Keywords: Zigbee, web-based modeling, measurements-based modeling, stack development, 802.15, TCP/IP, adaptive-transmission protocol, frequency-hop spread spectrum, wireless network protocols, mobile communications.

* *Ass.-Prof. at the "1 Dec.1918"-Univ. of Alba-Iulia*

** *Lecturer at the University of Petrosani*

1. INTRODUCTION IN ZIGBEE TECHNOLOGY

Introduction on semiconductor devices for low power wireless networks

Comprehensive monitoring and control of industrial processes and equipment is crucial to achieving efficient production, minimizing cost, and ensuring safety of staff and public. However, providing enough wired sensors – perhaps thousands - to monitor and control an average industrial process is costly and complex business. Applications range from meter reading, through pipeline flow measurement, to machine control. Sensors might simply be for temperature, or for specialist gas detection. Wiring is expensive, and even more expensive to change. Wireless systems can offer a good solution if the sensors and controllers are low cost, easy to install, and can provide a robust transmission method to guarantee the signal gets through. Apart from being cheaper and more flexible, wireless sensors can also be used in hazardous environments inaccessible to normal wired systems.

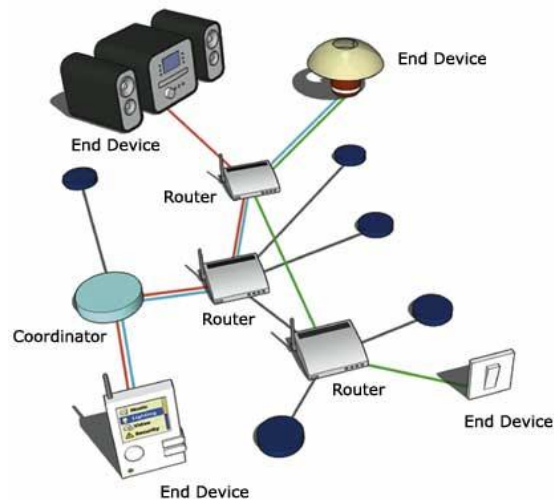


Fig. 8 Suggestive image of integrated automation

In this paper, we deal with the problem of mutual understanding the differences between IEEE 802.11 WLANs (Wireless Local Area Networks) and short-range radio systems based on the Zigbee technology, or equivalently, IEEE 802.15 WPANs (Wireless Personal Area Networks). These systems will operate in the ISM (Industrial, Medical and Scientific) frequency bands, i.e., the unlicensed spectrum at 2.4 GHz. IEEE 802.15 uses a FHSS (Frequency Hopping Spread Spectrum) scheme, while IEEE In this paper, we present a coexistence mechanism based on a simple traffic shaping technique. The proposed mechanism is to be performed at the WLAN stations in presence of a 802.15 voice link. It does not require a centralized traffic scheduler and can be implemented in non-collaborative mode, thus allowing for interference mitigation between co-located and non co-located 802.11 and 802.15 devices. Performance, as well as advantages and disadvantages, of the presented algorithm are compared with those of the so called MEHTA scheme, which is a collaborative algorithm proposed within the IEEE 802.15 Working Group.

1.2 802.11xx vs 802.15 comparison

IEEE 802.11 and IEEE 802.15.3 target at designing PHY and MAC specifications for wireless local area network (WLAN) and wireless personal area network (WPAN), respectively [1]. They adopt different philosophies for MAC design,

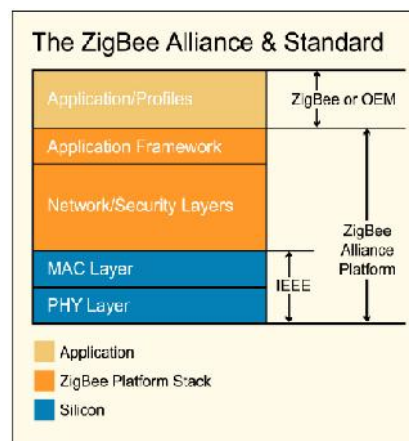
namely CSMA/CA in 802.11 and TDMA in 802.15.3. An interesting problem is the performance of each MAC working on the same physical layer, e.g., ultra wideband (UWB). The results show that the newly added mechanisms of 802.11e, such as transmission opportunity (TXOP) and Block Ack, improve its throughput greatly, making it comparable to that of 802.15.3. In addition, 802.15.3 MAC has easier power management by utilizing its TDMA access method.

ZigBee fills yet another niche. It is a PAN technology based on the IEEE 802.15.4 standard. Unlike Bluetooth or wireless USB devices, ZigBee devices have the ability to form a mesh network between nodes. Meshing is a type of daisy chaining from one device to another. This technique allows the short range of an individual node to be expanded and multiplied, covering a much larger area. The chipset and the stack are incomplete without a profile, which defines the module application. As mentioned previously, there are public profiles and private profiles. For public profiles, ZigBee Logo Certification is available; private profiles are not intended to interoperate and therefore cannot be certified.

Implementing profiles, either public or private, is no small undertaking. In addition to the need to license development tools from the stack providers and attending a training class, we have to be prepared to spend a fair amount of time studying the various firmware components that constitute the ZigBee stack. Also we have to make sure that the firmware engineers are familiar with the microcontroller used in the platform. While none of these items is insurmountable, they do add to development costs and time to market.

2. ANALYZING STACK COMPONENT OF ZIGBEE TECHNOLOGY

In our approach we used smart sensor system and it is based on 8-bit single-chip microcontroller 78K0/KF1+ (μ PD78F0148HGK) 128KB Flash, 512KB serial Flash, 8KB RAM, A/D converter, with 2420 radio transceiver. For our purpose we built up a client application packet for using Object Oriented approach around a Xmesh server. Before running real time measurements we have built up a virtual sender (local emulator) (figure 4) where we have programmed fixed packets, for comparison and errors checking.



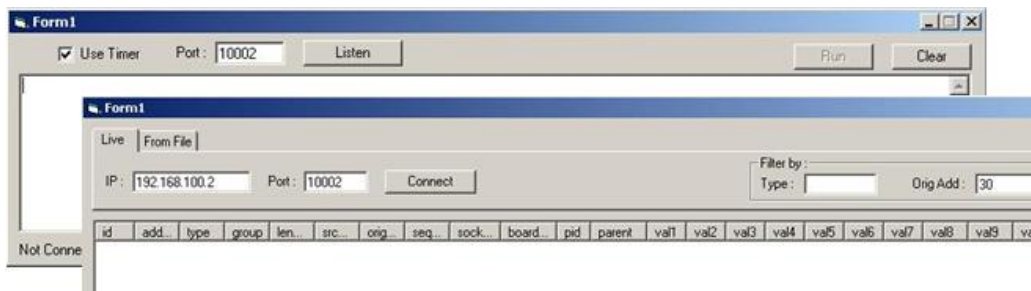


Fig. 9 Emulator & client application

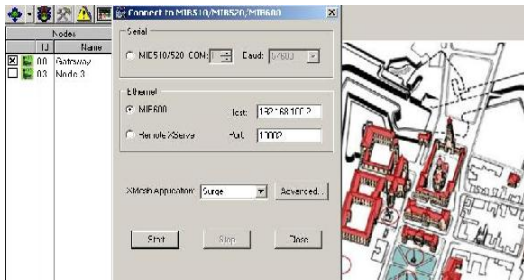


Fig. 10 Configuration interface

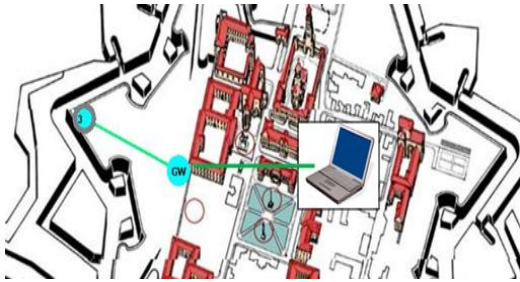


Fig. 11 Sensors positioning

database on the machine when that option is checked. The installation requires administrative privileges on the system, including the ability to create a new user called *postgres*. The Data tab on the application interface displays the latest sensor readings received for each node in the network. Any column of data can be sorted by left clicking the top. This allows you to sort by node ID, parent, temperature, voltage, last result time, or any other sensor reading. For configuring the communication protocol between gateway (FFD) and measurement station some extra facilities have been developed.

Gateways, together with their related system software, are a key component of WSNs. Their duties include protocol conversion; acting as proxy servers (thus eliminating the need to poll every node from an application or management tool); and performing sensor management functions such as network definition, monitoring, deployment, and configuration. Additional duties may include alert and alarm processing; sensor logging and database management; application programming interfaces (APIs); security key management; traffic analysis and optimization;

On the other hand we have executed device control center for real measurements. This OEM application is designed to be an interface (“client tier”) between a user and a deployed network of wireless sensors. It provides users the tools to simplify deployment and monitoring (figure 5). It also makes it

easy to connect to a database, to analyze, and to graph sensor readings. The associated server protocol is a multihop mesh networking protocol that has various options including low-power listening, time synchronization, sleep modes, any-to-base and base-to-any routing. All of our sensor and data acquisition boards are supported with these enabled applications. The installation of database environment (*PostgreSQL*) will automatically install and configure a local *PostgreSQL 8.0*

application integration; and routing management. Gateway TCP/IP application programming interfaces enable developers to leverage WSN technology using familiar Internet programming paradigms. Protocol conversion will break down barriers between WSNs and other types of networks. Gateway standards such as Universal Plug and Play (UPnP) and OPC support integration of diverse devices, including computers, electronics, security and automation components, and other networked devices spanning wireless and wired networks.

3. WIRELESS MEASUREMENT- BASED SETUP

By implementing this setup, we have started measurement analysis. The data packets are framed (at the start and end) by 0x7e (126) (SYNC_BYTE) bytes. Each packet has the form: <packet type><data bytes 1...n><16-bit CRC>.

Each packet is framed on either end by a SYNC_BYTE. The value of the SYNC_BYTE is 0x7E. The type field indicates the type of packet sent. There are five packet frame types:

- *P_PACKET_NO_ACK* = 0x42(66): A user-packet with no acknowledgement required.
- *P_PACKET_ACK* = 0x41: A user-packet that requires acknowledgement.
- *P_ACK* = 0x40: Required response for P_PACKET_ACK packet.
- *P_UNKNOWN*: Unknown packet type received. Requires response of type P_UNKNOWN

Data is the packet payload. If the packet payload contains the special SYNC_BYTE, it is escaped out. The escaping algorithm is described below.

The 2-byte CRC is a redundancy check on the packet type and the data bytes. It is used by the receiving application to verify the packet is not been corrupted during transport. The CRC calculation includes the type byte through the end of the data payload. If the SYNC_BYTE is sent in data portion of the application it would confuse the receiving application by making prematurely end the packet. To avoid this, if a SYNC_BYTE is in the data portion of the packet, the byte is escaped out. Escape bytes are proceeded with 0x7d (ESC_BYTE), then the byte value XOR (exclusive or) with 0x20. For example, 0x7e is converted to 0x7d5e; 0x7d and 0x7e bytes must be escaped; 0x00 to 0x1f and 0x80 to 0x9f can be optionally escaped. By following XServe User's Manual (XServe_Users_Manual_7430-0111-01_B.pdf , pag 188) we have access to the programming environment of TinyOS as:

Bin	126,66,125,94,0,17,125,93,22,0,0,0,0,0,0,0,0,0,0,125,94,0,180,1,0,194,100,110,0,0,82,109,66,143,126
Hex	7E 42 7D 5E 00 11 7D 5D 16 00 00 00 00 00 00 00 00 00 00 00 7D 5E 00 B4 01 00 C2 64 6E 00 00 52 6D 42 8F 7E

After processing:

Bin	126,66,125,94,0,17,125,93,22,0,0,0,0,0,0,0,0,0,0,125,94,0,180,1,0,194,100,110,0,0,82,109,66,143,126
Hex	7E 00 11 7D 16 00 00 00 00 00 00 00 00 00 00 00 00 00 00 7E 00 B4 01 00 C2 64 6E 00 00 52 6D

Because the header of TinyOS is:

7E 00 11 7D 16 00 00 00 00 00 00 00 00 00 00 00 7E 00 B4 01 00 C2 64 6E 00 00 52 6D

With the associated commands:

- *dest_address* - Single hop destination address: 7E 00 (126, 0) => bytearray="0" length="2" type="uint16"
- *am_type* - Active message type: 11 (17) => bytearray="2" length="1" type="uint8"
- *group* - Active message group ID: 7D (125)=> bytearray="3" length="1" type="uint8"
- *length* - Length of entire message: 16(22) => bytearray="4" length="1" type="uint8"

And the associated chain header:

00 00 00 00 00 00 00 00 00 00 00 00 7E 00 B4 01 00 C2 64 6E 00 00 52 6D.

The XMesh header is:

00 00 00 00 00 00 00 00 00 00 00 00 7E 00 B4 01 00 C2 64 6E 00 00 52 6D

With the main associated commands:

- *sourceaddr* - Single hop sender address: 00 00 (0,0)=> bytearray="5" length="2" type="uint16"
- *originaddr* - Node ID of originator of message: 00 00 (0,0)=> bytearray="7" length="2" type="uint16"
- *seqno* - Sequence number for link estimation: 00 00 (0,0)=> bytearray="9" length="2" type="uint16"
- *Socket* - Application ID: 00 (0)=> bytearray="11" length="1" type="uint8"

And, the associated chain header is: 00 00 00 7E 00 B4 01 00 C2 64 6E 00 00 52 6D

The associated combined commands are:

- XSensor Header: 00 00 00 7E 00 B4 01 00 C2 64 6E 00 00 52 6D
- *board_id* - Sensor Board ID: 00 (0)=> bytearray="12" length="1" type="uint8"
- *packet_id* - Sensor Packet ID; 00 (0)=> bytearray="13" length="1" type="uint8"
- *Parent* - Sensor Parent: 00 7E (0,126)=> bytearray="14" length="2" type="uint16"

The main conclusion related to sensor analysis is that each sensor has own packet structure. The packet ends with a CRC that is calculated on the entire packet excluding the packet header and the CRC field itself. A CRC is calculated by XORing the current byte with a shifted CRC accumulator. The CRC is always 2 bytes. (XServe_Users_Manual_7430-0111-01_B.pdf , pag 68).So, by extracting the specofoc code from 7E 00 11 7D 16 00 00 00 00 00 00 00 00 00 00 00 7E 00 06 00 00 BE C0 7A 60 79 8E 74, result: 00 7E - parent; 00 06 - epoch; C0 - Light; 7A - Thermistor; 60 - magX; 79 - magY; 8E - accelX; 74 - accelY. Measured data (case study) exported into standard datasheet.

4. SELF-HEALTHING NETWORK. MULTI-HOPE PROTOCOL

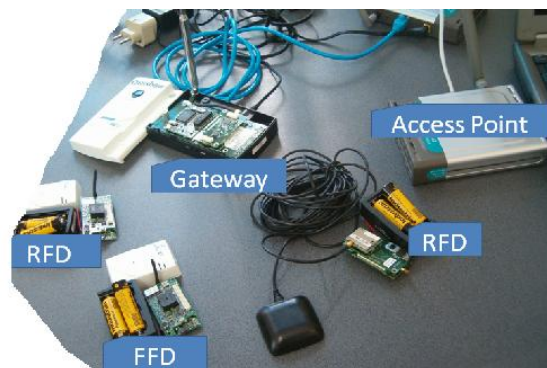


Fig. 12 Integrating the Zigbee devices with TCP/IP

In order to fit this requirement, the main components of the setup are: **End Devices**, also called Nodes, Edge Nodes, Devices, or Reduced Function Devices (RFDs), are battery-powered devices that wake up periodically and send data to a host. **Routers** also called Mesh Nodes, Coordinators, or Full Function Devices (FFDs), form a wireless backbone that ferries messages in a multi-hop fashion across the network. Routers allow messages to flow in various directions on demand and buffer messages for nearby End Devices that are currently sleeping. Routers need to expend energy handling traffic on behalf of other network devices and therefore tend to use more power than End Devices. In most implementations, Routers run their receivers continuously and thus require a continuous power source. Routers can also act as application nodes. **Gateways**, also called Bridges, Controllers, Internet Interfaces, or PAN Coordinators, are usually envisioned as Internet appliances that provide an interface between the WSN and the Internet. Gateways control and monitor the WSN, consolidate data from various nodes, execute business logic, and provide a TCP/IP interface to the outside world. Gateways provide scalability, enabling subnets of WSNs within the enterprise to operate in a collaborative fashion.

5. CONCLUSION. ENSURING MULTI-HOPE PROTOCOL

It is a goal at some point to add mesh routing support to this stack. The next figure shows the diagram form multi-hope and self-*healing* situation. In this approach, wireless sensor networks offer numerous benefits over previous networking solutions for many applications, including lowered costs, the ability to leverage infrastructure for multiple applications, and the capacity to restructure the network quickly and easily, as well as security, scalability, and ease of administration.

The catch-all phrase for low power, low data rate sensor networks targeted at condition monitoring, lighting and climate control as well as safety and security. The goal is to provide a standard, yet extensible, protocol stack for use with 802.15.4 radios with enough flexibility for use in limited power environments for low latency, single hop networks as well as longer distance, multi-hope mesh network configurations. So,

the main pros are: standards based sensor networking allows multi-sourcing, interoperability; multi-path mesh architecture can overcome difficult RF environments.

BIBLIOGRAPHY

[1] **Xin Wang, Yong Ren, Jun Zhao, Zihua Guo, Yao, R.** Comparison of IEEE 802.11e and IEEE 802.15.3 MAC, Emerging Technologies: Frontiers of Mobile and Wireless Communication, 2004. Proceedings of the IEEE 6th Circuits and Systems Symposium on Volume 2, Issue , 31 May-2 June 2004 Page(s): 675 - 680 Vol.2

[2] **xxx** A Zigbee-subset/IEEE 802.15.4, Multi-platform Protocol Stack, IEEE 802.xx, 2006

[3] **xxx** IEEE Std. 802.15.4, Part 15.4: Wireless Medium Access Control (MAC) and Physical Layer (PHY) Specifications for Low-Rate Wireless Personal Area Networks (LR-WPANs), pp. 679.

[4] **xxx** Zigbee Alliance, Zigbee SPecification Version 1.0, pp. 376. Available online at www.zigbee.org

THERMOENERGETIC BLOCK ON COAL. POLLUTION VECTOR: EVACUATED WATER

ANDREEA BRÎNDUȘA*, IOSIF KOVACS**

Abstract: In thermo energetic power stations which function on coal, the cooling of energetic aggregates and the steam production have as base collected water from surface sources. Evacuated water from the thermo energetic blocks is the polluting vector for the surface sources by modifying the physical dimension: temperature. The main problem in this case is keeping this dimension in admitted values that won't affect the bioaquatic fauna.

Keywords: industrial water, coal, thermo energetic block, pollution vector

1. INTRODUCTION

The energetic blocks, with installed powers of great values from our country, have as basis turbo- generators of an apparent power of 388 MVA, an active power of 330MW, the THA330-2 type and the steam turbine of the FIC 330 MW type.

The steam turbine of the FIC 330 MW type has the following technical characteristics:

- the maximum cont. power:330MW
- the revolution: 3000rpm
- the temperature in. IP:535C
- the pressure ot.IP: 49,8atm
- the debit ot. IP: 1023t/h
- the power of overcharge: 345MW
- the pressure in. IP: 186atm
- the debit in. IP: 1035t/h
- the temperature ot. IP:344C

The turbo-generator is of the THA330-2 type and of an apparent power of 388 MVA, an active power of 330 MW, the THA330-2 type shows the following technique characteristics:

- apparent power: 388MVA
- revolution: 3000rpm
- active power: 330MW
- frequency: 50Hz

* *PhD. Ec. University of Petrosani*

** *Professof PhD .eng. University of Petrosani*

- tension: 24kV
- electric current: 9334A
- number of phases:3
- the connection of phases: Y

The system of water alimentation, energetic group, is realized mainly on the basis of two channels, one of adduction and the other of industrial water evacuation.

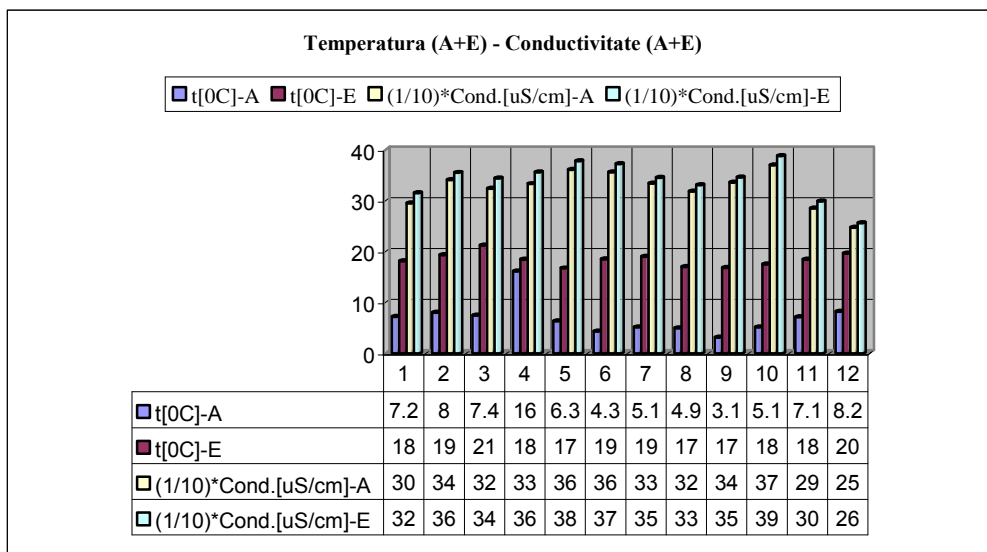
One of the most important physical parameters for establishing the brute qality of water which supplies the thermoelectrical power station and the evacuated industrial water made by them is temperature.

It is imposed the measurement of the physical-chemical parameters of the industrial water collected and evacuated from the energetic blocks.

2. WATER COLLECTED AND EVACUATED, ENERGETIC GROUPS. VARIATION PARAMETER: TEMPERATURE

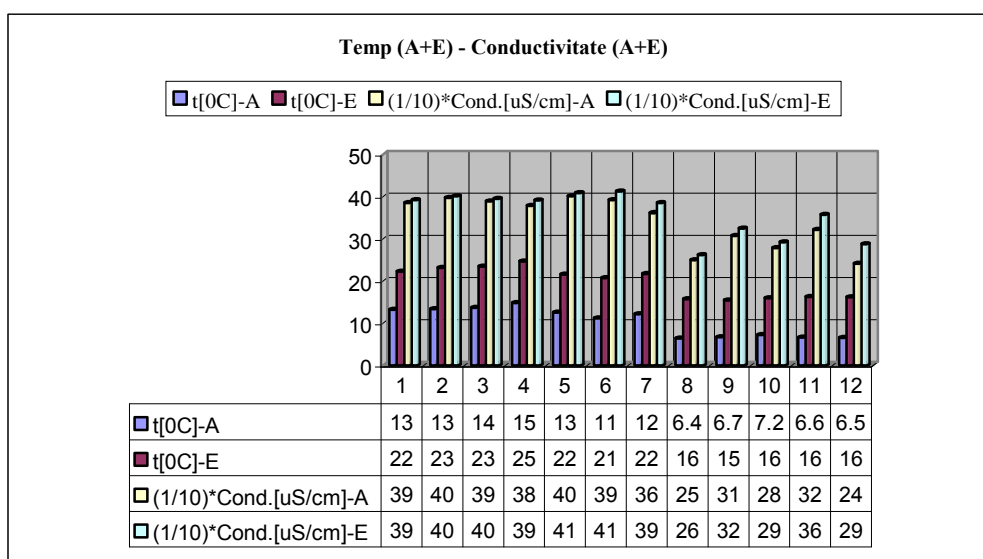
This case study has been made base don collected data from SC Thermoenergetic Complex Turceni on collected and evacuated industrial water from 330 MW Thermoenergetic blocks, duaring the II and IV trimester of 2006.

Values physical indicatoris Collected+Evacuated channels in the II trimester of 2006.



The important parameters for the industrial water used in the energetic groups are mainly the following:- temperature.

Values physical indicatoris Collected+Evacuated channels in the IV trimester of 2006.



The collected and evacuated water in and from the river Jiu is made through collectig and evacuating points and channels.

The supervision of the important phisical and chemical parameters is made all the time and in real time through some complex equipments, set in a observation cabin, with telemetrical transmission of the collected datas.

3. CONCLUSIONS

The evaluation of the environment performance of the industrial branch- Energetic industry- is absolutely necessary in an open and interconnected society specific to the XXI century, where the globalization phenomenon is present all over.

The biggest consumption of industrial water from the surface area lead to:

- the necessity of introducing solutions and technical methods which can stop the growth slope of the consumption of industrial water
- the necessity of permanent monitorisation of the physical-chemical parameters, water collected and evacuated from the industrial giants, Energetic Complex.

Thouse Energetic Complex have in common four big characteristics:

- big power installed: of order *1000 MW;
- they are situated in the same hydrographic basin, the river Jiu basin, which is situated in the neighborhood of the river;
- there are Energetic Complex which use as prime substance inferior coal of lignite type from the Oltenia miner basin;
- it polluted a commune region definite so, such from the commune geographical elements and the specific elements of activity (technological processes of production and socio-economical services) very close.

REFERENCES

[1]. **Brîndușa, A., Kovacs, I.**, *Physical-chemical parameters water collected and evacuated at the energetic blocks*, Simpozion internațional multidisciplinar “UNIVERSITARIA SIMPRO 2006”, Universitatea din Petroani, Petroani, 13-14 octombrie 2006.

[2]. **Brîndușa, A., Bulucea, A.**, *Considerations upon industrial wastewater purifying equipments*, Simpozion național “Ingineria mecanică și mediul”, Universitatea din Craiova, Craiova, 6-7 octombrie 2006.

[3]. **Brîndușa, A.**, *The factors of degradation of the environment and of the tourist potential specific to the autochthon relief*, Simpozion internațional multidisciplinar “UNIVERSITARIA SIMPRO 2006”, Universitatea din Petroani, Petroani, 13-14 octombrie 2006.

ONE CLASSIFICATION EXAMPLE OF DECISION SUPPORT SYSTEMS

PREDRAG DAŠIĆ* RATOMIR JEČMENICA** VEIS ŠERIFI***

Abstract: Application of modern manufacturing philosophies (CIM, EMS, JAT, JIT, PLM, SAT, TPM, TQEM, TQM etc.) in manufacturing conditions, demands greater speed and accuracy in information movement, which can not be done without modern system for decision support (DSS). Today, under modern DSS system we imply a system which is supported by powerful computer technique, which is more acceptable from the aspect of price, as of performance it offers. And its goal is to create good information that can be managed and to make a decision based on that information. In the paper is given clasification of DSS system by diffrent basics from from various areas of human influence.

Keywords: Information System (IS), Decision Support System (DSS)

1. INTRODUCTION

In forties in last centuries (from 1940. year and later), experts for computer science have begun to develop techniques which will enable computers to achieve more. Research efforts of scientists have been pointed in direction of computer development which are able to look and talk. These kind of systems were based as systems with elements of artificial intelligence.

During 1950 was begun development and application of TPS systems, in1960 development and application of MIS system and in 1970 development and application of DSS system.

In 1980 (from 1980. year until today) begins development of expert systems as software systems. In the beginning the research of expert systems was limited to a small number of research institutions usually university research laboratories. In 1985.

*¹ *High Technical Mechanical School, Trstenik and High Technological School, Kruševac, SERBIA, E-mail: dasicp@ptt.yu*

** *University of Kragujevac, Technical Faculty, Cacak, SERBIA, E-mail: jecmenica@tfc.kg.ac.yu*

*** *O.Š. "5. October", Dragaš, Kosovo, SERBIA, E-mail: veisserifi@yahoo.com*

year in some countries as USA, Japan, England, countries of Europe (EU), begin to accelerate research program with goal to develop and apply expert systems.

In that time about 500 corporations and national companies have formed departments of artificial intelligence, invested in equipment and technology on development of expert systems, all in cause of achieving better commercial success

Development of micro computing, led to new generation of computers which had better performances than before, with goal to operate more successfully than earlier and to enable work on expert systems (computers of V i VI generation).

In 1980 was developed and applied EIS, GDSS and ODSS systems. Inclusion of knowledge in IT led to development of so called KB-DSS or IDSS which were developed during 1990. In the new millennium was developed and applied in various areas WB-DSS systems.

Assignment of all information systems was to process input data into output data, usable for making certain decisions. Back link has for goal to control whether the output size is a real value, and if a expected real value is not achieved then it comes to correction of input values (adjusting of fault in input or in data processing).

2. DECISION SUPPORT SYSTEM

DSS (*Decision Support System*) system is based on computer which in given opportunity enables managing in way that it takes different information about organization and predicts effect of possible decisions. It is based on set of procedures that are used for processing data, managing informations, and decision making, supporting complex and hard decision making, and have begun to develop by appearance of program languages of fourth generation and so called application generators [1-4,8,10-12,15,17,18,20].

Unlike MIS (*Management Information System*) (figure 1) DSS system provides greater help in analysis and decision making. (figure 2).

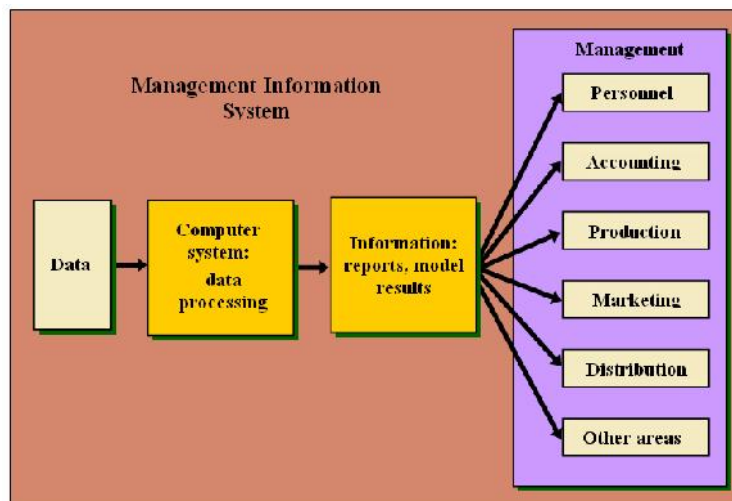


Figure 1: Information management in Management Information Systems (MIS)

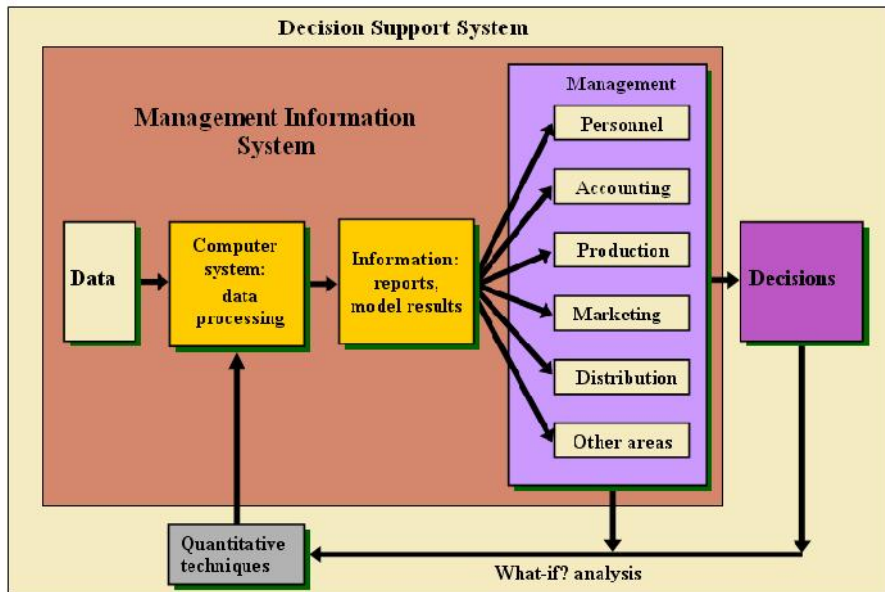


Figure 2: Information management and decision making in Decision Support Systems (DSS)

Beginning of development of Decision Support Systems (DSS) is tightly involved for theory development and quantity method and model (linear programming, network planning, simulation, dynamic programming, theory of lines etc.) during 1970. In middle of 1980 a concept appeared of GDSS i ODSS systems. During 1990 concepts OLAP and KB-DSS, and by the end of 1990 and beginning of 2000 concept WB-DSS (figure 3).

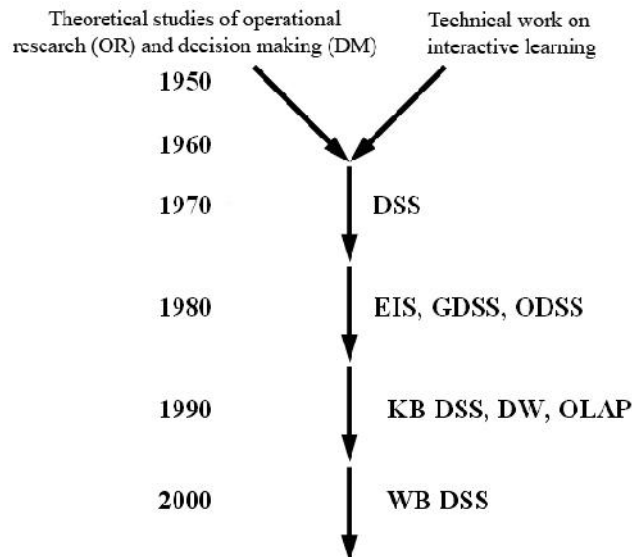


Figure 3: Brief graphical preview of historical development of DSS system

Basic goal of DSS system is to secure quality information for process of decision making in cause of increasing decision efficiency and to help decision makers to solve unstructured or weakly structured problems (decision making).

Main characteristics of these systems are:

- Orientation to decision making,
- Orientation to solving weakly structured problems decision making and orientation on end user,
- They give help in decision making on all levels of decision, but are of special importance for higher levels, and unlike MIS systems who mostly simplify horizontal flow of informations, DSS systems support vertical informational flows and by that help information integration that are used on different organization and managing levels.,
- They ease sintesis of informations from certain subsystems for strategic decision making and contribute automatisation of strategic planning and prediction,
- Easy to use, languages of communication are very simple, and structure of system is made that way that enables easy access to the data in interactive work etc.

Basic components of DSS system are: (Figure 4) [5,14]:

- Users with user interface,
- Databases,
- Models of decision making and bases of prediction, planning and decision making,
- Communication components and
- Special software which links users with data and models.

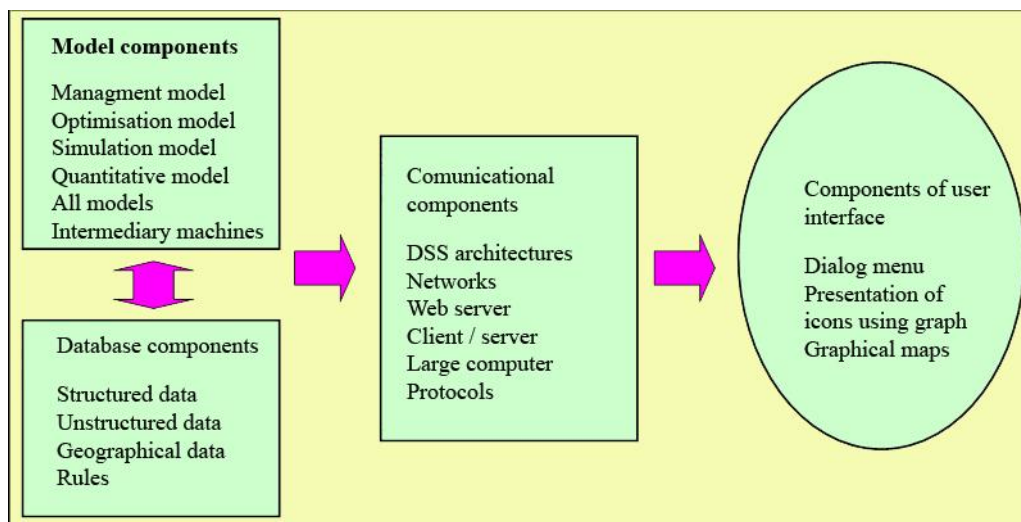


Figure 4: Traditional components of DSS system [5,14]

3. CLASSIFICATION OF DSS SYSTEMS

Different authors suggest different classifications. In the paper will be applied classification of DSS to:

- Classification of DSS systems according to user level,

- Classification of DSS systems according to conceptual level,
- Classification of DSS systems according to system level,
- Classification of DSS systems according to according to way of realization
- Classification of DSS systems according to according to concrete realization.

3.1. Classification of DSS systems according to user level

In user level the following differs [6]:

- *Passive DSS* systems, Which helps the process of *Decision Making* (DM) and can not give explicit output decision of suggestion or solution,
- *Active DSS* systems, which can give explicit output decision of suggestion or solution,
- *Cooperative DSS* systems, which suggests making of decision (or its advice) for modified, complete or ratified decision of suggestion prepared from system, which is in advance sent to him to the system for quality check.

3.2. Classification of DSS systems according to conceptual level

In conceptual level the following differs [15,16,20]:

- *Model-driven DSS* systems, which accentuate access to and manipulation of statistic, financial, optimization or simulation models, and use data and parameters delivered by DSS users for help in decision making in analyzed simulation, except when they are not intensive data (example model-driven DSS generator of open code is *Dicodess*),
- *Communication-driven DSS* systems, which supports work with more then one user on common work, and as an example includes integrated software tools like Microsoft NetMeeting or Groove,
- *Data-driven DSS* systems or *data-oriented DSS* systems, which accentuate access to and manipulation of time series of inter data of company and sometimes extern data,
- *Document-driven DSS* systems, who manages, rehabilitates and manipulates unstructured information in many electronic data and
- *Knowledge-driven DSS* systems, which ensures specialized problem solving of reserve expertise in form of facts, rules, procedures or in similar structures.

3.3. Classification of DSS systems according to system level

In system level the following differs [15,20]:

- *Enterprise-wide DSS* systems, which are connected with large data storage and serve managers in company and,
- *Desktop DSS* systems, which are small systems that are located on individual managers computers

3.4. Classification of DSS systems according to way of realization

DSS systems, according to way of realization split to [1,2,4,5,7,8,12-14,16,18,19]:

- EDSS (*Expert Decision Support System*) systems,
- GDSS (*Group Decision Support System*) systems,
- MDSS (*Multiparticipant Decision Support System*) systems,
- NSS (*Negotiation Support System*) systems,
- ODSS (*Organizational Decision Support System*) systems,
- PDSS (*Planning Decision Support System*) systems,
- TDSS (*Team Decision Support System*) systems,
- WB-DDS (*Web-Based Decision Support System*) systems.

3.4. Classification of DSS systems according to concrete realization

Concrete realized DSS systems, according to sort of given services, for wider geographical area are for example [3-5,9]:

- CDSS (*Consumer Decision Support System*) systems,
- EDSS (*Environmental Decision Support System*) systems,
- GSDSS (*Group Spatial Decision Support System*) systems,
- IDSS (*Intelligent Environmental Decision Support System*) systems,
- LADSS (*Land Allocation Decision Support System*) systems,
- MC-SDSS (*Multi-Criteria S Decision Support System*) systems,
- SDDS (*Spatial Decision Support System*) systems,
- TDSS (*Tactical Decision Support System*) systems,
- WebSDDS (*Web-Based Spatial Decision Support System*) systems and etc.

4. CONCLUSION

Modern business demands greater speed and accuracy during flow of informations, which can not be done without modern DSS system.

In areas of information systems is no common methodology of DSS classification, so different authors classify them differently, but there is a large number of developed DSS systems, among which according to way of realization are: EDSS, GDSS, MDSS, ODSS, PDSS, TDSS i WB-DSS, or by sort of given services: CDSS, EDSS, GSDSS. GSDSS, LADSS, MC-SDSS, TDSS i WebSDDS etc.

REFERENCES

[1] **Arsovski, Z.:** *Informations systems* (in Serbian language). Kragujevac: Faculty of Mechanical Engineering, CIM center, 2001. – 484 pp. ISBN 86-80581-36-4.

[2] **Britanica,** *On-Line Encyclopedia.* Available on Web site: <http://www.britanica.com/>.

[3] **Cortés, U.; Sánchez-Marré, M.; Ceccaronni, L.;** Rodríguez-Roda, I.; and Poch, M.: Artificial intelligence and environmental decision support systems. *Applied Intelligence*, 13 (2000.), No. 1, pp. 77-91. ISSN 0924-669X.

- [4] **Dašić, P.:** *Encyclopedia of the Technical and ICT Abbreviations* (in preparation in Serbian language). Electronic Edition. Trstenik: High Technical Mechanical School. ISBN 86-83803-12-0.
- [5] **Dašić, P.; Ječmenica, R.; Šerifi, V.:** Analysis of KB-DSS systems. In: *Proceedings on CD-ROM of 6th International Conference "Research and Development in Mechanical Industry - RaDMI 2006"*, Budva, Montenegro, 13-17. September 2006. Edited by Predrag Daši . Kraljevo: Faculty of Mechanical Engineering of and Trstenik: High Technical Mechanical School, 2006, pp. 751-757. ISBN 86-83803-21-X.
- [6] **Hättenschwiler, P.:** Neues anwenderfreundliches Konzept der Entscheidungsunterstützung. *Gutes Entscheiden in Wirtschaft, Politik und Gesellschaft*. Zurich, vdf Hochschulverlag AG: 1999, s. 189-208.
- [7] **Klein, M. R. and Methlie, L. B.:** *Knowledge-based DSS with applications in business*. 2nd edition. New York (NY – USA): John Wiley & Sons, Inc., 1995. – 544 pp. ISBN 0-471-95295-8.
- [8] **Kock E.:** *Decentralising the Codification of Rules in a Decision Support Expert Knowledge Base*. Master's Dissertation. Pretoria: Faculty of Engineering, Built Environment and Information Technology, University of Pretoria, 2003. – 165 pp.
- [9] **Matthews, K. B.; Sibbald, A. R. and Craw, S.:** Implementation of a spatial decision support system for rural land use planning: integrating geographical information system and environmental models with search and optimisation algorithms. *Computers and Electronics in Agriculture*, Vol, 23 (1999.), pp. 9-26.
- [10] **Mićić, J.; Je menica, R.:** *Operating systems with basis of information technology* (in Serbian language). a ak: Technical Faculty, 2000. – 174 pp. ISBN 86-81745-54-9.
- [11] **Parsaye, K, et al:** *Intelligent Databases: Object-Oriented, Deductive Hypermedia Technologies*. New York (NY – USA): John Wiley & Sons, Inc., 1989. – 479 pp. ISBN 0-471-50345-2.
- [12] **Power, D. J.:** *Decision support systems: concepts and resources for managers*. Westport, Conn., Quorum Books, 2002.
- [13] **Power, D. J.:** Web-based decision support systems. *The On-Line Executive Journal for Data-Intensive Decision Support*, Vol. 2 (1998.), No. 33-34. Available on Web site: <http://dssresources.com/papers/webdss/>.
- [14] **Power, D. J.:** Web-based and model-driven decision support systems: Concepts and issues. In: *Proceedings of Americas Conference on Information Systems*. Long Beach, California, 2000.
- [15] **Power, D. J.:** What is a DSS?. *The On-Line Executive Journal for Data-Intensive Decision Support*, Vol. 1 (1997.), No. 3.
- [16] **Power, D. J. and Kapauthi S.:** Building Web-based decision support systems. *Studies in Informatics and Control*, Vol. 11 (2002.), No. 4, pp. 291-302.
- [17] **Stadlmeyer, V.:** *Entscheidungsunterstützung zur technischen Planung im Fertigungsbereich*. Dissertation. Schriftenreihe Produktionstechnik, Band 8. Saarbrücken: Universität des Saarlandes, 1994. ISBN 3-930429-37-3.
- [18] **Turban, E.:** *Decision support and expert systems: Management support systems*. 4th edition. New York (NY – USA): Macmillan Publishing Company, 1995. – 1005 pp. ISBN: 0-02-421701-8.
- [19] **Turban, E.; McLean, E. and Wetherbe, J.:** *Information technology for management: Transforming business in the digital economy*. 3rd edition. New York (NY – USA): John Wiley & Sons, Inc., 2001. – 832 pp. ISBN 0-471-21533-3.
- [20] *Wikipedia, Free Encyclopedia*. Available on Web site: http://en.wikipedia.org/wiki/Main_Page.

IMPLEMENTING WITHIN AN OBJECT-ORIENTED LANGUAGE (JAVA) THE UML MODELLING CONCEPTS

LIVIU DUMITRASCU^{*}, GABRIEL MARCU^{**}, DOREL DUSMANESCU^{***}

Abstract: An verry important phase of developping software applications process consist in modelling the rality that need to be implemented as executable software, writed in some programming language. UML is an object-oriented modelling language that need to be translated into an programming languanges. This paper present a synthesis of the correspondences between the UML and the object –oriented language Java.

Keywords: model, object, class, diagram, interface, package, attribut

1. FROM UML TO JAVA

The UML language is a visual modelling language and Java or C# are textual programming languages. UML is richer than the programming languages in the sense that it offers stronger and more abstract ways of expressing.

Java is a rapid, elegant and strong programming language starting with the launching of the 1.02 version, Java attracting programmers by means of its friendly syntax, the object oriented characteristics, the memory administration and portability. Java 5.0 (versions 1.5 and newer ones) has brought major changes within the proper language, making it simpler for programmers and adding to it already popular characteristics.

The Java programming cycle is different from the model. The information contained by an UML model has as objective generating the application code. To accomplish an UML language it is not easier than writing a Java code. The information contained within the models has to be synchronised with the Java code. There is in this respect a privileged way of translating UML concepts into Java statements.

^{*} *Professor, Ph.D. at the Petroleum and Gas University of Ploiesti*

^{**} *Assoc. prof, Ph.D. at the Petroleum and GasUniversity of Ploiesti*

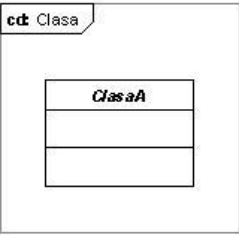
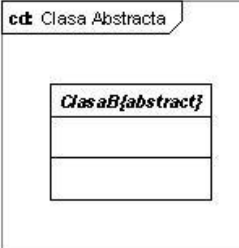
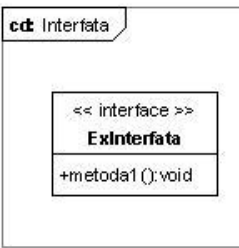
^{***} *Lecturer, Ph.D. at the Petroleum and GasUniversity of Ploiesti*

This paper offers you a synthesis of the major correspondences between the UML modelling concepts and the rules for generating the Java code.

2. UML CORRESPONDENCE RULES TOWARDS JAVA

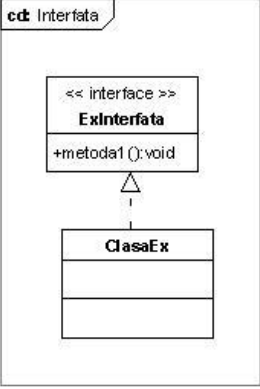
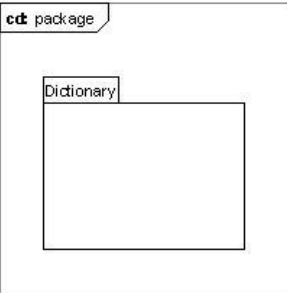
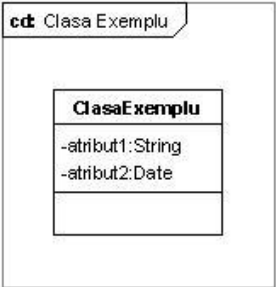
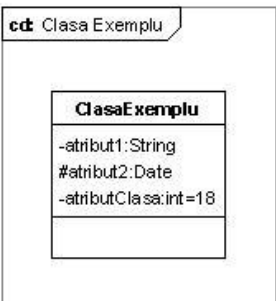
Table 1 presents a synthesis of the major correspondences between the UML modelling concepts and the way they are implemented within Java.

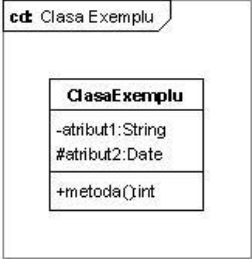
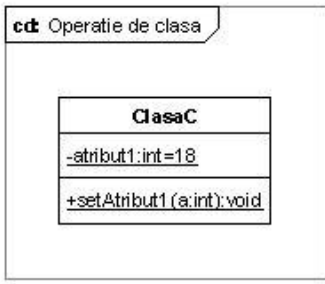
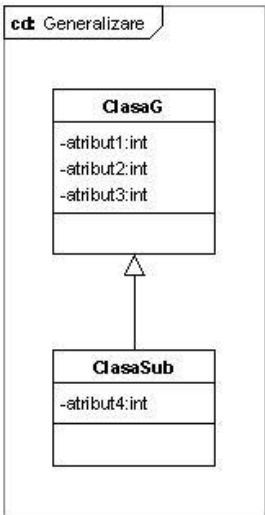
Table 1.

Concept	UML	Java
Class	 <p>The UML diagram shows a class named 'Clasa' with a compartment containing 'ClasaA'. The class has two empty compartments below the name, representing attributes and operations.</p>	<pre>public class A { ... }</pre>
Class(abstract)	 <p>The UML diagram shows an abstract class named 'Clasa Abstracta' with a compartment containing 'ClasaB{abstract}'. The class has two empty compartments below the name, representing attributes and operations.</p>	<pre>public abstract class B { ... }</pre>
Interface	 <p>The UML diagram shows an interface named 'Interfata' with a compartment containing '<< interface >>' and 'ExInterfata'. Below the name, there is a compartment containing '+metoda1():void'.</p>	<pre>interface ExInterfata { void metoda1 (); }</pre>

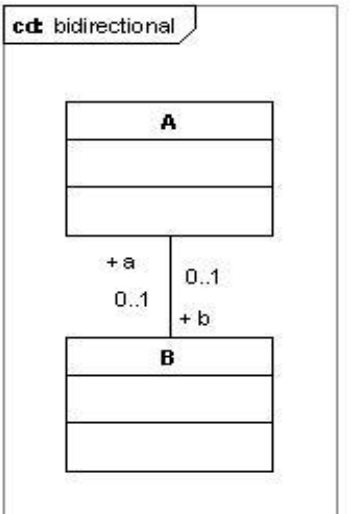
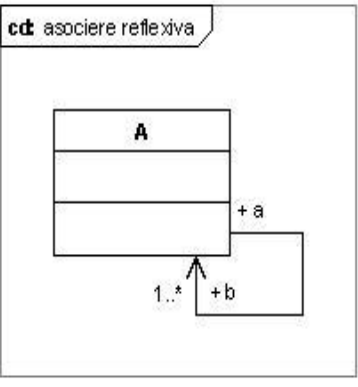
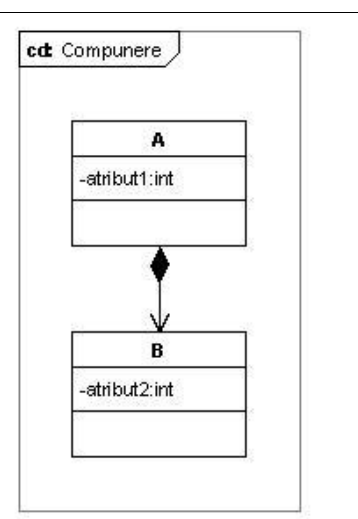
Implementing within an object-oriented language (java) the
UML modelling concepts

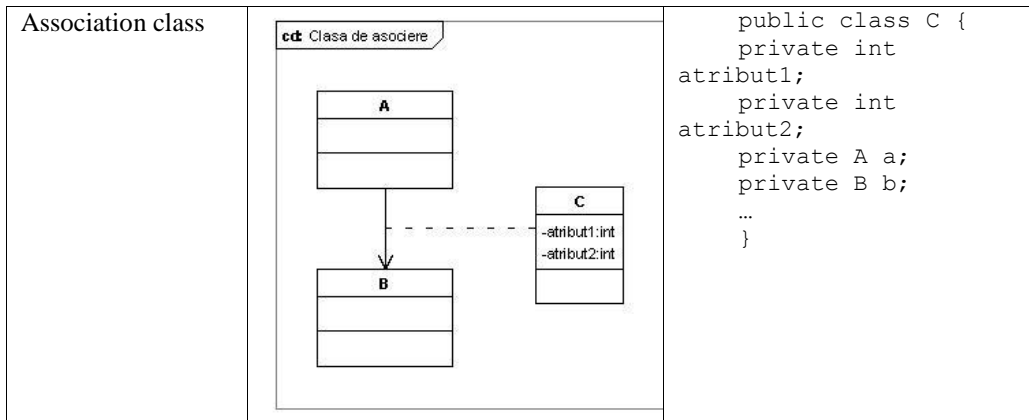
-394-

	 <pre> classDiagram class ExInterfata { <<interface>> +metoda1():void } class ClasaEx ExInterfata < -- ClasaEx </pre>	
package		package dictionary;
Attribute		<pre> import java.util. Date; public class ClasaExemplu { private String atribut1; private Date atribut2; ... } </pre>
Attribute (of class)		<pre> abstract public class clasaExemplu { private String atribut 1; protected Date atribut 2; private static int atributClasa=18; } </pre>

<p>Operation</p>	 <pre> classDiagram class ClasaExemplu { -atribut1:String #atribut2:Date +metoda():int } </pre>	<pre> public class ClasaExemplu { private String atribut1; protected Date atribut2; public int metoda() { ... } } </pre>
<p>Operation (of class)</p>	 <pre> classDiagram class ClasaC { -atribut1:int=18 +setAtribut1(a:int):void } </pre>	<pre> public class clasaC { private static int atribut1= 18; public static void setatribut1 (int a) { ... } } </pre>
<p>Generalisation</p>	 <pre> classDiagram ClasaSub < -- ClasaG class ClasaG { -atribut1:int -atribut2:int -atribut3:int } class ClasaSub { -atribut4:int } </pre>	<pre> public class ClasaSub extends ClasaG { private int atribut4; ... } </pre>

<p>Realisation</p>	<pre> classDiagram class A { <<interface>> +op1():void +op2():void } class B { <<interface>> +op3():void } class C { -atribut1:String -atribut2:String +op1():void +op2():void +op3():void } A < .. C B < .. C </pre>	<pre> public class C implements B, A { private String atribut1; private String atribut2; public void op3 () { ... } public void op1 () { ... } public void op2 () { ... } } </pre>
<p>Navigable association</p>	<pre> classDiagram class A1 class B1 A1 --> B1 </pre>	<pre> public class A1 { private B1 b1; } </pre>
<p>Navigable association</p>	<pre> classDiagram class A2 class B2 A2 --> "*" B2 </pre>	<pre> public class A2 { private B2[] b2; } </pre>
<p>Navigable association</p>	<pre> classDiagram class A3 class B3 A3 --> "*" B3 : {ordered} </pre>	<pre> public class A3 { private List<B3> b3= new ArrayList<B3>(); } </pre>

<p>Bidirectional association</p>	<p>cd bidirectional</p> 	<pre>public class A { private B b; ... } public class B { private A a; ... }</pre>
<p>Reflexive association</p>	<p>cd asociere reflexiva</p> 	<pre>public class A { private A b []; ... }</pre>
<p>Composition</p>	<p>cd Compunere</p> 	<pre>public class A { private int atribut1; private B b; private static class B { private int atribut2; ... } }</pre>



Remarks

- The UML tools transforms any UML class into Java class stored in separate file;
- The UML interface is translated in Java language using keyword *interface*;
- In Java language the attributes become class member variable. The attribute type could be simple (int, double, float, long, char etc.) or could be a class (String, Date etc.);
- The UML class attribute become static member variable in Java language;
- The UML operations are class methods in Java language and class operations become private static methods of class;
- The generalization in Java language is the inheritance feature of object oriented programming and will be introduced by keyword *extends*;
- The realisation of one UML interface is done by Java language keywords *implements*;
- A navigable association of multiplicity 1 is translated in Java language using a member variable of referred class type. A multiplicity of kind <<*>> is translated in Java language using a collection of referred class.
- The bidirectional association is translated into Java language by one member variable of referred class type in each class. The variables identifier is the name of the role placed at the end of the association.
- The UML reflexive association is translated into Java by a member variable of same class type.

In the figure 1. are presents the class structure for some documents like: check, invoice and receipt.

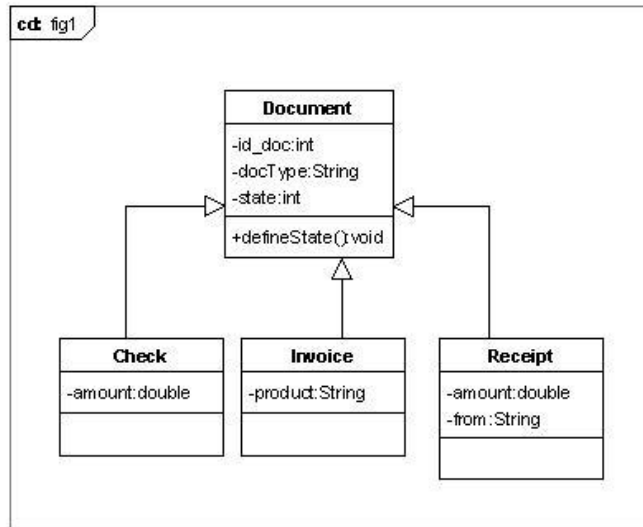


Fig. 1. Class structure

The next Java code are generated starting from the classes Check, Invoice and Receipt, presented in figure 1.

```

public class Document {
    private int ID_doc;
    private String tipdoc;
    private int state;
    public void defineState() {
        // your code here
    }
}
public class Check extends Document {
    private int amount;
}
public class Invoice extends Document {
    private String product;
}
public class Receipt extends Document {
    private int amount ;
    private String from;
}
  
```

3. SOFTWARE TOOLS FOR UML 2

3.1. UML Software Tools Market

UML has been created in order to be also used by (brand) software applications which allow both the construction of UML diagrams and the code generating process (Java, C#, PHP etc.) in order to accomplish object-oriented application projects.

The market for UML software tools has not yet reached full maturity since there are still hundreds of instruments with different philosophies and qualities. Generally, the UML tools provide various features but the most important factors are: user interface look and feel, support for code generation and code import, conformance with the latest UML standard, and integration with the environment. The UML tools must not save the UML diagrams in their own formats which is not compatible with the formats of other UML tools.

The UML software tools increase the program developer productivity as well as the quality of software application modelled.

A recent market study of the UML tools identifies three categories of software products: multi-purpose software tools, code generating software tools and MDA (Model Driven Architecture) software tools.

3.2. Multi- Purpose Software Tools

Multipurpose software tools belong to the first generation of UML tools and can be used in the analysis, conception and code generating phases of the development of software applications.

The main UML software products pertaining to this category are: IBM-Rational Rose; Borland Together Control Centre; Softeam Objecteering, Embarcadero Describe; Gentleware Poseidon for UML; Popkin Support Architect; Tigris ArgoUML; Visual Paradigm for UML; Enterprise Architect etc.

3.3. Code Generating Software Tools

Code generating software tools grant the data application generators the possibility to immediately visualise the structure of the code by synchronising the generated code and the edited UML class diagrams.

The main software products which form part of this category are: Borland Together; IBM Rational XDE; Oracle JDeveloper 10g; Omondo UML; IDE Visual Studio 8 etc.

Figure 2 presents the architecture of the product Borland Together.

3.4. MDA TOOLS

MDA is an approach to software development that provides a set of guidelines for structuring specifications expressed as models.

MDA standard is mainly based on two standards of OMG: MOF (Meta-Object Facility) for the model data and XMI (XML Metadata Interchange) for the exchange between tools, but is related to other multiple standards including EDOC (Enterprise Distributed Object Computing), SPEM (Software Process Engineering Metamodel), CWM (Common Warehouse Metamodel).

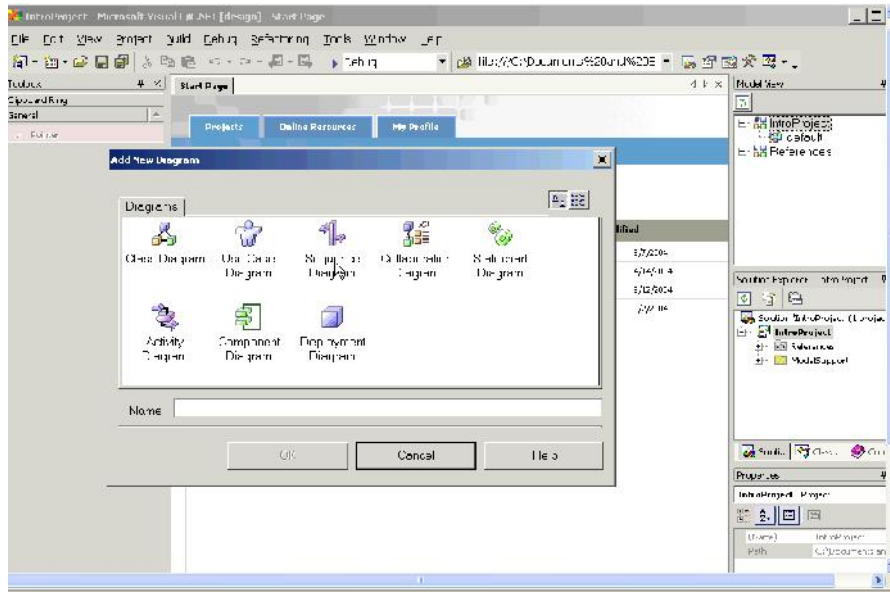


Fig. 2. The product Borland Together

The analysis of the UML software tools market has demonstrated that there is no clear demarcation between the software products approaching MDA and the software tools belonging to the other two categories.

The main software products which represent MDA solutions are the following: Compuware Optimal J; Arcstyler; Codagen Architect; AndromDA; Kabira; Kennedy Carter UML; I-Logix Rhapsody etc.

REFERENCES

- [1]. Balzert, H. *UML 2 compacts*, Eyrolles, Paris, 2005
- [2]. Blanc, X., Mounier, I., Besse, C. *UML 2 pour les developpeurs*, Eyrolles, Paris, 2006
- [3]. Charroux, B., Osmani, S., Thierry-Mieg, Y. *UML 2*, Pearson Education France, Collection Syntex, 2005
- [4]. Debrauner, L., Karam, N. *UML 2, Entraînez-vous à la modelisation*, ENI, Paris, 2006
- [5]. Pilone, D, Pitman, N. *UML 2. En concentre. Manuel de reference*, O'Reilly, Paris, 2006

INDEX OF AUTHORS

A

ACHIM M., 111
ALBOTEANU L., 357
ARAD S., 28
ARAD V., 28

B

BACIU I., 83, 192
BERZAN F.M., 147, 164
BLĂNARU, L., 34, 133, 196
BOBORA, B., 28
BOBORA, M., 28
BOCIAT A., 205,
BORON S., 126
BRÎNDUȘA A., 215, 218, 381
BRINDUSA, C., 67, 183, 188, 222
237
BUCUR G., 260
BUCUR L., 260
BURIAN S., 37, 43, 120
BUSONI, A., 91

C

CASAVELA V., 338
CANGEA O., 320
CAZACU D., 16
CÂRLAN, M., 49
CECLAN, A., 72
CERNAT M., 97
CORCĂU J. I., 174, 232
COVACIU C., 111
CSASZAR, T., 43
CUNȚAN, C., 83, 192
CURČIĆ S., 6
CURELEANU S., 34, 133, 196

D

DAN N., 160, 211
DAN, V., 160, 211, 226
DARIE M., 37, 43, 120

DAŠIĆ P., 6, 385
DEACONU, S., 22, 77, 107
DOBRA R., 242
DOJCSAR D., 278
DUMITRAȘCU, L., 392
DUSMANESCU D., 392
DZIȚAC S., 49, 55,

E

EGRI A., 326

F

FELEA, I., 55
FOTĂU I., 168

G

GAWOR P., 126
GHICIOI E., 199
GROFU F., 286, 292
GOIA H., 49, 55

I

IONESCU J., 37, 120
IRIMIA R.A., 266

J

JURCA A., 147, 199

K

KOVACS I., 215, 218, 381

L

LEBA M., 254,
LUPU L., 87, 164

M

MÂNDRESCU C., 246, 365
MANOLEA G., 357
MARCU I., 91
MARCU M., 153
MARCU G., 392
MARDARE D., 91
MICU D., 72
MICU D. D., 72
MOLDOVAN L., 37

N

NEDEFF V., 6
NOUR A., 357

O

OLARU O., 292
ORBAN M., 133,

P

PANĂ L., 153, 168,
PĂRĂIAN M., 199,
PĂSCULESCU D., 67, 183, 188, 222,
237
PĂSCULESCU M., 183, 188, 222
PĂTRASCIOIU C, 298
PĂTRASCIOIU N, 309, 351
PĂUN F., 87, 164,
POANTA A., 278,
POP E., 254, 343
POP E., 343
POPA G.N., 22, 77, 107,
POPA I., 22, 77, 107,
POPESCU C., 133, 298,
POPESCU F., 153,
POPESCU L., 283,
POPESCU M., 283, 292,
POPESCU M. C, 312
POPESCU C-na., 332

R

RATOMIR J., 385
RAVIGAN F., 357
RISTEIU M., 111, 272, 373
RODEAN I., 107

S

SIMION, E., 72
SÎRB V. C., 326
SOCHIRCA B., 278
STANESCU C., 16
STOIA, D., 97,
STOICHITOIU A., 34, 196
STOICUȚA O., 246, 365

Ș

ȘERBAN H., 168

T

TĂBĂCARU-BARBU T., 61,
TĂBĂCARU-BARBU C. I., 343,
TOMUȘ A. M., 309, 351
TULBURE A., 111, 272, 373

U

UTU I., 133,

V

VAIDA V., 138
VAMVU P., 254,
VASIU I., 205,
VĂTAVU N., 87, 147, 199,
VEIS Ș., 385
VIȘAN, D., 91,
VLĂSCEANU A.N., 266,

Z

ZOLLER C., 226